FINAL REPORT

Strength Envelopes for Florida Rock and Intermediate Geomaterials

FDOT Contract No: BDV31-977-51
UF Project No: 00125485

Submitted to:
Rodrigo Herrera, P.E.
David Horhota, Ph.D., P.E.
Project Managers
Florida Department of Transportation

Principal Investigators:
Michael C. McVay, Ph.D.
Xiaoyu Song, Ph.D.
Scott Wasman, Ph.D.

Graduate Assistant:
Thai Nguyen, Ph.D., P.E.
Kaiqi Wang

May 2019

University of Florida
Department of Civil and Coastal Engineering

DISCLAIMER

The opinions, findings, and conclusions expressed in this publication are those of the authors and not necessarily those of the Florida Department of Transportation or the U.S. Department of Transportation.

Prepared in cooperation with the State of Florida Department of Transportation and the U.S. Department of Transportation.

SI (MODERN METRIC) CONVERSION FACTORS (from FHWA)

APPROXIMATE CONVERSIONS TO SI UNITS

SYMBOL	WHEN YOU KNOW	MULTIPLY BY	TO FIND	SYMBOL
LENGTH				
in	inches	25.4	millimeters	mm
ft	feet	0.305	meters	m
yd	yards	0.914	meters	m
mi	miles	1.61	kilometers	km

SYMBOL	WHEN YOU KNOW	MULTIPLY BY	TO FIND	SYMBOL
AREA				
in^2	square inches	645.2	square millimeters	mm^2
ft^2	square feet	0.093	square meters	m^2
yd^2	square yard	0.836	square meters	m^2
ac	acres	0.405	hectares	ha
mi^2	square miles	2.59	square kilometers	km^2

SYMBOL	WHEN YOU KNOW	MULTIPLY BY	TO FIND	SYMBOL
VOLUME				
fl oz	fluid ounces	29.57	milliliters	mL
gal	gallons	3.785	liters	L
ft^3	cubic feet	0.028	cubic meters	m^3
yd^3	cubic yards	0.765	cubic meters	m^3
NOTE: volumes greater than 1000 L shall be shown in m^3				

SYMBOL	WHEN YOU KNOW	MULTIPLY BY	TO FIND	SYMBOL
MASS				
oz	ounces	28.35	grams	g
lb	pounds	0.454	kilograms	kg
T	short tons (2000 lb)	0.907	megagrams (or "metric ton")	Mg (or "t")

SYMBOL	WHEN YOU KNOW	MULTIPLY BY	TO FIND	SYMBOL
TEMPERATURE (exact degrees)				
°F	Fahrenheit	5 (F-32)/9 or (F-32)/1.8	Celsius	°C

SYMBOL	WHEN YOU KNOW	MULTIPLY BY	TO FIND	SYMBOL
ILLUMINATION				
fc	foot-candles	10.76	lux	lx
fl	foot-Lamberts	3.426	candela/m^2	cd/m^2

SYMBOL	WHEN YOU KNOW	MULTIPLY BY	TO FIND	SYMBOL
FORCE and PRESSURE or STRESS				
Lbf*	poundforce	4.45	newtons	N
kip	kip force	1000	pounds	lbf
lbf/in^2 (psi)	poundforce per square inch	6.89	kilopascals	kPa
ksf	kips per square foot	0.04788	Megapascals	Mpa
tsf	tons per square foot	0.09576	Megapascals	Mpa

APPROXIMATE CONVERSIONS TO SI UNITS

SYMBOL	WHEN YOU KNOW	MULTIPLY BY	TO FIND	SYMBOL
LENGTH				
mm	millimeters	0.039	inches	in
m	meters	3.28	feet	ft
m	meters	1.09	yards	yd
km	kilometers	0.621	miles	mi

SYMBOL	WHEN YOU KNOW	MULTIPLY BY	TO FIND	SYMBOL
AREA				
mm^2	square millimeters	0.0016	square inches	in^2
m^2	square meters	10.764	square feet	ft^2
m^2	square meters	1.195	square yards	yd^2
ha	hectares	2.47	acres	ac
km^2	square kilometers	0.386	square miles	mi^2

SYMBOL	WHEN YOU KNOW	MULTIPLY BY	TO FIND	SYMBOL
VOLUME				
mL	milliliters	0.034	fluid ounces	fl oz
L	liters	0.264	gallons	gal
m^3	cubic meters	35.314	cubic feet	ft^3
m^3	cubic meters	1.307	cubic yards	yd^3

SYMBOL	WHEN YOU KNOW	MULTIPLY BY	TO FIND	SYMBOL
MASS				
g	grams	0.035	ounces	oz
kg	kilograms	2.202	pounds	lb
Mg (or "t")	megagrams (or "metric ton")	1.103	short tons (2000 lb)	T

SYMBOL	WHEN YOU KNOW	MULTIPLY BY	TO FIND	SYMBOL
TEMPERATURE (exact degrees)				
°C	Celsius	1.8C+32	Fahrenheit	°F

SYMBOL	WHEN YOU KNOW	MULTIPLY BY	TO FIND	SYMBOL
ILLUMINATION				
lx	lux	0.0929	foot-candles	fc
cd/m^2	candela/m^2	0.2919	foot-Lamberts	fl

SYMBOL	WHEN YOU KNOW	MULTIPLY BY	TO FIND	SYMBOL
FORCE and PRESSURE or STRESS				
N	newtons	0.225	poundforce	lbf
kPa	kilopascals	0.145	poundforce per square inch	lbf/in^2

*SI is the symbol for International System of Units. Appropriate rounding should be made to comply with Section 4 of ASTM E380. (Revised March 2003)

TECHNICAL REPORT DOCUMENTATION PAGE

1. Report No.	2. Government Accession No.	3. Recipient's Catalog No.

4. Title and Subtitle	5. Report Date
Strength Envelopes of Florida Rock and Intermediate Geomaterials	May 2019
	6. Performing Organization Code

7. Author(s)	8. Performing Organization Report No.
Michael McVay, Xiaoyu Song, Scott Wasman, Thai Nguyen, and Kaiqi Wang	

9. Performing Organization Name and Address	10. Work Unit No. (TRAIS)
University of Florida – Dept. of Civil and Coastal Engineering Engineering School of Sustainable Infrastructure and Environment 365 Weil Hall – P.O. Box 116580 Gainesville, FL 32611-6580	11. Contract or Grant No. BDV31-977-51

12. Sponsoring Agency Name and Address	13. Type of Report and Period Covered
Florida Department of Transportation 605 Suwannee Street, MS 30 Tallahassee, FL 32399	Final Report 1/25/16 – 5/01/19
	14. Sponsoring Agency Code

15. Supplementary Notes

16. Abstract: For the design of a shallow foundation on Florida limestone, a calibrated bearing capacity equation based on a material-specific strength envelope is required. In this study, two large data sets containing samples from across the state of Florida were studied. Data set #1 contained over 8,000 results of unconfined compression tests (q_u), split tension (q_t), and bulk dry unit weight (γ_{dt}), and set #2 with 570 results contained q_u, q_t, γ_{dt}, as well as rock formation identification, carbonate content, and porosity components. The data sets show Florida carbonate rocks are porous to very porous with porosity up to 60% and median porosity of 37%. The data sets were used to develop strong correlations for q_t and q_u from bulk dry unit weight, carbonate content, and formation factor. Next, (conventional triaxial compression (CTC) testing (>300) with cell pressures up to 1,500 psi was performed to evaluate the ductile and brittle nature of Florida limestone. It was concluded that most of Florida's near surface rocks are in the ductile range when subjected to confining stresses typical for shallow foundation loadings. Based on the test results, a threshold for rocks to change from brittle to ductile behavior has been identified. Most significantly, strength envelopes for the rocks in the study have been developed from all the triaxial results. In general, the envelopes show significant downward slope after reaching peak values, at much steeper rate than the envelopes for brittle rocks. Additionally, guidelines to establish the strength envelope for other rock formations in Florida are provided.

Subsequently, a constitutive model representative of the nonlinear strength envelope of Florida limestone was implemented into a 2D and 3D finite element code, and simulations were carried out for potential shallow foundation scenarios (homogenous or rock over sand). Each characterization (B, B/L, and D/B) was simulated with the full range of expected strength properties. Finally, an analytical bearing capacity equation was developed for both the homogeneous and rock-over-sand scenario. The Florida bearing capacity equation was calibrated using the numerical simulation results, and it can be applied to any footing shape, depth from 0 to B, and any rock thickness, even rock overlying a soil layer, such as the case in south Florida, where cap rock Is usually encountered atop a thick sand layer.

17. Key Words	18. Distribution Statement
Florida limestone, Shallow Foundation Design, Bearing Capacity, Strength Envelope, Triaxial Compression Testing, Index Testing and Unconfined Compression Strength.	No restrictions.

19. Security Classif. (of this report)	20. Security Classif. (of this page)	21. No. of Pages	22. Price
Unclassified	Unclassified	271	

Form DOT F 1700.7 (8-72) Reproduction of completed page authorized

ACKNOWLEDGEMENTS

The researchers would like to thank the Florida Department of Transportation (FDOT) for the financial support to carry out this research. In addition, special thanks are given to the Central Office, State Materials Office and District Offices for the collection as well as assistance in testing (chemical, XRD, index, and triaxial) of all Florida limestone samples.

EXECUTIVE SUMMARY

For shallow foundation bearing capacity, a strength envelope is required. For soils, the well-known Mohr-Coulomb linear envelope with two parameters, cohesion, c, and internal friction, φ, is typically used. For rocks with brittle stress-strain behavior, either the Mohr-Coulomb or the Hoek-Brown envelope is applicable. However, rocks with ductile stress-strain behavior within the range of shallow foundation confining stress have never been explored for bearing capacity analyses. Therefore, for Florida carbonate rocks, there are two concerns: (i) what are strength envelopes for Florida carbonate rocks, and are they following envelopes for brittle or ductile behavior? (ii) coring Florida rock typically provides poor recoveries with limited specimens that are long enough to satisfy the unconfined compression strength test standard requirements; thus, there is a need to correlate rock index parameters to basic strength parameters.

In this study, two large data sets containing test results of rock core samples from across the state of Florida were studied. Data set #1 contained more than 8,000 results of the unconfined compression test (q_u), splitting tension test (q_t), and bulk dry unit weight (γ_{dt}). Data set #2 contained approximately 570 data points with q_u, q_t, γ_{dt}, rock formation identification, carbonate content, and porosity components (vug and inner porosities). The study indicates that Florida carbonate rocks are porous to very porous, with porosity up to 60% and a median porosity of 37%. Due to high porosity, recent deposition (many rock formations deposited within the last 2 million years, which is a relatively short time for rock deposition/sedimentation), and low carbonate content; Florida near surface rocks have low strengths, with median q_t of 0.6 MPa (90 psi) and median q_u of 3 MPa (435 psi). The study has established strong correlations to estimate q_t and q_u from bulk dry unit weight, formation identification, and carbonate content.

A rock triaxial system with a modified volume change measurement device was used to analyze Florida carbonate rocks' stress-strain and volumetric responses. Based on more than 200 triaxial test results, it was concluded that most Florida rocks display ductile behavior when subjected to confining stresses typical for shallow foundation loadings. Based on the test results, a threshold for several rock foundations to change from brittle to ductile behavior was summarized. Most significantly, strength envelopes were developed from the triaxial test results. These envelopes show significant downward slopes beyond the point the peak strength, at much steeper rate than the envelopes for brittle rocks. Additionally, guidelines to establish the strength envelope for other Florida rock formation is recommended in the appendix.

As part of the numerical modeling, a material model was developed for Florida limestone based on the strength envelopes from the experimental test and validation of the material model. The material model was validated, and the parametric studies was performed for one rock layer and two-layer (rock overlying sand) systems. Finally, bearing capacity equations were developed for shallow foundations resting on a rock or rock overlying sand.

The Florida bearing capacity equation was calibrated using numerical simulation results, which can be applied to any footing shape, any depth, and any rock thickness, even rock overlying a soil layer, such as the case in south Florida, where a caprock is usually encountered atop a thick sand layer:

$$Q_u = \min (Q_{u1}, Q_{u2}) * \xi / N_R \quad \text{(vii-1)}$$

$$Q_{u1} = n\, c\, N_c + qN_q \quad \text{(vii-2)}$$

$$Q_{u2} = n\, [c\, N'_c + p_p\, N_\gamma\,] + qN_q \quad \text{(vii-3)}$$

where the width factor (n), shape factor (ξ), rock thickness reduction factor (N_R), and other related terms are defined in Chapter 8 and summarized in Chapter 9

TABLE OF CONTENTS

page

DISCLAIMER II

SI (MODERN METRIC) CONVERSION FACTORS (FROM FHWA) III

TECHNICAL REPORT DOCUMENTATION PAGE V

ACKNOWLEDGEMENTS VI

EXECUTIVE SUMMARY VII

LIST OF TABLES XII

LIST OF FIGURES XIV

CHAPTER 1 INTRODUCTION 1

CHAPTER 2 FLORIDA SURFACE ROCK GEOLOGY AND GENERAL TERMINOLOGIES 4

2.1 Geology of Florida Surface Rocks 4
2.2 Example Pictures of Florida Rocks 9
2.3 General Carbonate Rock Terminologies 13

CHAPTER 3 OVERVIEW OF CONVENTIONAL LABORATORY TESTS FOR CARBONATE ROCKS 15

3.1 Porosity and Unit Weight Tests 15
3.2 Carbonate Content Test 20
3.3 Powder X-ray Diffraction (XRD) 21
3.4 Splitting Tension Strength Test 23
3.5 Unconfined Compression Test 27

CHAPTER 4 PROPERTIES OF CARBONATE ROCKS AND IGMS 29

4.1 Florida Data 29
4.2 Florida Carbonate Rock Porosity and Unit Weight Results 31
4.3 Florida Carbonate Rock Minerals 35
4.4 Subsurface Spatial Variability 40
4.5 Summary 42

CHAPTER 5 SPLITTING TENSION AND UNCONFINED COMPRESSION STRENGTHS OF FLORIDA CARBONATE ROCKS AND IGMS 43

5.1 Necessity for Florida Rock Strength Correlation 43
5.2 Splitting Tension Strength Test (q_t) 44

5.3 Unconfined Compression Strength (q_u)....55
5.4 Unconfined Strengths of Marls....63
5.5 Stress-Strain Behavior....64
5.6 Summary....65

CHAPTER 6 STRENGTH ENVELOPES OF FLORIDA CARBONATE ROCKS AND IGMS....67

6.1 Existing Strength Envelopes....67
6.2 Triaxial System for Rock Testing....74
6.3 Triaxial Hoek cell....75
6.4 Displacement or Strain Measurements....79
6.5 Range of Triaxial Confining Pressures....81
6.6 Triaxial Stress-Strain and Volumetric Responses of Florida Carbonate rocks....83
6.7 Extension Test Results....89
6.8 Intact-rock Strength Envelope....92
6.9 Simplified Intact-rock Strength Envelope....102
6.10 Rock Mass Strength Envelope....111
6.10.1. Weight-adjusted Strength Envelope....113
6.10.2. Recovery-adjusted Strength Envelope....114
6.11 Summary....116

CHAPTER 7 NUMERICAL MODELING – SHALLOW FOUNDATIONS ON FLORIDA ROCKS....118

7.1 Material model....118
7.2 Validation of FEM code and material model....119
7.2.1. Validation of elastic, perfectly plastic model....120
7.2.2. Validation of Drucker-Prager-Cap model....127
7.3 Parametric Studies – Rock Subsurface....129
7.4 Parametric Studies – Rock over Sand Subsurface....146

CHAPTER 8 BEARING EQUATIONS – SHALLOW FOUNDATIONS ON FLORIDA ROCKS....166

8.1 Bearing Equations – Shallow foundation on Rock Subsurface....166
8.1.1. Strip footings of width B = 4 m at ground surface, D = 0 m....166
8.1.2. Strip footings B = 4 m below surface, D = 2 m....168
8.1.3. Strip footings with different widths....169
8.1.4. Shape factors....170
8.1.5. Bearing Capacity Bias Ratios – Rock Subsurface....171
8.2 Bearing Equations – Shallow Foundation on Rock over Sand Subsurface....174
8.2.1. N_R reduction factor....174
8.2.2. Bearing Capacity Bias Ratios – Rock over Sand Subsurface....175
8.3 Bearing capacity comparison with existing method....182
8.4 Design examples....188

8.4.1. Case (1): Rectangular footing with embedment D = 0 ft 190
8.4.2. Case (2): Rectangular footing with embedment D = 10 ft 191
8.4.3. Case (3): Rectangular footing supported on a thin layer of rock overlying sand 192

CHAPTER 9 CONCLUSIONS AND RECOMMENDATIONS 194

LIST OF REFERENCES 200

APPENDIX A ROCK CORE DESCRIPTIONS 205

APPENDIX B ROCK CORE PICTURES 207

APPENDIX C ROCK TRIAXIAL TEST PROCEDURE 217

C.1 Sigma-1 Features 217
C.2 Sample Preparation 218
C.3 Isotropic Loading to σ_{3max} 219
C.4 Deviatoric (Shear) Loading 220
C.5 End Test 220

APPENDIX D PICTURES OF SPECIMENS AFTER TRIAXIAL TESTS 221

APPENDIX E REPRESENTATIVE INDIVIDUAL TEST RESULTS 224

APPENDIX F RECOMMENDED PROCEDURE TO ESTABLISH STRENGTH ENVELOPE OF A DESIGN PROJECT 239

APPENDIX G FEM SIMULATION RESULTS IN SI UNIT 246

LIST OF TABLES

Table page

Table 3-1. Mineral specific gravities from literature 18
Table 3-2. Proposed vug descriptions 20
Table 3-3. Proposed porosity descriptions 20
Table 3-4. Typical carbonate rock strengths 28
Table 4-1. List of projects in data set #1 29
Table 4-2. List of projects in data set #2 31
Table 4-3. Carbonate content versus XRD interpreted results 38
Table 4-4. Estimated mineral components from carbonate content and specific gravity results ..39
Table 5-1. Splitting tension formation factor (F_t) 50
Table 5-2. Average carbonate content from data set #2 62
Table 5-3. Compression formation factors (F_u) 62
Table 6-1. Values of the constant m_i for carbonate rocks (after Marinos and Hoek 2000) 69
Table 6-2. Approximate behavior type table of Florida carbonate rocks based on σd/σ3 ratio ...86
Table 6-3. Approximate behavior type table of Florida carbonate rocks 86
Table 6-4. Value of 2nd slope (ω) on Florida strength envelopes 109
Table 7-1. Material parameters used in the simulation 125
Table 7-2. FEM simulation parameters 131
Table 7-3. FEM simulation results – Bearing capacity (tsf) on rock subsurface 137
Table 7-4. FEM simulation results – Bearing capacity (tsf) on 4.9 to 6.6-ft rock over sand subsurface – Plane strain only 147
Table 7-5. FEM simulation results – Bearing capacity (tsf) on 6.6 to 13.2-ft rock over sand subsurface – Plane strain only 156
Table 7-6. Additional FEM simulations - Bearing capacities (tsf) on rock subsurface 165
Table 7-7. Additional FEM simulations – Bearing capacities (tsf) on rock (E = 43.51 ksi) over sand subsurface 165
Table 8-1. Hoek Brown GSI values versus REC values in new bearing capacity equation 186
Table 8-2. Comparison data for REC=100, GSI=81 186
Table 8-3. Miami rock for REC=100, GSI=81 and parameters for Florida bearing capacity equations 190
Table 8-4. Bearing capacity for case (1) 191
Table 8-5. Bearing capacity for case (2) 192
Table 8-6. Bearing capacity for case (3) 193
Table 9-1. Proposed vug descriptions 195
Table F-1. Example data 242
Table G-1. FEM simulation results – Bearing capacity (MPa) on rock subsurface 246
Table G-2. FEM simulation results – Bearing capacity (MPa) on 1.5 to 2-m rock over sand subsurface – Plane strain only 252
Table G-3. FEM simulation results – Bearing capacity (MPa) on 2 to 4-m rock over sand subsurface – Plane strain only 259
Table G-4. Additional FEM simulations – Bearing capacities (MPa) on rock subsurface 265

Table G-5. Additional FEM simulation – Bearing capacities (MPa) on rock (E = 300 MPa) over sand subsurface 266

LIST OF FIGURES

Figure page

Figure 2-1. Stratigraphy of the Burnt Store Road and Nelson Road Pits in Lee County, Florida (Missimer and Scott 2001) 4
Figure 2-2. Geologic units of Florida geology (Scott et al. 2001) 5
Figure 2-3. Newberry quarry excavation (Bullock, 2004) 10
Figure 2-4. Heterogeneous rock specimens: (a) Half vuggy limestone, half coralline specimen; (b) "Scaled" coralline limestone specimen; (c) Two different limestones within one specimen; (d) Half solid, half porous specimen; (e) Solid rock with vug; (f) Vuggy and porous limestone specimens; (g) Fresh roots living in the vugs of limestone specimens 11
Figure 2-5. Weak, poorly cemented silt, sand, and limestone mixture in a core run 12
Figure 2-6. Examples of core runs with low RQD 13
Figure 3-1. Rock phase diagram 17
Figure 3-2. XRD major 2θ peaks for typical minerals 22
Figure 3-3. Example XRD patterns of Miami and Key Largo limestone specimens 23
Figure 3-4. q_t versus q_{dt} relationship 24
Figure 3-5. Examples of center splitting 25
Figure 3-6. q_t test on sample 543-1: (a) Splitting on center on one face; (b) Splitting off-center on the other face 25
Figure 3-7. Non-center splitting−tests on samples 534-1 and 541-6 26
Figure 3-8. q_t test on sample 545-2: (a) Compression crushing occurred at contact between the steel platen and specimen; (b) Splitting occurred after significant crushing; (c) Splitting stress versus displacement 26
Figure 3-9. q_t tests on vuggy porous limestones:(a) Splitting; (b) Crushing thorough soft end; (c) Crushing through weak zone 26
Figure 3-10. q_t test on sample 624-3 with uneven diameter 27
Figure 4-1. Data set #1 – Range of unit weights 32
Figure 4-2. Data set #1 – Dry unit weight histogram 33
Figure 4-3. Data set #1 – Porosity histogram 33
Figure 4-4. Vug porosity versus bulk porosity: (a) Plotted using data from this study; (b) Plotted using text data from Hester & Schmoker (1985) 34
Figure 4-5. Porosities of Florida carbonate rocks: (a) Vug and permeable porosities; (b) Vug porosity only 35
Figure 4-6. Carbonate content versus bulk dry unit weight γdt 36
Figure 4-7. Examples of rock core records: (a) Ft. Thompson site; (b) Anastasia site 41
Figure 4-8. Bulk dry unit weight γ_{dt} with depth 41
Figure 5-1. Data set #1 – Histogram of splitting tension strength q_t 46
Figure 5-2. Data set #1−q_t results versus bulk porosity 46
Figure 5-3. Data set #2−q_t results versus bulk porosity 47
Figure 5-4. Data set #1−q_t results versus bulk dry unit weight 47
Figure 5-5. Data set #2−q_t results versus bulk dry unit weight 48
Figure 5-6. Data set #2−q_t and bulk dry unit weight for different formations 49
Figure 5-7. Data set #2−$Bias_1$ for each project site 49

Figure 5-8. Splitting tension formation factor F_t 50
Figure 5-9. Types of porosities: (a) Sketch of porosity types; (b) Vuggy specimen; (c) Example of porosities at γ_{dt} = 15.7 kN/m^3 (100 pcf) 50
Figure 5-10. Data set #2−q_t correlation with γ_{dt}, F_t, and C 53
Figure 5-11. Statistical results for Miami formation only - q_t correlation with γ_{dt}, F_t, and C: (a) F_t = 0.75, 0.9, and 1.0; (b) F_t = 0.9 for all 3 sites 54
Figure 5-12. Data set # 2 - $Bias_2$ and n_v 55
Figure 5-13. Data set #1−Histogram of unconfined compression strength q_u 56
Figure 5-14. Data set #1−q_u results versus bulk dry unit weight 56
Figure 5-15. Data sets #1a and 2−q_u and bulk dry unit weight for different formations 57
Figure 5-16. Bullock (2004) q_u versus q_t relationship 59
Figure 5-17. q_u versus q_t relationship: (a) For typical Florida rocks; (b) For rocks outside of typical Florida strengths. Notes: 1, LS – Limestone; 2, Johnston relationship is for direct tension test result, q_{dt} 60
Figure 5-18. Data sets #1a and 2 – q_u correlations: (a) Correlation against 1 parameter (γ_{dt}); (b) Correlation against 3 parameters (γ_{dt}, F_u, and C) 62
Figure 5-19. q_t results for marl 63
Figure 5-20. q_u results for marl 64
Figure 5-21. Example of stress-strain results from q_u tests: (a) Site 8-I95 on the Fuller Warren Bridge, St. Johns River; (b) Site 21-SR 8 over Choctawhatchee River 65
Figure 6-1. Sketch of strength envelopes 68
Figure 6-2. Rock unconfined compression strength, bulk dry unit weight, and porosity 72
Figure 6-3. Triaxial modular setup 76
Figure 6-4. Schematic of Hoek triaxial cell test 76
Figure 6-5. Hoek cell design 77
Figure 6-6. Hoek cell hydraulic fluid filling 78
Figure 6-7. Triaxial system with accumulator and volume change device 80
Figure 6-8. Triaxial system with Digiflow pump 80
Figure 6-9. Volume change with membrane displacement 81
Figure 6-10. Pressure under a footing: (a) Active and passive zones (Adapted from Carter and Kulhawy, 1988); (b) Possible contact stresses 82
Figure 6-11. Stress paths and strength envelope 83
Figure 6-12. Examples of triaxial results−Key Largo formation: (a) γ_{dt} = 18.9 kN/m^3 = 120 pcf, σ_3 = 345 kPa = 50 psi; (b) γ_{dt} = 15.7 kN/m^3 = 100 pcf, σ_3 = 3,100 kPa = 450 psi 84
Figure 6-13. Normalized deviatoric stress and volumetric strain: (a) Combination plots of multiple specimens; (b) Example of “transition” behavior 85
Figure 6-14. Crushing of porous rocks: (a) isotropic loading; (b) isotropic then deviatoric loadings 87
Figure 6-15. Unconfined compression test and extension test results 89
Figure 6-16. Triaxial compression test and extension test results: (a) σ_3 = 130 psi; (b) σ_3 = 600 psi 90
Figure 6-17. Triaxial extension test stress – strain curve for specimen 813 91
Figure 6-18. Outlier extension test specimens: (a) Hole on specimen; (b) One end of specimen is much softer 91
Figure 6-19. Schematic of strength envelope construction 92
Figure 6-20. Key Largo normalized deviatoric stress results 93

Figure 6-21. Examples of incorrectly constructed strength envelopes: (a) Specimens A and B pairing; (b) Specimens C and D pairing 94
Figure 6-22. Strength envelope – Key Largo Formation 95
Figure 6-23. Strength envelope – Anastasia Formation 96
Figure 6-24. Strength envelope – Miami Formation 97
Figure 6-25. Strength envelope – Shallow Ft. Thompson Formation 98
Figure 6-26. Strength envelope – Hawthorn Formation 98
Figure 6-27. Example of lower bound and upper bound of intact rock strength envelope 99
Figure 6-28. Verification for using $0.7q_t$ as q_{dt} value: (a) Key Largo Formation; (b) Anastasia Formation 101
Figure 6-29. Schematic of bilinear strength envelope for intact rock 103
Figure 6-30. 2nd slope ω correlation – Key Largo Formation 105
Figure 6-31. 2nd slope ω correlation – Shallow Ft. Thompson Formation 105
Figure 6-32. 2nd slope ω correlation – Miami Formation 106
Figure 6-33. 2nd slope ω correlation – Anastasia Formation 106
Figure 6-34. 2nd slope ω correlation – Hawthorn Formation 106
Figure 6-35. Bilinear strength envelope – Key Largo Formation 107
Figure 6-36. Bilinear strength envelope – Anastasia Formation 107
Figure 6-37. Bilinear strength envelope – Miami Formation 108
Figure 6-38. Bilinear strength envelope – Shallow Ft Thompson Formation 108
Figure 6-39. Bilinear strength envelope – Hawthorn Formation 109
Figure 6-40. Scatter of predicted normalized stresses back-calculated from bilinear envelopes 111
Figure 6-41. Rock mass strength envelopes in relative to intact rock strength envelope: (a) q_u = 0.5 MPa; (b) q_u = 1 MPa; (c) q_u = 3 MPa; (d) q_u = 10 MPa 112
Figure 6-42. Bilinear strength envelope for rock mass from intact rock 115
Figure 7-1. Yield function in Lambe's p-q diagram 118
Figure 7-2. Variables in the τ - σ diagram 119
Figure 7-3. (a) Geometry of meshed model and boundary conditions; (b) Parameters in p-q diagram 120
Figure 7-4. Plastic shear strain 121
Figure 7-5. Comparison of bearing contact stress-computed center displacement curve 122
Figure 7-6. (a) Geometry of meshed model and boundary conditions; (b) Parameters in p-q diagram 123
Figure 7-7. Plastic shear strain 124
Figure 7-8. Comparison of bearing contact stress-computed center displacement curve 124
Figure 7-9. Geometry of meshed model and boundary conditions 125
Figure 7-10. (a) Deviatoric stress vs. axial strain from FEM simulation; (b) Deviatoric stress/confining stress vs. axial strain from laboratory testing 126
Figure 7-11. (a) Volumetric strain vs. axial strain for three different confining pressures from FEM simulation; (b) Volumetric strain vs. axial strain from laboratory testing 127
Figure 7-12. Mesh model and boundary conditions 128
Figure 7-13. Plastic shear strain 128
Figure 7-14. Comparison of the simulation results and Vesic's bearing equation results 129
Figure 7-15. Variables in the τ - σ diagram 130
Figure 7-16. Meshed model and boundary conditions – B/L = 0 and D ≥ 0 130
Figure 7-17. Meshed model and boundary conditions – B/L > 0 and D ≥0 131

Figure 8-1. Strip footing correlation for N_c 166
Figure 8-2. Strip footing bias statistical result 167
Figure 8-3. N_q correlation 169
Figure 8-4. Bearing ratios of non-strip footing versus strip footing 171
Figure 8-5. Bearing bias ratios – FEM versus bearing equation; rock subsurface 172
Figure 8-6. Bearing bias ratios – rock to rock-over-sand results 176
Figure 8-7. Rock-over-sand N_R reduction factor 177
Figure 8-8. Bearing bias ratios – FEM versus bearing equation; rock over sand subsurface 178
Figure 8-9. Capacity comparison for intact rock – Strip footing on rock subsurface 184
Figure 8-10. Capacity comparison for rock mass – Strip footing on rock subsurface 185
Figure 8-11. Design examples: (a) Rectangular footing with embedment D = 0 ft; (b) Rectangular footing with embedment D = 10 ft; (c) Rectangular footing supported on a thin layer of rock overlying sand 188
Figure B-1. Site 1, Bore hole RC-1 207
Figure B-2. Site 1, Bore hole RC-2 207
Figure B-3. Site 1, Bore hole RC-3 207
Figure B-4. Site 1, Bore hole RC-4 208
Figure B-5. Site 1, Bore hole RC-5 208
Figure B-6. Site 1, Bore hole RC-6 208
Figure B-7. Site 1, Bore hole RC-7 208
Figure B-8. Site 2, Bore hole RC-1 209
Figure B-9. Site 2, Bore hole RC-2 209
Figure B-10. Site 2, Bore hole RC-3 209
Figure B-11. Site 2, Bore hole RC-4 210
Figure B-12. Site 3, Bore hole RC-1 210
Figure B-13. Site 3, Bore hole RC-2 210
Figure B-14. Site 3, Bore hole RC-3 211
Figure B-15. Site 4, Bore hole RC-1 211
Figure B-16. Site 4, Bore hole RC-2 211
Figure B-17. Site 4, Bore hole RC-3 212
Figure B-18. Site 4, Bore hole RC-4 212
Figure B-19. Site 5, Bore hole RC-1 213
Figure B-20. Site 5, Bore hole RC-2 213
Figure B-21. Site 5, Bore hole RC-3 214
Figure B-22. Site 5, Bore hole RC-4 214
Figure B-23. Site 6, Bore hole RC-1 215
Figure B-24. Site 6, Bore hole RC-2 215
Figure B-25. Site 6, Bore hole RC-3 216
Figure B-26. Site 6, Bore hole RC-4 216
Figure C-1. Hand pump valves 218
Figure C-2. Sample preparation screen: (a) Load-control tab; (b) Sample dimensions 218
Figure C-3. Volume control tab 219
Figure C-4. Pressure ramp schedule 220
Figure D-1. Rock at failure surface apparently weaker than overall rock specimen 221
Figure D-2. Specimens tested at 130-psi chamber pressure: (a) γ_{dt} > 130 pcf; (b) γ_{dt} = 120 - 130 pcf; (c) γ_{dt} = 110 - 120 pcf 222

Figure D-3. Specimens deformed at 3,000 psi chamber pressure 223
Figure E-1. Test results at σ_3 = 50 psi.....225
Figure E-2. Test results at σ_3 = 130 psi.....227
Figure E-3. Test results at σ_3 = 200 psi.....229
Figure E-4. Test results at σ_3 = 300 psi.....231
Figure E-5. Test results at σ_3 = 600 psi.....233
Figure E-6. Test results at σ_3 = 1,000 psi.....234
Figure E-7. Test results at σ_3 = 3,000 psi.....236
Figure E-8. Specimens crushed during isotropic loading 237
Figure E-9. Extension triaxial tests.....238
Figure F-1. First portion of bilinear curve.....241
Figure F-2. Example of test triaxial results at 600-psi.....241
Figure F-3. Estimate representative triaxial results for the rock layer.....241
Figure F-4. First part of the bilinear envelope.....244
Figure F-5. Obtaining σ_d/σ_3 corresponding to γ_{dtw} 244
Figure F-6. Completion of bilinear envelope for intact rock.....244
Figure F-7. Envelopes for intact rock and rock mass.....245

CHAPTER 1
INTRODUCTION

Most of the Florida Department of Transportation (FDOT) bridges are founded on deep foundations (especially drilled shafts and driven piles). Many of these deep foundation elements derive their bearing capacities from the Florida carbonate rocks and intermediate geomaterials (IGM). In some areas where shallow rock formations exist (i.e., rocks encountered at a starting depth of less than 5 m, or 15 ft), designers have proposed the use of shallow foundations (i.e., spread footings) for support of bridge piers or bents. Required for design is the assessment of the rocks' bearing capacity, which requires strength envelopes for the rock material as well as identifying the stress-strain response to assess the failure modes (general, local, and punching). One option is to modify and use existing strength envelope models. One such model is the well-known Hoek-Brown criterion (Hoek and Brown 1980, 1988, and 2018), originally developed for underground excavation (tunnel) in hard rock. Another model is the Johnston (1985) criterion, which is very similar to Hoek-Brown criterion.

However, the rocks tested by Hoek and Brown (1980, 1988, and 2018) and Johnston (1985) typically had high strengths with brittle rupture failure responses. The problem with the adoption of these strength criteria is that Florida carbonate rock is generally weaker than rock formations in other areas of the world, due to its recent deposition as the Florida peninsula underwent varying degrees of submersion prior to its current geologic sate. Florida materials, especially at shallow depths, are porous to very porous and their stress-strain responses are not necessarily brittle. Given the differences, the recommended parameters suggested in the literature for use in Hoek-Brown or Johnston criteria have been brought into question when applied to Florida rock.

Due to the heterogeneous nature of Florida carbonate rock, the rock core recovery, REC = (total length of rock recovered) / (total length of the core run), and the rock quality designation, RQD = (sum of lengths of sound pieces that are longer than 4 inches) / (total length of the core run), are typically less than 100%, and frequently less than 50%. In addition, specimens for unconfined compression or triaxial strength tests are required to have a length / diameter ratio of 2.0 (i.e., the core pieces need to be longer than 5 or 8 inches for 2.5-in or 4.0-in core barrels, respectively). Therefore, there are often not enough pieces that are long enough for strength tests, and the pieces that can be tested represent the strongest rock. Thus, the first two objectives of this research are to:

Investigate the Florida rock index properties.

Establish correlations from rock index properties to conventional strength results (splitting tension – q_t and unconfined compression – q_u) to enable rock strength estimates from index testing of available core pieces from the core runs (too small to be tested).

Then, the research aims to:

1. Develop strength envelopes for both compression (underneath the footing) and extension (outside the footing) loading of Florida carbonate rock.

Develop stress-strain and volumetric strain models for Florida carbonate rock.

To address these objectives, this report is organized as follows:

- Chapter 2: Overview of Rock Identification and Geological Setting. This chapter presents a literature review into rock descriptions, with a focus on the shallow formations found in Florida.
- Chapter 3: Overview of Laboratory Tests. This chapter presents a literature review into the procedures of laboratory tests commonly performed on rock in Florida.
- Chapter 4: Properties of Carbonate Rocks and IGMs. Shown in this chapter are the results characterizing the index properties from two data sets of Florida carbonate rocks.
- Chapter 5: Splitting Tension and Unconfined Compression Strengths of Florida Carbonate Rocks and IGMs.

- Chapter 6: Strength Envelopes of Florida Carbonate Rocks and IGMs. The chapter has three main parts:

    a) Review of conventional strength envelopes (Mohr – Coulomb, Hoek-Brown, and Johnston)

    b) Description of the triaxial system and its modification to perform tests on Florida carbonate rocks

    c) Test results and strength envelope construction for Florida carbonate rocks.

- Chapter 7: Numerical simulation using results from Chapter 6
- Chapter 8: Empirical bearing equation, based on results from Chapter 7.

The study highlights the following key findings: i) different components of porosities, porous and vuggy scales, are recommended as there is no consistent grading scale that is available; ii) basic strength parameters are correlated to index rock parameters based on equations provided in Chapter 5, which are helpful when the recovered rock specimens are too short for strength tests; and iii) Florida carbonate rocks were found to have a predominantly ductile stress-strain response when the unconfined compression strength, q_u, is less than 9 MPa (1,300 psi), making strength envelopes for brittle rock unsuitable and necessitated the development of a strength envelope model for the different Florida formations that can be applied in evaluating shallow foundation bearing capacity on Florida carbonate rocks.

CHAPTER 2
FLORIDA SURFACE ROCK GEOLOGY AND GENERAL TERMINOLOGIES

2.1 Geology of Florida Surface Rocks

Florida carbonate rocks are chemical and/or biochemical sedimentary rocks. Chemical/biochemical sedimentary rocks are composed of minerals precipitated mainly from ocean or lake water by inorganic (chemical) and/or organic (biogenic) processes. The sediment and the cementation processes were governed by many factors, including the changes in water level. During the Holocene Epoch, the sea water level apparently fluctuated as much as 120 m (400 ft) (Chappell, 2009). As a result, the shallow soils and rocks have high spatial variability, or heterogeneity. This heterogeneous feature of Florida materials is depicted in Figure 2-1, which shows the stratigraphy of shallow materials within two pits in Lee County (Missimer and Scott 2001).

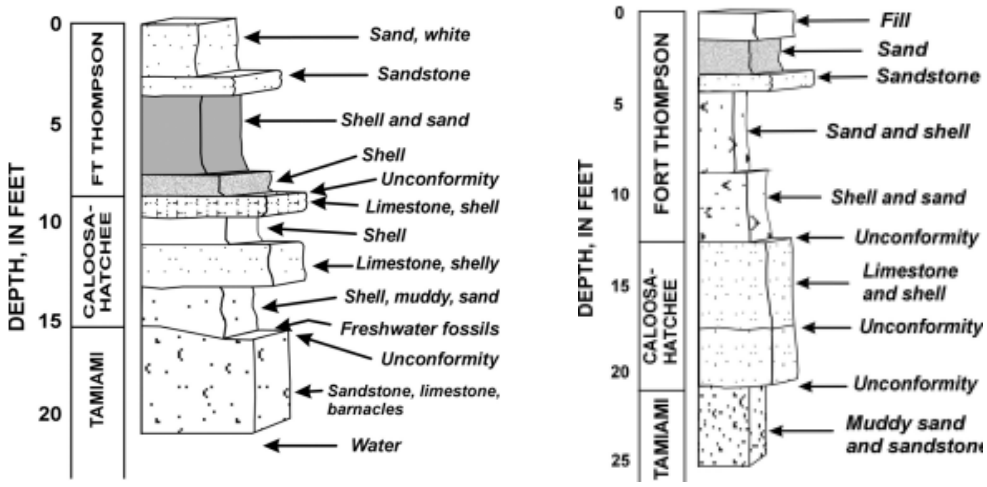

Figure 2-1. Stratigraphy of the Burnt Store Road and Nelson Road Pits in Lee County, Florida (Missimer and Scott 2001)

According to Figure 2-2, the Florida carbonate rocks are very young. The oldest rock in the state only dates back to the Eocene Epoch, which is only approximately 1% of the maximum time

scale of 4.6 billion years presented in Figure 2-2. As the Florida carbonate rocks are very young, many believe that some Florida carbonate rocks are still in the process of "forming", which may take millions or hundreds of millions of years. Therefore, while still in the forming process, some of Florida rocks have already been exposed to the weathering process, weakening the rock strengths.

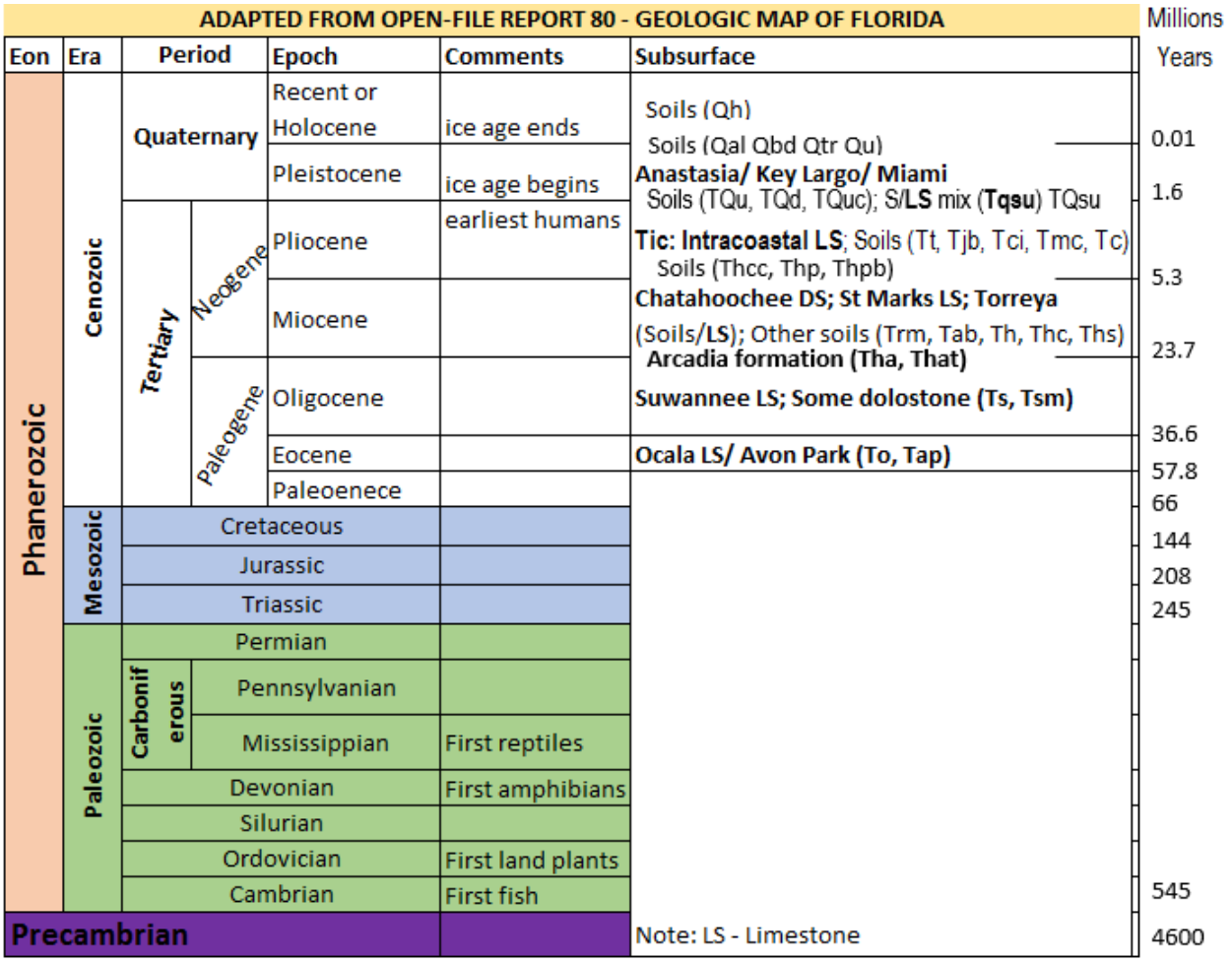

Figure 2-2. Geologic units of Florida geology (Scott et al. 2001)

The Florida carbonate rocks can be divided into: (i) limestone, (ii) dolostone, (iii) and marls. Limestones are composed mainly of the mineral calcium carbonate $CaCO_3$. The same chemical composition $CaCO_3$ can exist in different crystalline structures: (1) Rhombohedral for Calcite, and

(2) Orthorhombic for Aragonite. Per Boggs (2006), the modern shallow-water carbonate sediments are composed mainly of aragonite. Aragonite is metastable at the low pressures near the Earth's surface and is thus commonly replaced by calcite in fossils. As such, most limestones in Florida are calcite while some mollusk shells and calcareous coral endoskeletons are aragonite. Aragonite has a range of specific gravities (GS) from 2.85 to 2.94, which is higher than that for calcite (GS = 2.70 to 2.72) per Hester & Schmoker (1985). Using measured specific gravity results, Hester & Schmoker (1985) estimated that the aragonite content is substantially high (91% to 99%) for the Bahamian Oolites (Holocene epoch). However, for the older Pleistocene Miami limestones, aragonite has been replaced by calcite, thus the aragonite content reduces to typically between 30% and 5%. Apart from pure calcite, limestones can also contain several percent of magnesium in their content; for example, their chemical composition can be described as $Mg_{0.06}Ca_{0.94}CO_3$ with an informal name of mgcalcite.

Dolostones are composed mainly of the mineral dolomite $MgCa(CO_3)_2$. Dolomitization is a process by which limestone is altered into dolomite. When limestone comes into contact with magnesium-rich water, the mineral dolomite, $MgCa(CO_3)_2$, replaces the calcite, $CaCO_3$, in the rock, volume for volume. Dolomitization involves recrystallization on a large scale. The dolomite mineral grains often show distinct faces, are fairly uniformly sized throughout, and are larger than the calcite crystals in the limestone. When the recrystallization is not complete, the dolomite crystals are scattered throughout a calcite matrix. Sometimes rocks are formed that show zones of dolomite mottling the limestone where the magnesium-rich waters are thought to have filtered through the rock. In the process of dolomitization the dolomite crystals cut across original calcite grains, fossils, and oölites (spherical modules of calcite) and sometimes include quartz grains within their boundaries. Dolomites do not preserve the textures of the original limestone nor the

fossils therein. Fossils are uncommon in dolomites but sometimes remain as faint shadows outlining the original shape without showing internal detail or as molds with poor detail and filled with tiny dolomite crystals.

Marl or marlstone is a calcium carbonate or lime-rich mud or mudstone which contains variable amounts of clays and silt. The dominant carbonate mineral in most marls is calcite, but other carbonate minerals such as aragonite, dolomite, and siderite may be present. Marl was originally an older term loosely applied to a variety of materials, most of which occur as loose, earthy deposits consisting chiefly of an intimate mixture of clay and calcium carbonate, formed under freshwater conditions; specifically, an earthy substance containing 35–65% clay, silt, or sand and 65–35% carbonate. Marl specimens subjected to prolong air-dry condition gain significant strength. In the opposite direction, marl specimens subjected to prolong moisture condition lose their strengths and will not retain their own cylindrical shapes. Therefore, it is critical to preserve the natural moisture content of the cores and test the specimens right away. Once the marl specimens have been subjected to air-dry condition, their strengths have been naturally altered and should not be evaluated.

Most carbonate rocks have micro-crystallite structure, i.e., the rock grain contains small crystals visible only through microscopic examination. Rocks with very large grain size – when the grains are visible under human vision – are calcarenite and coquina (for example, the Anastasia Formation). Calcarenite is a clastic (cementation of sand and/or mud by calcite) sedimentary rock that is made up predominantly of recycled carbonate particles of sand size while coquina is composed of either wholly or almost entirely of the transported, abraded, and mechanically sorted fragments of shells.

Quartz (sand) is also a major component of Florida rocks, with contents of up to 50% by weight. The higher the quartz content, the lower the cementation of the rocks. Apart from four major minerals of calcite, aragonite, dolomite, and quartz, Boggs (2006) stated that minor amount of feldspars and clay minerals are present in most carbonate rocks, with minor to trace elements of Al, K, Mn, Na, Fe, Zn, B, Be, Ba, Sr, Br, Cl, Co, Cr, Cu, Ga, Ge, and Li. Many organisms concentrate and incorporate trace elements into their skeletal structures.

In urban or suburban areas of Florida where bridges are constructed, the following carbonate rock formations are typically encountered at shallow depths:

Qm: Miami Formation consists of two facies, an oolitic facies and a bryozoan facies. The oolitic facies is poorly to moderately indurated. The bryozoan facies are poorly to well indurated and tends to have more concentrations of fossils (Scott 2001).

Qk: Key Largo Formation is moderately to well indurated fossiliferous, coralline limestone composed of coral heads encased in a calcarenitic matrix (Scott 2001).

Qa: Anastasia Formation is composed of interbedded sands and coquinoid limestones. It is nonindurated to moderately indurated, coquina of whole and fragmented mollusk shells in a matrix of sand often cemented by sparry, i.e., coarse-grained, calcite (Scott 2001).

Tqsu: Shelly sediments of Plio-Pleistocene age (informal name as Okeechobee shelly sediments), formerly known as Caloosahatchee/Bermont/Fort Thompson Formations (Scott 2001). They are sands to limestone mixtures. The Fort Thompson Formation is typically found around Hendry County and may extend toward Palm Beach and Broward counties. Caloosahatchee Formation is typically found in Lee County. The Bermont Formation is typically found in Charlotte and/or Glades Counties and it overlies the Caloosahatchee Formation and underlies the Fort Thompson Formation.

To: Ocala Limestone: the lower Ocala Limestone is poorly to moderately indurated, very fossiliferous limestone. Where present, dolomite content increases with depth in the Ocala Limestone, especially in the southwestern part where the base of the unit is often dolomitized (Arthur et al. 2008). These dolostones can be either (1) friable, light to medium brown, sucrosic (i.e., coarsely recrystallized), or (2) indurated, dark gray to dark brown, dense, crystalline. The upper part of the Ocala Limestone is poorly to well indurated, very fossiliferous limestone. It tends to be more mud-supported (i.e., mudstone to wackestone) and chalky. Mineralogy of the Ocala Limestone unit is predominantly calcite, and to a lesser extent, dolomite. Siliciclastics are rare; however, chert occurs throughout the formation and is generally more common where the unit occurs at or near land surface.

Hawthorn Formation: The Hawthorn Formation can be divided into many subgroups (Scott 2001) and is typically encountered at depths deeper than 30 feet. Two following subgroups are evaluated in this research:

i) Marl: carbonate contents can be as high as 80% or as low as 20%. Core specimens subjected to prolong air-dry condition would gain significant strength. At low carbonate contents (such as below 50%), core specimens subjected to prolong moisture condition would lose their strengths and could not retain their own cylindrical shapes. Therefore, it is critical to preserve the natural moisture content of the cores and test the specimen right away. Once the core specimens have been subjected to air-dry condition, their strengths have been naturally altered and should not be evaluated.

ii) Hawthorn limestone/dolostone: this subgroup contains a mixture of calcite and dolomite, as well as quartz sand.

2.2 Example Pictures of Florida Rocks

Some example pictures of the Florida carbonate rocks are presented in Figure 2-3 through Figure 2-6, which highlight the heterogeneity of Florida rocks. Therefore, it is expected that all test results should display considerable scatter and the coefficient of determination R^2 is expected

to be low when correlating rock strength parameters. Additionally, despite having abundant holes (vugs) or scales (such as of coral heads), no distinctive rock joint or joint face could be identified in Florida carbonate rocks (Truzman 2016).

Figure 2-3. Newberry quarry excavation (Bullock, 2004)

a)

b)

c)

Figure 2-4. Heterogeneous rock specimens: (a) Half vuggy limestone, half coralline specimen; (b) "Scaled" coralline limestone specimen; (c) Two different limestones within one specimen

d) 

e) 

f) 

g) 

Figure 2-4. Continued; (d) Half solid, half porous specimen; (e) Solid rock with vug; (f) Vuggy and porous limestone specimens; (g) Fresh roots living in the vugs of limestone specimens

Figure 2-5. Weak, poorly cemented silt, sand, and limestone mixture in a core run

Figure 2-6. Examples of core runs with low RQD

2.3 General Carbonate Rock Terminologies

This section presents some common terminologies commonly used for rocks:

REC: Recovery - length of recovered rock divided by the total length of the core run.

RQD: Rock Quality Designation - a core recovery percentage that is intended to be an indicator of the number of fractures and the amount of softening in the rock mass that is observed from the drill cores. Only the intact pieces with a length greater than 100 mm (4 in.) are summed and divided by the total length of the core run.

GSI: Geological Strength Index - an engineering judgement index, based on rock mass evaluation of the rock blocks and joints (Hoek and Brown 1980, 1988, and 2018). For Florida

rocks and IGMs, the materials appear as having no joints, thus making it very difficult to judge the GSI value.

RMR: Rock Mass Rating - also an engineering judgement index, which is based on six parameters: strength, RQD, joint spacing, joint condition, and joint orientation. Similar to the GSI, the RMR is not commonly used in Florida due to the jointless appearance of Florida rocks.

CHAPTER 3
OVERVIEW OF CONVENTIONAL LABORATORY TESTS FOR CARBONATE ROCKS

3.1 Porosity and Unit Weight Tests

For saturated soil, there are two volumes of interest: (1) Volume of solids, V_s, and (2) Volume of water, V_w, which is assumed to be unbound (free to move). In the case of saturated rock, there are actually four volumes of interest with diagram shown in Figure 3-1: (1) Solid, V_s, (2) Inner impermeable void (bound water in occluded pores), V_i, (3) Inner permeable (i.e. unbound) void, V_p, and (4) Vug, V_v respectively. In unsaturated medium, both soil or rock materials will have one more volume, air. To account for all four volumes in describing Florida carbonate rocks, all related parameters are defined below.

γ_w = water unit weight = 9.81 kN/m^3 (62.43 pcf).

SSD = Saturated Surface Dry condition, this is the condition where the inner porous volume of the sample is saturated, but the surface is damp-dry for laboratory test per American Association of State Highway and Transportation Officials (AASHTO) Method T-85 or American Society for Testing and Materials (ASTM) Method D6473.

$V = (\pi\ L\ D^2/4)$ = Total (true) cylindrical volume of the core specimen.

V_s = Solid volume, this is the volume of the rock particles which is difficult to evaluate. Hester & Schmoker (1985) described a porosimeter used in the Petroleum industry to measure V_s based on the volume of sample not occupied by helium at 0.7 MPa (100 psi) in a carefully calibrated chamber that accommodates 1-in diameter samples. The porosimeter is expensive ($15,000 in 2016) and has a sample diameter limitation of 2.5-cm (1-in), which is much smaller than the most common diameters of 6-cm to 10-cm (2.4-in to 4-in) for rock cores in Florida practice. Therefore,

the specific gravity method for soil, AASHTO T-100 or ASTM D-854 (Specific Gravity by Water Pycnometer for soils passing #4 sieve), was improvised so that it can be applied to Florida rocks. All rock specimens were pulverized to powder (100% passing through #40 sieve and 80% passing through #200 sieve), satisfying the sieve requirement to be tested per AASHTO T-100 or ASTM D-854. Furthermore, the powder can also be used for Powder X-ray Diffraction (XRD) test – see Section 3.3

V_{sa} = Apparent solid volume, to include the impermeable pore volume V_i that water is unable to enter under submerged condition (Figure 3-1).

V_{ta} = Apparent total volume. This is the total displaced volume when the SSD sample is submerged under water (Figure 3-1).

V_v = Volume of vugs, which are holes significantly larger than the rock particle size (Sowers 1996). As rock cores are sufficiently small in diameter compared to the rock mass size, vugs are typically exposed on the outer face of the core. Therefore, in the laboratory testing condition, the vugs will not be able to retain free-standing water and the rock volume will be different than the cylindrical volume of the rock core specimen. As such, conventional test methods (ASTM D6473) will not yield meaningful moisture contents because the water will immediately drain from the free-standing core.

V_p = Volume of permeable voids, which are connected inner voids and can retain saturated water under laboratory testing condition so that saturated surface-dry (SSD) test condition per ASTM D6473 can be obtained. The mass of saturated water occupying V_p volume is Q_w (Figure 3-1).

V_i = Impermeable voids, which are occluded voids and the pore water can be evaporated in the drying oven. However, during the laboratory water submersion time (typically 24 ± 4 hours),

they are essentially waterproof. The size of impermeable voids is very small. However, many well-distributed voids throughout the rock could sum up to a considerable volume, such as the case for Key Largo Formation. In fact, when tested according to the ASTM D6473, some Key Largo rock pieces initially float in water before sinking very slowly to the bottom. The impermeable porosity is part of the coherent rock structure and is not as detrimental to their unconfined strengths (as opposed to the case of n_v and n_p); thus, the existence of the impermeable porosity makes the rocks light weight, but still they retain their unconfined strengths.

A = Dry mass in air (the notations A, B, and C below are used by ASTM D6473).

B = SSD mass in air; $B = Q_w + A = V_p \gamma_w + A$.

C = Buoyant mass of submerged specimen in water; however, as there may be internal pores, V_i, that is not permeable, the water does not come in all the pores; $C = A - V_{sa}\gamma_w$

$(B-C)/\gamma_w$ is supposed to present the total specimen volume. However, $(B-C)/\gamma_w = V_p + V_{sa}$ actually presents the apparent total specimen volume as vugs do not retain water, thus are not part of the SSD mass B, Figure 3-1.

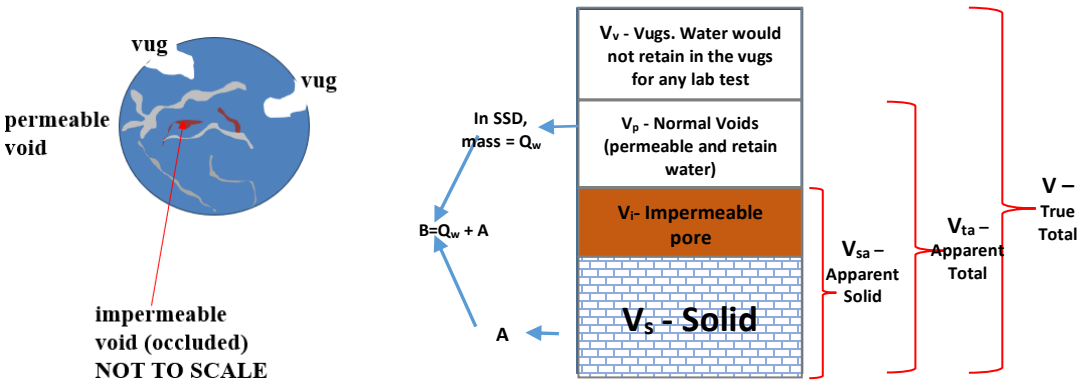

Figure 3-1. Rock phase diagram

The A, B, and C notations are also used in the AASHTO T-85 for specific gravity of rock and coarse aggregate. In the following equations, the ones denoted with an asterisk (i.e., Eqs. 3-3 and 3-5) are derived from A, B, and C per AASHTO T-85/ ASTM D6473.

$$C = A - V_{sa}*62.43 = B - V_{ta}*62.43 \quad (3\text{-}1)$$

Dry bulk (true) dry unit weight $\gamma_{dt} = A / V$ (3-2)

Dry apparent dry unit weight (*) $\gamma_{da} = A / V_{ta} = \gamma_w A / (B-C)$ (3-3)

Solid true unit weight $\gamma_{st} = GS\ \gamma_w$ (3-4)

Solid apparent unit weight (*) $\gamma_{sa} = A / V_{sa} = \gamma_w A / (A-C)$ (3-5)

In Eq. 3-4, the GS value is obtained from AASHTO T-100/ ASTM D-854. This is the true solid specific gravity, which is in fact a weighted average value of the mineral specific gravities, depending on the percentage of each mineral in the rock specimen. Mineral specific gravities cited in literature are presented in Table 3-1.

Table 3-1. Mineral specific gravities from literature

Mineral	Jumikis (1983)	Goodman (1989)	Lambe & Whitman (1969)	Hester & Schmoker (1985)
Calcite	2.71 - 3.72	2.7	2.72	2.71
Aragonite				2.91-2.94
Dolomite	2.80 - 3.00	2.8-3.1	2.85	
Quartz		2.65	2.65	2.65

It should be noted that most index parameter tests are performed on the same specimens that are tested for strength (i.e. q_u or q_t), after the specimen have been fractured. Thus, extreme care needs to be taken to collect every single broken piece to obtain the total oven-dried weight of the

specimen. In addition to the traditional bulk porosity parameter in Eq. 3-6 below, additional porosity components are evaluated in Eqs. 3-7 through 3-9:

Bulk porosity is defined as $n = V_{v+p+i} / V = 1 - \gamma_{dt}/\gamma_{st} = n_i + n_p + n_v$ (3-6)

Impermeable porosity: $n_i = V_i/V = \gamma_{dt}(1/\gamma_{sa} - 1/\gamma_{st}) = \frac{A}{V}(\frac{V_{sa}}{A} - \frac{V_s}{A})$ (3-7)

Permeable porosity: $n_p = V_p/V = \gamma_{dt}(1/\gamma_{da} - 1/\gamma_{sa}) = \frac{A}{V}(\frac{V_{ta}}{A} - \frac{V_{sa}}{A})$ (3-8)

Vug porosity: $n_v = V_v/V = 1 - \gamma_{dt}/\gamma_{da} = 1 - \frac{V_{ta}}{V}$ (3-9)

where n_v is termed as "wash content" by Hester & Schmoker (1985), as there might be insitu soft materials in the vugs before being washed away during the rock coring process.

Limestones in literature, such as those listed by Goodman (1989), are very dense with corresponding low bulk porosity: Solenhofen limestone, n = 5%; Great Britain limestone, n = 6%; Salem/ Bedford limestone, n = 12% to 13%. Therefore, the perception of "porous" rocks is very different from that of Florida rocks. For instance, Fereidooni and Khajevand (2018) indicated that travertine samples with n of 7% were porous; Schwartz (1964) considered the Pottsville sandstone and Indiana limestone as porous rocks, with porosities of n = 14% to 20%, respectively. Gowd and Rummel (1980) considered n = 15% as porous. In Mogi (1966), rocks with n = 1% to 10% were grouped as porous, and n > 10% as very porous, with a highest porosity cited as n = 22%. In comparison, 90% of Florida limestone has a porosity n ≥ 20% and only 10% of Florida limestone has porosities between 5% and 20%. In general, the rocks that are typically considered porous in literature are considered "dense" and "outlier" data for Florida. Due to the fact that there is no consistent grading scale in the literature to identify a rock as vuggy or porous, Tables 3-2 and 3-3 are proposed to describe the rocks based on magnitudes of different porosities.

Table 3-2. Proposed vug descriptions

n_v	0 to 5%	5 to 10%	10 to 15%	15 to 20%	>20%
Vug porosity	No vug, relatively smooth rock	Slightly vuggy	Vuggy to Very vuggy	Very vuggy	Extremely vuggy

Table 3-3. Proposed porosity descriptions

n	0 to 15%	15 to 30%	30 to 45%	>45%
Bulk porosity	Dense	Slightly porous	Porous	Very porous

3.2 Carbonate Content Test

Florida Method FM 5-514 details a procedure to obtain total carbonate contents (which can be CaCO3, MgCO3, $CaMg(CO_3)_2$, etc.). A summary of the short method contained in FM 5-514 is itemized below.

For aggregates:

- Obtain a 50-lb gross sample at air dried condition.
- Quarter (split) the sample to 3 to 5-lb fractions. Then oven dry the fraction at 230^0F for 12-hr.
- Continue per steps below.

For rock cores and quartered aggregates:

- Crush the carbonate rock to fragments of sand-sized particles. Then quarter (split) the sample to a ¼ to 1-lb sample.
- Pass one fraction through a finer grinder so that 100% material passes through #10 sieve and 90% material passes #40 sieve (which is the limiting sieve for fine sand). In reality, the finer the material, the easier it takes to perform the carbonate content test. Therefore, most of the Florida rocks were pulverized to much finer than the minimum requirement, with 100% passing #40 sieve (fine sand-sized particles) and approximately 40% to 80% passing #200 sieve (silt-sized particles).
- Stir sample with spatula.

- Weight out a 1-gram specimen using a scale with an accuracy of 0.0001 gram. Transfer the specimen to a 300-mL beaker by brushing.
- Add 20 mL of 1:5 hydrochloric acid HCl to the beaker slowly. The following reaction occurs:

$$CaCO_3 + 2HCl = CaCl_2 + CO_2 + H_2O \quad (3\text{-}10)$$

$$CaMg(CO_3)_2 + 4HCL = CaCl_2 + MgCl_2 + 2CO_2 + 2H_2O \quad (3\text{-}11)$$

- To aid the above chemical reaction, momentarily boil the beaker over a Bunsen burner flame or hot plate. Let stand until the last gas has been produced.
- Drop three drops phenolphthalein $C_{20}H_{14}O_4$ - which is a weak acid.
- Neutralize to a faint pink color using 1:5 ammonium hydroxide, NH_4OH, which is a weak base (phenolphthalein turns pink in bases).
- Momentary boil the solution, then allow it to cool until the precipitate has settled enough for rapid filtration. Filter the solution through No. 41 paper and transfer all the precipitate to the filter paper by washing with water. Wash the paper five times, allowing paper to drain between washings.
- Ignite the content wrapped in the filter paper in a porcelain crucible at 1,550°F to 1,750°F until all carbon is destroyed (30 minutes or longer). The filter paper will burn out without any ash as No. 41 paper is an ashless filter paper.
- Then cool the crucible and weight the crucible contents in grams. These contents are the insoluble residue (R), which contain non-carbon portions of the rocks, such as quartz and metals such as Al, Fe, etc.
- Carbonate content then is (w - R)/w x 100%.

3.3 Powder X-ray Diffraction (XRD)

Powder X-ray Diffraction (XRD) is one of the primary techniques used by mineralogists and solid-state chemists to examine the physical-chemical make-up of unknown materials. The XRD technique takes a powdered sample in a holder, then the sample is illuminated with x-rays of a fixed wave-length and the intensity of the reflected radiation is recorded using a goniometer. This data is then analyzed for the reflection angle to calculate the inter-atomic spacing (D value in Angstrom units or 10^{-8} cm). The intensity (λ) is measured to discriminate the various D spacings.

The results are plotted as reflected angle, 2θ, versus intensity, where $2\theta = 2\{\text{acsin}(\lambda/(2D))\}$. Figure 3-2 presents the XRD patterns for typical minerals dolomite, aragonite, calcite, and quartz. Figure 3-3 presents the XRD results for actual specimens. Rietveld refinement technique - a signal matching analysis between simulation and measured intensity graphs - is then performed to estimate the percentage of each mineral within the specimen. For example, specimens 4434 and 5246 in Figure 3-3 are estimated by the Rietveld refinement signal-matching program to have 94% and 99% calcite, respectively. The signals of these two specimens resemble the calcite intensity peaks shown in Figure 3-2. Specimen 4337 in Figure 3-3 has intensity peaks that resemble both calcite and aragonite in Figure 3-2. The Rietveld refinement signal-matching program estimated that this specimen has 63% calcite and 36% aragonite.

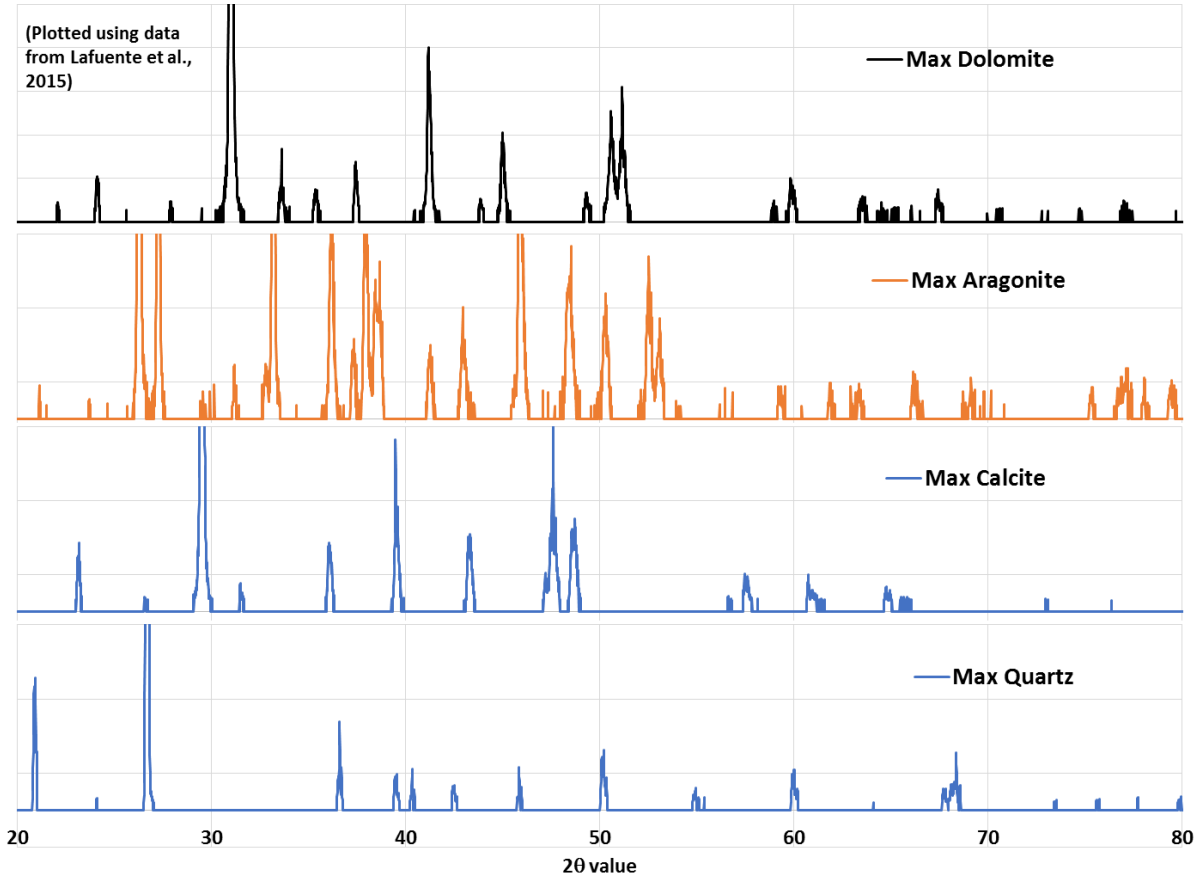

Figure 3-2. XRD major 2θ peaks for typical minerals

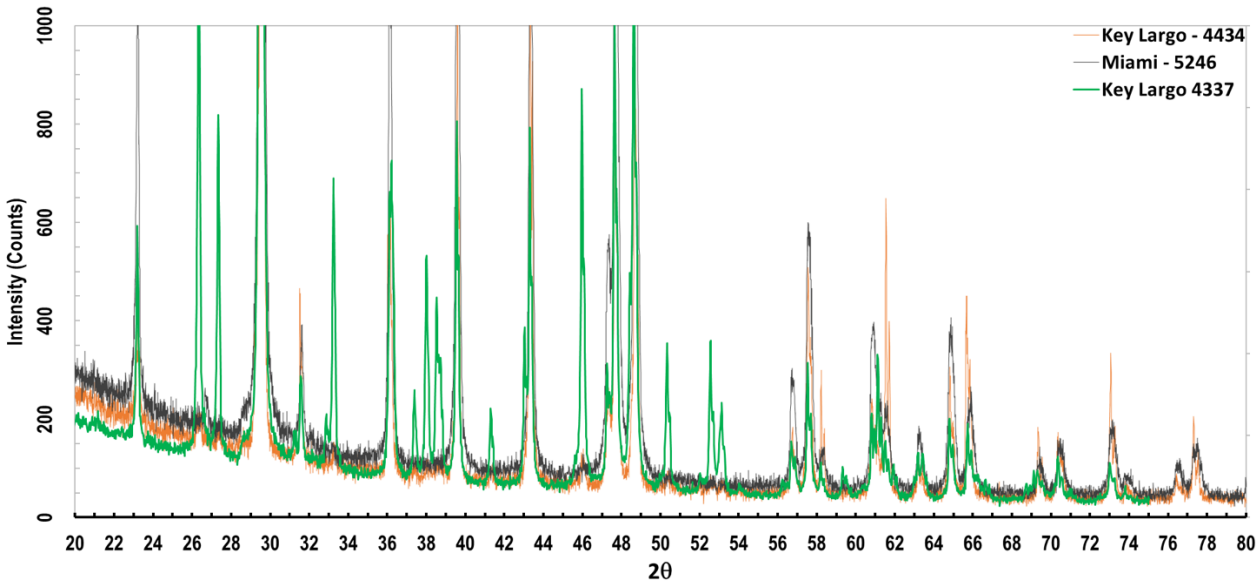

Figure 3-3. Example XRD patterns of Miami and Key Largo limestone specimens

3.4 Splitting Tension Strength Test

The Splitting Tension Strength Test (q_t), is used to evaluate indirectly the tension strength of rocks. In this test, the compressive loads are line loads applied parallel to the core's axis by steel bearing plates between which the specimen is placed horizontally. Loading is applied continuously at a constant rate of deformation – typically 0.015 to 0.03 in/min – such that failure occurs within one to ten minutes so that the specimens are reasonably free from rapid loading effects. The splitting tensile strength of the specimen is calculated as $2P/(\pi LD)$, where P is the applied load, L is the length, and D is the diameter of the specimen. Tests were performed in accordance with ASTM D-3967 except that the minimum L/D (length-to-diameter) ratio was greater, approximately L/D = 1, due to the nature of Florida carbonate rocks (FDOT 2018). The splitting tension strength is sometimes denoted as $q_{st,}$ however in order to use terminology that is consistent

with FDOT practice (FDOT's Soils and Foundations Handbook, 2019) at large, it will be denoted as q_t in this report to highlight the distinction with the direct tension test, q_{dt}.

Per Perras and Diederichs (2014), the q_{dt}/q_t ratio of the test results of the two methods (direct tension strength versus q_t) for sedimentary rock ranges from 0.4 to 1.2, with a mean value of 0.7, as shown in Figure 3-4. For concrete, the scatter of the q_{dt}/q_t spread is less, and thus Hannant et al. (1973) suggests a factor of $q_{dt}/q_t = 0.9$ for concrete.

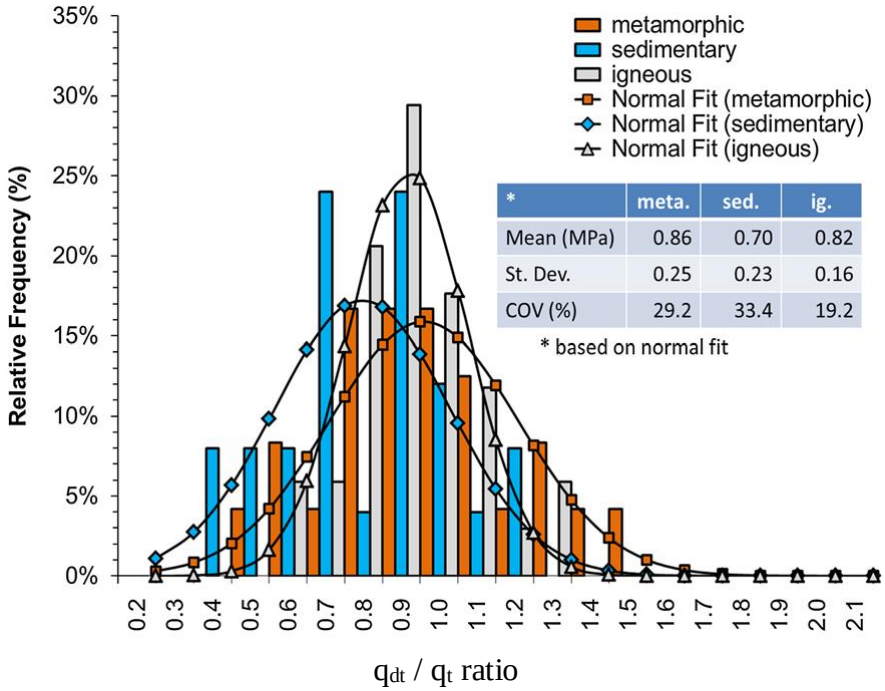

Figure 3-4. q_t versus q_{dt} relationship

Impacting the strength results are the orientations and distributions of the vugs within the specimens relative to the loading line. Figure 3-5 to Figure 3-9 illustrate different splitting behavior of Florida carbonate rocks. If the rocks are relatively uniform without vugs, the specimens likely exhibit center splitting. However, when the rocks are not uniform or contain vugs, the q_t strengths are likely to be low due to the failures through the weakest path as well as off center. Figure 3-7 to Figure 3-9 presents some examples of these types of q_t results. For these types of samples, the

splitting tension strength through the center would be expected to be higher, but the specimens already failed elsewhere before the center splitting happened. Figure 3-10 presents an example where an uneven diameter specimen could introduce local stress concentrations from the steel platen of the q_t test, resulting in a lower q_t result than expected.

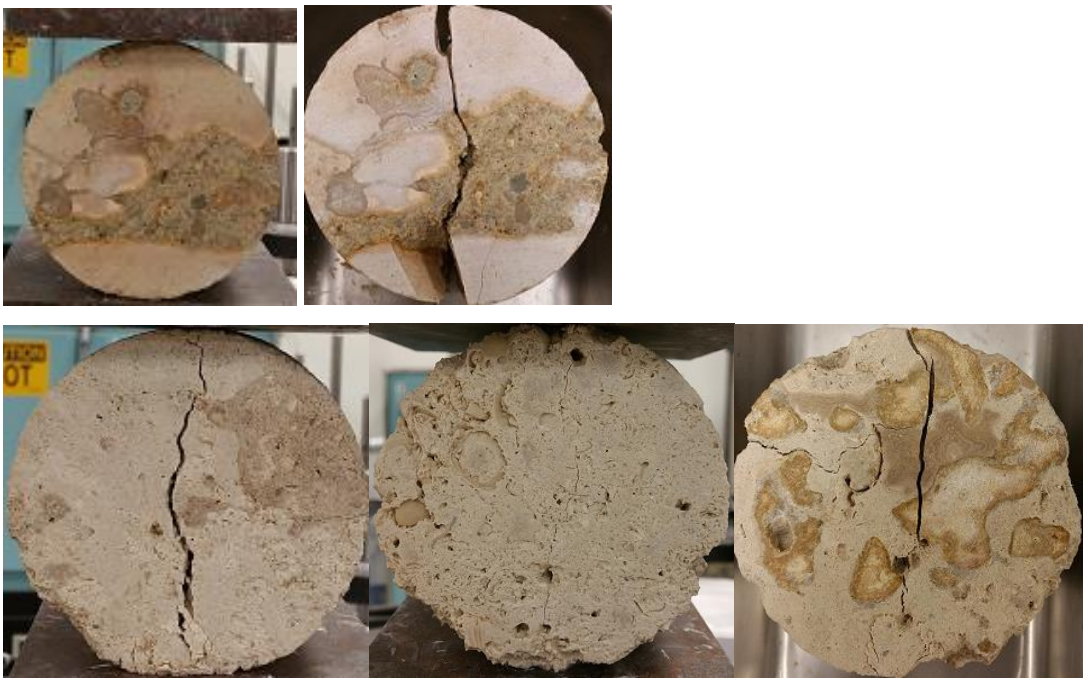

Figure 3-5. Examples of center splitting

a) b)

Figure 3-6. q_t test on sample 543-1: (a) Splitting on center on one face; (b) Splitting off-center on the other face

Figure 3-7. Non-center splitting−tests on samples 534-1 and 541-6

a) b) c)

Figure 3-8. q_t test on sample 545-2: (a) Compression crushing occurred at contact between the steel platen and specimen; (b) Splitting occurred after significant crushing; (c) Splitting stress versus displacement

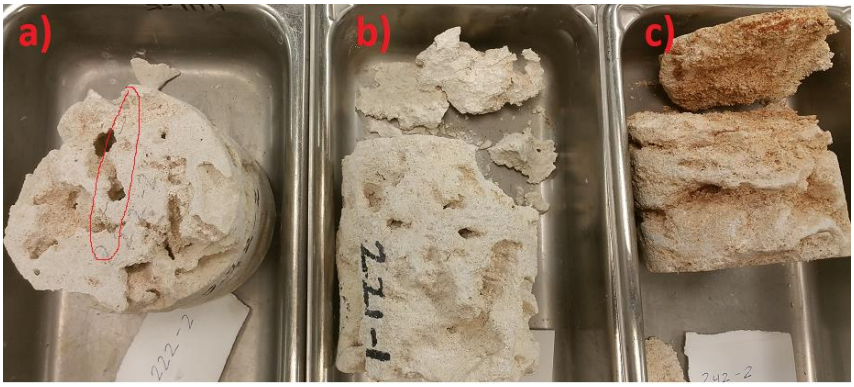

Figure 3-9. q_t tests on vuggy porous limestones:(a) Splitting; (b) Crushing thorough soft end; (c) Crushing through weak zone

Figure 3-10. q_t test on sample 624-3 with uneven diameter

3.5 Unconfined Compression Test

Unconfined compression tests are performed in accordance with ASTM D-7012 (formerly D2938). The specimen is placed in the testing machine and loaded axially at an approximately constant rate such that failure occurs within 2 to 15 minutes. The axial compression pressure at failure is the unconfined compression strength, q_u. This is the most common parameter to describe rock strengths. Some carbonate rocks q_u values in literature are presented in Table 3-4, which indicate high strength values. In contrast, Florida carbonate rocks, with high porosities (from 10% to 60%) and younger geological age, typically have much lower strengths than those shown in Table 3-4 and their strengths will be discussed in detail in Chapter 5.

Table 3-4. Typical carbonate rock strengths

Source	q_u (ksi)	q_u (MPa)
Solenhofen Limestone (Jaeger and Cook 1969; Goodman 1989)	32 to 36	220 to 250
Bedford Limestone (Goodman 1989)	7 to 8	48 to 55
Tarvernalle Limestone (Goodman 1989)	14	100
Malaysian Limestone (Nazir et al. 2013)	8 to 16	55 to 110
Virginia Limestone (Jaeger and Cook 1969)	48	330
Australian Limestone and Dolostone (Johnston 1985)	6 to 75	38 to 520
Limestone (Hoek and Brown 1980)	6.4 to 29	44 to 200
Dolostone (Hoek and Brown 1980)	21 to 73	150 to 500

CHAPTER 4

PROPERTIES OF CARBONATE ROCKS AND IGMS

4.1 Florida Data

Two sets of data for carbonate rocks and Intermediate Geo-Materials (IGM) throughout the state of Florida were utilized in this study with results presented in the subsequent sections:

Data set #1 contains over 8,000 historical data points, which were collected by the Florida Department of Transportation (FDOT) for projects from 1990 to 2017, listed in Table 4-1. Data set #1 includes the following three parameters: 1) Unconfined compression strength results – q_u, 2) splitting tension strength results – q_t, and 3) bulk dry unit weight results – γ_{dt}. Data set #1 includes a subset #1a of 98 data points, where rock formation identifications were available.

Table 4-1. List of projects in data set #1

Name	ID	District	Location
I-75 over Manatee River	1	1	27°31'26.50"N 82°30'21.21"W
I-75 over Golden Gate Canal	2	1	26°10'06.6"N 81°43'50.0"W
Edison Farm	3	1	Not provided
I275 over Yukon St	14	7	28°01'45.1"N 82°27'18.6"W
SR-20 @ Lochloosa Creek, Alachua Co.	4	2	29.600716, -82.144517
SR-25 @ Santa Fe River	5	2	29°51'11.18"N 82°36'30.74"W
SR-10 @ CSX RR (Beaver St. Viaduct), Duval Co.	6	2	30.334805, -81.685905
SR-9 (I-95) Overland	7	2	30.31361, -81.65231
I 95 (Fuller Warren Bridge) over St. Johns River	8	2	30°18'53.7"N 81°40'10.7"W
CR-326 @ Waccasa River	9	2	29°13'17.40"N 82°45'29.03"W
I-295 Dames Point Bridge	10	2	30°23'8.09"N 81°33'26.24"W
I-295 Buckman Bridge over St Johns River	11	2	30.1901°N 81.6665°W
I-95 @ I-295 Cloverleaf	12	2	30°10'00.4"N 81°33'16.9"W
Acosta Bridge Research (Modulus)	13	2	30°19'18.6"N 81°39'52.2"W
US-98 / SR-30 @ Wakulla River	15	3	30°10'32.8"N 84°14'43.6"W
Bridge #530022 US 98 over Wakulla	16	3	Not provided
Rob Forehand Road Over Little Creek	17	3	30°53'53.6"N 85°43'06.5"W
Lost Creek Bridge #590048	18	3	30°09'38.4"N 84°22'53.2"W
I 10, SR 8 over Ochlockonee River (#550089EB, #550050WB)	19	3	30°29'06.5"N 84°23'50.9"W
SR 63, US 27 Ochlockonee Relief Bridge	20	3	30°33'14.2"N 84°23'03.1"W
SR 8 over Choctawhatchee River	21	3	30.7557092, -85.8298427

Table 4-1. Continued

Name	ID	District	Location
I 10, SR 8 Over Apalachicola River (#500087)	22	3	30.6335607, -84.9045483
I 10, SR 8 over Chipola River (#530052)	23	3	30.7245131, -85.1997390
SR-20 over Chipola River	24	3	30.4310665, -85.1718566
SR 166 over Chipola River	25	3	30.7928089, -85.2217664
I 10, SR 8 Over CSX, Little River	26	3	Not provided
US 90 over Little River	27	3	30°28'48.2"N 83°32'49.1"W
Sr 267 over Rocky Comfort Creek (#500027, 28)	28	3	30°29'33.3"N 84°36'49.2"W
Dry Creek SR 73 (#530089) (actually Chipola River)	29	3	30°41'22.1"N 85°14'10.3"W
SR30/US98 @ Aucilla River	30	3	30°08'47.2"N 83°58'24.5"W
SR-2 Bridge over Choctawhatchee River	31	3	30.9500870, -85.8431570
SR-10 (US90) Bridge over Choctawhatchee River	32	3	30°46'31.84"N, 85°49'37.56"W
Merritts Mill Pond US-90 SR-10	33	3	30°45'12.8"N 85°11'36.3"W
SR-166 Rock Slope Design	34	3	30.78819, -85.18632
Fisher Creek Bridge CR 2203	35	3	30°18'52.4"N 84°23'57.2"W
CR 166 Alligator Creek Bridge	36	3	30°47'30" N, 85°33'47" W
SR-8 (I-10) @ CR-286 High Mast	37	3	30°38'11.0"N 84°56'41.0"W
Holmes Creek - Cr 166 Bridge	38	3	30°47'58.3"N 85°36'08.9"W
CR 12A (Kemp Road Bridge)	39	3	30°37'38.4"N 84°22'06.3"W
Natural Bridge over St. Marks River	40	3	30°17'02.7"N 84°09'02.8"W
SR 71 over Rocky Creek	42	3	30°39'26.5"N 85°09'44.8"W
SR-20 @ Blountstown (Apalachicola river)	43	3	30°26'13.6"N 85°00'03.6"W
US-90 Victory Bridge	44	3	30°42'05.6"N 84°51'32.3"W
SR-2 Cowarts Creek	45	3	30°56'50.6"N 85°15'30.4"W
SR-2 Marshall Creek Jackson Co.	46	3	30°56'10.9"N 85°17'47.6"W
SR-2 Spring Branch Jackson Co.	47	3	30°56'14.4"N 85°19'26.0"W
SR-261 Capital Circle	48	3	30°27'13.9"N 84°13'35.1"W
US-98 / SR-30 @ St. Marks river	49	3	30°11'56.6"N 84°10'41.0"W
I-10 Tower site @ Snead's weigh station	50	3	30°38'23.5"N 84°58'58.3"W
SR A1A Flagler Memorial Bridge	51	4	26.718431, -80.047041
SR A1A over Sebastian Inlet	52	4/5	27.860028, -80.448415
US 1 over Dania Cutoff Canal	64	4	26.059517, -80.143883
SR 858 (Hallandale Beach Bridge) over Intercoastal	65	4	25.986404, -80.121659
SR 600 (Broadway Bridge) over Halifax River	66	5	29.216332, -81.015482
SR40 WB over Tomoka River 1991	67	5	29.254847, -81.123547
NW 36th Street Bridge Replacement	53	6	25°48'30.4"N 80°15'42.7"W
NW 12th Ave (SR 933) Miami River Bridge	54	6	25°46'58.83"N 80°12'53.34"W
MIC- People Mover Project	55	6	Not provided
Verona Ave Bridge over Grand Canal	56	6	25°57'36.8"N 80°07'18.6"W
HEFT / SR 874 PD&E	57	6	25°39'00.8"N 80°23'05.0"W
Wall @ Service Rd. South of Snake Creek	58	6	24.95092, -80.59129
17th St. Causeway, Miami	59	6	26°06'02.4"N 80°07'06.8"W
96th St. & Indian Creek (Pump Station @ Bal Harbour)	60	6	25°53'12.7"N 80°07'41.6"W
Jewfish Creek	61	6	25°11'04.2"N 80°23'17.2"W
NW 5th Street Bridge over Miami River	62	6	25°46'41.8"N 80°12'24.9"W
Radio Tower Everglades Academy (Florida City) Pump Station	63	6	Not provided

Data set #2 consists of approximately 573 data points (270 q_t, 80 q_u, and 223 triaxial test results) performed specifically for this study. The data comes from 8 different sites across Florida, as shown in Table 4-1. For data set #2, in addition to the three parameters referenced above, the following rock index parameters were obtained: 4) rock formation identification, 5) carbonate content, and 6) vug and inner porosity. The rock core descriptions for data set #2 and photographs of the cores are presented in Appendices A and B, respectively.

Table 4-2. List of projects in data set #2

Site	Address	Area	Notes	Geology	Triaxial tests
1	I-75/ I-595	Davie (Broward)	Interchange; 75-ft from a wet retention pond	Qm overlays Tqsu; Specimens below 8-ft, identified as Tqsu (Ft Thompson)	Yes
2	SW 13th St	Miami	Underpass; no near-by body of water	Qm (Miami); 0.5 miles from the ocean	Yes
3	SR80 Bingham Island	West Palm	Bridge end bent; 35-ft from sea water	Qa (Anastasia)	Yes
4	SR 5-Marvin Adams Way	Key Largo	Bridge end bent; 25-ft from sea water	Qk (Key Largo)	Yes
5	SR 836 Ext - NW 12 St-MDX	Miami	Underpass; closest fresh water is 500-ft away	Qm (Miami), poor induration	Yes
6	SR 997-Krome Avenue		Existing culvert (no bridge) over a small canal	Qm (Miami), poor to moderate induration	Yes
7	S Tamiami Trail over Catfish creek	Sarasota	Small bridge. Limited specimens for q_u and q_t tests only	Tha (Arcadia formation)	No
8	Fuller-Warren bridge	Jackson-ville	This is a deep foundation project. Data was collected for rock characterization.	Th (undifferentiated Hawthorn group)	Yes

4.2 Florida Carbonate Rock Porosity and Unit Weight Results

Moist unit weights (γ) are presented along with bulk dry unit weights (γ_{dt}) in Figure 4-1. This figure indicates that the tested rock specimens were at different degrees of saturation. For example,

when γ_{dt} = 70 pcf, γ could vary from approximately 70 pcf (i.e., specimen was dry) to 110 pcf (i.e., specimen was fully saturated). In the field, most of the rocks are fully saturated due to the depth of the rocks and the relative shallow groundwater table depths in Florida. However, it is not possible to prevent the water from running out of the vugs in the laboratory. Therefore, as described in Chapter 5, rock strengths were not correlated to the laboratory moisture content, but rather they were correlated to the bulk dry unit weight or porosity.

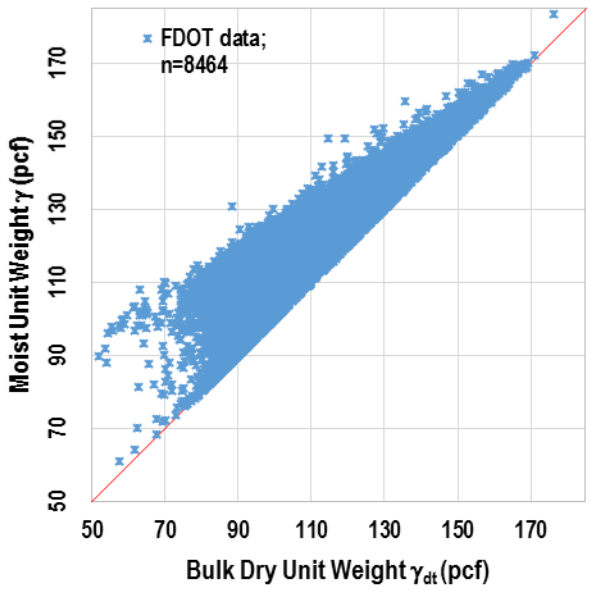

Figure 4-1. Data set #1 – Range of unit weights

From data set #1, most (80%) of the specimens have dry unit weights (γ_{dt}) between 80 and 130 pcf (Figure 4-2). Specimens having γ_{dt} of less than 80 pcf are typically very porous, vuggy (Figure 4-3), and of low strengths, and thus, not typically suited to support foundation structures. Specimens having γ_{dt} higher than 130 pcf are typically not encountered consistently or in substantial lengths (i.e., rock layers are typically only a few inches or a foot thick). Therefore, outlier samples with γ_{dt} greater than 130 pcf should be conservatively assigned the same strengths as those samples with γ_{dt} = 130 pcf. Also, from Figures 4-2 and 4-3, the median bulk dry unit

weight and median bulk porosity for Florida carbonate rocks are approximately 105 pcf and 37%, respectively, which indicate that Florida carbonate rocks are much more porous than other rocks in literature (Section 3.1).

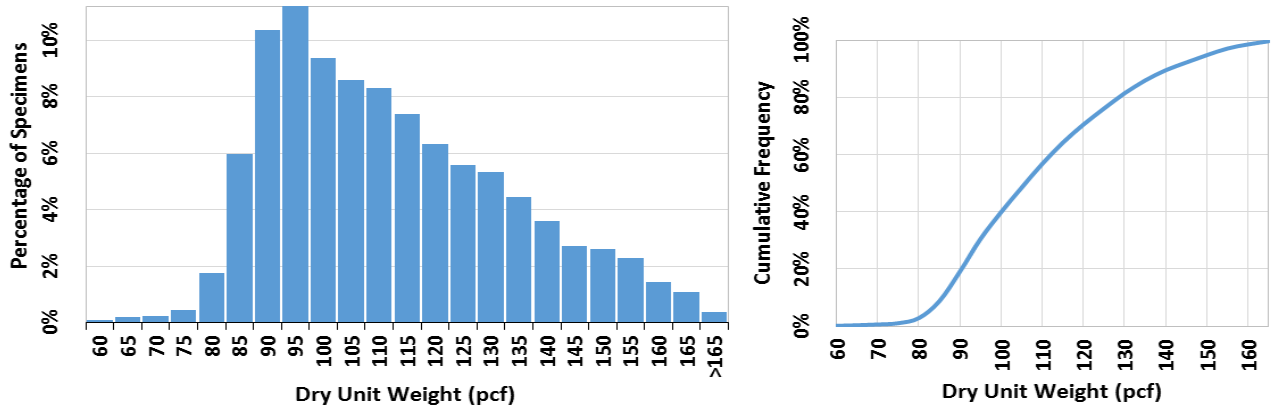

Figure 4-2. Data set #1 – Dry unit weight histogram

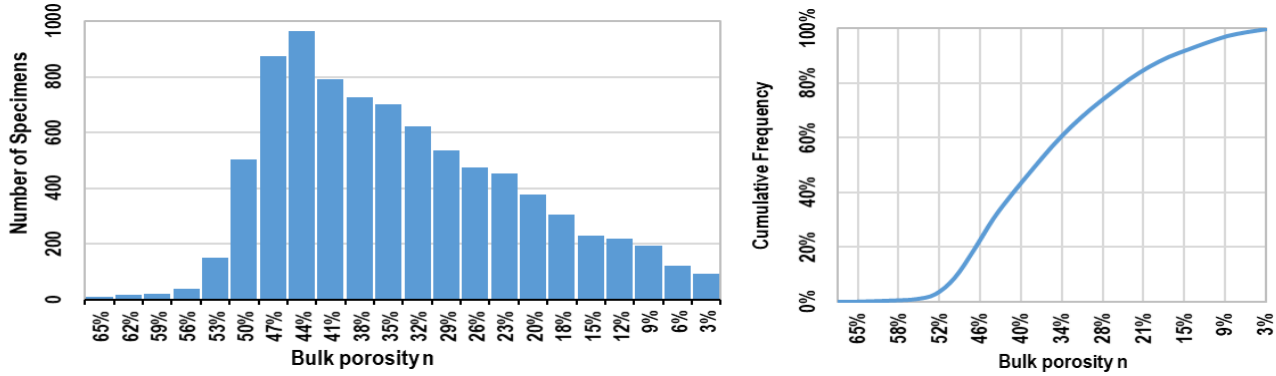

Figure 4-3. Data set #1 – Porosity histogram

Figure 4-4.a presents the bulk porosity versus vug porosity of the FDOT carbonate rock specimens. These results agree with data collected by Hester and Schmoker (1985), and plotted by Thai Nguyen in Figure 4-4.b. As shown in Figure 4-4, they have a wide range of bulk porosity, n, from approximately 5% (relatively dense rock) to 60% (very porous rock) and a vug porosity, n_v, from 0% (no vugs) to 35% (extremely vuggy). Figure 4-5 highlights different proportions of

porosities, namely vug (n_v) and permeable porosity (n_p), within the bulk porosities (n) of multiple Florida rock formations.

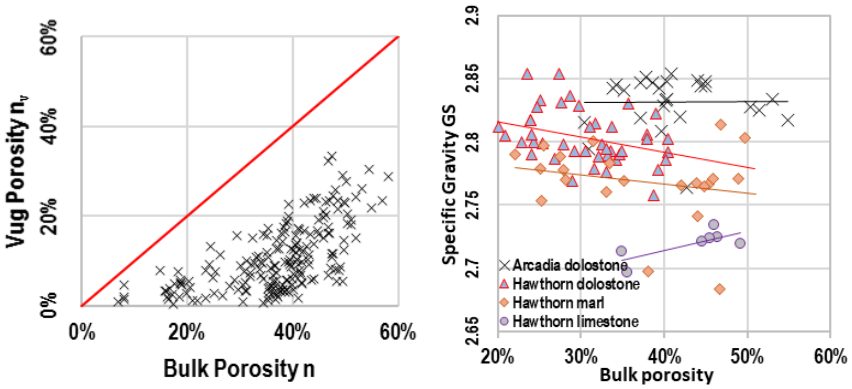

a)

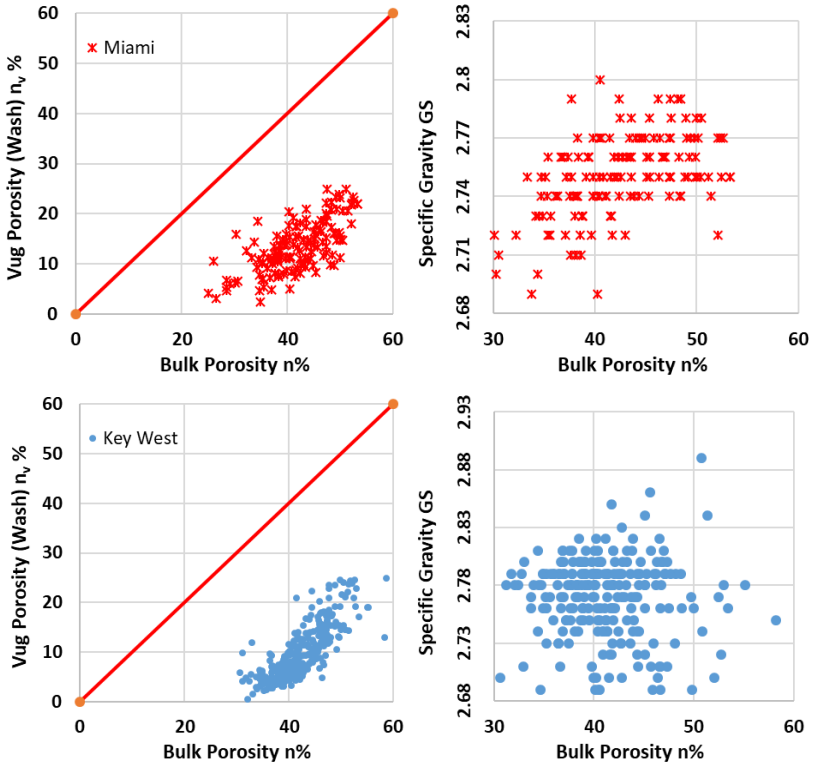

b)

Figure 4-4. Vug porosity versus bulk porosity: (a) Plotted using data from this study; (b) Plotted using text data from Hester & Schmoker (1985)

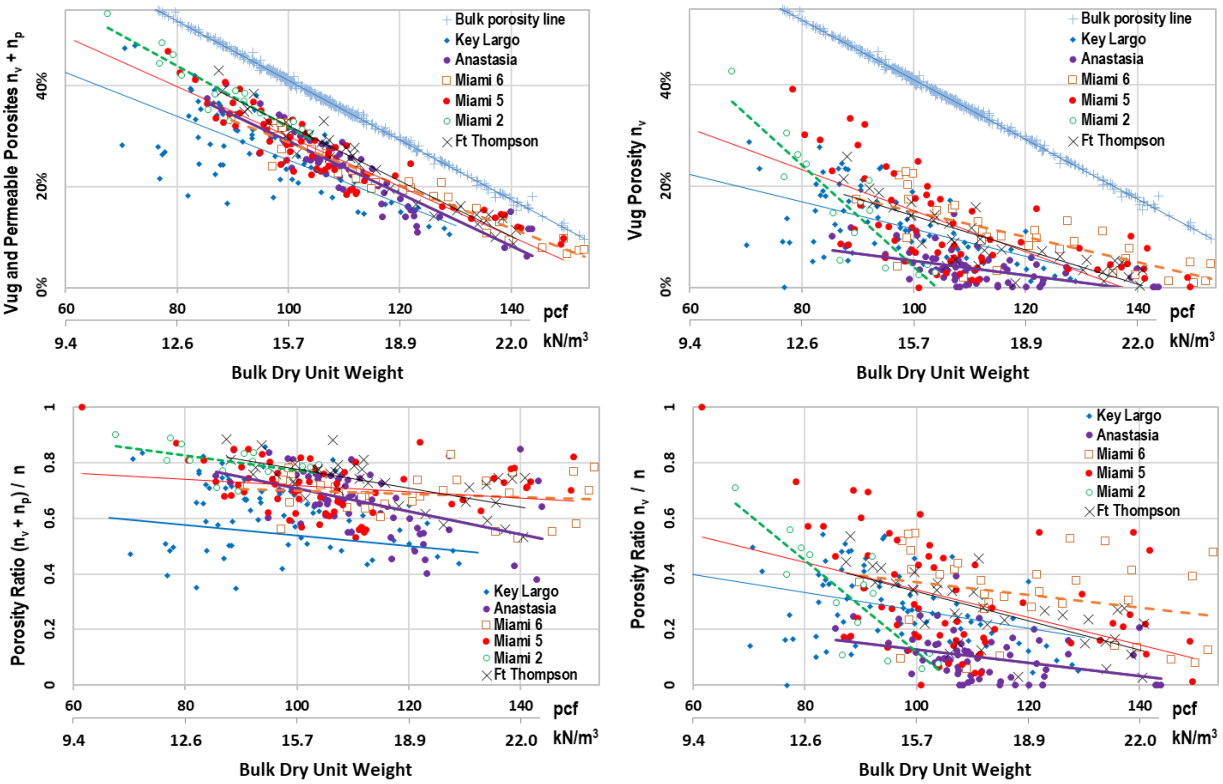

Figure 4-5. Porosities of Florida carbonate rocks: (a) Vug and permeable porosities; (b) Vug porosity only

4.3 Florida Carbonate Rock Minerals

The key component of the carbonate rocks is carbonate content. To quantify the mineral components of Florida rocks, carbonate contents per Florida Method FM 5-514 (FDOT 2015) and Powder X-ray Diffraction (XRD) tests were conducted in this study. The carbonate contents are presented in Figure 4-6 and are described below.

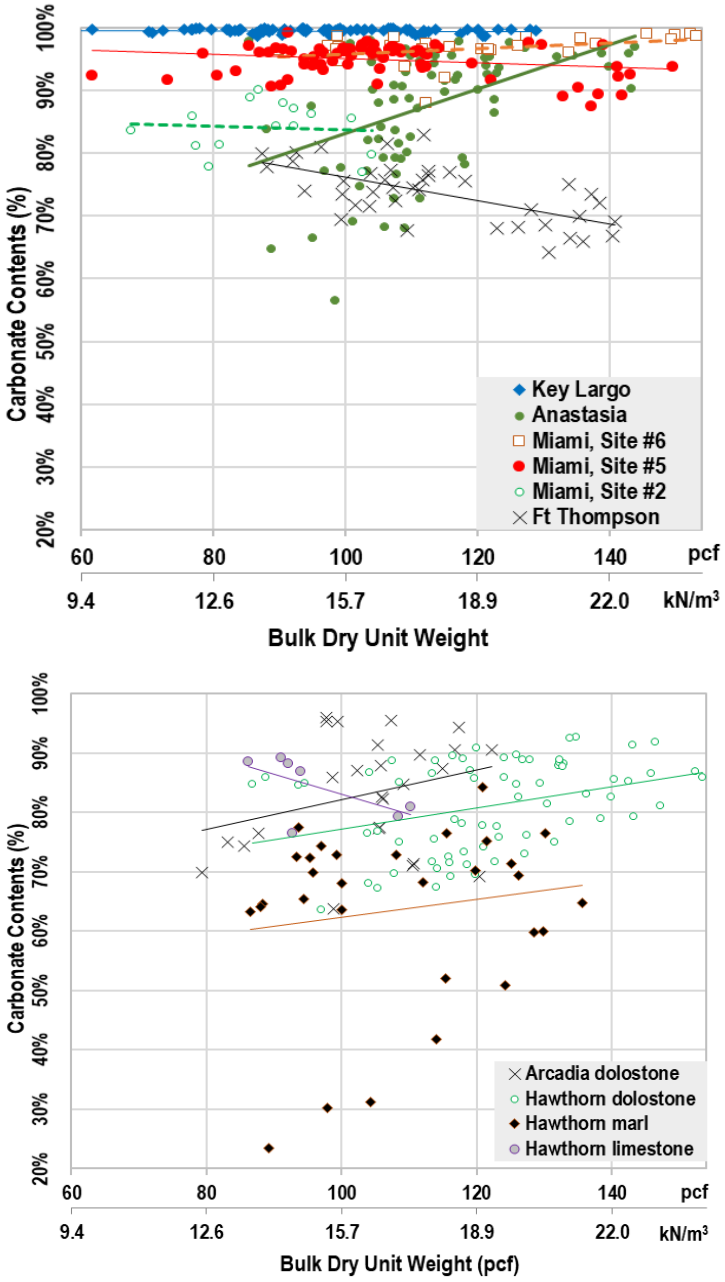

Figure 4-6. Carbonate content versus bulk dry unit weight γ_{dt}

Fort Thompson of shelly sediments of the Plio-Pleistocene age (Tqsu): Typically, this formation is a calcite limestone and quartz. The Fort Thompson Formation has a low carbonate content compared to other Florida rock formations, and ranges from 65% to 80%.

Anastasia (Qa): Anastasia Formation has a wider range of carbonate content, typically from 65% to 95%, and the remaining component is quartz. The carbonate is typically calcite, with a minor percentage of aragonite.

Miami (Qm): This formation is also a calcite, with a minor percentage of aragonite, and quartz. Depending on the location of the Miami Formation, which can be the oolitic facies (Atlantic Coastal Ridge) or the bryozoan facies (toward the Everglades) and depending on degree of induration, the carbonate content of Miami Formation can range from 80% at one location to 98% at another location, as shown in Figure 4-6 for three different Miami sites.

Key Largo (Qk): This formation has the highest carbonate contents (near 100%), which consist of mainly calcite, averaging about 80%, and a minor amount of aragonite averaging 20%.

Undifferentiated Hawthorn Group (Th): Among this group, there are two subgroups of carbonate rocks that were tested in this study:

i) Hawthorn dolostone/limestone: in this subgroup, the carbonate contents typically range from 65% to 95%, with feldspar/ quartz as the remaining mineral component. The carbonates are mixtures of dolomite and calcite.
ii) Hawthorn marl: the marl has the same main minerals as the other Hawthorn rocks: dolomite, calcite, and an earthy mineral (quartz). However, the carbonate content is much lower in the marl. For marl, the natural moisture contents of the specimens control the strengths of the material. If the specimens lose their moisture content, their dry strengths (i.e., unconfined compression or splitting tension) are typically much higher than their true strengths. However, if the specimens are subject to higher moisture (such as in a moisture room, without the natural overburden confining pressure), the material will disintegrate (lose strength). In Figure 4-6, marl specimens typically have carbonate contents less than 65%. However, many marl specimens had the same properties (dry unit weights, and carbonate contents between 65% and 85%) as the Hawthorn dolostone. Due to exposure issues (quartz located at surface of the cores), it was decided to classify them as Hawthorn marl; whereas, for cores that the marl was not exposed (i.e., dolostone on the surface of the cores and marl lens buried inside), the specimens with carbonate content exceeding 65% are categorized as dolostone. The reason is that when marl is exposed at the surface of the cores, the marl on the surface of the core would collapse or chip away during strength tests (q_t or q_u), and test would be stopped due to excessive deformation.

Arcadia Formation of the Hawthorn Group (Tha): This formation is somewhat similar to the subgroup of the undifferentiated Hawthorn group. The Arcadia Formation is also a dolostone, with carbonate contents typically from 70% to 90%.

The XRD tests were performed on a limited number of specimens and the mineral components of the rocks are calculated using Rietveld Refinement analyses in columns 5 through 11 of Table 4-3. The sum of columns 6 through 11 is the total carbonate content, which is presented in column 4. The results in column 4 agree well with the total carbonate content results using FM 5-514in column 3. From Table 4-3, each formation contains three main minerals. For the youngest formations (approximately less than 2 million years old), the three minerals are calcite, aragonite, and quartz. For older formations, aragonite typically does not exist as it is replaced by calcite (refer to Section 2.1), and at the same time, some dolomitization occurred due to the flow of magnesium-rich water. Thus, the three main minerals for older formations are calcite, dolomite, and quartz.

Table 4-3. Carbonate content versus XRD interpreted results

Formations ①	Number of XRD specimens ②	% Carbonate content (FM5-514) ③	% of mineral by XRD results							
			Carbonate Content ④	Quartz ⑤	limestone			dolostone (dolomite) ⑨	portlandite $Ca(OH)_2$ ⑩	periclase MgO ⑪
					Calcite ⑥	Mgcalcite ⑦	Aragonite ⑧			
Ft. Thompson	4	64 - 77	68 - 79	18 - 32	66 - 76	0 - 0.5	0 - 5.5	0	0	0.5 - 1
Anastasia	6	67 - 98	66 - 99	1 - 34	62 - 90	0 - 5	2 - 9	0	0	0 - 2
Key Largo	6	99 - 100	99 - 100	0 - 1	26 - 98	0 - 5	1 - 72	0 - 1	0	0
Poor indurated Miami	3	77 - 89	82 - 91	9 - 18	70 - 80	0 - 1.5	0 - 20	0 - 1	0 - 3	0
Medium indurated Miami	3	89 - 98	89 - 100	0 - 11	82 - 98	0 - 4	0 - 3	0	0	0 - 1
Medium to well-indurated Miami	4	88 - 99	88 - 100	0 - 11	78 - 98	0 - 5	0 - 6	0 - 1	0	0 - 1
Arcadia dolostone	5	64 - 96	64 - 100	0 - 36	0 - 2	0	0	63 - 100	0 - 1	0 - 1
Hawthorn dolostone	7	67 - 93	66 - 93	7 - 34	0 - 2	0	0	60 - 92	0	0 – 3
Hawthorn marl	6	23 - 65	24 - 65	35 - 76	0 - 0.5	0	0	23 - 64	0	0 – 2
Hawthorn limestone	2	76 - 88	71 - 88	12 - 29	68 - 77	0 - 1	0 - 1	9 - 10	0 - 1	0

For example, the specific gravity of specimen #4337, performed per ASTM D854, is GS = 2.77. XRD result indicates that specimen #4337 has 63.5% calcite with $GS_{calcite}$ = 2.70, 36.3% aragonite with $GS_{aragonite}$ = 2.91, and 0.2% quartz with GS_{quartz} = 2.65. Therefore, the specimen's specific gravity is 63.5% * 2.70 + 36.3% * 2.91 + 0.2% * 2.65 = 2.77, which confirms the GS value performed by ASTM D854. For specimens having no XRD results, the aragonite (for young formations of less than 2 million years old) or dolomite (for older formations) content can be back calculated from GS and carbonate test results. For example, specimen #3221 (Anastasia Formation, Quaternary Period - young formation) has 91.6% carbonate (based on the FM 5-514 test result), 8.4% quartz, and GS = 2.73 (based on the ASTM D854 test result); therefore, the aragonite content, C_a, is back calculated as: (91.6% - C_a) * 2.7 + C_a * 2.91 + 8.4% * 2.65 = 2.73, thus C_a = 17%. From these back calculations of the aragonite or dolomite contents, Table 4-4 presents a summary of the calculated mineral contents of various Florida formations.

Table 4-4. Estimated mineral components from carbonate content and specific gravity results

Formations	Number of specimens	% carbonate		% calcite		% aragonite		% dolomite		% quartz	
		range	average	range	average	range	average	range	average	range	average
Ft. Thompson	14	64-80	72	55-78	67	0-15	5			20-36	28
Anastasia	40	66-98	90	50-98	84	0-47	6			2-34	10
Key Largo	39	99-100	99.5	39-95	79	5-61	20			0-1	0.5
poor indurated Miami	12	77-90	84	52-82	70	0-34	14			10-23	16
medium indurated Miami	34	89-98	95	74-97	91	0-22	4			2-11	5
medium to well indurated Miami	14	88-99	96	76-99	91	0-21	5			1-12	4
Arcadia dolostone	26	64-96	84	0-18	2			49-94	82	4-36	16
Hawthorn marl	22	23-77	64	0-40	12			12-73	51	23-77	36
Hawthorn dolostone	49	67-93	81	0-38	12			38-87	69	7-33	19
Hawthorn limestone	7	77-89	84	62-83	76			0-16	8	11-23	16

4.4 Subsurface Spatial Variability

With the exception of some isolated areas of Florida where a few carbonate rocks are dense with low porosity, many Florida carbonate rocks (as shown in Section 2.2) are nonuniform, porous, and often times vuggy to the extent that plant roots are able to grow through a connected vug structure. The rock core recovery (REC) and rock quality designation (RQD) are generally poor when at least one of the following conditions is encountered: poor cementation (poor induration, generally low strength rocks), or brittle rocks, and/or interbedded rock/soil types, and/or extreme vugs/voids. An example of coring logs is presented in Figure 4-7 where each curve represents one borehole for a project site. In the figure, the recovery was poor to decent (typically 40% to 80%) and RQD was very poor to decent (typically 0% to 60%). All parameters (REC, RQD, and coring time) in the figure would indicate significant subsurface spatial variability. Furthermore, when presenting the bulk dry unit weight, γ_{dt}, with depth (Figure 4-8), the subsurface spatial variability stands out. For each site, within a very short vertical distance, γ_{dt} can vary up to 8 kN/m^3 (50 pcf) indicating a very wide range of rock densities - from very porous (γ_{dt} = 12.5 kN/m^3 or 80 pcf) to dense (γ_{dt} = 20.5 kN/m^3 or 130 pcf). This reflects the extreme heterogenous nature of Florida carbonate rocks.

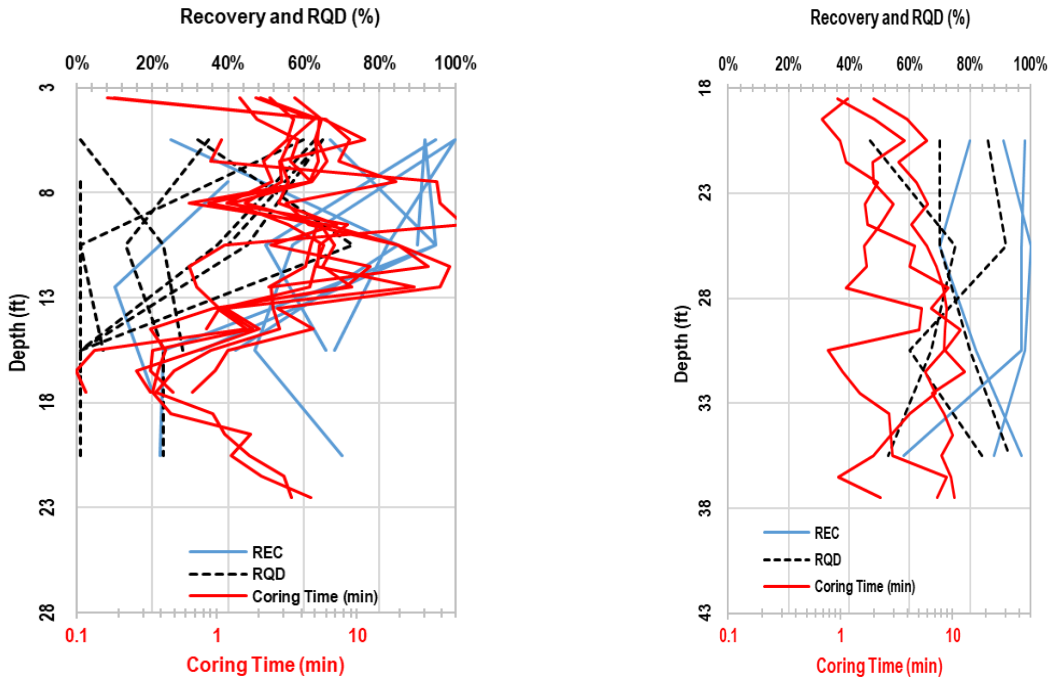

Figure 4-7. Examples of rock core records: (a) Ft. Thompson site; (b) Anastasia site

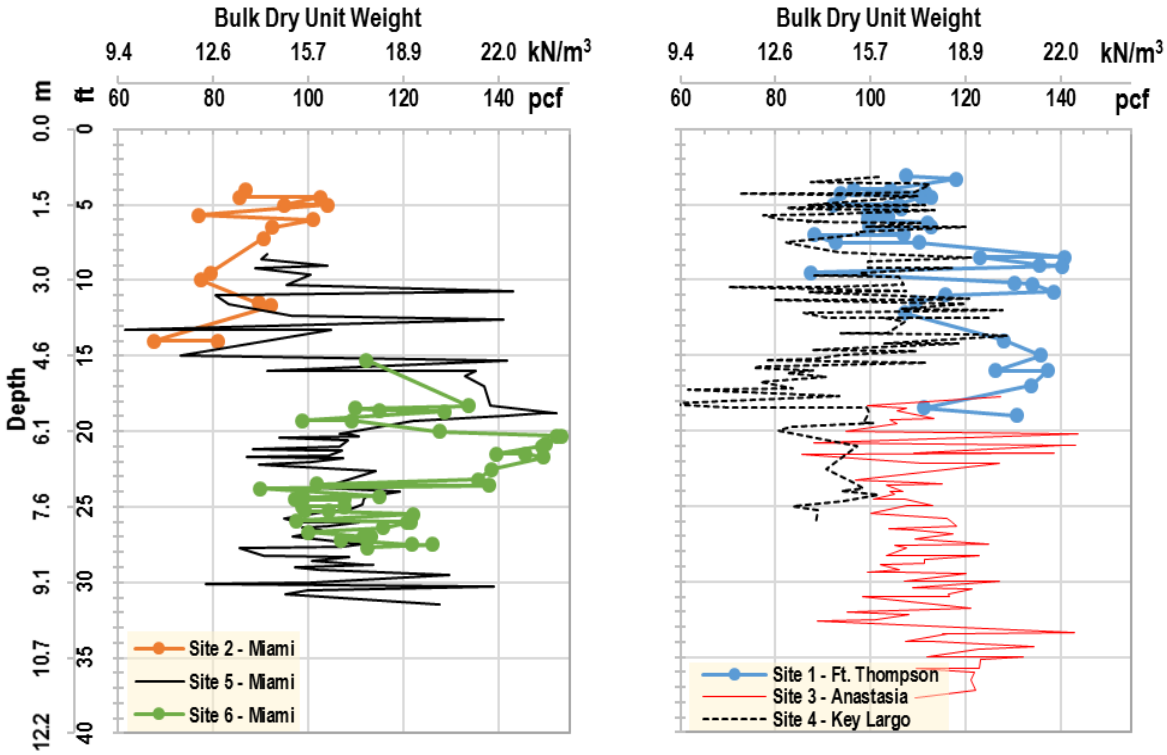

Figure 4-8. Bulk dry unit weight γ_{dt} with depth

4.5 Summary

Florida carbonate rocks and IGMs are geologically young and thus their crystal bonding strengths may influence their unique geotechnical properties. They are generally very porous, with porosities up to 60%. The carbonate, such as $CaCO_3$ or $CaMg(CO_3)_2$, acts as a binder for the cementation of the material. However, some formations have very low carbonate contents of only 80% but may be as low as 65%. Below 65% carbonate content, the IGMs are typically not testable for unconfined compression nor splitting tension strengths as specimens can easily disintegrate during handling for strength testing.

Based on the results of carbonate content tests, X-ray diffraction (XRD) tests, and determination of rock porosities for many Florida formations, different strength correlations may exist among the formations. The strengths are a function of the material characteristics, such as dry unit weight (porosity), carbonate content, and crystalline structure. These correlations were investigated and presented in Chapter 5.

CHAPTER 5
SPLITTING TENSION AND UNCONFINED COMPRESSION STRENGTHS OF FLORIDA CARBONATE ROCKS AND IGMS

5.1 Necessity for Florida Rock Strength Correlation

To describe rock strengths, the two most common rock strength parameters are unconfined compression strength (q_u) and splitting tension strength (q_t), which are obtained via laboratory tests (ASTM D7012 and ASTM D3967, respectively) on rock core specimens. In a difficult terrain or deep exploration (e.g., for petroleum engineering projects), it is expensive to retrieve rock cores for laboratory tests. As a result, many authors have published correlations to obtain rock strengths from the rock physical, index, and mechanical parameters. However, a number of publications contain a very limited number of specimens per rock formation, sometimes only three specimens per rock formation. Fereidooni and Khajevand (2018), using a database of 12 rock specimens of 4 different rock formations with porosities (n) between 0.04 to 0.10 (4% to 10%), presented correlations to estimate q_u and q_t based on a single input parameter – either Schmidt rebound hardness, point load index, block punch index, or cylindrical punch index. Chang et al. (2006) gathered the results from 12 different authors from 1971 to 2001, using rocks from all over the world, and tabulated 31 different empirical equations to estimate q_u and q_t, typically from a single input parameter, such as porosity, modulus, or shear wave velocity. The carbonate rocks (limestone and dolostone) examined had a typical porosity of 0% to 20%. Chang et al. (2006) noted that many correlations do a poor job in fitting measured data because they were originally proposed to fit a subset of the data only. All the mentioned rocks, especially carbonate rocks (limestone or dolostone), have a much lower porosity than Florida carbonate rocks, and subsequently have much higher strengths than Florida rocks.

It is evident that Florida carbonate rocks have lower strengths, higher porosities, and higher variability. As such, the definition of "porous" rock is very different between Florida rocks and those cited in literature. Fereidooni and Khajevand (2018) indicated travertine samples with n of 0.07 as porous. In Schwartz (1964), the Pottsville sandstone and Indiana limestone were considered as typical porous rocks, and their porosities are n = 0.14 and 0.20, respectively. Gowd and Rummel (1980) considered n=0.15 as porous. In Mogi (1966), rocks with n = 0.01 to 0.10 were grouped as porous, and n > 0.10 as very porous. In comparison, Figure 4-3 in the previous chapter shows that 90% of the Florida limestone sampled ha porosities $n \geq 0.20$ and only 10% of had porosities between 0.05 and 0.20 (i.e., the limestone or dolostone that are typically considered porous in literature are considered "dense" and "outlier" data in Florida). In addition, Section 4.4 indicates that within short vertical distances (cm or inches) of one another, one Florida rock specimen may have a bulk dry unit weight (γ_{dt}) of 20.5 kN/m^3 (130 pcf) and the adjoining rock specimen may have γ_{dt} of 12.5 kN/m^3 (80 pcf), indicating extreme differences in rock porosities. As a result, the Rock Designation Quality (RQD) values are often low as seen in Figure 2-6, with specimens having insufficient lengths for strength testing, but of sufficient size for rock index testing. In this case, it would be beneficial to be able to estimate the unconfined strengths from the index parameters.

The following sections present the correlations developed between the strength parameters (q_t and q_u) and the rock's index parameters for different Florida formations.

5.2 Splitting Tension Strength Test (q_t)

Shown in Figure 5-1, the majority of splitting tension strength (q_t) results in data set #1 are less than 1.7 MPa (250 psi), with a median q_t = 0.6 MPa (90 psi). Figures 5-2 and 5-3 show the

relationship between q_t and bulk porosity n. It should be noted that bulk porosity, n, and bulk dry unit weight, γ_{dt}, have a direct relationship of $n = 1 - \gamma_{dt}/(GS*\gamma_w)$, where GS is the sample specific gravity and γ_w is water unit weight. Because GS is generally a constant in Florida rocks (i.e., it varies within a narrow range depending on the percentage of calcite, quartz, dolomite, or aragonite within the carbonate rocks), for a given bulk dry unit weight, the porosity fluctuates within a margin of typically 3%. For example, γ_{dt} = 15.7 kN/m^3 = 100 pcf, then n could vary from 0.405 to 0.418, or 40.5% to 41.8% when GS = 2.69 to 2.75. The rock's GS is difficult to measure while γ_{dt} is very easy to obtain – simply the oven-dried weight divided by the cylindrical volume. Therefore, the key correlation for the Florida rock strength was based on the bulk dry unit weight, γ_{dt}. Figure 5-4 presents the q_t results versus bulk dry unit weight for data set #1 with a general correlation between the predicted q_t and dry unit weight as:

$$q_t \text{ (kPa)} = 26.64 \exp(0.191 \gamma_{dt} B) \quad \text{(5-1a)}$$

$$q_t \text{ (psi)} = 3.864 \exp(0.03 \gamma_{dt} B) \quad \text{(5-1b)}$$

where,

γ_{dt} - the bulk dry unit weight (kN/m^3 or pcf)

$B = 1$ if $\gamma_{dt} < \gamma_{dt0}$

$B = \sqrt{\gamma_{dt}/\gamma_{dt0}}$ if $\gamma_{dt} \geq \gamma_{dt0}$

γ_{dt0} = 22 kN/m^3 (140 pcf)

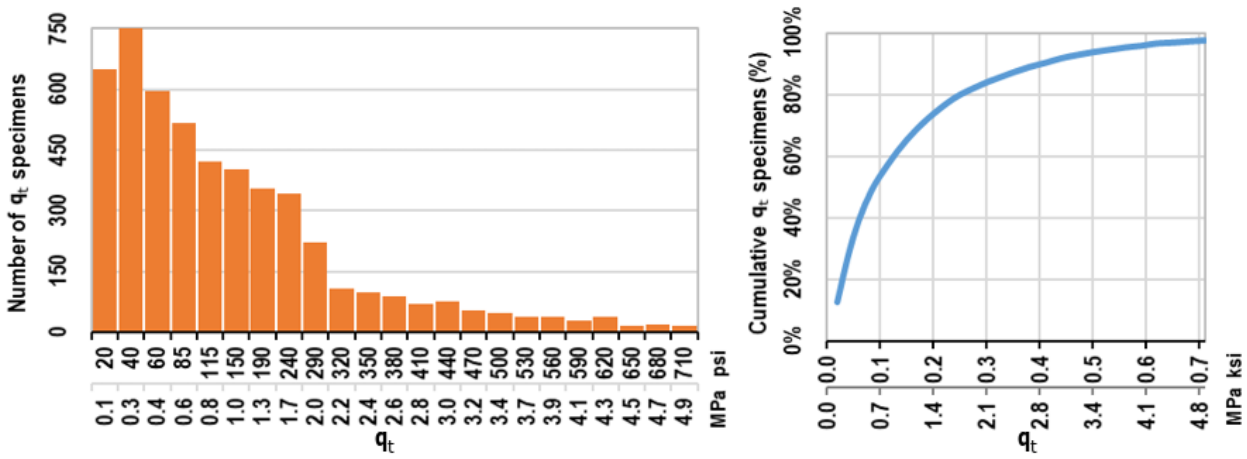

Figure 5-1. Data set #1 – Histogram of splitting tension strength q_t

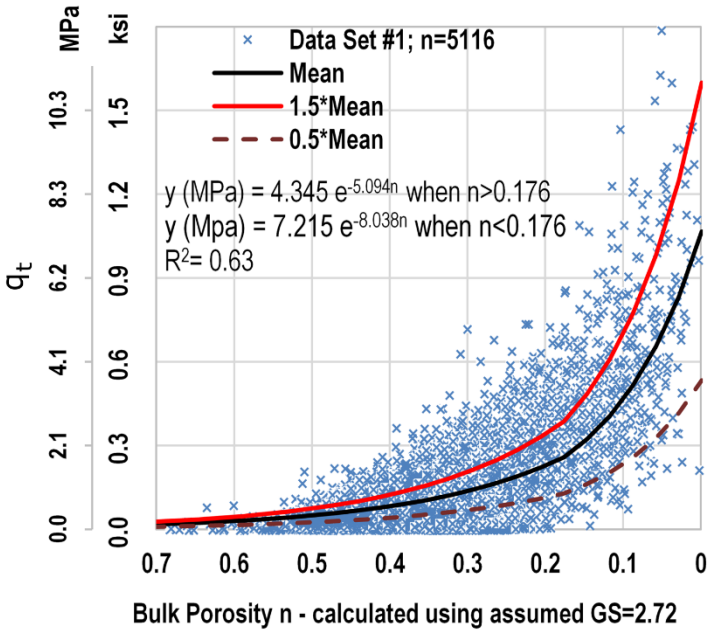

Figure 5-2. Data set #1−q_t results versus bulk porosity

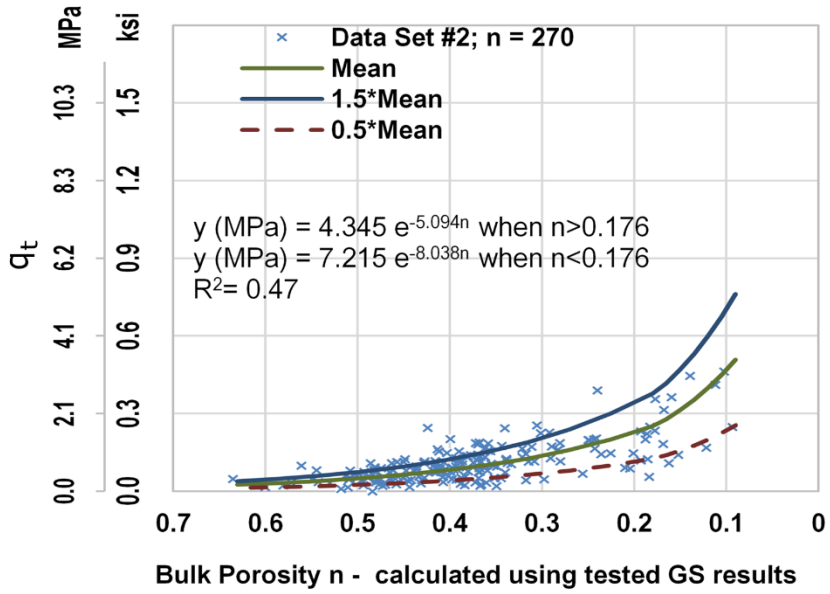

Figure 5-3. Data set #2−q_t results versus bulk porosity

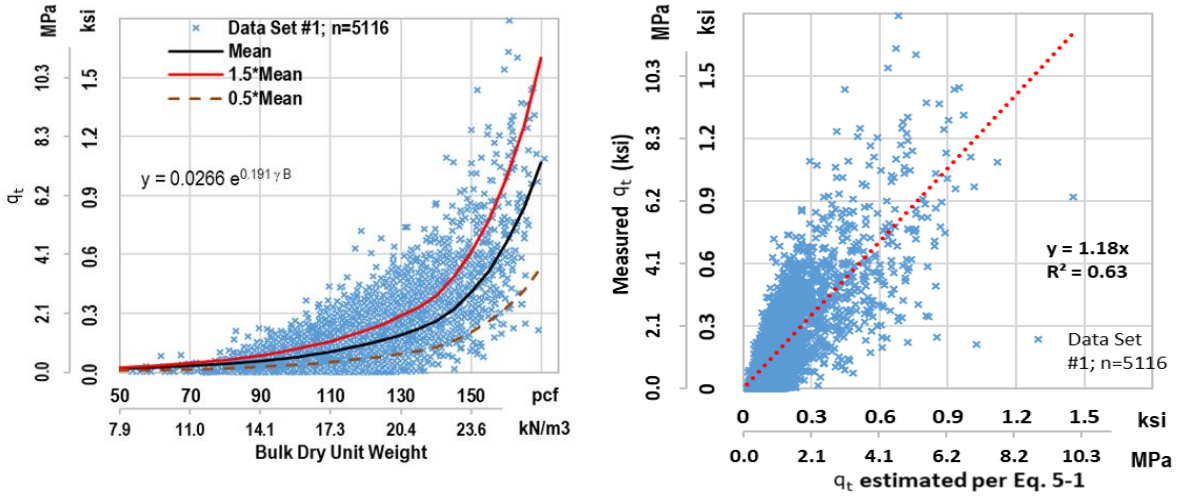

Figure 5-4. Data set #1−q_t results versus bulk dry unit weight

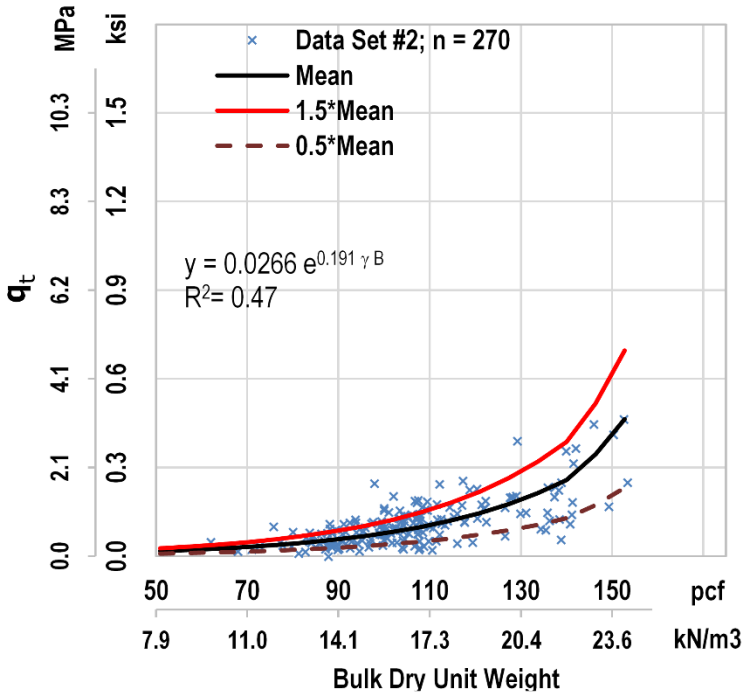

Figure 5-5. Data set #2—q_t results versus bulk dry unit weight

The very large data set (5,116 data points) has a coefficient of determination of $R^2 = 0.63$. It can be seen that there exists a large scatter in the data in Figure 5-4. For the data set #2 in Figure 5-5, the coefficient of determination for the same regression analysis was 0.47. This lower value may be attributed to the difference in sample properties of each formation. As stated earlier, in addition to bulk dry unit weight, other index parameters are available for data set #2. One of the most important additional parameters is the rock formation identification, which relates to the mineral structure (i.e., calcite, aragonite, dolomite, etc.), as well as weathering state (i.e., carbonate content and porosities). As shown in Figure 5-6, each formation has a distinctive trendline with regard to the bulk dry unit weight. To discern the formation factor, the bias ratio ($Bias_1$) between measured values (q_{t_m}) and predicted values using Eq. 5-1 ($Bias_1 = q_{t\_m}$/ Eq. 5-1) was plotted for each project site (Figure 5-7): Sites 2, 5, and 6 in Miami Formation[1], Site 1 in shallow Ft.

[1] Per Scott (2001), the Miami formation forms the Atlantic Coastal Ridge

Thompson Formation[2], Site 3 in Anastasia Formation, site 4 in Key Largo Formation, site 7 in Arcadia dolostone, and site 8 in Hawthorn Formation. The average $Bias_1$ ratio value presented in Figure 5-7 is the splitting tension formation factor, F_t. F_t is then generalized in Figure 5-8 and Table 5-1.

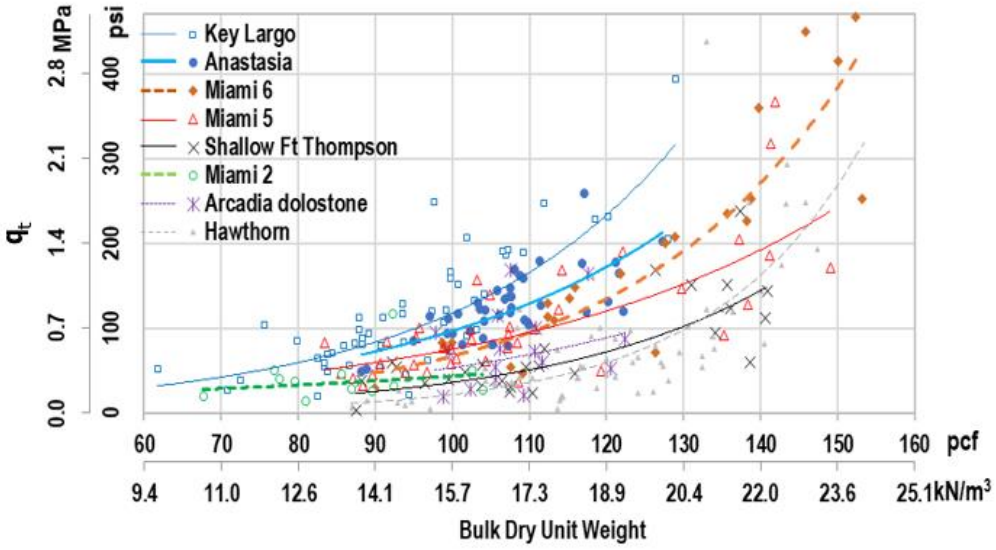

Figure 5-6. Data set #2−q_t and bulk dry unit weight for different formations

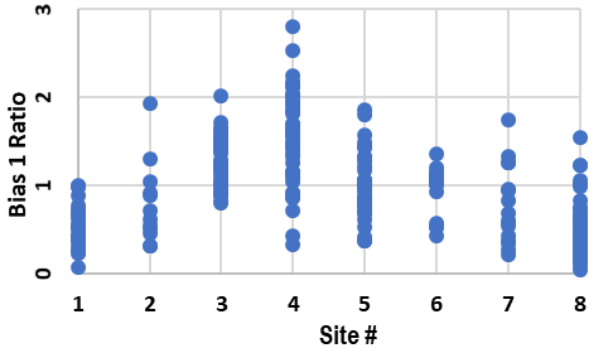

Figure 5-7. Data set #2−$Bias_1$ for each project site

[2] Shallow Ft. Thompson formation exists near the ground surface to the west and north-west of the Atlantic Coastal Ridge. In the Atlantic Coastal Ridge, the deeper Ft. Thompson formation is overlaid by the Miami formation. In data set #2, only shallow Ft. Thompson formation samples were recovered and analyzed.

Table 5-1. Splitting tension formation factor (F_t)

Formation	Ft	
Anastasia	1.3	
Key Largo	1.5	
Shallow Ft. Thompson	0.6	
Miami, poor induration	0.75	Average 0.9
Miami, moderate induration	0.9	for the
Miami, moderate/well induration	1	Miami
Miami, well induration	>1	formation
Arcadia dolostone	0.8	
Hawthorn	0.7	

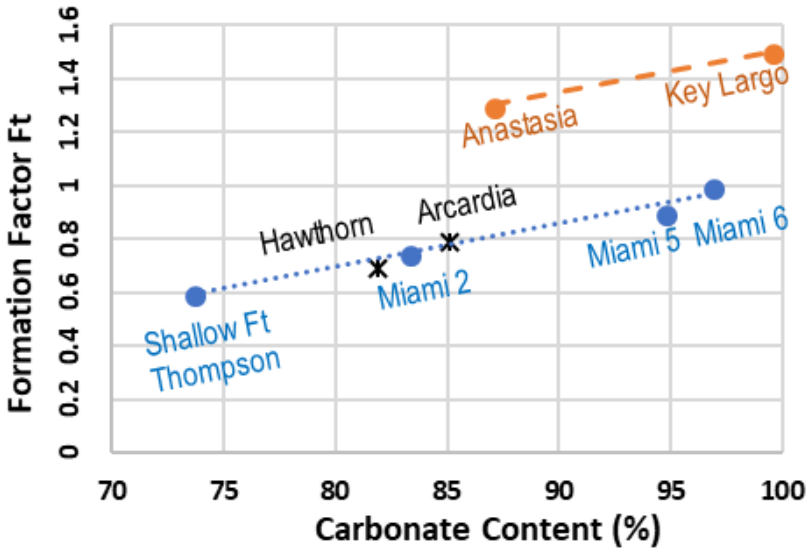

Figure 5-8. Splitting tension formation factor F_t

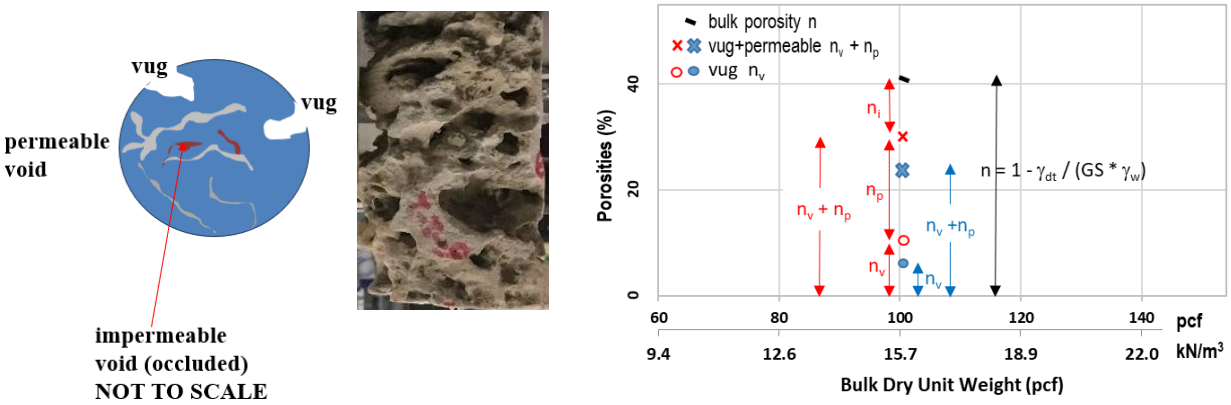

Figure 5-9. Types of porosities: (a) Sketch of porosity types; (b) Vuggy specimen; (c) Example of porosities at γ_{dt} = 15.7 kN/m^3 (100 pcf)

Based on Figure 5-8, for Florida carbonate rocks having different index properties than the rocks presented in this study, F_t can be estimated as:

$$F_t = 1.6C_{ave} - 0.43 + P_n \quad (5\text{-}2)$$

C_{ave} - the average carbonate content for the formation;

P_n - porosity structure factor with suggested value varying from -0.2 to +0.3 as:

If porosity ratio $n_v / n < 0.1$ or $(n_v + n_p)/ n < 0.6$, then $P_n = +0.3$

If porosity ratio $n_v / n > 0.2$ and $(n_v + n_p)/ n > 0.7$, then $P_n = -0.2$

P_n is an empirical factor, as presented above based on the quantitative estimates of vug porosity or the sum of vug and permeable porosities. To examine the formation factor (F_t) or its related porosity structure factor (P_n) refer to Figure 5-9.c - both have the same bulk dry unit weight γ_{dt} = 15.7 kN/m^3 (100 pcf), thus both have approximately the same bulk porosity (n). However, the red specimen (A) has a higher vug porosity and smaller impermeable porosity. Therefore, the failure surface would more likely go through the weakest path connecting the vugs and the permeable porosity in the red specimen. Thus, the blue specimen (B) would likely have a higher unconfined strength. This is the same reason for the Key Largo and Anastasia having a higher trend of splitting tension formation factors, F_t, while other formations would have a lower trend of F_t values (corresponding to a given carbonate content) in Figure 5-8.

For the Anastasia Formation, there are two factors affecting the formation factor, F_t:

a) The detrimental porosities ($n_v + n_p$), despite being higher than the Key Largo Formation, is still lower than other the formations (Figure 4-5.a);

b) The vug porosity (n_v) is the lowest for Anastasia Formation (Figure 4-5.b).

For the Key Largo Formation, detrimental porosities ($n_v + n_p$) are the lowest among the tested formations (Figure 4-5.a). The lower the detrimental porosity, the higher the porosity structure factor P_n. For example, a P_n factor of +0.3 can be used for Key Largo, since its P_n factor is much less than the other formations.

The $Bias_1$ ratio was correlated the against carbonate content (C) and formation factor (F_t) as follows:

$$Bias_1 = 0.64\, F_t \exp(0.4214C) \tag{5-3}$$

Substituing Eq. 5-3 into 5-1, a revised predicted q_t value based on γ_{dt}, C, and F_t is presented as Eq. 5-4:

$$q_t \text{ (kPa)} = 17.05 * F_t \exp(0.191\gamma_{dt} B) \exp(0.4214C) \tag{5-4a}$$

$$q_t \text{ (psi)} = 2.47 * F_t \exp(0.03\gamma_{dt} B) \exp(0.4214C) \tag{5-4b}$$

This correlation yields an improved coefficient of determination of 0.66. The power parameter 0.4214 for carbonate content, C, was simplified to a value of 0.5 and it was found that the coefficient of determination stays the same as (Figure 5-10):

$$Bias_1 = 0.639\, F_t \exp(0.5C) \tag{5-5}$$

And substituting Eq. 5-5 into 5-1:

$$q_t \text{ (kPa)} = 17\, F_t \exp(0.191\gamma_{dt} B) \exp(0.5C) \tag{5-6a}$$

$$q_t \text{ (psi)} = 2.468\, F_t \exp(0.03\gamma_{dt} B) \exp(0.5C) \tag{5-6b}$$

It is noted that this is the same population of n=270 for data set #2, but the R^2 improved significantly from 0.47 when the correlation uses one parameter (Figure 5-5) versus 0.66 when the correlation employs three index parameters (Figure 5-10), namely γ_{dt}, F_t (Table 5-1), and C.

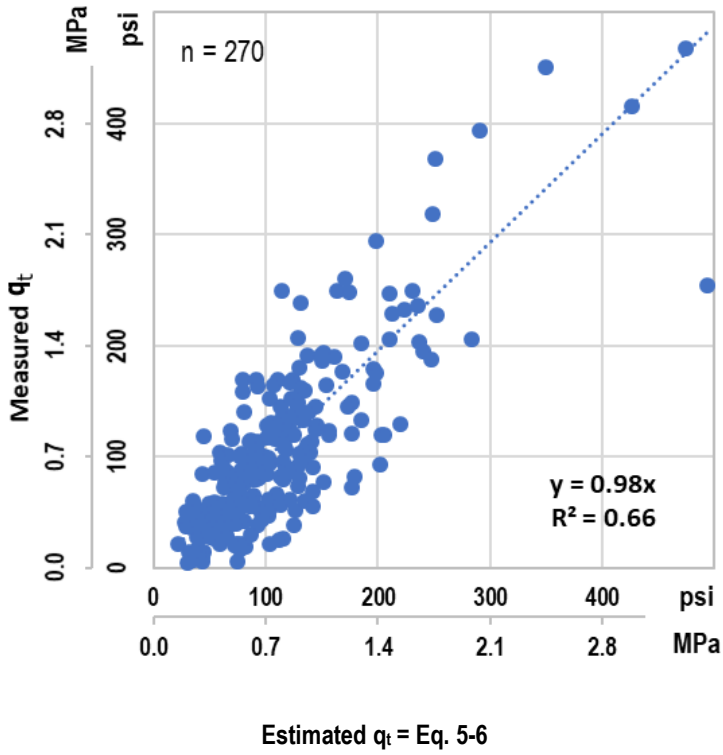

Figure 5-10. Data set #2−q_t correlation with γ_{dt}, F_t, and C

For Miami Formation, the Florida Geological Survey (Scott 2001) describes it as having two distinct facies -- an eastern oolitic facies that forms along the Atlantic Coastal Ridge, and the bryozoan facies to the west toward the Everglades. In some areas, the two facies may intermix with each other. The oolitic facies can be further be divided into a cross-bedded and a bioturbated facies. Rock samples from three Miami sites showed completely different magnitudes of indurations. Therefore, it may be logical to use separate formation factors for Miami formation depending on degrees of indurations - as shown in Table 5-1. If the degree of induration is uncertain, a single formation factor of 0.9, also shown in Table 5-1, can be used. Figure 5-11 indicates that both methods would yield a good coefficient of determination R^2.

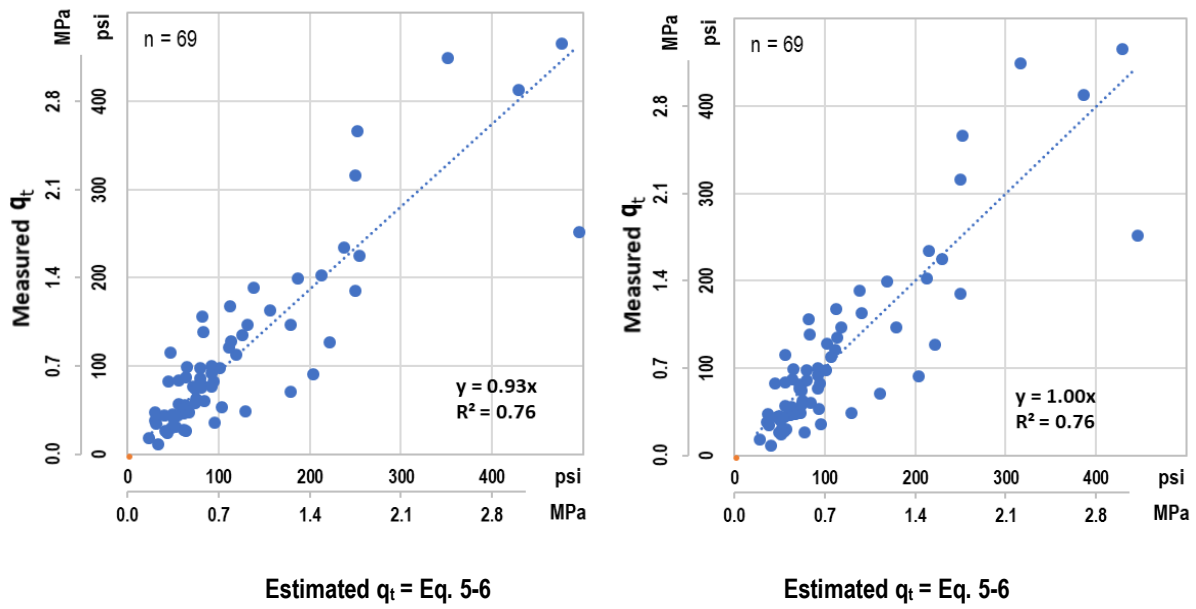

Figure 5-11. Statistical results for Miami formation only - q_t correlation with γ_{dt}, F_t, and C: (a) F_t = 0.75, 0.9, and 1.0; (b) F_t = 0.9 for all 3 sites

A new bias ratio between the measured and predicted values ($Bias_2 = q_{t\_m}$/ Eq. 5-6) was plotted versus the vug porosity (n_v) to see if strength correlations could be improved using the numerical values of these porosity properties. As seen in Figure 5-12, no clear relationship was found to exist. As discussed earlier, impacting the strength results are the orientations and distributions of the vugs within the specimens relative to the loading line. If the vugs are aligned with the loading line, then the failure loads and the associated strengths are lower than the rocks with the same vug porosity (n_v) but with a different orientation of the vugs. The vugs play a very significant role in scattering the resulting strengths without any clear numerical correlations.

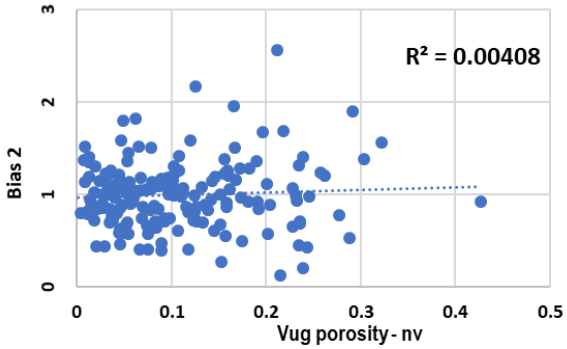

Figure 5-12. Data set # 2 - Bias$_2$ and n_v

5.3 Unconfined Compression Strength (q_u)

As a result of the geological history (described in Chapter 2) and physical properties of Florida carbonate rock (including the carbonate content, dry unit weight, and porosity as reported in Chapter 4), strengths for Florida rock are generally low, and as seen in Figure 5-13, the majority (80%) of the rocks have unconfined compression strengths, q_u, less than 9 MPa (1,300 psi), with a median q_u = 3 MPa (435 psi). Figure 5-14 presents q_u versus bulk dry unit weights from data set #1. In this figure, the coefficient of determination of R^2 = 0.69 does show, despite the scatter, that there is a good correlation between unconfined compression strength, q_u, and the single index parameter of bulk dry unit weight, γ_{dt}. The equation is presented below, which is quite similar to q_t Eq. 5-1:

$$q_u \text{ (kPa)} = 40.3 \exp(0.255\gamma_{dt} B) \quad (5\text{-}7a)$$

$$q_u \text{ (psi)} = 5.89 \exp(0.04\gamma_{dt} B) \quad (5\text{-}7b)$$

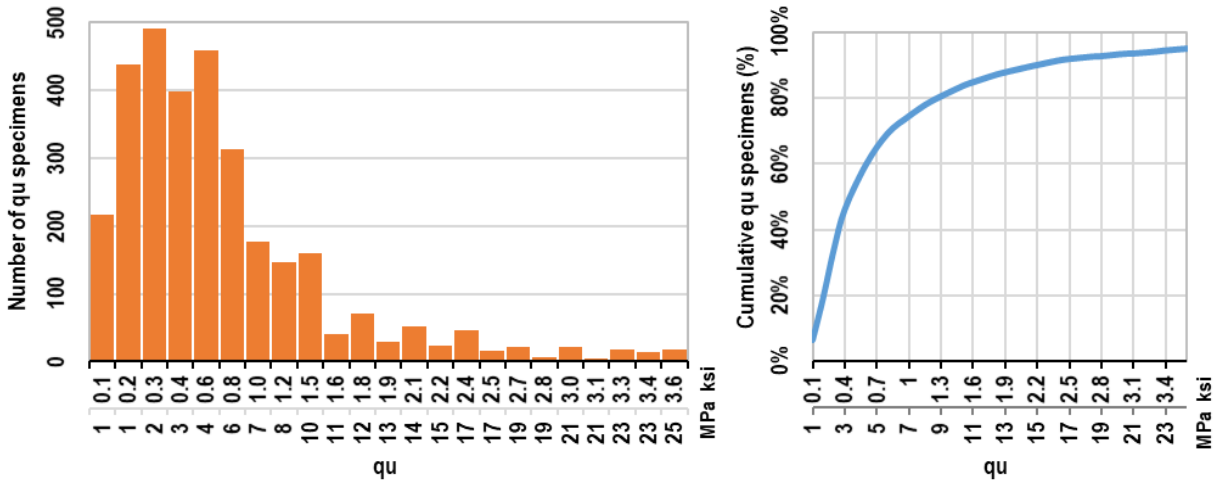

Figure 5-13. Data set #1−Histogram of unconfined compression strength q_u

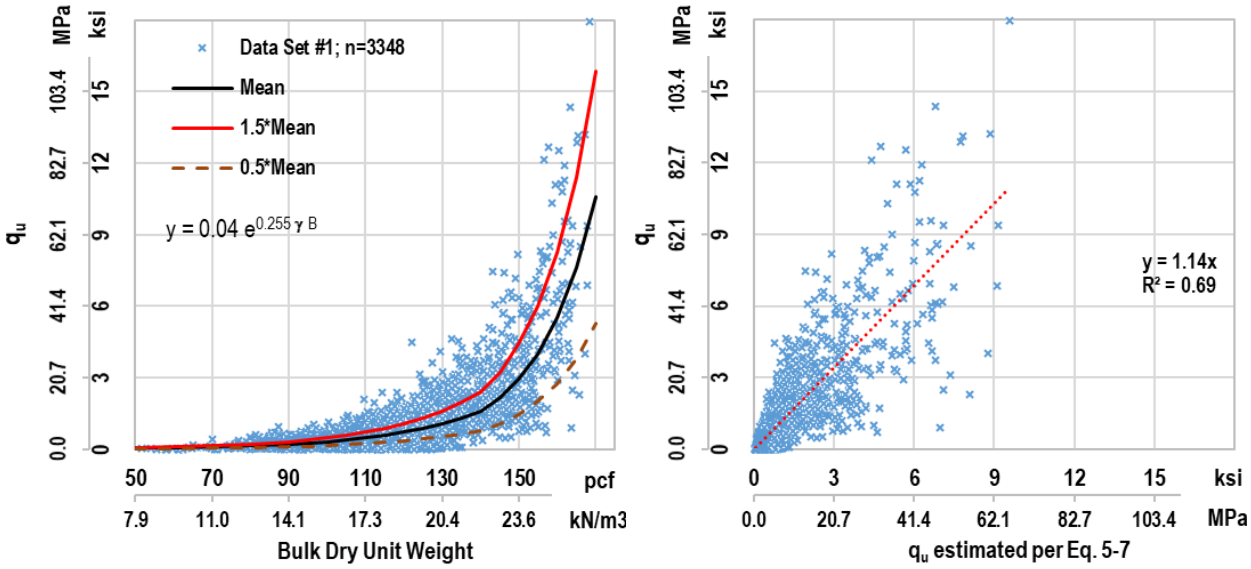

Figure 5-14. Data set #1−q_u results versus bulk dry unit weight

The population for q_u results in data set #2, n = 80, is significantly less than the population for q_t results (n = 270). Furthermore, 71 of these 80 q_u results belong to only one formation (Anastasia), while the other three formations have only 2 to 5 q_u data points. The reason is that most of the available long specimens were used for triaxial tests, with those results presented in Chapter 6. Due to the small population of q_u results in data set #2, especially when only 2 to 5 data points were available per formation, a different approach was employed to establish a correlation

between q_u and the index parameters of γ_{dt}, C, and compression formation factor, F_u. The approach, utilizing a combination of data set #2 and subset #1a with a total population of 178 (Figure 5-15), is described below.

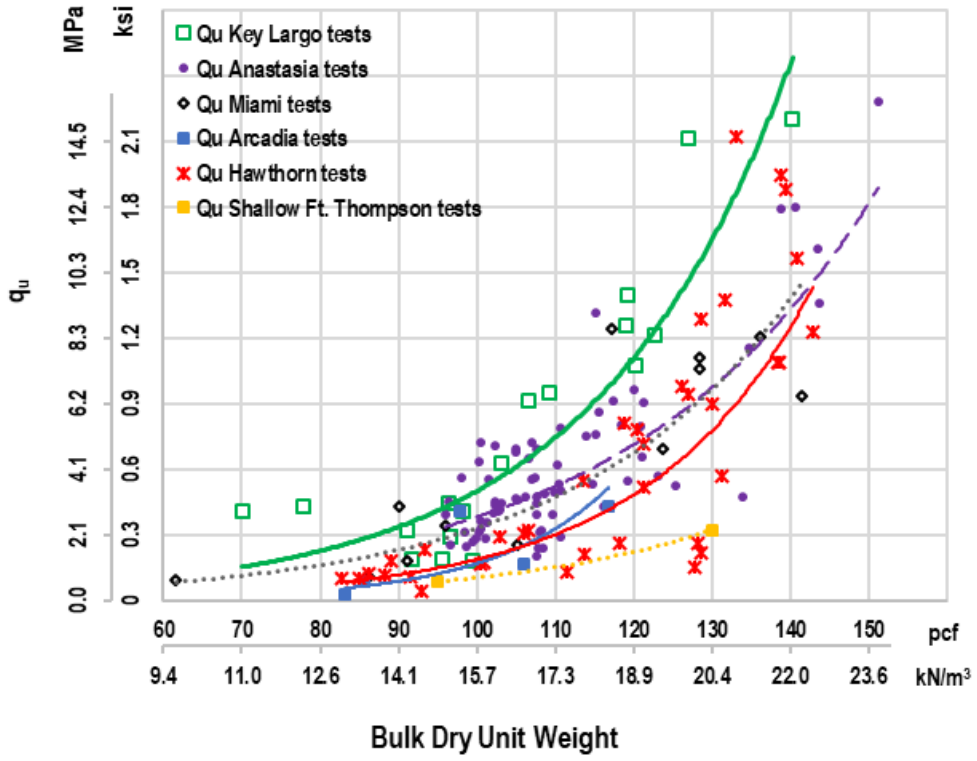

Figure 5-15. Data sets #1a and 2−q_u and bulk dry unit weight for different formations

First, by comparing Eq. 5-7 to 5-1, a general relationship between q_u and q_t was established:

$$q_u \text{ (kPa)} = 0.51 * q_t^{4/3} \quad (5\text{-}8a)$$

$$q_u \text{ (psi)} = 0.97 * q_t^{4/3} \quad (5\text{-}8b)$$

Solving for q_t, the equations are: $q_t \text{ (kPa)} = 1.96 * q_u^{3/4}$ (5-9a)

$$q_t \text{ (psi)} = 1.03 * q_u^{3/4} \quad (5\text{-}9b)$$

Relationships for q_t/q_u have been proposed by many authors for many materials. For example, a comparison of q_t with q_u for concrete is quite simple because it is easy to pair a q_t

specimen to another q_u specimen that have the same index properties. Arioglu et al. (2006) developed the following equation for concrete:

$$q_t \text{ (MPa)} = 0.387 q_u^{0.63} \quad \text{(5-10a)}$$

$$q_t \text{ (psi)} = 2.44039 * q_u^{0.63} \quad \text{(5-10b)}$$

For carbonate rocks, it is much more difficult and sometimes impossible to find a pair of q_u and q_t specimens that have similar index properties (i.e., same mineral components, porosities, dry weights, etc.). As identified in Section 4.4, within short vertical distances (cm or inches) of one another, one Florida rock specimen may have γ_{dt} of 20.5 kN/m^3 (130 pcf) and the adjoining rock specimen may have γ_{dt} of 12.5 kN/m^3 (80 pcf). Thus, pairing these two specimens is not recommended despite being at almost the same depth. Johnston (1985) - based on an Australian rock database, paired triaxial test and direct tension test results versus q_u results by selecting only measured q_u values that fell within 50% of the estimated q_u values; thereby, best-fitting the strength envelope connecting the tension test result and the triaxial test result. Johnston (1985) then recommended the following equation for carbonate rocks, which exhibit q_u in the range of 38 to 520 MPa (5,500 to 75,400 psi) in his database:

$$q_{dt} \text{ (kPa)} / q_u \text{ (kPa)} = (1\text{-}0.0172\log^2 q_u) / (2.065\text{+}0.170 \log^2 q_u) \quad \text{(5-11)}$$

For mudstones (different crystal or cleavage structure than carbonate rocks), Johnston (1985) suggested a lower q_{dt}/q_u ratio of:

$$q_{dt} \text{ (kPa)} / q_u \text{ (kPa)} = (1\text{-}0.0172\log^2 q_u) / (2.065\text{+}0.231 \log^2 q_u) \quad \text{(5-12)}$$

It is noted that Eqs. 5-11 and 5-12 use a direct tension test result, q_{dt}. Per Perras and Diederichs (2014), the q_{dt}/q_t ratio for sedimentary rocks ranges between 0.4 to 1.2, with a mean value of 0.7. For concrete, Arioglu et al. (2006) used a ratio of 0.9 for q_{dt}/q_t.

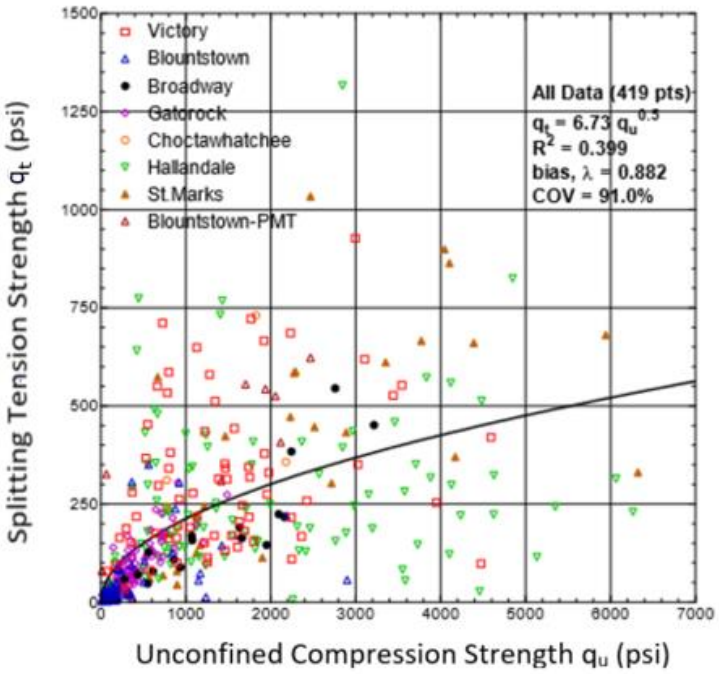

Figure 5-16. Bullock (2004) q_u versus q_t relationship

Bullock (2004) tabulated q_t versus q_u by pairing specimen at similar depths and similar densities (reproduced in Figure 5-16) and yielded the following relationship:

$$q_t \text{ (psi)} = 6.73\ q_u^{0.5} \quad (5\text{-}13)$$

This relationship is almost identical to the American Concrete Institute (ACI 2014) relationship for concrete:

$$q_t \text{ (kPa)} = 17.59\ q_u^{0.5} \quad (5\text{-}14a)$$

$$q_t \text{ (psi)} = 6.7\ q_u^{0.5} \quad (5\text{-}14b)$$

Rodgers (2016) established the following relationship based on data from Little River (Gadsden County, Florida) carbonate rocks:

$$q_t \text{ (kPa)} = 0.765\ q_u^{0.825} \quad (5\text{-}15a)$$

$$q_t \text{ (psi)} = 0.545\ q_u^{0.825} \quad \text{(5-15b)}$$

For the Little River project, Rodgers (2016) converts q_t to q_{dt} by a factor of 0.8 and arrived at the following equation:

$$q_{dt} \text{ (kPa)} = 0.612\ q_u^{0.825} \quad \text{(5-16a)}$$

$$q_{dt} \text{ (psi)} = 0.436\ q_u^{0.825} \quad \text{(5-16b)}$$

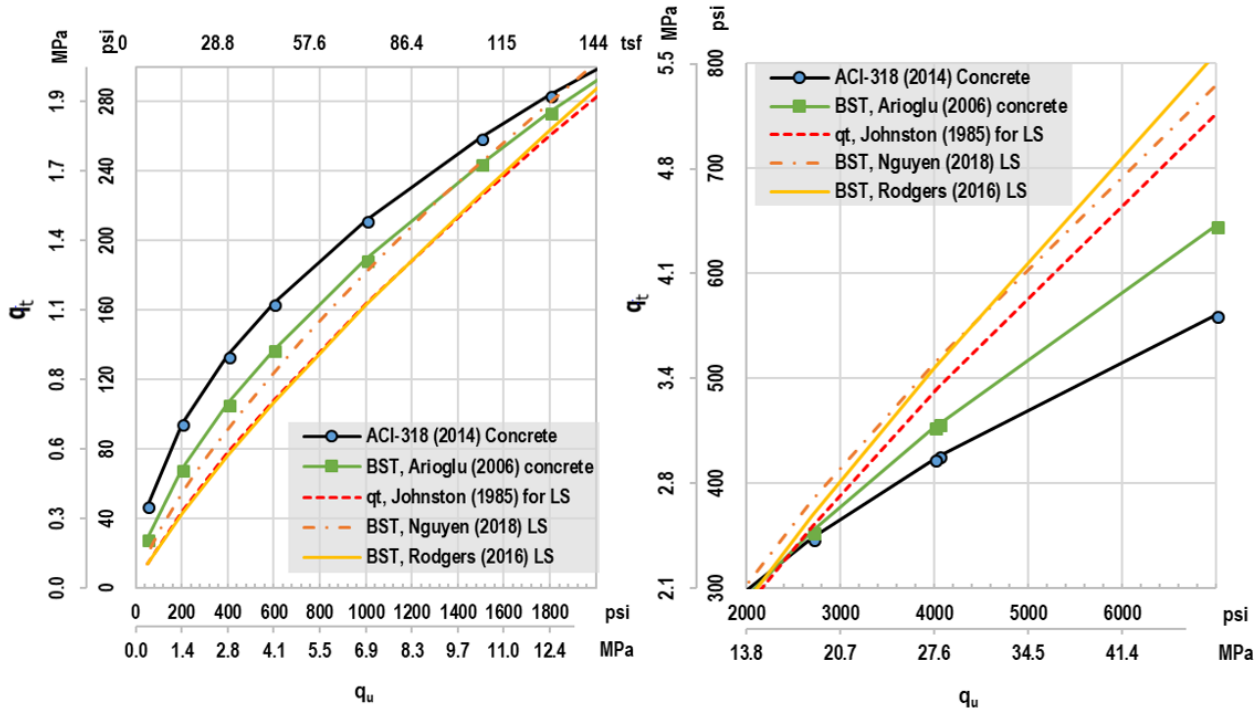

Figure 5-17. q_u versus q_t relationship: (a) For typical Florida rocks; (b) For rocks outside of typical Florida strengths. Notes: 1, LS – Limestone; 2, Johnston relationship is for direct tension test result, q_{dt}

Finally, these different q_t versus q_u relationships are plotted together in Figure 5-17, where the proposed relationship is described earlier in Eq. 5-8 or 5-9. As shown in Figure, the proposed relationship is in good agreement to the other relationships, especially when plotted within the range of typical Florida rock strengths (Figure 5-17.a). For rocks that are outside of typical Florida strengths (Figure 5-17.b), the relationships still agree with each other, with the exception that concrete shows a different trend than the carbonate rock relationships.

Substituting Eq. 5-6 into Eq. 5-8, the following equation can be used to estimate q_u based on dry unit weight, γ_{dt}, compression formation factor F_u, and carbonate content C:

$$q_u \text{ (kPa)} = 22.34\ F_u\ e^{2C/3} * e^{0.255\ \gamma_{dt}\ B} \quad (5\text{-}17a)$$

$$q_u \text{ (psi)} = 3.24\ F_u\ e^{2C/3} * e^{0.04\ \gamma_{dt}\ B} \quad (5\text{-}17b)$$

The compression formation factor, F_u, is derived as follows:

- Measured q_u results, only for specimens with known rock formation identifications, were tabulated (Figure 5-15). The majority of the data in Figure 5-15 came from data subset #1a.
- As the carbonate contents were not recorded for this set of data, the average carbonate content values obtained from data set #2, tabulated in Table 5-2, were used in Eq. 5-17.
- F_{ui} was then calculated for each q_u data point by solving Eq. 5-17:
- $F_{ui} = q_{u\ measured} / (22.34\ e^{2C/3} * e^{0.255\ \gamma_{dt}\ B})$
- The average F_u for each formation is presented in Table 5-3. It is noted that the F_u factor is different than the F_t factor due to the differing boundary conditions of the two different test methods and differing loading orientation. Statistical results using Eq. 5-7 are presented in Figure 5-18. a, whereas the results using Eq. 5-17, plugging in the F_u value from Table 5-3, are presented in Figure 5-18. b.

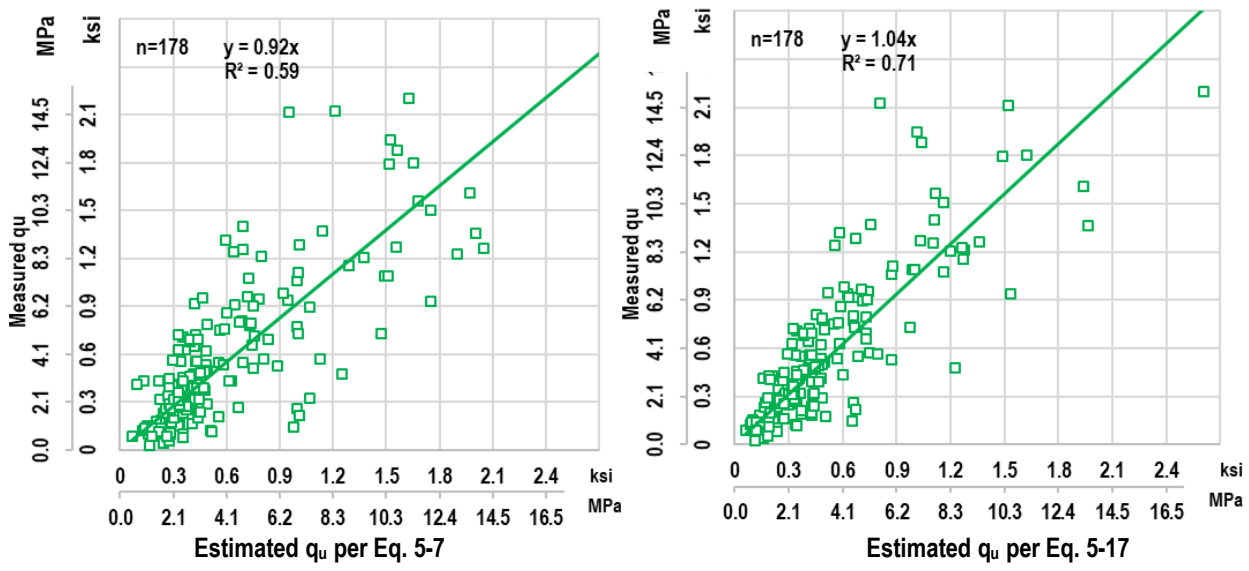

(a) (b)

Figure 5-18. Data sets #1a and 2 – q_u correlations: (a) Correlation against 1 parameter (γ_{dt}); (b) Correlation against 3 parameters (γ_{dt}, F_u, and C)

It can be seen that the correlation was improved when using three index parameters versus one parameter. Due to limited population in data set #2 and the assumption that carbonate content for each formation in subset #1a equals the average carbonate content from data set #2, it is recommended that the compression factor F_u be calibrated for available local data when Eq. 5-17 is used.

Table 5-2. Average carbonate content from data set #2

Formation	Key Largo	Anastasia	Miami	Shallow Ft. Thompson	Arcadia	Hawthorn dolostone
Average Carbonate Content	99.5%	87.0%	93.9%	73.6%	84.9%	81.7%

Table 5-3. Compression formation factors (F_u)

Formation	Key Largo	Anastasia	Miami	Shallow Ft. Thompson	Arcadia dolostone	Hawthorn
Fu	1.5	1.0	0.85	0.5	0.7	0.7

5.4 Unconfined Strengths of Marls

A limited quantity of marl specimens from the Hawthorn Formation were provided from Site #8 (Fuller Warren Bridge) and unconfined strength tests were performed on these specimens. No specimens were available for triaxial tests. Unfortunately, the rock cores' natural moistures had not been preserved. When the cores arrived at the laboratory, they had already been air-dried. The unconfined strengths of these air-dried specimens are presented in Figure 5-19 and Figure 5-20 for q_t and q_u, respectively. Some other marl specimens were placed in the moisture room. However, depending on the locations of the specimens in the moisture room, many of them disintegrated and were not testable. The remaining were tested as "moist" specimens and are also presented in Figures 5-19 and 5-20. These figures show that the air-dried specimens have significantly higher unconfined strengths than the moist specimens. In summary, the marl strength is highly sensitive to the specimen moistures, and it is critical to test the specimens at their natural moisture contents, otherwise their strengths would be altered and are not reliable.

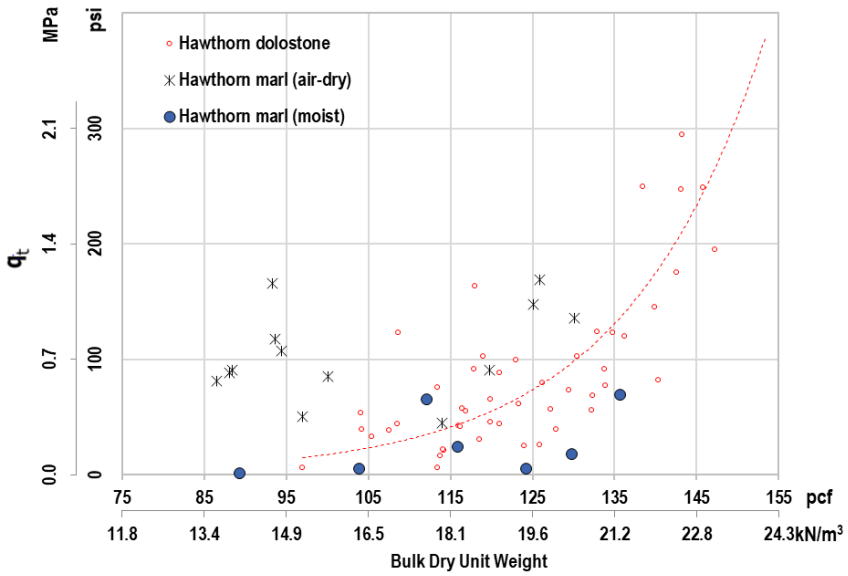

Figure 5-19. q_t results for marl

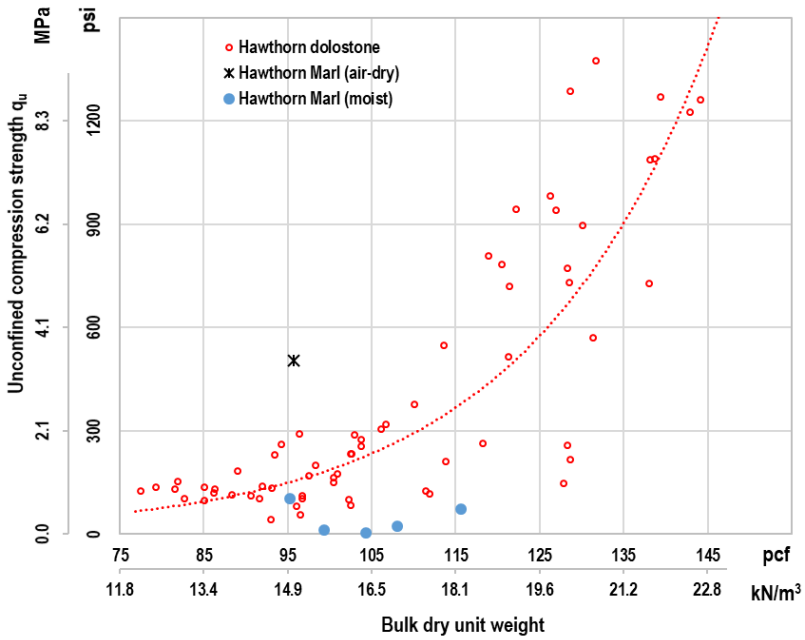

Figure 5-20. q_u results for marl

5.5 Stress-Strain Behavior

A relationship that should also be identified in addition to peak strengths (splitting tension and unconfined compression) is the stress-strain response of unconfined compression tests. Examples of stress-strain curves from data set #1 are presented in Figure 5-21. As the figure shows, the low strength materials with q_u < 5 MPa (725 psi), which are classified as IGM typically exhibit ductile behavior (minimal loss of strength with increased axial strain) or transition between brittle and ductile. This is unique characteristic of Florida porous rocks, as most rocks cited in literature (Schwartz 1964, Hoek and Brown 1980 and 1988, Gowd and Rummel 1980) would display a brittle rupture response under no confinement. The higher strength rocks with q_u > 9 MPa (1,305 psi) typically exhibit brittle behavior (a significant drop in strength after the peak). As shown by authors above, this brittle behavior typically transitions to ductile behavior under increasing confining pressure in triaxial testing (presented in Chapter 6). This type of behavior is helpful to

the engineers when selecting an applicable stress-strain model for Florida carbonate rocks, especially for finite element model analyses.

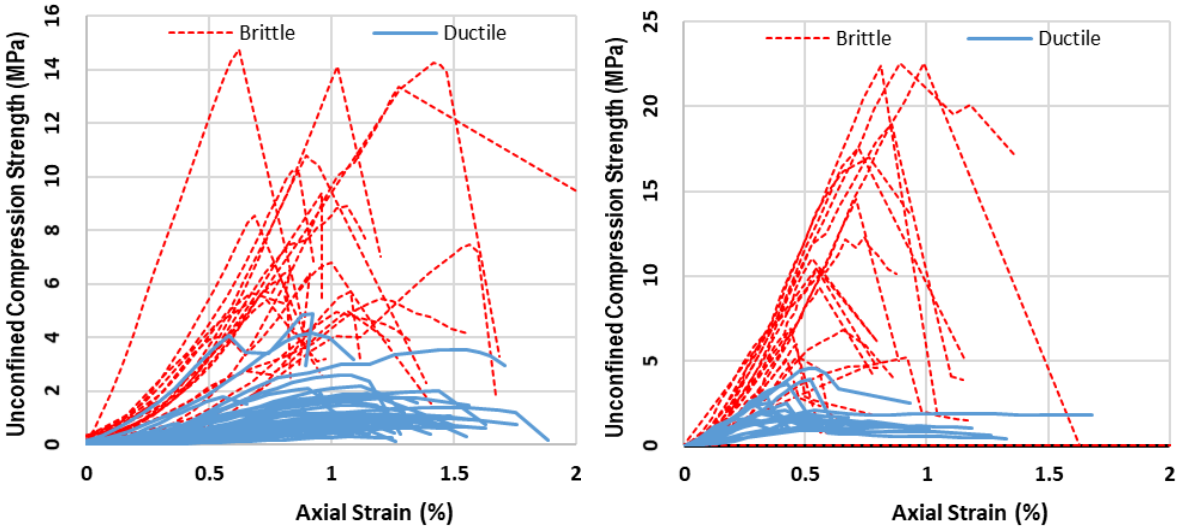

a) b)

Figure 5-21. Example of stress-strain results from q_u tests: (a) Site 8-I95 on the Fuller Warren Bridge, St. Johns River; (b) Site 21-SR 8 over Choctawhatchee River

5.6 Summary

Florida carbonate rock is among the youngest sedimentary rock in the world. It is generally very porous, with porosity sometimes exceeding 50%, i.e., more voids than solids. In addition, some rock formations have very low carbonate content, which reduces the binding cementation and, in turn, reduces the rock strength.

The unconfined strength – both split tension and unconfined compression – are strongly correlated to the material bulk porosity, which is inversely represented by the bulk dry unit weight, γ_{dt} are presented in Eqs. 5-1 and 5-7. Unconfined strength was also found as a function of rock formation, which is represented by the porosity structure (proportion of vug and permeable, and impermeable porosities), and average carbonate content. For each formation, the carbonate content can vary from specimen to specimen. The relationship between unconfined strength and three key

parameters (bulk dry unit weight, formation factor, and carbonate content) is present in Eqs. 5-6 and 5-17.

Since Florida rocks are highly variable, with intermixing of hard and soft lenses with highly variable recoveries and rock quality designation (RQD), obtaining a significant number of core pieces of sufficient length for strength testing for a particular stratum can be difficult. However, index rock parameter testing as discussed is an alternative approach when it is not feasible to perform strength tests due to the required specimen's minimum L/D ratio. Therefore, a comprehensive and continuous rock strength profile with depth can be established using estimated strengths correlated to index parameters. The established correlations are not only helpful in explaining the unconfined strength behaviors of Florida carbonate rocks, but also crucial in the economical and safe design of shallow or deep foundations relying on continuous strength profiles.

The findings of the work presented in this chapter can be summarized as follows: i) based on an examination of a large volume of data of Florida carbonate rocks, it was discovered that a majority are much more porous than other carbonate rocks typically cited in literature, ii) it is recommended that the strength correlations involving three input parameters be used to improve the reliability of the correlations, and iii) the input parameters (rock index properties) are relatively easy to obtain.

CHAPTER 6
STRENGTH ENVELOPES OF FLORIDA CARBONATE ROCKS AND IGMS

6.1 Existing Strength Envelopes

Many of the Florida Department of Transportation (FDOT) bridges are supported on deep foundations (typically drilled shafts or driven piles). Most of these foundations derive their bearing capacities from embedment in carbonate rocks. The design practices for these deep foundations are described below.

Driven pile resistances are designed not based on laboratory rock testing results, but based on correlations with in situ testing results, e.g., SPT or CPT (McVay et al. 2017).

Drilled shafts: (a) toe bearing capacity of shafts that are not post-grouted is typically ignored, and when utilized it is assigned only a fraction of the anticipated ultimate resistance to account for strain incompatibility between side resistance and end bearing; (b) side resistance (f_s) approximately equals the adhesion between concrete and rocks. McVay et al. (1992) proved that the linear Mohr-Coulomb portion (red continuous line in Figure 6-1), tangent with Mohr circles of the unconfined compression (q_u) and direct tension results (q_{dt}), could be used to calculate the cohesion, which is the intercept between the linear portion and the y-axis, and has been shown to have a good correlation with the adhesion between drilled shaft concrete and the surrounding rock material in side resistances:

$$f_s = 0.5\sqrt{q_u q_{dt}} \tag{6-1}$$

A number of locations across Florida, especially the southeastern portion of the state, have shallow rock formations (i.e., rocks encountered at a depth less than about 10 m or 30 ft), and designers have recently proposed the use of shallow foundations for bridge piers or bents. An

assessment of the rocks' bearing capacity is needed for design, including strength envelopes for the rock identifying the stress-strain response of the rocks to assess foundation deformations, and bearing failure modes (general, local, and punching). The dashed black lines in Figure 6-1 are the portion of the strength envelope that have not been explored for the shallow and porous Florida carbonate rocks.

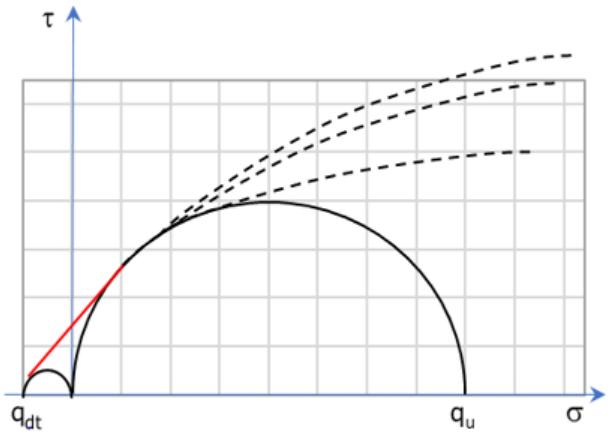

Figure 6-1. Sketch of strength envelopes

One option is to modify and use existing strength envelope models for the design. One such model is the Hoek and Brown criterion, which is widely accepted and has been used on many projects around the world (Hoek and Brown 1980, 1988, and 2018), that was originally developed for rock with of brittle failure (rupture) behavior and expressed as:

$$\sigma_1 = \sigma_3 + q_u \left(m\frac{\sigma_3}{q_u} + s\right)^a \quad (6\text{-}2)$$

where,

σ_1 and σ_3 = specimen principal stresses.

s = rock mass discontinuity factor.

$$s = e^{(GSI-100)/(9-3D)} \quad (6\text{-}3)$$

GSI is the Geological Strength Index, which approaches 80 to 100 for intact or massive rock (blocky, very well interlocked undisturbed rock mass), and reduces to as low as 10 for very weathered, heavily broken rock mass.

$$m = m_i\, e^{(GSI-100)/(28-14D)}. \quad (6\text{-}4)$$

m_i ranges from approximately 8±3 to 12±3 for different carbonate rocks (Table 6-1). A typical value of m_i = 10 for Florida carbonate rocks was used when applying the Hoek-Brown criterion for this study.

Table 6-1. Values of the constant m_i for carbonate rocks (after Marinos and Hoek 2000)

Texture	Coarse	Medium	Fine	Very Fine
Rock	Crystalline Limestone	Sparitic Limestone	Micritic Limestone	Dolomite
m_i	12 ± 3	10 ± 5	8 ± 3	9 ± 3

D = disturbance factor caused by the rock removal methodology. For shallow foundation excavation, D=0.

$$a = 0.5 + (e^{-GSI/15} - e^{-20/3})/6; \text{ Typically, a} = 0.5 \quad (6\text{-}5)$$

Note, setting $\sigma_3 = 0$ in Eq. 6-2 results in:

$$\sigma_1 = q_u s^a \quad (6\text{-}6)$$

For intact rock, s =1.0 and $\sigma_1 = q_u$. When comparing the strength envelopes to laboratory test results, s is always 1.0 regardless of rock mass qualities because each individual rock piece is intact (otherwise, σ_1 would not equal to q_u at $\sigma_3 = 0$).

When setting $\sigma_1 = 0$ in Eq. 6-2, then σ_3 would be the direct tension strength, $\sigma_3 = 0.5(m - \sqrt{m^2 + 4s})q_u$. Therefore, for intact rock (i.e., s=1 and $m = m_i$), this equation becomes

$\sigma_3 = 0.5(m_i - \sqrt{m_i^2 + 4})q_u$. Since direct tension strength $q_{dt} = -\sigma_3$ in this case, the direct tension strength over unconfined compression strength ratio for intact rock is:

$$q_{dt} / q_u = 0.5(\sqrt{m_i^2 + 4} - m_i) \approx 0.1 \quad (6\text{-}7)$$

Hoek and Brown (2018) found out that this q_{dt} / q_u ratio per Eq. 6-7 is higher than measured values, when q_{dt} test results were available. Thus, a tension strength limiting value was introduced, where the estimated q_{dt} value is reduced to the following value (Hoek and Brown 2018):

$$q_{dt} = q_u / (0.81m_i + 7) \quad (6\text{-}8)$$

In shallow foundation analyses or triaxial testing, it is more convenient to express the strength envelope in terms of Lambe's p-q diagram (Lambe and Whitman, 1969), as defined below:

$$p = (\sigma_1 + \sigma_3)/2 \quad (6\text{-}9)$$

$$q = (\sigma_1 - \sigma_3)/2 \quad (6\text{-}10)$$

Therefore, the Hoek-Brown criterion becomes:

$$q = 0.5\, q_u (m\frac{\sigma_3}{q_u} + s)^a \quad (6\text{-}11)$$

$$p = q + \sigma_3 = 0.5\, q_u (m\frac{\sigma_3}{q_u} + s)^a + \sigma_3 \quad (6\text{-}12)$$

For intact tested specimens, using typical carbonate rock parameters of $m_i = 10$, s=1, a=0.5:

$$q = 0.5\, q_u (10\frac{\sigma_3}{q_u} + 1)^{0.5} \quad (6\text{-}13)$$

$$p = q + \sigma_3 = 0.5\, q_u (10\frac{\sigma_3}{q_u} + 1)^{0.5} + \sigma_3 \quad (6\text{-}14)$$

Similar to the Hoek-Brown criterion, Johnston (1985) developed the following criterion that did not include a recommended range for the rock mass parameter, s, but only that for intact rock, s = 1:

$$\sigma_1 = q_u \left(\frac{M}{B}\frac{\sigma_3}{q_u} + s\right)^B \quad (6\text{-}15)$$

$$B = (1\text{-}0.0172\log^2 q_u) \quad (6\text{-}16)$$

$$M = (2.065\text{+}0.170\log^2 q_u) \text{ for limestone} \quad (6\text{-}17)$$

These criteria, as stated, are suitable for rocks with brittle rupture failure behavior. Numerous authors have studied the transitions from brittle to ductile flow, characterized as compactive cataclastic flow. These studies generally provide important physical insights into earthquake-related rock mechanics and tectonic processes in relation to faulting (Mogi 1966; Wong et al. 1997). Schwartz (1964) studied four different rocks with void ratio, e, from 0.02 to 0.24, or porosities, n, from 3% to 20%. For the "porous" Indiana limestone with n = 20%, the results indicated that the stress-strain response transitioned from brittle to ductile at a confining pressure exceeding 34 MPa (5 ksi) and when the stress ratio of σ_d/σ_3 reduced to approximately 3.0 or below. Mogi (1967) evaluated the transition from brittle to ductile in 45 different rocks with porosities from 0% to 21.6% and found that the average transition is defined by $\sigma_d/\sigma_3 = 3.4$. It is noted that Mogi (1967) grouped rocks with porosities above 10% as "highly porous". The confining pressure in the Mogi (1967) study typically ranged between 30 MPa and 300 MPa (4.3 to 43 ksi) when the rocks changed from brittle to ductile flow. Elliott and Brown (1985) and Wong et al. (1997) studied other "highly porous" rocks, where the porosities exceeded 18%. Both studies showed that the rock responses changed from brittle faulting to compactive cataclastic flow at or above confining pressures of 10 MPa (1.5 ksi). In terms of unconfined compression strength, q_u, the original Hoek

and Brown (1980) study consisted of 923 data points, with the majority of q_u exceeding 100 MPa (14.5 ksi), and the remaining minority exceeding 40 MPa (5.8 ksi). The q_u = 23 MPa (3.3 ksi) for the Bath oolitic limestone in Elliott and Brown (1985) study was among the lowest unconfined compression strengths in the above studies. These rock properties are characterized in Figure 6-2.

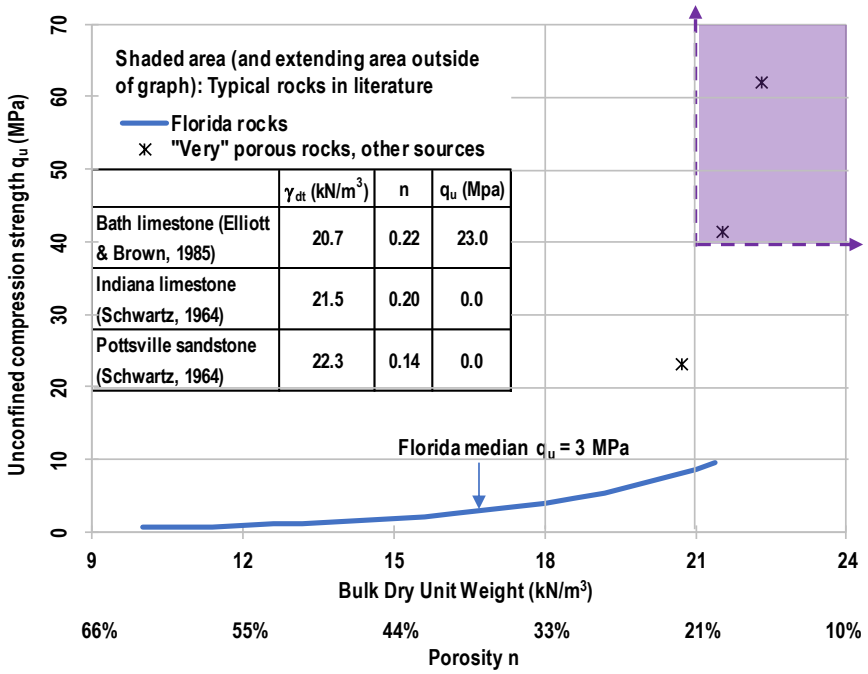

	γ_{dt} (kN/m^3)	n	q_u (Mpa)
Bath limestone (Elliott & Brown, 1985)	20.7	0.22	23.0
Indiana limestone (Schwartz, 1964)	21.5	0.20	0.0
Pottsville sandstone (Schwartz, 1964)	22.3	0.14	0.0

Figure 6-2. Rock unconfined compression strength, bulk dry unit weight, and porosity

Considering the aforementioned results in the literature, it is logical to adopt the Hoek and Brown criterion for the evaluation of shallow foundation (spread footing) bearing capacities as most rocks would be expected to be in the brittle zone. That is: (i) the overburden lateral stress within the spread footing influence zone only ranges from 0 to 0.2 MPa (0 to 30 psi); (ii) due to the expected foundation load and spread footing size, the vertical stress under a spread footing is typically 0.2 to below 5 MPa (30 to 725 psi). To give some perspectives: (i) the 169-m (555-ft) Washington Monument had a shallow foundation loading stress of approximately 0.5 MPa (70 psi)

(Briaud et al. 2009), (ii) The 110-story World Trade Center Towers 1 and 2 were not on shallow foundations; however, based on the dead weight of 4,900 MN (500,000 tons) and a foot print of 4,100 m^2 (44,000 ft^2), (Eagar and Musso 2001), the dead-weight pressure would be 1.2 MPa (170 psi). All of these values are well below the threshold range between 10 and 300 MPa (1.4 to 43 ksi) determined in the previous studies for rocks to start changing to ductile flow. Adopting the Hoek-Brown criterion can also be justified by using the ductile threshold of $\sigma_d/\sigma_3 \approx 3$, which was found in the above studies. With the low confinement under spread footings, σ_d/σ_3 ratio would overwhelmingly exceed 10 for typical rocks with strength exceeding 20 MPa (2.9 ksi), which means the rocks are would be expected to be in the brittle zone. Consequently, Carter and Kulhawy (1988) utilized the Hoek-Brown criterion in recommending Eq. 6-18 to evaluate the ultimate bearing capacity (p_u) of shallow foundation on rock, which is cited in Transportation Research Board (TRB) Report 651 (Paikowsky et al 2010).

$$p_u = \left[\sqrt{s} + \sqrt{m\sqrt{s} + s}\right] q_u \tag{6-18}$$

The Carter and Kulhawy (1988) method is the only semi-empirical bearing capacity evaluation method for rocks that is referenced in the current FHWA publication for shallow foundations (Kimmerling 2002), as well as in the current AASHTO LRFD Bridge Design Specification (AASHTO 2017).

As the ductile stress-strain behavior, or the compactive cataclastic flow, would typically never occur under minimal confining pressure (shallow foundation bearing capacity scenario), this ductile regime has never been explored under low confining pressure for rocks.

In contrast, Florida carbonate rocks are generally much weaker as a result of their recent deposition in the Florida peninsula and their porous nature. Based on more than eight thousand

data points from 1990 to 2017 in data set #1 (Chapter 5), the median q_u value is 3 MPa (435 psi) and the median porosity is 37%. The cementation of Florida rocks is apparently significantly lower than carbonate rocks reported in other regions. For example, at a same porosity of n = 20% to 21%, the Bath limestone and Indiana limestone are anticipated to have q_u value three times higher than those for Florida limestone (Figure 6-2). Given this difference, it is critical to explore the ductile zone behavior regarding lower confining pressures and corresponding strength parameters suitable for Florida carbonate rocks. In this chapter, 223 triaxial tests on Florida rock were performed using a unique method to measure the volumetric behaviors of the porous specimens. These results expand the knowledge on the σ_d/σ_3 threshold for ductile response under low confinement pressures, which are applicable for shallow foundation application in soft rocks and IGM. Finally, the method leads to the development of rock strength envelopes for many of the Florida rock formations that may be used for shallow foundation design.

6.2 Triaxial System for Rock Testing

Directly under a spread footing, the lateral stress may be 50% of the applied vertical stress; whereas, at the edge of the footing, it could be greater than the vertical stress at the center (i.e., extension loading). To capture these loading scenarios, a triaxial testing device is required, which is capable of testing material under different confining pressures. Typical soil triaxial cells have maximum confining pressures (lateral stress) of approximately 0.9 MPa (130 psi) or less and employ air and water for confinement. The rock triaxial device must be capable of testing in both compression and extension (higher lateral vs. vertical stress). Also, the device must be capable of strain control loading for measuring strain softening (i.e., loss of strength), as well as measuring volumetric behavior.

The triaxial system used for this study to test Florida limestone was designed to satisfy the above objectives. The system is modular and consists of (1) a 180-kN (40,000-lb) capacity strain-controlled Sigma-1 load frame by GEOTAC, (2) GEOTAC Sigma-1 CU SI software and instrumentation for controlling the load frame strain rate and sample monitoring (load, deformation, cell pressure, etc.), (3) a Hoek cell by RocTest with cell pressure rated for 69 MPa (10,000 psi), and (4) a volume change measurement device.

The modular system offers the greatest flexibility of testing any material (soil and rock). For instance, under lower cell pressures, the Hoek cell may be replaced with a standard soil triaxial cell for testing soil and intermediate geomaterials (IGM). A discussion of each component as well as their integration into the test system, is presented in the next section.

6.3 Triaxial Hoek cell

The Hoek-cell, made of hardened stainless steel, was acquired from RocTest, Ltd. of Industry, Pennsylvania. The parts and dimensions of the Hoek cell used for this study are shown in Figure 6-4 and Figure 6-5. The Hoek cell system consists of:

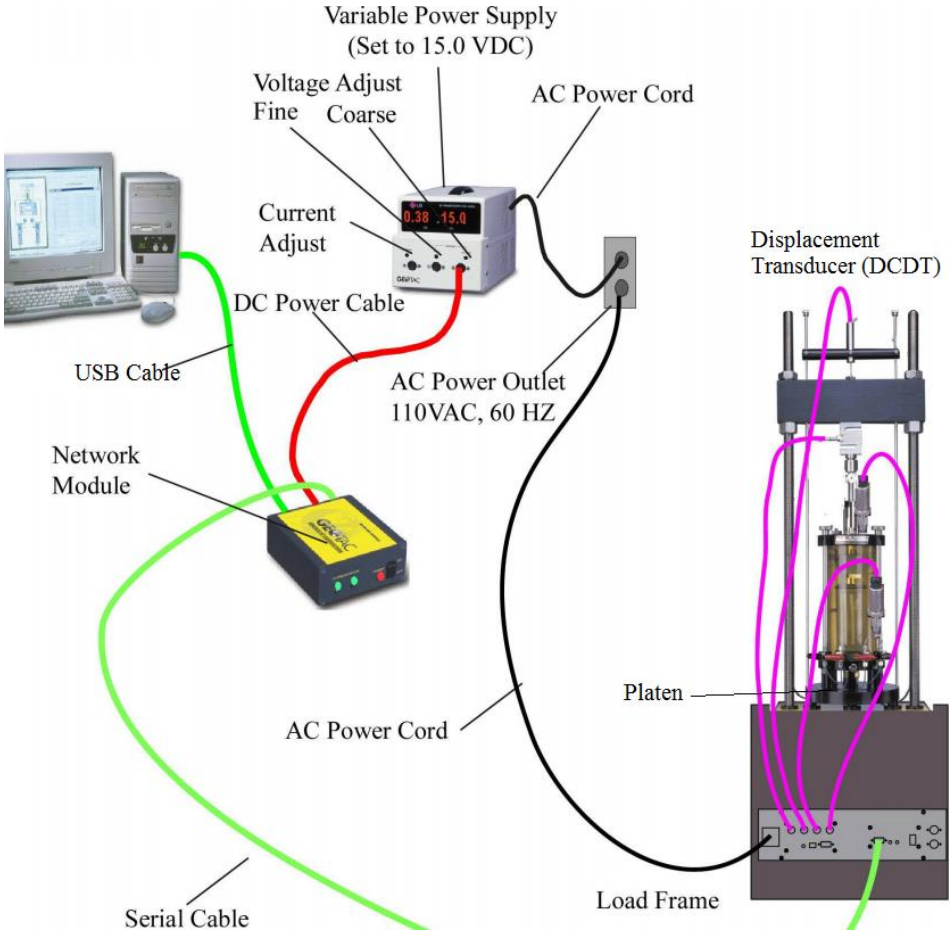

Figure 6-3. Triaxial modular setup

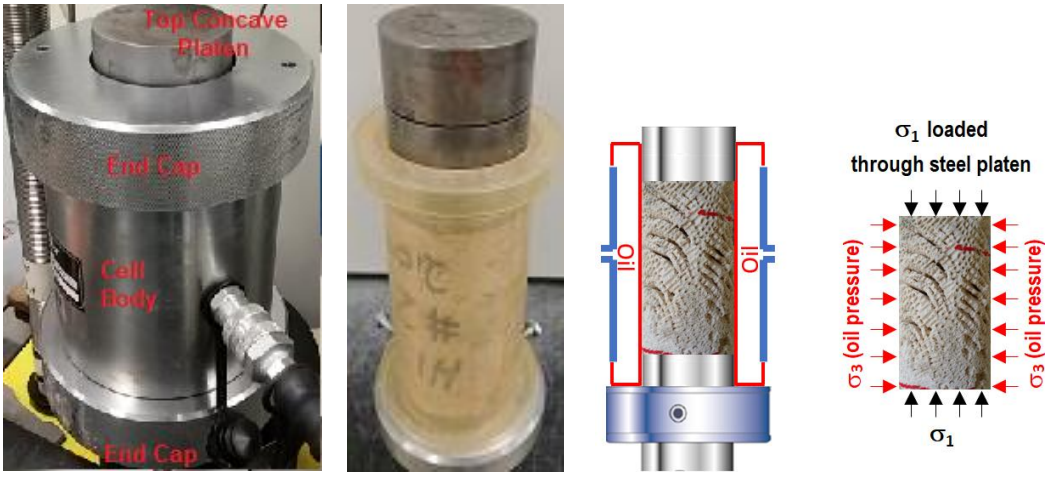

Figure 6-4. Schematic of Hoek triaxial cell test

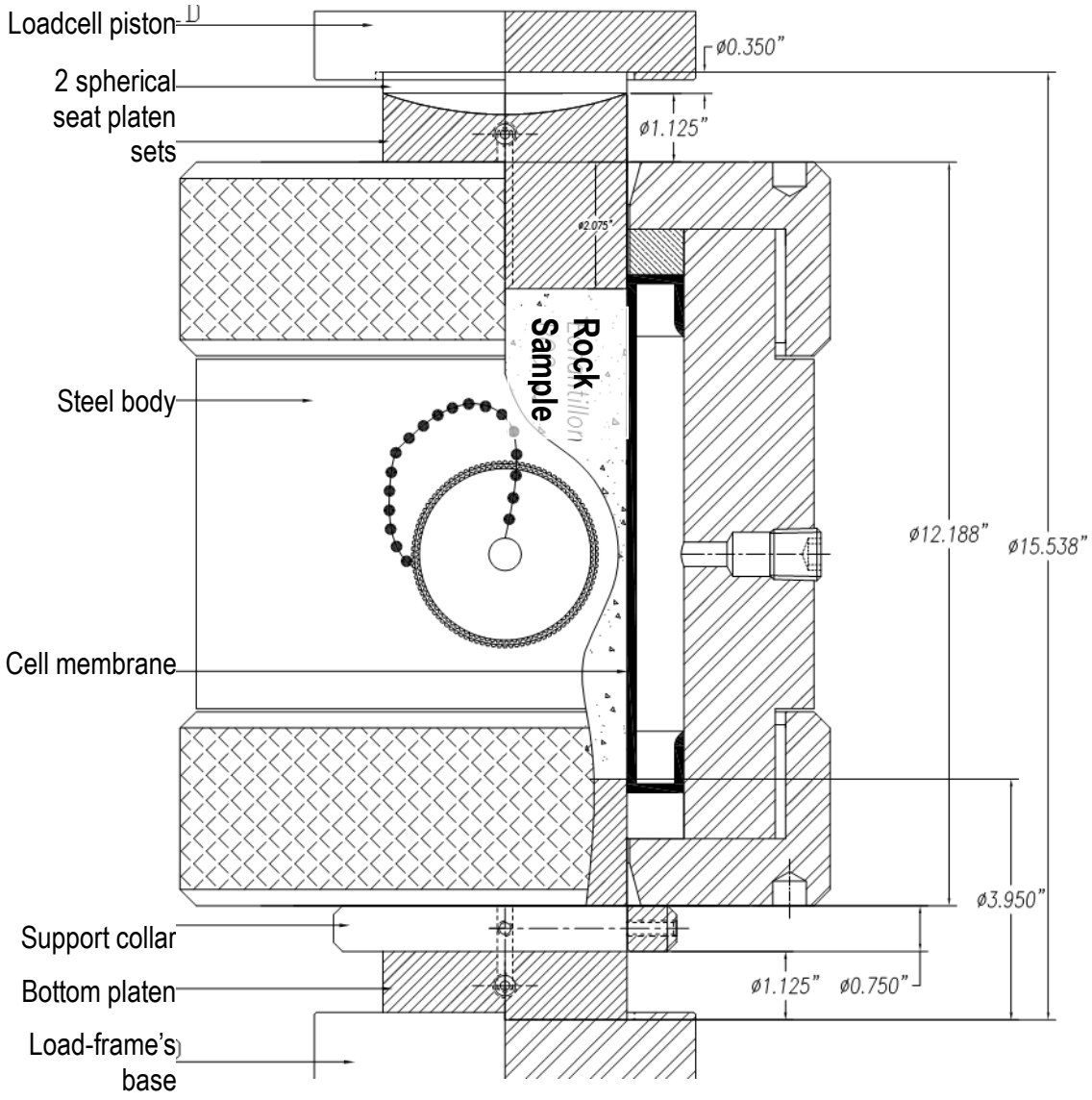

Figure 6-5. Hoek cell design

1. One main steel cylindrical body with end caps (Figure 6-4) that screw onto the body. The manufacturer recommends white grease on the cap's thread (Lubriplate white lubricant l0034, Dow Corning Molykote 33 light grease, or Kleen-Flo #907);

2. One set of steel platens (top and bottom), which include a set of concave and convex end platens (to center the load); and

3. One specimen membrane made of Adiprene urethane, capable of withstanding 69-MPa (10,000-psi) hydraulic cell pressure.

Once the central section of the cell is attached to the bottom end cap (Figure 6-5), the urethane membrane is placed within the cell (greased top and bottom) and the top end cap is screwed onto the central section. Next, two quick-release self-sealing Simplex hydraulic couplings are screwed onto the cell to provide circulation of the hydraulic fluid and for the coupling of a pressure transducer. This device allows the hydraulic fluid to stay, without the need to drain it nor dismantling of the cell between tests of different specimens. Dismantling of the cell is only needed to replace the worn out or damaged membrane, which typically lasts for about 20 to 30 triaxial tests. Figure 6-6 shows the hydraulic fluid filling the annulus between the outer cell steel wall and the urethane membrane. Finally, the operator inserts the specimen into the cell and place the top platen with the spherical seats. The spherical seats are provided so that the rock core ends do not need to be parallel (they only need to be flat), and the spherical seats, without lubricant, will help minimize bending to the specimen.

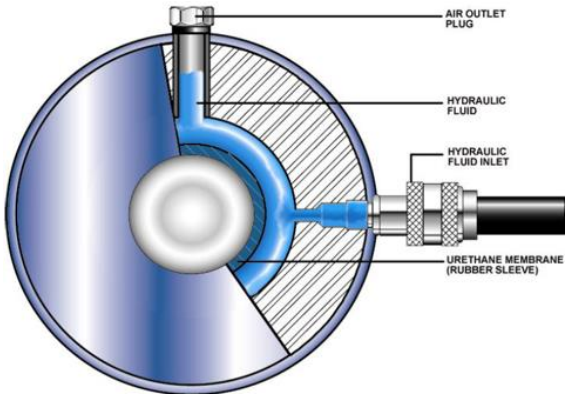

Figure 6-6. Hoek cell hydraulic fluid filling

It is noted that the cell pressure in a Hoek cell is only acting on the membrane surrounding the specimen, but not the top and bottom of the specimen. Therefore, during the initial pumping of the oil to reach the target confining pressure in the isotropic loading phase, the axial load should

also be gradually applied to maintain initial vertical stress σ_1 equal to the confining pressure σ_3. The procedure to perform a rock triaxial test is presented in Appendix C.

6.4 Displacement or Strain Measurements

To measure the vertical displacement of the rock specimen during shear, a direct current displacement transducer (DCDT) is attached to the top of the Hoek cell assembly. Hoek and Franklin (1968) recommended lateral strains to be measured via strain gauges, which are typically glued to the surface of the rock specimens. However, due to the vugs and large amount of shells in Florida carbonate rocks, it is typically infeasible to attach strain gauges to the rock surface, such as the specimen in Figure 6-4 or other specimens previously presented in Chapter 4. To overcome this challenge, a method to capture the hydraulic oil movement inward or outward of the closed system was implemented. In Figure 6-7, the volume measurement device is simply an inactive piston, moving in or out depending on the oil flow direction. The piston is attached to a linear variable displacement transducer (LVDT), and the linear movement is correlated to the oil volume (ΔV). Also shown in this figure, a dry inert gas accumulator is used to stabilize the oil pressure (i.e. confining pressure) at the prescribed pressure, σ_3. Later in the study, the volume measurement mechanism was improved to the configuration shown in Figure 6-8, where a custom made Digiflow pump was used. The Digiflow pump is an active piston, where upon any change in oil pressure, a signal is sent to the piston to run in or out to get the pressure back to the target pressure. Similarly, the piston displacement is correlated to the volume change (ΔV) of the supplied hydraulic oil. The lateral strain and volumetric strain are as follows:

$$\varepsilon_L = \Delta R/R = \frac{\Delta V}{A_{surface}} / R = \frac{\Delta V}{2\pi H R^2} \quad (6\text{-}19)$$

$$\varepsilon_v = \varepsilon + \varepsilon_L + \varepsilon_H = \varepsilon + 2\varepsilon_L \quad (6\text{-}20)$$

where,

R, ΔR, and H: dimensions as shown in Figure 6-9.

ΔV: oil volume change.

$A_{surface}$: Surface area of specimen.

ε, ε_L, ε_H, ε_V: axial, lateral, horizontal, and volumetric strains during triaxial shearing test, respectively.

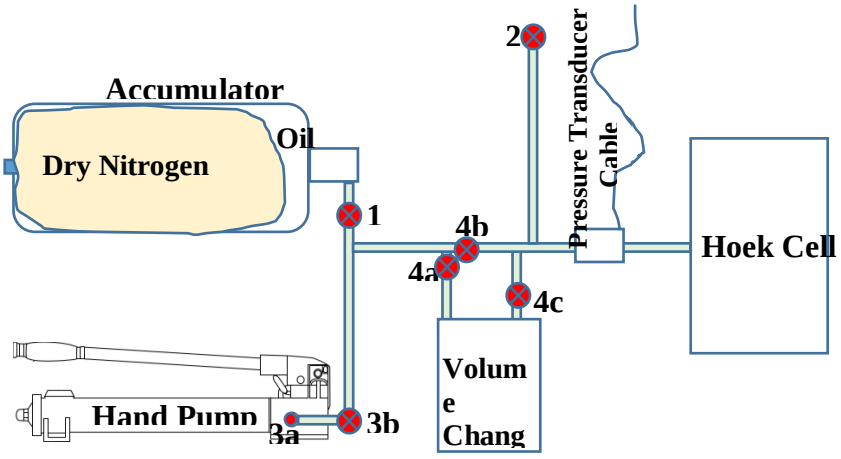

Figure 6-7. Triaxial system with accumulator and volume change device

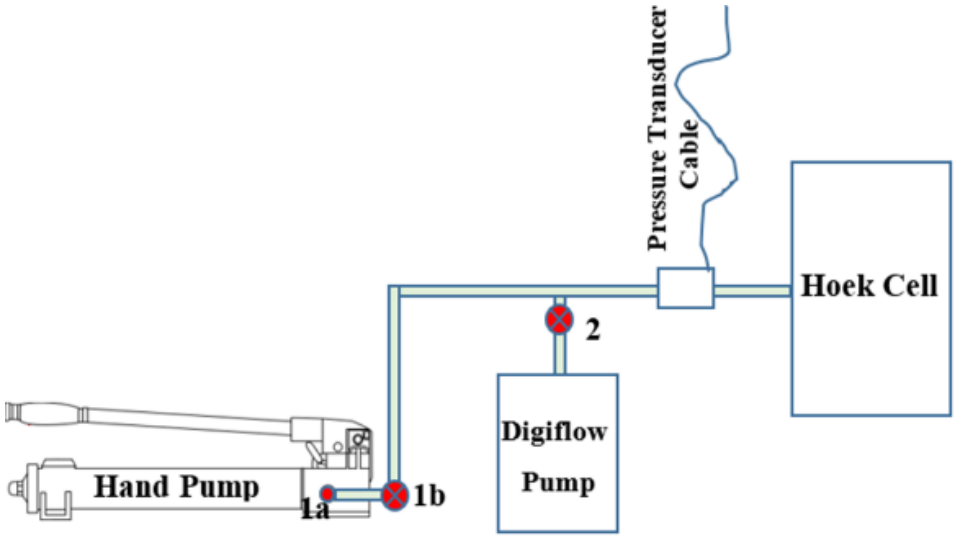

Figure 6-8. Triaxial system with Digiflow pump

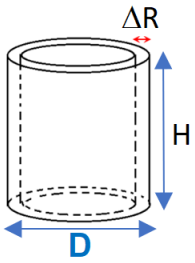

Figure 6-9. Volume change with membrane displacement

6.5 Range of Triaxial Confining Pressures

Due to the limited depth of a shallow foundation, the initial confining stress is minimal. However, as the major principal stress (σ_1) increases under the foundation loading, the confining stress (σ_3) increases as well. In Zone 1 (outside of the footing) in Figure 6-10.a, at ground surface (i.e., depth = 0), $\sigma_{3\_zone\ 1} = \sigma_v = 0$ and $\sigma_{1\_zone\ 1} = q_u\, s^a$ using the simple approximation by Carter and Kulhawy (1988). Using the median undrained shear strength value for Florida rock and IGM of q_u = 3 MPa (435 psi) and typical s = 0.3 to 0.8, then $\sigma_{1\_zone\ 1}$ = 1.6 to 2.8 MPa (230 to 400 psi). The q_u value for Florida material frequently attains 9 MPa (1,300 psi), and it is not uncommon for certain formations to exceed that value. In this case, $\sigma_{1\_zone\ 1}$ can exceed 5 MPa (700 psi), potentially reaching 10 to 20 MPa (1,500 to 3,000 psi).

In Zone 2 (underneath the footing), the confining pressure, $\sigma_{3\_zone\ 2}$, in equilibrium will be equal to $\sigma_{1\_zone\ 1}$. The confining pressure under a footing starts at a minimal value, such as 0.0 to 0.2 MPa depending on the rock's depth. However, as foundation loading increases, the stress-path induced confining pressure can eventually reach 2.0 to 6.9 MPa (300 to 1,000 psi), and could exceed those values, either during extreme event conditions or due to concentrated contact pressures that are higher than the average pressure (as in the diagram depicted in Figure 6-10.b) or both.

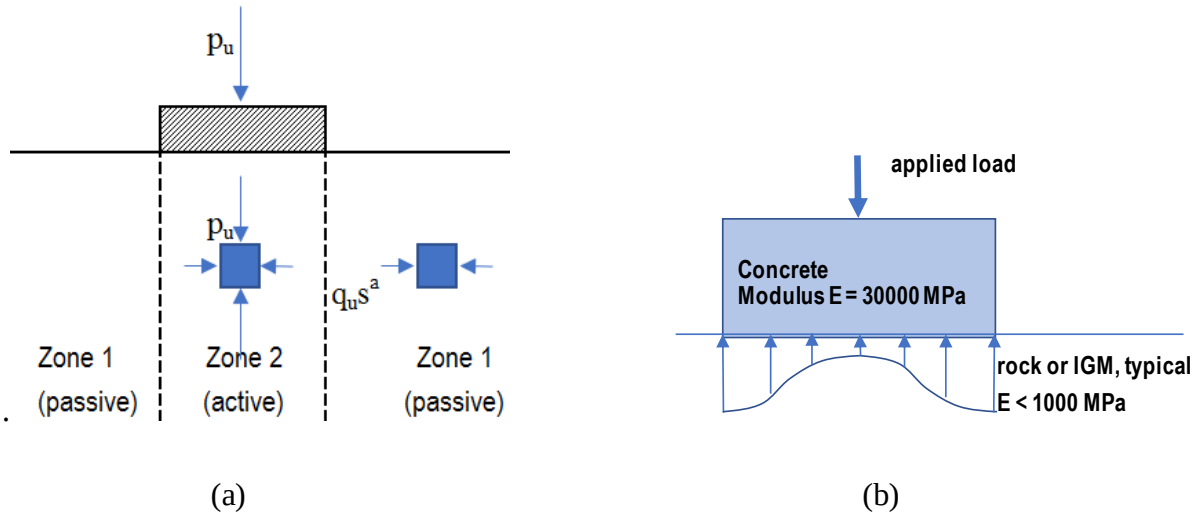

(a) (b)

Figure 6-10. Pressure under a footing: (a) Active and passive zones (Adapted from Carter and Kulhawy, 1988); (b) Possible contact stresses

The above discussion can also be illustrated using the stress paths in Figure 6-11. In a triaxial test, the σ_3 is maintained to be constant. However, σ_3 under a footing will keep increasing along with the applied load (σ_1). As such, depending on Finite Element Method (FEM) simulation, the possible stress path under a footing could be such as the dashed line example in Figure 6-11. The final confining pressure for this dashed line example would be 4 MPa (580 psi), despite having a minimal starting confining pressure. Therefore, a majority of the triaxial tests were performed at a chamber pressure at or less than 6.9 MPa (1,000 psi), and a small portion of the triaxial tests were performed at a chamber pressure up to 20.7 MPa (3,000 psi).

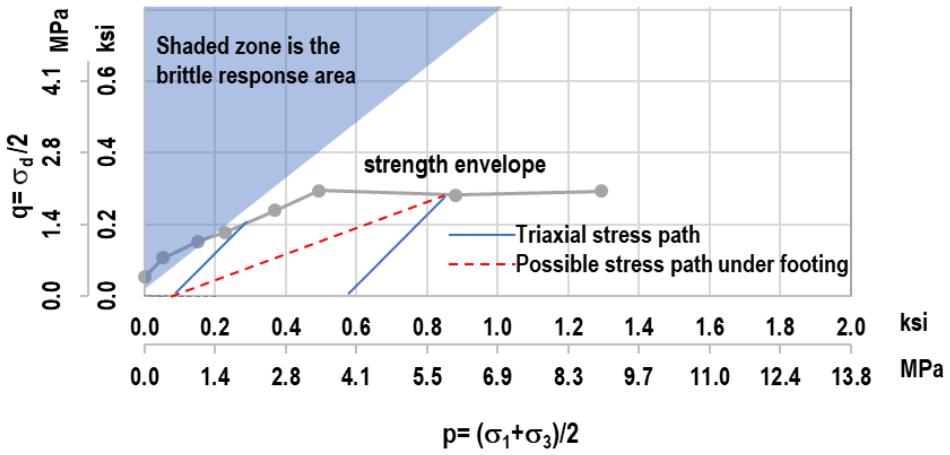

Figure 6-11. Stress paths and strength envelope

6.6 Triaxial Stress-Strain and Volumetric Responses of Florida Carbonate rocks

In this study, the rock specimens were cored at 7 different sites across the state of Florida. The encountered Florida rock formations are: Key Largo, Miami, Anastasia, Hawthorn, and Ft. Thompson. Triaxial tests were performed using confining pressures ranging from 0.35 to 20.7 MPa (50 to 3,000 psi), which covers the expected shallow foundation range of stresses, which is less than the typical threshold of 20 to 300 MPa (3,000 to 43,000 psi) for the response to change from brittle to ductile for rocks found in literature. Pictures of rock specimens after triaxial testing are presented in Appendix D and representative individual triaxial test results are presented in Appendix E. Typical normalized deviatoric stress (σ_d /σ_3) versus vertical strain, ε, plots of the triaxial results are shown in Figure 6-12, where $\sigma_d = \sigma_1 - \sigma_3$ is the deviatoric stress. It was found that a few Florida carbonate rocks have a brittle rupture failure (Figure 6-12.a), with a sharp rise in stress versus strain, then a sudden drop in deviatoric stress at failure. A large number of the specimens have ductile responses (Figure 6-12.b), where the stress is rising gradually with strain, and there is no sudden drop in deviatoric stress at failure. Shown in Figure 6-13 are the stress-

strain responses from 223 triaxial specimens obtained from different Florida formations using the triaxial testing. A summary of the findings are as follows:

1. The red curves represent triaxial results for low confining pressure of σ_3 = 0.35 MPa (50 psi). It was discovered that:

    1) 30% of the specimens had brittle rupture failures, and they experienced moderate to large volumetric dilation. The latter specimens were all dense rocks, with bulk dry unit weight (γ_{dt}) typically exceeding 20 kN/m^3 (127 pcf), associating with high rock strengths. Note, the bulk dry unit weight is the ratio between the dry weight of specimen and its cylindrical core volume.

    2) 42% of the specimens experienced ductile failures, and it was found that ductile stress-strain behavior would be indicative of contractive volumetric responses. Also, some of the specimens' behavior would be described as "transition" (Figure 6-13.b), where there is a sharp rise in stress in the first part of the curve, but in the subsequent parts, the deviatoric stress only drops to 0% to 20% of the peak load.

2. In the case of higher confining pressure, σ_3 = 0.9 MPa (130 psi, black curves), more (76%) specimens experienced ductile behavior. As the confining pressures exceeded 4.1 MPa (600 psi, purple and orange curves), almost no specimen experienced brittle rupture failure. Even in the unconfined pressure condition, the Chapter 5 results indicated that the very porous Florida rocks exhibit transition and ductile behavior when the unconfined strength q_u is approximately less than 5 MPa (725 psi), i.e., σ_d/σ_3 = 50, using atmospheric pressure of σ_3 = 0.1 MPa.

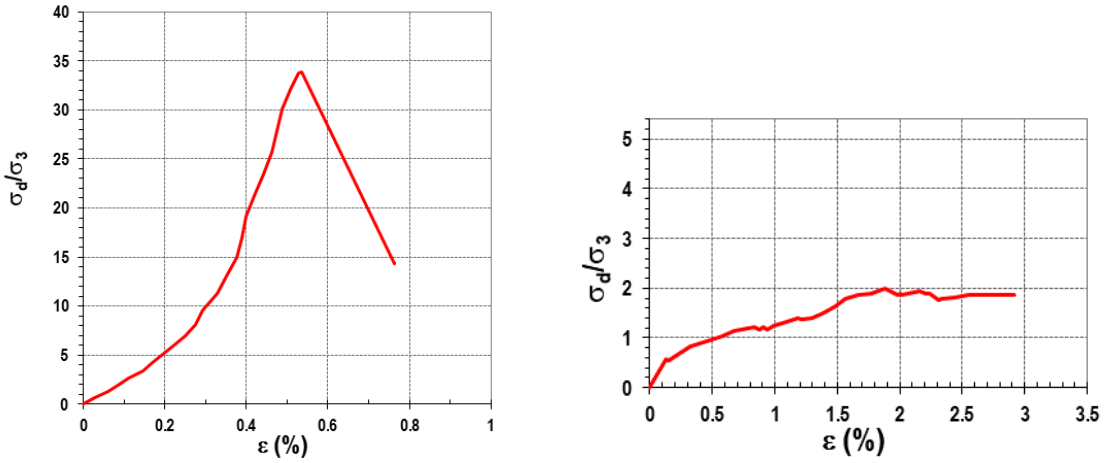

(a) (b)

Figure 6-12. Examples of triaxial results−Key Largo formation: (a) γ_{dt} = 18.9 kN/m^3 = 120 pcf, σ_3 = 345 kPa = 50 psi; (b) γ_{dt} = 15.7 kN/m^3 = 100 pcf, σ_3 = 3,100 kPa = 450 psi

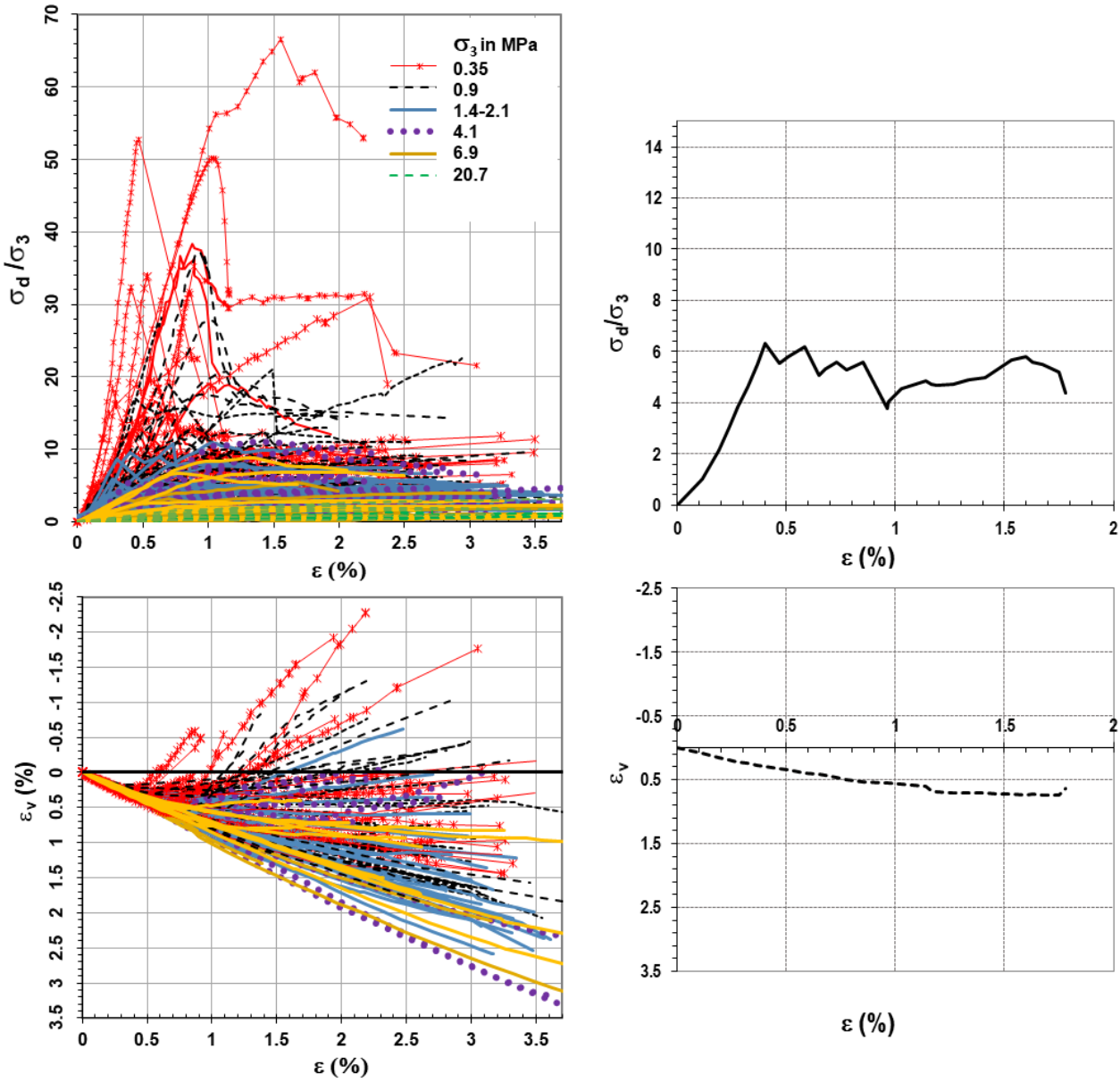

(a) (b)

Figure 6-13. Normalized deviatoric stress and volumetric strain: (a) Combination plots of multiple specimens; (b) Example of "transition" behavior

The above observations are summarized in Tables 6-2 and 6-3, where ductile/ brittle responses are categorized per confining pressure ranges and σ_d / σ_3 ratios or rock porosities. Table 6-2 supplements the σ_d / σ_3 thresholds to cover all ranges of confining pressures, and not just at high pressures (i.e., at or above 20 MPa, or 3,000 psi) as was previously studied. For example, a weak

rock with $\sigma_d / \sigma_3 = 10$ at $\sigma_3 = 0.3$ would be in the ductile flow zone per Table 6-2. However, if the existing threshold ratio of 3 were to be used, it would mistakenly be categorized as brittle. It is noted that depending on carbonate content, mineral structure, and rock grain size, some rock specimens would behave more or less ductile than the indicated ranges in Table 6-3.

Table 6-2. Approximate behavior type table of Florida carbonate rocks based on σ_d/σ_3 ratio

σ_3 (MPa)	σ_3 (psi)	σ_d/σ_3 for transitional response	σ_d/σ_3 for ductile response
0.1	15	50	20
0.3	50	17	10
0.9	130	10	7
1.4	200	9	6
2.1	300	8	5.5
4.1	600	7	5
6.9	1,000	6.5	4.5
20.7	3,000	*	3
**	**	**	**

Note: * Florida carbonate rock specimens tested at $\sigma_3 = 20.7$ MPa all had $\sigma_d/\sigma_3 \leq 3$

** For $\sigma_3 > 20$ MPa, the transitional and ductile thresholds of $\sigma_d/\sigma_3 \approx 3$, as in Schwartz (1964) and Mogi (1967) could be applicable.

Table 6-3. Approximate behavior type table of Florida carbonate rocks

		Bulk Dry Unit Weight Range (pcf)					
σ_3 (MPa)	σ_3 (psi)	60-65	66-85	86-110	111-120	121-130	130-135
0.1	15	Transition	Transition	Brittle	Brittle	Brittle	Brittle
0.3	50	Ductile	Transition	Transition	Brittle	Brittle	Brittle
0.9	130	Ductile	Ductile	Transition	Transition	Brittle	Brittle
1.4	200	Ductile	Ductile	Ductile	Transition	Transition	Brittle
2.1	300	Ductile	Ductile	Ductile	Ductile	Transition	Transition
4.1-6.9	600-1,000	Ductile	Ductile	Ductile	Ductile	Ductile	Transition
6.9-20.7	1,000-3,000	Ductile	Ductile	Ductile	Ductile	Ductile	Ductile

One of the phenomena of the triaxial response when testing porous carbonate rocks is the crushing or breaking of the rock's cemented grain structure, leading to structural rearrangement

with appreciable porosity reduction, as indicated by the contractive volumetric strains in Figure 6-12.b. When the rocks have very high porosity (low bulk dry unit weight), under high isotropic stress, the rock grain cementation breaks and subsequently crushes due to the extent and size of the void structure. Consider the case of Figure 6-14.a, the deviatoric stress is $\sigma_d = 0$, i.e. the sample is subject to an isotropic stress state. As confining pressure is increased, several drops in stress are observed at vertical strains of 1.1%, 1.4%, and 1.7%, which are due to crushing of some cementation structure. At these points, the strain-rate controlled loading frame and the hydraulic oil could not initially maintain the confining stress during the crushing but recovered when the crushing stopped. However, as the confining pressure increased, the crushing resumed and collapse ensued.

In the case of medium isotropic stress states, the sample will still exhibit shearing resistance. That is, the rock structure may crush, forming granular assemblages within the sample, and they will exhibit friction between granular particles as well as cementation within the non-crushed zones. For example, consider Figure 6-14.b which shows isotropic loading followed by deviatoric (shear) loading. Under isotropic loading, crushing is observed at strains of 1.1%, 1.4%, and 1.7%. Subsequently for the triaxial shearing phase, the sample carried an increasing deviatoric stress and observed further crushing and shear failures at axial strains of 2.7% and 3.5%.

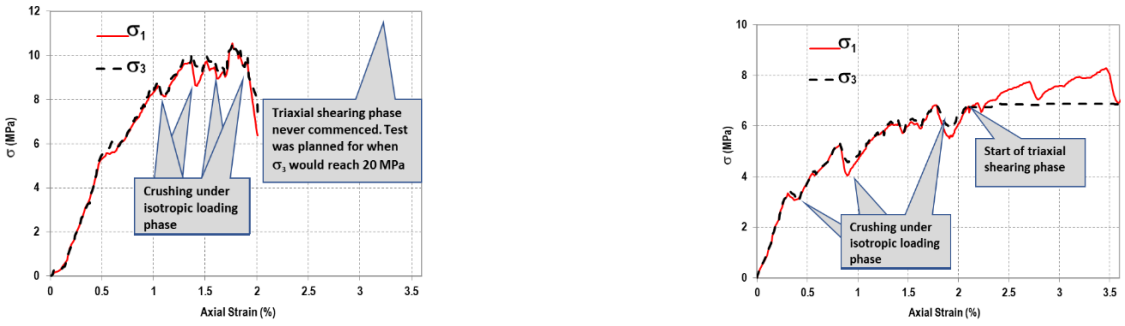

(a) (b)

Figure 6-14. Crushing of porous rocks: (a) isotropic loading; (b) isotropic then deviatoric loadings

It should be noted that porous Florida carbonate rocks generally do not experience natural crushing under their own overburden pressure due to their limited depths and due to the recent rock deposition (i.e., pre-consolidation pressure is about the same order of magnitude as the current overburden pressure). The formations investigated in this research are typically encountered at depths of 1 to 10 m (3 to 30 ft), thus the overburden pressure is less than 0.2 MPa (30 psi). The very porous Florida rock formations likely experience breaking of cemented grain structure and a collapse of some void structure under high isotropic or deviatoric stress applications. This phenomenon may result in a downward curvature of the strength envelopes as function of dry unit weight or porosity (Section 6.8).

The crushing phenomena, especially at confining pressures of 0.1 to 4.1 MPa (10 to 600 psi), is less frequently encountered in rocks cited in literature due to their low porosities; thus, the perception of "porous" rock is very different from that of Florida rock. For instance, Fereidooni and Khajevand (2018) indicated travertine samples with n=7% were porous; Schwartz (1964) considered the Pottsville sandstone and Indiana limestone as porous rocks, with porosities of n = 14% to 20%, respectively. Gowd and Rummel (1980) considered n = 15% as porous. In Mogi (1966), rocks with n = 1% to 10% were grouped as porous, and n > 10% as very porous, with a highest porosity cited as n = 21.6%. In comparison, 90% of Florida carbonate rocks have porosities greater than 20% and only 10% of Florida carbonate rocks have porosities between 5% and 20% (Chapter 4). In general, the rocks that are typically considered porous in literature are considered "dense" and "outlier" data for Florida.

6.7 Extension Test Results

In a conventional compression triaxial test, the cell pressure (σ_3) is applied, and then the vertical stress (σ_1), is increased to failure. In the case of extension loading, the isotropic pressure is applied initially as in the above case. However, while the vertical stress is maintained constant, the cell pressure is increased to induce shearing. For the shearing phase, the cell pressure is the major principal stress, σ_1, and the constant vertical stress is now the minor principal stress, σ_3.

For the extension test results at vertical stress of $\sigma_3 = 0$, the failure value of σ_1 is called q_e. The q_e value is generally at least the same or higher than the unconfined compression strength (q_u) trendlines (shown in Figure 6-15).

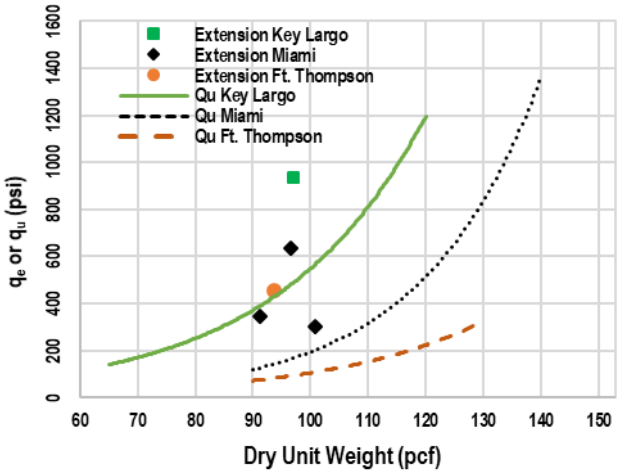

Figure 6-15. Unconfined compression test and extension test results

Similarly, for extension tests at higher vertical stress (such as σ_3 = 0.35 MPa = 130 psi), the failure normalized stress (σ_d/σ_3) is approximately the same or slightly higher than, the compression test normalized results (as shown in Figure 6-16.a).

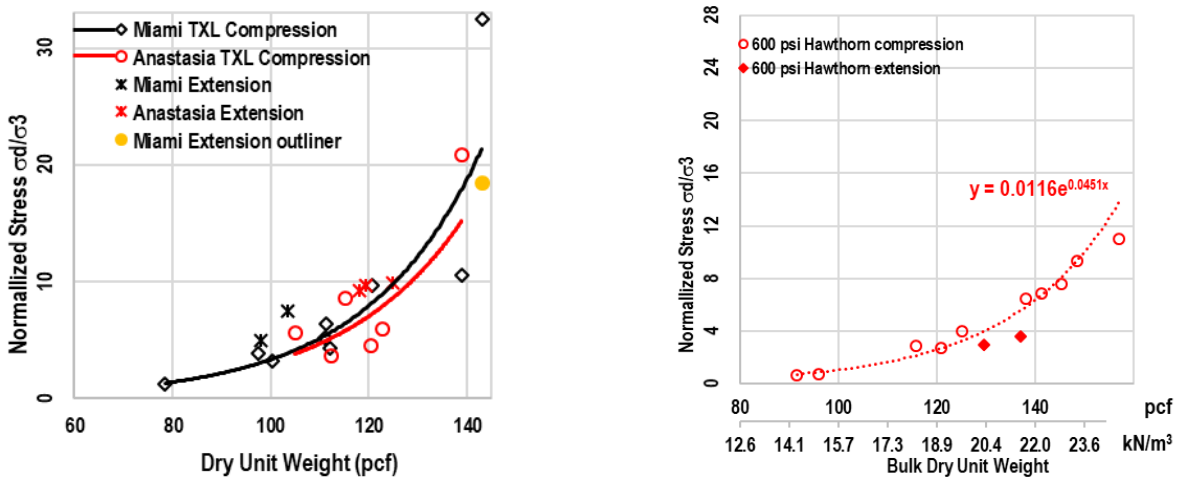

(a) (b)

Figure 6-16. Triaxial compression test and extension test results: (a) σ_3 = 130 psi; (b) σ_3 = 600 psi

There are outlier points where the extension test results have lower normalized stress ratios (σ_d/σ_3) than those from the compression triaxial tests, listed below:

- The orange dot in Figure 6-16.a for a Miami specimen: the specimen had a large vug (hole) within the specimen (Figure 6-18.a). As the cell pressure (σ_1) was increasing on the flexible membrane, the cell pressure failed the sample at this location, splitting the specimen and damaged the membrane without failing the hard rock above and below this location. Thus, the strength of this specimen is lower than expected. In conventional compression tests, under a constant chamber pressure of 130 psi, the membrane would survive even if there were anomalies in the specimens.
- The two solid dots in Figure 6-16.b for two Hawthorn specimens: The specimens had very soft ends (Figure 6-18.b), while the remaining sections of the specimens were harder rock. As the pressure was being increased, the membrane kept squeezing in,

thus the lateral pressure reached a limit and would not increase (Figure 6-17). These tests were stopped to prevent membrane damage.

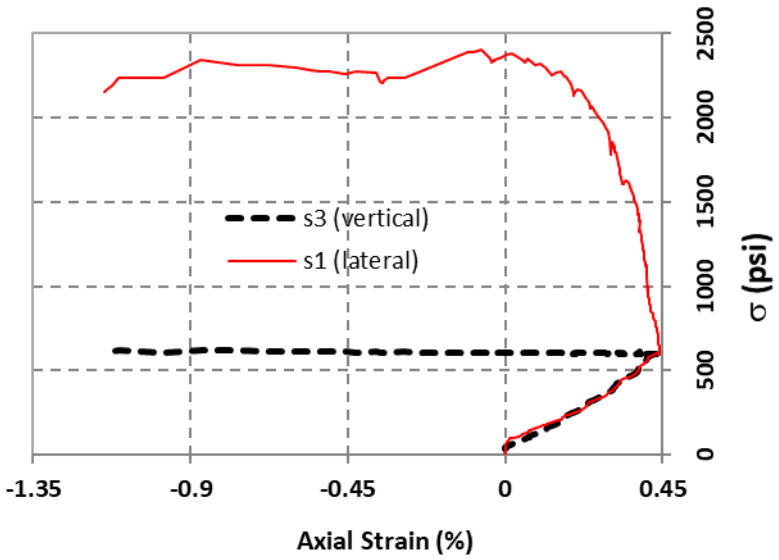

Figure 6-17. Triaxial extension test stress – strain curve for specimen 813

a) b)

Figure 6-18. Outlier extension test specimens: (a) Hole on specimen; (b) One end of specimen is much softer

If these specimens for the above cases were to be tested in a conventional compression, the very rigid loading steel platen would transfer the axial load to a wider area, instead of being

localized as in the case of the flexible membrane, which could lead to membrane puncture due to excessive displacement.

In summary, the extension test strengths and envelopes are generally expected to be at least the same as those of the compression test results. There were occasional outlier results due to nonhomogeneity of specimens and the flexibility of the membrane, which would be punctured and damaged due to the anomalies of the specimen under high pressure.

6.8 Intact-rock Strength Envelope

Obtaining a typical strength envelope requires a series of triaxial tests, tension strength tests, and unconfined compression strength tests to be performed (Figure 6-19). Ideally, all the specimens are the same or at least have similar index properties. For Florida carbonate rocks, it is difficult and sometimes impossible to find a pair of specimens that have similar index properties (i.e., same mineral components, porosities, dry weights, etc.) at the same depth. As identified in Chapter 4, within short vertical distances (cm or inches) of one another, one Florida rock specimen may have a bulk dry unit weight (γ_{dt}) of 20.5 kN/m^3 (130 pcf) and the adjoining rock specimen may have γ_{dt} of 12.5 kN/m^3 (80 pcf). Thus, pairing these two specimens is not recommended despite being at almost the same depth.

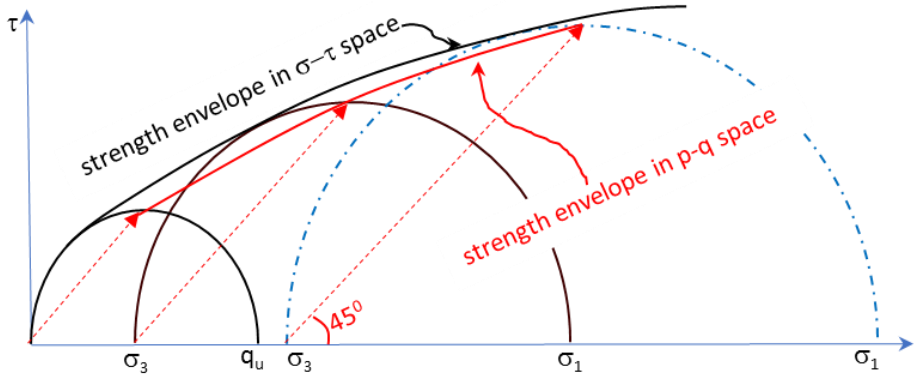

Figure 6-19. Schematic of strength envelope construction

Furthermore, assuming a pair of specimens with same index properties were to be found, the results of the triaxial tests could still exhibit scatter from the mean value (due to orientation and distribution of vugs within each specimen), yielding erroneous strength envelopes. For example, specimen A and B in Figure 6-20 (from the Key Largo Formation) both have the same carbonate content of approximately 99.5%, and the same bulk dry unit weight of approximately 12.7 kN/m^3 (81 pcf). Due to point A being lower than the mean value for the 345 kPa (50 psi) tests (blue dash line in Figure 6-20) and point B being higher than the mean value for the 900 kPa (130 psi) tests (green continuous line in Figure 6-20), the strength envelope (blue continuous line in Figure 6-21.a) would have an erroneous upward curve instead of downward curve, or at least a straight line for a Mohr-Coulomb envelope. In an opposite example, specimen C and D also in Figure 6-20 (again from the Key Largo Formation) have the same index properties. However, the paring of C and D would result in an extreme and erroneous downward curve for the resulting strength envelope (blue continuous line in Figure 6-21.b)

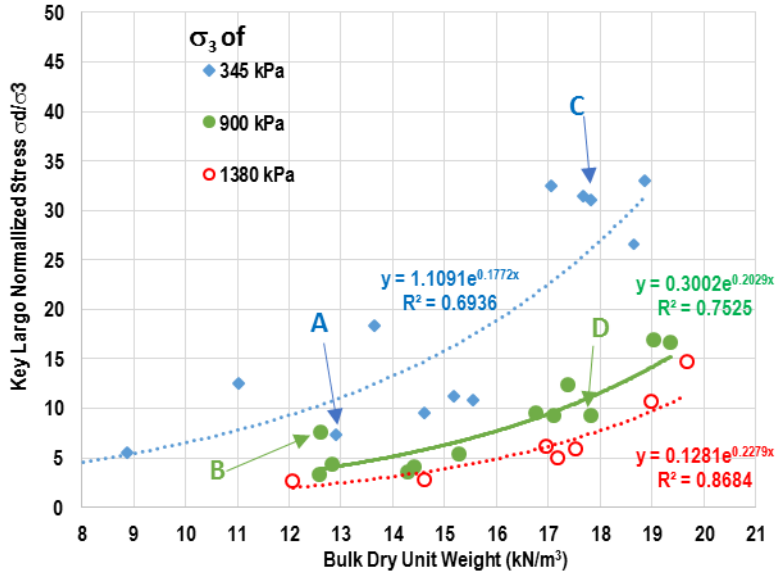

Figure 6-20. Key Largo normalized deviatoric stress results

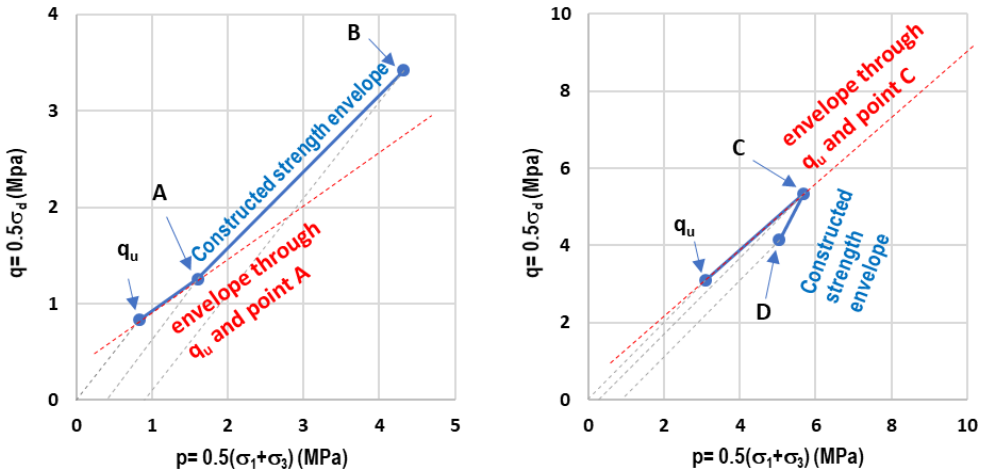

(a) (b)

Figure 6-21. Examples of incorrectly constructed strength envelopes: (a) Specimens A and B pairing; (b) Specimens C and D pairing

To resolve this issue of incompatible paring when constructing strength envelopes, the following procedures were followed:

The mean values for the normalized stress are utilized by establishing an individual correlation between the normalized stress (σ_d/σ_3) at failure along with the bulk dry unit weight (γ_{dt}) for each formation, at each level of confining pressure (e.g., Figure 6-20). As identified in Chapter 4, it is simple for practitioners to obtain bulk dry unit weight (γ_{dt}), which is directly related to porosity: $n = 1 - \gamma_{dt}/ (GS*\gamma_w)$, where GS is the sample specific gravity and γ_w is water unit weight. Therefore, instead of correlating to porosity (n), strength correlations were based on the bulk dry unit weight as the primary input parameter.

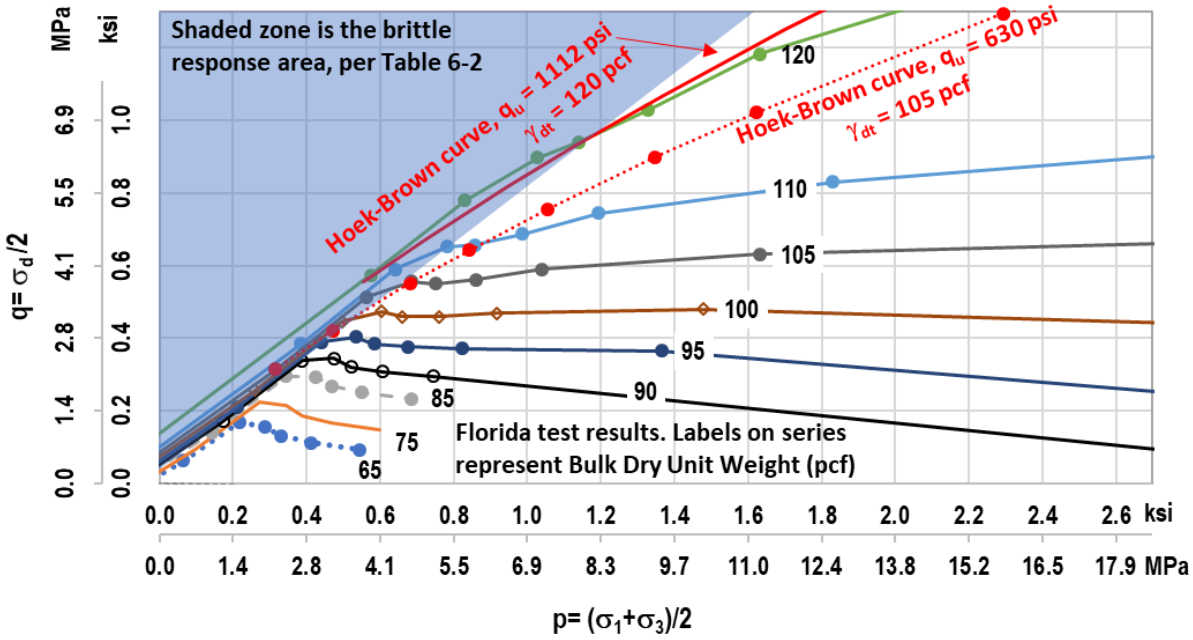

Figure 6-22. Strength envelope – Key Largo Formation

The correlations (e.g., Figure 6-20) were then used to calculate the σ_d/σ_3 at failure for each increment of dry unit weight (e.g., 5 pcf). The resulted values are presented in individual graphs for each of the formations (Figure 6-22 through Figure 6-26, with detailed descriptions presented in the subsequent discussion). Shown in Figure 6-22 are strength envelopes for the Key Largo Formation. Also shown in this figure are two curves obtained using the Hoek-Brown criterion, for comparison purposes with Florida materials. Summarizing the results in Figure 6-22:

- The red continuous Hoek-Brown curve corresponds to an unconfined compression result of q_u = 7.9 MPa = 1112 psi and bulk dry unit weight of 18.8 kN/m^3 = 120 pcf, which would be among the densest Key Largo limestones. This Hoek-Brown curve matches well with the tested results, which is expected as these very dense Key Largo limestone specimens had brittle rupture failures in the triaxial tests (Figure 6-12.a).

- The red dash Hoek-Brown curve (Figure 6-22) corresponds to an unconfined compression result of q_u = 4.3 MPa = 630 psi and bulk dry unit weight of 16.5 kN/m^3 = 105 pcf. The test result for this rock (at 105 pcf) indicates a much lower strength envelope than the Hoek-Brown one. The triaxial test results for these specimens typically show ductile behavior (Figure 6-

12.b), which explains why the Hoek-Brown criterion does not apply for the more porous Florida limestones.

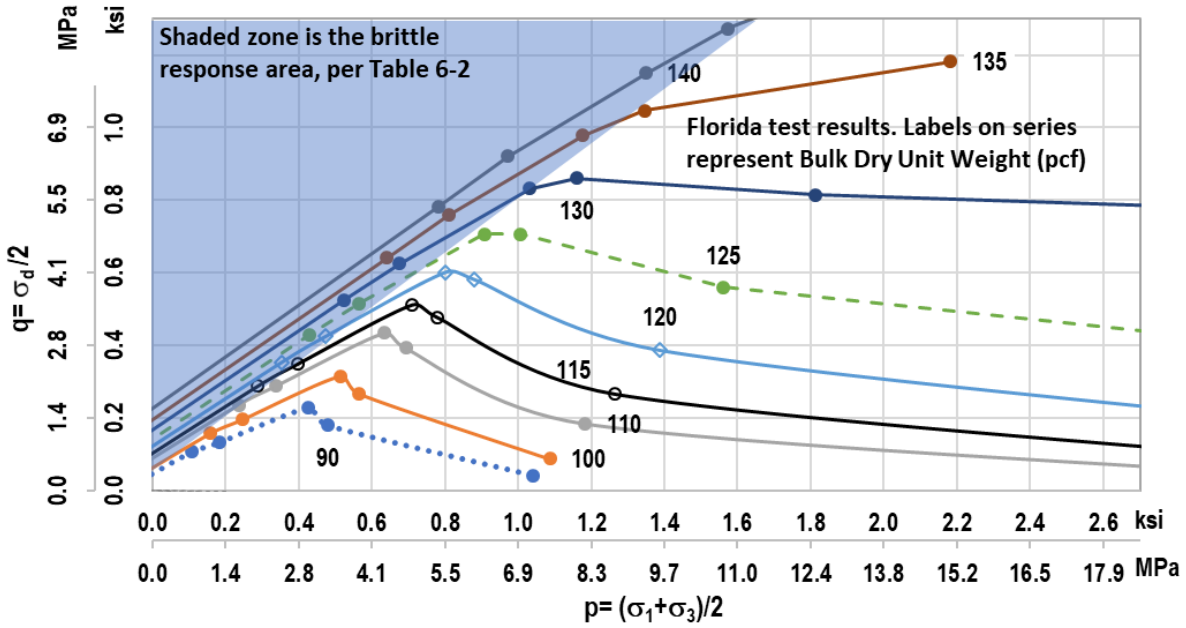

Figure 6-23. Strength envelope – Anastasia Formation

Similarly, shown in Figure 6-23 are strength envelopes for the Anastasia Formation. As shown in Chapter 5, Florida rock formations that have a high proportion of vug and permeable porosities (i.e., low proportion of impermeable porosity) have lower unconfined strengths. Those with a higher proportion of impermeable porosity, such as of the Key Largo or Anastasia Formations, will have higher unconfined compression strength at a given bulk porosity (i.e., bulk dry unit weight) than other Florida formations. However, at sufficiently high confining pressures in triaxial tests, all the different voids associated with the specimen's porosity will collapse (i.e., crush) - not just the vug and permeable portions in the case of unconfined strength tests. Therefore, the strength envelopes for the porous specimens of these two formations have very steep downward slopes (Figure 6-22 and Figure 6-23). For other formations (Hawthorn, Miami, and Ft Thompson), due to the low carbonate content or low proportion of impermeable porosity, their starting points on

the strength envelopes (from q_u results) are already low, thus the downward slopes in Figure 6-24 to Figure 6-26 for these formations are not as steep as in the case of the Key Largo or Anastasia Formations. Based on Figure 6-22 through Figure 6-26, dense Florida rocks with q_u higher than 9 MPa (1,300 psi) typically display brittle behavior when loaded under minimal confinement, e.g., under shallow foundations. Thus, the Hoek-Brown envelope would be applicable. However, more than 80% of Florida specimens (Chapter 4) are more porous and have q_u less than 9 MPa (1,300 psi). As shown in Figure 6-22 through Figure 6-26, they display ductile behavior, even under minimal confinement, and the strength envelopes of these porous rocks have much steeper downward slopes than those in the brittle zone.

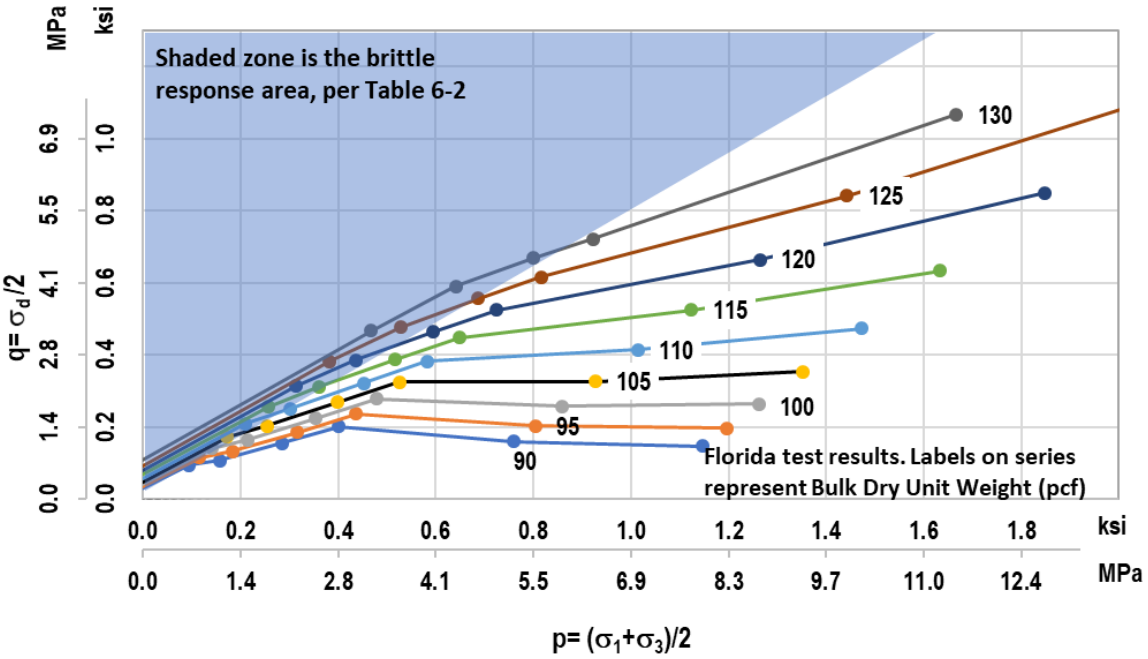

Figure 6-24. Strength envelope – Miami Formation

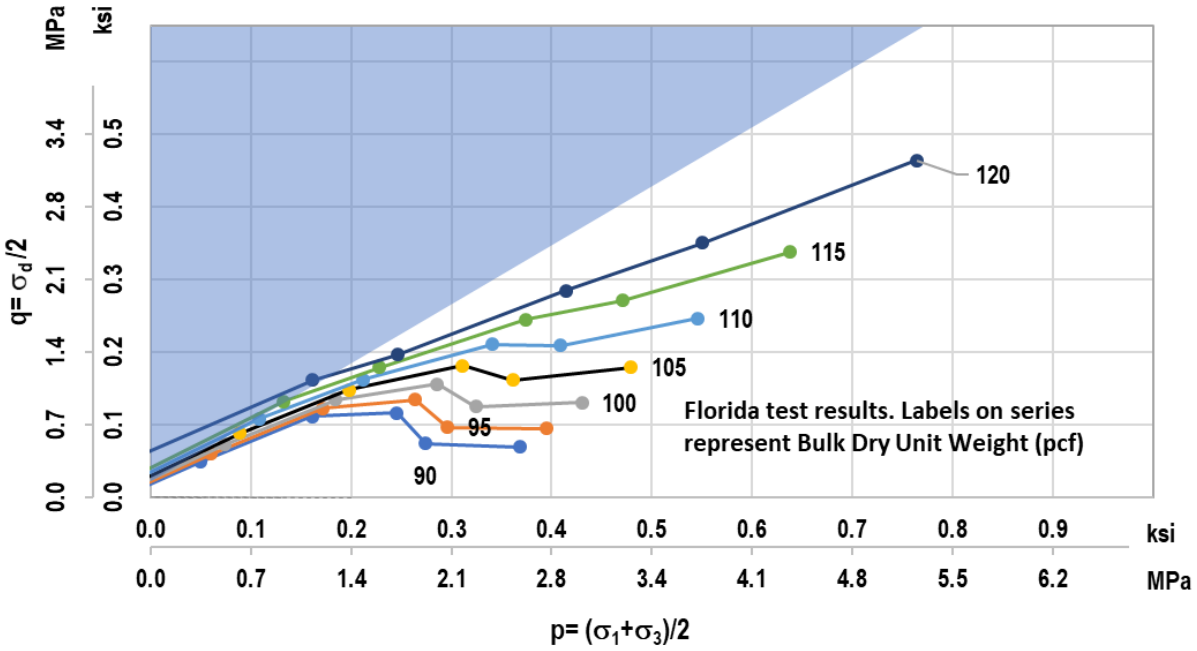

Figure 6-25. Strength envelope – Shallow Ft. Thompson Formation

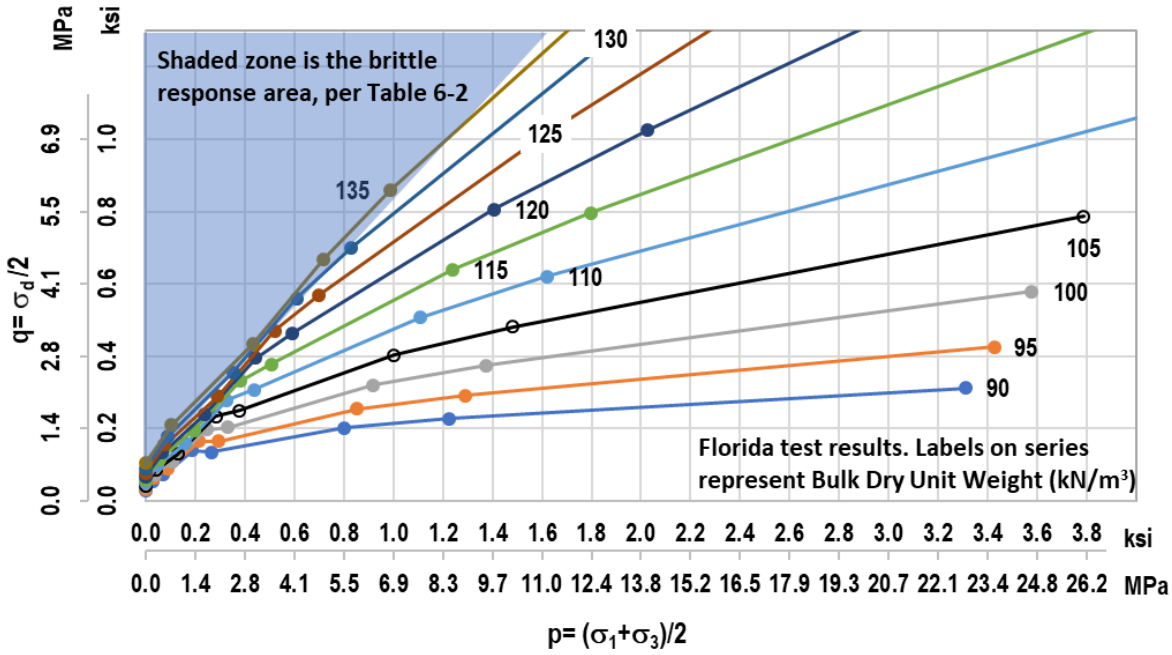

Figure 6-26. Strength envelope – Hawthorn Formation

a) Discussion regarding data variability

In addition to rock crushing, which is already discussed in Section 6.5 there is an additional dip in the middle of several constructed envelopes such as in Figure 6-23 for γ_{dt} = 14 to 16 kN/m^3 (90 to 100 pcf) when σ_3 = 2.1 MPa (300 psi). This concavity in the strength envelopes could be the result of a lower bias at σ_3 = 2.1 MPa (300 psi) a higher bias at $\sigma_3 \neq$ 2.1 MPa (300 psi). This is due to the scatter of the test results and the statistical population (the number of tests performed) for the data set.

The bias ratio, $(\sigma_d/\sigma_3)_{measured}$ / $(\sigma_d/\sigma_3)_{predicted}$, has a standard deviation of 0.33 from the triaxial test results. Therefore, the upper bound and lower bound of the σ_d/σ_3 value can be calculated as (1.00 ± 0.33) * $(\sigma_d/\sigma_3)_{predicted}$. The strength enveloped constructed based on the lower bound of the σ_d/σ_3 value, with an example presented in Figure 6-27, would be recommended for a conservative approach.

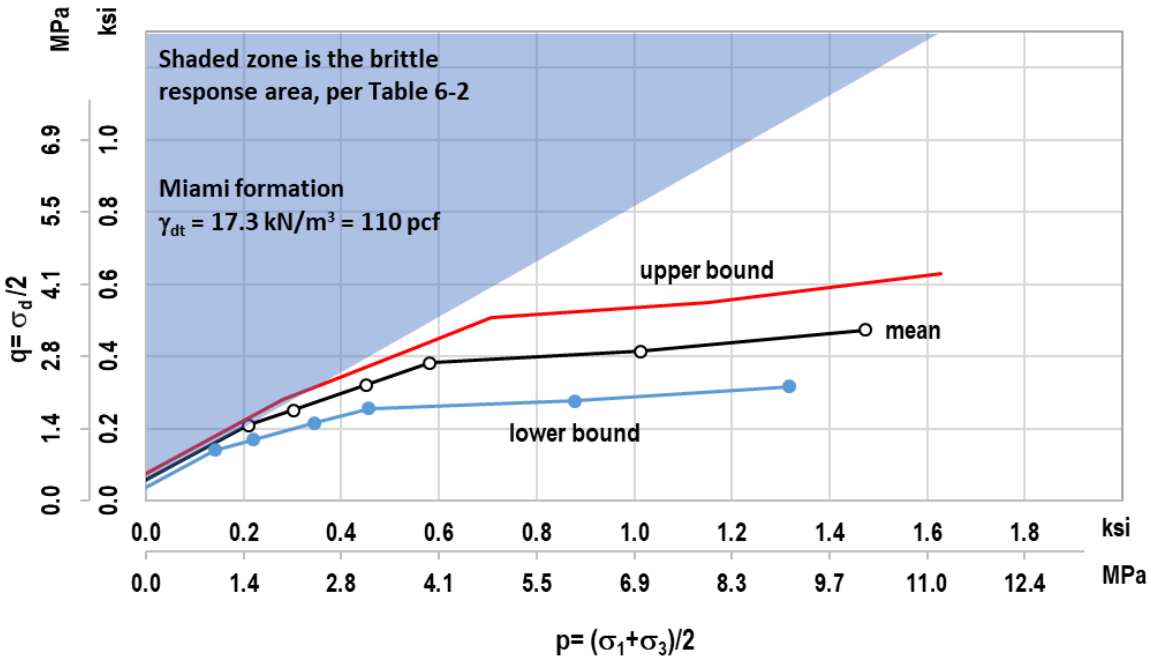

Figure 6-27. Example of lower bound and upper bound of intact rock strength envelope

b) Discussion regarding splitting tension (q_t) and direct tension (q_{dt}) relationship

The direct tension test is difficult to perform (Perras and Diederichs 2014). This is especially true for Florida carbonate rocks with porosities commonly ranging from 25% to 50% (Chapter 4), as it would be practically infeasible to reshape the vuggy and poorly cemented rock specimens to the dog-bone shape required for direct tension tests. Thus, q_t has become the standard laboratory test to evaluate tension strengths for Florida materials, and it is required test method reference in the FDOT Soil and Foundations Handbook (FDOT 2018). Perras and Diederichs (2014) identified that q_{dt} / q_t could vary from 0.4 to 1.2, with a mean value of 0.7 for sedimentary rocks. Therefore, a q_{dt} value of $0.7q_t$ for Florida carbonate rocks was used as starting point in this study. Figure 6-28 plots the early portions of the strength envelopes, connecting three values of q_{dt} (at $0.7q_t$), q_u, and triaxial test results at a low confinement of σ_3 = 0.345 MPa (50 psi) on the Lambe's p-q diagram. As examples, Figure 6-28.a and Figure 6-28.b are essentially the zoomed-in portions of Figure 6-22 and Figure 6-23, respectively, where the early portions of the strength envelopes are practically linear. As shown in lower left corners of Figure 6-22 through Figure 6-26 and in Figure 6-28, a few of the lines could be straighter if one of the following scenarios occur: i) the q_{dt} values are higher, such as to q_{dt} = (1.0 or 1.2) q_t; or ii) the q_u values are lower, or the triaxial strengths are higher at σ_3 = 0.345 MPa (50 psi), while keeping $q_{dt} = 0.7q_t$. Either of these scenarios are possible due to the scatter of the test results and the limited sample population (number of tests performed), which is similar to the discussion (a) above. In summary, Florida carbonate rock test results support $q_{dt} = 0.7q_t$ as a reasonable and conservative assumption.

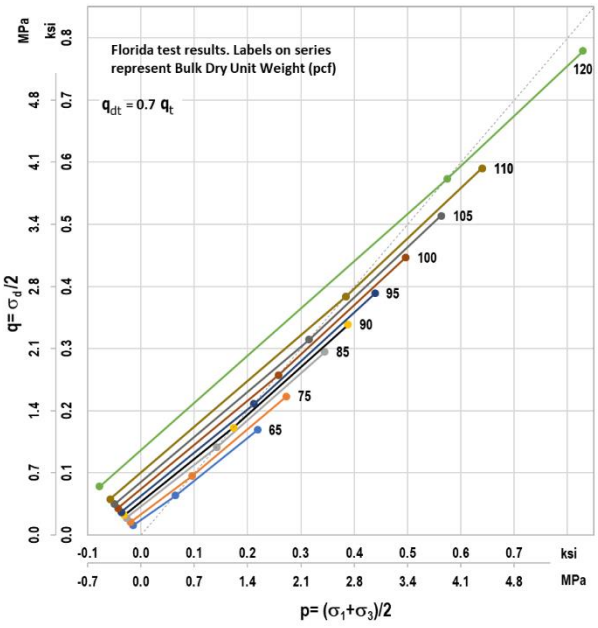

(a)

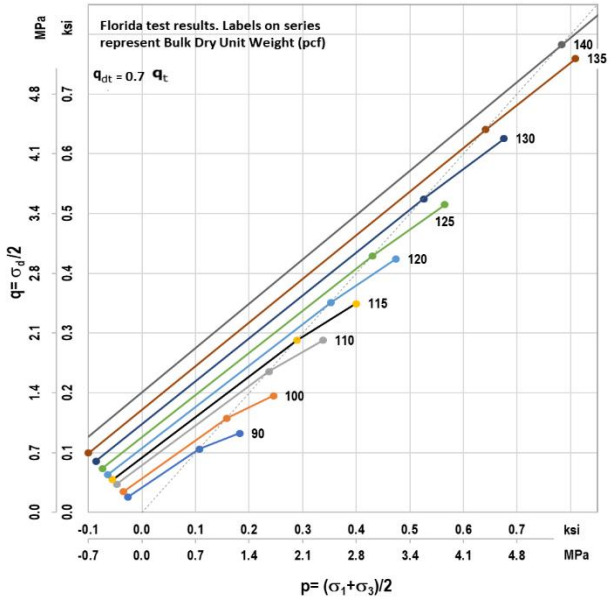

(b)

Figure 6-28. Verification for using $0.7q_t$ as q_{dt} value: (a) Key Largo Formation; (b) Anastasia Formation

6.9 Simplified Intact-rock Strength Envelope

Hoek et al. (2002) stated that it is necessary to determine equivalent Mohr-Coulomb angles of friction and cohesive strengths for each rock mass and stress range. This is done by fitting an average linear relationship to the Hoek-Brown curve to balance the areas above and below the Mohr-Coulomb plot. Thus, the slightly curved Hoek-Brown envelope becomes a straight-line Mohr-Coulomb envelope. The reason for this simplification is so that it can be used by geotechnical applications that employ various bearing capacity theories and numerical models, such as the finite element method (FEM). Hoek et al. (2002) derived the equivalent Mohr-Coulomb envelope as follow:

$$\varphi = \arcsin\left[\frac{6am(s+m\sigma_{3n})^{a-1}}{2(1+a)(2+a)+6am(s+m\sigma_{3n})^{a-1}}\right] \quad (6\text{-}21)$$

$$c = \frac{q_u[(1+2a)s+(1-a)m\sigma_{3n}](s+m\sigma_{3n})^{a-1}}{(1+a)(2+a)\sqrt{1+(6am(s+m\sigma_{3n})^{a-1})/((1+a)(2+a))}} \quad (6\text{-}22)$$

where s, m, a are from Eqs. 6-3 to 6-5, and σ_{3n} is σ_{3max} / q_u, with σ_{3max} as the maximum confining stress over which the Hoek-Brown curve is approximated to the linear Mohr-Coulomb envelope.

Similarly, there is a need to simplify strength envelopes for Florida carbonate rocks for finite element simulation of boundary value problems (e.g., bearing capacity of spread footings). Due to the general shape of the Florida strength envelopes, a bilinear simplification is proposed which allows a general modeling of Florida carbonate rocks at a specified dry unit weight in a finite element method simulation. For Florida carbonate rocks, rock heterogeneity is another reason to use the bilinear simplification for practical engineering projects. For one project site, one rock layer (for example, at 5-m or 15-ft thick) will have a wide range of bulk dry weights. As such, either there will not be enough specimens (30 to 50 specimens are required) to perform triaxial

tests for all different confining pressures at different bulk dry unit weights, or it will be expensive for the designer to complete all 30 to 50 triaxial tests. Thus, it is anticipated that only 5 to 8 triaxial tests to be performed at one specific confining pressure. The recommended pressure is 4.1 MPa (600 psi) to cover the typical range of confining pressures under a shallow foundation (Appendix F).

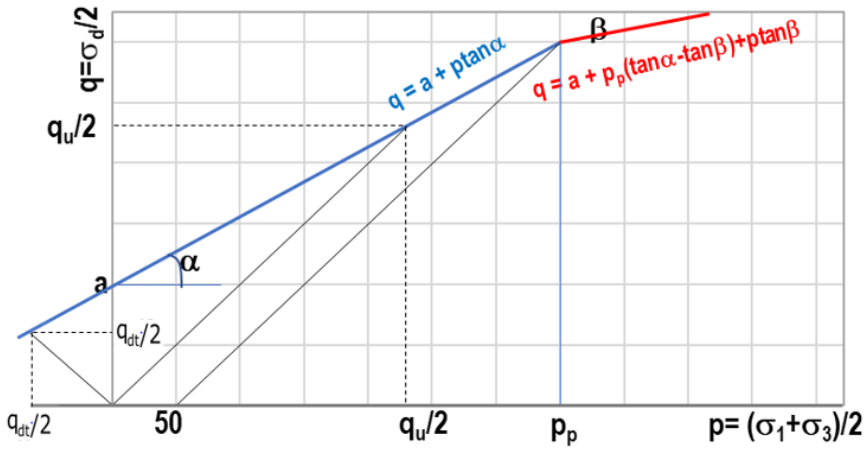

Figure 6-29. Schematic of bilinear strength envelope for intact rock

The four parameters that define the bilinear strength envelopes are: initial friction angle (φ), location of slope change (p_p), which can be considered as the onset of cementation breakage and crushing (onset of the ductile flow), second slope of the envelope (ω), and cementation (c). The term cementation is used because unlike cohesion, the cementation strength is not recoverable once the rock grains have been reorganized. It is noted that the strength envelopes are presented as Lambe's p-q diagram (Figure 6-29), and the relatable geotechnical terms have direct relationships to Lambe's p-q diagram parameters as follow:

$$c = a / \cos\varphi \text{ or } a = c\cos\varphi \tag{6-23}$$

$$\sin\varphi = \tan\alpha \text{ and } \sin\omega = \tan\beta \tag{6-24}$$

These output parameters are obtained via four input parameters: q_{dt}, q_u, γ_{dt}, and Florida carbonate formation identification, as identified below:

The cementation c (or a in Lambe's p-q diagram), is the y-axis intercept between the initial straight portion of the envelope (between q_{dt} and q_u results):

$$c = 0.5\sqrt{q_u q_{dt}} \tag{6-25}$$

The friction angle, φ (or α in p-q diagram) is the slope of the initial straight portion of the envelope (between q_{dt} and q_u results):

$$\sin\varphi = \frac{q_u - q_{dt}}{q_u + q_{dt}} \qquad \text{(in p-q diagram: } \tan\alpha = \frac{q_u - q_{dt}}{q_u + q_{dt}}\text{)} \tag{6-26}$$

The p location at the peak of the initial straight portion of the envelope corresponds to a triaxial chamber pressure of 0.35 MPa (50 psi), shown in Figure 6-29. This is a conservative representation of the peak point, since Figure 6-22 to Figure 6-26 indicate that the initial straight portion of the envelopes extends out to a triaxial chamber pressure (σ_3) of between 0.35 and 1.40 MPa (50 psi and 200 psi).

$$p_p \text{ (psi)} = \frac{50 + a}{1 - \tan\alpha} = \frac{50 + c\cos\varphi}{1 - \sin\varphi} \tag{6-27}$$

The second slope on the strength envelope (β in p-q diagram, or ω in σ-τ diagram) is calculated between the peak point, p, and the end of the curve, presented in Figure 6-30 through Figure 6-34. The ω value is best fitted using bulk dry unit weight and rock formations due to (i) different proportions of vug, permeable, or impermeable porosities within the bulk porosity; (ii) mineral bonds (i.e., calcite, dolomite, and/or the sum of them – represented as carbonate content); (iii) rock grain size. The ω correlation is presented in Table 6-4. In the case where rock formation is not known, a general value (approximate lower bound) for ω is suggested in Table 6-4 under

Generic Florida formation. Using the above parameters, the simplified bilinear envelopes for the formations tested in this study are presented in Figure 6-35 through Figure 6-39.

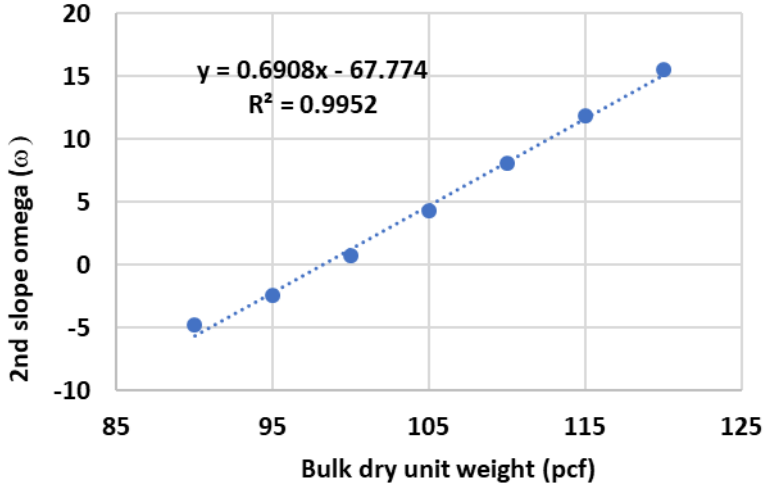

Figure 6-30. 2nd slope ω correlation – Key Largo Formation

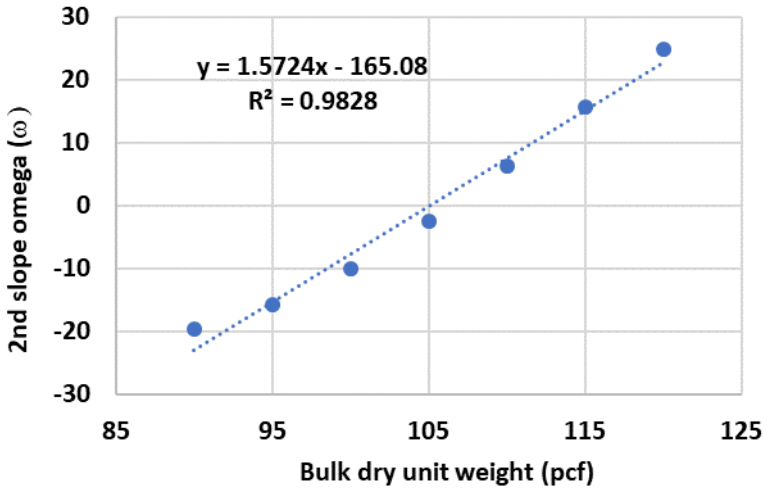

Figure 6-31. 2nd slope ω correlation – Shallow Ft. Thompson Formation

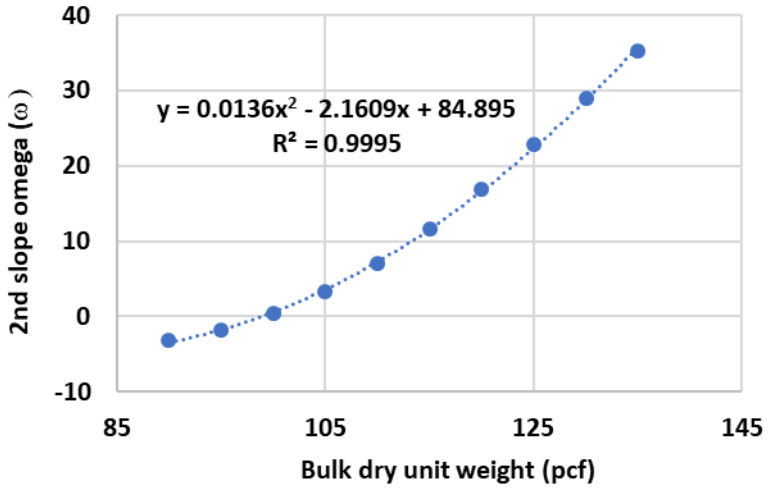

Figure 6-32. 2nd slope ω correlation – Miami Formation

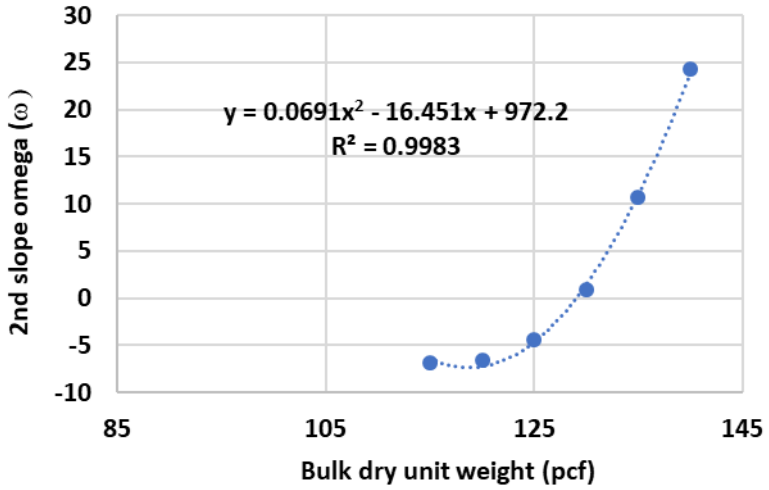

Figure 6-33. 2nd slope ω correlation – Anastasia Formation

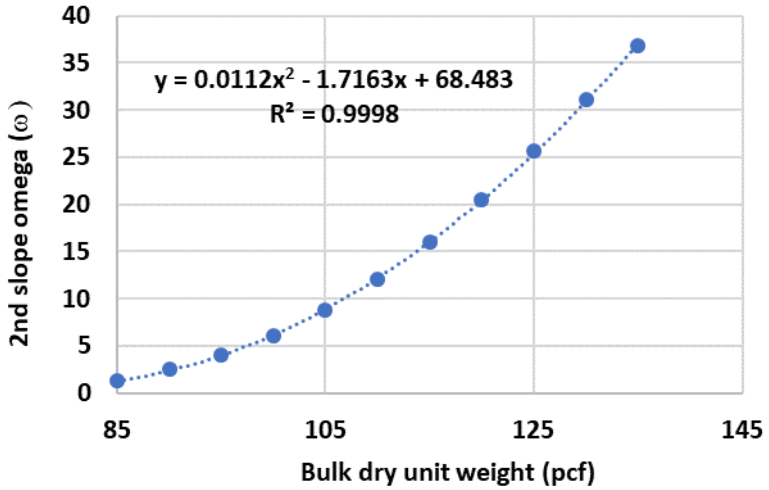

Figure 6-34. 2nd slope ω correlation – Hawthorn Formation

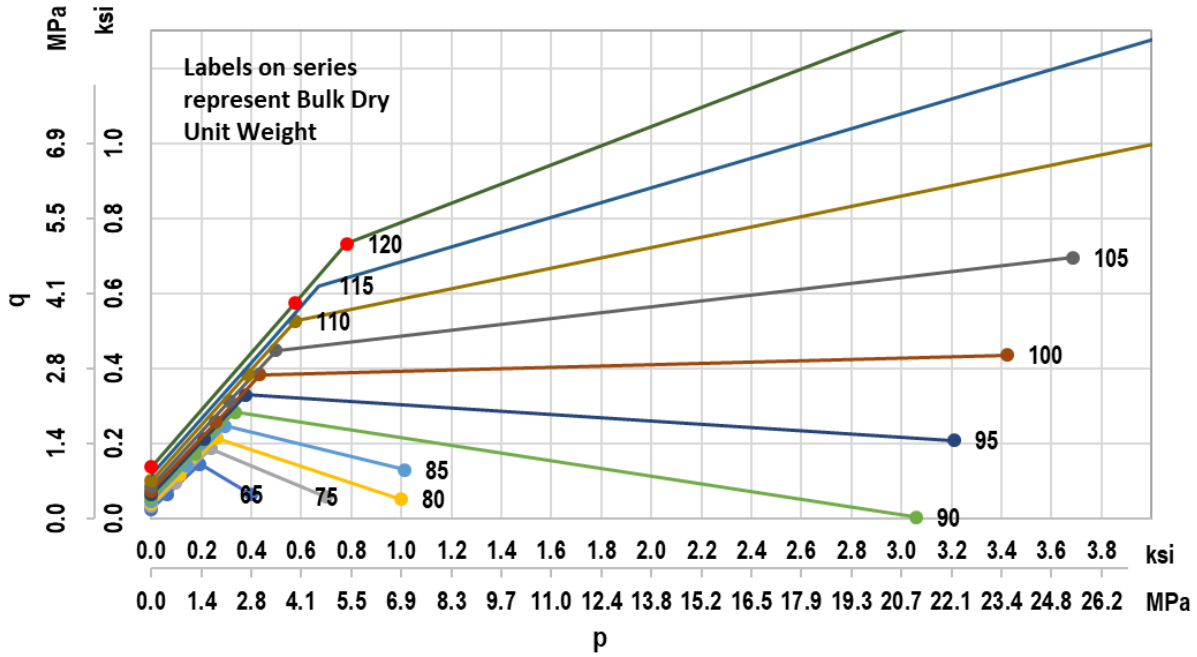

Figure 6-35. Bilinear strength envelope – Key Largo Formation

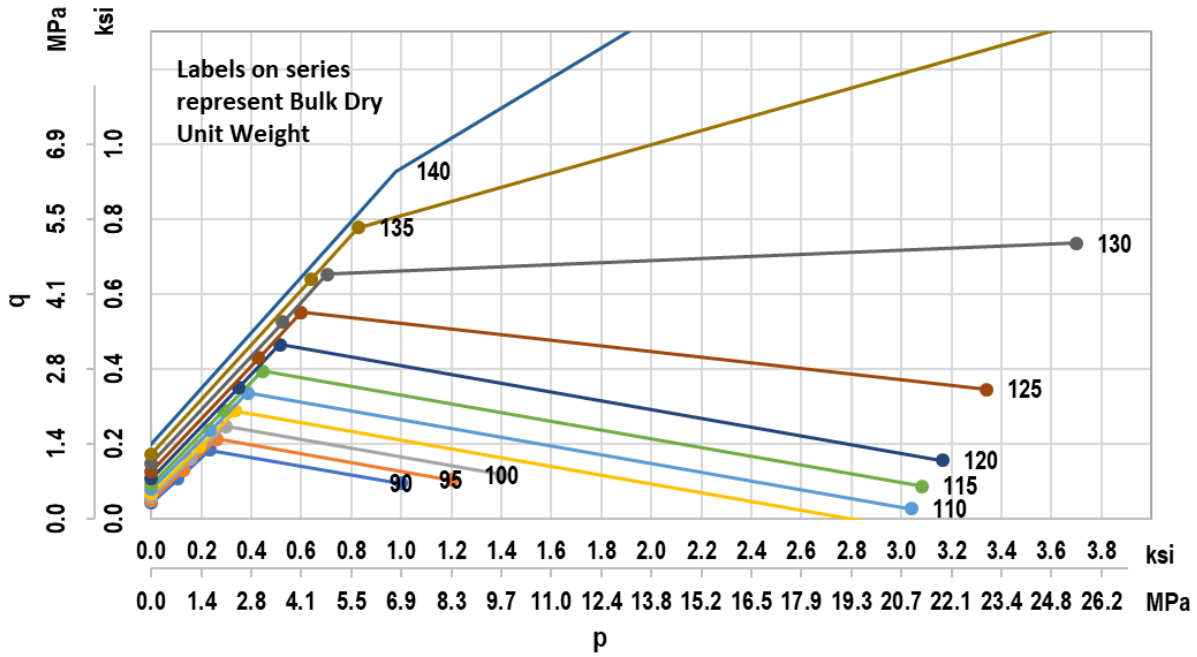

Figure 6-36. Bilinear strength envelope – Anastasia Formation

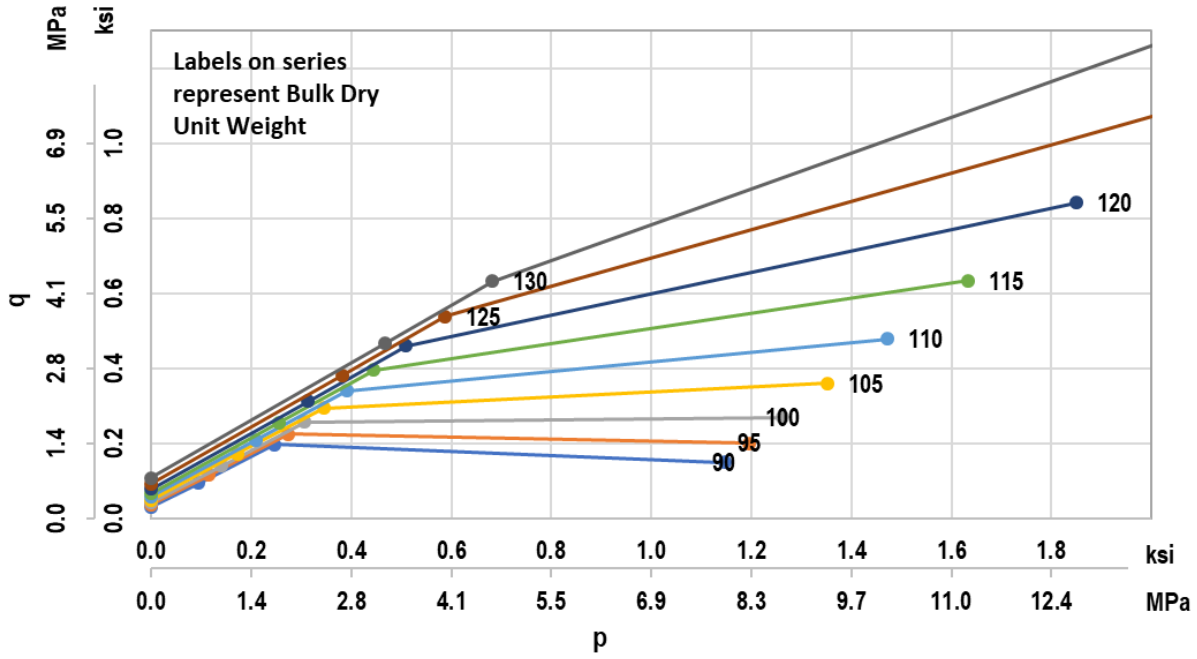

Figure 6-37. Bilinear strength envelope – Miami Formation

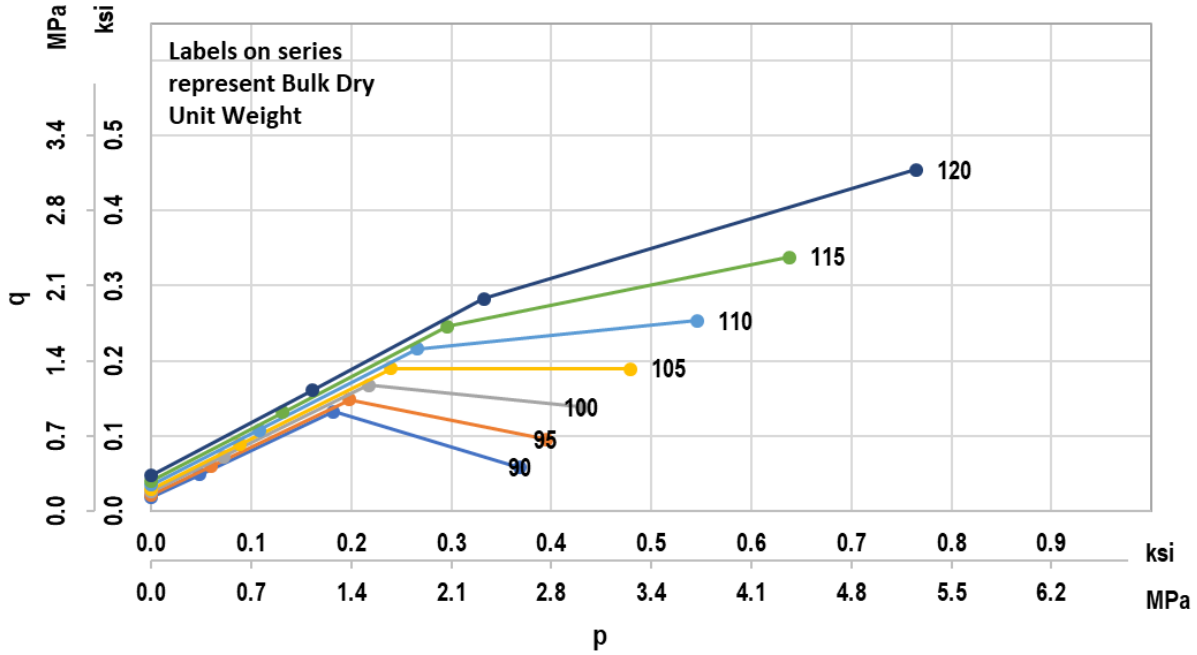

Figure 6-38. Bilinear strength envelope – Shallow Ft Thompson Formation

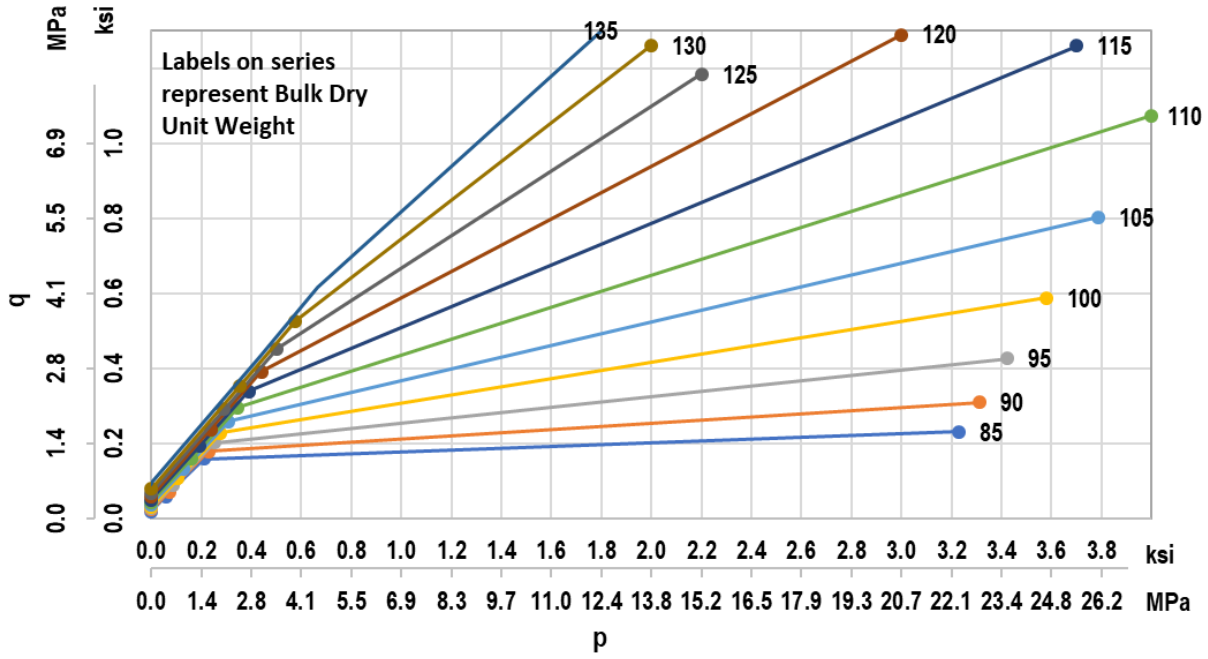

Figure 6-39. Bilinear strength envelope – Hawthorn Formation

Table 6-4. Value of 2nd slope (ω) on Florida strength envelopes

Formation	ω value for γ_{dt} in pcf	ω value for γ_{dt} in kN/m^3
Key Largo	$0.69\,\gamma_{dt} - 68$	$4.4\,\gamma_{dt} - 68$
Shallow Ft. Thompson	$1.57\,\gamma_{dt} - 165$	$10\,\gamma_{dt} - 165$
Miami	$0.0136\gamma_{dt}^2 - 2.2\,\gamma_{dt} + 85$	$0.55\gamma_{dt}^2 - 14\,\gamma_{dt} + 85$
Anastasia	$0.0691\gamma_{dt}^2 - 16.45\,\gamma_{dt} + 972$ $\omega = -6.7$ for $\gamma_{dt} < 120$ pcf	$2.8\gamma_{dt}^2 - 104.7\,\gamma_{dt} + 972$ $\omega = -6.7$ for $\gamma_{dt} < 19$ kN/m^3
Hawthorn	$0.011\gamma_{dt}^2 - 1.72\,\gamma_{dt} + 68$	$0.45\gamma_{dt}^2 - 11\,\gamma_{dt} + 68$
Generic Florida formation	$0.79\gamma_{dt} - 90$	$5\gamma_{dt} - 90$

A bias statistical analysis was performed to evaluate the scatter of the triaxial test results compared to the recommended bilinear strength envelopes on 223 tested specimens. One example of the bias calculation is presented below using the trigonometry from Figure 6-29:

- Key Largo test specimen results: bulk dry unit weight γ_{dt} = 80.1 pcf, carbonate content of 98.2%, and the measured triaxial normalized stress $(\sigma_d/\sigma_3)_{measured}$ = 3.37 at chamber pressure of σ_3 = 130.5 psi. Thus, the triaxial stress path is:

  $$q = -130.5 + p \quad (6\text{-}28)$$

- Unconfined compression strength q_u = 230.4 psi and split tension strength q_t = 46.8 psi.
- Per Eq. 6-25, c = 51.9 psi
- Per Eq. 6-26, $\tan\alpha = 0.66$, $\varphi = 41.5^0$, $\cos\varphi = 0.75$
- Per Eq. 6-23, a = 38.9 psi
- Per Eq. 6-27, p_p = 263.2 psi
- Per Table 6-4, $\omega = 0.69\ \gamma_{dt} - 68 = -12.7^0$, thus $\sin\omega = \tan\beta = -0.22$
- Therefore, the recommended bilinear strength envelope is:

  For $p \le p_p$: $q = 38.9 + 0.66p$ (6-29)

  For $p > p_p$: $q = 38.9 + 263.3\ (0.66+0.22) - 0.22p = 271.3 - 0.22p$ (6-30)

- Eq. 6-28 intersects with Eq. 6-30 at p = 328.8 psi and q = 198.3 psi, therefore the predicted deviatoric stress based on the bilinear envelope is $\sigma_d = 2q$ = 396.6 psi, and $(\sigma_d / \sigma_3)_{predicted}$ = 3.04.
- The (σ_d/σ_3) bias for this specimen is $(\sigma_d/\sigma_3)_{measured} / (\sigma_d/\sigma_3)_{predicted}$ = 3.37 / 3.04 = 1.11.

Figure 6-40 shows the (σ_d / σ_3) bias scatter representation for all 223 tested specimens, which indicates that the bilinear strength envelopes are quite acceptable (R^2 = 0.88, with a conservative bias higher than 1.0) in representing the Florida rock strengths.

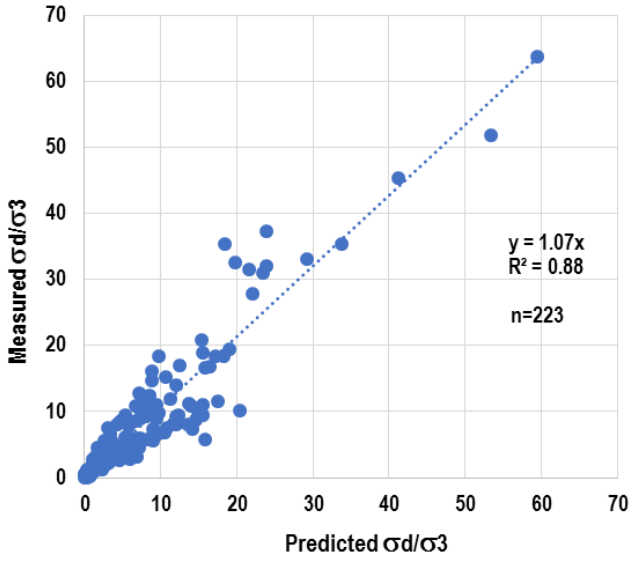

Figure 6-40. Scatter of predicted normalized stresses back-calculated from bilinear envelopes

6.10 Rock Mass Strength Envelope

In engineering practice, there is a need in characterizing Florida's rock masses from intact rock specimens and coring information. In cases of a jointed rock mass, the overall Hoek-Brown envelope for the rock mass is lower than that for intact rock, via parameters m, s, and a as shown in Eq. 6-2. The resulting $q_{rock\text{-}mass} = (\sigma_{1rock\text{-}mass} - \sigma_3)/2$ value on the rock mass strength envelope is reduced by a factor approximately proportional to GSI/100, compared to the $q = (\sigma_1 - \sigma_3)/2$ of intact rock, with examples presented in Figure 6-41. For jointed rock, the GSI/100 value is approximately proportional to the RQD or REC values. Therefore, the rock mass strength envelope is expected to be proportional to RQD or REC with respect to the intact rock strength.

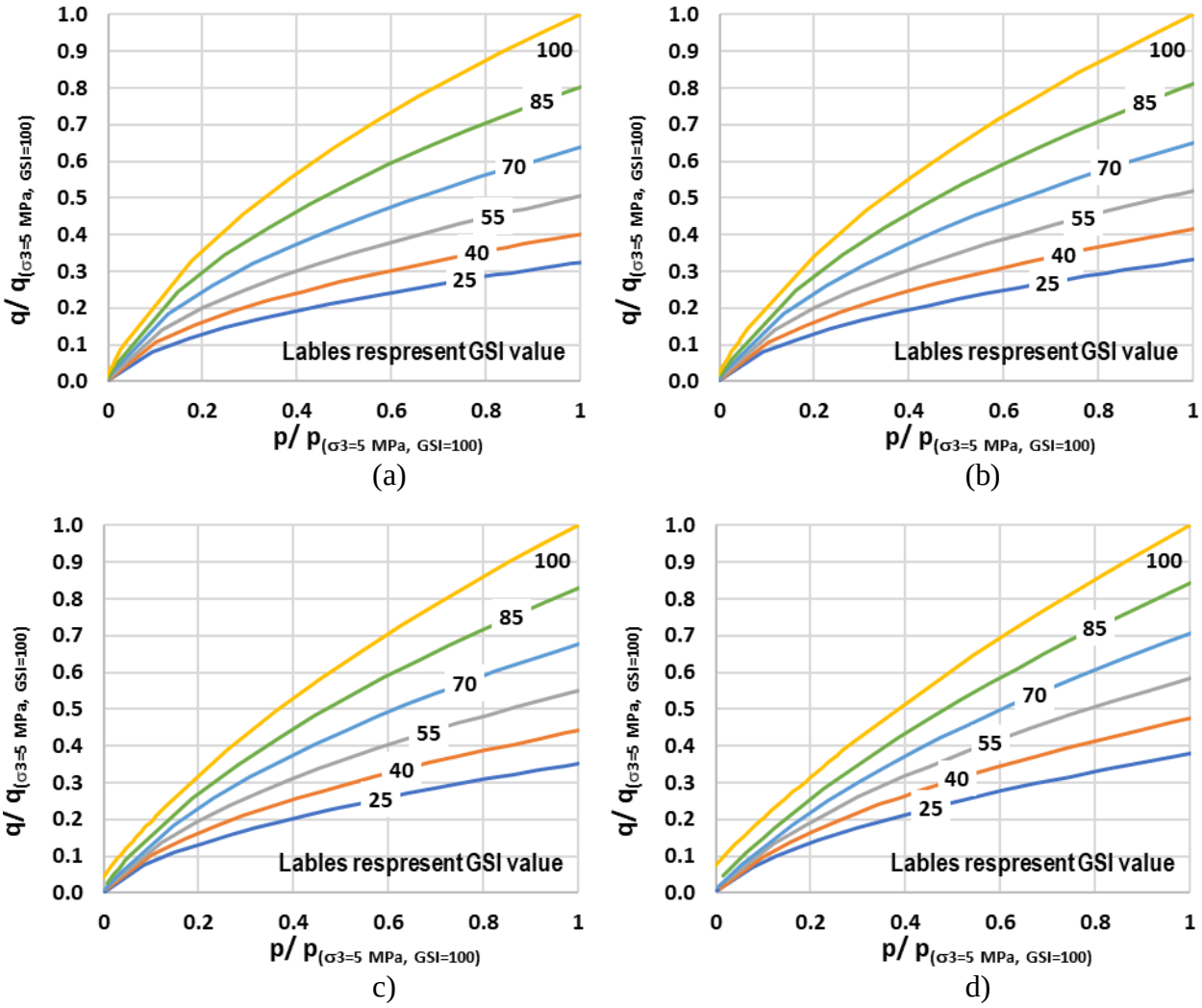

Figure 6-41. Rock mass strength envelopes in relative to intact rock strength envelope: (a) q_u = 0.5 MPa; (b) q_u = 1 MPa; (c) q_u = 3 MPa; (d) q_u = 10 MPa

Florida rocks and IGMs appear to be jointless (Truzman 2016); the appearance of the intact or massive rock mass can be misinterpreted and it is not feasible to directly apply the GSI index. Therefore, further studies are needed regarding the reduction of rock mass strength envelopes for Florida materials. Pending further studies, a provisional procedure is suggested below.

6.10.1. Weight-adjusted Strength Envelope

Determine the bulk dry unit weights on as many specimens (Length, L_i) as possible from the recovered rocks, and a weighted average unit weight is obtained:

$$\gamma_{dtw} = \Sigma(\gamma_{dti}\, L_i) / \Sigma L_i \quad (6\text{-}31)$$

The three subscripts are: d for dry, t for total (or bulk, to differentiate from the apparent dry unit weight, obtained from ASTM D6473, presented in Eq. 3-3), and w for weighted average.

For the rock layer that is being evaluated, determine the weighted average dry unit weight for those specimens that were strength tested, γ_{dts} (the three subscripts are: d for dry, t for total, and s for strength tested specimens). The same procedure can be done for carbonate content to arrive at the weighted average carbonate content (C_w) and strength test only carbonate content C_s. Despite varying from one formation to the next, the carbonate content may not vary much within a site-specific rock layer and it can be assumed that for a specific rock layer, $C_w \approx C_s$. For the porous Florida rocks, q_t is estimated to be $2.468F_t e^{0.03\gamma_{dt}} e^{0.5C}$ and q_u is estimated to be $3.24F_u e^{0.04\gamma_{dt}} e^{2C/3}$ (Chapter 5). Therefore, the weighted q_t (or direct tension, q_{dt}) and q_u values for the evaluated rock layer are obtained from the values of the intact specimens as:

$$q_{tw} = q_{dt} * e^{0.03(\gamma_{dtw}-\gamma_{dts})} e^{0.5(C_w-C_s)} \approx q_{dt} * e^{0.03(\gamma_{dtw}-\gamma_{dts})} \quad (6\text{-}32)$$

$$q_{uw} = q_u * e^{0.04(\gamma_{dtw}-\gamma_{dts})} e^{2/3(C_w-C_s)} \approx q_u * e^{0.04(\gamma_{dtw}-\gamma_{dts})} \quad (6\text{-}33)$$

where q_{dt} (based on $0.7*q_t$) and q_u are site specific test results for the evaluated rock layer. When many specimens are tested for q_t and q_u, then the statistical procedure in Appendix A of FDOT Soil and Foundations Handbook can be followed to arrive at a single mean value of q_t and q_u for the rock layer. After step 1, instead of a strength envelope based on intact

properties of q_{dt}, q_u, and γ_{dts}, a weight-adjusted strength envelope based on q_{tw}, q_{uw}, and γ_{dtw} should be used in Eqs. 6-25 to 6-27 and Table 6-4.

For example, in the last core run of Figure 2-12, REC = 78%, there are two pieces (labelled as 1 and 2 in the figure) that have strength (q_t or q_u) and dry unit weight results. Index parameters (no strength test) would be obtained from the other specimens in the core run. For the specimens tested for strengths, assume the mean values are: q_t = 66.9 psi, q_{dt} = 0.7*66.9 = 46.8 psi, q_u = 230.4 psi, and γ_{dts} = 80.1 pcf. When including all specimens, the weighted value is γ_{dtw} = 70.1 pcf. Thus, we have lower weighted strength values of: $q_{tw} = 46.8 * e^{0.03(70.1-80.1)} = 34.7$ psi and $q_{uw} = 230.4 * e^{0.04(70.1-80.1)} = 154.4$ psi. Then, after step 1, instead of a strength envelope based on intact properties of 46.8 psi, 230.4 psi, and 80.1 pcf, a weight-adjusted strength envelope based on 34.7 psi, 154.4 psi, and 70.1 pcf should be used in Eqs. 6-25 to 6-27 and Table 6-4.

6.10.2. Recovery-adjusted Strength Envelope

In the Florida Department of Transportation practice (FDOT 2018), the rock mass strength is reduced by rock recovery (REC%) compared to the intact specimen strength to account for uncoreable materials. For example, $q_{um} = q_u * REC$ and $q_{tm} = q_{dt} * REC$, thus $f_{su\_design} = REC * 0.5\sqrt{q_u * q_{dt}}$ for drilled shaft side resistance calculation. This strength reduction accounts for the uncoreable weak rock or soil within the core run. Additional advantages of using REC to reduce the rock strength estimation during the design phase include:

i) If low recovery indicates suspected voids.

ii) If low recovery is due to the drilling process, resulting in no or few specimens to be tested, then an additional subsurface exploration plan can be considered to increase the number of samples that can be tested.

It is therefore recommended that the Florida strength envelope for the rock mass to be reduced by a factor of REC as illustrated in Figure 6-42 and in the equation below:

$$q_m = q * REC \qquad (6\text{-}34)$$

which would result in the following parameters, based on the weighted values from Step 1:

$$a_m = REC*a = REC*0.5\sqrt{q_{uw}q_{tw}}\cos\left(\arcsin\frac{q_{uw}-q_{tw}}{q_{uw}+q_{tw}}\right) \qquad (6\text{-}35)$$

$$tan\alpha_m = REC*\tan\alpha = REC\frac{q_{uw}-q_{tw}}{q_{uw}+q_{tw}} \qquad (6\text{-}36)$$

$$tan\beta_m = REC*\tan\beta = REC*\sin\omega \qquad (6\text{-}37)$$

$$p_{pm} = p_p \qquad (6\text{-}38)$$

It is noted that the above Eq. 6-34 and its derivations for rock mass would yield a more conservative rock mass's cementation value than the conventional $REC*\ 0.5\sqrt{q_{uw} * q_{tw}}$ value:

$$c_m = a_m / cos\varphi_m = REC*\ c\ *\ \cos\varphi / \cos\varphi_m$$

$$c_m = REC*\ 0.5\sqrt{q_{uw} * q_{tw}}\ *\ \cos\varphi / \cos\varphi_m \le REC*\ 0.5\sqrt{q_{uw} * q_{tw}} \qquad (6\text{-}39)$$

Therefore, due to its simplicity and conservatism, Eq. 6-34 was used to model the rock mass envelope in the finite element method analyses in the next chapter.

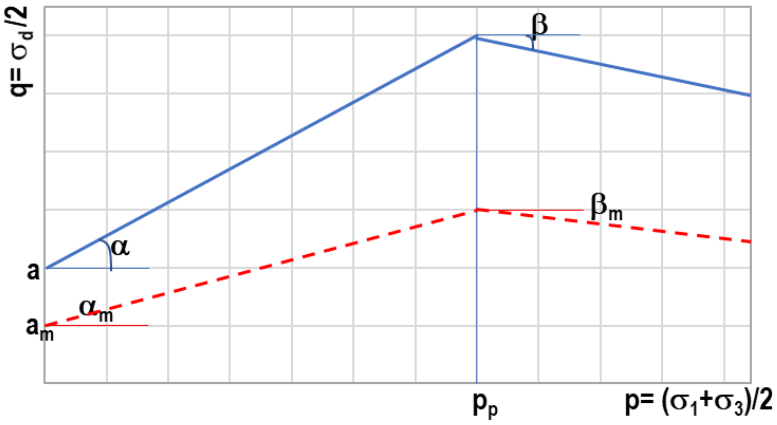

Figure 6-42. Bilinear strength envelope for rock mass from intact rock

6.11 Summary

The main focus of this chapter is the development of strength envelopes for the shallow Florida rock formations, with the ultimate goal of estimating shallow foundation (spread footing) bearing capacity. The encountered Florida carbonate rocks for the shallow depths are porous, with some porosities exceeding 50%, or bulk dry unit weight less than 13.4 kN/m^3 (85 pcf). Their strengths are low, with the median value for unconfined compression strength of 3 MPa (435 psi). Due to the difficulty in attaching strain gauges to the vuggy and shelly surface of Florida carbonate rocks, a volume measurement device was added to the Hoek cell triaxial system, enabling the researchers to measure the volumetric responses of Florida carbonate rocks in triaxial tests. Based on triaxial testing, it was shown that when the unconfined compression strength, q_u, is higher than 9 MPa (1.3 ksi), the material typically exhibits brittle stress-strain behavior for shallow foundation loading conditions. In this case, the Hoek-Brown criterion, developed for brittle rupture failure, is applicable. However, most of the porous Florida carbonate rocks have weaker strengths with a ductile stress-strain response, associated with contractive volumetric behavior. In the case of Florida limestone, the σ_d/σ_3 threshold for the material to transition from brittle to ductile responses occurs at much lower confining pressures as shown in Table 6-2. Accordingly, the strength envelopes for these materials slope downward at a much steeper rate than those for the brittle zone and occur at lower confining pressures. In addition, the envelopes vary between formations, due to different cementations (different minerals, carbonate contents, and rock grain sizes) and different proportions of void structures (vug, permeable, and impermeable voids). Consequently, it is recommended that different Florida carbonate rock formations have their own strength

envelopes based on dry unit weights. When sufficient specimens can be collected, strength envelopes should be established based on triaxial testing as discussed herein. Furthermore, it is not recommended to reduce the strength envelope of Florida carbonate rocks using the GSI index since it is not readily available. Pending further study, a provisional procedure is recommended to develop a rock mass strength envelope from the intact strength envelope, weighted-average of the dry unit weights, and rock recovery ratio (REC).

CHAPTER 7 NUMERICAL MODELING –
SHALLOW FOUNDATIONS ON FLORIDA ROCKS

7.1 Material model

Based on the measured strength envelope and stress-strain response of Florida carbonate rock (Chapter 6), a new elastic, perfectly plastic material model to describe the behavior of Florida's rock has been proposed in Chapter 6 via four parameters (a, α, β, p_p) in Lambe's p-q diagram (Lambe and Whitman, 1969). In the case of sand, the Drucker-Prager-Cap model (Souza Neto et al. 2011) is used to simulate the sand behavior for the case of rock over sand.

The rock's stress-strain response is characterized as elastic up to the yield/failure surface where it is plastic. The strength function/surface is written in Lambe's p-q diagram (Figure 7-1) with the 4 parameters (a, α, β, p_p) as,

$$F = \begin{cases} q - (tan\alpha)p - a & if\ p \leq p_p \\ q - (tan\alpha - tan\beta)p_p - (tan\beta)p - a & if\ p > p_p \end{cases}, \quad (7\text{-}1)$$

where p = $(\sigma_1 + \sigma_3)/2$ is the mean stress and q = $(\sigma_1 - \sigma_3)/2$ is half of the deviatoric stress

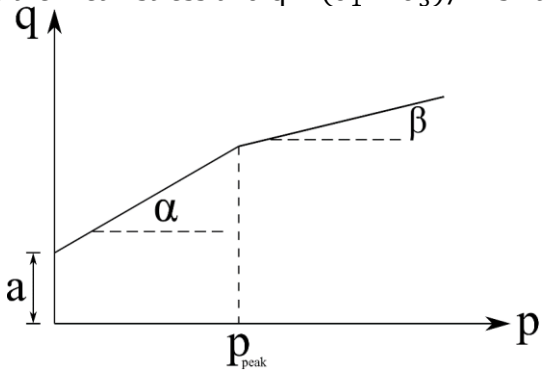

Figure 7-1. Yield function in Lambe's p-q diagram

In order to compare the simulation results with the traditional bearing equation terms, one can easily convert a $p - q$ diagram to the $\tau - \sigma$ diagram (Figure 7-2). The relationship between the two stress systems strength envelopes are,

$$\varphi = sin^{-1}(tan\alpha); \qquad \omega = sin^{-1}(tan\beta); \qquad c = a/cos\varphi. \tag{7-2}$$

Where c is the cohesion intercept, φ is the initial friction angle, and ω is the second slope of the strength envelope.

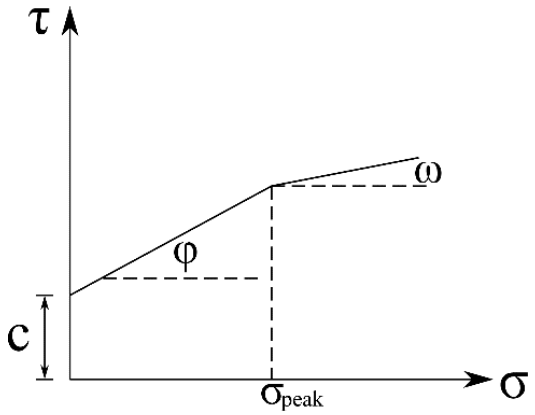

Figure 7-2. Variables in the τ - σ diagram

7.2 Validation of FEM code and material model

Since the FEM simulations were to be used in developing bearing capacity equations, validation of the material model and FEM code was required. The first validation (Section 7.2.1.) was for a strip footing on an elastic, perfectly plastic material (purely cohesive material only) based on Lambe and Whitman (1969). The second validation was a strip footing resting on a c - φ material (straight line strength envelope) based on Vesic's results (Das, 2015). The final validation used the laboratory triaxial stress-stress results of a typical Florida carbonate rock. The final validation (Section 7.2.2.) was a strip footing resting on a sand layer with Drucker-Prager-Cap model which was compared to Vesic's results.

7.2.1. Validation of elastic, perfectly plastic model

Three simulations were conducted to validate both the FEM code and elastic, perfectly plastic material model. Two different strength envelopes were used to model the material. The first simulation dealt with a strip footing resting on a cohesive-only soil layer. Due to symmetry, only half of the homogeneous soil layer of 26.5ft height and 26.5ft length (Figure 7-3.a) was discretized using a regular grid of quadrilateral elements. Vertical and horizontal displacements were constrained at the bottom boundary. The left and right sides were fixed in horizontal directions. An external contact stress, Figure 7-3.a, was applied to the surface to characterize the strip footing. The mechanical behavior of the soil was modeled using the elastic, perfectly plastic model. The material parameters (c = 1.72 tsf and φ = 0) used in the simulations are listed as Table 7-1 and were given by Lambe and Whitman (1969). All the parameters, based on $\tau - \sigma$ diagram, were converted to p-q diagram (Figure 7-3.b) for the analysis.

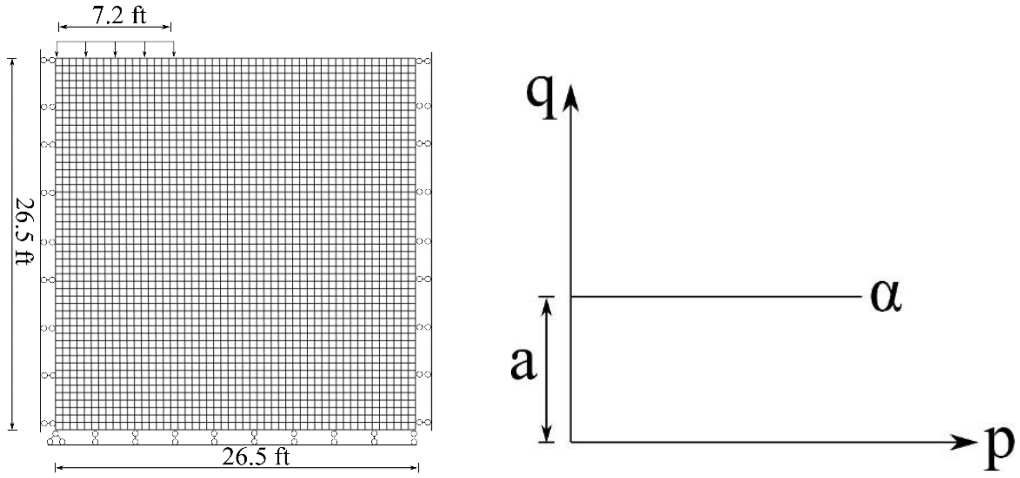

(a) (b)

Figure 7-3. (a) Geometry of meshed model and boundary conditions; (b) Parameters in p-q diagram

The contours of the computed plastic shear strain for a loading state are shown in Figure 7-4. It appears that a rupture surface is developing beneath and to the right of the loaded area, i.e.

general shear failure. Figure 7.5 compares the bearing contact stress versus computed center displacement of the footing to the reported results (Whitman and Hoeg, 1966). For the reported boundary conditions and material properties, Vesic's bearing capacity is:

$$q_u = cN_c = 1.72 \times 5.14 = 8.84\ tsf.$$

The simulation and reported load to deformation agree with one another as well as with Vesic's estimated bearing capacity (Figure 7.5).

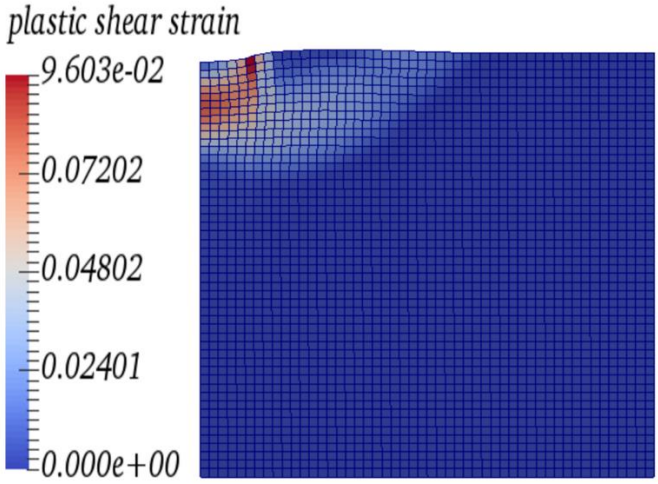

Figure 7-4. Plastic shear strain

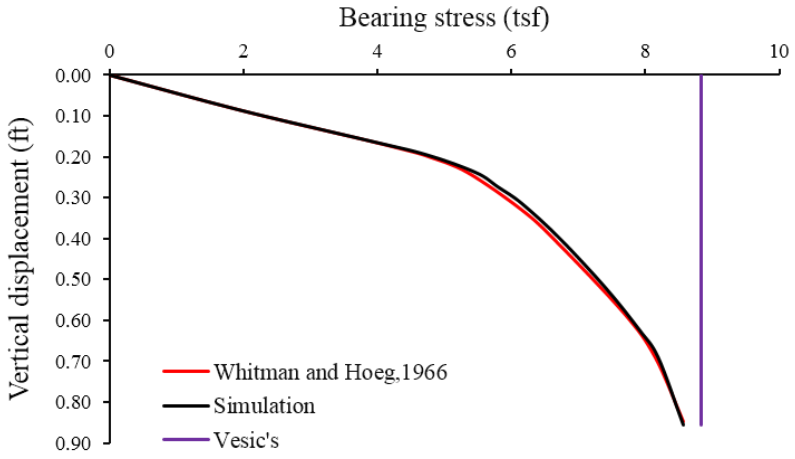

Figure 7-5. Comparison of bearing contact stress-computed center displacement curve

The second simulation involves a strip footing resting on a single layer of c - φ material (e.g. carbonate rock). Due to symmetry, only half of the layer of homogeneous material was discretized using a regular grid of quadrilateral elements, 26.5ft height and 26.5ft length (Figure 7.6 (a)). Vertical and horizontal displacements were constrained at the bottom surface. The left and right sides were fixed in horizontal directions. An external contact stress was applied to represent the strip footing. The mechanical behavior of the carbonate rock was modeled using an elastic plastic model. The material parameters used in the simulations are listed in Table 7-1. All the parameters are based on a $\tau - \sigma$ diagram and were converted from a p-q diagram (Figure 7.6 (b)).

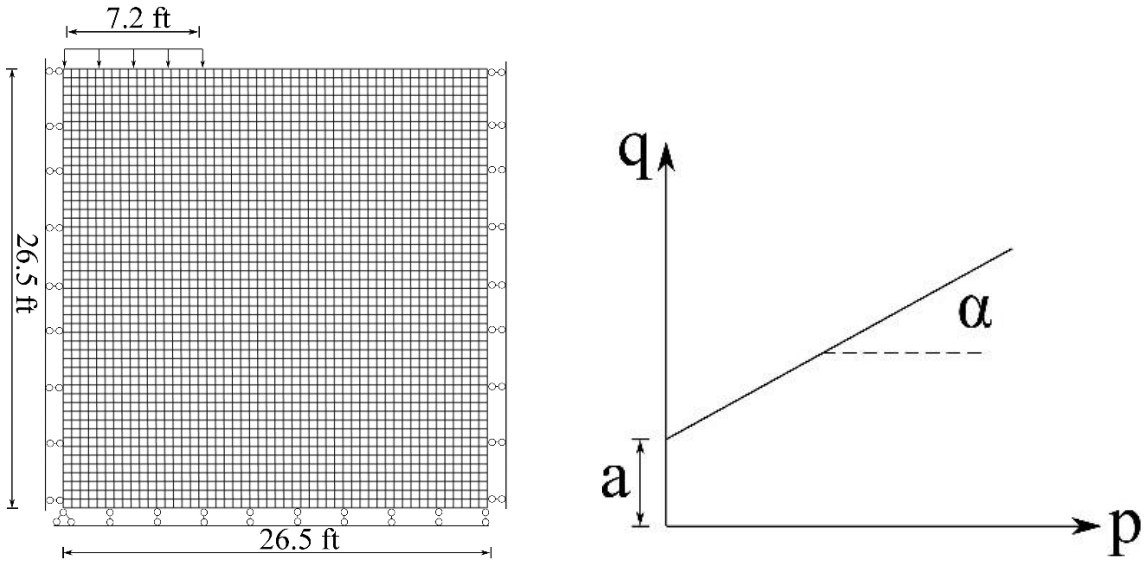

(a) (b)

Figure 7-6. (a) Geometry of meshed model and boundary conditions; (b) Parameters in p-q diagram

The Lambe and Whitman (1969) solution with the cohesion equal to $1.72tsf$ was used in the in the simulation, but a friction angles (φ) of 30°as added. The computed plastic shear strain beneath and outside of the loaded area is shown in Figure 7.7. A bearing failure slip surface, representative of generalized shear failure, is developed. Shown in Figure 7.8 is the footing contact stress versus the center displacement of the footing. As shown in Figures 7.7 and 7.8, the footing is on the verge of bearing failure. Vesic's bearing equation for this problem gives:

$$q_u = cN_c + 0.5\gamma BN_\gamma = 1.72 \times 30.14 + 0.5 \times 100 \times 14.4 \times 22.40 \times 0.0005 = 60.7 \text{ tsf.}$$

Comparison between the simulation and Vesic's bearing capacity is quite good, shown in Figure 7.8.

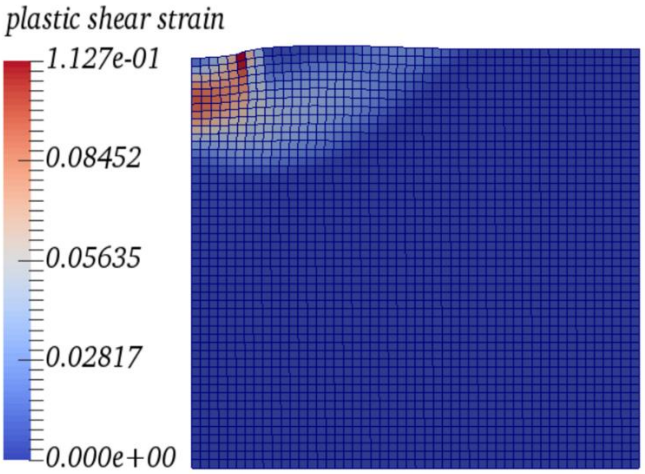

Figure 7-7. Plastic shear strain

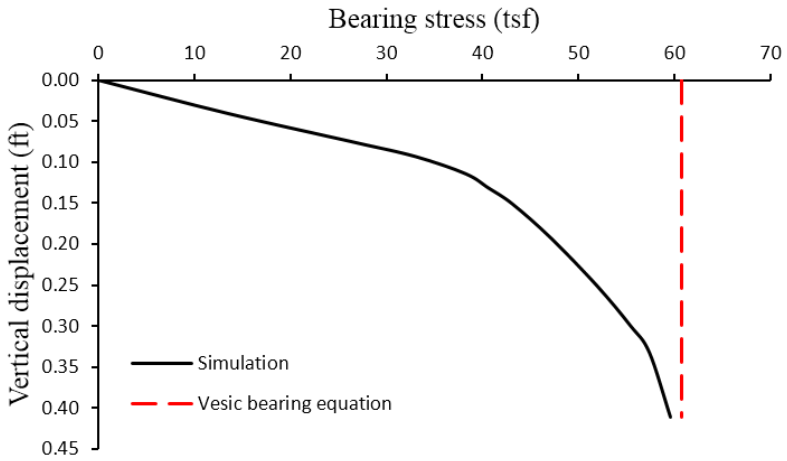

Figure 7-8. Comparison of bearing contact stress-computed center displacement curve

The third simulation for the elastic, perfectly plastic model (i.e. carbonate rock) were the laboratory 3D triaxial test results. The geometry of the 3D model mesh and boundary conditions are shown in Figure 7.9. The material parameters used in the simulations are given in Table 7-1. Results for deviatoric stress versus axial strain are given for a confining pressure equal to 200 psi, and volumetric strain versus axial strain for confining pressures equal to 50, 150, and 200 psi.

Table 7-1. Material parameters used in the simulation

	Validation of elastic, perfectly plastic model		3D triaxial test simulation
	Cohesion only material	c - φ material	
Porosity	0.4	0.3	0.3
Dry unit weight	110 pcf	110 pcf	110 pcf
Young's modulus	5,000 psi	43,511 psi	43,511 psi
Poisson's ratio	0.3	0.23	0.23
Friction angle (φ)	0^0	30^0	30^0
2^{nd} slope (ω)	0^0	30^0	0^0
Cohesion intercept	1.72 tsf	1.72 tsf	1.72 tsf

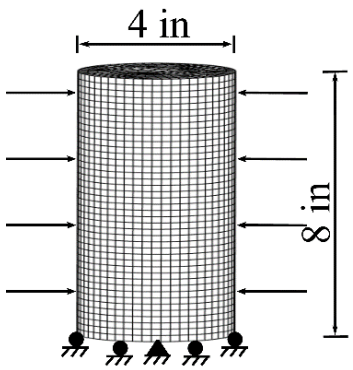

Figure 7-9. Geometry of meshed model and boundary conditions

Figure 7.10 shows the deviatoric stress versus axial strain for the 200 psi confining pressure results along with the normalized deviatoric stress (deviatoric/ confining stress) from the laboratory testing. The figure shows that the shape of the predicted deviatoric stress versus axial strain is very similar to the laboratory results (Figure 7.10b).

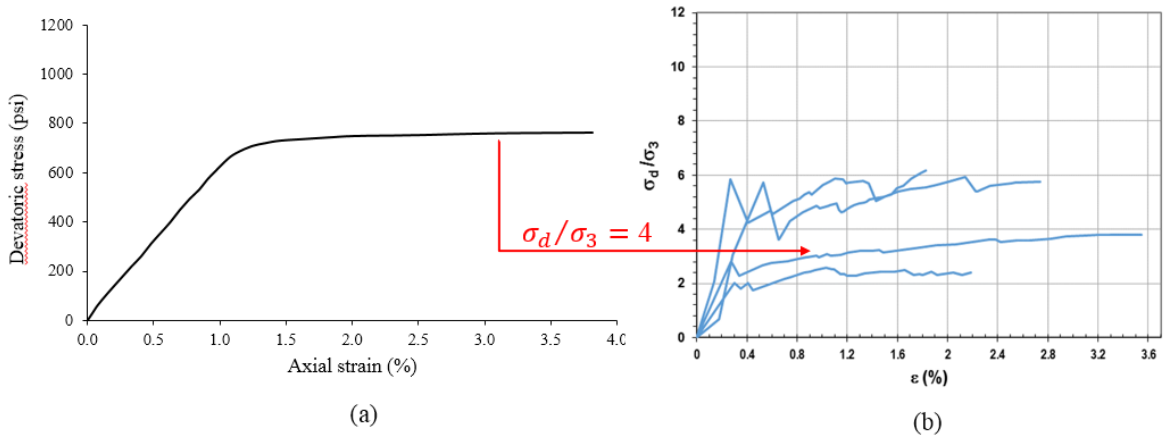

Figure 7-10. (a) Deviatoric stress vs. axial strain from FEM simulation; (b) Deviatoric stress/confining stress vs. axial strain from laboratory testing

In the case of volumetric versus axial strain at different confining stresses, the simulation using a Poisson's ratio of 0.2 matches the lower measured volumetric response (Figure 7.11b). To match the higher volumetric response, a lower Poisson's ratio of 0.1 is needed.

The lower Poisson's ratio has a significant impact on the load versus deformation results and estimated bearing capacity values. Specifically, a Poisson's ratio of 0.1 results in only local shear failure (Figure 7.7 – i.e. no plastic shear outside footprint). This results in a reduced bearing contact stresses versus displacement and much lower estimated capacities compared to Vesic's result. Since the lower Poisson's ratio is conservative (i.e. lower bearing capacity values), it will be used in the next section for the parametric studies to represent the different formations to develop a bearing capacity equation for Florida carbonate rock.

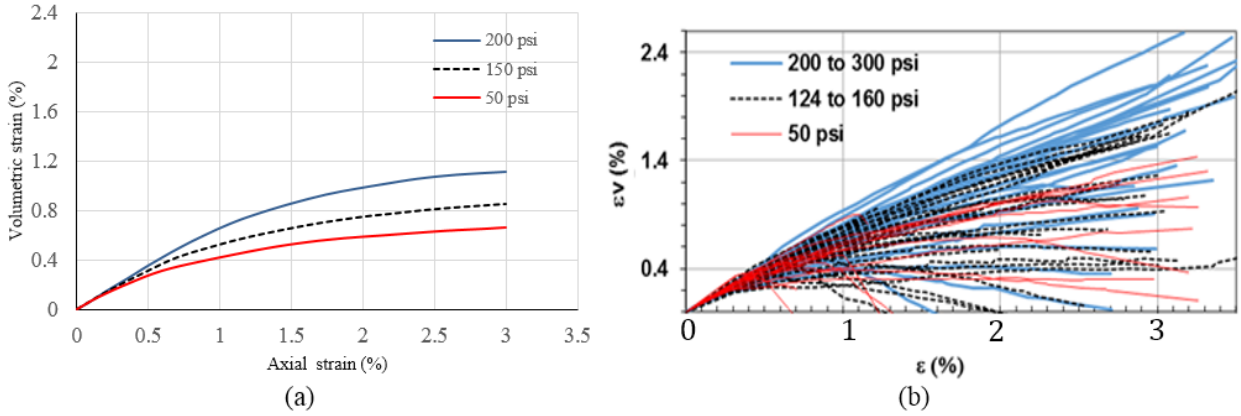

Figure 7-11. (a) Volumetric strain vs. axial strain for three different confining pressures from FEM simulation; (b) Volumetric strain vs. axial strain from laboratory testing

7.2.2. Validation of Drucker-Prager-Cap model

To characterize sand, a Drucker–Prager-Cap model was employed which captures both volumetric compression and dilation. For the validation, a strip footing resting on a sand layer was characterized. The width of the strip footing was 4m and due to symmetry, a half-model with a homogeneous soil layer of 15 m height and 15 m length (Figure 7.12) was discretized using a regular grid of quadrilateral elements. Vertical and horizontal displacements were constrained at the bottom surface. The left and right sides were fixed in horizontal directions. An external contact stress was applied to represent the strip footing.

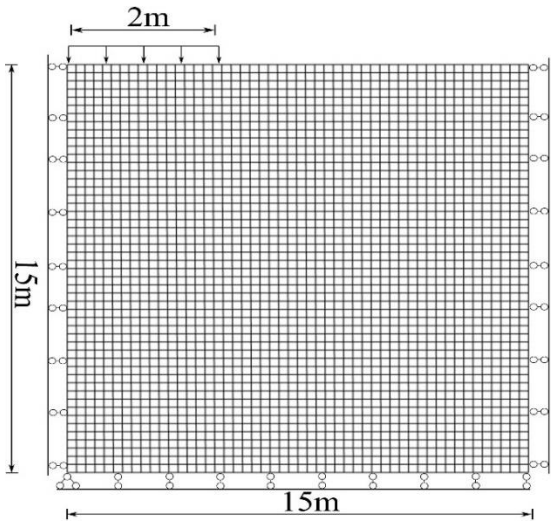

Figure 7-12. Mesh model and boundary conditions

In the simulation, the cohesion = 0, φ = 30˚, and Young's modulus was 10MPa. The dry unit weight of sand was 16.50kN/m^3. The failure mechanism is shown in the plastic shear strain plot, Figure 7.13. The simulation results (contact stress versus displacement) are given in in Figure 7.14.

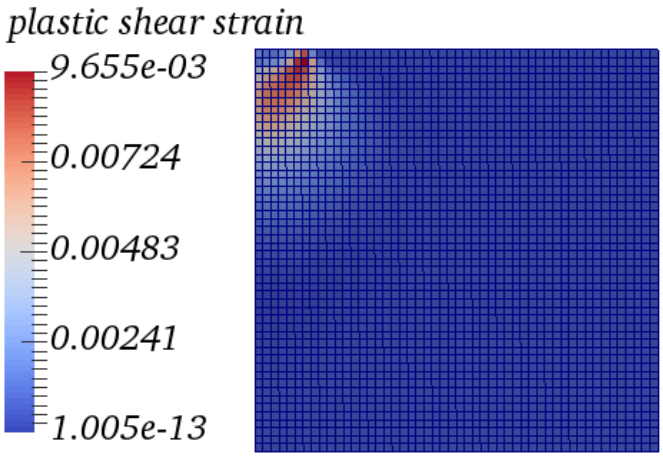

Figure 7-13. Plastic shear strain

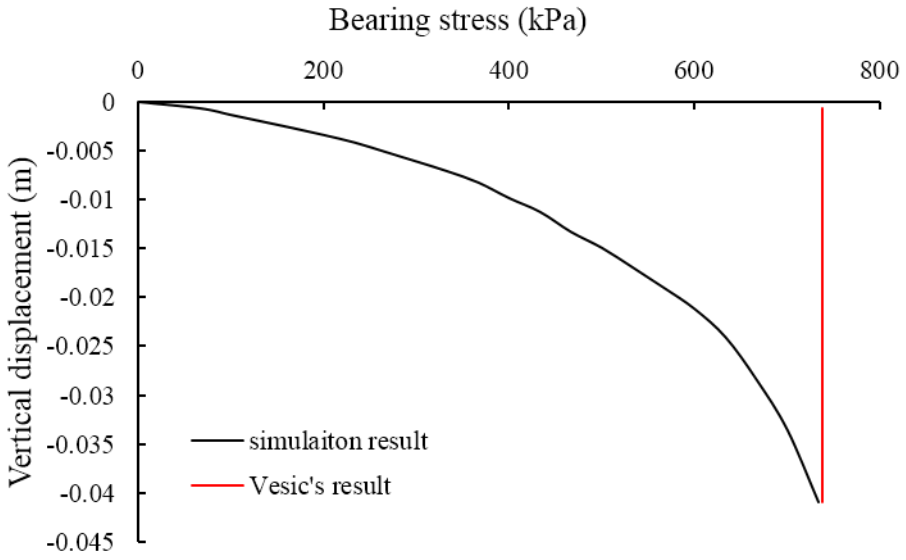

Figure 7-14. Comparison of the simulation results and Vesic's bearing equation results

Vesic's bearing capacity for this problem is given as,

$$q_u = cN_c + 0.5 \times B \times \gamma \times N_\gamma = 0 + 0.5 \times 4 \times 16.5 \times 22.4 = 739.2\ kPa$$

The simulated bearing stress results and Vesic's bearing capacity (Figure 7.14) agrees reasonably well.

7.3 Parametric Studies – Rock Subsurface

Over 300 simulations were performed to study the influence of rock parameters on the bearing capacity of strip and rectangular footings, on or within (i.e. embedded) a single layer of carbonate rock. In the parametric studies, the variables changed were cohesion intercept (c), initial friction angle (φ), second slope (ω), and σ_{peak} as shown in the Figure 7.15. All the simulations used a Poisson ratio of 0.1 as discussed in Section 3.3.2. For all of the simulations, only one parameter was changed while keeping the other three parameters constant in order to study its influence on bearing capacity.

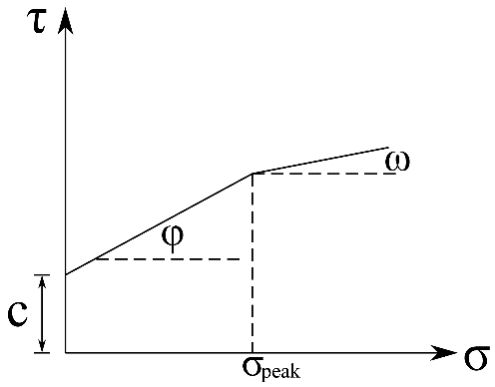

Figure 7-15. Variables in the τ - σ diagram

The meshed model and boundary conditions is shown in Figure 7-16 and Figure 7-17. For the simulations where B/L >0, a full 3D FEM mesh was used. The bottom surface was fixed in all three directions, a roller was added for surfaces # 1 and #3 (Figure 7-17) in the x-direction and another roller for surfaces # 2 and #4 in the y-direction. Table 7-2 provides the parameters in both p-q and τ-σ diagram. The results of all simulations are presented in Table 7-3.

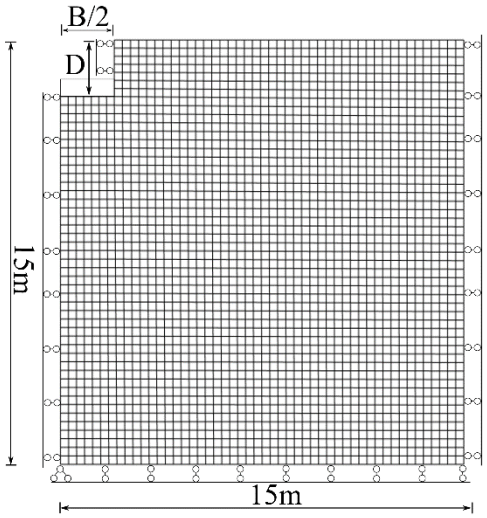

Figure 7-16. Meshed model and boundary conditions – B/L = 0 and D ≥ 0

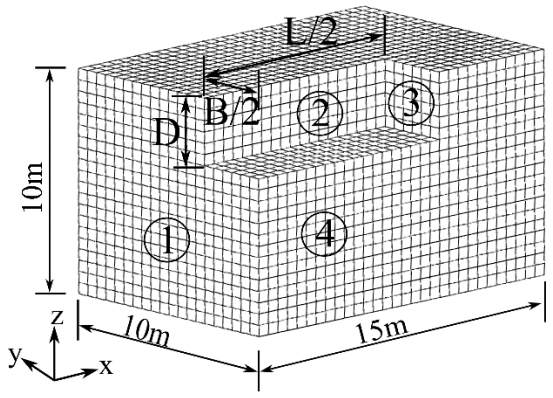

Figure 7-17. Meshed model and boundary conditions – B/L > 0 and D ≥0

Table 7-2. FEM simulation parameters

	p-q diagram						τ-σ diagram					
No.	a (MPa)	a (tsf)	α (°)	β (°)	p_p (MPa)	p_p (tsf)	c (MPa)	c (tsf)	φ (°)	ω (°)	σ_p (MPa)	σ_p (tsf)
1	0.1	1.04	27	-20	1.2	12.53	0.116	1.21	30.63	-21.34	1.91	19.94
2	0.1	1.04	27	-20	1.3	13.57	0.116	1.21	30.63	-21.34	2.06	21.51
3	0.1	1.04	27	-20	1.5	15.66	0.116	1.21	30.63	-21.34	2.36	24.64
4	0.1	1.04	27	-15	1.2	12.53	0.116	1.21	30.63	-15.54	1.91	19.94
5	0.1	1.04	27	-15	1.3	13.57	0.116	1.21	30.63	-15.54	2.06	21.51
6	0.1	1.04	27	-15	1.5	15.66	0.116	1.21	30.63	-15.54	2.36	24.64
7	0.1	1.04	27	-10	1.2	12.53	0.116	1.21	30.63	-10.16	1.91	19.94
8	0.1	1.04	27	-10	1.3	13.57	0.116	1.21	30.63	-10.16	2.06	21.51
9	0.1	1.04	27	-10	1.5	15.66	0.116	1.21	30.63	-10.16	2.36	24.64
10	0.1	1.04	27	-5	1.2	12.53	0.116	1.21	30.63	-5.02	1.91	19.94
11	0.1	1.04	27	-5	1.3	13.57	0.116	1.21	30.63	-5.02	2.06	21.51
12	0.1	1.04	27	-5	1.5	15.66	0.116	1.21	30.63	-5.02	2.36	24.64
13	0.1	1.04	27	0	1.2	12.53	0.116	1.21	30.63	0.00	1.91	19.94
14	0.1	1.04	27	0	1.3	13.57	0.116	1.21	30.63	0.00	2.06	21.51
15	0.1	1.04	27	0	1.5	15.66	0.116	1.21	30.63	0.00	2.36	24.64
16	0.1	1.04	27	5	1.2	12.53	0.116	1.21	30.63	5.02	1.91	19.94
17	0.1	1.04	27	5	1.3	13.57	0.116	1.21	30.63	5.02	2.06	21.51
18	0.1	1.04	27	5	1.5	15.66	0.116	1.21	30.63	5.02	2.36	24.64
19	0.1	1.04	27	10	1.2	12.53	0.116	1.21	30.63	10.16	1.91	19.94
20	0.1	1.04	27	10	1.3	13.57	0.116	1.21	30.63	10.16	2.06	21.51
21	0.1	1.04	27	10	1.5	15.66	0.116	1.21	30.63	10.16	2.36	24.64
22	0.1	1.04	27	15	1.2	12.53	0.116	1.21	30.63	15.54	1.91	19.94
23	0.1	1.04	27	15	1.3	13.57	0.116	1.21	30.63	15.54	2.06	21.51
24	0.1	1.04	27	15	1.5	15.66	0.116	1.21	30.63	15.54	2.36	24.64
25	0.1	1.04	27	20	1.2	12.53	0.116	1.21	30.63	21.34	1.91	19.94
26	0.1	1.04	27	20	1.3	13.57	0.116	1.21	30.63	21.34	2.06	21.51
27	0.1	1.04	27	20	1.5	15.66	0.116	1.21	30.63	21.34	2.36	24.64
28	0.1	1.04	31	-20	1.2	12.53	0.125	1.31	36.93	-21.34	2.02	21.09
29	0.1	1.04	31	-20	1.3	13.57	0.125	1.31	36.93	-21.34	2.18	22.76
30	0.1	1.04	31	-20	1.5	15.66	0.125	1.31	36.93	-21.34	2.5	26.10
31	0.1	1.04	31	-15	1.2	12.53	0.125	1.31	36.93	-15.54	2.02	21.09
32	0.1	1.04	31	-15	1.3	13.57	0.125	1.31	36.93	-15.54	2.18	22.76
33	0.1	1.04	31	-15	1.5	15.66	0.125	1.31	36.93	-15.54	2.5	26.10
34	0.1	1.04	31	-10	1.2	12.53	0.125	1.31	36.93	-10.16	2.02	21.09
35	0.1	1.04	31	-10	1.3	13.57	0.125	1.31	36.93	-10.16	2.18	22.76
36	0.1	1.04	31	-10	1.5	15.66	0.125	1.31	36.93	-10.16	2.5	26.10
37	0.1	1.04	31	-5	1.2	12.53	0.125	1.31	36.93	-5.02	2.02	21.09

Table 7-2. Continued

	p-q diagram						τ-σ diagram					
No.	a (MPa)	a (tsf)	α (°)	β (°)	p_p (MPa)	p_p (tsf)	c (MPa)	c (tsf)	φ (°)	ω (°)	σ_p (MPa)	σ_p (tsf)
38	0.1	1.04	31	-5	1.3	13.57	0.125	1.31	36.93	-5.02	2.18	22.76
39	0.1	1.04	31	-5	1.5	15.66	0.125	1.31	36.93	-5.02	2.5	26.10
40	0.1	1.04	31	0	1.2	12.53	0.125	1.31	36.93	0.00	2.02	21.09
41	0.1	1.04	31	0	1.3	13.57	0.125	1.31	36.93	0.00	2.18	22.76
42	0.1	1.04	31	0	1.5	15.66	0.125	1.31	36.93	0.00	2.5	26.10
43	0.1	1.04	31	5	1.2	12.53	0.125	1.31	36.93	5.02	2.02	21.09
44	0.1	1.04	31	5	1.3	13.57	0.125	1.31	36.93	5.02	2.18	22.76
45	0.1	1.04	31	5	1.5	15.66	0.125	1.31	36.93	5.02	2.5	26.10
46	0.1	1.04	31	10	1.2	12.53	0.125	1.31	36.93	10.16	2.02	21.09
47	0.1	1.04	31	10	1.3	13.57	0.125	1.31	36.93	10.16	2.18	22.76
48	0.1	1.04	31	10	1.5	15.66	0.125	1.31	36.93	10.16	2.5	26.10
49	0.1	1.04	31	15	1.2	12.53	0.125	1.31	36.93	15.54	2.02	21.09
50	0.1	1.04	31	15	1.3	13.57	0.125	1.31	36.93	15.54	2.18	22.76
51	0.1	1.04	31	15	1.5	15.66	0.125	1.31	36.93	15.54	2.5	26.10
52	0.1	1.04	31	20	1.2	12.53	0.125	1.31	36.93	21.34	2.02	21.09
53	0.1	1.04	31	20	1.3	13.57	0.125	1.31	36.93	21.34	2.18	22.76
54	0.1	1.04	31	20	1.5	15.66	0.125	1.31	36.93	21.34	2.5	26.10
55	0.1	1.04	35	-20	1.2	12.53	0.140	1.46	44.44	-21.34	2.14	22.34
56	0.1	1.04	35	-20	1.3	13.57	0.140	1.46	44.44	-21.34	2.31	24.12
57	0.1	1.04	35	-20	1.5	15.66	0.140	1.46	44.44	-21.34	2.65	27.67
58	0.1	1.04	35	-15	1.2	12.53	0.140	1.46	44.44	-15.54	2.14	22.34
59	0.1	1.04	35	-15	1.3	13.57	0.140	1.46	44.44	-15.54	2.31	24.12
60	0.1	1.04	35	-15	1.5	15.66	0.140	1.46	44.44	-15.54	2.65	27.67
61	0.1	1.04	35	-10	1.2	12.53	0.140	1.46	44.44	-10.16	2.14	22.34
62	0.1	1.04	35	-10	1.3	13.57	0.140	1.46	44.44	-10.16	2.31	24.12
63	0.1	1.04	35	-10	1.5	15.66	0.140	1.46	44.44	-10.16	2.65	27.67
64	0.1	1.04	35	-5	1.2	12.53	0.140	1.46	44.44	-5.02	2.14	22.34
65	0.1	1.04	35	-5	1.3	13.57	0.140	1.46	44.44	-5.02	2.31	24.12
66	0.1	1.04	35	-5	1.5	15.66	0.140	1.46	44.44	-5.02	2.65	27.67
67	0.1	1.04	35	0	1.2	12.53	0.140	1.46	44.44	0.00	2.14	22.34
68	0.1	1.04	35	0	1.3	13.57	0.140	1.46	44.44	0.00	2.31	24.12
69	0.1	1.04	35	0	1.5	15.66	0.140	1.46	44.44	0.00	2.65	27.67
70	0.1	1.04	35	5	1.2	12.53	0.140	1.46	44.44	5.02	2.14	22.34
71	0.1	1.04	35	5	1.3	13.57	0.140	1.46	44.44	5.02	2.31	24.12
72	0.1	1.04	35	5	1.5	15.66	0.140	1.46	44.44	5.02	2.65	27.67
73	0.1	1.04	35	10	1.2	12.53	0.140	1.46	44.44	10.16	2.14	22.34
74	0.1	1.04	35	10	1.3	13.57	0.140	1.46	44.44	10.16	2.31	24.12
75	0.1	1.04	35	10	1.5	15.66	0.140	1.46	44.44	10.16	2.65	27.67
76	0.1	1.04	35	15	1.2	12.53	0.140	1.46	44.44	15.54	2.14	22.34
77	0.1	1.04	35	15	1.3	13.57	0.140	1.46	44.44	15.54	2.31	24.12
78	0.1	1.04	35	15	1.5	15.66	0.140	1.46	44.44	15.54	2.65	27.67
79	0.1	1.04	35	20	1.2	12.53	0.140	1.46	44.44	21.34	2.14	22.34
80	0.1	1.04	35	20	1.3	13.57	0.140	1.46	44.44	21.34	2.31	24.12
81	0.1	1.04	35	20	1.5	15.66	0.140	1.46	44.44	21.34	2.65	27.67
82	0.1	1.04	38	-20	1.2	12.53	0.160	1.67	51.38	-21.34	2.24	23.39
83	0.1	1.04	38	-20	1.3	13.57	0.160	1.67	51.38	-21.34	2.42	25.26
84	0.1	1.04	38	-20	1.5	15.66	0.160	1.67	51.38	-21.34	2.77	28.92
85	0.1	1.04	38	-15	1.2	12.53	0.160	1.67	51.38	-15.54	2.24	23.39
86	0.1	1.04	38	-15	1.3	13.57	0.160	1.67	51.38	-15.54	2.42	25.26
87	0.1	1.04	38	-15	1.5	15.66	0.160	1.67	51.38	-15.54	2.77	28.92
88	0.1	1.04	38	-10	1.2	12.53	0.160	1.67	51.38	-10.16	2.24	23.39
89	0.1	1.04	38	-10	1.3	13.57	0.160	1.67	51.38	-10.16	2.42	25.26
90	0.1	1.04	38	-10	1.5	15.66	0.160	1.67	51.38	-10.16	2.77	28.92
91	0.1	1.04	38	-5	1.2	12.53	0.160	1.67	51.38	-5.02	2.24	23.39
92	0.1	1.04	38	-5	1.3	13.57	0.160	1.67	51.38	-5.02	2.42	25.26

Table 7-2. Continued

	p-q diagram						τ-σ diagram					
No.	a (MPa)	a (tsf)	α (°)	β (°)	p_p (MPa)	p_p (tsf)	c (MPa)	c (tsf)	φ (°)	ω (°)	σ_p (MPa)	σ_p (tsf)
93	0.1	1.04	38	-5	1.5	15.66	0.160	1.67	51.38	-5.02	2.77	28.92
94	0.1	1.04	38	0	1.2	12.53	0.160	1.67	51.38	0.00	2.24	23.39
95	0.1	1.04	38	0	1.3	13.57	0.160	1.67	51.38	0.00	2.42	25.26
96	0.1	1.04	38	0	1.5	15.66	0.160	1.67	51.38	0.00	2.77	28.92
97	0.1	1.04	38	5	1.2	12.53	0.160	1.67	51.38	5.02	2.24	23.39
98	0.1	1.04	38	5	1.3	13.57	0.160	1.67	51.38	5.02	2.42	25.26
99	0.1	1.04	38	5	1.5	15.66	0.160	1.67	51.38	5.02	2.77	28.92
100	0.1	1.04	38	10	1.2	12.53	0.160	1.67	51.38	10.16	2.24	23.39
101	0.1	1.04	38	10	1.3	13.57	0.160	1.67	51.38	10.16	2.42	25.26
102	0.1	1.04	38	10	1.5	15.66	0.160	1.67	51.38	10.16	2.77	28.92
103	0.1	1.04	38	15	1.2	12.53	0.160	1.67	51.38	15.54	2.24	23.39
104	0.1	1.04	38	15	1.3	13.57	0.160	1.67	51.38	15.54	2.42	25.26
105	0.1	1.04	38	15	1.5	15.66	0.160	1.67	51.38	15.54	2.77	28.92
106	0.1	1.04	38	20	1.2	12.53	0.160	1.67	51.38	21.34	2.24	23.39
107	0.1	1.04	38	20	1.3	13.57	0.160	1.67	51.38	21.34	2.42	25.26
108	0.1	1.04	38	20	1.5	15.66	0.160	1.67	51.38	21.34	2.77	28.92
109	0.5	5.22	27	-20	2	20.88	0.581	6.07	30.63	-21.34	3.52	36.75
110	0.5	5.22	27	-20	2.5	26.10	0.581	6.07	30.63	-21.34	4.27	44.58
111	0.5	5.22	27	-20	3	31.32	0.581	6.07	30.63	-21.34	5.02	52.41
112	0.5	5.22	27	-15	2	20.88	0.581	6.07	30.63	-15.54	3.52	36.75
113	0.5	5.22	27	-15	2.5	26.10	0.581	6.07	30.63	-15.54	4.27	44.58
114	0.5	5.22	27	-15	3	31.32	0.581	6.07	30.63	-15.54	5.02	52.41
115	0.5	5.22	27	-10	2	20.88	0.581	6.07	30.63	-10.16	3.52	36.75
116	0.5	5.22	27	-10	2.5	26.10	0.581	6.07	30.63	-10.16	4.27	44.58
117	0.5	5.22	27	-10	3	31.32	0.581	6.07	30.63	-10.16	5.02	52.41
118	0.5	5.22	27	-5	2	20.88	0.581	6.07	30.63	-5.02	3.52	36.75
119	0.5	5.22	27	-5	2.5	26.10	0.581	6.07	30.63	-5.02	4.27	44.58
120	0.5	5.22	27	-5	3	31.32	0.581	6.07	30.63	-5.02	5.02	52.41
121	0.5	5.22	27	0	2	20.88	0.581	6.07	30.63	0.00	3.52	36.75
122	0.5	5.22	27	0	2.5	26.10	0.581	6.07	30.63	0.00	4.27	44.58
123	0.5	5.22	27	0	3	31.32	0.581	6.07	30.63	0.00	5.02	52.41
124	0.5	5.22	27	5	2	20.88	0.581	6.07	30.63	5.02	3.52	36.75
125	0.5	5.22	27	5	2.5	26.10	0.581	6.07	30.63	5.02	4.27	44.58
126	0.5	5.22	27	5	3	31.32	0.581	6.07	30.63	5.02	5.02	52.41
127	0.5	5.22	27	10	2	20.88	0.581	6.07	30.63	10.16	3.52	36.75
128	0.5	5.22	27	10	2.5	26.10	0.581	6.07	30.63	10.16	4.27	44.58
129	0.5	5.22	27	10	3	31.32	0.581	6.07	30.63	10.16	5.02	52.41
130	0.5	5.22	27	15	2	20.88	0.581	6.07	30.63	15.54	3.52	36.75
131	0.5	5.22	27	15	2.5	26.10	0.581	6.07	30.63	15.54	4.27	44.58
132	0.5	5.22	27	15	3	31.32	0.581	6.07	30.63	15.54	5.02	52.41
133	0.5	5.22	27	20	2	20.88	0.581	6.07	30.63	21.34	3.52	36.75
134	0.5	5.22	27	20	2.5	26.10	0.581	6.07	30.63	21.34	4.27	44.58
135	0.5	5.22	27	20	3	31.32	0.581	6.07	30.63	21.34	5.02	52.41
136	0.5	5.22	31	-20	2	20.88	0.626	6.54	36.93	-21.34	3.7	38.63
137	0.5	5.22	31	-20	2.5	26.10	0.626	6.54	36.93	-21.34	4.5	46.98
138	0.5	5.22	31	-20	3	31.32	0.626	6.54	36.93	-21.34	5.3	55.33
139	0.5	5.22	31	-15	2	20.88	0.626	6.54	36.93	-15.54	3.7	38.63
140	0.5	5.22	31	-15	2.5	26.10	0.626	6.54	36.93	-15.54	4.5	46.98
141	0.5	5.22	31	-15	3	31.32	0.626	6.54	36.93	-15.54	5.3	55.33
142	0.5	5.22	31	-10	2	20.88	0.626	6.54	36.93	-10.16	3.7	38.63
143	0.5	5.22	31	-10	2.5	26.10	0.626	6.54	36.93	-10.16	4.5	46.98
144	0.5	5.22	31	-10	3	31.32	0.626	6.54	36.93	-10.16	5.3	55.33
145	0.5	5.22	31	-5	2	20.88	0.626	6.54	36.93	-5.02	3.7	38.63
146	0.5	5.22	31	-5	2.5	26.10	0.626	6.54	36.93	-5.02	4.5	46.98
147	0.5	5.22	31	-5	3	31.32	0.626	6.54	36.93	-5.02	5.3	55.33

Table 7-2. Continued

	p-q diagram						τ-σ diagram					
No.	a (MPa)	a (tsf)	α (°)	β (°)	p_p (MPa)	p_p (tsf)	c (MPa)	c (tsf)	φ (°)	ω (°)	σ_p (MPa)	σ_p (tsf)
148	0.5	5.22	31	0	2	20.88	0.626	6.54	36.93	0.00	3.7	38.63
149	0.5	5.22	31	0	2.5	26.10	0.626	6.54	36.93	0.00	4.5	46.98
150	0.5	5.22	31	0	3	31.32	0.626	6.54	36.93	0.00	5.3	55.33
151	0.5	5.22	31	5	2	20.88	0.626	6.54	36.93	5.02	3.7	38.63
152	0.5	5.22	31	5	2.5	26.10	0.626	6.54	36.93	5.02	4.5	46.98
153	0.5	5.22	31	5	3	31.32	0.626	6.54	36.93	5.02	5.3	55.33
154	0.5	5.22	31	10	2	20.88	0.626	6.54	36.93	10.16	3.7	38.63
155	0.5	5.22	31	10	2.5	26.10	0.626	6.54	36.93	10.16	4.5	46.98
156	0.5	5.22	31	10	3	31.32	0.626	6.54	36.93	10.16	5.3	55.33
157	0.5	5.22	31	15	2	20.88	0.626	6.54	36.93	15.54	3.7	38.63
158	0.5	5.22	31	15	2.5	26.10	0.626	6.54	36.93	15.54	4.5	46.98
159	0.5	5.22	31	15	3	31.32	0.626	6.54	36.93	15.54	5.3	55.33
160	0.5	5.22	31	20	2	20.88	0.626	6.54	36.93	21.34	3.7	38.63
161	0.5	5.22	31	20	2.5	26.10	0.626	6.54	36.93	21.34	4.5	46.98
162	0.5	5.22	31	20	3	31.32	0.626	6.54	36.93	21.34	5.3	55.33
163	0.5	5.22	35	-20	2	20.88	0.700	7.31	44.44	-21.34	3.9	40.72
164	0.5	5.22	35	-20	2.5	26.10	0.700	7.31	44.44	-21.34	4.73	49.38
165	0.5	5.22	35	-20	3	31.32	0.700	7.31	44.44	-21.34	5.6	58.46
166	0.5	5.22	35	-15	2	20.88	0.700	7.31	44.44	-15.54	3.9	40.72
167	0.5	5.22	35	-15	2.5	26.10	0.700	7.31	44.44	-15.54	4.73	49.38
168	0.5	5.22	35	-15	3	31.32	0.700	7.31	44.44	-15.54	5.6	58.46
169	0.5	5.22	35	-10	2	20.88	0.700	7.31	44.44	-10.16	3.9	40.72
170	0.5	5.22	35	-10	2.5	26.10	0.700	7.31	44.44	-10.16	4.73	49.38
171	0.5	5.22	35	-10	3	31.32	0.700	7.31	44.44	-10.16	5.6	58.46
172	0.5	5.22	35	-5	2	20.88	0.700	7.31	44.44	-5.02	3.9	40.72
173	0.5	5.22	35	-5	2.5	26.10	0.700	7.31	44.44	-5.02	4.73	49.38
174	0.5	5.22	35	-5	3	31.32	0.700	7.31	44.44	-5.02	5.6	58.46
175	0.5	5.22	35	0	2	20.88	0.700	7.31	44.44	0.00	3.9	40.72
176	0.5	5.22	35	0	2.5	26.10	0.700	7.31	44.44	0.00	4.73	49.38
177	0.5	5.22	35	0	3	31.32	0.700	7.31	44.44	0.00	5.6	58.46
178	0.5	5.22	35	5	2	20.88	0.700	7.31	44.44	5.02	3.9	40.72
179	0.5	5.22	35	5	2.5	26.10	0.700	7.31	44.44	5.02	4.73	49.38
180	0.5	5.22	35	5	3	31.32	0.700	7.31	44.44	5.02	5.6	58.46
181	0.5	5.22	35	10	2	20.88	0.700	7.31	44.44	10.16	3.9	40.72
182	0.5	5.22	35	10	2.5	26.10	0.700	7.31	44.44	10.16	4.73	49.38
183	0.5	5.22	35	10	3	31.32	0.700	7.31	44.44	10.16	5.6	58.46
184	0.5	5.22	35	15	2	20.88	0.700	7.31	44.44	15.54	3.9	40.72
185	0.5	5.22	35	15	2.5	26.10	0.700	7.31	44.44	15.54	4.73	49.38
186	0.5	5.22	35	15	3	31.32	0.700	7.31	44.44	15.54	5.6	58.46
187	0.5	5.22	35	20	2	20.88	0.700	7.31	44.44	21.34	3.9	40.72
188	0.5	5.22	35	20	2.5	26.10	0.700	7.31	44.44	21.34	4.73	49.38
189	0.5	5.22	35	20	3	31.32	0.700	7.31	44.44	21.34	5.6	58.46
190	0.5	5.22	38	-20	2	20.88	0.801	8.36	51.38	-21.34	4.06	42.39
191	0.5	5.22	38	-20	2.5	26.10	0.801	8.36	51.38	-21.34	4.95	51.68
192	0.5	5.22	38	-20	3	31.32	0.801	8.36	51.38	-21.34	5.84	60.97
193	0.5	5.22	38	-15	2	20.88	0.801	8.36	51.38	-15.54	4.06	42.39
194	0.5	5.22	38	-15	2.5	26.10	0.801	8.36	51.38	-15.54	4.95	51.68
195	0.5	5.22	38	-15	3	31.32	0.801	8.36	51.38	-15.54	5.84	60.97
196	0.5	5.22	38	-10	2	20.88	0.801	8.36	51.38	-10.16	4.06	42.39
197	0.5	5.22	38	-10	2.5	26.10	0.801	8.36	51.38	-10.16	4.95	51.68
198	0.5	5.22	38	-10	3	31.32	0.801	8.36	51.38	-10.16	5.84	60.97
199	0.5	5.22	38	-5	2	20.88	0.801	8.36	51.38	-5.02	4.06	42.39
200	0.5	5.22	38	-5	2.5	26.10	0.801	8.36	51.38	-5.02	4.95	51.68
201	0.5	5.22	38	-5	3	31.32	0.801	8.36	51.38	-5.02	5.84	60.97
202	0.5	5.22	38	0	2	20.88	0.801	8.36	51.38	0.00	4.06	42.39

Table 7-2. Continued

	p-q diagram						τ-σ diagram					
No.	a (MPa)	a (tsf)	α (°)	β (°)	p_p (MPa)	p_p (tsf)	c (MPa)	c (tsf)	φ (°)	ω (°)	σ_p (MPa)	σ_p (tsf)
203	0.5	5.22	38	0	2.5	26.10	0.801	8.36	51.38	0.00	4.95	51.68
204	0.5	5.22	38	0	3	31.32	0.801	8.36	51.38	0.00	5.84	60.97
205	0.5	5.22	38	5	2	20.88	0.801	8.36	51.38	5.02	4.06	42.39
206	0.5	5.22	38	5	2.5	26.10	0.801	8.36	51.38	5.02	4.95	51.68
207	0.5	5.22	38	5	3	31.32	0.801	8.36	51.38	5.02	5.84	60.97
208	0.5	5.22	38	10	2	20.88	0.801	8.36	51.38	10.16	4.06	42.39
209	0.5	5.22	38	10	2.5	26.10	0.801	8.36	51.38	10.16	4.95	51.68
210	0.5	5.22	38	10	3	31.32	0.801	8.36	51.38	10.16	5.84	60.97
211	0.5	5.22	38	15	2	20.88	0.801	8.36	51.38	15.54	4.06	42.39
212	0.5	5.22	38	15	2.5	26.10	0.801	8.36	51.38	15.54	4.95	51.68
213	0.5	5.22	38	15	3	31.32	0.801	8.36	51.38	15.54	5.84	60.97
214	0.5	5.22	38	20	2	20.88	0.801	8.36	51.38	21.34	4.06	42.39
215	0.5	5.22	38	20	2.5	26.10	0.801	8.36	51.38	21.34	4.95	51.68
216	0.5	5.22	38	20	3	31.32	0.801	8.36	51.38	21.34	5.84	60.97
217	0.7	7.31	27	-20	3	31.32	0.814	8.50	30.63	-21.34	5.22	54.50
218	0.7	7.31	27	-20	3.5	36.54	0.814	8.50	30.63	-21.34	5.98	62.43
219	0.7	7.31	27	-20	4	41.76	0.814	8.50	30.63	-21.34	6.73	70.26
220	0.7	7.31	27	-15	3	31.32	0.814	8.50	30.63	-15.54	5.22	54.50
221	0.7	7.31	27	-15	3.5	36.54	0.814	8.50	30.63	-15.54	5.98	62.43
222	0.7	7.31	27	-15	4	41.76	0.814	8.50	30.63	-15.54	6.73	70.26
223	0.7	7.31	27	-10	3	31.32	0.814	8.50	30.63	-10.16	5.22	54.50
224	0.7	7.31	27	-10	3.5	36.54	0.814	8.50	30.63	-10.16	5.98	62.43
225	0.7	7.31	27	-10	4	41.76	0.814	8.50	30.63	-10.16	6.73	70.26
226	0.7	7.31	27	-5	3	31.32	0.814	8.50	30.63	-5.02	5.22	54.50
227	0.7	7.31	27	-5	3.5	36.54	0.814	8.50	30.63	-5.02	5.98	62.43
228	0.7	7.31	27	-5	4	41.76	0.814	8.50	30.63	-5.02	6.73	70.26
229	0.7	7.31	27	0	3	31.32	0.814	8.50	30.63	0.00	5.22	54.50
230	0.7	7.31	27	0	3.5	36.54	0.814	8.50	30.63	0.00	5.98	62.43
231	0.7	7.31	27	0	4	41.76	0.814	8.50	30.63	0.00	6.73	70.26
232	0.7	7.31	27	5	3	31.32	0.814	8.50	30.63	5.02	5.22	54.50
233	0.7	7.31	27	5	3.5	36.54	0.814	8.50	30.63	5.02	5.98	62.43
234	0.7	7.31	27	5	4	41.76	0.814	8.50	30.63	5.02	6.73	70.26
235	0.7	7.31	27	10	3	31.32	0.814	8.50	30.63	10.16	5.22	54.50
236	0.7	7.31	27	10	3.5	36.54	0.814	8.50	30.63	10.16	5.98	62.43
237	0.7	7.31	27	10	4	41.76	0.814	8.50	30.63	10.16	6.73	70.26
238	0.7	7.31	27	15	3	31.32	0.814	8.50	30.63	15.54	5.22	54.50
239	0.7	7.31	27	15	3.5	36.54	0.814	8.50	30.63	15.54	5.98	62.43
240	0.7	7.31	27	15	4	41.76	0.814	8.50	30.63	15.54	6.73	70.26
241	0.7	7.31	27	20	3	31.32	0.814	8.50	30.63	21.34	5.22	54.50
242	0.7	7.31	27	20	3.5	36.54	0.814	8.50	30.63	21.34	5.98	62.43
243	0.7	7.31	27	20	4	41.76	0.814	8.50	30.63	21.34	6.73	70.26
244	0.7	7.31	31	-20	3	31.32	0.876	9.15	36.93	-21.34	5.5	57.42
245	0.7	7.31	31	-20	3.5	36.54	0.876	9.15	36.93	-21.34	6.3	65.77
246	0.7	7.31	31	-20	4	41.76	0.876	9.15	36.93	-21.34	7.1	74.12
247	0.7	7.31	31	-15	3	31.32	0.876	9.15	36.93	-15.54	5.5	57.42
248	0.7	7.31	31	-15	3.5	36.54	0.876	9.15	36.93	-15.54	6.3	65.77
249	0.7	7.31	31	-15	4	41.76	0.876	9.15	36.93	-15.54	7.1	74.12
250	0.7	7.31	31	-10	3	31.32	0.876	9.15	36.93	-10.16	5.5	57.42
251	0.7	7.31	31	-10	3.5	36.54	0.876	9.15	36.93	-10.16	6.3	65.77
252	0.7	7.31	31	-10	4	41.76	0.876	9.15	36.93	-10.16	7.1	74.12
253	0.7	7.31	31	-5	3	31.32	0.876	9.15	36.93	-5.02	5.5	57.42
254	0.7	7.31	31	-5	3.5	36.54	0.876	9.15	36.93	-5.02	6.3	65.77
255	0.7	7.31	31	-5	4	41.76	0.876	9.15	36.93	-5.02	7.1	74.12
256	0.7	7.31	31	0	3	31.32	0.876	9.15	36.93	0.00	5.5	57.42
257	0.7	7.31	31	0	3.5	36.54	0.876	9.15	36.93	0.00	6.3	65.77

Table 7-2. Continued

	p-q diagram						τ-σ diagram					
No.	a (MPa)	a (tsf)	α (°)	β (°)	p_p (MPa)	p_p (tsf)	c (MPa)	c (tsf)	φ (°)	ω (°)	σ_p (MPa)	σ_p (tsf)
258	0.7	7.31	31	0	4	41.76	0.876	9.15	36.93	0.00	7.1	74.12
259	0.7	7.31	31	5	3	31.32	0.876	9.15	36.93	5.02	5.5	57.42
260	0.7	7.31	31	5	3.5	36.54	0.876	9.15	36.93	5.02	6.3	65.77
261	0.7	7.31	31	5	4	41.76	0.876	9.15	36.93	5.02	7.1	74.12
262	0.7	7.31	31	10	3	31.32	0.876	9.15	36.93	10.16	5.5	57.42
263	0.7	7.31	31	10	3.5	36.54	0.876	9.15	36.93	10.16	6.3	65.77
264	0.7	7.31	31	10	4	41.76	0.876	9.15	36.93	10.16	7.1	74.12
265	0.7	7.31	31	15	3	31.32	0.876	9.15	36.93	15.54	5.5	57.42
266	0.7	7.31	31	15	3.5	36.54	0.876	9.15	36.93	15.54	6.3	65.77
267	0.7	7.31	31	15	4	41.76	0.876	9.15	36.93	15.54	7.1	74.12
268	0.7	7.31	31	20	3	31.32	0.876	9.15	36.93	21.34	5.5	57.42
269	0.7	7.31	31	20	3.5	36.54	0.876	9.15	36.93	21.34	6.3	65.77
270	0.7	7.31	31	20	4	41.76	0.876	9.15	36.93	21.34	7.1	74.12
271	0.7	7.31	35	-20	3	31.32	0.980	10.23	44.44	-21.34	5.8	60.55
272	0.7	7.31	35	-20	3.5	36.54	0.980	10.23	44.44	-21.34	6.65	69.43
273	0.7	7.31	35	-20	4	41.76	0.980	10.23	44.44	-21.34	7.5	78.30
274	0.7	7.31	35	-15	3	31.32	0.980	10.23	44.44	-15.54	5.8	60.55
275	0.7	7.31	35	-15	3.5	36.54	0.980	10.23	44.44	-15.54	6.65	69.43
276	0.7	7.31	35	-15	4	41.76	0.980	10.23	44.44	-15.54	7.5	78.30
277	0.7	7.31	35	-10	3	31.32	0.980	10.23	44.44	-10.16	5.8	60.55
278	0.7	7.31	35	-10	3.5	36.54	0.980	10.23	44.44	-10.16	6.65	69.43
279	0.7	7.31	35	-10	4	41.76	0.980	10.23	44.44	-10.16	7.5	78.30
280	0.7	7.31	35	-5	3	31.32	0.980	10.23	44.44	-5.02	5.8	60.55
281	0.7	7.31	35	-5	3.5	36.54	0.980	10.23	44.44	-5.02	6.65	69.43
282	0.7	7.31	35	-5	4	41.76	0.980	10.23	44.44	-5.02	7.5	78.30
283	0.7	7.31	35	0	3	31.32	0.980	10.23	44.44	0.00	5.8	60.55
284	0.7	7.31	35	0	3.5	36.54	0.980	10.23	44.44	0.00	6.65	69.43
285	0.7	7.31	35	0	4	41.76	0.980	10.23	44.44	0.00	7.5	78.30
286	0.7	7.31	35	5	3	31.32	0.980	10.23	44.44	5.02	5.8	60.55
287	0.7	7.31	35	5	3.5	36.54	0.980	10.23	44.44	5.02	6.65	69.43
288	0.7	7.31	35	5	4	41.76	0.980	10.23	44.44	5.02	7.5	78.30
289	0.7	7.31	35	10	3	31.32	0.980	10.23	44.44	10.16	5.8	60.55
290	0.7	7.31	35	10	3.5	36.54	0.980	10.23	44.44	10.16	6.65	69.43
291	0.7	7.31	35	10	4	41.76	0.980	10.23	44.44	10.16	7.5	78.30
292	0.7	7.31	35	15	3	31.32	0.980	10.23	44.44	15.54	5.8	60.55
293	0.7	7.31	35	15	3.5	36.54	0.980	10.23	44.44	15.54	6.65	69.43
294	0.7	7.31	35	15	4	41.76	0.980	10.23	44.44	15.54	7.5	78.30
295	0.7	7.31	35	20	3	31.32	0.980	10.23	44.44	21.34	5.8	60.55
296	0.7	7.31	35	20	3.5	36.54	0.980	10.23	44.44	21.34	6.65	69.43
297	0.7	7.31	35	20	4	41.76	0.980	10.23	44.44	21.34	7.5	78.30
298	0.7	7.31	38	-20	3	31.32	1.121	11.70	51.38	-21.34	6.04	63.06
299	0.7	7.31	38	-20	3.5	36.54	1.121	11.70	51.38	-21.34	6.93	72.35
300	0.7	7.31	38	-20	4	41.76	1.121	11.70	51.38	-21.34	7.83	81.75
301	0.7	7.31	38	-15	3	31.32	1.121	11.70	51.38	-15.54	6.04	63.06
302	0.7	7.31	38	-15	3.5	36.54	1.121	11.70	51.38	-15.54	6.93	72.35
303	0.7	7.31	38	-15	4	41.76	1.121	11.70	51.38	-15.54	7.83	81.75
304	0.7	7.31	38	-10	3	31.32	1.121	11.70	51.38	-10.16	6.04	63.06
305	0.7	7.31	38	-10	3.5	36.54	1.121	11.70	51.38	-10.16	6.93	72.35
306	0.7	7.31	38	-10	4	41.76	1.121	11.70	51.38	-10.16	7.83	81.75
307	0.7	7.31	38	-5	3	31.32	1.121	11.70	51.38	-5.02	6.04	63.06
308	0.7	7.31	38	-5	3.5	36.54	1.121	11.70	51.38	-5.02	6.93	72.35
309	0.7	7.31	38	-5	4	41.76	1.121	11.70	51.38	-5.02	7.83	81.75
310	0.7	7.31	38	0	3	31.32	1.121	11.70	51.38	0.00	6.04	63.06
311	0.7	7.31	38	0	3.5	36.54	1.121	11.70	51.38	0.00	6.93	72.35
312	0.7	7.31	38	0	4	41.76	1.121	11.70	51.38	0.00	7.83	81.75

Table 7-2. Continued

	p-q diagram						τ-σ diagram					
No.	a (MPa)	a (tsf)	α (°)	β (°)	p_p (MPa)	p_p (tsf)	c (MPa)	c (tsf)	φ (°)	ω (°)	σ_p (MPa)	σ_p (tsf)
313	0.7	7.31	38	5	3	31.32	1.121	11.70	51.38	5.02	6.04	63.06
314	0.7	7.31	38	5	3.5	36.54	1.121	11.70	51.38	5.02	6.93	72.35
315	0.7	7.31	38	5	4	41.76	1.121	11.70	51.38	5.02	7.83	81.75
316	0.7	7.31	38	10	3	31.32	1.121	11.70	51.38	10.16	6.04	63.06
317	0.7	7.31	38	10	3.5	36.54	1.121	11.70	51.38	10.16	6.93	72.35
318	0.7	7.31	38	10	4	41.76	1.121	11.70	51.38	10.16	7.83	81.75
319	0.7	7.31	38	15	3	31.32	1.121	11.70	51.38	15.54	6.04	63.06
320	0.7	7.31	38	15	3.5	36.54	1.121	11.70	51.38	15.54	6.93	72.35
321	0.7	7.31	38	15	4	41.76	1.121	11.70	51.38	15.54	7.83	81.75
322	0.7	7.31	38	20	3	31.32	1.121	11.70	51.38	21.34	6.04	63.06
323	0.7	7.31	38	20	3.5	36.54	1.121	11.70	51.38	21.34	6.93	72.35
324	0.7	7.31	38	20	4	41.76	1.121	11.70	51.38	21.34	7.83	81.75

Table 7-3. FEM simulation results – Bearing capacity (tsf) on rock subsurface

	B=6.6 ft; D=0 ft				B=13.2 ft; D=0 ft					B=6.6 ft; D=3.3 ft			B=13.2 ft; D=6.6 ft			
#	Strip B/L=0	L/B=10 B/L=0.1	L/B=5 B/L=0.2	square	Strip v=0.2	Strip v=0.1	L/B=10 B/L=0.1	L/B=5 B/L=0.2	square	L/B=10 B/L=0.1	L/B=5 B/L=0.2	square	Strip B/L=0	L/B=10 B/L=0.1	L/B=5 B/L=0.2	square
1	5.85	6.06	6.37	7.31	16.81	6.06	6.26	6.58	7.52	7.52	7.83	8.98	7.20	7.73	8.14	9.29
2-27	same	results														
28	7.52	7.83	8.35	9.60	21.72	7.93	8.14	8.67	9.92	9.71	10.34	11.80	9.40	10.13	10.75	12.32
29	7.52	7.83	8.35	9.60	23.28	7.93	8.14	8.67	9.92	9.71	10.34	11.80	9.40	10.13	10.75	12.32
30	7.52	7.83	8.35	9.60	26.62	7.93	8.14	8.67	9.92	9.71	10.34	11.80	9.40	10.13	10.75	12.32
31	7.52	7.83	8.35	9.60	21.92	7.93	8.14	8.67	9.92	9.71	10.34	11.80	9.40	10.13	10.75	12.32
32	7.52	7.83	8.35	9.60	23.49	7.93	8.14	8.67	9.92	9.71	10.34	11.80	9.40	10.13	10.75	12.32
33	7.52	7.83	8.35	9.60	26.83	7.93	8.14	8.67	9.92	9.71	10.34	11.80	9.40	10.13	10.75	12.32
34	7.52	7.83	8.35	9.60	22.13	7.93	8.14	8.67	9.92	7.52	10.34	11.80	9.40	7.73	10.75	12.32
35	7.52	7.83	8.35	9.60	23.70	7.93	8.14	8.67	9.92	9.71	10.34	11.80	9.40	10.13	10.75	12.32
36	7.52	7.83	8.35	9.60	27.14	7.93	8.14	8.67	9.92	9.71	10.34	11.80	9.40	10.13	10.75	12.32
37	7.52	7.83	8.35	9.60	22.55	7.93	8.14	8.67	9.92	9.71	10.34	11.80	9.40	10.13	10.75	12.32
38	7.52	7.83	8.35	9.60	24.01	7.93	8.14	8.67	9.92	9.71	10.34	11.80	9.40	10.13	10.75	12.32
39	7.52	7.83	8.35	9.60	27.46	7.93	8.14	8.67	9.92	9.71	10.34	11.80	9.40	10.13	10.75	12.32
40	7.52	7.83	8.35	9.60	22.86	7.93	8.14	8.67	9.92	9.71	10.34	11.80	9.40	10.13	10.75	12.32
41	7.52	7.83	8.35	9.60	24.53	7.93	8.14	8.67	9.92	7.52	10.34	11.80	9.40	7.73	10.75	12.32
42	7.52	7.83	8.35	9.60	27.87	7.93	8.14	8.67	9.92	9.71	10.34	11.80	9.40	10.13	10.75	12.32
43	7.52	7.83	8.35	9.60	23.18	7.93	8.14	8.67	9.92	9.71	10.34	11.80	9.40	10.13	10.75	12.32
44	7.52	7.83	8.35	9.60	25.06	7.93	8.14	8.67	9.92	9.71	10.34	11.80	9.40	10.13	10.75	12.32
45	7.52	7.83	8.35	9.60	28.19	7.93	8.14	8.67	9.92	9.71	10.34	11.80	9.40	10.13	10.75	12.32
46	7.52	7.83	8.35	9.60	23.70	7.93	8.14	8.67	9.92	9.71	10.34	11.80	9.40	10.13	10.75	12.32

Table 7-3. Continued

	B=6.6 ft; D=0 ft				B=13.2 ft; D=0 ft				B=6.6 ft; D=3.3 ft				B=13.2 ft; D=6.6 ft			
#	Strip B/L=0	L/B=10 B/L=0.1	L/B=5 B/L=0.2	square	Strip v=0.2	Strip v=0.1	L/B=10 B/L=0.1	L/B=5 B/L=0.2	square	L/B=10 B/L=0.1	L/B=5 B/L=0.2	square	Strip B/L=0	L/B=10 B/L=0.1	L/B=5 B/L=0.2	square
47	7.52	7.83	8.35	9.60	25.58	7.93	8.14	8.67	9.92	9.71	10.34	11.80	9.40	10.13	10.75	12.32
48	7.52	7.83	8.35	9.60	28.50	7.93	8.14	8.67	9.92	7.52	10.34	11.80	9.40	7.73	10.75	12.32
49	7.52	7.83	8.35	9.60	24.64	7.93	8.14	8.67	9.92	9.71	10.34	11.80	9.40	10.13	10.75	12.32
50	7.52	7.83	8.35	9.60	26.10	7.93	8.14	8.67	9.92	9.71	10.34	11.80	9.40	10.13	10.75	12.32
51	7.52	7.83	8.35	9.60	29.34	7.93	8.14	8.67	9.92	9.71	10.34	11.80	9.40	10.13	10.75	12.32
52	7.52	7.83	8.35	9.60	25.89	7.93	8.14	8.67	9.92	9.71	10.34	11.80	9.40	10.13	10.75	12.32
53	7.52	7.83	8.35	9.60	27.35	7.93	8.14	8.67	9.92	9.71	10.34	11.80	9.40	10.13	10.75	12.32
54	7.52	7.83	8.35	9.60	30.48	7.93	8.14	8.67	9.92	9.71	10.34	11.80	9.40	10.13	10.75	12.32
55	15.56	16.18	17.12	19.52	23.70	16.29	16.70	17.75	20.25	19.94	21.19	24.22	19.31	20.67	21.92	25.06
56	15.56	16.18	17.12	19.52	25.58	16.29	16.70	17.75	20.25	19.94	21.19	24.22	19.31	20.67	21.92	25.06
57	15.56	16.18	17.12	19.52	29.34	16.29	16.70	17.75	20.25	19.94	21.19	24.22	19.31	20.67	21.92	25.06
58	15.56	16.18	17.12	19.52	24.12	16.29	16.70	17.75	20.25	19.94	21.19	24.22	19.31	20.67	21.92	25.06
59	15.56	16.18	17.12	19.52	26.10	16.29	16.70	17.75	20.25	19.94	21.19	24.22	19.31	20.67	21.92	25.06
60	15.56	16.18	17.12	19.52	29.65	16.29	16.70	17.75	20.25	19.94	21.19	24.22	19.31	20.67	21.92	25.06
61	15.56	16.18	17.12	19.52	24.74	16.29	16.70	17.75	20.25	19.94	21.19	24.22	19.31	20.67	21.92	25.06
62	15.56	16.18	17.12	19.52	26.41	16.29	16.70	17.75	20.25	19.94	21.19	24.22	19.31	20.67	21.92	25.06
63	15.56	16.18	17.12	19.52	30.07	16.29	16.70	17.75	20.25	19.94	21.19	24.22	19.31	20.67	21.92	25.06
64	15.56	16.18	17.12	19.52	25.37	16.29	16.70	17.75	20.25	19.94	21.19	24.22	19.31	20.67	21.92	25.06
65	15.56	16.18	17.12	19.52	27.25	16.29	16.70	17.75	20.25	19.94	21.19	24.22	19.31	20.67	21.92	25.06
66	15.56	16.18	17.12	19.52	30.69	16.29	16.70	17.75	20.25	19.94	21.19	24.22	19.31	20.67	21.92	25.06
67	15.56	16.18	17.12	19.52	26.00	16.29	16.70	17.75	20.25	19.94	21.19	24.22	19.31	20.67	21.92	25.06
68	15.56	16.18	17.12	19.52	27.98	16.29	16.70	17.75	20.25	19.94	21.19	24.22	19.31	20.67	21.92	25.06
69	15.56	16.18	17.12	19.52	31.63	16.29	16.70	17.75	20.25	19.94	21.19	24.22	19.31	20.67	21.92	25.06
70	15.56	16.18	17.12	19.52	26.62	16.29	16.70	17.75	20.25	19.94	21.19	24.22	19.31	20.67	21.92	25.06
71	15.56	16.18	17.12	19.52	28.50	16.29	16.70	17.75	20.25	19.94	21.19	24.22	19.31	20.67	21.92	25.06
72	15.56	16.18	17.12	19.52	32.68	16.29	16.70	17.75	20.25	19.94	21.19	24.22	19.31	20.67	21.92	25.06
73	15.56	16.18	17.12	19.52	27.98	16.29	16.70	17.75	20.25	19.94	21.19	24.22	19.31	20.67	21.92	25.06
74	15.56	16.18	17.12	19.52	29.96	16.29	16.70	17.75	20.25	19.94	21.19	24.22	19.31	20.67	21.92	25.06
75	15.56	16.18	17.12	19.52	34.45	16.29	16.70	17.75	20.25	19.94	21.19	24.22	19.31	20.67	21.92	25.06
76	15.56	16.18	17.12	19.52	29.86	16.29	16.70	17.75	20.25	19.94	21.19	24.22	19.31	20.67	21.92	25.06
77	15.56	16.18	17.12	19.52	32.16	16.29	16.70	17.75	20.25	19.94	21.19	24.22	19.31	20.67	21.92	25.06
78	15.56	16.18	17.12	19.52	36.12	16.29	16.70	17.75	20.25	19.94	21.19	24.22	19.31	20.67	21.92	25.06
79	15.56	16.18	17.12	19.52	33.09	16.29	16.70	17.75	20.25	19.94	21.19	24.22	19.31	20.67	21.92	25.06

Table 7-3. Continued

	B=6.6 ft; D=0 ft				B=13.2 ft; D=0 ft				B=6.6 ft; D=3.3 ft				B=13.2 ft; D=6.6 ft			
#	Strip B/L=0	L/B=10 B/L=0.1	L/B=5 B/L=0.2	square	Strip v=0.2	Strip v=0.1	L/B=10 B/L=0.1	L/B=5 B/L=0.2	square	L/B=10 B/L=0.1	L/B=5 B/L=0.2	square	Strip B/L=0	L/B=10 B/L=0.1	L/B=5 B/L=0.2	square
80	15.56	16.18	17.12	19.52	36.23	16.29	16.70	17.75	20.25	19.94	21.19	24.22	19.31	20.67	21.92	25.06
81	15.56	16.18	17.12	19.52	40.40	16.29	16.70	17.75	20.25	19.94	21.19	24.22	19.31	20.67	21.92	25.06
82	21.82	22.76	24.01	27.56	25.37	22.86	23.49	24.85	28.50	27.98	29.65	34.03	27.04	29.02	30.80	35.29
83	23.91	24.74	26.20	29.96	27.46	24.95	25.68	27.04	31.01	30.69	32.26	37.06	29.55	31.74	33.51	38.42
84	27.56	28.50	30.17	34.45	31.22	28.71	29.55	31.11	35.60	35.29	37.17	42.49	34.03	36.54	38.52	44.06
85	22.13	22.97	24.33	27.77	26.10	23.07	23.70	25.06	28.71	28.29	29.96	34.24	27.35	29.34	31.01	35.60
86	24.12	24.95	26.52	30.17	28.19	25.16	25.89	27.35	31.22	30.90	32.68	37.27	29.75	32.05	33.83	38.63
87	27.77	28.71	30.38	34.66	32.05	28.92	29.75	31.42	35.91	35.50	37.48	42.91	34.24	36.85	38.94	44.47
88	22.45	23.18	24.64	28.08	26.83	23.39	24.01	25.37	29.02	28.71	30.28	34.66	27.67	29.75	31.42	35.91
89	24.53	25.37	26.94	30.59	28.81	25.58	26.31	27.77	31.74	31.42	33.20	37.90	30.28	32.57	34.35	39.36
90	27.98	28.92	30.69	34.97	32.89	29.13	29.96	31.63	36.23	35.70	37.79	43.22	34.45	37.06	39.15	44.89
91	23.07	23.80	25.26	28.81	27.46	24.01	24.74	26.10	29.86	29.55	31.11	35.60	28.40	30.59	32.36	36.96
92	24.74	25.58	27.14	30.90	29.44	25.79	26.52	27.98	32.05	31.63	33.41	38.31	30.59	32.78	34.66	39.67
93	28.19	29.23	31.01	35.29	33.72	29.44	30.28	31.95	36.54	36.12	38.11	43.64	34.87	37.48	39.57	45.21
94	23.18	24.01	25.47	29.02	28.92	24.22	24.95	26.31	30.07	29.75	31.42	35.91	28.71	30.90	32.57	37.27
95	24.85	25.68	27.25	31.01	31.01	25.89	26.62	28.08	32.16	31.74	33.51	38.42	30.69	32.99	34.77	39.78
96	28.40	29.44	31.22	35.60	35.18	29.65	30.48	32.16	36.85	36.33	38.42	43.95	35.08	37.69	39.78	45.62
97	23.28	24.12	25.58	29.13	29.44	24.33	25.06	26.41	30.17	29.96	31.53	36.02	28.81	31.01	32.68	37.38
98	24.95	25.79	27.35	31.11	31.42	26.00	26.73	28.19	32.26	31.84	33.62	38.52	30.80	33.09	34.87	39.99
99	28.61	29.55	31.32	35.70	36.44	29.75	30.59	32.26	36.96	36.54	38.52	44.16	35.29	37.90	39.99	45.73
100	23.59	24.43	25.89	29.55	31.53	24.64	25.37	26.73	30.59	30.28	31.95	36.54	29.23	31.42	33.09	37.90
101	25.16	26.10	27.67	31.53	33.72	26.31	27.04	28.50	32.68	32.26	34.03	39.05	31.11	33.51	35.29	40.51
102	28.71	29.75	31.53	36.02	38.31	29.96	30.80	32.47	37.27	36.75	38.73	44.47	35.50	38.11	40.19	46.14
103	23.80	24.64	26.10	29.86	34.56	24.85	25.58	26.94	30.90	30.48	32.16	36.85	29.44	31.63	33.30	38.31
104	25.58	26.41	27.98	31.95	37.17	26.62	27.35	28.92	33.09	32.68	34.56	39.57	31.53	33.83	35.81	41.03
105	29.13	29.86	31.63	36.12	41.66	30.07	30.90	32.68	37.38	36.85	39.05	44.58	35.60	38.31	40.51	46.25
106	24.12	24.95	26.52	30.17	38.94	25.16	25.89	27.35	31.22	30.90	32.68	37.27	29.75	32.05	33.83	38.63
107	25.79	26.73	28.29	32.36	42.07	26.94	27.67	29.23	33.51	32.99	34.87	39.99	31.95	34.24	36.23	41.55
108	29.44	30.17	31.95	36.44	47.61	30.38	31.22	32.99	37.79	37.27	39.36	45.10	36.02	38.63	51.26	46.77
109	30.59	31.53	33.41	38.11	38.73	31.74	32.57	34.45	39.46	38.84	41.13	47.08	37.38	40.30	42.70	48.86
110	30.59	31.53	33.41	38.11	46.04	31.74	32.57	34.45	39.46	38.84	41.13	47.08	37.38	40.30	42.70	48.86
111	30.59	31.53	33.41	38.11	53.97	31.74	32.57	34.45	39.46	38.84	41.13	47.08	37.38	40.30	42.70	48.86
112	30.59	31.53	33.41	38.11	39.36	31.74	32.57	34.45	39.46	38.84	41.13	47.08	37.38	40.30	42.70	48.86

Table 7-3. Continued

	B=6.6 ft; D=0 ft				B=13.2 ft; D=0 ft				B=6.6 ft; D=3.3 ft				B=13.2 ft; D=6.6 ft			
#	Strip B/L=0	L/B=10 B/L=0.1	L/B=5 B/L=0.2	square	Strip v=0.2	Strip v=0.1	L/B=10 B/L=0.1	L/B=5 B/L=0.2	square	L/B=10 B/L=0.1	L/B=5 B/L=0.2	square	Strip B/L=0	L/B=10 B/L=0.1	L/B=5 B/L=0.2	square
113	30.59	31.53	33.41	38.11	46.46	31.74	32.57	34.45	39.46	38.84	41.13	47.08	37.38	40.30	42.70	48.86
114	30.59	31.53	33.41	38.11	54.29	31.74	32.57	34.45	39.46	38.84	41.13	47.08	37.38	40.30	42.70	48.86
115	30.59	31.53	33.41	38.11	39.99	31.74	32.57	34.45	39.46	38.84	41.13	47.08	37.38	40.30	42.70	48.86
116	30.59	31.53	33.41	38.11	46.98	31.74	32.57	34.45	39.46	38.84	41.13	47.08	37.38	40.30	42.70	48.86
117	30.59	31.53	33.41	38.11	55.02	31.74	32.57	34.45	39.46	38.84	41.13	47.08	37.38	40.30	42.70	48.86
118	30.59	31.53	33.41	38.11	41.03	31.74	32.57	34.45	39.46	38.84	41.13	47.08	37.38	40.30	42.70	48.86
119	30.59	31.53	33.41	38.11	48.02	31.74	32.57	34.45	39.46	38.84	41.13	47.08	37.38	40.30	42.70	48.86
120	30.59	31.53	33.41	38.11	55.33	31.74	32.57	34.45	39.46	38.84	41.13	47.08	37.38	40.30	42.70	48.86
121	30.59	31.53	33.41	38.11	42.07	31.74	32.57	34.45	39.46	38.84	41.13	47.08	37.38	40.30	42.70	48.86
122	30.59	31.53	33.41	38.11	49.17	31.74	32.57	34.45	39.46	38.84	41.13	47.08	37.38	40.30	42.70	48.86
123	30.59	31.53	33.41	38.11	56.17	31.74	32.57	34.45	39.46	38.84	41.13	47.08	37.38	40.30	42.70	48.86
124	30.59	31.53	33.41	38.11	43.43	31.74	32.57	34.45	39.46	38.84	41.13	47.08	37.38	40.30	42.70	48.86
125	30.59	31.53	33.41	38.11	50.01	31.74	32.57	34.45	39.46	38.84	41.13	47.08	37.38	40.30	42.70	48.86
126	30.59	31.53	33.41	38.11	56.69	31.74	32.57	34.45	39.46	38.84	41.13	47.08	37.38	40.30	42.70	48.86
127	30.59	31.53	33.41	38.11	44.79	31.74	32.57	34.45	39.46	38.84	41.13	47.08	37.38	40.30	42.70	48.86
128	30.59	31.53	33.41	38.11	51.78	31.74	32.57	34.45	39.46	38.84	41.13	47.08	37.38	40.30	42.70	48.86
129	30.59	31.53	33.41	38.11	57.84	31.74	32.57	34.45	39.46	38.84	41.13	47.08	37.38	40.30	42.70	48.86
130	30.59	31.53	33.41	38.11	47.29	31.74	32.57	34.45	39.46	38.84	41.13	47.08	37.38	40.30	42.70	48.86
131	30.59	31.53	33.41	38.11	53.97	31.74	32.57	34.45	39.46	38.84	41.13	47.08	37.38	40.30	42.70	48.86
132	30.59	31.53	33.41	38.11	60.03	31.74	32.57	34.45	39.46	38.84	41.13	47.08	37.38	40.30	42.70	48.86
133	30.59	31.53	33.41	38.11	52.41	31.74	32.57	34.45	39.46	38.84	41.13	47.08	37.38	40.30	42.70	48.86
134	30.59	31.53	33.41	38.11	58.05	31.74	32.57	34.45	39.46	38.84	41.13	47.08	37.38	40.30	42.70	48.86
135	30.59	31.53	33.41	38.11	62.85	31.74	32.57	34.45	39.46	38.84	41.13	47.08	37.38	40.30	42.70	48.86
136	37.38	38.42	40.72	46.46	42.07	38.73	39.88	42.18	48.13	47.61	50.32	57.52	46.35	49.38	52.20	59.61
137	44.47	45.83	48.55	55.33	50.32	46.14	47.50	50.32	57.32	56.69	60.03	68.49	54.91	58.78	62.33	70.99
138	44.79	46.14	48.86	55.75	58.78	46.46	47.82	50.63	57.73	57.00	60.45	68.90	55.44	59.19	62.74	71.51
139	37.58	38.73	41.03	46.88	43.12	39.05	40.19	42.60	48.55	47.92	50.84	57.94	46.67	49.69	52.72	60.13
140	44.47	45.83	48.55	55.33	51.16	46.14	47.50	50.32	57.32	56.69	60.03	68.49	54.91	58.78	62.33	70.99
141	44.79	46.14	48.86	55.75	59.72	46.46	47.82	50.63	57.73	57.00	60.45	68.90	55.44	59.19	62.74	71.51
142	38.00	39.15	41.55	47.40	43.95	39.46	40.61	43.01	49.07	48.44	51.36	58.57	47.19	50.22	53.24	60.76
143	44.47	45.83	48.55	55.33	52.10	46.14	47.50	50.32	57.32	56.69	60.03	68.49	54.91	58.78	62.33	70.99
144	44.79	46.14	48.86	55.75	60.66	46.46	47.82	50.63	57.73	57.00	60.45	68.90	55.44	59.19	62.74	71.51
145	38.21	38.63	41.76	47.61	45.21	39.67	40.82	43.22	49.28	48.75	51.57	58.88	47.40	50.53	53.56	61.07

Table 7-3. Continued

	B=6.6 ft; D=0 ft				B=13.2 ft; D=0 ft				B=6.6 ft; D=3.3 ft				B=13.2 ft; D=6.6 ft			
#	Strip B/L=0	L/B=10 B/L=0.1	L/B=5 B/L=0.2	square	Strip v=0.2	Strip v=0.1	L/B=10 B/L=0.1	L/B=5 B/L=0.2	square	L/B=10 B/L=0.1	L/B=5 B/L=0.2	square	Strip B/L=0	L/B=10 B/L=0.1	L/B=5 B/L=0.2	square
146	44.47	45.83	48.55	55.33	53.56	46.14	47.50	50.32	57.32	56.69	60.03	68.49	54.91	58.78	62.33	70.99
147	44.79	46.14	48.86	55.75	61.91	46.46	47.82	50.63	57.73	57.00	60.45	68.90	55.44	59.19	62.74	71.51
148	38.63	39.78	42.18	48.13	47.19	40.09	41.24	43.74	49.80	49.17	52.20	59.51	47.92	51.05	54.18	61.70
149	44.47	45.83	48.55	55.33	55.65	46.14	47.50	50.32	57.32	56.69	60.03	68.49	54.91	58.78	62.33	70.99
150	44.79	46.14	48.86	55.75	64.00	46.46	47.82	50.63	57.73	57.00	60.45	68.90	55.44	59.19	62.74	71.51
151	38.84	39.88	42.28	48.23	49.07	40.19	41.34	43.85	49.90	49.38	52.41	59.61	48.02	51.16	54.29	61.80
152	44.47	45.83	48.55	55.33	57.21	46.14	47.50	50.32	57.32	56.69	60.03	68.49	54.91	58.78	62.33	70.99
153	44.79	46.14	48.86	55.75	65.56	46.46	47.82	50.63	57.73	57.00	60.45	68.90	55.44	59.19	62.74	71.51
154	38.94	40.09	42.49	48.34	52.30	40.40	41.55	44.06	50.11	49.59	52.62	59.82	48.34	51.47	54.60	62.12
155	44.47	45.83	48.55	55.33	60.55	46.14	47.50	50.32	57.32	56.69	60.03	68.49	55.23	58.78	62.33	70.99
156	44.79	46.14	48.86	55.75	68.80	46.46	47.82	50.63	57.73	57.00	60.45	68.90	55.44	59.19	62.74	71.51
157	39.25	40.40	42.80	48.86	56.06	40.72	41.86	44.37	50.63	49.90	52.93	60.45	48.65	51.78	54.91	62.74
158	44.47	45.83	48.55	55.33	64.52	46.14	47.50	50.32	57.32	56.69	60.03	68.49	55.23	58.78	62.33	70.99
159	44.79	46.14	48.86	55.75	73.18	46.46	47.82	50.63	57.73	57.00	60.45	68.90	55.44	59.19	62.74	71.51
160	39.57	40.72	43.12	49.17	63.06	41.03	42.18	44.68	50.95	50.32	53.35	60.87	49.07	52.20	55.33	63.06
161	44.47	45.83	48.55	55.33	72.66	46.14	47.50	50.32	57.32	56.69	60.03	68.49	55.23	58.78	62.33	70.99
162	44.79	46.14	48.86	55.75	80.18	46.46	47.82	50.63	57.73	57.00	60.45	68.90	55.44	59.19	62.74	71.51
163	40.51	41.66	44.16	50.43	45.52	41.97	43.22	45.73	52.20	51.57	54.60	62.33	50.22	53.45	56.58	64.62
164	48.86	50.32	53.24	60.76	55.02	50.63	52.10	55.23	62.95	62.12	65.98	75.17	60.66	64.52	68.38	77.99
165	57.21	58.88	62.43	71.20	64.00	59.30	60.97	64.62	73.71	72.77	77.15	88.01	70.99	75.48	80.07	91.25
166	41.03	42.18	44.68	51.16	46.67	42.49	43.74	46.35	52.93	52.30	55.33	63.16	50.84	54.18	57.42	65.56
167	49.49	50.95	53.97	61.49	55.85	51.26	52.72	55.85	63.79	62.95	66.71	76.21	61.39	65.25	69.22	79.03
168	57.52	59.19	62.74	71.62	65.46	59.61	61.28	64.94	74.23	73.18	77.57	88.64	71.41	75.90	80.39	91.98
169	41.55	42.91	45.52	51.89	48.34	43.22	44.47	47.08	53.77	53.04	56.17	64.21	51.78	55.02	58.26	66.61
170	50.01	51.57	54.60	62.33	57.42	51.89	53.35	56.58	64.52	63.68	67.55	77.05	62.12	65.98	70.05	79.87
171	57.84	59.61	63.16	72.14	66.82	60.03	61.80	65.46	74.65	73.71	78.20	89.16	71.93	76.53	81.01	92.50
172	42.28	43.53	46.14	52.62	50.43	43.85	45.10	47.82	54.50	53.77	57.11	65.04	52.51	55.85	59.19	67.55
173	50.43	51.99	55.02	62.85	60.24	52.30	53.77	57.00	65.04	64.21	68.07	77.67	62.74	66.50	70.57	80.60
174	58.26	60.03	63.58	72.56	68.90	60.45	62.22	65.88	75.17	74.23	78.61	89.78	72.35	77.05	81.54	93.12
175	42.80	44.16	46.77	53.35	52.93	44.47	45.73	48.44	55.33	54.60	57.84	66.09	53.24	56.58	60.03	68.49
176	50.95	52.51	55.54	63.48	62.54	52.83	54.39	57.63	65.77	64.94	68.80	78.51	63.27	67.34	71.41	81.43
177	58.78	60.55	64.10	73.29	72.24	60.97	62.74	66.50	75.90	74.85	79.45	90.62	72.98	77.67	82.37	94.06
178	43.53	44.89	47.61	54.29	55.02	45.21	46.46	49.28	56.17	55.44	58.88	67.02	54.18	57.52	61.07	69.53

Table 7-3. Continued

	B=6.6 ft; D=0 ft				B=13.2 ft; D=0 ft				B=6.6 ft; D=3.3 ft				B=13.2 ft; D=6.6 ft			
#	Strip B/L=0	L/B=10 B/L=0.1	L/B=5 B/L=0.2	square	Strip v=0.2	Strip v=0.1	L/B=10 B/L=0.1	L/B=5 B/L=0.2	square	L/B=10 B/L=0.1	L/B=5 B/L=0.2	square	Strip B/L=0	L/B=10 B/L=0.1	L/B=5 B/L=0.2	square
179	51.36	53.04	56.17	64.00	65.46	53.35	54.91	58.15	66.29	65.56	69.43	79.14	63.89	67.96	72.04	82.16
180	58.99	60.76	64.41	73.60	75.27	61.18	62.95	66.71	76.21	75.17	79.66	91.04	73.18	77.88	82.58	94.38
181	44.68	46.04	48.75	55.65	59.61	46.35	47.71	50.53	57.63	56.90	60.34	68.80	55.54	59.09	62.54	71.41
182	52.10	53.66	56.90	64.94	70.05	54.08	55.65	58.99	67.23	66.40	70.47	80.28	64.73	68.90	73.08	83.31
183	59.51	61.39	65.04	74.23	79.87	61.80	63.58	67.34	76.84	75.90	80.39	91.77	74.02	78.72	83.42	95.21
184	45.83	47.29	50.11	57.11	65.98	47.61	48.96	51.89	59.19	58.46	61.91	70.68	57.00	60.55	64.21	73.29
185	53.04	54.60	57.84	65.98	76.42	55.02	56.58	60.03	68.38	67.55	71.72	81.64	65.88	70.05	74.33	84.67
186	60.13	62.01	65.67	74.96	87.49	62.43	64.21	68.07	77.67	76.63	81.22	92.71	74.75	79.45	84.36	96.26
187	47.40	48.86	51.78	59.09	76.53	49.17	50.63	53.56	61.18	60.45	63.89	73.18	58.88	62.74	66.29	75.79
188	54.18	55.85	59.19	67.55	89.05	56.27	57.94	61.39	69.95	69.11	73.29	83.52	67.44	71.72	76.00	86.65
189	61.49	63.37	67.13	76.63	99.28	63.79	65.67	69.53	79.34	78.40	83.00	94.80	76.42	81.22	86.13	98.24
190	42.91	44.16	46.77	53.45	48.34	44.47	45.73	48.44	55.33	54.60	57.84	66.09	53.24	56.58	60.03	68.49
191	52.10	53.66	56.90	64.94	58.57	54.08	55.65	58.99	67.23	66.40	70.47	80.28	64.73	68.90	73.18	83.31
192	61.07	62.95	66.71	76.11	68.17	63.37	65.15	69.11	78.82	77.78	82.48	94.17	75.90	80.60	85.61	97.61
193	43.64	44.89	47.61	54.18	49.69	45.21	46.46	49.28	56.17	55.44	58.88	67.02	54.18	57.52	61.07	69.63
194	52.83	54.39	57.63	65.77	59.82	54.81	56.38	59.72	68.17	67.23	71.31	81.43	65.67	69.74	73.92	84.46
195	61.60	63.48	67.23	76.73	70.26	63.89	65.77	69.63	79.45	78.51	83.10	94.90	76.53	81.43	86.23	98.45
196	44.58	45.94	48.65	55.54	51.78	46.25	47.61	50.43	57.52	56.79	60.24	68.70	55.33	58.88	62.43	71.20
197	53.45	55.02	58.36	66.50	62.22	55.44	57.00	60.45	68.90	67.96	72.14	82.27	66.40	70.57	74.85	85.29
198	62.43	64.31	68.07	77.67	72.77	64.73	66.61	70.57	80.49	79.45	84.25	96.15	77.57	82.48	87.38	99.70
199	45.73	47.08	49.90	57.00	53.87	47.40	48.75	51.68	58.99	58.15	61.70	70.47	56.79	60.34	64.00	73.18
200	54.50	56.06	59.40	67.86	64.41	56.48	58.15	61.60	70.26	69.43	73.50	83.94	67.65	71.93	76.32	87.07
201	63.37	65.25	69.11	78.82	75.17	65.67	67.55	71.62	81.64	80.60	85.50	97.51	78.61	83.62	88.74	101.16
202	46.67	48.02	50.84	58.05	57.42	48.34	49.69	52.72	60.13	59.30	62.95	71.83	57.94	61.49	65.25	74.44
203	55.44	57.11	60.55	69.01	67.96	57.52	59.19	62.74	71.51	70.68	74.96	85.40	68.90	73.29	77.67	88.53
204	64.21	66.19	70.05	79.97	78.93	66.61	68.49	72.66	82.79	81.75	86.76	98.87	79.76	84.77	89.99	102.52
205	47.19	48.65	51.47	58.78	61.07	48.96	50.32	53.35	60.87	60.03	63.68	72.66	58.67	62.33	66.09	75.38
206	56.17	57.84	61.28	69.95	71.93	58.26	59.93	63.48	72.45	71.51	75.79	86.55	69.74	74.12	78.61	89.78
207	65.15	67.13	71.10	81.01	83.21	67.55	69.53	73.60	83.94	83.00	87.90	100.22	80.91	86.03	91.14	103.98
208	49.17	50.63	53.56	61.18	65.46	50.95	52.41	55.54	63.37	62.54	66.29	75.69	61.07	64.83	68.80	78.51
209	57.84	59.51	63.06	71.93	77.99	59.93	61.70	65.35	74.54	73.60	77.99	89.05	71.83	76.32	80.91	92.29
210	66.50	68.49	72.45	82.79	89.26	68.90	70.89	75.06	85.71	84.56	89.58	102.31	82.58	87.70	92.92	106.17
211	50.63	52.20	55.23	63.06	73.39	52.51	53.97	57.21	65.35	64.41	68.28	78.09	62.85	66.82	70.89	80.91

Table 7-3. Continued

	B=6.6 ft; D=0 ft				B=13.2 ft; D=0 ft				B=6.6 ft; D=3.3 ft				B=13.2 ft; D=6.6 ft			
#	Strip B/L=0	L/B=10 B/L=0.1	L/B=5 B/L=0.2	square	Strip v=0.2	Strip v=0.1	L/B=10 B/L=0.1	L/B=5 B/L=0.2	square	L/B=10 B/L=0.1	L/B=5 B/L=0.2	square	Strip B/L=0	L/B=10 B/L=0.1	L/B=5 B/L=0.2	square
212	59.61	61.39	65.04	74.23	87.28	61.80	63.58	67.34	76.84	75.90	80.39	91.77	74.02	78.72	83.42	95.21
213	68.38	70.37	74.54	85.09	98.97	70.89	72.98	77.26	88.11	87.07	92.29	105.24	84.88	90.31	95.63	109.10
214	53.24	54.81	58.15	66.29	85.61	55.23	56.79	60.24	68.70	67.76	71.93	82.06	66.19	70.26	74.65	85.09
215	62.22	64.10	67.86	77.46	101.27	64.52	66.40	70.37	80.18	79.24	84.04	95.73	77.26	82.16	87.17	99.28
216	70.99	72.98	77.46	88.43	114.74	73.60	75.69	80.28	91.56	90.31	95.84	109.31	88.11	93.65	99.39	113.38
217	42.49	43.85	46.46	65.88	57.42	44.16	45.41	48.13	68.28	54.18	57.42	81.54	53.14	56.17	59.61	84.56
218	42.49	43.85	46.46	65.88	65.04	44.16	45.41	48.13	68.28	54.18	57.42	81.54	53.14	56.17	59.61	84.56
219	42.49	43.85	46.46	65.88	72.66	44.16	45.41	48.13	68.28	54.18	57.42	81.54	53.14	56.17	59.61	84.56
220	42.49	43.85	46.46	65.88	58.15	44.16	45.41	48.13	68.28	54.18	57.42	81.54	53.14	56.17	59.61	84.56
221	42.49	43.85	46.46	65.88	65.56	44.16	45.41	48.13	68.28	54.18	57.42	81.54	53.14	56.17	59.61	84.56
222	42.49	43.85	46.46	65.88	73.18	44.16	45.41	48.13	68.28	54.18	57.42	81.54	53.14	56.17	59.61	84.56
223	42.49	43.85	46.46	65.88	59.19	44.16	45.41	48.13	68.28	54.18	57.42	81.54	53.14	56.17	59.61	84.56
224	42.49	43.85	46.46	65.88	66.29	44.16	45.41	48.13	68.28	54.18	57.42	81.54	53.14	56.17	59.61	84.56
225	42.49	43.85	46.46	65.88	73.81	44.16	45.41	48.13	68.28	54.18	57.42	81.54	53.14	56.17	59.61	84.56
226	42.49	43.85	46.46	65.88	60.13	44.16	45.41	48.13	68.28	54.18	57.42	81.54	53.14	56.17	59.61	84.56
227	42.49	43.85	46.46	65.88	67.34	44.16	45.41	48.13	68.28	54.18	57.42	81.54	53.14	56.17	59.61	84.56
228	42.49	43.85	46.46	65.88	74.85	44.16	45.41	48.13	68.28	54.18	57.42	81.54	53.14	56.17	59.61	84.56
229	42.49	43.85	46.46	65.88	61.91	44.16	45.41	48.13	68.28	54.18	57.42	81.54	53.14	56.17	59.61	84.56
230	42.49	43.85	46.46	65.88	68.80	44.16	45.41	48.13	68.28	54.18	57.42	81.54	53.14	56.17	59.61	84.56
231	42.49	43.85	46.46	65.88	76.21	44.16	45.41	48.13	68.28	54.18	57.42	81.54	53.14	56.17	59.61	84.56
232	42.49	43.85	46.46	65.88	63.16	44.16	45.41	48.13	68.28	54.18	57.42	81.54	53.14	56.17	59.61	84.56
233	42.49	43.85	46.46	65.88	70.26	44.16	45.41	48.13	68.28	54.18	57.42	81.54	53.14	56.17	59.61	84.56
234	42.49	43.85	46.46	65.88	77.26	44.16	45.41	48.13	68.28	54.18	57.42	81.54	53.14	56.17	59.61	84.56
235	42.49	43.85	46.46	65.88	65.88	44.16	45.41	48.13	68.28	54.18	57.42	81.54	53.14	56.17	59.61	84.56
236	42.49	43.85	46.46	65.88	72.24	44.16	45.41	48.13	68.28	54.18	57.42	81.54	53.14	56.17	59.61	84.56
237	42.49	43.85	46.46	65.88	79.34	44.16	45.41	48.13	68.28	54.18	57.42	81.54	53.14	56.17	59.61	84.56
238	42.49	43.85	46.46	65.88	69.74	44.16	45.41	48.13	68.28	54.18	57.42	81.54	53.14	56.17	59.61	84.56
239	42.49	43.85	46.46	65.88	75.79	44.16	45.41	48.13	68.28	54.18	57.42	81.54	53.14	56.17	59.61	84.56
240	42.49	43.85	46.46	65.88	82.68	44.16	45.41	48.13	68.28	54.18	57.42	81.54	53.14	56.17	59.61	84.56
241	42.49	43.85	46.46	65.88	75.90	44.16	45.41	48.13	68.28	54.18	57.42	81.54	53.14	56.17	59.61	84.56
242	42.49	43.85	46.46	65.88	81.54	44.16	45.41	48.13	68.28	54.18	57.42	81.54	53.14	56.17	59.61	84.56
243	42.49	43.85	46.46	65.88	86.97	44.16	45.41	48.13	68.28	54.18	57.42	81.54	53.14	56.17	59.61	84.56
244	53.97	55.75	59.09	67.44	62.33	56.17	57.73	61.18	69.84	68.90	73.18	83.42	67.96	71.41	75.79	86.55

Table 7-3. Continued

	B=6.6 ft; D=0 ft				B=13.2 ft; D=0 ft				B=6.6 ft; D=3.3 ft				B=13.2 ft; D=6.6 ft			
#	Strip B/L=0	L/B=10 B/L=0.1	L/B=5 B/L=0.2	square	Strip v=0.2	Strip v=0.1	L/B=10 B/L=0.1	L/B=5 B/L=0.2	square	L/B=10 B/L=0.1	L/B=5 B/L=0.2	square	Strip B/L=0	L/B=10 B/L=0.1	L/B=5 B/L=0.2	square
245	62.12	64.10	67.86	77.36	70.78	64.52	66.40	70.37	80.18	79.24	84.04	95.73	77.99	82.16	87.17	99.28
246	62.12	64.10	67.86	77.36	79.03	64.52	66.40	70.37	80.18	79.24	84.04	95.73	77.99	82.16	87.17	99.28
247	54.29	56.06	59.40	67.86	63.68	56.48	58.15	61.60	70.26	69.43	73.50	83.94	68.28	71.93	76.32	87.07
248	62.12	64.10	67.86	77.36	71.83	64.52	66.40	70.37	80.18	79.24	84.04	95.73	77.99	82.16	87.17	99.28
249	62.12	64.10	67.86	77.36	80.07	64.52	66.40	70.37	80.18	79.24	84.04	95.73	77.99	82.16	87.17	99.28
250	54.71	56.38	59.72	68.17	65.04	56.79	58.46	61.91	70.57	69.74	73.92	84.25	68.70	72.35	76.63	87.38
251	62.12	64.10	67.86	77.36	73.39	64.52	66.40	70.37	80.18	79.24	84.04	95.73	77.99	82.16	87.17	99.28
252	62.12	64.10	67.86	77.36	81.75	64.52	66.40	70.37	80.18	79.24	84.04	95.73	77.99	82.16	87.17	99.28
253	55.02	56.79	60.24	68.80	66.82	57.21	58.88	62.33	71.10	70.26	74.44	84.88	69.22	72.87	77.15	88.11
254	62.12	64.10	67.86	77.36	75.27	64.52	66.40	70.37	80.18	79.24	84.04	95.73	77.99	82.16	87.17	99.28
255	62.12	64.10	67.86	77.36	83.42	64.52	66.40	70.37	80.18	79.24	84.04	95.73	77.99	82.16	87.17	99.28
256	56.06	57.84	61.28	69.95	69.63	58.26	59.93	63.48	72.45	71.51	75.79	86.55	70.47	74.12	78.61	89.78
257	62.12	64.10	67.86	77.36	77.88	64.52	66.40	70.37	80.18	79.24	84.04	95.73	77.99	82.16	87.17	99.28
258	62.12	64.10	67.86	77.36	86.23	64.52	66.40	70.37	80.18	79.24	84.04	95.73	77.99	82.16	87.17	99.28
259	56.38	58.15	61.60	70.37	72.77	58.57	60.24	63.89	72.87	71.93	76.32	87.07	70.89	74.54	79.14	90.31
260	62.12	64.10	67.86	77.36	80.70	64.52	66.40	70.37	80.18	79.24	84.04	95.73	77.99	82.16	87.17	99.28
261	62.12	64.10	67.86	77.36	89.47	64.52	66.40	70.37	80.18	79.24	84.04	95.73	77.99	82.16	87.17	99.28
262	56.79	58.57	62.01	70.89	76.94	58.99	60.66	64.31	73.39	72.35	76.73	87.70	71.41	75.06	79.66	90.93
263	62.12	64.10	67.86	77.36	85.29	64.52	66.40	70.37	80.18	79.24	84.04	95.73	77.99	82.16	87.17	99.28
264	62.12	64.10	67.86	77.36	93.23	64.52	66.40	70.37	80.18	79.24	84.04	95.73	77.99	82.16	87.17	99.28
265	57.11	58.88	62.43	71.20	82.68	59.30	60.97	64.62	73.71	72.77	77.15	88.01	71.72	75.48	80.07	91.35
266	62.12	64.10	67.86	77.36	91.56	64.52	66.40	70.37	80.18	79.24	84.04	95.73	77.99	82.16	87.17	99.28
267	62.12	64.10	67.86	77.36	100.22	64.52	66.40	70.37	80.18	79.24	84.04	95.73	77.99	82.16	87.17	99.28
268	57.52	59.30	62.85	71.72	94.06	59.72	61.39	65.15	74.23	73.29	77.78	88.64	72.24	76.00	80.70	91.98
269	62.12	64.10	67.86	77.36	101.58	64.52	66.40	70.37	80.18	79.24	84.04	95.73	77.99	82.16	87.17	99.28
270	62.12	64.10	67.86	77.36	110.66	64.52	66.40	70.37	80.18	79.24	84.04	95.73	77.99	82.16	87.17	99.28
271	60.13	62.01	65.67	74.96	67.55	62.43	64.31	68.07	77.67	76.73	81.22	92.81	75.69	79.55	84.25	96.26
272	68.80	70.89	75.17	85.82	76.94	71.41	73.50	77.88	88.84	87.70	93.02	106.17	86.55	90.93	96.47	110.04
273	76.94	79.34	84.04	95.84	86.34	79.87	82.16	87.07	99.28	98.03	103.98	118.60	96.78	101.69	107.85	122.98
274	60.76	62.64	66.29	75.69	69.22	63.06	64.83	68.70	78.40	77.36	82.06	93.65	76.42	80.28	85.09	97.09
275	69.43	71.51	75.79	86.44	78.61	72.04	74.12	78.51	89.58	88.43	93.75	107.01	87.28	91.77	97.20	110.98
276	77.46	79.87	84.56	96.47	87.70	80.39	82.68	87.59	99.91	98.66	104.61	119.33	97.41	102.31	108.47	123.71
277	61.49	63.37	67.13	76.63	71.31	63.79	65.67	69.53	79.34	78.40	83.00	94.80	77.26	81.33	86.13	98.24

Table 7-3. Continued

	B=6.6 ft; D=0 ft				B=13.2 ft; D=0 ft				B=6.6 ft; D=3.3 ft				B=13.2 ft; D=6.6 ft			
#	Strip B/L=0	L/B=10 B/L=0.1	L/B=5 B/L=0.2	square	Strip v=0.2	Strip v=0.1	L/B=10 B/L=0.1	L/B=5 B/L=0.2	square	L/B=10 B/L=0.1	L/B=5 B/L=0.2	square	Strip B/L=0	L/B=10 B/L=0.1	L/B=5 B/L=0.2	square
278	70.05	72.14	76.42	87.17	80.70	72.66	74.75	79.24	90.31	89.16	94.59	107.85	88.01	92.50	98.14	111.81
279	78.09	80.49	85.19	97.30	90.10	81.01	83.31	88.32	100.75	99.39	105.44	120.27	98.14	103.15	109.41	123.71
280	62.12	64.00	67.76	77.36	74.23	64.41	66.29	70.26	80.07	79.14	83.94	95.63	78.09	82.06	86.97	99.18
281	70.68	72.77	77.15	88.01	83.62	73.29	75.38	79.87	91.14	89.99	95.32	108.89	88.84	93.33	98.87	112.86
282	78.72	81.12	85.92	98.14	93.23	81.64	84.04	88.95	101.58	100.33	106.17	121.31	98.97	103.98	110.14	125.80
283	63.27	65.25	69.11	78.82	77.99	65.67	67.55	71.62	81.64	80.60	85.50	97.51	79.55	83.62	88.74	101.16
284	71.10	73.29	77.67	88.64	87.70	73.81	75.90	80.49	91.77	90.51	96.15	109.62	89.47	94.06	99.70	113.69
285	79.24	81.64	86.44	98.66	97.30	82.16	84.56	89.58	102.21	100.95	106.91	122.04	99.60	104.71	110.98	126.64
286	63.89	65.88	69.74	79.66	82.16	66.29	68.17	72.24	82.48	81.33	86.23	98.45	80.28	84.36	89.47	102.21
287	71.62	73.81	78.20	89.26	92.19	74.33	76.42	81.01	92.39	91.14	96.78	110.35	90.10	94.59	100.33	114.42
288	79.66	82.16	86.97	99.28	102.00	82.68	85.09	90.10	102.83	101.58	107.53	122.77	100.22	105.34	111.60	127.37
289	64.94	66.92	70.89	80.81	88.64	67.34	69.32	73.39	83.73	82.68	87.59	100.02	81.64	85.82	90.93	103.67
290	72.56	74.75	79.24	90.41	98.45	75.27	77.46	82.06	93.65	92.39	97.93	111.81	91.25	95.84	101.58	116.09
291	80.60	83.10	88.01	100.43	109.20	83.62	86.03	91.14	103.98	102.63	108.89	124.13	101.37	106.49	112.86	128.83
292	66.40	68.49	72.45	82.79	97.41	68.90	70.89	75.06	85.71	84.56	89.58	102.31	83.42	87.70	92.92	106.17
293	74.02	76.32	80.81	92.29	108.26	76.84	79.03	83.73	95.53	94.27	100.02	114.11	93.12	97.82	103.67	118.29
294	81.85	84.25	89.26	101.89	119.02	84.88	87.28	92.50	105.55	104.19	110.46	126.01	102.83	108.05	114.53	130.71
295	68.17	70.26	74.44	84.98	113.07	70.78	72.87	77.15	88.01	86.97	92.08	105.13	85.82	90.20	95.53	108.99
296	76.00	78.30	82.89	94.69	124.55	78.82	81.12	85.92	98.03	96.78	102.63	117.03	95.53	100.43	106.38	121.42
297	83.31	85.82	90.93	103.88	135.82	86.44	88.95	94.27	107.53	106.17	112.54	128.41	104.71	110.14	116.72	133.21
298	64.31	66.19	70.05	79.97	71.72	66.61	68.49	72.66	82.79	81.75	86.76	98.87	81.22	84.77	89.99	102.63
299	73.50	75.69	80.18	91.56	81.43	76.21	78.40	83.10	94.80	93.54	99.18	113.17	92.92	97.09	102.94	117.45
300	81.75	84.25	89.16	101.79	91.77	84.77	87.17	92.39	105.44	103.98	110.35	125.91	103.36	107.85	114.42	130.60
301	65.15	67.13	71.10	81.12	74.12	67.55	69.53	73.60	84.04	83.00	87.90	100.33	82.37	86.03	91.14	104.09
302	74.33	76.53	81.01	92.50	83.83	77.05	79.24	84.04	95.84	94.59	100.33	114.42	93.86	98.03	104.09	118.70
303	82.79	85.19	90.31	103.04	93.86	85.82	88.32	93.54	106.70	105.34	111.71	127.47	104.61	109.31	115.88	132.17
304	66.19	68.17	72.14	82.37	76.21	68.59	70.57	74.75	85.29	84.25	89.26	101.89	83.62	87.38	92.60	105.65
305	75.48	77.67	82.27	93.86	86.76	78.20	80.49	85.29	97.20	96.05	101.79	116.09	95.32	99.60	105.65	120.37
306	83.73	86.13	91.25	104.09	97.30	86.76	89.26	94.59	107.85	106.49	112.96	128.83	105.76	110.46	117.14	133.63
307	67.13	69.01	73.18	83.52	80.07	69.53	71.51	75.79	86.44	85.29	90.51	103.25	84.77	88.53	93.86	107.11
308	76.32	78.61	83.21	95.00	90.51	79.14	81.43	86.23	98.45	97.20	102.94	117.55	96.47	100.75	106.80	121.94
309	84.98	87.49	92.71	105.76	100.95	88.11	90.62	96.05	109.52	108.16	114.63	130.81	107.43	112.13	118.91	135.62
310	68.90	70.89	75.17	85.82	84.56	71.41	73.50	77.88	88.84	87.70	93.02	106.07	87.07	90.93	96.47	110.04

Table 7-3. Continued

	B=6.6 ft; D=0 ft				B=13.2 ft; D=0 ft				B=6.6 ft; D=3.3 ft				B=13.2 ft; D=6.6 ft			
#	Strip B/L=0	L/B=10 B/L=0.1	L/B=5 B/L=0.2	square	Strip v=0.2	Strip v=0.1	L/B=10 B/L=0.1	L/B=5 B/L=0.2	square	L/B=10 B/L=0.1	L/B=5 B/L=0.2	square	Strip B/L=0	L/B=10 B/L=0.1	L/B=5 B/L=0.2	square
311	77.26	79.55	84.25	96.15	95.32	80.07	82.37	87.28	99.60	98.24	104.19	118.91	97.61	102.00	108.05	123.40
312	86.23	88.74	94.06	107.32	106.38	89.37	91.98	97.41	111.19	109.72	116.30	132.80	108.89	113.80	120.58	137.70
313	69.95	72.04	76.32	87.07	89.99	72.56	74.65	79.14	90.20	89.05	94.48	107.74	88.43	92.39	98.03	111.71
314	78.72	81.12	85.92	98.14	100.95	81.64	84.04	88.95	101.58	100.33	106.17	121.31	99.49	103.98	110.14	125.80
315	88.01	90.62	96.05	109.62	112.44	91.25	93.86	99.49	113.48	112.02	118.81	135.51	111.19	116.20	123.19	140.52
316	71.72	73.81	78.20	89.26	97.41	74.33	76.42	81.01	92.50	91.14	96.78	110.46	90.62	94.59	100.33	114.63
317	81.33	83.73	88.64	101.16	109.52	84.25	86.65	91.87	104.82	103.36	109.72	125.18	102.73	107.22	113.80	129.87
318	89.68	92.29	97.72	111.60	121.63	92.92	95.63	101.27	115.57	114.11	120.90	138.02	113.27	118.39	125.38	143.13
319	75.17	77.36	81.95	93.54	108.89	77.88	80.07	84.88	96.88	95.53	101.37	115.68	94.90	99.08	105.13	120.06
320	83.42	85.82	90.93	103.88	121.83	86.44	88.95	94.27	107.53	106.17	112.54	128.41	105.34	110.14	116.72	133.21
321	91.45	94.17	99.70	113.80	134.78	94.80	97.51	103.36	117.87	116.41	123.40	140.73	115.57	120.69	127.99	146.06
322	79.03	81.43	86.23	98.34	128.52	81.95	84.36	89.37	101.89	100.64	106.70	121.83	100.02	104.50	110.66	126.22
323	87.17	89.68	95.00	108.47	142.61	90.31	92.92	98.45	112.33	110.87	117.55	134.15	110.04	115.05	121.94	139.17
324	94.80	97.61	103.46	118.08	156.50	98.34	101.16	107.22	122.25	120.69	128.10	145.95	119.85	125.18	132.80	151.48

7.4 Parametric Studies – Rock over Sand Subsurface

In south Florida, shallow foundations may not just reside over rock, but may have a sand layer underlying the cap-rock. Consequently, any bearing capacity assessment must consider the case of punching of the footing through the rock into the underlying sand. Using the FEM code with the elastic, perfectly plastic model for the rock, Figures 7.1 and 7.2, the underlying sand was characterized as a Drucker-Prager material with a cap. Three different thickness, T, of 1.5m, 2m and 4m for the rock layer (the distance between the bottom of strip footing and bottom of the rock layer), were used to study bearing capacity. Also investigated was the stiffness of the sand with two different Young's moduli of 5 and 10 MPa. The rock variables: cohesion intercept (c), initial friction angle (φ), second slope (ω), and σ_{peak} are the same as in Section 7.3 (Table 7-2). The

simulation results are presented in Table 7-4 and Table 7-5. The simulation results in SI unit are shown in Appendix G.

Table 7-4. FEM simulation results – Bearing capacity (tsf) on 4.9 to 6.6-ft rock over sand subsurface – Plane strain only

#	Rock (T) = 4.9 ft				Rock (T) = 4.9 ft				Rock (T) = 6.6 ft			
	E: 1.5 ksi B: 6.6ft D: 0ft	E: 1.5ksi B: 13.2ft D: 0ft	E: 1.5ksi B: 13.2ft D: 6.6ft	E: 1.5ksi B: 13.2ft D: 3.3ft	E: 0.7ksi B: 6.6ft D: 0ft	E: 0.7ksi B: 13.2ft D: 0ft	E: 0.7ksi B: 13.2ft D: 6.6ft	E: 0.7ksi B: 6.6ft D: 3.3ft	E: 1.5ksi B: 6.6ft D: 0ft	E: 1.5ksi B: 13.2ft D: 0ft	E:1.5ksi B: 13.2ft D: 6.6ft	E: 1.5ksi B: 6.6ft D: 3.3ft
1	3.65	3.76	4.59	4.38	3.03	3.13	3.86	3.55	3.86	3.97	4.91	4.70
2-27	same	results										
28	4.70	4.91	6.06	5.85	3.86	4.07	5.01	4.80	5.01	5.22	6.37	6.16
29	4.70	4.91	6.06	5.85	3.86	4.07	5.01	4.80	5.01	5.22	6.37	6.16
30	4.70	4.91	6.06	5.85	3.86	4.07	5.01	4.80	5.01	5.22	6.37	6.16
31	4.70	4.91	6.06	5.85	3.86	4.07	5.01	4.80	5.01	5.22	6.37	6.16
32	4.70	4.91	6.06	5.85	3.86	4.07	5.01	4.80	5.01	5.22	6.37	6.16
33	4.70	4.91	6.06	5.85	3.86	4.07	5.01	4.80	5.01	5.22	6.37	6.16
34	4.70	4.91	6.06	5.85	3.86	4.07	5.01	4.80	5.01	5.22	6.37	6.16
35	4.70	4.91	6.06	5.85	3.86	4.07	5.01	4.80	5.01	5.22	6.37	6.16
36	4.70	4.91	6.06	5.85	3.86	4.07	5.01	4.80	5.01	5.22	6.37	6.16
37	4.70	4.91	6.06	5.85	3.86	4.07	5.01	4.80	5.01	5.22	6.37	6.16
38	4.70	4.91	6.06	5.85	3.86	4.07	5.01	4.80	5.01	5.22	6.37	6.16
39	4.70	4.91	6.06	5.85	3.86	4.07	5.01	4.80	5.01	5.22	6.37	6.16
40	4.70	4.91	6.06	5.85	3.86	4.07	5.01	4.80	5.01	5.22	6.37	6.16
41	4.70	4.91	6.06	5.85	3.86	4.07	5.01	4.80	5.01	5.22	6.37	6.16
42	4.70	4.91	6.06	5.85	3.86	4.07	5.01	4.80	5.01	5.22	6.37	6.16
43	4.70	4.91	6.06	5.85	3.86	4.07	5.01	4.80	5.01	5.22	6.37	6.16
44	4.70	4.91	6.06	5.85	3.86	4.07	5.01	4.80	5.01	5.22	6.37	6.16
45	4.70	4.91	6.06	5.85	3.86	4.07	5.01	4.80	5.01	5.22	6.37	6.16
46	4.70	4.91	6.06	5.85	3.86	4.07	5.01	4.80	5.01	5.22	6.37	6.16
47	4.70	4.91	6.06	5.85	3.86	4.07	5.01	4.80	5.01	5.22	6.37	6.16
48	4.70	4.91	6.06	5.85	3.86	4.07	5.01	4.80	5.01	5.22	6.37	6.16
49	4.70	4.91	6.06	5.85	3.86	4.07	5.01	4.80	5.01	5.22	6.37	6.16
50	4.70	4.91	6.06	5.85	3.86	4.07	5.01	4.80	5.01	5.22	6.37	6.16
51	4.70	4.91	6.06	5.85	3.86	4.07	5.01	4.80	5.01	5.22	6.37	6.16
52	4.70	4.91	6.06	5.85	3.86	4.07	5.01	4.80	5.01	5.22	6.37	6.16
53	4.70	4.91	6.06	5.85	3.86	4.07	5.01	4.80	5.01	5.22	6.37	6.16
54	4.70	4.91	6.06	5.85	3.86	4.07	5.01	4.80	5.01	5.22	6.37	6.16

Table 7-4. Continued

#	Rock (T) = 4.9 ft				Rock (T) = 4.9 ft				Rock (T) = 6.6 ft			
	E: 1.5 ksi B: 6.6ft D: 0ft	E: 1.5ksi B: 13.2ft D: 0ft	E: 1.5ksi B: 13.2ft D: 6.6ft	E: 1.5ksi B: 13.2ft D: 3.3ft	E: 0.7ksi B: 6.6ft D: 0ft	E: 0.7ksi B: 13.2ft D: 0ft	E: 0.7ksi B: 13.2ft D: 6.6ft	E: 0.7ksi B: 6.6ft D: 3.3ft	E: 1.5ksi B: 6.6ft D: 0ft	E: 1.5ksi B: 13.2ft D: 0ft	E:1.5ksi B: 13.2ft D: 6.6ft	E: 1.5ksi B: 6.6ft D: 3.3ft
55	9.81	10.13	12.53	12.11	8.04	8.35	10.44	9.92	10.23	10.65	13.15	12.74
56	9.81	10.13	12.53	12.11	8.04	8.35	10.44	9.92	10.23	10.65	13.15	12.74
57	9.81	10.13	12.53	12.11	8.04	8.35	10.44	9.92	10.23	10.65	13.15	12.74
58	9.81	10.13	12.53	12.11	8.04	8.35	10.44	9.92	10.23	10.65	13.15	12.74
59	9.81	10.13	12.53	12.11	8.04	8.35	10.44	9.92	10.23	10.65	13.15	12.74
60	9.81	10.13	12.53	12.11	8.04	8.35	10.44	9.92	10.23	10.65	13.15	12.74
61	9.81	10.13	12.53	12.11	8.04	8.35	10.44	9.92	10.23	10.65	13.15	12.74
62	9.81	10.13	12.53	12.11	8.04	8.35	10.44	9.92	10.23	10.65	13.15	12.74
63	9.81	10.13	12.53	12.11	8.04	8.35	10.44	9.92	10.23	10.65	13.15	12.74
64	9.81	10.13	12.53	12.11	8.04	8.35	10.44	9.92	10.23	10.65	13.15	12.74
65	9.81	10.13	12.53	12.11	8.04	8.35	10.44	9.92	10.23	10.65	13.15	12.74
66	9.81	10.13	12.53	12.11	8.04	8.35	10.44	9.92	10.23	10.65	13.15	12.74
67	9.81	10.13	12.53	12.11	8.04	8.35	10.44	9.92	10.23	10.65	13.15	12.74
68	9.81	10.13	12.53	12.11	8.04	8.35	10.44	9.92	10.23	10.65	13.15	12.74
69	9.81	10.13	12.53	12.11	8.04	8.35	10.44	9.92	10.23	10.65	13.15	12.74
70	9.81	10.13	12.53	12.11	8.04	8.35	10.44	9.92	10.23	10.65	13.15	12.74
71	9.81	10.13	12.53	12.11	8.04	8.35	10.44	9.92	10.23	10.65	13.15	12.74
72	9.81	10.13	12.53	12.11	8.04	8.35	10.44	9.92	10.23	10.65	13.15	12.74
73	9.81	10.13	12.53	12.11	8.04	8.35	10.44	9.92	10.23	10.65	13.15	12.74
74	9.81	10.13	12.53	12.11	8.04	8.35	10.44	9.92	10.23	10.65	13.15	12.74
75	9.81	10.13	12.53	12.11	8.04	8.35	10.44	9.92	10.23	10.65	13.15	12.74
76	9.81	10.13	12.53	12.11	8.04	8.35	10.44	9.92	10.23	10.65	13.15	12.74
77	9.81	10.13	12.53	12.11	8.04	8.35	10.44	9.92	10.23	10.65	13.15	12.74
78	9.81	10.13	12.53	12.11	8.04	8.35	10.44	9.92	10.23	10.65	13.15	12.74
79	9.81	10.13	12.53	12.11	8.04	8.35	10.44	9.92	10.23	10.65	13.15	12.74
80	9.81	10.13	12.53	12.11	8.04	8.35	10.44	9.92	10.23	10.65	13.15	12.74
81	9.81	10.13	12.53	12.11	8.04	8.35	10.44	9.92	10.23	10.65	13.15	12.74
82	13.89	14.41	17.64	17.02	11.38	11.90	14.72	13.99	14.51	15.03	18.37	17.75
83	15.14	15.66	19.21	18.48	12.42	12.84	15.97	15.14	15.76	16.39	20.04	19.31
84	17.43	18.06	22.13	21.30	14.30	14.82	18.48	17.43	18.17	18.79	23.07	22.24
85	13.99	14.51	17.85	17.23	11.48	11.90	14.82	14.09	14.62	15.14	18.58	17.96
86	15.24	15.76	19.42	18.69	12.42	12.95	16.18	15.35	15.87	16.50	20.25	19.52
87	17.54	18.17	22.34	21.51	14.30	14.93	18.58	17.64	18.37	19.00	23.28	22.45
88	14.20	14.72	18.06	17.43	11.59	12.11	15.03	14.30	14.82	15.35	18.79	18.17

Table 7-4. Continued

#	Rock (T) = 4.9 ft				Rock (T) = 4.9 ft				Rock (T) = 6.6 ft			
	E: 1.5 ksi B: 6.6ft D: 0ft	E: 1.5ksi B: 13.2ft D: 0ft	E: 1.5ksi B: 13.2ft D: 6.6ft	E: 1.5ksi B: 13.2ft D: 3.3ft	E: 0.7ksi B: 6.6ft D: 0ft	E: 0.7ksi B: 13.2ft D: 0ft	E: 0.7ksi B: 13.2ft D: 6.6ft	E: 0.7ksi B: 6.6ft D: 3.3ft	E: 1.5ksi B: 6.6ft D: 0ft	E: 1.5ksi B: 13.2ft D: 0ft	E:1.5ksi B: 13.2ft D: 6.6ft	E: 1.5ksi B: 6.6ft D: 3.3ft
89	15.45	16.08	19.73	19.00	12.63	13.26	16.39	15.56	16.18	16.81	20.57	19.84
90	17.64	18.27	22.45	21.61	14.41	15.03	18.69	17.75	18.48	19.11	23.49	22.65
91	14.62	15.14	18.48	17.85	11.90	12.42	15.35	14.62	15.24	15.76	19.31	18.58
92	15.56	16.18	19.94	19.21	12.74	13.36	16.60	15.76	16.29	16.91	20.78	20.04
93	17.85	18.48	22.76	21.92	14.62	15.24	19.00	17.96	18.58	19.31	23.70	22.86
94	14.72	15.24	18.69	18.06	12.01	12.53	15.56	14.82	15.35	15.87	19.52	18.79
95	15.66	16.29	19.94	19.21	12.84	13.36	16.60	15.76	16.39	17.02	20.88	20.15
96	17.96	18.58	22.86	22.03	14.72	15.35	19.00	18.06	18.69	19.42	23.91	23.07
97	14.72	15.24	18.79	18.17	12.01	12.53	15.66	14.93	15.45	15.97	19.63	18.90
98	15.66	16.29	20.04	19.31	12.84	13.36	16.70	15.87	16.50	17.12	20.98	20.25
99	18.06	18.69	22.97	22.13	14.72	15.35	19.11	18.17	18.79	19.52	24.01	23.18
100	14.93	15.45	19.00	18.27	12.21	12.74	15.87	15.03	15.56	16.18	19.84	19.11
101	15.87	16.50	20.25	19.52	12.95	13.57	16.91	15.97	16.60	17.23	21.19	20.46
102	18.17	18.79	23.07	22.24	14.82	15.45	19.21	18.27	18.90	19.63	24.12	23.28
103	15.14	15.66	19.21	18.48	12.42	12.84	15.97	15.14	15.66	16.29	20.04	19.31
104	16.08	16.70	20.57	19.84	13.15	13.78	17.12	16.29	16.81	17.43	21.40	20.67
105	18.27	18.90	23.18	22.34	14.93	15.56	19.31	18.37	19.00	19.73	24.22	23.39
106	15.24	15.76	19.42	18.69	12.42	12.95	16.18	15.35	15.87	16.50	20.25	19.52
107	16.29	16.91	20.78	20.04	13.36	13.89	17.33	16.50	17.02	17.64	21.72	20.98
108	18.37	19.11	23.49	22.65	15.03	15.76	19.52	18.58	19.21	19.94	24.43	23.59
109	19.21	19.94	24.53	23.70	15.66	16.39	20.46	19.42	20.25	20.98	25.79	24.85
110	19.21	19.94	24.53	23.70	15.66	16.39	20.46	19.42	20.25	20.98	25.79	24.85
111	19.21	19.94	24.53	23.70	15.66	16.39	20.46	19.42	20.25	20.98	25.79	24.85
112	19.21	19.94	24.53	23.70	15.66	16.39	20.46	19.42	20.25	20.98	25.79	24.85
113	19.21	19.94	24.53	23.70	15.66	16.39	20.46	19.42	20.25	20.98	25.79	24.85
114	19.21	19.94	24.53	23.70	15.66	16.39	20.46	19.42	20.25	20.98	25.79	24.85
115	19.21	19.94	24.53	23.70	15.66	16.39	20.46	19.42	20.25	20.98	25.79	24.85
116	19.21	19.94	24.53	23.70	15.66	16.39	20.46	19.42	20.25	20.98	25.79	24.85
117	19.21	19.94	24.53	23.70	15.66	16.39	20.46	19.42	20.25	20.98	25.79	24.85
118	19.21	19.94	24.53	23.70	15.66	16.39	20.46	19.42	20.25	20.98	25.79	24.85
119	19.21	19.94	24.53	23.70	15.66	16.39	20.46	19.42	20.25	20.98	25.79	24.85
120	19.21	19.94	24.53	23.70	15.66	16.39	20.46	19.42	20.25	20.98	25.79	24.85
121	19.21	19.94	24.53	23.70	15.66	16.39	20.46	19.42	20.25	20.98	25.79	24.85
122	19.21	19.94	24.53	23.70	15.66	16.39	20.46	19.42	20.25	20.98	25.79	24.85

Table 7-4. Continued

#	Rock (T) = 4.9 ft				Rock (T) = 4.9 ft				Rock (T) = 6.6 ft			
	E: 1.5 ksi B: 6.6ft D: 0ft	E: 1.5ksi B: 13.2ft D: 0ft	E: 1.5ksi B: 13.2ft D: 6.6ft	E: 1.5ksi B: 13.2ft D: 3.3ft	E: 0.7ksi B: 6.6ft D: 0ft	E: 0.7ksi B: 13.2ft D: 0ft	E: 0.7ksi B: 13.2ft D: 6.6ft	E: 0.7ksi B: 6.6ft D: 3.3ft	E: 1.5ksi B: 6.6ft D: 0ft	E: 1.5ksi B: 13.2ft D: 0ft	E:1.5ksi B: 13.2ft D: 6.6ft	E: 1.5ksi B: 6.6ft D: 3.3ft
123	19.21	19.94	24.53	23.70	15.66	16.39	20.46	19.42	20.25	20.98	25.79	24.85
124	19.21	19.94	24.53	23.70	15.66	16.39	20.46	19.42	20.25	20.98	25.79	24.85
125	19.21	19.94	24.53	23.70	15.66	16.39	20.46	19.42	20.25	20.98	25.79	24.85
126	19.21	19.94	24.53	23.70	15.66	16.39	20.46	19.42	20.25	20.98	25.79	24.85
127	19.21	19.94	24.53	23.70	15.66	16.39	20.46	19.42	20.25	20.98	25.79	24.85
128	19.21	19.94	24.53	23.70	15.66	16.39	20.46	19.42	20.25	20.98	25.79	24.85
129	19.21	19.94	24.53	23.70	15.66	16.39	20.46	19.42	20.25	20.98	25.79	24.85
130	19.21	19.94	24.53	23.70	15.66	16.39	20.46	19.42	20.25	20.98	25.79	24.85
131	19.21	19.94	24.53	23.70	15.66	16.39	20.46	19.42	20.25	20.98	25.79	24.85
132	19.21	19.94	24.53	23.70	15.66	16.39	20.46	19.42	20.25	20.98	25.79	24.85
133	19.21	19.94	24.53	23.70	15.66	16.39	20.46	19.42	20.25	20.98	25.79	24.85
134	19.21	19.94	24.53	23.70	15.66	16.39	20.46	19.42	20.25	20.98	25.79	24.85
135	19.21	19.94	24.53	23.70	15.66	16.39	20.46	19.42	20.25	20.98	25.79	24.85
136	23.49	24.33	29.86	28.81	19.21	20.04	24.85	23.59	24.64	25.58	31.42	30.28
137	27.98	29.02	35.60	34.35	22.86	23.91	29.65	28.19	29.44	30.48	37.48	36.12
138	28.19	29.23	35.81	34.56	23.07	24.12	29.86	28.40	29.65	30.69	37.69	36.33
139	23.70	24.53	30.17	29.13	19.42	20.15	25.16	23.91	24.85	25.79	31.74	30.59
140	27.98	29.02	35.60	34.35	22.86	23.91	29.65	28.19	29.44	30.48	37.48	36.12
141	28.19	29.23	35.81	34.56	23.07	24.12	29.86	28.40	29.65	30.69	37.69	36.33
142	23.91	24.85	30.48	29.34	19.52	20.46	25.37	24.12	25.16	26.10	32.05	30.90
143	27.98	29.02	35.60	34.35	22.86	23.91	29.65	28.19	29.44	30.48	37.48	36.12
144	28.19	29.23	35.81	34.56	23.07	24.12	29.86	28.40	29.65	30.69	37.69	36.33
145	24.01	24.95	30.59	29.44	19.63	20.57	25.47	24.12	25.26	26.20	32.26	31.11
146	27.98	29.02	35.60	34.35	22.86	23.91	29.65	28.19	29.44	30.48	37.48	36.12
147	28.19	29.23	35.81	34.56	23.07	24.12	29.86	28.40	29.65	30.69	37.69	36.33
148	24.22	25.16	30.90	29.75	19.84	20.67	25.79	24.43	25.58	26.52	32.57	31.42
149	27.98	29.02	35.60	34.35	22.86	23.91	29.65	28.19	29.44	30.48	37.48	36.12
150	28.19	29.23	35.81	34.56	23.07	24.12	29.86	28.40	29.65	30.69	37.69	36.33
151	24.33	25.26	31.01	29.86	19.84	20.78	25.79	24.53	25.68	26.62	32.68	31.53
152	27.98	29.02	35.60	34.35	22.86	23.91	29.65	28.19	29.44	30.48	37.48	36.12
153	28.19	29.23	35.81	34.56	23.07	24.12	29.86	28.40	29.65	30.69	37.69	36.33
154	24.43	25.37	31.22	30.07	19.94	20.88	26.00	24.64	25.79	26.73	32.78	31.63
155	27.98	29.02	35.60	34.35	22.86	23.91	29.65	28.19	29.44	30.48	37.48	36.12
156	28.19	29.23	35.81	34.56	23.07	24.12	29.86	28.40	29.65	30.69	37.69	36.33

Table 7-4. Continued

#	Rock (T) = 4.9 ft				Rock (T) = 4.9 ft				Rock (T) = 6.6 ft			
	E: 1.5 ksi B: 6.6ft D: 0ft	E: 1.5ksi B: 13.2ft D: 0ft	E: 1.5ksi B: 13.2ft D: 6.6ft	E: 1.5ksi B: 13.2ft D: 3.3ft	E: 0.7ksi B: 6.6ft D: 0ft	E: 0.7ksi B: 13.2ft D: 0ft	E: 0.7ksi B: 13.2ft D: 6.6ft	E: 0.7ksi B: 6.6ft D: 3.3ft	E: 1.5ksi B: 6.6ft D: 0ft	E: 1.5ksi B: 13.2ft D: 0ft	E:1.5ksi B: 13.2ft D: 6.6ft	E: 1.5ksi B: 6.6ft D: 3.3ft
157	24.64	25.58	31.42	30.28	20.15	21.09	26.20	24.85	26.00	26.94	33.09	3194.64
158	27.98	29.02	35.60	34.35	22.86	23.91	29.65	28.19	29.44	30.48	37.48	36.12
159	28.19	29.23	35.81	34.56	23.07	24.12	29.86	28.40	29.65	30.69	37.69	36.33
160	25.47	25.79	31.63	30.48	20.78	21.19	26.31	25.06	26.20	27.14	33.30	3215.52
161	27.98	29.02	35.60	34.35	22.86	23.91	29.65	28.19	29.44	30.48	37.48	36.12
162	28.19	29.23	35.81	34.56	23.07	24.12	29.86	28.40	29.65	30.69	37.69	36.33
163	25.47	26.41	32.36	31.22	20.78	21.72	26.94	25.58	26.83	27.77	34.03	32.78
164	30.69	31.84	39.05	37.69	25.06	26.20	32.57	30.90	32.36	33.51	41.13	39.67
165	35.91	37.27	45.73	44.06	29.34	30.69	38.11	36.12	37.90	39.25	48.13	46.46
166	25.79	26.73	32.78	31.63	21.09	22.03	27.35	26.00	27.04	28.08	34.45	33.20
167	31.11	32.26	39.57	38.11	25.47	26.52	32.99	31.22	32.68	33.93	41.66	40.19
168	36.12	37.48	46.04	44.37	29.55	30.90	38.31	36.44	38.11	39.46	48.44	46.77
169	26.20	27.14	33.30	32.16	21.40	22.34	27.77	26.41	27.56	28.61	35.08	33.83
170	31.42	32.57	40.09	38.63	25.68	26.83	33.41	31.74	33.09	34.35	42.18	40.72
171	36.33	37.69	46.35	44.68	29.75	31.01	38.63	36.64	38.21	39.67	48.75	46.98
172	26.62	27.56	33.83	32.57	21.72	22.65	28.19	26.73	27.98	29.02	35.60	34.35
173	31.74	32.89	40.40	38.94	26.00	27.04	33.62	31.95	33.30	34.56	42.49	41.03
174	36.64	38.00	46.67	45.00	29.96	31.32	38.84	36.96	38.52	39.99	49.07	47.29
175	26.94	27.98	34.35	33.09	22.03	23.07	28.61	27.14	28.40	29.44	36.12	34.87
176	32.05	33.20	40.72	39.25	26.20	27.35	33.93	32.16	33.72	34.97	42.91	41.34
177	36.96	38.31	47.08	45.41	30.17	31.53	39.25	37.27	38.84	40.30	49.49	47.71
178	27.35	28.40	34.87	33.62	22.34	23.39	29.02	27.56	28.81	29.86	36.75	35.50
179	32.26	33.51	41.13	39.67	26.41	27.56	34.24	32.57	34.03	35.29	43.33	41.76
180	37.06	38.42	47.19	45.52	30.28	31.63	39.36	37.38	38.94	40.40	49.69	47.92
181	28.08	29.13	35.81	34.56	22.97	24.01	29.86	28.40	29.65	30.69	37.58	36.23
182	32.78	34.03	41.76	40.30	26.83	27.98	34.77	33.09	34.45	35.70	43.95	42.39
183	37.48	38.84	47.71	46.04	30.59	31.95	39.78	37.79	39.36	40.82	50.22	48.44
184	28.92	29.96	36.75	35.39	23.59	24.64	30.59	29.02	30.28	31.42	38.63	37.27
185	33.30	34.56	42.49	40.92	27.25	28.50	35.39	33.62	35.08	36.33	44.68	43.12
186	37.90	39.25	48.13	46.35	31.01	32.36	40.09	38.00	39.78	41.24	50.74	48.96
187	29.75	30.90	37.90	36.54	24.33	25.47	31.53	29.96	31.32	32.47	39.88	38.42
188	34.14	35.39	43.43	41.86	27.87	29.13	36.23	34.35	35.81	37.17	45.73	44.06
189	38.63	40.09	49.28	47.50	31.53	32.99	41.03	38.94	40.72	42.18	51.78	49.90
190	26.94	27.98	34.35	33.09	22.03	23.07	28.61	27.14	28.40	29.44	36.12	34.87

Table 7-4. Continued

#	Rock (T) = 4.9 ft				Rock (T) = 4.9 ft				Rock (T) = 6.6 ft			
	E: 1.5 ksi B: 6.6ft D: 0ft	E: 1.5ksi B: 13.2ft D: 0ft	E: 1.5ksi B: 13.2ft D: 6.6ft	E: 1.5ksi B: 13.2ft D: 3.3ft	E: 0.7ksi B: 6.6ft D: 0ft	E: 0.7ksi B: 13.2ft D: 0ft	E: 0.7ksi B: 13.2ft D: 6.6ft	E: 0.7ksi B: 6.6ft D: 3.3ft	E: 1.5ksi B: 6.6ft D: 0ft	E: 1.5ksi B: 13.2ft D: 0ft	E:1.5ksi B: 13.2ft D: 6.6ft	E: 1.5ksi B: 6.6ft D: 3.3ft
191	32.78	34.03	41.76	40.30	26.83	27.98	34.77	33.09	34.45	35.70	43.95	42.39
192	38.31	39.78	48.86	47.08	31.32	32.78	40.72	38.63	40.40	41.86	51.47	49.69
193	27.35	28.40	34.87	33.62	22.34	23.39	29.02	27.56	28.81	29.86	36.75	35.50
194	33.20	34.45	42.28	40.72	27.14	28.40	35.18	33.41	34.97	36.23	44.47	42.91
195	38.73	40.19	49.28	47.50	31.63	33.09	41.03	38.94	40.82	42.28	51.89	50.01
196	27.98	29.02	35.70	34.45	22.86	23.91	29.75	28.29	29.55	30.59	37.58	36.23
197	33.62	34.87	42.80	41.24	27.46	28.71	35.70	33.83	35.39	36.64	45.00	43.43
198	39.25	40.72	49.90	48.13	32.05	33.51	41.55	39.46	41.24	42.80	52.51	50.63
199	28.71	29.75	36.54	35.18	23.49	24.53	30.48	28.81	30.28	31.42	38.52	37.17
200	34.24	35.50	43.53	41.97	27.98	29.23	36.23	34.45	36.02	37.38	45.83	44.16
201	39.78	41.24	50.63	48.86	32.47	33.93	42.18	40.09	41.86	43.43	53.35	51.47
202	29.34	30.38	37.27	35.91	24.01	25.06	31.01	29.44	30.80	31.95	39.25	37.90
203	34.87	36.12	44.37	42.80	28.50	29.75	36.96	35.08	36.64	38.00	46.67	45.00
204	40.40	41.86	51.36	49.49	32.99	34.45	42.80	40.61	42.49	44.06	54.08	52.30
205	29.65	30.80	37.79	36.44	24.22	25.37	31.53	29.86	31.22	32.36	39.78	38.31
206	35.29	36.64	45.00	43.33	28.81	30.17	37.48	35.50	37.17	38.52	47.29	45.62
207	40.92	42.49	52.10	50.22	33.41	34.97	43.43	41.24	43.12	44.68	54.81	52.83
208	30.90	32.05	39.36	37.90	25.26	26.41	32.78	31.11	32.57	33.72	41.34	39.88
209	36.33	37.69	46.25	44.58	29.75	31.01	38.52	36.54	38.21	39.57	48.65	46.88
210	41.76	43.33	53.14	51.26	34.14	35.70	44.27	42.07	43.85	45.52	55.96	53.97
211	31.84	32.99	40.51	39.05	26.00	27.14	33.72	32.05	33.51	34.77	42.60	41.13
212	37.48	38.84	47.71	46.04	30.59	31.95	39.78	37.79	39.36	40.82	50.22	48.44
213	43.01	44.58	54.71	52.72	35.18	36.75	45.62	43.22	45.21	46.88	57.52	55.44
214	33.41	34.66	42.60	41.03	27.35	28.50	35.50	33.62	35.29	36.54	44.79	43.22
215	39.05	40.51	49.80	48.02	31.95	33.30	41.45	39.36	41.13	42.70	52.41	50.53
216	44.58	46.25	56.79	54.71	36.44	38.11	47.29	44.89	46.88	48.65	59.72	55.54
217	26.73	27.77	34.03	32.78	21.82	22.86	28.40	26.94	28.19	29.23	35.81	34.56
218	26.73	27.77	34.03	32.78	21.82	22.86	28.40	26.94	28.19	29.23	35.81	34.56
219	26.73	27.77	34.03	32.78	21.82	22.86	28.40	26.94	28.19	29.23	35.81	34.56
220	26.73	27.77	34.03	32.78	21.82	22.86	28.40	26.94	28.19	29.23	35.81	34.56
221	26.73	27.77	34.03	32.78	21.82	22.86	28.40	26.94	28.19	29.23	35.81	34.56
222	26.73	27.77	34.03	32.78	21.82	22.86	28.40	26.94	28.19	29.23	35.81	34.56
223	26.73	27.77	34.03	32.78	21.82	22.86	28.40	26.94	28.19	29.23	35.81	34.56
224	26.73	27.77	34.03	32.78	21.82	22.86	28.40	26.94	28.19	29.23	35.81	34.56

Table 7-4. Continued

#	Rock (T) = 4.9 ft				Rock (T) = 4.9 ft				Rock (T) = 6.6 ft			
	E: 1.5 ksi B: 6.6ft D: 0ft	E: 1.5ksi B: 13.2ft D: 0ft	E: 1.5ksi B: 13.2ft D: 6.6ft	E: 1.5ksi B: 13.2ft D: 3.3ft	E: 0.7ksi B: 6.6ft D: 0ft	E: 0.7ksi B: 13.2ft D: 0ft	E: 0.7ksi B: 13.2ft D: 6.6ft	E: 0.7ksi B: 6.6ft D: 3.3ft	E: 1.5ksi B: 6.6ft D: 0ft	E: 1.5ksi B: 13.2ft D: 0ft	E:1.5ksi B: 13.2ft D: 6.6ft	E: 1.5ksi B: 6.6ft D: 3.3ft
225	26.73	27.77	34.03	32.78	21.82	22.86	28.40	26.94	28.19	29.23	35.81	34.56
226	26.73	27.77	34.03	32.78	21.82	22.86	28.40	26.94	28.19	29.23	35.81	34.56
227	26.73	27.77	34.03	32.78	21.82	22.86	28.40	26.94	28.19	29.23	35.81	34.56
228	26.73	27.77	34.03	32.78	21.82	22.86	28.40	26.94	28.19	29.23	35.81	34.56
229	26.73	27.77	34.03	32.78	21.82	22.86	28.40	26.94	28.19	29.23	35.81	34.56
230	26.73	27.77	34.03	32.78	21.82	22.86	28.40	26.94	28.19	29.23	35.81	34.56
231	26.73	27.77	34.03	32.78	21.82	22.86	28.40	26.94	28.19	29.23	35.81	34.56
232	26.73	27.77	34.03	32.78	21.82	22.86	28.40	26.94	28.19	29.23	35.81	34.56
233	26.73	27.77	34.03	32.78	21.82	22.86	28.40	26.94	28.19	29.23	35.81	34.56
234	26.73	27.77	34.03	32.78	21.82	22.86	28.40	26.94	28.19	29.23	35.81	34.56
235	26.73	27.77	34.03	32.78	21.82	22.86	28.40	26.94	28.19	29.23	35.81	34.56
236	26.73	27.77	34.03	32.78	21.82	22.86	28.40	26.94	28.19	29.23	35.81	34.56
237	26.73	27.77	34.03	32.78	21.82	22.86	28.40	26.94	28.19	29.23	35.81	34.56
238	26.73	27.77	34.03	32.78	21.82	22.86	28.40	26.94	28.19	29.23	35.81	34.56
239	26.73	27.77	34.03	32.78	21.82	22.86	28.40	26.94	28.19	29.23	35.81	34.56
240	26.73	27.77	34.03	32.78	21.82	22.86	28.40	26.94	28.19	29.23	35.81	34.56
241	26.73	27.77	34.03	32.78	21.82	22.86	28.40	26.94	28.19	29.23	35.81	34.56
242	26.73	27.77	34.03	32.78	21.82	22.86	28.40	26.94	28.19	29.23	35.81	34.56
243	26.73	27.77	34.03	32.78	21.82	22.86	28.40	26.94	28.19	29.23	35.81	34.56
244	34.03	35.29	43.33	41.76	27.87	29.02	36.12	34.24	35.81	37.17	45.62	44.06
245	39.05	40.51	49.80	48.02	31.95	33.30	41.45	39.36	41.13	42.70	52.41	50.53
246	39.05	40.51	49.80	48.02	31.95	33.30	41.45	39.36	41.13	42.70	52.41	50.53
247	34.24	35.50	43.53	41.97	27.98	29.23	36.23	34.45	36.02	37.38	45.83	44.16
248	39.05	40.51	49.80	48.02	31.95	33.30	41.45	39.36	41.13	42.70	52.41	50.53
249	39.05	40.51	49.80	48.02	31.95	33.30	41.45	39.36	41.13	42.70	52.41	50.53
250	34.45	35.70	43.85	42.28	28.19	29.44	36.54	34.66	36.23	37.58	46.14	44.47
251	39.05	40.51	49.80	48.02	31.95	33.30	41.45	39.36	41.13	42.70	52.41	50.53
252	39.05	40.51	49.80	48.02	31.95	33.30	41.45	39.36	41.13	42.70	52.41	50.53
253	34.66	35.91	44.16	42.60	28.29	29.55	36.75	34.97	36.44	37.79	46.46	44.79
254	39.05	40.51	49.80	48.02	31.95	33.30	41.45	39.36	41.13	42.70	52.41	50.53
255	39.05	40.51	49.80	48.02	31.95	33.30	41.45	39.36	41.13	42.70	52.41	50.53
256	35.29	36.64	45.00	43.33	28.81	30.17	37.48	35.50	37.17	38.52	47.29	45.62
257	39.05	40.51	49.80	48.02	31.95	33.30	41.45	39.36	41.13	42.70	52.41	50.53
258	39.05	40.51	49.80	48.02	31.95	33.30	41.45	39.36	41.13	42.70	52.41	50.53

Table 7-4. Continued

#	Rock (T) = 4.9 ft				Rock (T) = 4.9 ft				Rock (T) = 6.6 ft			
	E: 1.5 ksi B: 6.6ft D: 0ft	E: 1.5ksi B: 13.2ft D: 0ft	E: 1.5ksi B: 13.2ft D: 6.6ft	E: 1.5ksi B: 13.2ft D: 3.3ft	E: 0.7ksi B: 6.6ft D: 0ft	E: 0.7ksi B: 13.2ft D: 0ft	E: 0.7ksi B: 13.2ft D: 6.6ft	E: 0.7ksi B: 6.6ft D: 3.3ft	E: 1.5ksi B: 6.6ft D: 0ft	E: 1.5ksi B: 13.2ft D: 0ft	E:1.5ksi B: 13.2ft D: 6.6ft	E: 1.5ksi B: 6.6ft D: 3.3ft
259	35.50	36.85	45.21	43.53	29.02	30.38	37.69	35.70	37.38	38.73	47.50	45.83
260	39.05	40.51	49.80	48.02	31.95	33.30	41.45	39.36	41.13	42.70	52.41	50.53
261	39.05	40.51	49.80	48.02	31.95	33.30	41.45	39.36	41.13	42.70	52.41	50.53
262	35.70	37.06	45.52	43.85	29.23	30.48	37.90	36.02	37.69	39.05	47.92	46.25
263	39.05	40.51	49.80	48.02	31.95	33.30	41.45	39.36	41.13	42.70	52.41	50.53
264	39.05	40.51	49.80	48.02	31.95	33.30	41.45	39.36	41.13	42.70	52.41	50.53
265	35.91	37.27	45.73	44.06	29.34	30.69	38.11	36.12	37.90	39.25	48.13	46.46
266	39.05	40.51	49.80	48.02	31.95	33.30	41.45	39.36	41.13	42.70	52.41	50.53
267	39.05	40.51	49.80	48.02	31.95	33.30	41.45	39.36	41.13	42.70	52.41	50.53
268	36.12	37.48	46.04	44.37	29.55	30.90	38.31	36.44	38.11	39.46	48.44	46.77
269	39.05	40.51	49.80	48.02	31.95	33.30	41.45	39.36	41.13	42.70	52.41	50.53
270	39.05	40.51	49.80	48.02	31.95	33.30	41.45	39.36	41.13	42.70	52.41	50.53
271	37.90	39.25	48.13	46.35	31.01	32.36	40.09	38.00	39.78	41.24	50.74	48.96
272	43.33	44.89	55.12	53.14	35.39	36.96	45.94	43.64	45.52	47.19	57.94	55.85
273	48.44	50.22	61.60	59.40	39.57	41.34	51.36	48.75	50.95	52.83	64.83	62.54
274	38.21	39.67	48.65	46.88	31.22	32.68	40.51	38.42	40.19	41.66	51.16	49.38
275	43.64	45.31	55.54	53.56	35.70	37.27	46.25	43.95	45.94	47.61	58.46	56.38
276	48.75	50.53	62.01	59.82	39.88	41.55	51.68	49.07	51.26	53.14	65.25	62.95
277	38.63	40.09	49.28	47.50	31.53	32.99	41.03	38.94	40.72	42.18	51.78	49.90
278	43.95	45.62	56.06	54.08	35.91	37.58	46.67	44.37	46.35	48.02	58.99	56.90
279	49.07	50.95	62.54	60.24	40.09	41.97	52.10	49.38	51.68	53.56	65.77	63.48
280	39.05	40.51	49.69	47.92	31.95	33.30	41.45	39.36	41.03	42.60	52.30	50.43
281	44.37	46.04	56.58	54.50	36.23	37.90	47.19	44.68	46.67	48.44	59.51	57.42
282	49.38	51.26	62.95	60.66	40.40	42.18	52.41	49.80	52.10	53.97	66.29	63.89
283	39.78	41.24	50.63	48.86	32.47	33.93	42.18	40.09	41.86	43.43	53.35	51.47
284	44.68	46.35	57.00	54.91	36.54	38.21	47.50	45.10	46.98	48.75	59.93	57.84
285	49.80	51.68	63.37	61.07	40.72	42.60	52.83	50.11	52.41	54.29	66.71	64.31
286	40.19	41.66	51.16	49.28	32.89	34.24	42.60	40.40	42.28	43.85	53.87	51.99
287	45.00	46.67	57.32	55.23	36.75	38.42	47.71	45.31	47.40	49.17	60.34	58.26
288	50.11	51.99	63.79	61.49	40.92	42.80	53.14	50.43	52.72	54.71	67.13	64.73
289	40.72	42.28	51.99	50.11	33.30	34.77	43.33	41.13	42.91	44.47	54.71	52.72
290	45.62	47.29	58.05	55.96	37.27	38.94	48.34	45.94	48.02	49.80	61.07	58.88
291	50.63	52.51	64.52	62.22	41.45	43.22	53.77	51.05	53.35	55.33	67.86	65.46
292	41.76	43.33	53.14	51.26	34.14	35.70	44.27	42.07	43.85	45.52	55.96	53.97

Table 7-4. Continued

#	Rock (T) = 4.9 ft				Rock (T) = 4.9 ft				Rock (T) = 6.6 ft			
	E: 1.5 ksi B: 6.6ft D: 0ft	E: 1.5ksi B: 13.2ft D: 0ft	E: 1.5ksi B: 13.2ft D: 6.6ft	E: 1.5ksi B: 13.2ft D: 3.3ft	E: 0.7ksi B: 6.6ft D: 0ft	E: 0.7ksi B: 13.2ft D: 0ft	E: 0.7ksi B: 13.2ft D: 6.6ft	E: 0.7ksi B: 6.6ft D: 3.3ft	E: 1.5ksi B: 6.6ft D: 0ft	E: 1.5ksi B: 13.2ft D: 0ft	E:1.5ksi B: 13.2ft D: 6.6ft	E: 1.5ksi B: 6.6ft D: 3.3ft
293	46.56	48.34	59.30	57.21	38.11	39.78	49.38	46.98	49.07	50.84	62.43	60.24
294	51.47	53.35	65.46	63.06	42.07	43.95	54.50	51.68	54.08	56.06	68.90	66.50
295	42.91	44.47	54.60	52.62	35.08	36.64	45.52	43.12	45.10	46.77	57.42	55.44
296	47.71	49.49	60.87	58.67	39.05	40.72	50.74	48.13	50.22	52.10	64.00	61.70
297	52.30	54.29	66.71	64.31	42.80	44.68	55.54	52.72	55.12	57.11	70.16	67.65
298	40.40	41.86	51.36	49.49	32.99	34.45	42.80	40.61	42.49	44.06	54.08	52.20
299	46.25	47.92	58.78	56.69	37.79	39.46	48.96	46.46	48.65	50.43	61.91	59.72
300	51.36	53.24	65.46	63.06	41.97	43.85	54.50	51.68	54.08	56.06	68.80	66.40
301	40.92	42.49	52.10	50.22	33.41	34.97	43.43	41.24	43.12	44.68	54.81	52.83
302	46.67	48.44	59.51	57.32	38.11	39.88	49.59	46.98	49.17	50.95	62.54	60.34
303	51.99	53.97	66.19	63.79	42.49	44.47	55.12	52.30	54.71	56.69	69.63	67.13
304	41.55	43.12	52.93	51.05	33.93	35.50	44.06	41.86	43.74	45.31	55.65	53.66
305	47.40	49.17	60.34	58.15	38.73	40.51	50.32	47.71	49.80	51.68	63.48	61.18
306	52.51	54.50	66.92	64.52	42.91	44.89	55.75	52.93	55.23	57.32	70.47	67.96
307	42.18	43.74	53.66	51.68	34.45	36.02	44.68	42.39	44.27	45.94	56.48	54.50
308	47.92	49.69	61.07	58.88	39.15	40.92	50.84	48.34	50.43	52.30	64.21	61.91
309	53.35	55.33	67.96	65.56	43.64	45.52	56.58	53.77	56.17	58.26	71.51	69.01
310	43.33	44.89	55.12	53.14	35.39	36.96	45.94	43.64	45.52	47.19	57.94	55.85
311	48.55	50.32	61.80	59.61	39.67	41.45	51.47	48.86	51.05	52.93	65.04	62.74
312	54.18	56.17	69.01	66.50	44.27	46.25	57.52	54.60	57.00	59.09	72.56	69.95
313	43.95	45.62	55.96	53.97	35.91	37.58	46.67	44.27	46.25	47.92	58.88	56.79
314	49.38	51.26	62.95	60.66	40.40	42.18	52.41	49.80	52.10	53.97	66.29	63.89
315	55.23	57.32	70.37	67.86	45.10	47.19	58.67	55.65	58.15	60.34	74.12	71.51
316	45.00	46.67	57.32	55.23	36.75	38.42	47.71	45.31	47.40	49.17	60.34	58.26
317	51.05	52.93	65.04	62.74	41.76	43.53	54.18	51.47	53.77	55.75	68.38	65.98
318	56.27	58.36	71.72	69.11	46.04	48.02	59.72	56.69	59.19	61.39	75.48	72.77
319	47.19	48.96	60.13	57.94	38.63	40.30	50.11	47.50	49.59	51.47	63.27	61.07
320	52.30	54.29	66.71	64.31	42.80	44.68	55.54	52.72	55.12	57.11	70.16	67.65
321	57.52	59.61	73.18	70.57	46.98	49.07	60.97	57.94	60.45	62.64	76.94	74.23
322	49.59	51.47	63.27	60.97	40.51	42.39	52.72	50.01	52.30	54.18	66.50	64.21
323	54.71	56.79	69.74	67.23	44.68	46.77	58.15	55.12	57.63	59.72	73.29	70.68
324	59.61	61.80	75.90	73.18	48.75	50.84	63.27	60.03	62.74	65.04	79.87	77.05

Table 7-5. FEM simulation results – Bearing capacity (tsf) on 6.6 to 13.2-ft rock over sand subsurface – Plane strain only

#	Rock (T) = 6.6 ft				Rock (T) = 13.2 ft				Rock (T) = 13.2 ft			
	E: 0.7ksi B: 6.6ft D: 0ft	E: 0.7ksi B: 13.2ft D: 0ft	E: 0.7ksi B: 13.2ft D: 6.6ft	E: 0.7ksi B: 6.6ft D: 3.3ft	E: 1.5ksi B: 6.6ft D: 0ft	E: 1.5ksi B: 13.2ft D: 0ft	E: 1.5ksi B: 13.2ft D: 6.6ft	E: 1.5ksi B: 6.6ft D: 3.3ft	E: 0.7ksi B: 6.6ft D: 0ft	E: 0.7ksi B: 13.2ft D: 0ft	E: 0.7ksi B: 13.2ft D: 6.6ft	E: 0.7ksi B: 6.6ft D: 3.3ft
1	3.45	3.45	4.38	4.18	5.01	5.22	6.47	6.26	5.01	5.22	6.47	6.26
2-27	same	results										
28	4.49	4.59	5.64	5.43	6.68	6.89	8.46	8.14	6.68	6.89	8.46	8.14
29	4.49	4.59	5.64	5.43	6.68	6.89	8.46	8.14	6.68	6.89	8.46	8.14
30	4.49	4.59	5.64	5.43	6.68	6.89	8.46	8.14	6.68	6.89	8.46	8.14
31	4.49	4.59	5.64	5.43	6.68	6.89	8.46	8.14	6.68	6.89	8.46	8.14
32	4.49	4.59	5.64	5.43	6.68	6.89	8.46	8.14	6.68	6.89	8.46	8.14
33	4.49	4.59	5.64	5.43	6.68	6.89	8.46	8.14	6.68	6.89	8.46	8.14
34	4.49	4.59	5.64	5.43	6.68	6.89	8.46	8.14	6.68	6.89	8.46	8.14
35	4.49	4.59	5.64	5.43	6.68	6.89	8.46	8.14	6.68	6.89	8.46	8.14
36	4.49	4.59	5.64	5.43	6.68	6.89	8.46	8.14	6.68	6.89	8.46	8.14
37	4.49	4.59	5.64	5.43	6.68	6.89	8.46	8.14	6.68	6.89	8.46	8.14
38	4.49	4.59	5.64	5.43	6.68	6.89	8.46	8.14	6.68	6.89	8.46	8.14
39	4.49	4.59	5.64	5.43	6.68	6.89	8.46	8.14	6.68	6.89	8.46	8.14
40	4.49	4.59	5.64	5.43	6.68	6.89	8.46	8.14	6.68	6.89	8.46	8.14
41	4.49	4.59	5.64	5.43	6.68	6.89	8.46	8.14	6.68	6.89	8.46	8.14
42	4.49	4.59	5.64	5.43	6.68	6.89	8.46	8.14	6.68	6.89	8.46	8.14
43	4.49	4.59	5.64	5.43	6.68	6.89	8.46	8.14	6.68	6.89	8.46	8.14
44	4.49	4.59	5.64	5.43	6.68	6.89	8.46	8.14	6.68	6.89	8.46	8.14
45	4.49	4.59	5.64	5.43	6.68	6.89	8.46	8.14	6.68	6.89	8.46	8.14
46	4.49	4.59	5.64	5.43	6.68	6.89	8.46	8.14	6.68	6.89	8.46	8.14
47	4.49	4.59	5.64	5.43	6.68	6.89	8.46	8.14	6.68	6.89	8.46	8.14
48	4.49	4.59	5.64	5.43	6.68	6.89	8.46	8.14	6.68	6.89	8.46	8.14
49	4.49	4.59	5.64	5.43	6.68	6.89	8.46	8.14	6.68	6.89	8.46	8.14
50	4.49	4.59	5.64	5.43	6.68	6.89	8.46	8.14	6.68	6.89	8.46	8.14
51	4.49	4.59	5.64	5.43	6.68	6.89	8.46	8.14	6.68	6.89	8.46	8.14
52	4.49	4.59	5.64	5.43	6.68	6.89	8.46	8.14	6.68	6.89	8.46	8.14
53	4.49	4.59	5.64	5.43	6.68	6.89	8.46	8.14	6.68	6.89	8.46	8.14
54	4.49	4.59	5.64	5.43	6.68	6.89	8.46	8.14	6.68	6.89	8.46	8.14
55	9.08	9.40	11.69	11.28	13.57	14.09	17.33	16.70	13.47	13.99	17.23	16.60
56	9.08	9.40	11.69	11.28	13.57	14.09	17.33	16.70	13.47	13.99	17.23	16.60
57	9.08	9.40	11.69	11.28	13.57	14.09	17.33	16.70	13.47	13.99	17.23	16.60
58	9.08	9.40	11.69	11.28	13.57	14.09	17.33	16.70	13.47	13.99	17.23	16.60

Table 7-5. Continued

#	Rock (T) = 6.6 ft				Rock (T) = 13.2 ft				Rock (T) = 13.2 ft			
	E: 0.7ksi B: 6.6ft D: 0ft	E: 0.7ksi B: 13.2ft D: 0ft	E: 0.7ksi B: 13.2ft D: 6.6ft	E: 0.7ksi B: 6.6ft D: 3.3ft	E: 1.5ksi B: 6.6ft D: 0ft	E: 1.5ksi B: 13.2ft D: 0ft	E: 1.5ksi B: 13.2ft D: 6.6ft	E: 1.5ksi B: 6.6ft D: 3.3ft	E: 0.7ksi B: 6.6ft D: 0ft	E: 0.7ksi B: 13.2ft D: 0ft	E: 0.7ksi B: 13.2ft D: 6.6ft	E: 0.7ksi B: 6.6ft D: 3.3ft
59	9.08	9.40	11.69	11.28	13.57	14.09	17.33	16.70	13.47	13.99	17.23	16.60
60	9.08	9.40	11.69	11.28	13.57	14.09	17.33	16.70	13.47	13.99	17.23	16.60
61	9.08	9.40	11.69	11.28	13.57	14.09	17.33	16.70	13.47	13.99	17.23	16.60
62	9.08	9.40	11.69	11.28	13.57	14.09	17.33	16.70	13.47	13.99	17.23	16.60
63	9.08	9.40	11.69	11.28	13.57	14.09	17.33	16.70	13.47	13.99	17.23	16.60
64	9.08	9.40	11.69	11.28	13.57	14.09	17.33	16.70	13.47	13.99	17.23	16.60
65	9.08	9.40	11.69	11.28	13.57	14.09	17.33	16.70	13.47	13.99	17.23	16.60
66	9.08	9.40	11.69	11.28	13.57	14.09	17.33	16.70	13.47	13.99	17.23	16.60
67	9.08	9.40	11.69	11.28	13.57	14.09	17.33	16.70	13.47	13.99	17.23	16.60
68	9.08	9.40	11.69	11.28	13.57	14.09	17.33	16.70	13.47	13.99	17.23	16.60
69	9.08	9.40	11.69	11.28	13.57	14.09	17.33	16.70	13.47	13.99	17.23	16.60
70	9.08	9.40	11.69	11.28	13.57	14.09	17.33	16.70	13.47	13.99	17.23	16.60
71	9.08	9.40	11.69	11.28	13.57	14.09	17.33	16.70	13.47	13.99	17.23	16.60
72	9.08	9.40	11.69	11.28	13.57	14.09	17.33	16.70	13.47	13.99	17.23	16.60
73	9.08	9.40	11.69	11.28	13.57	14.09	17.33	16.70	13.47	13.99	17.23	16.60
74	9.08	9.40	11.69	11.28	13.57	14.09	17.33	16.70	13.47	13.99	17.23	16.60
75	9.08	9.40	11.69	11.28	13.57	14.09	17.33	16.70	13.47	13.99	17.23	16.60
76	9.08	9.40	11.69	11.28	13.57	14.09	17.33	16.70	13.47	13.99	17.23	16.60
77	9.08	9.40	11.69	11.28	13.57	14.09	17.33	16.70	13.47	13.99	17.23	16.60
78	9.08	9.40	11.69	11.28	13.57	14.09	17.33	16.70	13.47	13.99	17.23	16.60
79	9.08	9.40	11.69	11.28	13.57	14.09	17.33	16.70	13.47	13.99	17.23	16.60
80	9.08	9.40	11.69	11.28	13.57	14.09	17.33	16.70	13.47	13.99	17.23	16.60
81	9.08	9.40	11.69	11.28	13.57	14.09	17.33	16.70	13.47	13.99	17.23	16.60
82	12.84	13.26	16.39	15.76	19.11	19.84	24.43	23.59	19.00	19.73	24.33	23.49
83	13.99	14.41	17.85	17.12	20.98	21.72	26.62	25.68	20.88	21.61	26.52	25.58
84	16.08	16.60	20.57	19.73	24.12	24.95	30.59	29.55	24.01	24.85	30.48	29.44
85	12.95	13.36	16.60	15.97	19.31	20.04	24.64	23.80	19.21	19.94	24.53	23.70
86	14.09	14.51	18.06	17.33	21.09	21.82	26.83	25.89	20.98	21.72	26.73	25.79
87	16.29	16.70	20.78	19.94	24.33	25.16	30.80	29.75	24.22	25.06	30.69	29.65
88	13.15	13.57	16.81	16.18	19.63	20.36	24.95	24.12	19.52	20.25	24.85	24.01
89	14.41	14.82	18.37	17.64	21.40	22.24	27.25	26.31	21.30	22.13	27.14	26.20
90	16.39	16.81	20.98	20.15	24.33	25.26	31.11	30.07	24.22	25.16	31.01	29.96
91	13.57	13.89	17.23	16.50	20.15	20.88	25.58	24.64	20.04	20.78	25.47	24.53
92	14.41	14.93	18.58	17.75	21.51	22.34	27.46	26.52	21.40	22.24	27.35	26.41
93	16.50	17.02	21.19	20.25	24.64	25.58	31.42	30.28	24.53	25.47	31.22	30.17

Table 7-5. Continued

#	Rock (T) = 6.6 ft				Rock (T) = 13.2 ft				Rock (T) = 13.2 ft			
	E: 0.7ksi B: 6.6ft D: 0ft	E: 0.7ksi B: 13.2ft D: 0ft	E: 0.7ksi B: 13.2ft D: 6.6ft	E: 0.7ksi B: 6.6ft D: 3.3ft	E: 1.5ksi B: 6.6ft D: 0ft	E: 1.5ksi B: 13.2ft D: 0ft	E: 1.5ksi B: 13.2ft D: 6.6ft	E: 1.5ksi B: 6.6ft D: 3.3ft	E: 0.7ksi B: 6.6ft D: 0ft	E: 0.7ksi B: 13.2ft D: 0ft	E: 0.7ksi B: 13.2ft D: 6.6ft	E: 0.7ksi B: 6.6ft D: 3.3ft
94	13.57	13.99	17.43	16.70	20.25	20.98	25.79	24.85	20.15	20.88	25.68	24.74
95	14.51	15.03	18.58	17.85	21.61	22.45	27.56	26.62	21.51	22.34	27.46	26.52
96	16.60	17.12	21.30	20.46	24.85	25.79	31.63	30.48	24.74	25.68	31.42	30.38
97	13.68	14.09	17.54	16.81	20.36	21.09	25.89	24.95	20.25	20.98	25.79	24.85
98	14.62	15.14	18.69	17.96	21.72	22.55	27.77	26.83	21.61	22.45	27.67	26.73
99	16.70	17.23	21.40	20.57	24.85	25.79	31.74	30.59	24.74	25.68	31.53	30.48
100	13.78	14.30	17.75	16.91	20.67	21.40	26.31	25.37	20.57	21.30	26.20	25.26
101	14.72	15.14	18.90	18.17	22.03	22.86	28.08	27.14	21.92	22.76	27.98	27.04
102	16.81	17.33	21.51	20.67	25.06	26.00	31.95	30.80	24.95	25.89	31.74	30.69
103	13.89	14.41	17.85	17.12	20.98	21.61	26.52	25.58	20.88	21.51	26.41	25.47
104	14.93	15.35	19.11	18.37	22.24	23.07	28.40	27.35	22.13	22.97	28.29	27.25
105	16.91	17.43	21.61	20.78	25.16	26.10	32.05	30.90	25.06	26.00	31.84	30.80
106	14.09	14.51	18.06	17.33	21.09	21.82	26.83	25.89	20.98	21.72	26.73	25.79
107	15.14	15.56	19.42	18.58	22.55	23.39	28.71	27.67	22.45	23.28	28.61	27.56
108	17.02	17.54	21.82	20.98	25.47	26.41	32.36	31.22	25.37	26.31	32.16	31.11
109	17.96	18.48	22.97	22.03	26.62	27.56	33.83	32.68	26.52	27.46	33.62	32.47
110	17.96	18.48	22.97	22.03	26.62	27.56	33.83	32.68	26.52	27.46	33.62	32.47
111	17.96	18.48	22.97	22.03	26.62	27.56	33.83	32.68	26.52	27.46	33.62	32.47
112	17.96	18.48	22.97	22.03	26.62	27.56	33.83	32.68	26.52	27.46	33.62	32.47
113	17.96	18.48	22.97	22.03	26.62	27.56	33.83	32.68	26.52	27.46	33.62	32.47
114	17.96	18.48	22.97	22.03	26.62	27.56	33.83	32.68	26.52	27.46	33.62	32.47
115	17.96	18.48	22.97	22.03	26.62	27.56	33.83	32.68	26.52	27.46	33.62	32.47
116	17.96	18.48	22.97	22.03	26.62	27.56	33.83	32.68	26.52	27.46	33.62	32.47
117	17.96	18.48	22.97	22.03	26.62	27.56	33.83	32.68	26.52	27.46	33.62	32.47
118	17.96	18.48	22.97	22.03	26.62	27.56	33.83	32.68	26.52	27.46	33.62	32.47
119	17.96	18.48	22.97	22.03	26.62	27.56	33.83	32.68	26.52	27.46	33.62	32.47
120	17.96	18.48	22.97	22.03	26.62	27.56	33.83	32.68	26.52	27.46	33.62	32.47
121	17.96	18.48	22.97	22.03	26.62	27.56	33.83	32.68	26.52	27.46	33.62	32.47
122	17.96	18.48	22.97	22.03	26.62	27.56	33.83	32.68	26.52	27.46	33.62	32.47
123	17.96	18.48	22.97	22.03	26.62	27.56	33.83	32.68	26.52	27.46	33.62	32.47
124	17.96	18.48	22.97	22.03	26.62	27.56	33.83	32.68	26.52	27.46	33.62	32.47
125	17.96	18.48	22.97	22.03	26.62	27.56	33.83	32.68	26.52	27.46	33.62	32.47
126	17.96	18.48	22.97	22.03	26.62	27.56	33.83	32.68	26.52	27.46	33.62	32.47
127	17.96	18.48	22.97	22.03	26.62	27.56	33.83	32.68	26.52	27.46	33.62	32.47
128	17.96	18.48	22.97	22.03	26.62	27.56	33.83	32.68	26.52	27.46	33.62	32.47

Table 7-5. Continued

#	Rock (T) = 6.6 ft				Rock (T) = 13.2 ft				Rock (T) = 13.2 ft			
	E: 0.7ksi B: 6.6ft D: 0ft	E: 0.7ksi B: 13.2ft D: 0ft	E: 0.7ksi B: 13.2ft D: 6.6ft	E: 0.7ksi B: 6.6ft D: 3.3ft	E: 1.5ksi B: 6.6ft D: 0ft	E: 1.5ksi B: 13.2ft D: 0ft	E: 1.5ksi B: 13.2ft D: 6.6ft	E: 1.5ksi B: 6.6ft D: 3.3ft	E: 0.7ksi B: 6.6ft D: 0ft	E: 0.7ksi B: 13.2ft D: 0ft	E: 0.7ksi B: 13.2ft D: 6.6ft	E: 0.7ksi B: 6.6ft D: 3.3ft
129	17.96	18.48	22.97	22.03	26.62	27.56	33.83	32.68	26.52	27.46	33.62	32.47
130	17.96	18.48	22.97	22.03	26.62	27.56	33.83	32.68	26.52	27.46	33.62	32.47
131	17.96	18.48	22.97	22.03	26.62	27.56	33.83	32.68	26.52	27.46	33.62	32.47
132	17.96	18.48	22.97	22.03	26.62	27.56	33.83	32.68	26.52	27.46	33.62	32.47
133	17.96	18.48	22.97	22.03	26.62	27.56	33.83	32.68	26.52	27.46	33.62	32.47
134	17.96	18.48	22.97	22.03	26.62	27.56	33.83	32.68	26.52	27.46	33.62	32.47
135	17.96	18.48	22.97	22.03	26.62	27.56	33.83	32.68	26.52	27.46	33.62	32.47
136	21.82	22.55	28.08	26.94	32.47	33.62	41.34	39.88	32.26	33.41	41.13	39.67
137	26.10	26.83	33.41	32.05	38.63	40.09	49.17	47.50	38.42	39.88	48.96	47.29
138	26.31	27.04	33.62	32.26	38.84	40.30	49.59	47.82	38.63	40.09	49.38	47.61
139	22.03	22.76	28.29	27.14	32.78	33.93	41.66	40.19	32.57	33.72	41.45	39.99
140	26.10	26.83	33.41	32.05	38.63	40.09	49.17	47.50	38.42	39.88	48.96	47.29
141	26.31	27.04	33.62	32.26	38.84	40.30	49.59	47.82	38.63	40.09	49.38	47.61
142	22.34	22.97	28.61	27.46	32.99	34.24	42.07	40.61	32.78	34.03	41.86	40.40
143	26.10	26.83	33.41	32.05	38.63	40.09	49.17	47.50	38.42	39.88	48.96	47.29
144	26.31	27.04	33.62	32.26	38.84	40.30	49.59	47.82	38.63	40.09	49.38	47.61
145	22.45	23.07	28.81	27.67	33.20	34.45	42.28	40.82	32.99	34.24	42.07	40.61
146	26.10	26.83	33.41	32.05	38.63	40.09	49.17	47.50	38.42	39.88	48.96	47.29
147	26.31	27.04	33.62	32.26	38.84	40.30	49.59	47.82	38.63	40.09	49.38	47.61
148	22.65	23.39	29.02	27.87	33.51	34.77	42.80	41.34	33.30	34.56	42.60	41.13
149	26.10	26.83	33.41	32.05	38.63	40.09	49.17	47.50	38.42	39.88	48.96	47.29
150	26.31	27.04	33.62	32.26	38.84	40.30	49.59	47.82	38.63	40.09	49.38	47.61
151	22.76	23.49	29.13	27.98	33.62	34.87	42.91	41.45	33.41	34.66	42.70	41.24
152	26.10	26.83	33.41	32.05	38.63	40.09	49.17	47.50	38.42	39.88	48.96	47.29
153	26.31	27.04	33.62	32.26	38.84	40.30	49.59	47.82	38.63	40.09	49.38	47.61
154	22.86	23.59	29.23	28.08	33.83	35.08	43.12	41.66	33.62	34.87	42.91	41.45
155	26.10	26.83	33.41	32.05	38.63	40.09	49.17	47.50	38.42	39.88	48.96	47.29
156	26.31	27.04	33.62	32.26	38.84	40.30	49.59	47.82	38.63	40.09	49.38	47.61
157	23.07	23.70	29.55	28.29	34.14	35.39	43.43	41.86	33.93	35.18	43.22	41.66
158	26.10	26.83	33.41	32.05	38.63	40.09	49.17	47.50	38.42	39.88	48.96	47.29
159	26.31	27.04	33.62	32.26	38.84	40.30	49.59	47.82	38.63	40.09	49.38	47.61
160	23.28	23.91	29.75	28.50	34.35	35.60	43.74	42.18	34.14	35.39	43.53	41.97
161	26.10	26.83	33.41	32.05	38.63	40.09	49.17	47.50	38.42	39.88	48.96	47.29
162	26.31	27.04	33.62	32.26	38.84	40.30	49.59	47.82	38.63	40.09	49.38	47.61
163	23.80	24.43	30.38	29.13	35.18	36.44	44.79	43.22	34.97	36.23	44.58	43.01

Table 7-5. Continued

#	Rock (T) = 6.6 ft				Rock (T) = 13.2 ft				Rock (T) = 13.2 ft			
	E: 0.7ksi B: 6.6ft D: 0ft	E: 0.7ksi B: 13.2ft D: 0ft	E: 0.7ksi B: 13.2ft D: 6.6ft	E: 0.7ksi B: 6.6ft D: 3.3ft	E: 1.5ksi B: 6.6ft D: 0ft	E: 1.5ksi B: 13.2ft D: 0ft	E: 1.5ksi B: 13.2ft D: 6.6ft	E: 1.5ksi B: 6.6ft D: 3.3ft	E: 0.7ksi B: 6.6ft D: 0ft	E: 0.7ksi B: 13.2ft D: 0ft	E: 0.7ksi B: 13.2ft D: 6.6ft	E: 0.7ksi B: 6.6ft D: 3.3ft
164	28.71	29.55	36.75	35.18	42.39	43.95	53.97	52.10	42.18	43.74	53.66	51.89
165	33.62	34.56	42.91	41.24	49.69	51.47	63.27	61.07	49.49	51.26	62.95	60.76
166	24.01	24.74	30.69	29.44	35.60	36.85	45.31	43.74	35.39	36.64	45.10	43.53
167	29.02	29.96	37.17	35.70	42.91	44.47	54.71	52.83	42.70	44.27	54.39	52.51
168	33.83	34.77	43.22	41.55	50.01	51.78	63.58	61.39	49.80	51.57	63.27	61.07
169	24.43	25.26	31.32	30.07	36.23	37.58	46.14	44.58	36.02	37.38	45.94	44.37
170	29.34	30.28	37.69	36.12	43.53	45.10	55.33	53.35	43.33	44.89	55.02	53.04
171	33.93	34.97	43.53	41.76	50.22	52.10	64.00	61.80	50.01	51.89	63.68	61.49
172	24.85	25.58	31.74	30.48	36.75	38.11	46.77	45.10	36.54	37.90	46.56	44.89
173	29.55	30.48	37.90	36.44	43.85	45.41	55.75	53.77	43.64	45.21	55.44	53.45
174	34.24	35.29	43.74	41.97	50.63	52.51	64.41	62.12	50.43	52.20	64.10	61.80
175	25.16	26.00	32.26	31.01	37.27	38.63	47.40	45.73	37.06	38.42	47.19	45.52
176	29.96	30.80	38.31	36.75	44.27	45.83	56.38	54.39	44.06	45.62	56.06	54.08
177	34.45	35.50	44.16	42.39	51.05	52.93	65.04	62.74	50.84	52.62	64.73	62.43
178	25.58	26.31	32.78	31.53	37.90	39.25	48.23	46.56	37.69	39.05	48.02	46.35
179	30.17	31.11	38.63	37.06	44.68	46.35	56.90	54.91	44.47	46.14	56.58	54.60
180	34.56	35.60	44.37	42.60	51.26	53.14	65.25	62.95	51.05	52.83	64.94	62.64
181	26.31	27.04	33.51	32.16	38.84	40.30	49.38	47.61	38.63	40.09	49.17	47.40
182	30.59	31.42	39.25	37.69	45.31	46.98	57.63	55.65	45.10	46.77	57.32	55.33
183	34.97	36.02	44.79	43.01	51.78	53.66	65.88	63.58	51.57	53.35	65.56	63.27
184	26.83	27.67	34.45	33.09	39.88	41.34	50.74	48.96	39.67	41.13	50.53	48.75
185	31.11	32.05	39.88	38.31	46.14	47.82	58.67	56.58	45.94	47.61	58.36	56.27
186	35.29	36.33	45.31	43.43	52.30	54.18	66.61	64.31	51.99	53.87	66.29	64.00
187	27.77	28.61	35.60	34.14	41.24	42.70	52.41	50.53	41.03	42.49	52.10	50.32
188	31.74	32.78	40.82	39.15	47.19	48.86	60.03	57.94	46.98	48.65	59.72	57.63
189	36.12	37.17	46.25	44.27	53.45	55.44	68.07	65.67	53.14	55.12	67.76	65.35
190	25.16	26.00	32.26	31.01	37.27	38.63	47.40	45.73	37.06	38.42	47.19	45.52
191	30.59	31.42	39.25	37.69	45.31	46.98	57.63	55.65	45.10	46.77	57.32	55.33
192	35.91	36.96	45.94	44.16	53.04	55.02	67.55	65.15	52.72	54.71	67.23	64.83
193	25.58	26.31	32.78	31.53	37.90	39.25	48.23	46.56	37.69	39.05	48.02	46.35
194	31.01	31.95	39.67	38.11	45.94	47.61	58.46	56.38	45.73	47.40	58.15	56.06
195	36.23	37.27	46.35	44.37	53.45	55.44	68.17	65.77	53.14	55.12	67.86	65.46
196	26.20	26.94	33.51	32.16	38.73	40.19	49.28	47.50	38.52	39.99	49.07	47.29
197	31.42	32.26	40.19	38.52	46.46	48.13	59.09	57.00	46.25	47.92	58.78	56.69
198	36.64	37.69	46.88	45.00	54.18	56.17	69.01	66.61	53.87	55.85	68.70	66.29

Table 7-5. Continued

#	Rock (T) = 6.6 ft				Rock (T) = 13.2 ft				Rock (T) = 13.2 ft			
	E: 0.7ksi B: 6.6ft D: 0ft	E: 0.7ksi B: 13.2ft D: 0ft	E: 0.7ksi B: 13.2ft D: 6.6ft	E: 0.7ksi B: 6.6ft D: 3.3ft	E: 1.5ksi B: 6.6ft D: 0ft	E: 1.5ksi B: 13.2ft D: 0ft	E: 1.5ksi B: 13.2ft D: 6.6ft	E: 1.5ksi B: 6.6ft D: 3.3ft	E: 0.7ksi B: 6.6ft D: 0ft	E: 0.7ksi B: 13.2ft D: 0ft	E: 0.7ksi B: 13.2ft D: 6.6ft	E: 0.7ksi B: 6.6ft D: 3.3ft
199	26.83	27.67	34.35	32.99	39.67	41.13	50.53	48.75	39.46	40.92	50.32	48.55
200	31.95	32.99	40.92	39.25	47.29	49.07	60.24	58.15	47.08	48.86	59.93	57.84
201	37.17	38.31	47.61	45.73	55.02	57.00	70.05	67.65	54.71	56.69	69.74	67.34
202	27.35	28.19	35.08	33.62	40.51	41.97	51.57	49.80	40.30	41.76	51.36	49.59
203	32.57	33.51	41.66	39.99	48.13	49.90	61.39	59.19	47.92	49.69	61.07	58.88
204	37.69	38.84	48.23	46.46	55.75	57.84	70.99	68.49	55.44	57.52	70.68	68.17
205	27.67	28.50	35.50	34.03	41.03	42.49	52.20	50.43	40.82	42.28	51.99	50.22
206	32.99	33.93	42.18	40.51	48.86	50.63	62.12	59.93	48.65	50.43	61.80	59.61
207	38.31	39.36	48.86	46.88	56.58	58.67	72.04	69.53	56.27	58.36	71.72	69.22
208	28.92	29.75	36.85	35.39	42.70	44.27	54.29	52.41	42.49	44.06	53.97	52.10
209	33.93	34.87	43.43	41.66	50.11	51.99	63.89	61.70	49.90	51.78	63.58	61.39
210	38.94	40.09	49.90	47.92	57.73	59.82	73.50	70.89	57.42	59.51	73.08	70.57
211	29.75	30.69	38.00	36.54	44.06	45.62	55.96	53.97	43.85	45.41	55.65	53.66
212	34.97	36.02	44.79	43.01	51.78	53.66	65.88	63.58	51.57	53.35	65.56	63.27
213	40.09	41.34	51.36	49.17	59.40	61.60	75.59	72.98	59.09	61.28	75.17	72.66
214	31.32	32.26	39.99	38.42	46.25	47.92	58.88	56.79	46.04	47.71	58.57	56.48
215	36.54	37.69	46.77	44.89	54.08	56.06	68.80	66.40	53.77	55.75	68.49	66.09
216	41.66	42.91	53.24	49.28	61.60	63.89	78.51	75.79	61.28	63.58	78.09	75.38
217	25.06	25.79	31.95	30.69	36.96	38.31	47.08	45.41	36.75	38.11	46.88	45.21
218	25.06	25.79	31.95	30.69	36.96	38.31	47.08	45.41	36.75	38.11	46.88	45.21
219	25.06	25.79	31.95	30.69	36.96	38.31	47.08	45.41	36.75	38.11	46.88	45.21
220	25.06	25.79	31.95	30.69	36.96	38.31	47.08	45.41	36.75	38.11	46.88	45.21
221	25.06	25.79	31.95	30.69	36.96	38.31	47.08	45.41	36.75	38.11	46.88	45.21
222	25.06	25.79	31.95	30.69	36.96	38.31	47.08	45.41	36.75	38.11	46.88	45.21
223	25.06	25.79	31.95	30.69	36.96	38.31	47.08	45.41	36.75	38.11	46.88	45.21
224	25.06	25.79	31.95	30.69	36.96	38.31	47.08	45.41	36.75	38.11	46.88	45.21
225	25.06	25.79	31.95	30.69	36.96	38.31	47.08	45.41	36.75	38.11	46.88	45.21
226	25.06	25.79	31.95	30.69	36.96	38.31	47.08	45.41	36.75	38.11	46.88	45.21
227	25.06	25.79	31.95	30.69	36.96	38.31	47.08	45.41	36.75	38.11	46.88	45.21
228	25.06	25.79	31.95	30.69	36.96	38.31	47.08	45.41	36.75	38.11	46.88	45.21
229	25.06	25.79	31.95	30.69	36.96	38.31	47.08	45.41	36.75	38.11	46.88	45.21
230	25.06	25.79	31.95	30.69	36.96	38.31	47.08	45.41	36.75	38.11	46.88	45.21
231	25.06	25.79	31.95	30.69	36.96	38.31	47.08	45.41	36.75	38.11	46.88	45.21
232	25.06	25.79	31.95	30.69	36.96	38.31	47.08	45.41	36.75	38.11	46.88	45.21
233	25.06	25.79	31.95	30.69	36.96	38.31	47.08	45.41	36.75	38.11	46.88	45.21

Table 7-5. Continued

#	Rock (T) = 6.6 ft				Rock (T) = 13.2 ft				Rock (T) = 13.2 ft			
	E: 0.7ksi B: 6.6ft D: 0ft	E: 0.7ksi B: 13.2ft D: 0ft	E: 0.7ksi B: 13.2ft D: 6.6ft	E: 0.7ksi B: 6.6ft D: 3.3ft	E: 1.5ksi B: 6.6ft D: 0ft	E: 1.5ksi B: 13.2ft D: 0ft	E: 1.5ksi B: 13.2ft D: 6.6ft	E: 1.5ksi B: 6.6ft D: 3.3ft	E: 0.7ksi B: 6.6ft D: 0ft	E: 0.7ksi B: 13.2ft D: 0ft	E: 0.7ksi B: 13.2ft D: 6.6ft	E: 0.7ksi B: 6.6ft D: 3.3ft
234	25.06	25.79	31.95	30.69	36.96	38.31	47.08	45.41	36.75	38.11	46.88	45.21
235	25.06	25.79	31.95	30.69	36.96	38.31	47.08	45.41	36.75	38.11	46.88	45.21
236	25.06	25.79	31.95	30.69	36.96	38.31	47.08	45.41	36.75	38.11	46.88	45.21
237	25.06	25.79	31.95	30.69	36.96	38.31	47.08	45.41	36.75	38.11	46.88	45.21
238	25.06	25.79	31.95	30.69	36.96	38.31	47.08	45.41	36.75	38.11	46.88	45.21
239	25.06	25.79	31.95	30.69	36.96	38.31	47.08	45.41	36.75	38.11	46.88	45.21
240	25.06	25.79	31.95	30.69	36.96	38.31	47.08	45.41	36.75	38.11	46.88	45.21
241	25.06	25.79	31.95	30.69	36.96	38.31	47.08	45.41	36.75	38.11	46.88	45.21
242	25.06	25.79	31.95	30.69	36.96	38.31	47.08	45.41	36.75	38.11	46.88	45.21
243	25.06	25.79	31.95	30.69	36.96	38.31	47.08	45.41	36.75	38.11	46.88	45.21
244	31.74	32.78	40.72	39.15	47.08	48.75	59.93	57.84	46.88	48.55	59.61	57.52
245	36.54	37.69	46.77	44.89	54.08	56.06	68.80	66.40	53.77	55.75	68.49	66.09
246	36.54	37.69	46.77	44.89	54.08	56.06	68.80	66.40	53.77	55.75	68.49	66.09
247	31.95	32.99	40.92	39.25	47.29	49.07	60.24	58.15	47.08	48.86	59.93	57.84
248	36.54	37.69	46.77	44.89	54.08	56.06	68.80	66.40	53.77	55.75	68.49	66.09
249	36.54	37.69	46.77	44.89	54.08	56.06	68.80	66.40	53.77	55.75	68.49	66.09
250	32.16	33.09	41.13	39.46	47.50	49.28	60.55	58.46	47.29	49.07	60.24	58.15
251	36.54	37.69	46.77	44.89	54.08	56.06	68.80	66.40	53.77	55.75	68.49	66.09
252	36.54	37.69	46.77	44.89	54.08	56.06	68.80	66.40	53.77	55.75	68.49	66.09
253	32.36	33.30	41.45	39.78	47.92	49.69	60.97	58.88	47.71	49.49	60.66	58.57
254	36.54	37.69	46.77	44.89	54.08	56.06	68.80	66.40	53.77	55.75	68.49	66.09
255	36.54	37.69	46.77	44.89	54.08	56.06	68.80	66.40	53.77	55.75	68.49	66.09
256	32.99	33.93	42.18	40.51	48.55	50.63	62.12	59.93	48.34	50.43	61.80	59.61
257	36.54	37.69	46.77	44.89	54.08	56.06	68.80	66.40	53.77	55.75	68.49	66.09
258	36.54	37.69	46.77	44.89	54.08	56.06	68.80	66.40	53.77	55.75	68.49	66.09
259	33.20	34.14	42.39	40.72	49.07	50.84	62.43	60.24	48.86	50.63	62.12	59.93
260	36.54	37.69	46.77	44.89	54.08	56.06	68.80	66.40	53.77	55.75	68.49	66.09
261	36.54	37.69	46.77	44.89	54.08	56.06	68.80	66.40	53.77	55.75	68.49	66.09
262	33.41	34.45	42.80	41.03	49.49	51.26	62.95	60.76	49.28	51.05	62.64	60.45
263	36.54	37.69	46.77	44.89	54.08	56.06	68.80	66.40	53.77	55.75	68.49	66.09
264	36.54	37.69	46.77	44.89	54.08	56.06	68.80	66.40	53.77	55.75	68.49	66.09
265	33.62	34.56	42.91	41.24	49.69	51.47	63.27	61.07	49.49	51.26	62.95	60.76
266	36.54	37.69	46.77	44.89	54.08	56.06	68.80	66.40	53.77	55.75	68.49	66.09
267	36.54	37.69	46.77	44.89	54.08	56.06	68.80	66.40	53.77	55.75	68.49	66.09
268	33.83	34.77	43.22	41.55	50.01	51.89	63.68	61.49	49.80	51.68	63.37	61.18

Table 7-5. Continued

#	Rock (T) = 6.6 ft				Rock (T) = 13.2 ft				Rock (T) = 13.2 ft			
	E: 0.7ksi B: 6.6ft D: 0ft	E: 0.7ksi B: 13.2ft D: 0ft	E: 0.7ksi B: 13.2ft D: 6.6ft	E: 0.7ksi B: 6.6ft D: 3.3ft	E: 1.5ksi B: 6.6ft D: 0ft	E: 1.5ksi B: 13.2ft D: 0ft	E: 1.5ksi B: 13.2ft D: 6.6ft	E: 1.5ksi B: 6.6ft D: 3.3ft	E: 0.7ksi B: 6.6ft D: 0ft	E: 0.7ksi B: 13.2ft D: 0ft	E: 0.7ksi B: 13.2ft D: 6.6ft	E: 0.7ksi B: 6.6ft D: 3.3ft
269	36.54	37.69	46.77	44.89	54.08	56.06	68.80	66.40	53.77	55.75	68.49	66.09
270	36.54	37.69	46.77	44.89	54.08	56.06	68.80	66.40	53.77	55.75	68.49	66.09
271	35.29	36.33	45.31	43.43	52.30	54.18	66.61	64.31	51.99	53.87	66.29	64.00
272	40.40	41.55	51.68	49.59	59.82	62.01	76.11	73.50	59.51	61.70	75.69	73.08
273	45.21	46.56	57.84	55.54	66.92	69.32	85.19	82.16	66.61	69.01	84.77	81.75
274	35.70	36.75	45.62	43.85	52.83	54.81	67.23	64.83	52.51	54.50	66.92	64.52
275	40.82	41.97	52.20	50.01	60.34	62.54	76.84	74.12	60.03	62.22	76.42	73.71
276	45.52	46.88	58.26	55.85	67.34	69.84	85.71	82.68	67.02	69.53	85.29	82.27
277	36.12	37.17	46.25	44.27	53.45	55.44	68.07	65.67	53.14	55.12	67.76	65.35
278	41.13	42.39	52.62	50.53	60.87	63.06	77.46	74.75	60.55	62.74	77.05	74.33
279	45.83	47.19	58.67	56.38	67.86	70.37	86.44	83.42	67.55	70.05	86.03	83.00
280	36.44	37.58	46.67	44.79	53.97	55.96	68.70	66.29	53.66	55.65	68.38	65.98
281	41.45	42.70	53.14	50.95	61.49	63.68	78.20	75.48	61.18	63.37	77.78	75.06
282	46.25	47.61	59.19	56.69	68.38	70.89	87.07	84.04	68.07	70.57	86.65	83.62
283	37.17	38.31	47.61	45.73	55.02	57.00	70.05	67.65	54.71	56.69	69.74	67.34
284	41.66	43.01	53.45	51.36	61.80	64.10	78.72	76.00	61.49	63.79	78.30	75.59
285	46.56	47.82	59.51	57.11	68.80	71.31	87.59	84.56	68.49	70.99	87.17	84.15
286	37.48	38.63	48.02	46.14	55.54	57.52	70.68	68.17	55.23	57.21	70.37	67.86
287	42.07	43.33	53.87	51.68	62.22	64.52	79.24	76.42	61.91	64.21	78.82	76.00
288	46.77	48.23	59.93	57.52	69.32	71.83	88.22	85.09	69.01	71.51	87.80	84.67
289	38.11	39.25	48.86	46.77	56.38	58.46	71.83	69.32	56.06	58.15	71.51	69.01
290	42.60	43.95	54.50	52.30	63.06	65.35	80.28	77.46	62.74	65.04	79.87	77.05
291	47.40	48.75	60.55	58.15	70.05	72.66	89.16	86.03	69.74	72.35	88.74	85.61
292	38.94	40.09	49.90	47.92	57.73	59.82	73.50	70.89	57.42	59.51	73.08	70.57
293	43.53	44.79	55.75	53.45	64.31	66.71	81.95	79.14	64.00	66.40	81.54	78.72
294	48.02	49.38	61.49	59.09	71.10	73.71	90.51	87.38	70.78	73.29	90.10	86.97
295	39.99	41.24	51.26	49.17	59.30	61.49	75.48	72.87	58.99	61.18	75.06	72.56
296	44.58	45.94	57.11	54.81	66.09	68.49	84.04	81.12	65.77	68.17	83.62	80.70
297	48.96	50.32	62.64	60.03	72.45	75.06	92.19	88.95	72.14	74.65	91.77	88.53
298	37.69	38.84	48.23	46.35	55.75	57.84	70.99	68.49	55.44	57.52	70.68	68.17
299	43.22	44.47	55.23	53.04	63.89	66.19	81.22	78.40	63.58	65.88	80.81	77.99
300	48.02	49.38	61.39	58.99	70.99	73.60	90.41	87.28	70.68	73.18	89.99	86.86
301	38.31	39.36	48.86	46.88	56.58	58.67	72.04	69.53	56.27	58.36	71.72	69.22
302	43.64	44.89	55.85	53.56	64.52	66.92	82.16	79.24	64.21	66.61	81.75	78.82
303	48.55	50.01	62.12	59.61	71.93	74.54	91.56	88.32	71.62	74.12	91.14	87.90

Table 7-5. Continued

#	Rock (T) = 6.6 ft				Rock (T) = 13.2 ft				Rock (T) = 13.2 ft			
	E: 0.7ksi B: 6.6ft D: 0ft	E: 0.7ksi B: 13.2ft D: 0ft	E: 0.7ksi B: 13.2ft D: 6.6ft	E: 0.7ksi B: 6.6ft D: 3.3ft	E: 1.5ksi B: 6.6ft D: 0ft	E: 1.5ksi B: 13.2ft D: 0ft	E: 1.5ksi B: 13.2ft D: 6.6ft	E: 1.5ksi B: 6.6ft D: 3.3ft	E: 0.7ksi B: 6.6ft D: 0ft	E: 0.7ksi B: 13.2ft D: 0ft	E: 0.7ksi B: 13.2ft D: 6.6ft	E: 0.7ksi B: 6.6ft D: 3.3ft
304	38.84	39.99	49.69	47.61	57.52	59.61	73.18	70.57	57.21	59.30	72.77	70.26
305	44.16	45.52	56.69	54.29	65.46	67.86	83.42	80.49	65.15	67.55	83.00	80.07
306	49.07	50.53	62.85	60.34	72.77	75.38	92.50	89.26	72.45	74.96	92.08	88.84
307	39.25	40.51	50.43	48.44	58.26	60.34	74.12	71.51	57.94	60.03	73.71	71.20
308	44.79	46.14	57.32	55.02	66.29	68.70	84.36	81.43	65.98	68.38	83.94	81.01
309	49.90	51.36	63.79	61.28	73.81	76.53	93.96	90.72	73.39	76.11	93.54	90.31
310	40.40	41.55	51.68	49.59	59.82	62.01	76.11	73.50	59.51	61.70	75.69	73.08
311	45.31	46.67	58.05	55.75	67.13	69.53	85.40	82.37	66.82	69.22	84.98	81.95
312	50.63	52.10	64.73	62.12	74.85	77.57	95.32	91.98	74.44	77.15	94.80	91.56
313	41.03	42.28	52.51	50.43	60.87	63.06	77.36	74.65	60.55	62.74	76.94	74.23
314	46.25	47.61	59.19	56.69	68.38	70.89	87.07	84.04	68.07	70.57	86.65	83.62
315	51.57	53.24	66.19	63.48	76.42	79.24	97.30	93.86	76.00	78.82	96.78	93.44
316	42.07	43.33	53.87	51.68	62.22	64.52	79.24	76.42	61.91	64.21	78.82	76.00
317	47.71	49.17	61.07	58.57	70.57	73.18	89.89	86.76	70.26	72.77	89.47	86.34
318	52.51	54.08	67.34	64.62	77.88	80.70	99.08	95.63	77.46	80.28	98.55	95.11
319	44.06	45.41	56.48	54.18	65.25	67.65	83.10	80.18	64.94	67.34	82.68	79.76
320	48.96	50.32	62.64	60.03	72.45	75.06	92.19	88.95	72.14	74.65	91.77	88.53
321	53.66	55.23	68.70	65.88	79.45	82.37	101.06	97.51	79.03	81.95	100.54	96.99
322	46.46	47.82	59.30	57.00	68.70	71.20	87.38	84.36	68.38	70.89	86.97	83.94
323	51.16	52.62	65.35	62.74	75.69	78.40	96.26	92.92	75.27	77.99	95.73	92.50
324	55.65	57.32	71.31	68.38	82.37	85.40	104.92	101.27	81.95	84.98	104.50	100.75

Finally, to augment the verification of the later bearing equation (presented in Chapter 8), additional FEM simulations are performed with parameters presented in Table 7-6 and Table 7-7.

Table 7-6. Additional FEM simulations - Bearing capacities (tsf) on rock subsurface

D	a (tsf)	α (°)	β (°)	p_p (tsf)	B=3.28 ft L=9.84 ft	B=3.28 ft L=32.8 ft	B=4.92 ft L=9.84 ft	B=4.92 ft L=49.2 ft	B=9.84 ft L=14.76 ft	B=9.84 ft L=98.4 ft
0ft	1.04	27	0	12.53	4.59	4.38	5.64	4.70	6.79	4.91
	5.22	29	10	20.88	26.94	25.37	34.24	27.35	49.49	28.61
	7.31	32	-10	31.32	42.60	40.09	54.08	41.86	75.27	45.10
	8.35	33	0	41.76	55.23	51.99	70.16	55.85	96.26	61.07
1.64ft	1.04	27	0	12.53	4.80	4.49	5.74	4.91	7.10	5.32
	5.22	29	10	20.88	28.81	26.52	36.02	28.71	50.84	31.22
	7.31	32	-10	31.32	49.49	45.62	61.39	50.32	90.41	54.39
	8.35	33	0	41.76	65.35	60.24	81.22	64.94	113.69	70.16
3.28ft	1.04	27	0	12.53	5.12	4.80	6.16	5.22	7.62	5.64
	5.22	29	10	20.88	30.59	28.40	38.42	30.59	54.08	32.99
	7.31	32	-10	31.32	57.32	53.35	70.05	57.52	103.15	61.91
	8.35	33	0	41.76	69.95	65.04	84.88	70.05	123.71	75.59

Table 7-7. Additional FEM simulations – Bearing capacities (tsf) on rock (E = 43.51 ksi) over sand subsurface

D	a (tsf)	α (°)	β (°)	p_p (tsf)	B = 1 m L = 3 m T = 9.84 ft E_{soil}=8.7 ksi	B = 1 m L = 10 m T = 13.12 ft E_{soil}=2.9 ksi	B=1.5 m L=3 m T = 9.84 ft E_{soil}=3.6 ksi	B=1.5 m L=15 m T =16.4 ft E_{soil}=2.17 ksi	B=3 m L=4.5 m T = 16.4 ft E_{soil}=2.9 ksi	B=3 m L=30 m T = 13.12 ft E_{soil}=3.6 ksi
0ft	1.04	27	0	12.53	4.18	3.86	4.28	4.59	6.68	4.38
	5.22	29	10	20.88	24.22	22.24	25.79	26.94	48.96	25.37
	7.31	32	-10	31.32	38.31	35.18	40.72	41.24	74.65	39.88
	8.35	33	0	41.76	45.59	45.62	52.83	55.02	95.11	54.39
1.64ft	1.04	27	0	12.53	4.28	3.97	4.28	4.80	6.99	4.91
	5.22	29	10	20.88	25.89	23.28	27.14	28.29	50.22	27.98
	7.31	32	-10	31.32	44.47	39.99	46.14	49.59	89.68	48.23
	8.35	33	0	41.76	58.78	52.83	61.07	64.00	112.33	62.54
3.28ft	1.04	27	0	12.53	4.59	4.18	4.59	5.12	7.52	5.12
	5.22	29	10	20.88	27.46	24.95	28.92	30.17	53.45	29.55
	7.31	32	-10	31.32	51.47	46.77	52.72	56.69	101.79	55.85
	8.35	33	0	41.76	62.85	57.00	63.89	69.01	122.88	67.13

CHAPTER 8 BEARING EQUATIONS – SHALLOW FOUNDATIONS ON FLORIDA ROCKS

8.1 Bearing Equations – Shallow foundation on Rock Subsurface

8.1.1. Strip footings of width B = 4 m at ground surface, D = 0 m

The bearing capacity equation was initially developed for the strip footing cases, using B = 4 m, D = 0 m, and L/B ≥ 10. Because of the bilinear strength envelope used for Florida carbonate rock, the ultimate bearing capacity is in the following form:

$$Q_u = \min (Q_{u1}, Q_{u2}) \quad (8\text{-}1)$$

$$Q_{u1} = c\, N_c \quad (8\text{-}2)$$

$$Q_{u2} = c\, N'_c + p_p\, N_\gamma \quad (8\text{-}3)$$

In the FEM analyses, where the stress paths intercept the first portion of the strength envelope, the N_c parameter was determined by solving the intercept of $q = a + p \tan\alpha = c \cos\varphi + p (1+ \sin\varphi)$ with the stress path, with the resulting correlation shown in Figure 8-1.

$$N_c = \frac{1.8\ cos\varphi}{0.8 - sin\varphi}$$

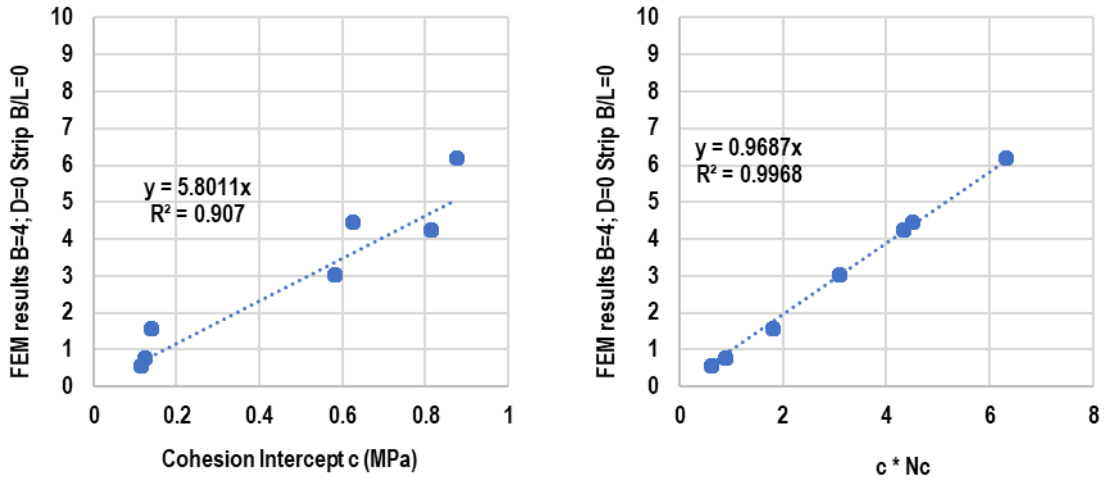

Figure 8-1. Strip footing correlation for N_c

Similarly, where the stress paths intercept the second portion of the strength envelope, the following parameters were obtained.

$$N'_c = \frac{1.8\ cos\varphi}{0.8-sin\omega} \tag{8-4}$$

$$N_\gamma = \frac{1.8\ [\ sin\varphi - sin\omega]}{0.8-\sin\omega} \tag{8-5}$$

The bias ratio (FEM bearing capacity result / bearing equation result) which is comparison between numerical results with the developed bearing equation is plotted in Figure 8-2. Evident,the bias is approximately 0.985 and has an excellent fit, or $R^2 = 0.9986$.

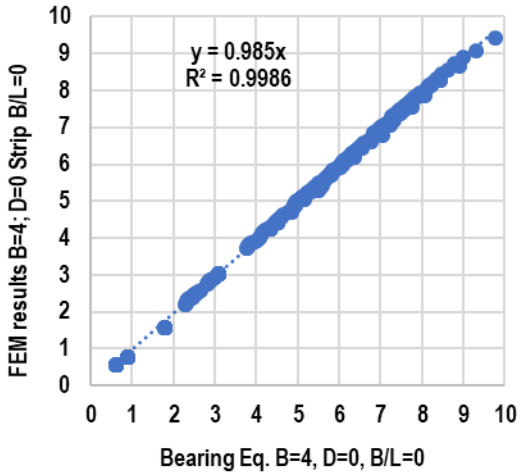

Figure 8-2. Strip footing bias statistical result

Therefore, the bearing equation for the strip footing can be summarized as:

$$Q_u = \min (Q_{u1}, Q_{u2}) \tag{8-6}$$

$$Q_{u1} = c\ N_c \tag{8-7}$$

$$Q_{u2} = c\ N'_c + p_p\ N_\gamma \tag{8-8}$$

$$N_c = \frac{1.8\ cos\varphi}{0.8-sin\varphi} \tag{8-9}$$

$$N'_c = \frac{1.8\ cos\varphi}{0.8-sin\omega} \tag{8-10}$$

$$N_\gamma = \frac{1.8\ [\ sin\varphi - sin\omega]}{0.8 - sin\omega} \quad (8\text{-}11)$$

The p_p is established based on triaxial test results. If the value is presented in a τ-σ diagram as σ_p, then p_p be determined by:

$$p_p = \frac{\sigma_p - c * cos\varphi}{1 + sin\varphi} \quad \text{or } \sigma_p = a + p_p\,(1 + \tan\alpha) = c * \cos\varphi + p_p\,(1 + \sin\varphi) \quad (8\text{-}12)$$

8.1.2. Strip footings B = 4 m below surface, D = 2 m

The depth of the footing contributes $q\,N_q$ to the bearing capacity, with $q = \gamma' * D$. To correlate the N_q parameter, the difference between FEM results of D=0 and D=2 was calculated:

$q\,N_q$ = (FEM results, strip footing, B=4, D=2) - (FEM results, strip footing, B=4, D=0)

Correlation between the calculated N_q and the input parameter p_p is presented in Figure 8-3, which was simplified to:

$$N_q = 15p_p - 10 \quad (8\text{-}13)$$

The bias ratio is then correlated against sinφ, which results in the following equation:

$$N_q = (1.5 * \frac{p_p}{\sigma_a} - 10) * (3 * sin\varphi - 1) \quad (8\text{-}14)$$

σ_a = Sea level standard atmospheric pressure

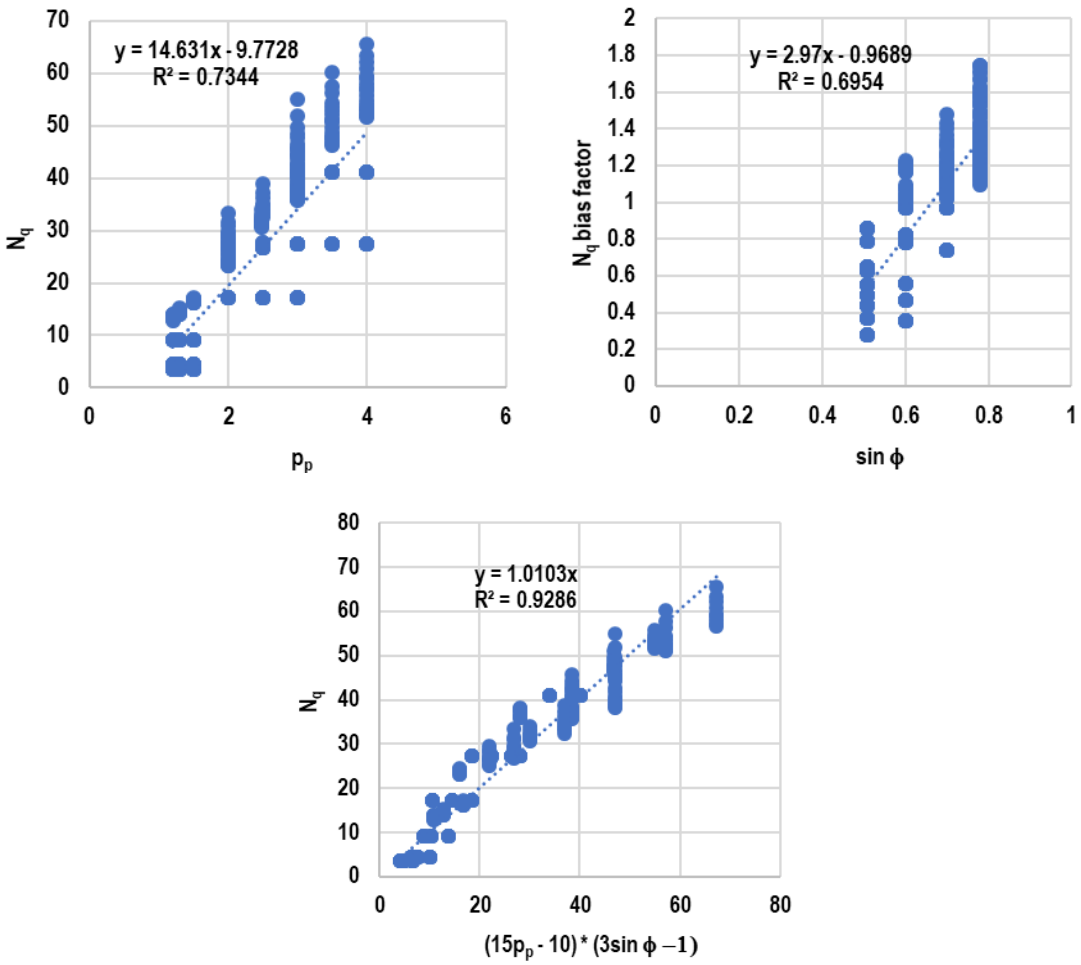

Figure 8-3. N_q correlation

8.1.3. Strip footings with different widths

Two different widths were modelled in FEM analyses: B = 2 m and B = 4 m. The difference in results of these two analyses are:

cN_c f(4) - cN_c f(2) = $cN_c * [f(4) – f(2)]$ for the first slope of the strength envelope.

$[cN_c' + p_pN_\gamma]$ f(4) - $[cN_c' + p_pN_\gamma]$ f(2) = $[cN_c' + p_pN_\gamma] * [f(4) – f(2)]$ for the second slope.

From the FEM results, the mean value for [f(4) – f(2)] is 0.037, with a standard deviation of 0.003.

Where f(B) is a function of footing width B, and f(4) = 1.0 as no modification factors were used with regards to the footing width in Sections 8.1 and 0, Thus, f(B) was assigned as $\left(\frac{4}{B}\right)^x$, which equals to 1.0 when B=4.

$\left(\frac{4}{4}\right)^x - \left(\frac{4}{2}\right)^x$=0.037, thus x = -0.055

Therefore, the bearing equation using different B value is:

$$Q_u = \min (Q_{u1}, Q_{u2}) \quad (8\text{-}15)$$

$$Q_{u1} = n\ c\ N_c\ + qN_q \quad (8\text{-}15a)$$

$$Q_{u2} = n\ [c\ N'_c + p_p\ N_\gamma\ ] + qN_q \quad (8\text{-}15b)$$

$$n = \left(\frac{4}{B}\right)^{-0.055} \quad (8\text{-}15c)$$

8.1.4. Shape factors

FEM analyses were performed using footings with different shapes: B/L = 0 (strip footing), B/L = 0.1, 0.2, and 1.0 (square). Based on results shown in Figure 8-4, the following correlation was established:

Shape factor $\xi = 1 + 0.245 \left(\frac{B}{L}\right)^{0.66}$

Therefore, the general equation for a shallow footing on a Florida carbonate rock subsurface is:

$$Q_u = \min (Q_{u1}, Q_{u2}) * \xi \quad (8\text{-}16)$$

$$Q_{u1} = n\ c\ N_c\ + qN_q \quad (8\text{-}16a)$$

$$Q_{u2} = n\ [c\ N'_c + p_p\ N_\gamma\ ] + qN_q \quad (8\text{-}16b)$$

$$n = \left(\frac{4}{B\ in\ meter}\right)^{-0.055} \text{ or } n = \left(\frac{4}{0.328B\ in\ ft}\right)^{-0.055} \quad (8\text{-}16c)$$

$$\xi = 1 + 0.245 \left(\frac{B}{L}\right)^{0.66} \quad (8\text{-}16d)$$

$$N_c = \frac{1.8\ cos\varphi}{0.8-sin\varphi} \quad (8\text{-}16e)$$

$$N'_c = \frac{1.8\ cos\varphi}{0.8-sin\omega} \quad (8\text{-}16f)$$

$$N_\gamma = \frac{1.8\ [sin\varphi - sin\omega]}{0.8-\sin\omega} \quad (8\text{-}16g)$$

$$q = \gamma' D \quad (8\text{-}16h)$$

$$N_q = (1.5 * \frac{p_p}{\sigma_a} - 10) * (3 * \sin\varphi - 1) \quad (8\text{-}16i)$$

σ_a = Sea level standard atmospheric pressure

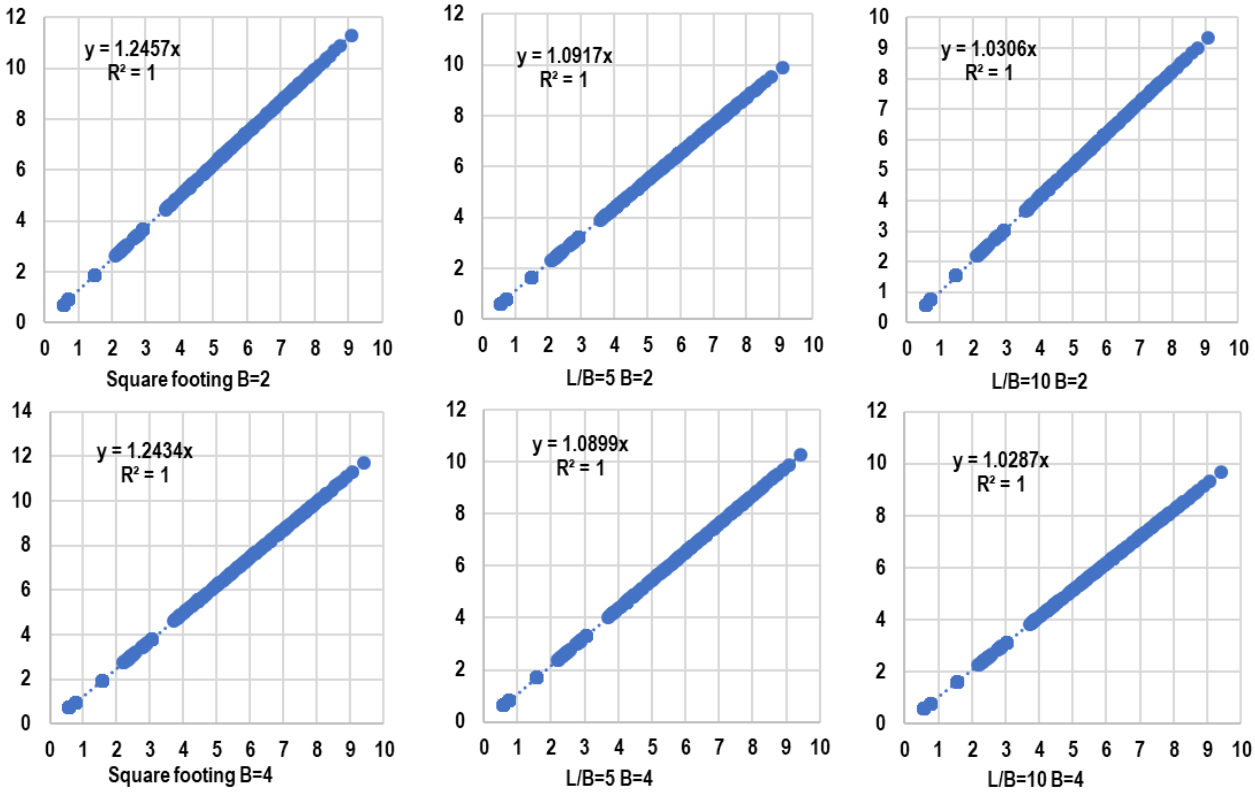

Note: The ratio on the figure = (Bearing capacity of non-strip footing) / (Bearing capacity of strip footing)

Figure 8-4. Bearing ratios of non-strip footing versus strip footing

8.1.5. Bearing Capacity Bias Ratios – Rock Subsurface

The bias ratio between the FEM and the derived bearing capacity equation results are plotted in Figure 8-5. For each individual plot, the bias ratio is very close to 1.0, with coefficient of determination (R^2) near 1.0, indicating excellent agreement between the results.

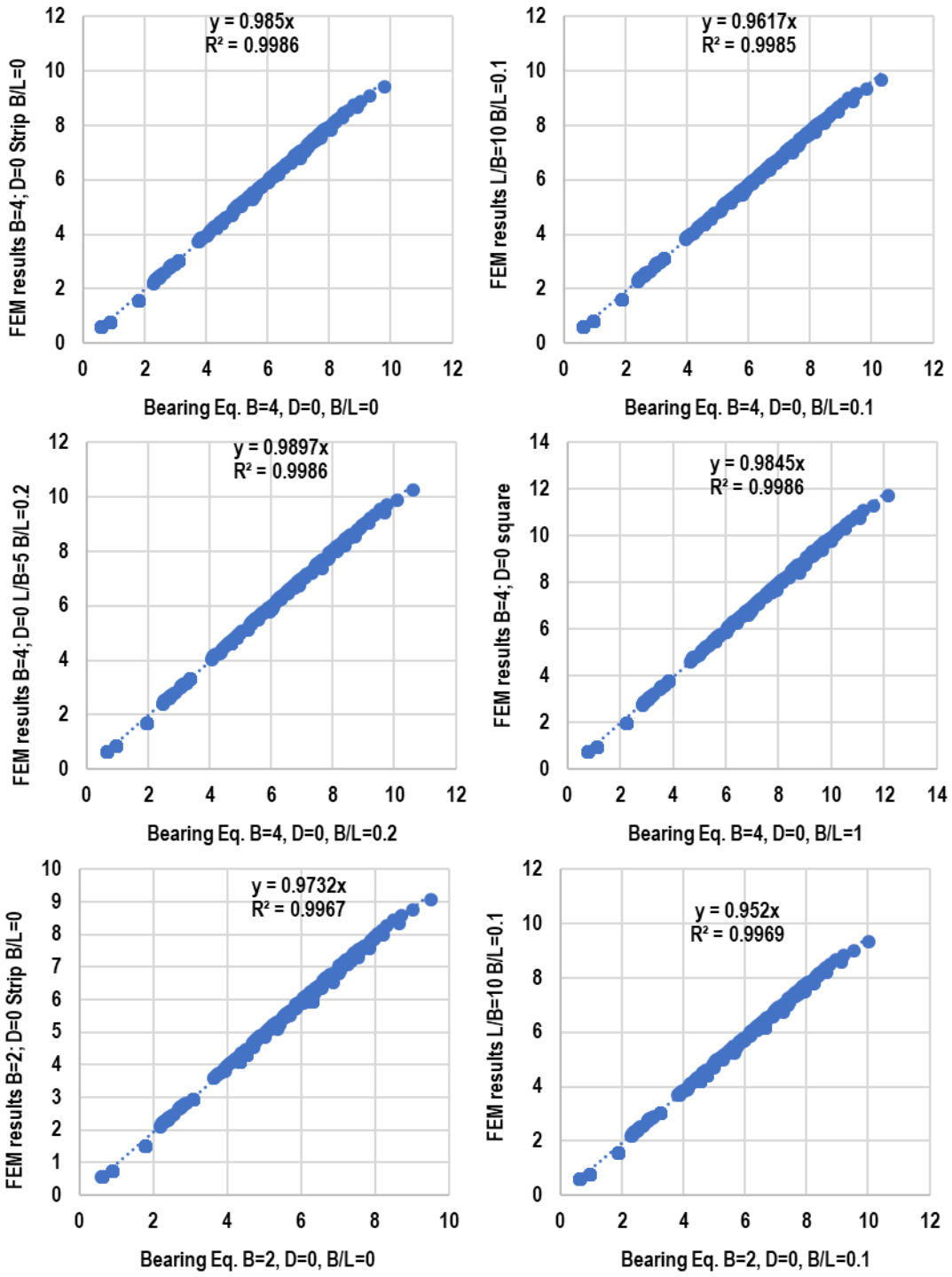

Figure 8-5. Bearing bias ratios – FEM versus bearing equation; rock subsurface

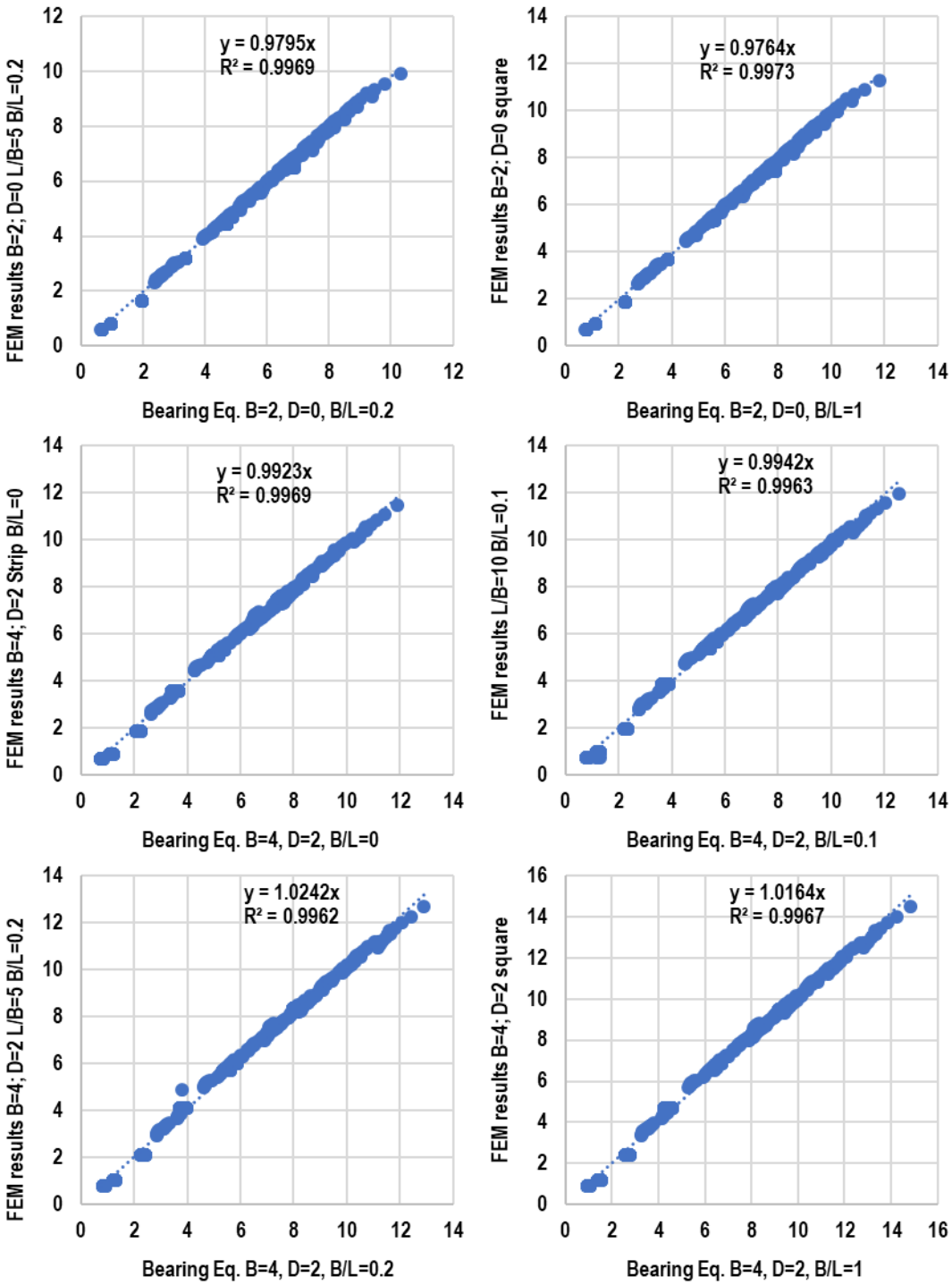

Figure 8-5. Bearing bias ratios (Cont.)

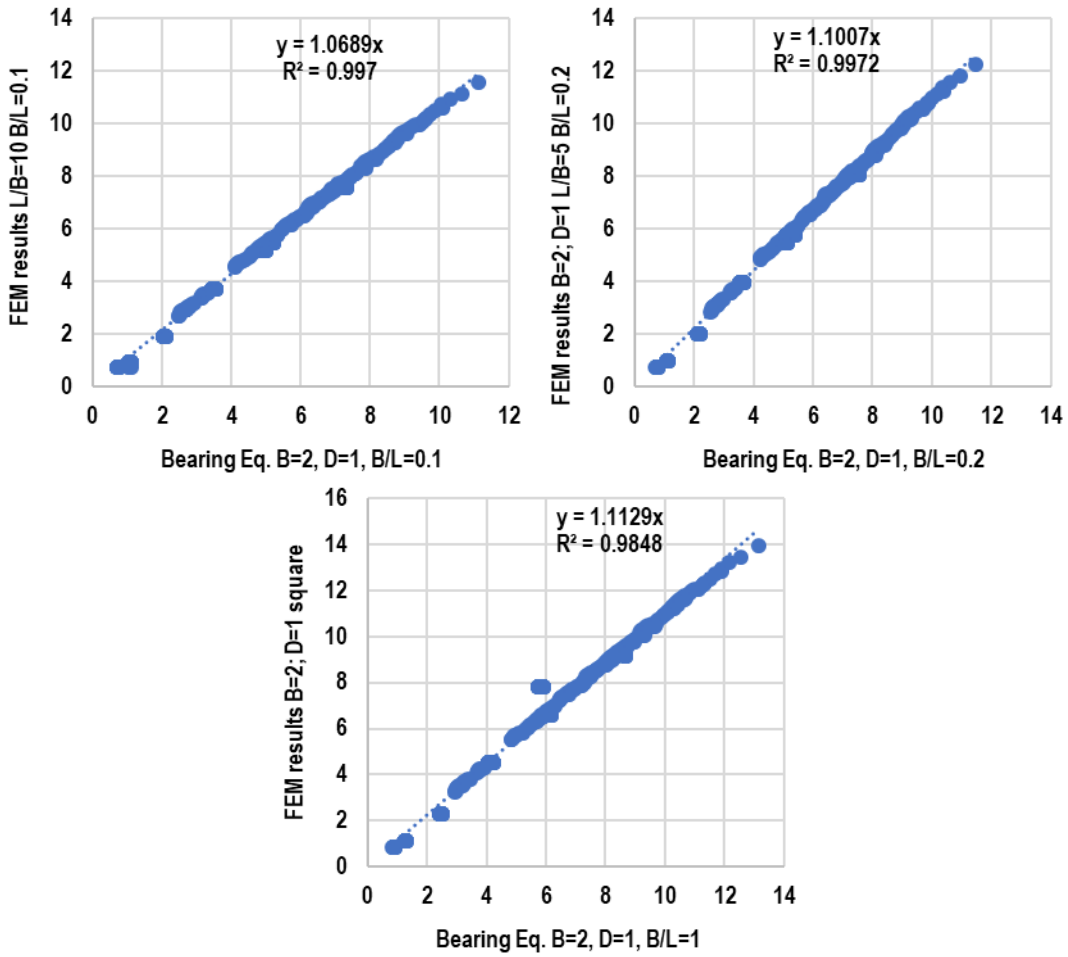

Figure 8-5. Bearing bias ratios (Cont.)

8.2 Bearing Equations – Shallow Foundation on Rock over Sand Subsurface

8.2.1. N_R reduction factor

Bearing bias ratios between the "Rock Subsurface" results and "Rock-Over-Sand Subsurface" results are plotted Figure 8-6. Based on the bearing ratio results the Rock-Over-Sand reduction factor N_R was determined, shown in Figure 8-7. The result is summarized as:

$$Q_{u,\,\text{Rock-Over-Sand}} = Q_{u,\,\text{Rock}} / N_R \qquad (8\text{-}17)$$

N_R – reduction factor compared to rock only subsurface.

$$N_R = 0.86 * R^{-0.25} \text{ if } R < 0.3 \quad (8\text{-}17a)$$

$$N_R = 1.2 - 0.1R \text{ if } R \geq 0.3 \quad (8\text{-}17b)$$

$$R = 0.093\, T^2 (E_{soil} / E_{rock}), \text{ limit R to 2.0} \quad (8\text{-}17c)$$

$$T = \text{Rock thickness in feet } \{\text{if T is in m, then } R = T^2 (E_{soil} / E_{rock})\} \quad (8\text{-}17d)$$

$$E_{soil} / E_{rock} = \text{Modulus ratio of soil and rock layers} \quad (8\text{-}17e)$$

Example, if the rock thickness is more than 25 ft (8 m) and $E_{soil} / E_{rock} > 0.03$, then the Rock over Sand bearing capacity results are expected to be the same as the Rock only results. This is reasonable, as the rock is thick enough. If the rock thickness is more than 10 ft (3 m) and $E_{soil}/E_{rock} > 0.25$, the Rock over Sand bearing capacity results are also expected to be the same. This is also reasonable, as E_{rock} is typically greater than 3,128 tsf (300 MPa), and E_{soil} of 783 tsf (75 MPa) is representative of a very dense soil with refusal SPT N blow counts ($N \geq 50$).

8.2.2. Bearing Capacity Bias Ratios – Rock over Sand Subsurface

The bearing bias ratio between the FEM and the derived bearing capacity equation results are plotted in Figure 8-8. For each individual plot, the bearing bias ratio is very close to 1.0, with coefficient of determination (R^2) near 1.0, indicating excellent agreement between the results.

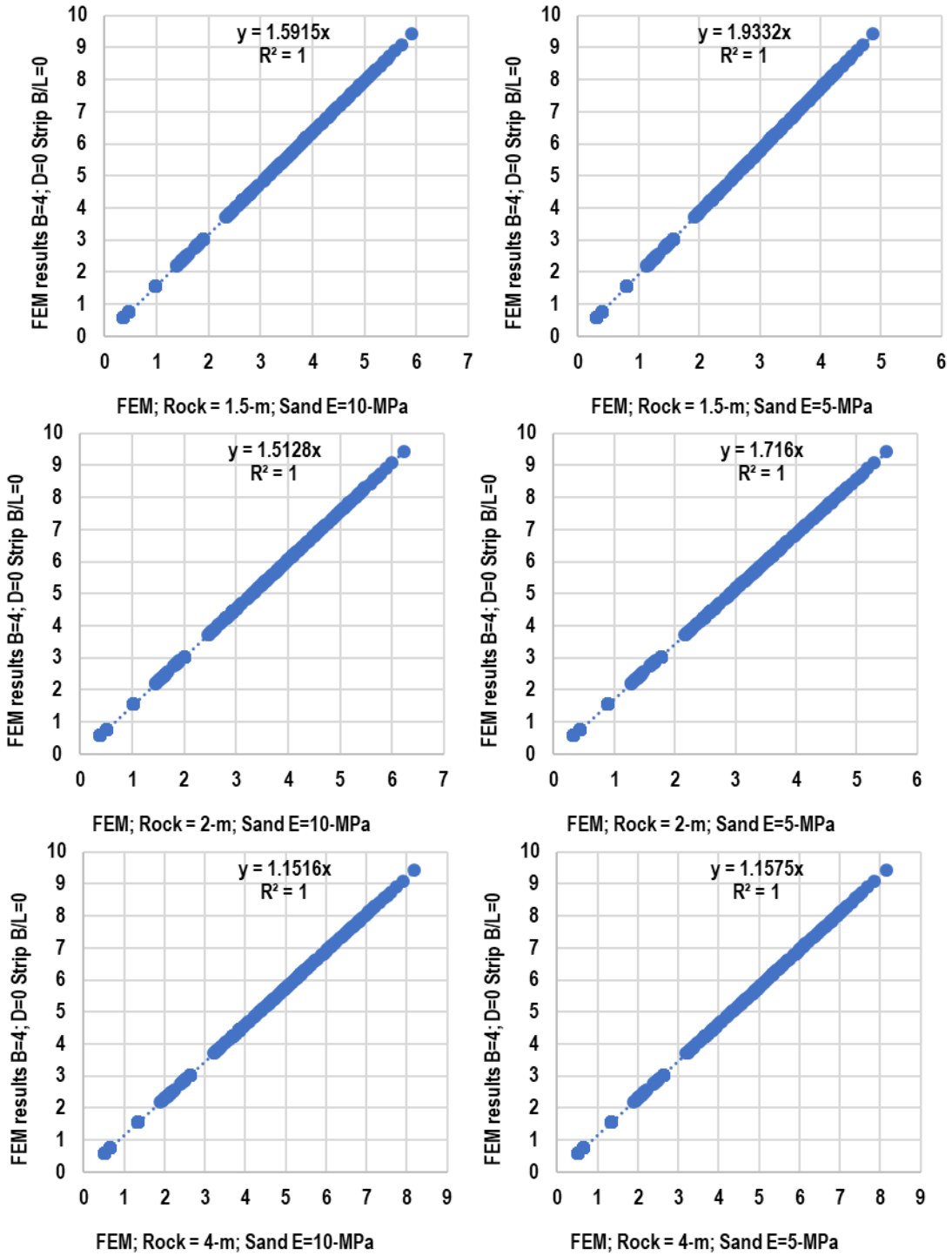

Figure 8-6. Bearing bias ratios – rock to rock-over-sand results

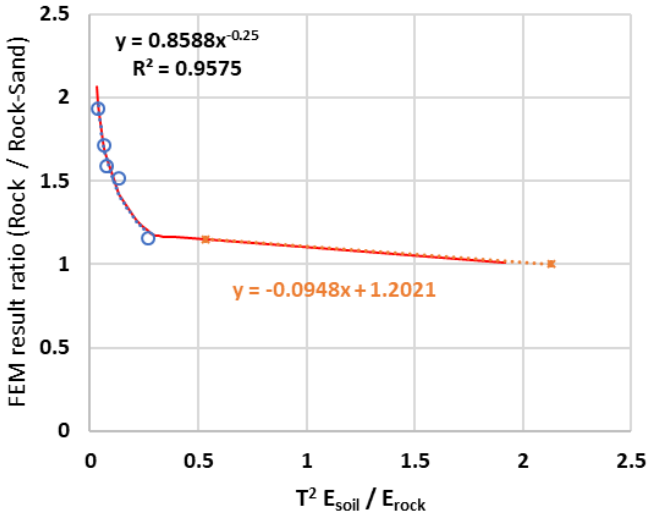

Figure 8-7. Rock-over-sand N_R reduction factor

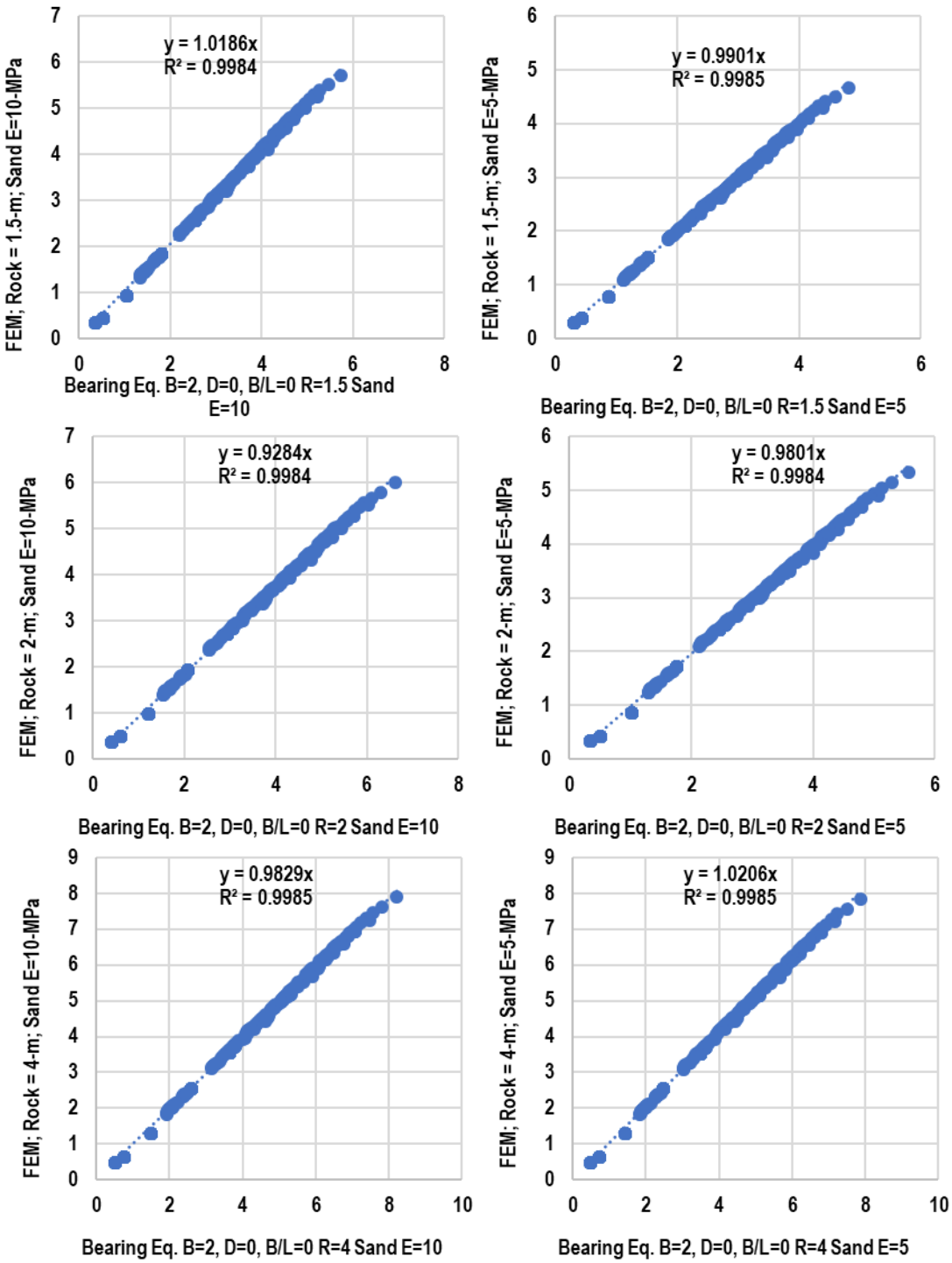

Figure 8-8. Bearing bias ratios – FEM versus bearing equation; rock over sand subsurface

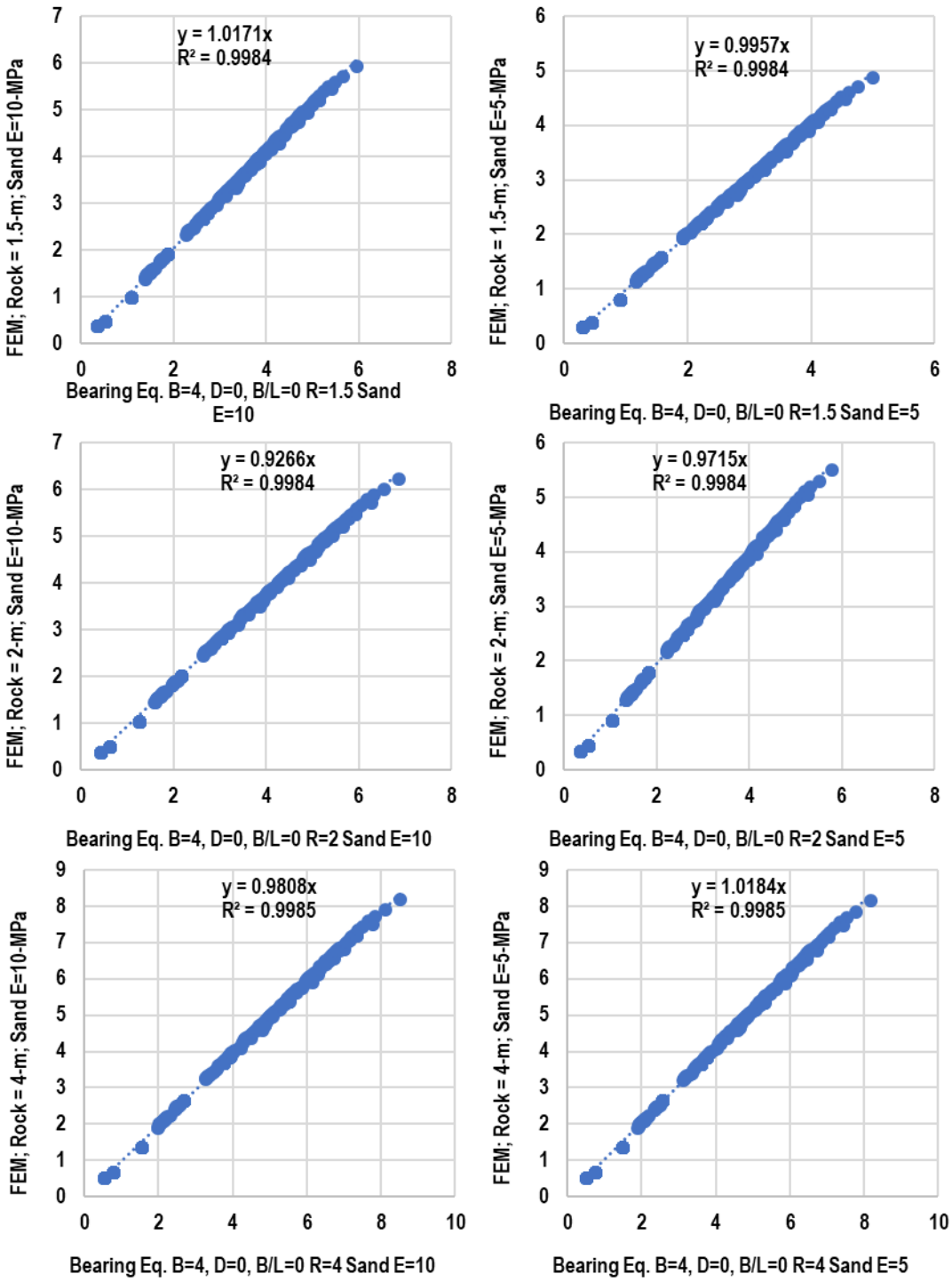

Figure 8-8. Bearing bias ratios – FEM versus bearing equation; rock over sand subsurface (Cont.)

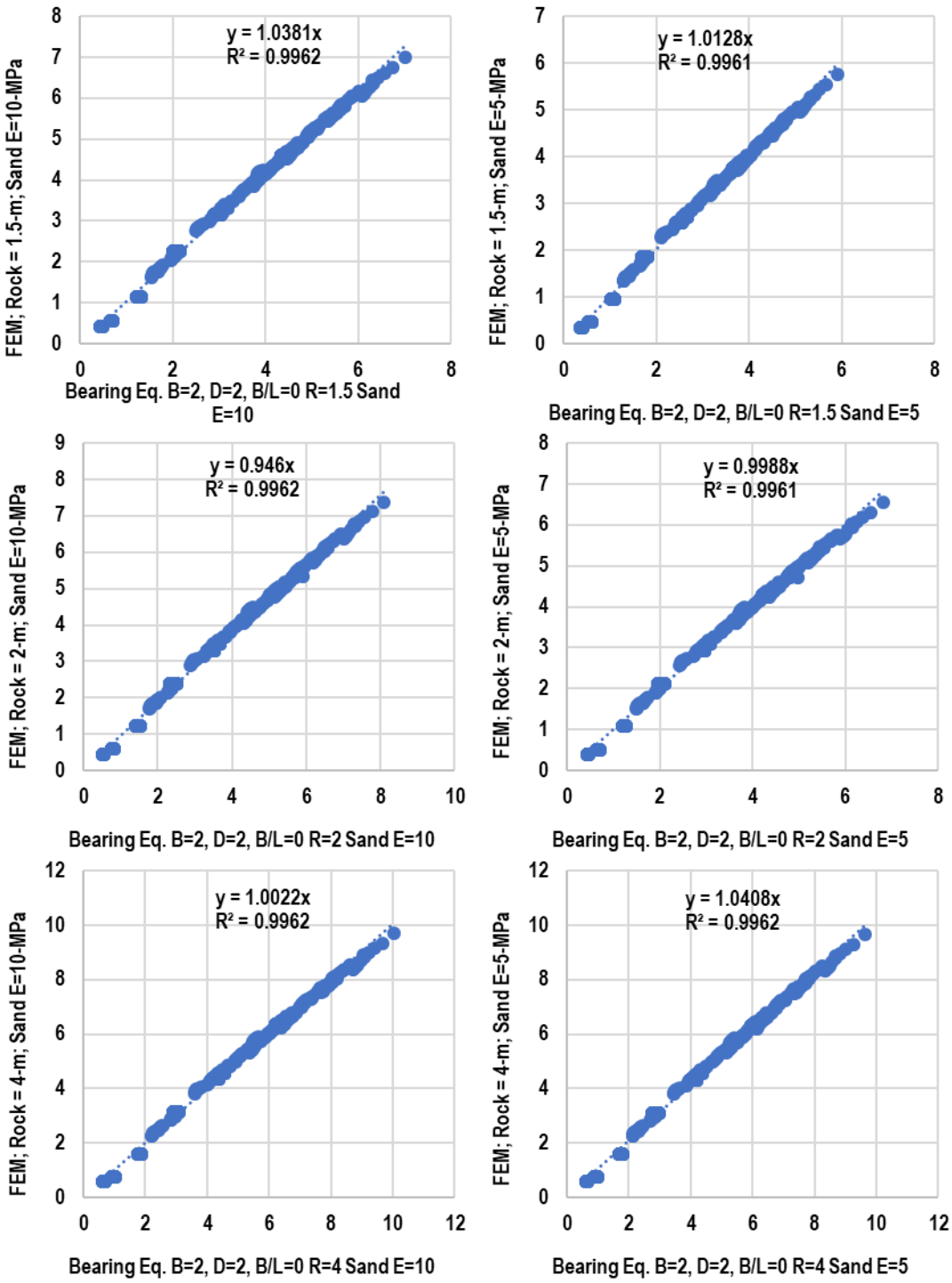

Figure 8-8. Bearing bias ratios – FEM versus bearing equation; rock over sand subsurface (Cont.)

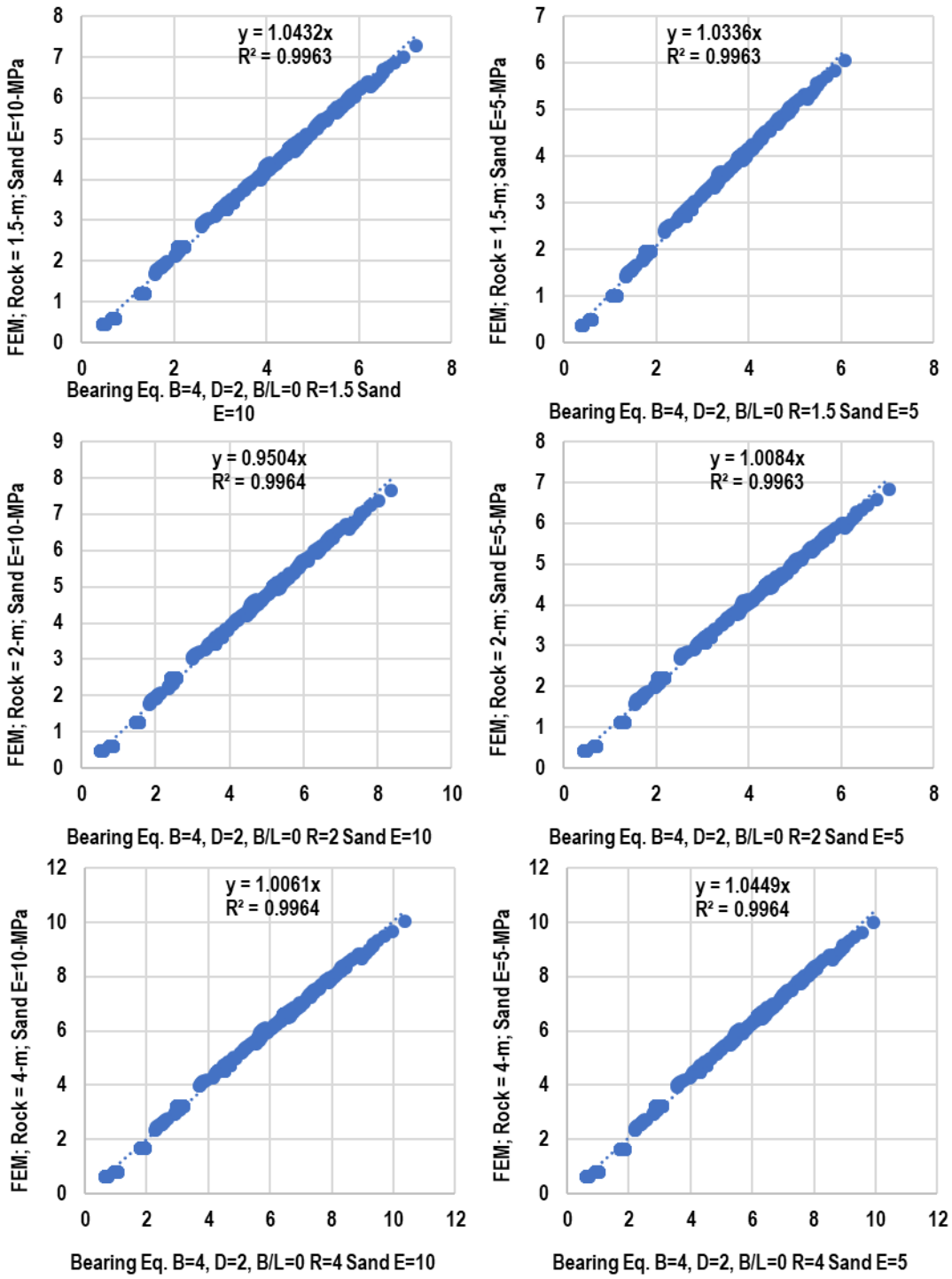

Figure 8-8. Bearing bias ratios – FEM versus bearing equation; rock over sand subsurface (Cont.)

8.3 Bearing capacity comparison with existing method

The Carter and Kulhawy (1988) method is the only semi-empirical bearing capacity analysis for rocks that is referenced in the current FHWA publication for shallow foundations (Kimmerling 2002), as well as in the current AASHTO LRFD Bridge Design Specification (AASHTO 2017). The Carter and Kulhawy (1988) bearing capacity equation is derived from the Hoek-Brown strength criterion. This method is derived only for the case of plane-strain condition (i.e., strip footing, B/L = 0 or L/B > 10) at the ground surface (D=0) of an infinite rock subsurface:

$$p_u = \left[\sqrt{s} + \sqrt{m\sqrt{s} + s}\right] q_u \quad (8\text{-}18)$$

q_u – unconfined compression strength

$$s = e^{(GSI\text{-}100)\,/\,9} \quad (8\text{-}18a)$$

$$m = m_i\, e^{(GSI\text{-}100)\,/\,28} \quad (8\text{-}18b)$$

m_i ranges from approximately 8±3 to 12±3 for different carbonate rocks. Assume $m_i = 10$ for the comparison analyses below.

GSI – Geological Strength Index, depending on rock joint spacing and rock joint quality.

As the Carter and Kulhawy (1988) results are only applicable for strip footing (e.g., B = 4 m, L > 40 m, shape factor $\xi = 1$, footing depth D = 0), the derived Florida bearing capacity equation was applied using the same strip footing configuration with a rock thickness reduction factor $N_R = 1$. While q_u was used in the Carter-Kulhawy equation, values of c and φ (as well as ω and p_p) were used in the Florida bearing equation. The parameters c and φ are related to q_u and q_{dt} as follow (Chapter 6):

$$c = 0.5\sqrt{q_u q_{dt}}\ ;\ q_{dt} = 0.7q_t \quad (8\text{-}19)$$

$$\sin\varphi = \frac{q_u - q_{dt}}{q_u + q_{dt}} \quad (8\text{-}20)$$

For rock mass:

$$c_{mass} = c * REC, \quad (8\text{-}21)$$

$$(\sin\varphi)_{mass} = (\tan\alpha)_{mass} = (\sin\varphi) * REC, \quad (8\text{-}22)$$

$$(\sin\omega)_{mass} = (\tan\beta)_{mass} = (\sin\omega) * REC. \quad (8\text{-}23)$$

For the case of intact rock, theoretically GSI is 100. However, in all charts presented by Hoek and Brown (1980, 1988, 2002, and 2018) as well as other publications (Rodegerdts et al., 2010, AASHTO 2017), the maximum GSI is shown as 80 to 90 for intact or massive rock. Therefore, Figure 8-9 presents the comparison for intact rock with GSI = 90 to 100, which indicates that the Florida bearing capacity equation would yield lower capacity results than those from Carter-Kulhawy's equation. However, using a GSI value of 81 (Figure 8-10.a and data presented in Table 8-2), the Carter-Kulhawy results would be approximately the same as the Florida bearing equation results. Additionally, Figure 8-10.b through f presents the capacity comparisons for rock mass using different values of rock recovery (REC) and GSI values. Using the REC-GSI value pairs in Figure 8-10, the results between the two methods are quite compatible. It should be noted that the REC value is a measured parameter from recovered rock cores, while GSI is subjectively evaluated based on the joint spacing and joint quality. When the rock appears as jointless as in the case of Florida carbonate rocks, the evaluation of the GSI value is very subjective. Therefore, the Florida bearing equation has several advantages: it utilizes measured parameters and it can be applied to any shallow foundation dimensions (i.e., any B/L ratio), any depths (D), and any layer thickness of surficial rock (T).

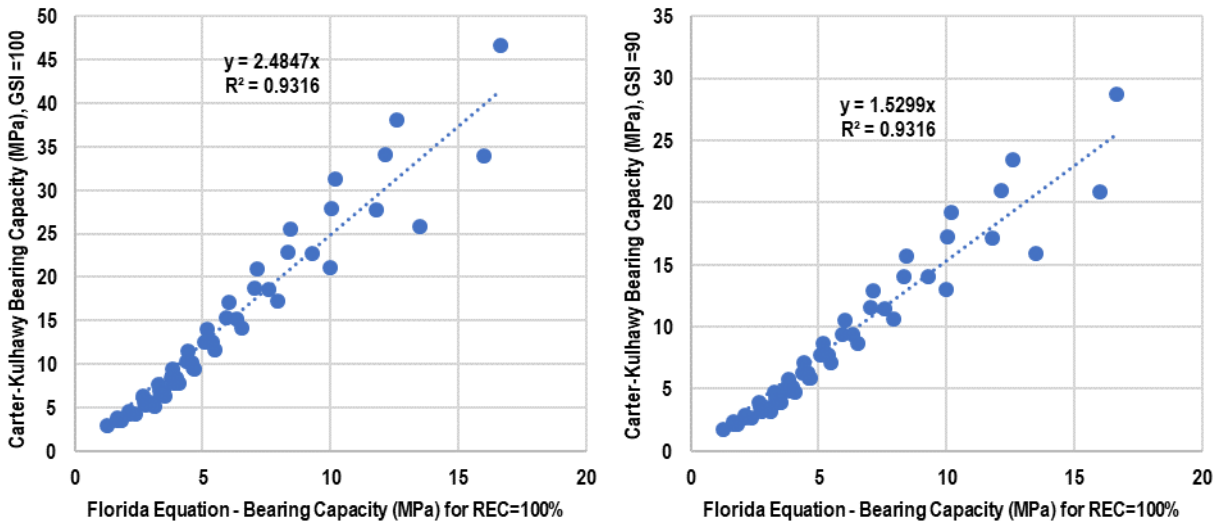

Figure 8-9. Capacity comparison for intact rock – Strip footing on rock subsurface

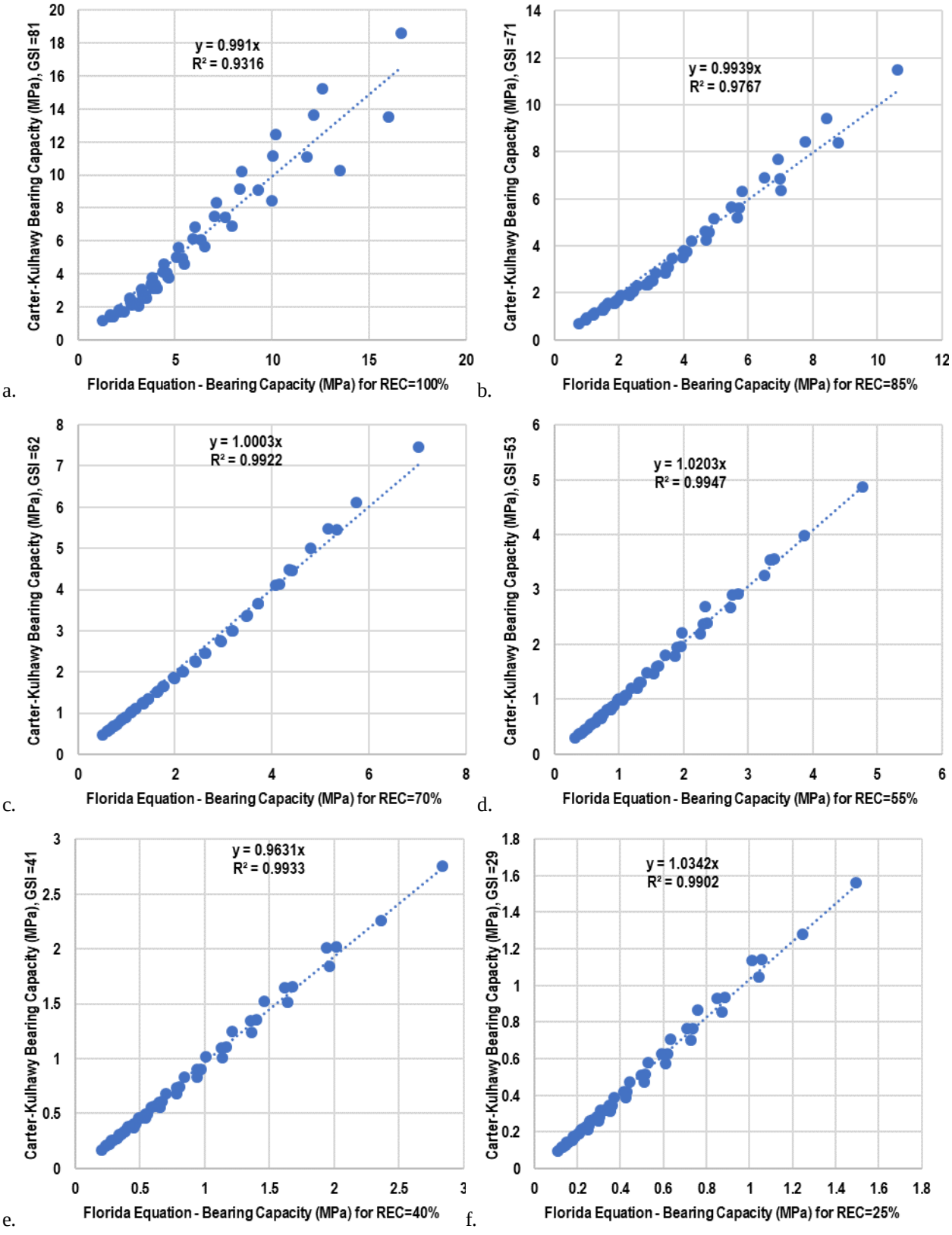

Figure 8-10. Capacity comparison for rock mass – Strip footing on rock subsurface

Table 8-1. Hoek Brown GSI values versus REC values in new bearing capacity equation

Analysis #	GSI	REC
#a	81	100%
#b	71	85%
#c	62	70%
#d	53	55%
#e	41	40%
#f	29	25%

Table 8-2. Comparison data for REC=100, GSI=81

Form-ation	q_{dt}	q_u	n	γ_{dt}		φ	ω	c		p_{peak}		Nc	Nc'	Nγ	Florida Eq.	Carter-Kulhawy
	psi			kN/m^3	pcf			psi	MPa	psi	MPa				MPa	MPa
Key Largo	30	127	0.62	10.2	65	38.2	-23.2	31	0.21	195	1.34	8	1.2	1.5	1.7	1.5
	35	155	0.59	11.0	70	39.3	-19.7	37	0.25	214	1.48	8	1.2	1.5	2.1	1.8
	40	189	0.56	11.8	75	40.4	-16.3	44	0.30	237	1.63	9	1.3	1.5	2.7	2.2
	47	231	0.53	12.6	80	41.5	-12.8	52	0.36	264	1.82	10	1.3	1.6	3.3	2.7
	55	283	0.50	13.4	85	42.6	-9.4	62	0.43	296	2.04	11	1.4	1.6	3.8	3.4
	63	345	0.47	14.1	90	43.6	-5.9	74	0.51	334	2.30	12	1.4	1.6	4.4	4.1
	74	422	0.44	14.9	95	44.6	-2.5	88	0.61	379	2.61	13	1.5	1.6	5.1	5.0
	86	515	0.41	15.7	100	45.6	1.0	105	0.72	433	2.99	15	1.6	1.6	6.0	6.1
	99	629	0.38	16.5	105	46.6	4.4	125	0.86	498	3.43	17	1.7	1.6	7.0	7.5
	116	768	0.35	17.3	110	47.6	7.9	149	1.03	575	3.97	20	1.8	1.6	8.4	9.1
	134	939	0.32	18.1	115	48.6	11.4	177	1.22	669	4.61	24	2.0	1.6	10.0	11.1
	156	1146	0.29	18.9	120	49.5	14.8	211	1.46	782	5.39	30	2.1	1.7	12.1	13.6
Anas-tasia	52	212	0.47	14.1	90	37.4	-6.7	52	0.36	233	1.61	7	1.6	1.4	2.7	2.5
	60	259	0.44	14.9	95	38.6	-6.7	62	0.43	262	1.81	8	1.5	1.5	3.3	3.1
	70	316	0.41	15.7	100	39.7	-6.7	74	0.51	296	2.04	9	1.5	1.5	3.8	3.8
	81	386	0.38	16.5	105	40.8	-6.7	88	0.61	337	2.32	9	1.5	1.5	4.4	4.6
	94	471	0.35	17.3	110	41.9	-6.7	105	0.73	386	2.66	10	1.5	1.5	5.2	5.6
	109	576	0.32	18.1	115	42.9	-6.7	125	0.86	445	3.06	11	1.4	1.6	6.0	6.8
	127	703	0.29	18.9	120	44.0	-6.7	149	1.03	515	3.55	12	1.4	1.6	7.1	8.3
	148	859	0.26	19.6	125	45.0	-4.3	178	1.23	600	4.14	14	1.5	1.6	8.4	10.2
	171	1049	0.23	20.4	130	46.0	1.6	212	1.46	702	4.84	15	1.6	1.6	10.2	12.5
	199	1281	0.20	21.2	135	47.0	10.9	253	1.74	826	5.70	18	2.0	1.6	12.6	15.2
	231	1565	0.18	22.0	140	47.9	23.7	301	2.07	977	6.73	21	3.0	1.5	16.6	18.6

Table 8-2. Continued

Form-ation	q_{dt}	q_u	n	γ_{dt}		φ	ω	c		p_{peak}		Nc	Nc'	Nγ	Florida Eq.	Carter-Kulhawy
	psi			kN/m^3	pcf			psi	MPa	psi	MPa				MPa	MPa
Ft. Thomp-son	22	97	0.47	14.1	90	38.7	-23.6	23	0.16	182	1.26	8	1.2	1.5	1.3	1.1
	26	118	0.44	14.9	95	39.9	-15.8	28	0.19	198	1.37	9	1.3	1.5	1.7	1.4
	30	144	0.41	15.7	100	40.9	-7.9	33	0.23	217	1.50	9	1.5	1.5	2.1	1.7
	35	176	0.38	16.5	105	42.0	-0.1	39	0.27	239	1.65	10	1.7	1.5	2.8	2.1
	41	216	0.35	17.3	110	43.1	7.8	47	0.32	265	1.83	11	2.0	1.5	3.4	2.6
	47	263	0.32	18.1	115	44.1	15.7	56	0.38	296	2.04	12	2.4	1.4	3.9	3.1
	55	322	0.29	18.9	120	45.1	23.5	66	0.46	332	2.29	14	3.2	1.4	4.6	3.8
Miami	37	188	0.47	14.1	90	42.2	-3.0	42	0.29	247	1.70	10	1.6	1.5	3.0	2.2
	43	230	0.44	14.9	95	43.3	-1.4	50	0.34	274	1.89	11	1.6	1.5	3.5	2.7
	50	281	0.41	15.7	100	44.3	0.8	59	0.41	306	2.11	13	1.6	1.6	4.0	3.3
	58	343	0.38	16.5	105	45.3	3.7	71	0.49	345	2.38	14	1.7	1.6	4.6	4.1
	67	419	0.35	17.3	110	46.3	7.3	84	0.58	390	2.69	16	1.8	1.6	5.4	5.0
	78	512	0.32	18.1	115	47.3	11.6	100	0.69	445	3.07	19	2.0	1.6	6.3	6.1
	91	626	0.29	18.9	120	48.3	16.5	119	0.82	510	3.52	22	2.3	1.6	7.6	7.4
	106	764	0.26	19.6	125	49.2	22.2	142	0.98	588	4.05	27	2.8	1.6	9.3	9.1
	123	934	0.23	20.4	130	50.1	28.5	169	1.17	682	4.70	35	3.6	1.6	11.8	11.1
	143	1140	0.20	21.2	135	51.0	35.5	202	1.39	795	5.48	50	5.1	1.6	16.0	13.5
Haw-thorn	23	117	0.50	13.4	85	41.9	1.4	26	0.18	209	1.44	10	1.7	1.5	1.8	1.4
	27	143	0.47	14.1	90	43.0	2.4	31	0.21	229	1.58	11	1.7	1.5	2.4	1.7
	31	175	0.44	14.9	95	44.0	4.1	37	0.26	251	1.73	12	1.8	1.5	3.1	2.1
	37	213	0.41	15.7	100	45.0	6.2	44	0.30	278	1.92	14	1.8	1.6	3.5	2.5
	42	261	0.38	16.5	105	46.0	9.0	53	0.36	309	2.13	16	1.9	1.6	4.1	3.1
	49	318	0.35	17.3	110	47.0	12.3	63	0.43	346	2.38	18	2.1	1.6	4.7	3.8
	57	389	0.32	18.1	115	48.0	16.1	75	0.51	389	2.68	21	2.3	1.6	5.5	4.6
	67	475	0.29	18.9	120	49.0	20.5	89	0.61	441	3.04	26	2.6	1.6	6.5	5.6
	77	580	0.26	19.6	125	49.9	25.5	106	0.73	503	3.47	33	3.1	1.6	7.9	6.9
	90	709	0.23	20.4	130	50.8	31.0	126	0.87	577	3.98	45	4.0	1.6	10.0	8.4
	104	866	0.20	21.2	135	51.7	37.1	150	1.04	665	4.59	73	5.7	1.7	13.5	10.3

8.4 Design examples

This section presents the use of the developed bearing capacity equations for typical shallow foundation design in Florida Limestones. Three cases are considered: (1) a rectangular footing residing on top of rock, i.e. embedment D = 0 ft; (2) a rectangular footing embedded 10 ft (D = 10 ft) into the rock; (3) a rectangular footing placed on top of a thin layer of rock overlying sand. Soil profiles for case (1), case (2) and case (3) are shown in Figure 8-11. (a), (b) and (c), respectively.

a)

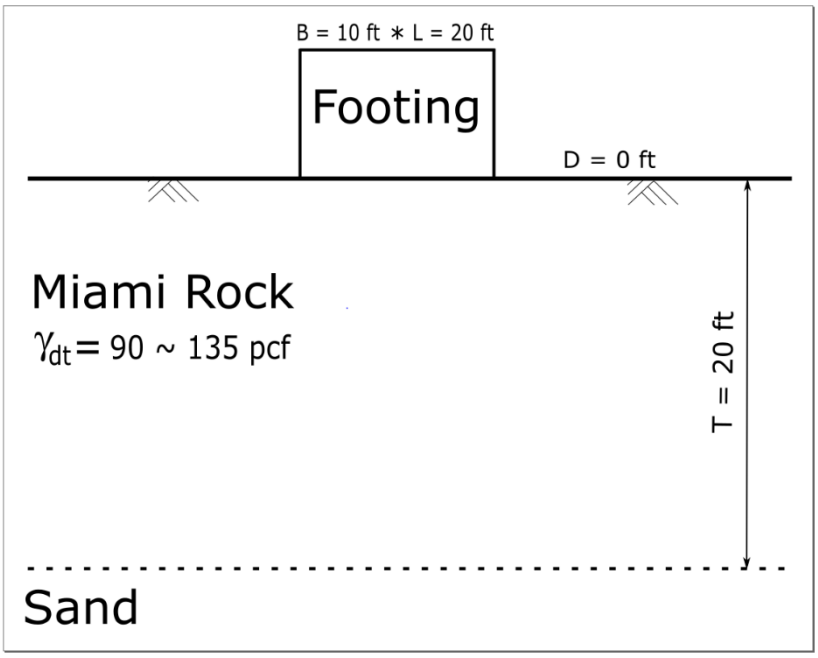

Figure 8-11. Design examples: (a) Rectangular footing with embedment D = 0 ft

b)

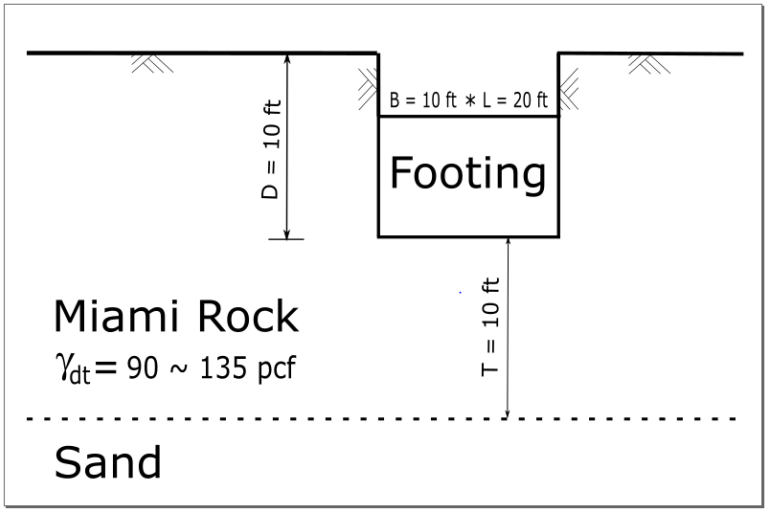

c)

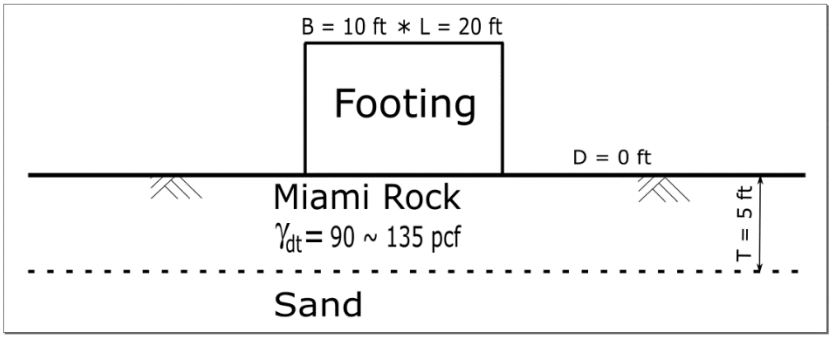

Figure 8-11. Continued: (b) Rectangular footing with embedment D = 10 ft; (c) Rectangular footing supported on a thin layer of rock overlying sand

For the analyses, the following dimensions and parameters are used: length (L) and width (B) of footing for three cases are 20 ft, and 10 ft, respectively; and E_{soil}/E_{rock} is 0.03. Table 8-2 in Section 8.3 (reproduced as Table 8-3) presents properties of Miami rock used. According to Equation (8-16e), (8-16f), (8-16g) and (8-16i) for N_c, N'_c, N_r and N_q are determined from strength parameters related to the dry bulk unit weight. Note, N_c, N'_c and N_q increase as dry bulk unit weight whereas the N_r decreases as dry bulk unit weight increases. Since the length (L) and width (B) of footing are known, Equation (8-16c) and (8-16d) determine n (0.99) and shape factor ξ (1.16), respectively. The rock thickness reduction factor, N_R varies with rock thickness;

the depth (D) of footing contributes $q*N_q$ to the bearing capacity and q varies with depth (D) of footing. Table 8.-3 presents the bearing capacity terms for all cases, as a function of the Miami rock properties.

Table 8-3. Miami rock for REC=100, GSI=81 and parameters for Florida bearing capacity equations

Form-ation	q_{dt}	q_u	γ_{dt}	φ	ω	c	p_{peak}	n	shape factor (ξ)	N_c	N_c'	N_γ	N_q
	Properties from Table 8-2							Equation (8-16c)	Equation (8-16d)	Equation (8-16e)	Equation (8-16f)	Equation (8-16g)	Equation (8-16i)
	psi		pcf	°		psi		–					
Miami	37	188	90	42.20	-3.00	42	247	0.99	1.16	10.39	1.56	1.53	15.74
	43	230	95	43.30	-1.40	50	274	0.99	1.16	11.47	1.59	1.55	19.40
	50	281	100	44.30	0.80	59	306	0.99	1.16	12.68	1.64	1.57	23.71
	58	343	105	45.30	3.70	71	345	0.99	1.16	14.19	1.72	1.58	29.10
	67	419	110	46.30	7.30	84	390	0.99	1.16	16.14	1.85	1.59	35.48
	78	512	115	47.30	11.60	100	445	0.99	1.16	18.76	2.04	1.60	43.43
	91	626	120	48.30	16.50	119	510	0.99	1.16	22.44	2.32	1.61	53.07
	106	764	125	49.20	22.20	142	588	0.99	1.16	27.35	2.79	1.62	64.50
	123	934	130	50.10	28.50	169	682	0.99	1.16	35.16	3.58	1.62	78.74
	143	1140	135	51.00	35.50	202	795	0.99	1.16	49.57	5.17	1.61	96.13

8.4.1. Case (1): Rectangular footing with embedment D = 0 ft

Case (1) calculates the bearing capacity of rectangular footing with embedment D = 0 ft, which has no contribution from the $q * Nq$ term (0) for case (1). Based on the rock thickness, T = 20 ft and Equation (8-17b) and (8-17c), the rock thickness reduction factor N_R, was computed as 1.08. Table 8-4 presents the bearing capacity values for the footing (case (1)), using Equations 8-16, 8-16a, 8-16b and 8-17 for the different rock strengths.

Table 8-4. Bearing capacity for case (1)

Form-ation	γ_{dt}	Q_{u1}	Q_{u2}	Q_U	Q_U
	Table 8-2	Equation (8-16a)	Equation (8-16b)	Equation (8-16) and (8-17)	Unit Conversion
	pcf	psi	psi	psi	tsf
Miami	90.00	430.11	436.81	461.65	33.24
	95.00	565.13	496.86	533.30	38.40
	100.00	737.11	567.76	609.40	43.88
	105.00	992.82	658.00	706.26	50.85
	110.00	1335.94	765.35	821.48	59.15
	115.00	1847.69	904.15	970.47	69.87
	120.00	2630.68	1082.91	1162.34	83.69
	125.00	3825.98	1326.23	1423.50	102.49
	130.00	5854.56	1681.83	1805.18	129.97
	135.00	9863.72	2290.80	2458.81	177.03

8.4.2. Case (2): Rectangular footing with embedment D = 10 ft

Case (2) calculates bearing capacity of a rectangular footing with embedment D = 10 ft, which contributes $q * Nq$ to the bearing capacity through Equation 8-16h. Rock thickness, T is 10 ft and Rock thickness reduction factor, N_R is determined as 1.17 by Equation (8-17b) and (8-17c). Table 8-5 presents the bearing capacity for the footing (case (2)), using Equations 8-16a, 8-16b, 8-16 and 8-17 for the different rock strengths.

Table 8-5. Bearing capacity for case (2)

Form-ation	γ_{dt}	Q_{u1}	Q_{u2}	Q_U	Q_U
	Table 8-2	Equation (8-16a)	Equation (8-16b)	Equation (8-16) and (8-17)	Unit Conversion
	pcf	psi	psi	psi	tsf
Miami	90.00	528.48	535.18	522.16	37.60
	95.00	693.18	624.90	617.43	44.46
	100.00	901.82	732.47	723.71	52.11
	105.00	1205.08	870.26	859.85	61.91
	110.00	1607.01	1036.41	1024.02	73.73
	115.00	2194.62	1251.08	1236.13	89.00
	120.00	3073.03	1525.26	1507.02	108.51
	125.00	4386.04	1886.28	1863.73	134.19
	130.00	6565.59	2392.86	2364.25	170.23
	135.00	10765.16	3192.24	3154.07	227.09

8.4.3. Case (3): Rectangular footing supported on a thin layer of rock overlying sand

Case (3) calculates bearing capacity of rectangular footing supported on a thin layer of rock overlying sand. The rock thickness (T) is known as 5 ft for case 3, Figure 8-11c, the rock thickness reduction factor, N_R is determined as 1.63 by using Equation (8-17a) and (8-17c). The embedment (D) of footing is same as case (1) with a value of 0, i.e. has no contribution to bearing capacity from $q * Nq$ term. Table 8-6 presents the bearing capacity for the footing (case (3)), using Equations 8-16a, 8-16b, 8-16 and 8-17 for each of the different rock strengths.

Table 8-6. Bearing capacity for case (3)

Form-ation	γ_{dt}	Q_{u1}	Q_{u2}	Q_U	Q_U
	Table 8-2	Equation (8-16a)	Equation (8-16b)	Equation (8-16) and (8-17)	Unit Conversion
	pcf	psi	psi	psi	tsf
Miami	90.00	430.11	436.81	304.72	21.94
	95.00	565.13	496.86	352.01	25.34
	100.00	737.11	567.76	402.24	28.96
	105.00	992.82	658.00	466.17	33.56
	110.00	1335.94	765.35	542.22	39.04
	115.00	1847.69	904.15	640.56	46.12
	120.00	2630.68	1082.91	767.20	55.24
	125.00	3825.98	1326.23	939.59	67.65
	130.00	5854.56	1681.83	1191.52	85.79
	135.00	9863.72	2290.80	1622.95	116.85

CHAPTER 9
CONCLUSIONS AND RECOMMENDATIONS

Florida carbonate rock strengths are very low; most of the splitting tension strength q_t values are less than 1.7 MPa (250 psi, Chapter 5), and most of the unconfined compression strength q_u values are less than 9 MPa (1,300 psi, Chapter 5), with a q_u median value of only 3 MPa (435 psi, Chapter 5). Cohesive IGM is defined by the FHWA as material that exhibits unconfined compressive strengths in the range of 0.5 to 5 MPa (70 to 700 psi). Thus, about 65% of the carbonate rocks tested in the historical FDOT database would be classified as IGM. The carbonate rocks in other regions reported in literature are typically much stronger, with q_u = 70 to 340 MPa (10,000 psi to 50,000 psi), including the rocks cited in the development of the strength envelop by Hoek and Brown (1980, 1988) and Johnston (1985). The low strengths of Florida carbonate rocks require unique study and correlations, which are presented in this study.

There are existing standard test methods for the evaluation of apparent rock index properties (e.g., D4673 or AASHTO T-85) and standard test methods for the evaluation of specimen solid specific gravity (e.g., ASTM D854 or AASHTO T-100). These standard test methods, however, do not differentiate the proportions of vug and permeable porosities, which are important index parameters for Florida rocks. Based on combinations of these standard test methods, Eqs. 3-7 to 3-9 (Chapter 3) have been derived to differentiate different proportions of porosities:

Impermeable porosity: $n_i = \gamma_{dt}(1/\gamma_{sa} - 1/\gamma_{st})$ (9-1)

Permeable porosity: $n_p = \gamma_{dt}(1/\gamma_{da} - 1/\gamma_{sa})$ (9-2)

Vug porosity: $n_v = 1 - \gamma_{dt}/\gamma_{da}$ (9-3)

where the apparent properties (γ_{sa} and γ_{da}) are obtained from D4673 or AASHTO T-85, the solid unit weight (γ_t) is obtained from ASTM D854 or AASHTO T-100 on rock powder, and

the bulk dry unit weight (γ_{dt}) is simply the oven-dried weight divided by the cylindrical volume of the specimen.

There is no consistent grading scale in literature to identify a rock as vuggy or porous as each author consider rock as "porous" or "highly porous" at different porosities. Furthermore, there is no grading scale for rock to be described as "slightly vuggy" or "vuggy". Therefore, Table 3-2 in Chapter 3 (reproduced as Table 9-1) is proposed to describe the Florida carbonate rock based on magnitudes of different porosities.

Table 9-1. Proposed vug descriptions

n_v	0 to 5%	5 to 10%	10 to 15%	15 to 20%	>20%
Vug porosity	No vug, relatively smooth rock	Slightly vuggy	Vuggy to Very vuggy	Very vuggy	Extremely vuggy

Results from Chapter 4 indicates that rocks in Florida are highly heterogeneous, containing a wide range of bulk dry unit weights (or porosities) within a given rock layer. The median porosity of Florida rocks is approximately 37%. In correlating the Florida carbonate rock strengths, the key parameter is porosity, $n = 1 - \gamma_{dt}/(GS * \gamma_w)$. As GS is relatively a constant, for a given bulk dry unit weight, the porosity (n) fluctuates within a margin about3% depending on the value of GS. For example, γ_{dt} = 15.7 kN/m^3 = 100 pcf, then n could vary from 0.405 to 0.418, or 40.5% to 41.8% when GS = 2.69 to 2.75. GS for rock is difficult to measure while γ_{dt} is very simple to obtain. Therefore, the key parameter used in this study to correlate the Florida rock strength was its bulk dry unit weight γ_{dt}.

The splitting tension strength q_t can be roughly estimated using Eq. 5-1 (Chapter 5) as follows:

$$q_t \text{ (psi)} = 3.864\, e^{0.03\gamma_{dt} B} \qquad (9\text{-}4)$$

However, Florida rock strengths are highly dependent on their rock formations. A more reliable estimate of q_t based on two additional parameters - formation factor, F_t, and carbonate content, C, is proposed:

$$q_t \text{ (psi)} = 2.468\ F_t\ e^{0.03\,\gamma_{dt}\,B}\ e^{0.5C} \tag{9-5}$$

where,

C is the carbonate content, typically ranging from 0.5 to 1.0 (i.e., 50% to 100%), and $e^{0.5C}$ would be 1.28 to 1.65. For C < 0.5, it would be considered a soil and would not be applicable for this correlation.

F_t is the formation factor, which is influenced by the rock formation identification. It is dependent on the vug or permeable porosity ratio (in relative to the bulk porosity). F_t are referenced in Table 5-1 or Figure 5-9 for rocks evaluated in this study. For other Florida formations not included in this study, F_t can be evaluated by using Eq. 5-2.

It is noted that when C = 89.5% and F_t = 1, which are the typical average value for carbonate content and formation factor of Florida rocks, then Eq. 5-6 turns into Eq. 5-1.

The direct tension strength q_{dt} can be estimated as 0.7*q_t for sedimentary rocks based on the statistical results from Perras and Diederichs (2014).

The unconfined compression strength q_u can be estimated using Eq. 5-7 or 5-17 depending on what rock index parameter is available. Eq. 5-17 is based on three index rock parameters; thus, the correlation has better coefficient of correlation than Eq. 5-7:

$$q_u \text{ (psi)} = 5.89\ e^{0.04\,\gamma_{dt}\,B} \tag{9-6}$$

$$q_u \text{ (psi)} = 3.24\ F_u\ e^{0.04\,\gamma_{dt}\,B}\ e^{2C/3} \tag{9-7}$$

The relationship between q_u and q_t is:

$$q_u \text{ (psi)} = 0.97 * q_t^{4/3} \quad (9\text{-}8)$$

Solving for q_t, the resulting relationship is:

$$q_t \text{ (psi)} = 1.03 * q_u^{3/4} \quad (9\text{-}9)$$

It was shown in Chapter 6 that when the unconfined compression strength, q_u, is higher than 9 MPa (1,300 psi), the material typically exhibits brittle stress-strain behavior for shallow foundation loading conditions. In this case, the Hoek-Brown criterion, developed for brittle rupture failure, is applicable. However, most of the porous Florida carbonate rocks have weaker strengths with ductile stress-strain response, associated with a contractive volumetric behavior. The σ_d/σ_3 threshold for the material to transition from a brittle to ductile response has been expanded beyond the conventional ductile pressure range (i.e., toward the minimal confining pressure range), presented in Table 6-2. Accordingly, the strength envelopes for these materials are sloping downward at a much steeper rate than those in the brittle zone. Moreover, the envelopes vary between formations, due to different cementations (different minerals, carbonate contents, and rock grain sizes) as well as different proportions of void structures (vug, permeable, and impermeable voids). Consequently, it is recommended that different Florida carbonate rock formations have their own strength envelopes based on dry unit weights (Figure 6-22 to Figure 6-26). For finite element method application, a simplified bilinear strength envelope can be used, with four parameters: cementation c, initial friction angle φ, onset of non-linear stress-strain (which is simplified to a linear line) p_p, and second slope of the bilinear envelope ω. The equations are shown in Eqs. 6-25 to 6-27 with presentations in Figure 6-35 to Figure 6-39. Appendix F describes a procedure to establish a rock strength envelope for a standard design project. Furthermore, it is not recommended to reduce the strength envelope of Florida carbonate rocks

using the GSI index since it is not readily available. Pending further study, a provisional procedure is recommended to develop the Florida rock mass strength envelope from the intact strength envelope, weighted-average value of dry unit weight, and rock recovery ratio (REC).

Florida bearing capacity equations (Chapter 8) were developed based on the bilinear strength envelope, which can be applied to any footing shape, any depth, and any rock thickness (which is applicable where a caprock is usually encountered atop a thick sand layer, such as the case in south Florida):

$$Q_u = \min (Q_{u1}, Q_{u2}) * \xi / N_R \quad (9\text{-}10)$$

$$Q_{u1} = n\ c\ N_c + qN_q \quad (9\text{-}10a)$$

$$Q_{u2} = n\ [c\ N'_c + p_p\ N_\gamma\ ] + qN_q \quad (9\text{-}10b)$$

c, φ, ω, and p_p are four parameters defining the bilinear strength envelope (Chapter 6). The relationships among the parameters in p-q diagram and in σ-τ diagram are:

$\sin\varphi = \tan\alpha$; $a = c\cos\varphi$; $\sin\omega = \tan\beta$; $c = 0.5\sqrt{q_u q_{dt}}$; $\sin\varphi = \frac{q_u - q_{dt}}{q_u + q_{dt}}$

$$p_p\ (\text{psi}) = \frac{50+a}{1-\tan\alpha} = \frac{50+c\cos\varphi}{1-\sin\varphi} \text{ or } p_p\ (\text{kPa}) = \frac{345+a}{1-\tan\alpha} = \frac{345+c\cos\varphi}{1-\sin\varphi} \quad (9\text{-}11)$$

The 2nd slope ω on the strength envelope is obtained via triaxial tests with recommended procedure in Appendix F. In case triaxial tests for a specific site are not available, preliminary values in Table 6-4 can be used.

$$n = \left(\frac{4}{B\ in\ meter}\right)^{-0.055} \quad \text{or } n = \left(\frac{4}{0.3B\ in\ ft}\right)^{-0.055} \quad (9\text{-}12)$$

$$\xi = \text{shape factor} = 1 + 0.245\left(\frac{B}{L}\right)^{0.66} \quad (9\text{-}12a)$$

N_R = Rock thickness reduction factor (9-12b)

$N_R = 0.86 * R^{-0.25}$ if $R < 0.3$

$N_R = 1.2 - 0.1R$ if $R \geq 0.3$

$R = 0.093T^2\ (E_{soil} / E_{rock})$, limit R to 2.0 (9-12c)

T = Rock thickness in feet {if T is in m, then $R = T^2\ (E_{soil} / E_{rock})$}

E_{soil} / E_{rock} = Modulus ratio of soil and rock layers

$$N_c = \frac{1.8\ cos\varphi}{0.8 - sin\varphi} \quad (9\text{-}12d)$$

$$N'_c = \frac{1.8\ cos\varphi}{0.8-sin\omega} \quad (9\text{-}12e)$$

$$N_\gamma = \frac{1.8\ [sin\varphi - sin\omega]}{0.8-\sin\omega} \quad (9\text{-}12f)$$

$$q = \gamma' D \quad (9\text{-}12g)$$

$$N_q = (1.5 * \frac{p_p}{\sigma_a} - 10) * (3 * \sin\varphi - 1) \quad (9\text{-}12h)$$

σ_a = Sea level standard atmospheric pressure

LIST OF REFERENCES

AASHTO. (2017). *AASHTO LRFD Bridge Design Specification. American Association of State Highway and Transportation Officials,* Washington, D.C.

AASHTO Standard T-100. (2015). *Standard Specifications for Transportation Materials and Methods of Sampling and Testing, and AASHTO Provisional Standards*, American Association of State Highway and Transportation Officials, Washington, D.C.

ACI 318-14. (2014). *Building Code Requirements for Structural Concrete and Commentary*, American Concrete Institute, Farmington Hills, MI.

Arioglu N., Girgin Z., Arioglu E. (2006). *Evaluation of Ratio between Splitting Tensile Strength and Compressive Strength for Concrete up to 120 MPa and its Application in Strength Criterion*. *ACI Materials Journal*, 103(1), 18-24.

Arthur, J. D., Fischler, C., Kromhout, C., Clayton, J., Kelley, G. M., Lee, R. A., & Werner, C. (2008). *Hydrogeologic framework of the southwest Florida water management district*. Florida Geological Survey Bulletin, 68, 175.

ASTM Standard D854 (2014). *Standard Test Methods for Specific Gravity of Soil Solids by Water Pycnometer*, ASTM International, West Conshohocken, PA.

ASTM Standard D3967 (2016). *Standard Test Method for Splitting Tensile Strength of Intact Rock Core Specimens",* ASTM International, West Conshohocken, PA.

ASTM Standard D6473 (2015). *Standard Test Method for Specific Gravity and Absorption of Rock for Erosion Control*, ASTM International, West Conshohocken, PA.

ASTM Standard D7012 (2014). *Standard Test Methods for Compressive Strength and Elastic Moduli of Intact Rock Core Specimens under Varying States of Stress and Temperatures*, ASTM International, West Conshohocken, PA.

Boggs Jr., S. (2006). *Principles of Sedimentology and Stratigraphy*. Pearson Prentice Hall Publishing.

Borja, Ronaldo I (2013). *Plasticity: modeling & computation*. Springer Science & Business Media.

Briaud J-L., Smith B., Rhee K-Y., Lacy H., Nicks J. (2009). "The Washington Monument Case History." *International Journal of Geoengineering Case Histories*, Vol.1, Issue 3, pp.170-188

Brown, D. A., Turner, J. P., & Castelli, R. J. (2010). Drilled shafts: construction procedures and LRFD design methods. Publication No. FHWA-NHI-10-016, Federal Highway Administration, Washington, DC.

Bullock, P. J. (2004). In-situ Rock Modulus Apparatus. Transportation Research Center, University of Florida. Florida Department of Transportation Project BC-354 TWO 13 Final Report. Gainesville, FL

Carter, J. P. and Kulhawy, F. H. (1988). "*Analysis and Design of Foundations Socketed into Rock*". Report No. EL-5918. Empire State Electric Engineering Research Corporation and Electric Power Research Institute, New York, pp. 158.

Chang C., Zobacka M.D., Khaksar A. (2006). "Empirical Relations between Rock Strength and Physical Properties in Sedimentary Rocks" in: *Journal of Petroleum Science and Engineering*, Vol 51(3), pp. 223-237.

Chappell, J.M. (2009). "Sea Level Change, Quaternary" in Vivien Gornitz, ed., *Encyclopedia of Paleoclimatology and Ancient Environments*, Springer, New York, NY. pp. 893-898.

Das, Braja M. (2015), "*Principles of foundation engineering*". Cengage learning.

Deer, D.U., and Miller, R.P. (1966). "*Engineering Classification and Index Properties for Intact Rock*", Technical Report No. AFWL-TR-65-116, Air Force Weapons Laboratory, Kirtland Air Force Base, Albuquerque, NM.

Eagar, T.W. and Musso, C. (2001). "Why did the world trade center collapse? Science, engineering, and speculation", in: The Journal of The Minerals, Vol 53, pp. 8-11.

Elliott G. M. and Brown E. T. (1985). "Yield of a soft, high porosity rock", in: *Geotechnique*, Vol 35, pp. 413-423.

Fereidooni, D. and Khajevand, R. (2018). "Determining the Geotechnical Characteristics of Some Sedimentary Rocks from Iran with an Emphasis on the Correlations between Physical, Index, and Mechanical Properties" in: *Geotechnical Testing Journal*, Vol 41(3), pp. 555-573.

Florida Department of Transportation (FDOT) (2015). "Florida Test Method for Carbonates and Organic Matter in Base Materials", State Materials Office, Florida.

Florida Department of Transportation (FDOT) (2018). "Soils and Foundations Handbook", State Materials Office, Florida.

Goodman, R.E. (1989). "Introduction to Rock Mechanics", John Wiley & Sons Publishing.

Gowd, T.N., Rummel, F. (1977). "Effect of fluid injection on the fracture behavior of porous rock" in *International Journal of Rock Mechanics and Mining Sciences & Geomechanics Abstracts*, Vol 14, pp. 203-208.

Gowd, T. N., & Rummel, F. (1980). Effect of confining pressure on the fracture behavior of a porous rock. In International Journal of Rock Mechanics and Mining Sciences & Geomechanics Abstracts (Vol. 17, No. 4, pp. 225-229). Pergamon.

Hannant, D. J.; Buckley, K. J.; and Croft, J. (1973). "The Effect of Aggregate Size on the Use of the Cylinder Splitting Test as a Measure of Tensile Strength" in *Materials and Structures,* Vol 6, No. 31, pp. 15-21.

Hester, T.C. and Schmoker, J.W. (1985). "Porosity, grain-density, and inferred aragonite-content data from the Miami Limestone, Miami area and lower Florida Keys", Open-File Report 85-21, U.S. Geological Survey, Reston, VA.

Hoek, E. and Brown, E. T. (1980). "Empirical strength criterion for rock masses", in *Journal of the Geotechnical Engineering Division,* Vol 106-9, pp. 1013-1035.

Hoek, E. and Brown, E. T. (1988). "The Hoek-Brown Failure Criterion - a 1988 Update." in "*Proceedings of the 15th Canadian Rock Mechanics Symposium*", editor Curran, J. H., Toronto, Civil Engineering Department, University of Toronto, pp 31–38.

Hoek, E. and Brown, E. T. (2018). "The Hoek-Brown failure criterion and GSI – 2018 edition", in: *Journal of Rock Mechanics and Geotechnical Engineering,* in press, accepted manuscript. doi.org/10.1016/j.jrmge.2018.08.001

Hoek, E., Carranza-Torres, C., and Corkum, B. (2002), "Hoek-Brown failure criterion – 2002 Edition" in *Proceedings of the NARMS-TAC Conference,* Toronto, Vol 1, pp. 267-273

Hoek, E. and Franklin, J.A. (1968). "Simple triaxial cell for field or laboratory testing of rock", in: *Transactions of the Institution of Mining and Metallurgy 77, Section A*, pp. 22-26

Jaeger, J.C. and Cook N.G. (1969). "Fundamentals of Rock Mechanics", The Chaucer Press, Ltd.

Johnston I. (1985). "Strength of Intact Geomechanical Materials", in: *ASCE Journal of Geotechnical Engineering 111,* pp. 730-749.

Jumikis, A.R (1983). "*Rock Mechanics*", Gulf Publishing Company.

Kimmerling, R. (2002). "Shallow Foundations", Geotechnical Engineering Circular No. 6, Federal Highway Administration, Washington D.C.

Lafuente, B., Downs, R.T., Yang, H., and Stone, N. (2015). "The power of databases: the RRUFF project" in: *Highlights in Mineralogical Crystallography*, Armbruster, T. and Danisi R.M., editors, Berlin, Germany, pp 1-30

Lambe, T.W. and Whitman, R.V. (1969). "Soil Mechanics", John Wiley & Sons Publishing, New York.

Marinos, P., & Hoek, E. (2000). GSI: a geologically friendly tool for rock mass strength estimation. In ISRM international symposium. International Society for Rock Mechanics and Rock Engineering.

McVay M.C, Chung J., Nguyen, T., Thiyyakkandi, S., Lyu, W., Schwartz, J., Huang, L., Le, V. (2017), "*Evaluation of Static Resistance of Deep Foundation*". Florida Department of Transportation, Final Report for BDV31-977-05. Gainesville, FL.

McVay M.C, Townsend F., Williams R. (1992), "Design of Socketed Drilled Shafts in Limestone" in: *ASCE Journal of Geotechnical Engineering 118*, pp.1626-1637.

Missimer, T.M. and Scott T.M. (2001). "Geology and Hydrogeology of Lee County, Florida - Special Publication No. 49", Florida Geological Survey.

Mogi K. (1966). "Pressure dependence of rock strength and transition from brittle to ductile flow", in *Bulletin of Earthquake Research Institution*, Vol 44, pp. 215-232.

Mogi, K. (1967). Effect of the intermediate principal stress on rock failure. Journal of Geophysical Research, 72(20), 5117-5131.

Nazir, R., Momeni, E., Armaghani, D. J., & Amin, M. M. (2013). Correlation between unconfined compressive strength and indirect tensile strength of limestone rock samples. Electronic Journal of Geotechnical Engineering, 18(1), 1737-1746.

Paikowsky, S.G., Canniff M.C., Lesny K., Kisse A., Amatya S., Muganga R. (2010). "*LRFD Design and Construction of Shallow Foundations for Highway Bridge Structures*", NCHRP Report 651. Transportation Research Board, Washington D.C.

Perras M.A. and Diederichs, M.S. (2014). "A Review of the Tensile Strength of Rock: Concepts and Testing" in *Geotechnical and Geological Engineering Journal*, Vol 32, pp. 525-546

Rodegerdts, L., Bansen, J., Tiesler, C., Knudsen, J., Myers, E., Johnson, M., and Isebrands, H. (2010). NCHRP Report 672. Roundabouts: An Informational Guide. Washington.

Rogers M. (2016). "Real time construction monitoring for drilled shafts socketed into Florida limestone" – Ph.D. Report, University of Florida, Gainesville, FL.

Scott, T.M. (2001). "Text to Accompany the Geologic Map of Florida", Open File Report 80, Florida Geological Survey, Tallahassee, FL.

Scott, T. M., Campbell, K. M., Rupert, F. R., Arthur, J. D., Missimer, T. M., Lloyd, J. M., Yon, J. W., and Duncan, J. G. (2001). "*Geologic Map of the State of Florida*", Map Series 146, Florida Geological Survey and Florida Department of Environmental Protection, Tallahassee, FL.

Schwartz, A.E. (1964). "Failure of rock in the triaxial shear test", in: *"Proceedings of the 6th U.S Symposium on Rock Mechanics"*, American Rock Mechanics Association. Rolla, MI; pp. 109-51

de Souza Neto, Eduardo A., Djordje Peric, and David RJ Owen (2011). "*Computational methods for plasticity: theory and applications*". John Wiley & Sons.

Sowers, G. (1996). "Building on Sinkholes*: Design and Construction of Foundations in Karst Terrain",* ISBN: 0784401764, American Society of Civil Engineers.

Truzman, M (2016). "Use of Geological Strength Index to Characterize the Miami Limestone for Shallow Foundation Design", in: "*Proceeding of the 50th U.S. Rock Mechanics/Geomechanics Symposium"*, American Rock Mechanics Association.

Whitman, R. V., and K. Hoeg, (1966). "Development of Plastic Zone Beneath a Footing," Report by M.I.T. Dept. of Civil Eng. to U.S. Army Eng. Waterways Experiment Station.

Wong, T., David, C., Zhu W. (1997). "The transition from brittle faulting to cataclastic flow in porous sandstones: Mechanical deformation", in: *Journal of Geophysical Research*, Vol 102-B2, pp: 3009-3025.

APPENDIX A
ROCK CORE DESCRIPTIONS

This appendix presents the detailed rock core descriptions for the six sites that were investigated for shallow foundation considerations. At the other sites, where the rocks were obtained for deep foundation design, only rock results (i.e., q_t, q_u, and triaxial results) are collected without detail rock core descriptions.

At site 1 near a wet retention pond of the I-75/ I-595 clover-leaf interchange in Davie, cores were obtained from a depth of 3 to 18 feet below ground surface. On the geological surface map, the site lies near the boundary of Miami limestone Formation (Qm) and Fort Thompson Formation, which is a subset of the Okeechobee shelly sediments group (Tqsu). Typically, the boundary area is where the subsurface is unpredictable and has great lateral variation due to geological formation changes. The consultant identified the acquired rocks as Fort Thompson. The recovery was poor to decent (typically 40% to 80%) and RQD was very poor to decent (typically 0% to 60%). Visually, the rocks are relatively smooth, a few rock cores have minor vugs. Overall, the rocks are relatively friable and weakly cemented.

At site 2 of SW 13th Street underpass in Miami, cores were obtained from depths of 3 to 28 feet below ground surface. On the geological surface map, the site is within the Miami Formation (Qm). The recovery was very poor to good (typically 0% to 80%) with typically very poor RQD (typically less than 20%). Most of the recovered rocks were broken in pieces indicating very poor cementation.

Site 3 is near one end bent of the SR-80 Bridge to Bingham Island in West Palm Beach. On the geological surface map, the site is within the Anastasia Formation (Qa). The recovery was

excellent (close to 100%) with decent to excellent RQD (typically 70% to 80%). Visually, the rock specimens were composed of cemented shell fossils (calcarenite to coquina) with no vugs.

At site 4 near one end bent of the SR-5 over Marvin Adams Waterway in Key Largo, cores were obtained from depths of 3 to 28 feet below ground surface. On the geological surface map, the site is within the Key Largo Formation (Qk). The recovery was good to excellent (60% to 100%) and variable RQD (0% to 100%), with the RQD typically worse with deeper depths. Overall, the rocks are very porous and light weight.

At site 5 of SR 836 Extension near NW 12 Street in Miami, cores were obtained from depths of 8 to 33 feet below ground surface. On the geological surface map, the site is within the Miami Formation (Qm). The recovery was average to excellent (typically 50% to 90%) with very poor to average RQD (typically 0% to 50%). The rock texture varies greatly from very vuggy to relatively smooth limestone.

At site 6 of SR 997 (Krome Avenue) over a man-made canal in Miami, cores were obtained from depths of 3 to 28 feet below ground surface. On the geological surface map, the site is within the Miami Formation (Qm). The recovery was very poor near the ground surface (less than 40%), then approached excellent (near 100%) at deeper depths. Similarly, the RQD was very poor (0%) near the ground surface, then became average to good (50% to 80%) at deeper depths. Similar to site #5, the rock texture varies greatly from very vuggy to relatively smooth limestone.

APPENDIX B
ROCK CORE PICTURES

Figure B-1. Site 1, Bore hole RC-1

Figure B-2. Site 1, Bore hole RC-2

Figure B-3. Site 1, Bore hole RC-3

Figure B-4. Site 1, Bore hole RC-4

Figure B-5. Site 1, Bore hole RC-5

Figure B-6. Site 1, Bore hole RC-6

Figure B-7. Site 1, Bore hole RC-7

Figure B-8. Site 2, Bore hole RC-1

Figure B-9. Site 2, Bore hole RC-2

Figure B-10. Site 2, Bore hole RC-3

Figure B-11. Site 2, Bore hole RC-4

Figure B-12. Site 3, Bore hole RC-1

Figure B-13. Site 3, Bore hole RC-2

Figure B-14. Site 3, Bore hole RC-3

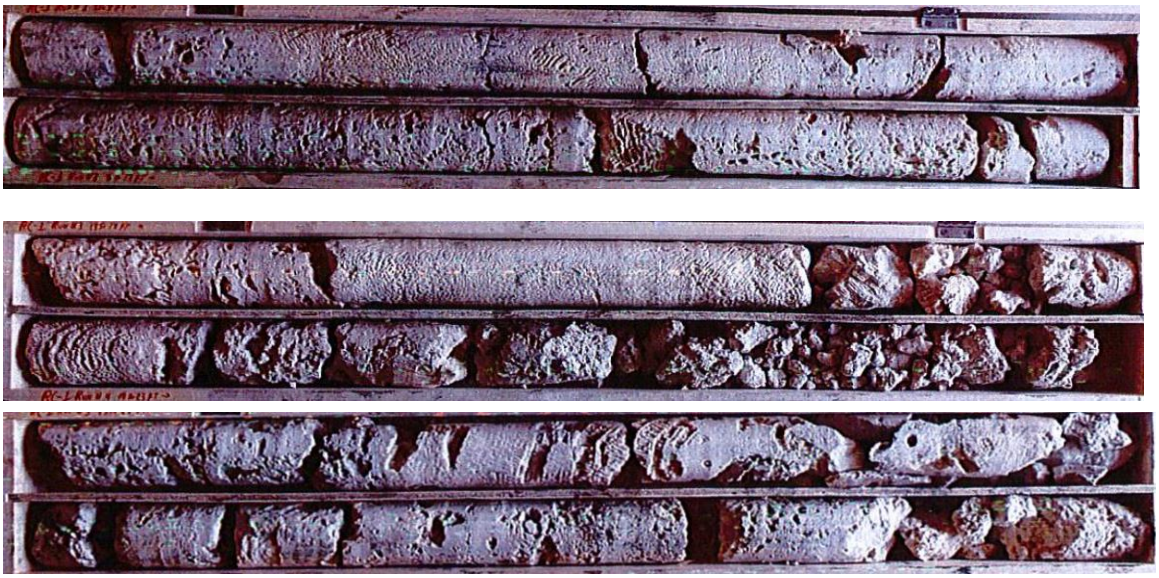

Figure B-15. Site 4, Bore hole RC-1

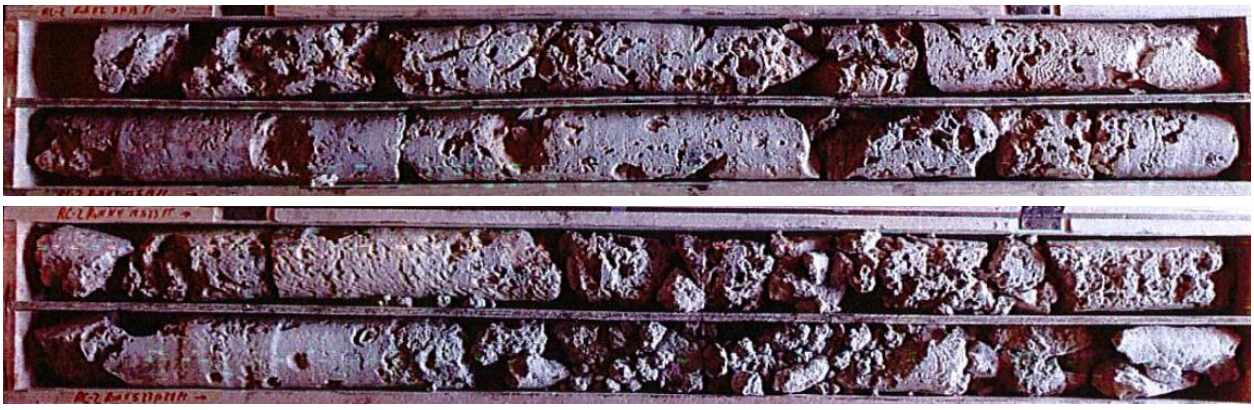

Figure B-16. Site 4, Bore hole RC-2

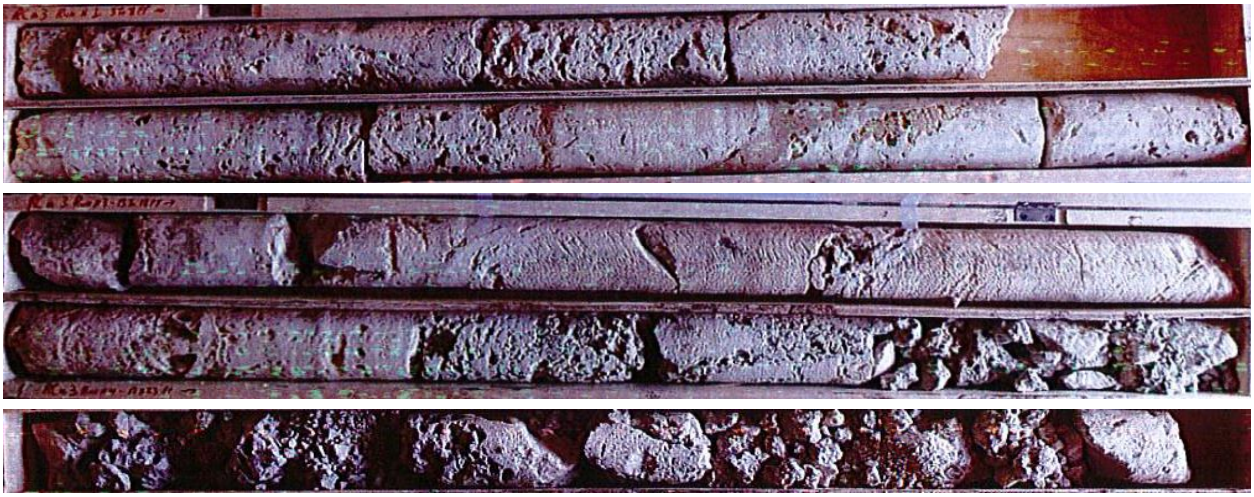

Figure B-17. Site 4, Bore hole RC-3

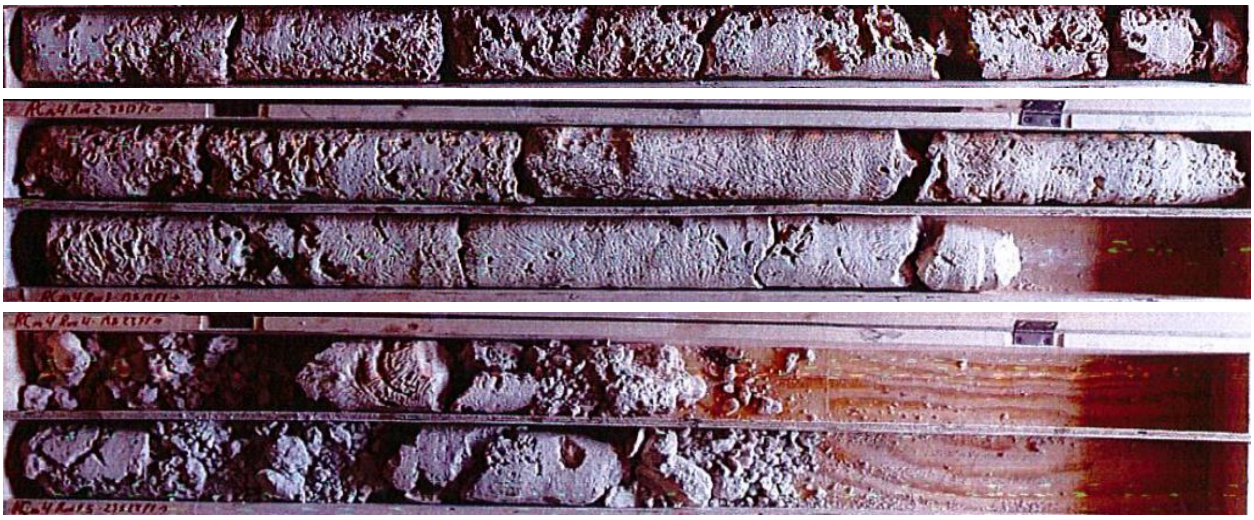

Figure B-18. Site 4, Bore hole RC-4

Figure B-19. Site 5, Bore hole RC-1

Figure B-20. Site 5, Bore hole RC-2

Figure B-21. Site 5, Bore hole RC-3

Figure B-22. Site 5, Bore hole RC-4

Figure B-23. Site 6, Bore hole RC-1

Figure B-24. Site 6, Bore hole RC-2

Figure B-25. Site 6, Bore hole RC-3

Figure B-26. Site 6, Bore hole RC-4

APPENDIX C
ROCK TRIAXIAL TEST PROCEDURE

C.1 Sigma-1 Features

The triaxial test can be terminated upon reaching any of the following action:

1. the button “END TEST” is manually clicked,

2. or the platen reaches its limit (per internal optical encoder),

3. or the load-cell reaches its limit (40,000 lbs, which is the limit of the frame even though the load-cell is rated for 50,000 lbs),

4. or the DCDT reaches its end of travel (maximum travel is 3 inches),

5. or the vertical strain ε reaches its shear strain limit, typically set at 3.5%.

6. or the stress drops by a user input threshold, typically 30% stress.

There are 2 different data recording modes:

- Data acquisition mode: data is recorded into a with file name “*.dat” whenever “new task” submenu is clicked. The data is recorded per time schedule, for example 1 read per every 10 seconds, regardless of whether the actual triaxial test is being run or not.
- Triaxial test mode: data is recorded into a with file name “*.trx” only when the “START TEST" button is clicked. The data is recorded per strain schedule, for example 1 read per every axial strain of 0.01%.

The hand-pump, shown in Figure C-1, is fitted with 2 valves. Valve 1 on the side of the pump is a one-way valve: when closed, Valve 1 only closes oil from coming back into the pump, but still allows oil to travel one-way from the pump out. Therefore, the seal on pump 1 is not 100% seal. Therefore, when there is no need to hand-pump, then valve 2 would be closed to prevent oil leaks back to the pump.

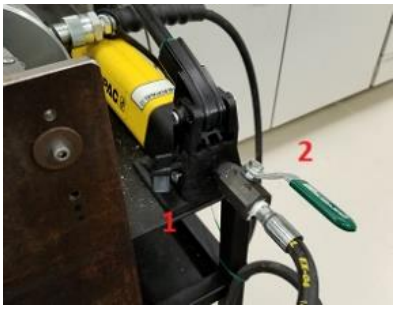

Figure C-1. Hand pump valves

C.2 Sample Preparation

1. Determine specimen dimensions and weight prior to test.

2. Insert rock sample into Hoek-cell with the cell laying horizontal on the working cart.

3. When inserting sample, or removing sample from Hoek-cell, make sure to have the oil not trapped by opening both Valves 1 and 2 of hand-pump.

4. Place bottom steel platen into Hoek-cell

5. Stand the Hoek-cell upright on its bottom platen

6. Place top steel platen into the cell

7. Using "Load Control" tab (Figure C-2.a), make the Load-Cell to contact the top platen for a seating load of about 10 to 20 lbs.
Be sure to re-center the Hoek cell before contact.

8. While the loading frame is in the process of moving to automatically reach that 20 lbs of seating load, type in the specimen data, using Menu File – Specimen Data (Figure C-2.b). Specify a maximum strain rate of 3.5% for the Deviatoric (shear) loading phase (the software identifies the moment the "START TEST" is clicked as the start of the Deviatoric loading).

9. Close Valve 1 on hand-pump (Valve 2 still open).

a)
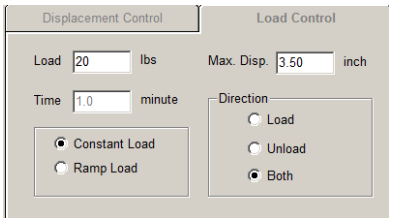

b)
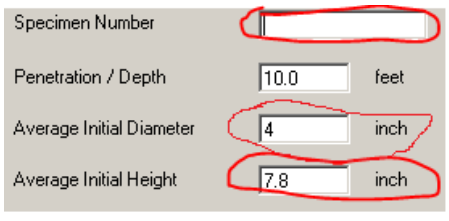

Figure C-2. Sample preparation screen: (a) Load-control tab; (b) Sample dimensions

C.3 Isotropic Loading to σ_{3max}

1. Prepare the DigiFlow pump (The pump total volume is 73 ml oil):

a) Make sure the DigiFlow pump piston is at the bottom position (i.e., the DigiFlow is full of oil), otherwise it would not have enough oil to supply to Hoek cell during isotropic loading.

b) If DigiFlow pump piston is not at the bottom position, move the pump piston down by using "Volume Control" (Figure C-3) and move the piston down to the target of Volume = 1.0 mL. At the same time that the piston is moving down, make sure to use hand-pump to supply oil to the upper chamber of the DigiFlow pump, so that the cell or pump pressure to be between 1 to 5 psi while hand pumping

2. Close valve 2 on hand-pump. (Valve 1 was already closed earlier)

3. On DigiFlow, use "Pressure Control" tab, set DigiFlow pump = σ_{3max}

4. On Main window, use "Load Control" tab, set Load = Specimen Area (A) * $\boldsymbol{\sigma_{3max}}$ (example 2.38-in rock specimen, A = 4.45in$^{2"}$)

5. Set Ramp Pressure and Ramp Load, both to same times as in Figure C-4.

6. Hit Start Pump for both the DigiFlow and Start for Load to increase. That way, the σ_3 (from Digiflow) and σ_1 (from loading frame) would gradually increase to the targets set above during the ramping time.

7. Once the σ_{3max} target has reached, the pressure would stay at σ_{3max}

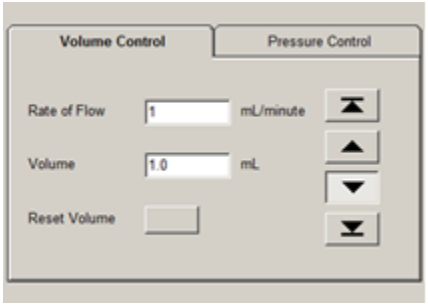

Figure C-3. Volume control tab

σ_{3max}	Target Ramp Time
50-100	2
100-200	3
200-500	5
500-1000	10
1000-1500	12-15

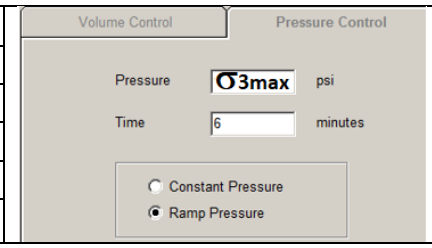

Figure C-4. Pressure ramp schedule

C.4 Deviatoric (Shear) Loading

1. Start the shearing process by hitting the "START TEST", the load frame would increase axial load beyond the load specifying in step 9 to begin the deviatoric loading.

2. Sometimes, the technician would have to interfere to end the test prematurely by hitting "Pause" button if:

c) There is oil leak (for example, due to membrane is damaged)

d) Or if the rock is too porous, and when it is crushed unevenly (only on 1 side of the specimen), the top platen may be excessively inclined.

3. The test would automatically "Paused" if a 30% drop in stress is detected, or if maximum strain (of 3.5%) has reached.

C.5 End Test

1. Hit End Test on the Load frame, also, Hit Stop on DigiFlow Pump so that it won't maintain the σ_{3max}

2. Unload to 0 lbs using Full Speed on the load frame

3. When load is about 0 lbs, there would be confining pressure left (possibly around 100 to 200 psi). Use "Pressure control" on the Digiflow pump to bring the pressure down to 1 psi.

4. Gradually opening Valves 2 and 1 on hand-pump to release pressure.

5. Remove rock specimen

6. Weight the specimen after test

7. Dry the specimen in oven and determine dry weight.

APPENDIX D
PICTURES OF SPECIMENS AFTER TRIAXIAL TESTS

Many rock specimens had a number of inclusions within each piece, especially for some of the longer specimens which were up to 8 inches long. The shear failure surface then would typically go through the softest portion of the specimen – see Figure D-1 for some examples. As the dry unit weight of the softest portion of the specimen is typically lower than that of the denser portion of the specimen, shear strength correlations of the highly variable Florida rocks and IGM would naturally exhibit more scatter and poorer coefficient of determination R^2 than correlations of uniform rocks.

Most specimens would become stuck within the Hoek-cell membrane and require an extruder to push the specimens out after shearing. In that case, there would be many mechanical breaks in the specimens. A small number of specimens could be extruded by hand, and examples of the failure surfaces of those specimens are presented in Figure D-1 and Figure D-2.

Figure D-1. Rock at failure surface apparently weaker than overall rock specimen

Figure D-1. Continued

a) 

Figure D-2. Specimens tested at 130-psi chamber pressure: (a) γ_{dt} > 130 pcf

b) 

c) 

Figure D-2. Continued: (b) γ_{dt} = 120 - 130 pcf, (c) γ_{dt} = 110 - 120 pcf

Figure D-3. Specimens deformed at 3,000 psi chamber pressure

APPENDIX E
REPRESENTATIVE INDIVIDUAL TEST RESULTS

The following sign convention is used: compression is positive. Thus, the vertical strain, ε, is always positive, while the lateral strain ε_L is negative as the specimen diameter increases during triaxial shearing ($-\varepsilon_L$ is positive). The slope of the volumetric ε_v curve is positive when rock contracts and negative when rock dilates. Triaxial tests, whenever performed with a volume control device, are presented with ε_v results. In the beginning of the study, when the volume control device was not yet ready, no volumetric strain (ε_v) was recorded. However, as demonstrated in the study, an adequate number of specimens have later been tested for the generalization of the volumetric behavior of Florida carbonate rocks.

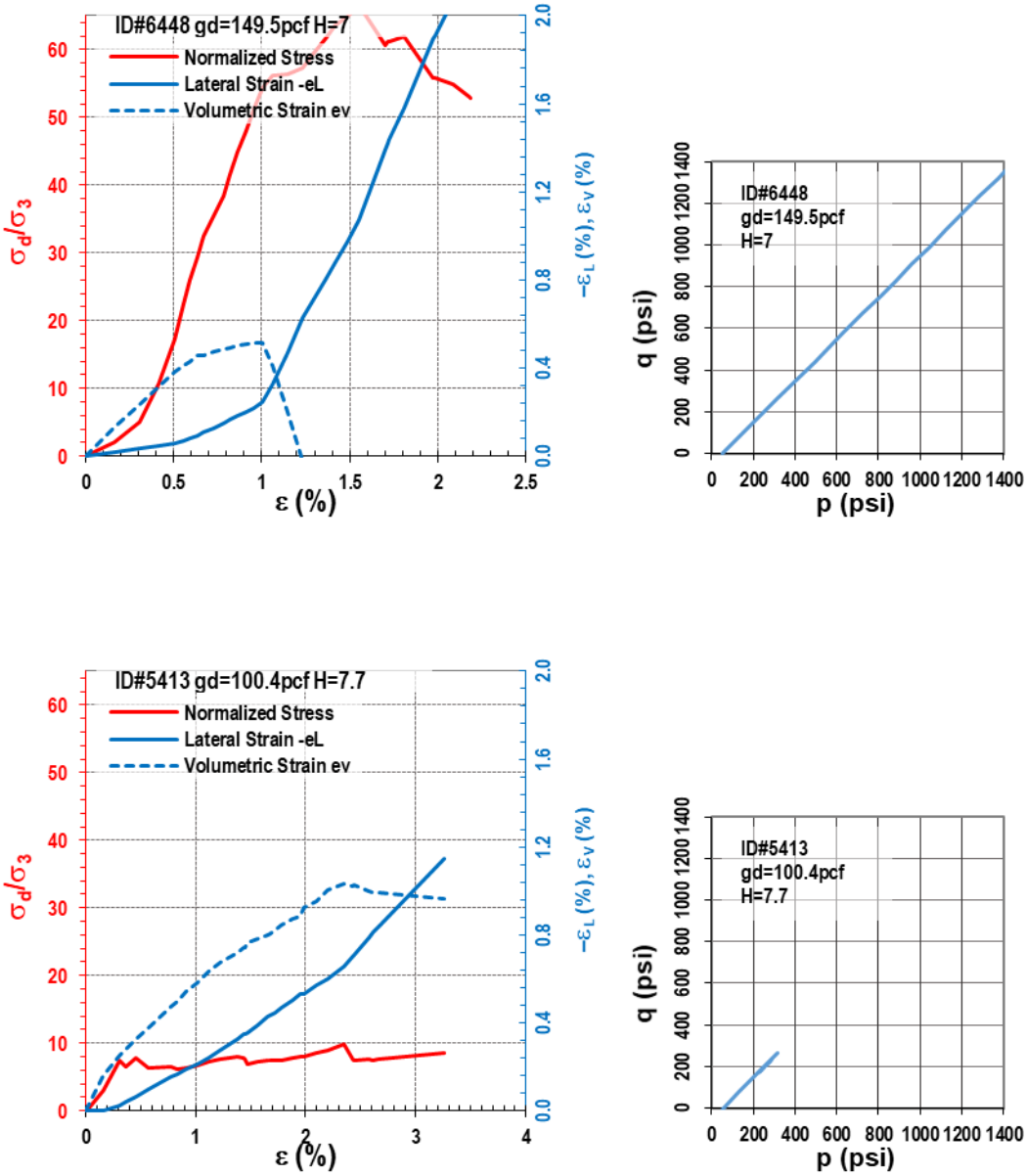

Figure E-1. Test results at σ_3 = 50 psi

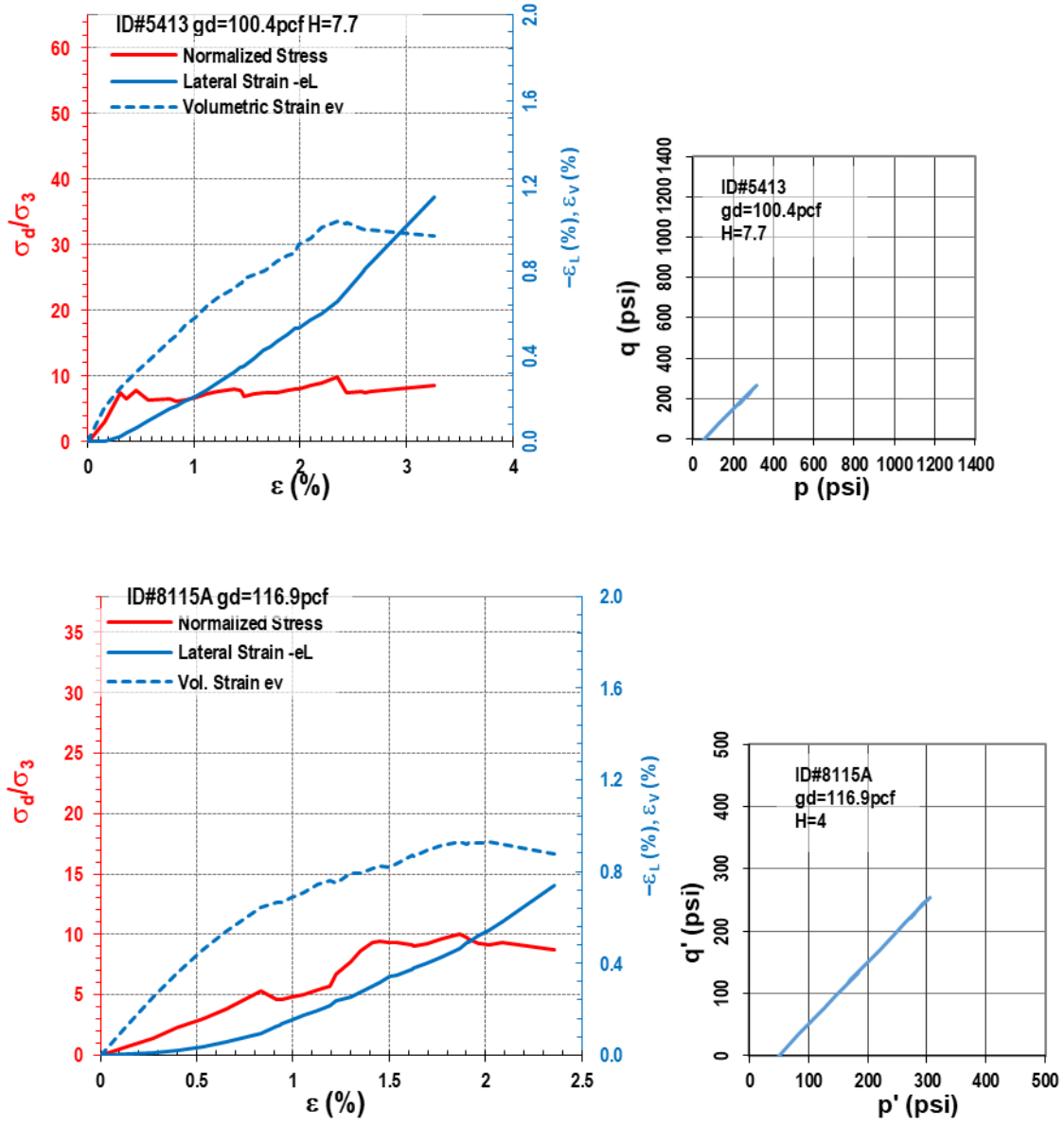

Figure E-1. Continued

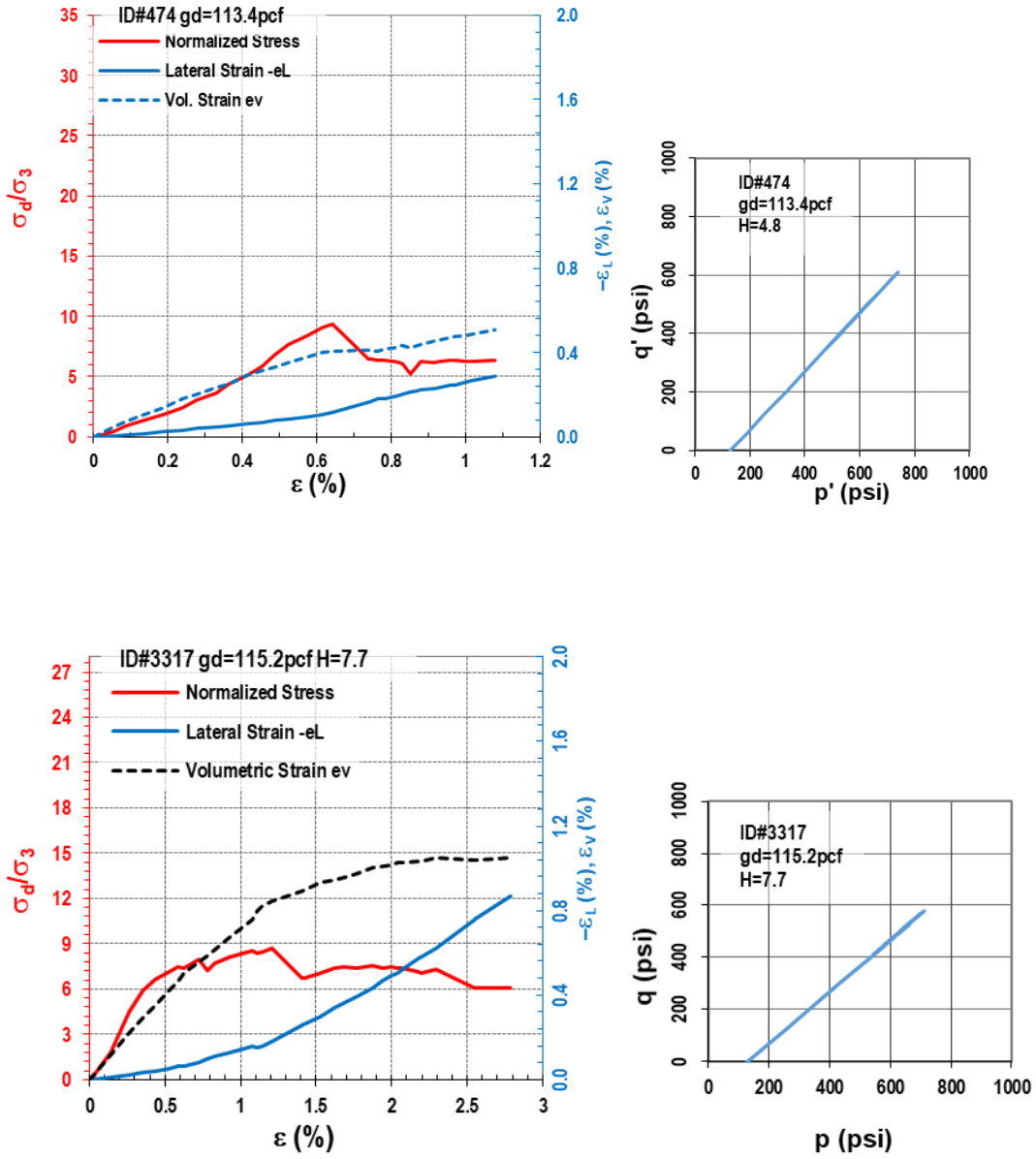

Figure E-2. Test results at σ_3 = 130 psi

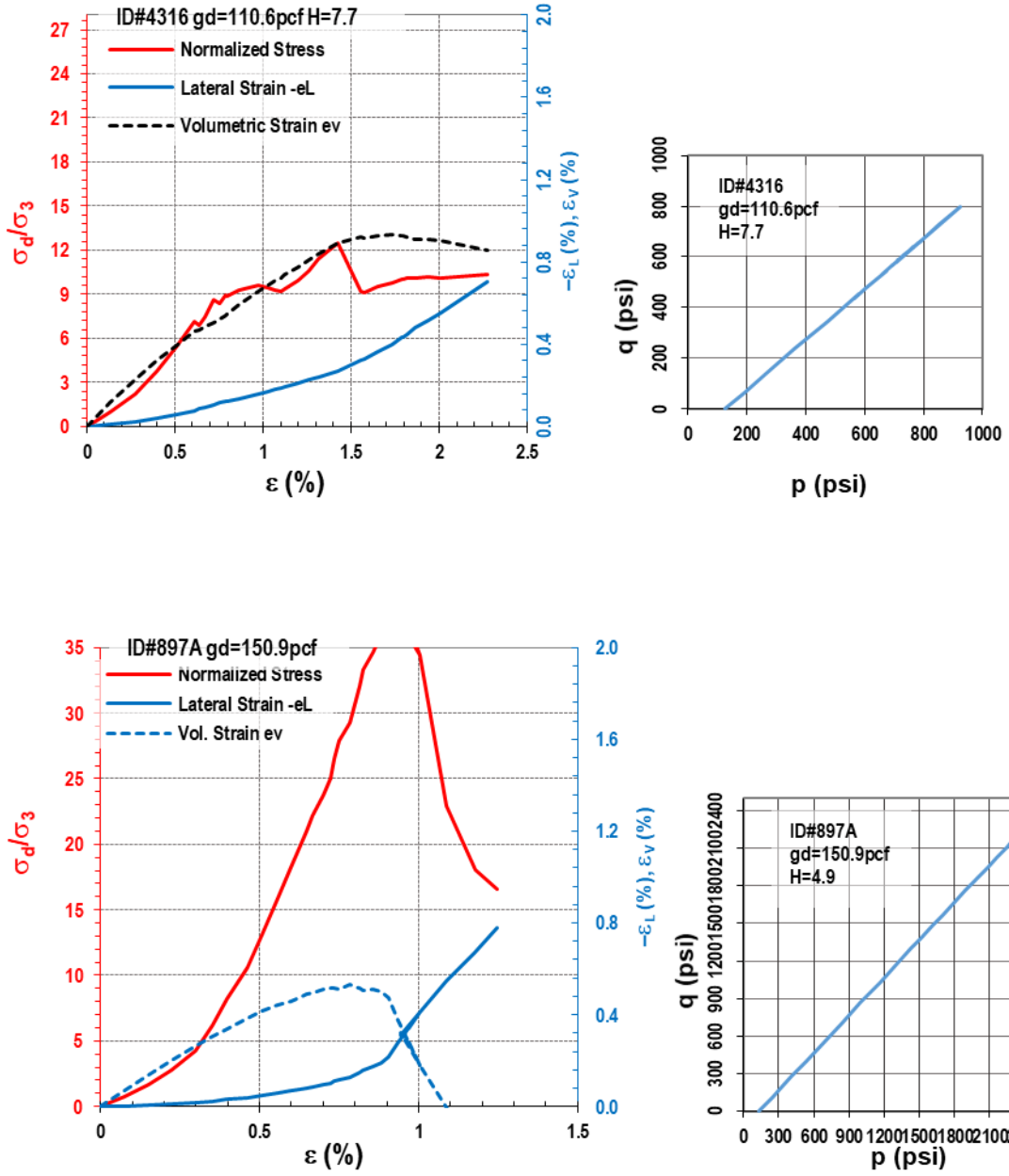

Figure E-2. Continued

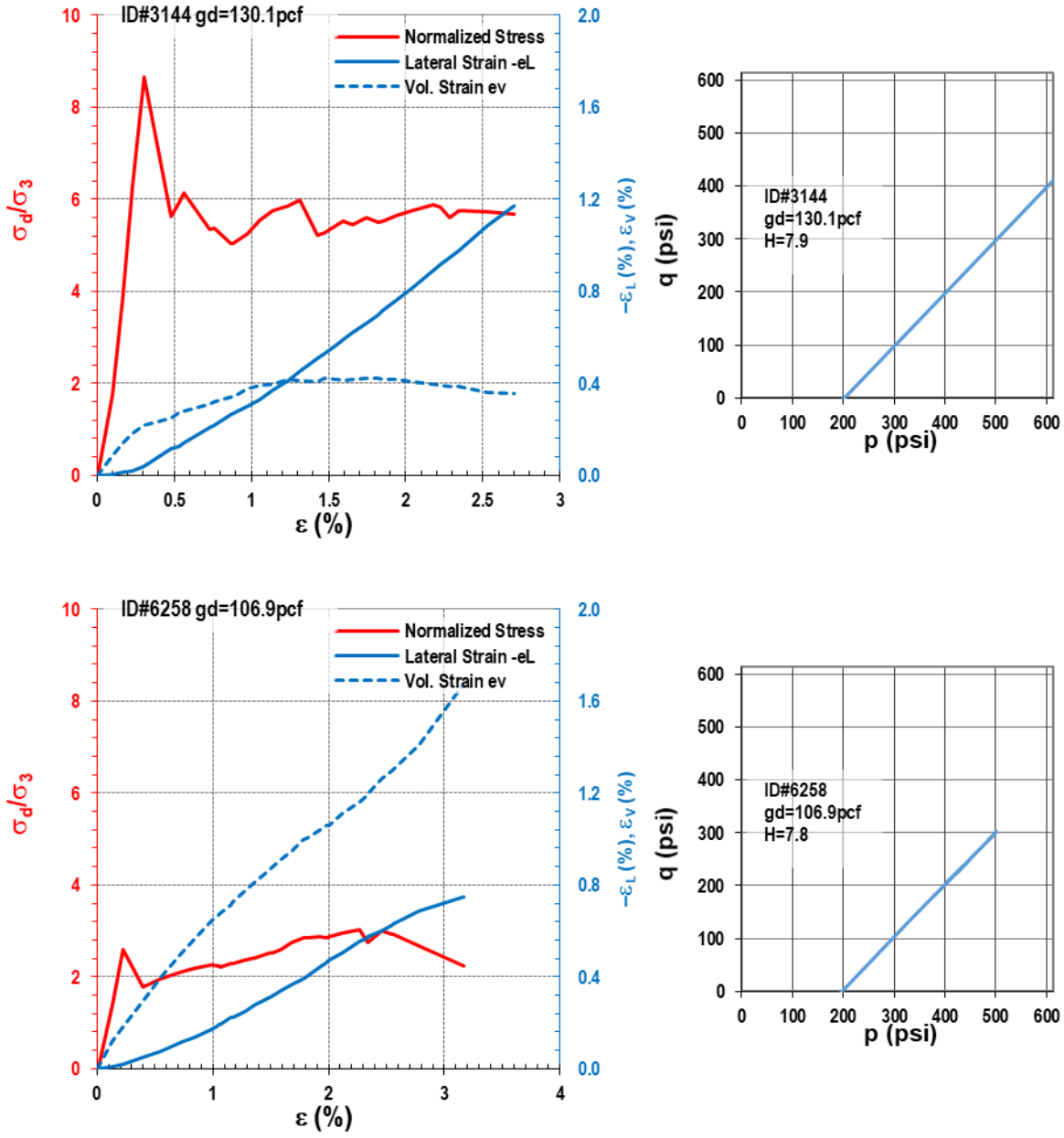

Figure E-3. Test results at σ_3 = 200 psi

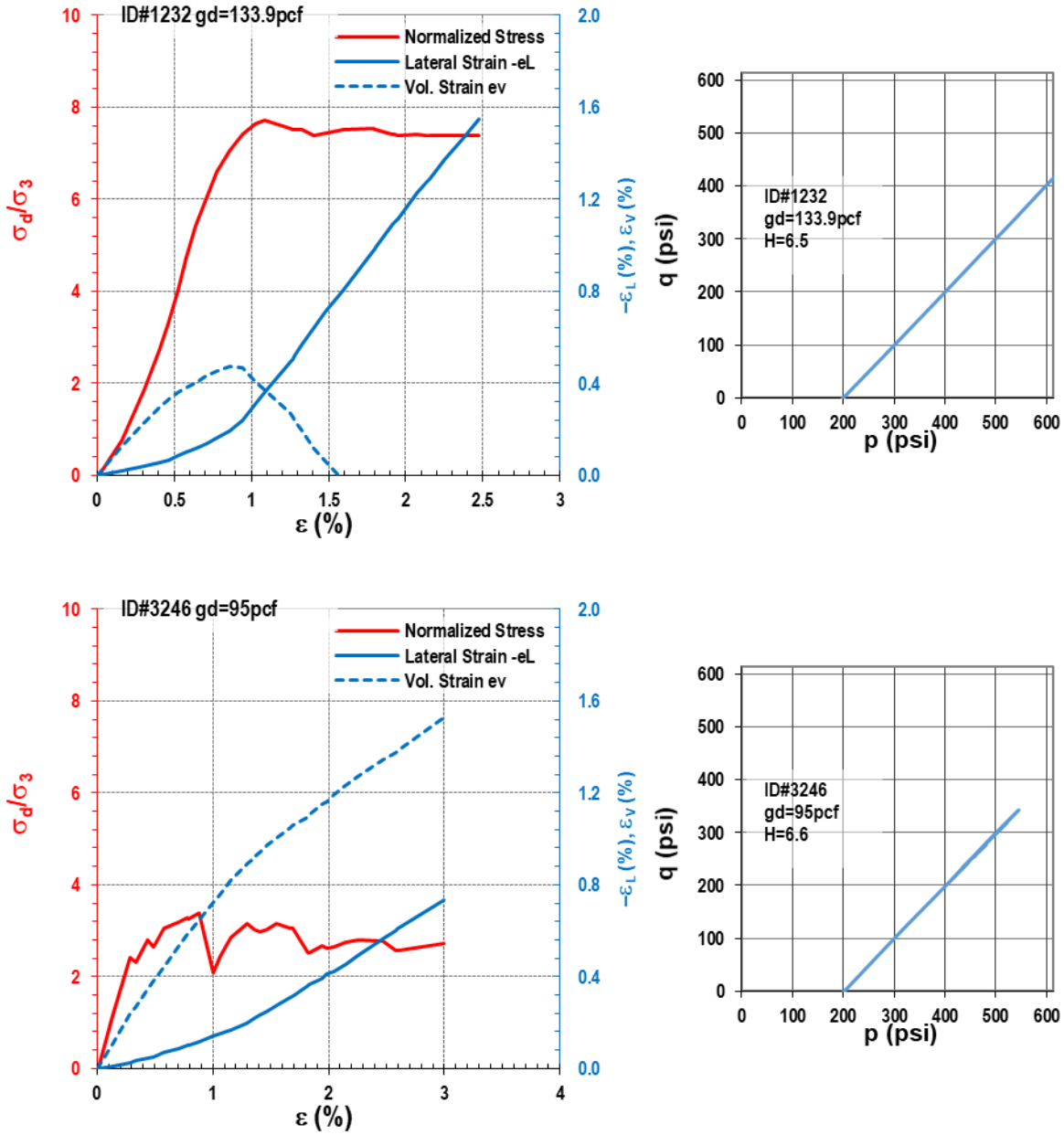

Figure E-3. Continued

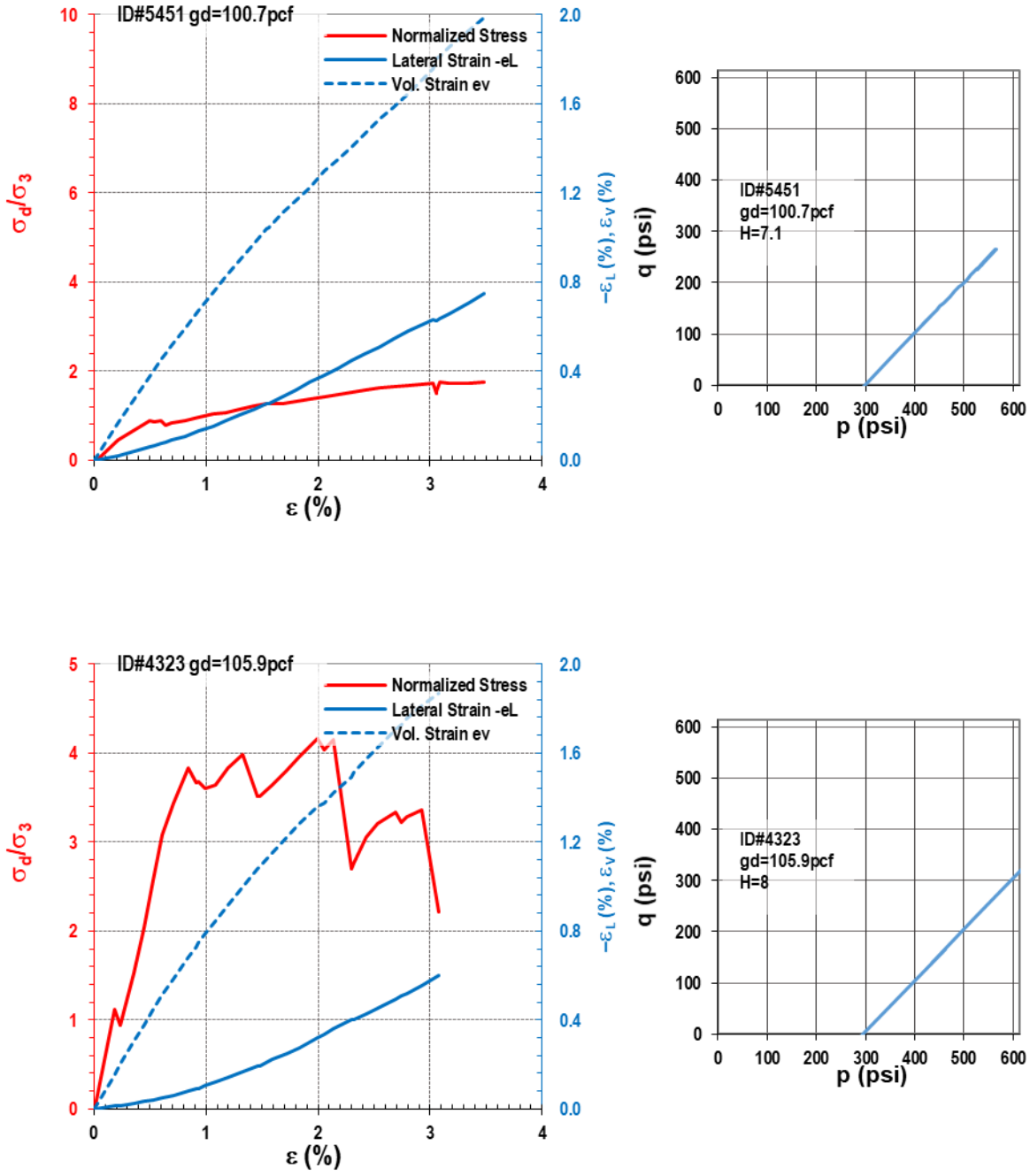

Figure E-4. Test results at σ_3 = 300 psi

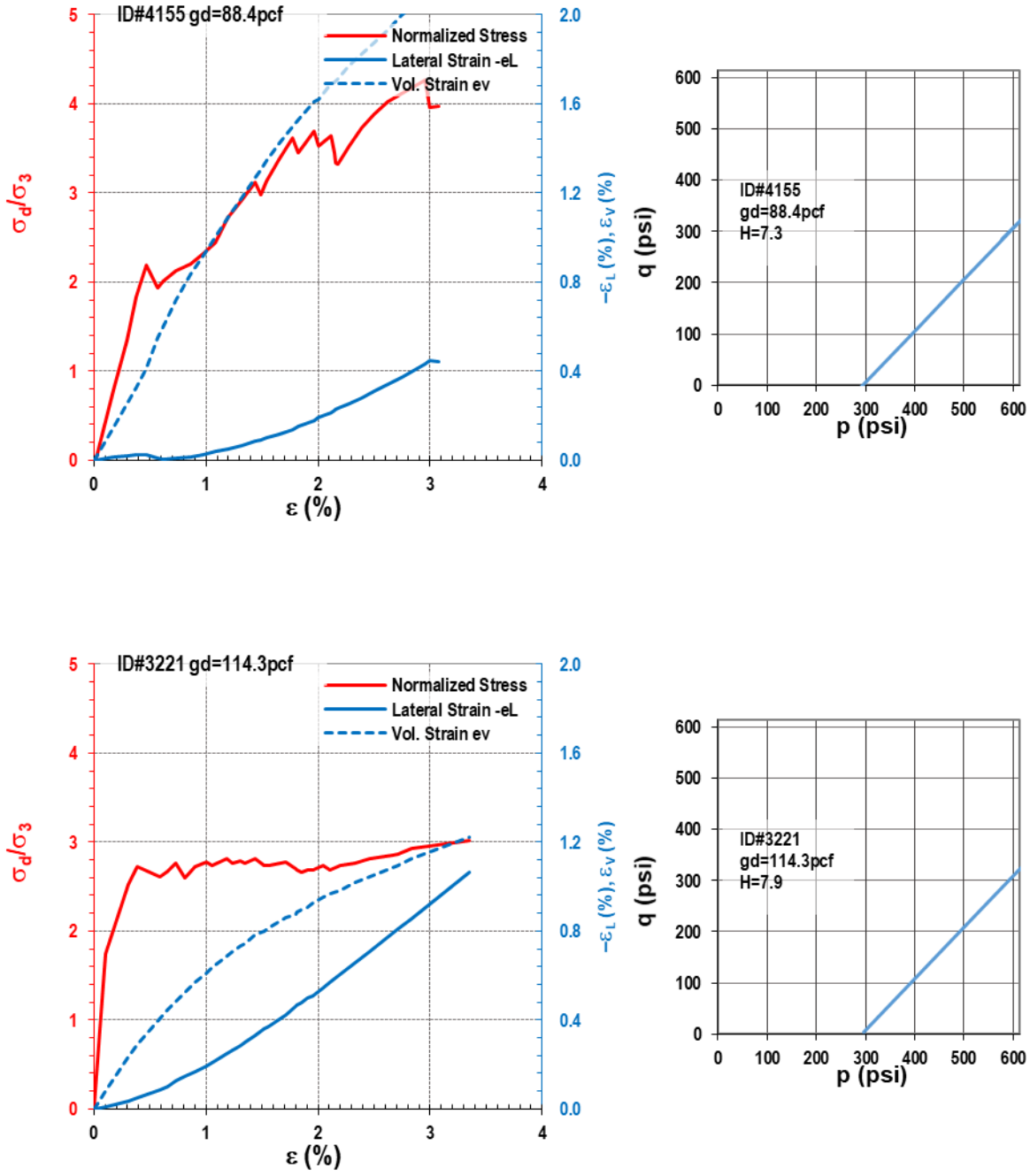

Figure E-4. Continued

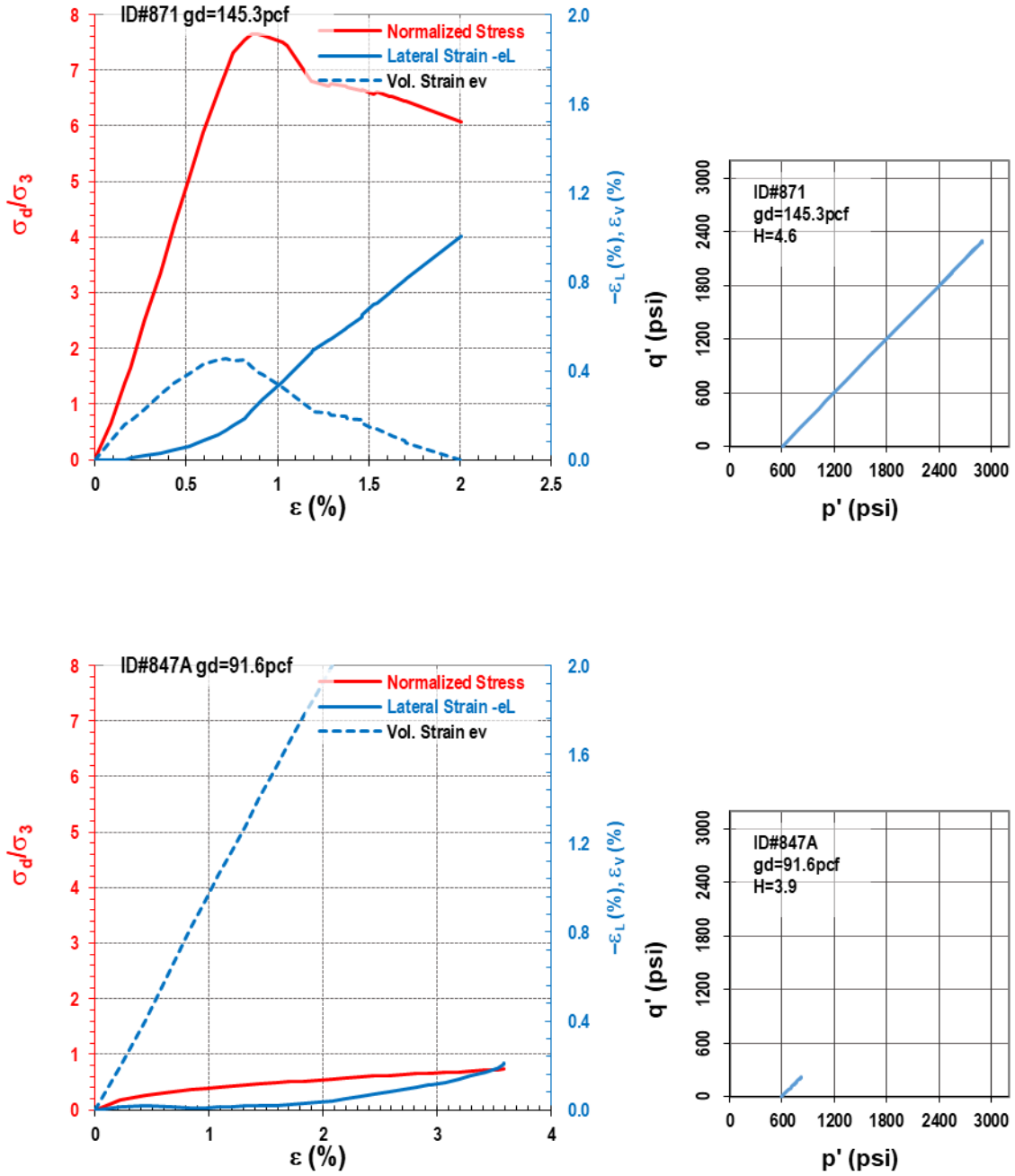

Figure E-5. Test results at σ_3 = 600 psi

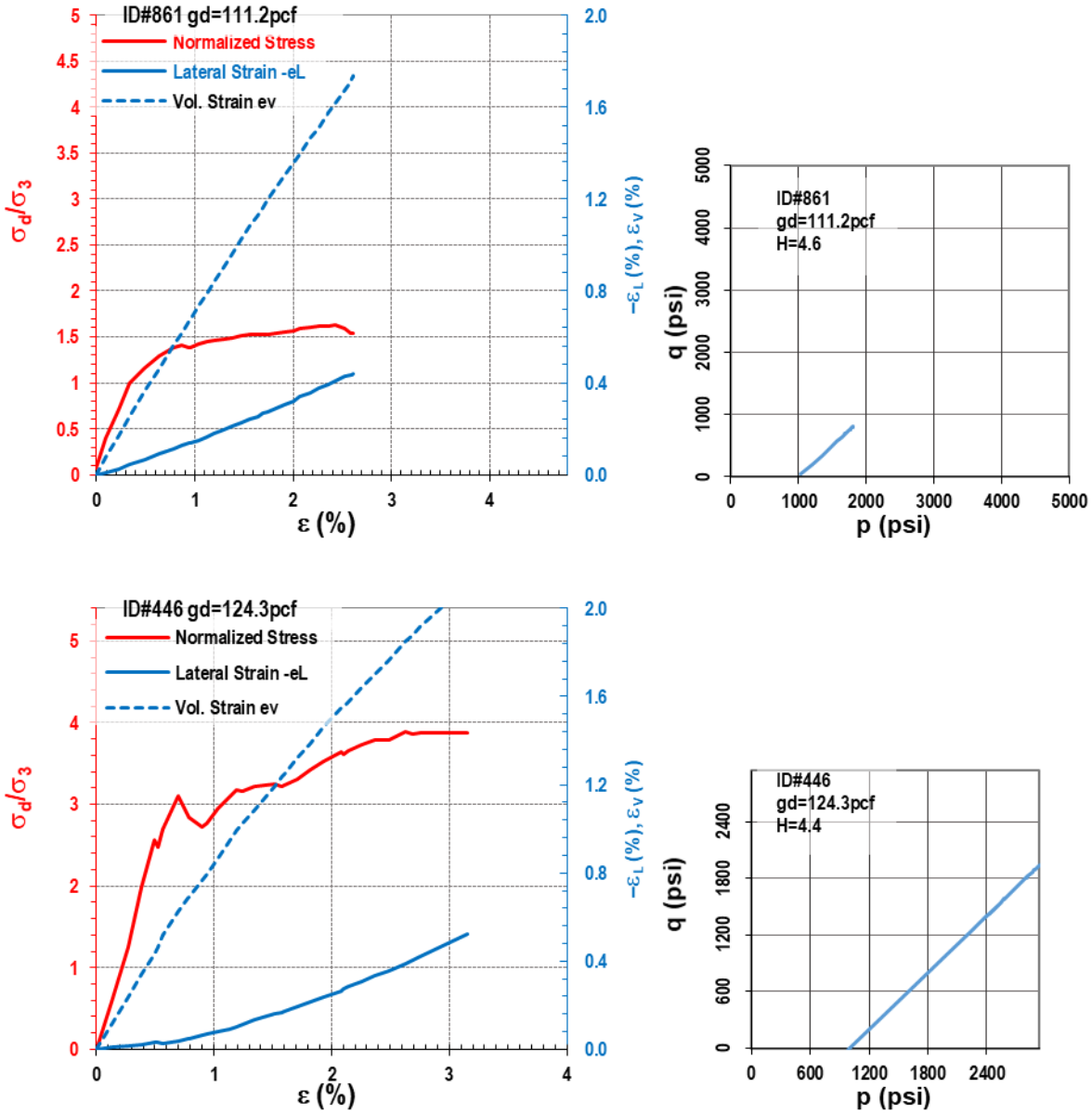

Figure E-6. Test results at σ_3 = 1,000 psi

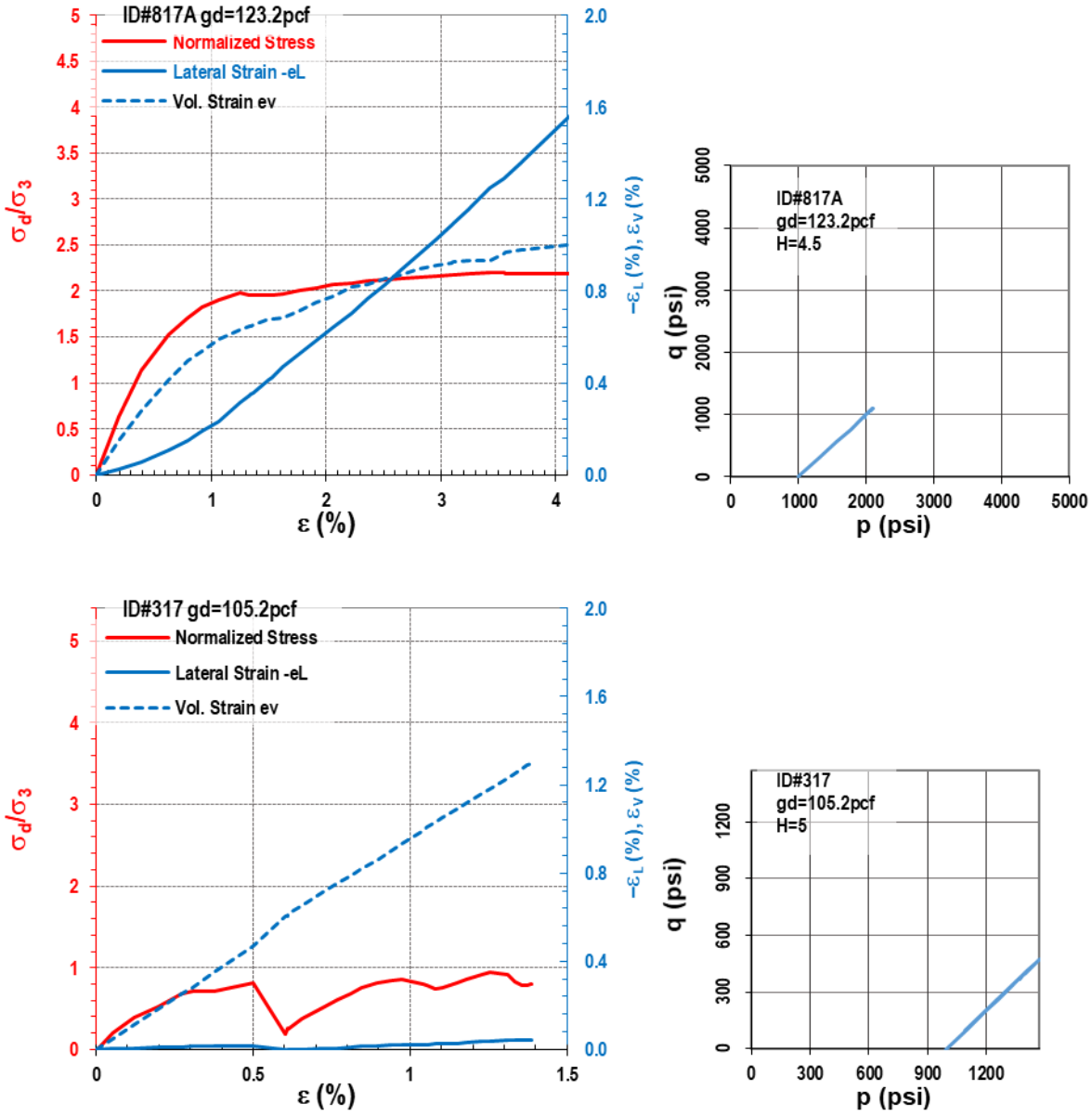

Figure E-6. Continued

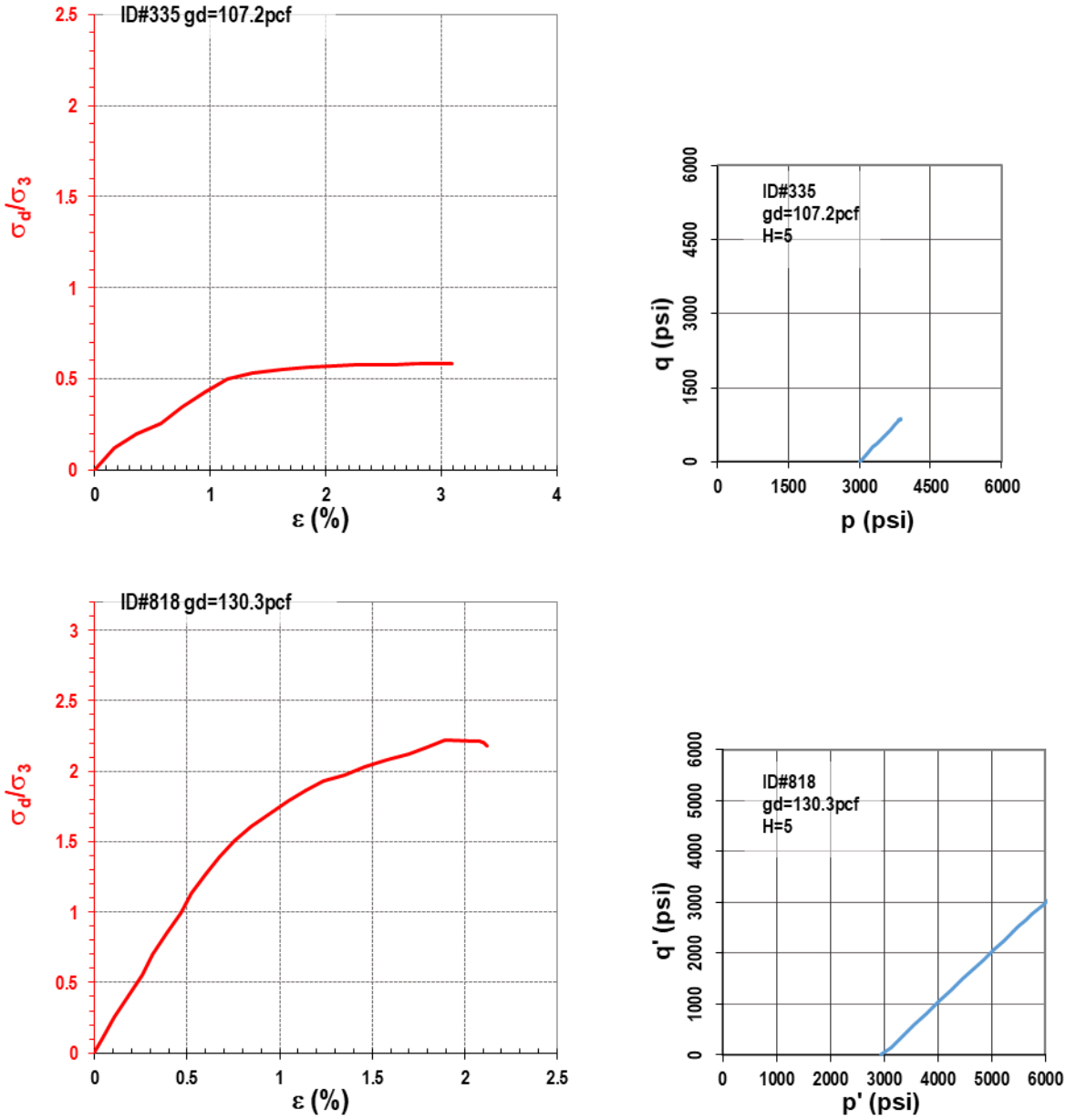

Figure E-7. Test results at σ_3 = 3,000 psi

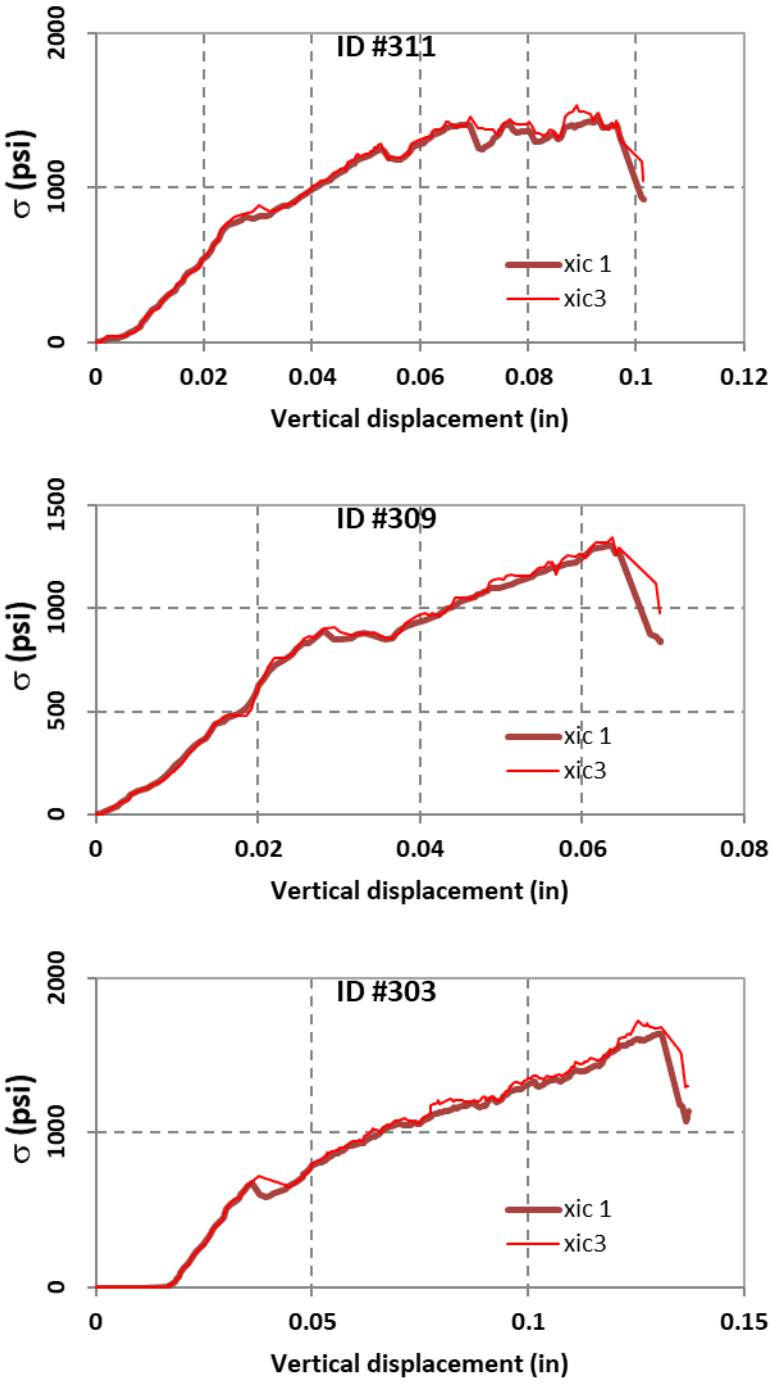

Figure E-8. Specimens crushed during isotropic loading

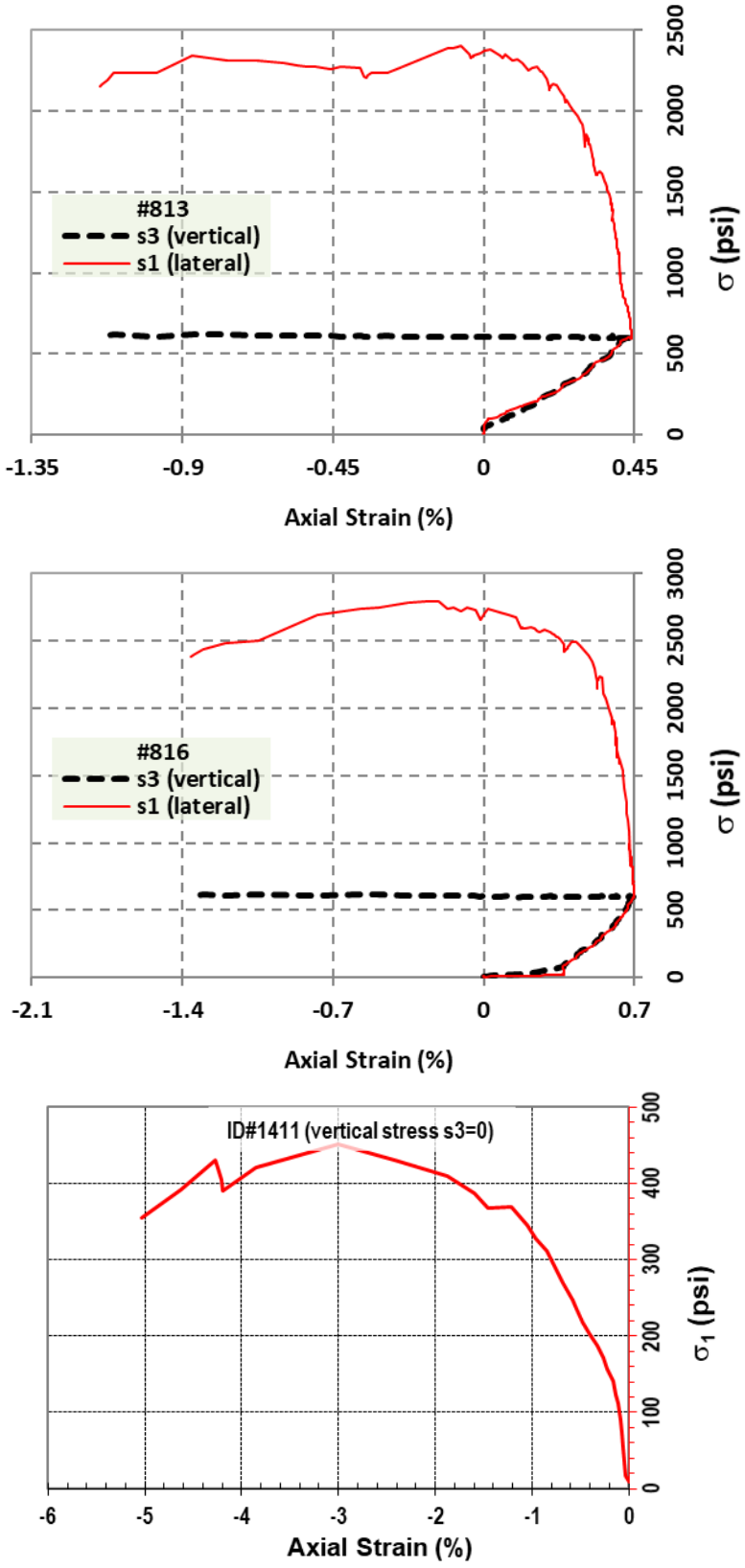

Figure E-9. Extension triaxial tests

APPENDIX F
RECOMMENDED PROCEDURE TO ESTABLISH STRENGTH ENVELOPE OF A DESIGN PROJECT

From the study's investigation, it was shown that the strength envelope from 0.7 q_t past q_u and up to a triaxial results with a confining pressure of σ_3 = 0.345 MPa (50 psi), the strength envelope is approximately linear with a slope angle of α in Lambe's p-q diagram. From σ_3 = 0.345 MPa (50 psi) to 4.1 MPa (600 psi), the sloping strength envelope portion can be simplified by a straight line with a slope angle of β in a p-q diagram. Confining pressures in the range of 0 to 4.1MPa (600 psi) cover the possible pressures underneath a shallow foundation.

Therefore, the proposed procedure for a production project is:

Obtain a minimum of 10 q_u and 10 q_t samples, calculate the mean values for q_u and q_t.

Estimate the equivalent direct tension strength, q_{dt}, based on $0.7 * q_t$.

Obtain dry unit weight, γ_{dti}, of each rock specimen. γ_{dti} is the ratio between dry weight and cylindrical volume of the specimen:

$$\gamma_{dti} = \frac{Oven\ Dry\ Weight}{0.25\pi D^2 L_i} \quad \text{(F-1)}$$

where D is the rock core diameter

L_i is the specimen length

Obtain weighted average γ_{dts} from strength-test specimens (i.e., q_u, q_t, as well as triaxial test specimens)

$$\gamma_{dts} = \Sigma(\gamma_{dti} L_i) / \Sigma L_i \quad \text{(F-2)}$$

i represents the strength-test-specimen #i

Obtain the dry unit measurements of all non-tested material in the core runs. Obtain the dry unit weighted average for the whole rock layer γ_{dtw}.

$$\gamma_{dtw} = \Sigma(\gamma_{dti} L_i) / \Sigma L_i \quad \text{(F-3)}$$

i represents either the strength-test-specimen or the non-strength-test-specimen

For the rubbles in the recovered rocks, where they do not retain the cylindrical shape, there are two options:

i) Either calculate the dry unit weight of the rubbles, using rock core diameter (i.e., inner diameter of the core barrel), and the length of the rubbles placed in the core box.

ii) Or ignore this rubble portion and count it as uncoreable material. Thus, the REC needs to be revised to a lower value, not counting the rubble.

Use Equations 32 & 33, use the average unit weight γ_{dtw} to reduce the q_u and q_{dt} values:

$$q_{tw} \approx q_{dt} * e^{0.03(\gamma_{dtw}-\gamma_{dts})} \quad \text{(F-4)}$$

$$q_{uw} \approx q_u * e^{0.04(\gamma_{dtw}-\gamma_{dts})} \quad \text{(F-5)}$$

Calculate c (or a) – intercept, Eq. F-5

$$c = 0.5\sqrt{q_{uw}q_{tw}} \quad \text{(F-6)}$$

$$c = a / \cos\varphi \text{ or } a = c\cos\varphi \quad \text{(F-7)}$$

Calculate φ (or α) – initial slope, Eq. F-7

$$\sin\varphi = \frac{q_{uw}-q_{tw}}{q_{uw}+q_{tw}} \quad \text{(in p-q diagram: } \tan\alpha = \frac{q_{uw}-q_{tw}}{q_{uw}+q_{tw}}\text{)} \quad \text{(F-8)}$$

Calculate p_p – onset of structure rearrangement, Eq. (F-8).

$$p_p \text{ (psi)} = \frac{50+a}{1-\tan\alpha} = \frac{50+c\cos\varphi}{1-\sin\varphi} \quad \text{(F-9)}$$

Thus, after step 9, the first portion of the bilinear curve in Figure F-1would be:

$$q = a + p\tan\alpha \quad \text{(F-10)}$$

Obtain an additional 4 to 8 samples for triaxial testing to estimate ω. The samples should cover the range of dry unit weights in the q_u and q_t samples above. All of them would be tested using the same σ_3 at 600 psi. The results will be scattered and should be displayed in a similar format as the example in Figure F-2.

Use the γ_{dtw} from step 3 to get σ_d/σ_3. For example, γ_{dtw} =103 and σ_d/σ_3 = 0.8 in Figure F-3.

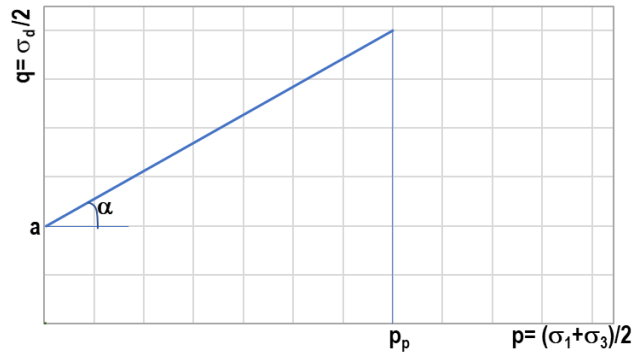

Figure F-1. First portion of bilinear curve

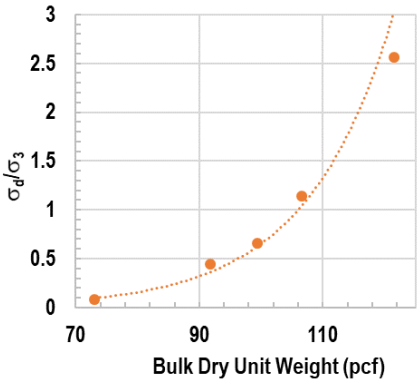

Figure F-2. Example of test triaxial results at 600-psi

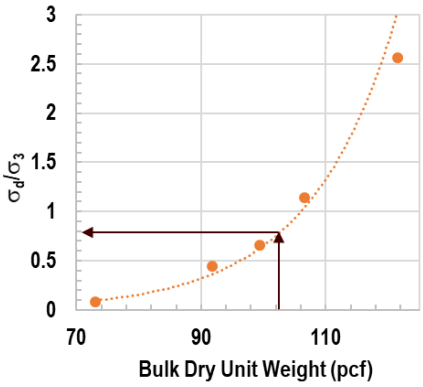

Figure F-3. Estimate representative triaxial results for the rock layer

Thus, σ_d = 600 * 0.8 = 480 psi, and $q_{600} = \sigma_d / 2 = 240$, $p_{600} = q_{600} + \sigma_3 = 840$ psi

Plot this point on Figure F-1 to obtain, the β slope in p-q diagram:

$$\tan\beta = \frac{q_{600} - q_p}{p_{600} - p_p}$$

then $\sin\omega = \tan\beta$

Adjust all parameters based on %REC. Since each core run should be the same length (5 ft), the weighted average of REC would be the same as average. Therefore, it is recommended that REC = average (REC_i) from all core runs.

$$q_m = q * REC \quad \text{(F-11)}$$

$$a_m = REC*a \quad \text{(F-12)}$$

$$tan\alpha_m = REC*\tan\alpha \quad \text{(F-13)}$$

$$tan\beta_m = REC*\tan\beta \quad \text{(F-14)}$$

$$p_{pm} = p_p \quad \text{(F-15)}$$

Table F-1. Example data

All γ_{dt}	γ_{dt} for strength specimens	q_u (psi)	q_t (psi)	σ_d/σ_3
105.1	105.1	133.7		
136.3	136.3	641.0		
90.1	90.1	228.3		
61.6	61.6	47.8		
91.2	91.2	97.3		
123.8	123.8	366.6		
95.9	95.9	180.2		
128.4	128.4	562.2		
141.6	141.6	496.7		
117.2	117.2	658.7		
108.2	108.2		61.2	
88.3	88.3		24.3	
104.3	104.3		44.8	
98.7	98.7		56.8	
129.6	129.6		107.0	
141.8	141.8		265.5	
137.1	137.1		148.1	
138.2	138.2		93.0	
110.5	110.5		72.1	
107.3	107.3		73.9	
91.8	91.8			0.45
99.4	99.4			0.66
106.6	106.6			1.14
121.6	121.6			2.56
73.1	73.1			0.08
79.5				
87.7				
79.0				
81.5				
94.2				

Table F- 1. Continued

All γ_{dt}	γ_{dt} for strength specimens	q_u (psi)	q_t (psi)	σ_d/σ_3
69.7				
104.6				
106.0				
83.0				
91.6				
109.7				
97.0				
90.2				
111.9				
108.9				
102.8				
82.6				

Mean values from a minimum of 10 q_u and 10 q_t lab tests: q_u = 341.3 psi, q_t = 94.7 psi

Equivalent q_{dt} = 0.7 * 94.7 = 66.3 psi

Mean value from 25 strength tests (10 q_u , 10 q_t and 5 triaxial tests): γ_{dts} =109.9 pcf

Mean value from all 42 specimens (25 strength tests, and 17 no strength tests): γ_{dtw} =103 pcf

Dry-unit-weight-adjusted strength values for q_{uw} & q_{tw}:

$q_{uw} = 341.3 * e^{0.04(103-109.9)} = 258.9$

$q_{tw} = 66.3 * e^{0.03(103-109.9)} = 53.9$

$c = 0.5\sqrt{q_{uw}q_{tw}} = 59.1$ psi

$\sin\varphi = \tan\alpha = \frac{q_{uw}-q_{tw}}{q_{uw}+q_{tw}} = 0.6555$ => $\varphi = 41$

$a = c*\cos\varphi = 44.6$

$p_p = \frac{50+a}{1-\sin\varphi} = 274.6$ and $q_p = p_p - 50 = 224.6$ (or $q_p = 44.6 + 0.6555*274.6 = 224.6$)
thus, the first portion of the bilinear envelope would be (in Figure F-4): q=44.6 + 0.6555 p

From triaxial tests, all performed at the same σ_3 = 600-psi in Figure F-5. γ_{dtw} =103 pcf => σ_d / σ_3 = 0.8. $\sigma_d = 600 * 0.8 = 480$ psi, and $q_{600} = \sigma_d / 2 = 240$, $p_{600} = q_{600} + \sigma_3 = 840$.

Add this coordinate (840,240) to the envelope chart, and the complete envelope for intact rock is obtained, as shown in Figure F-6.

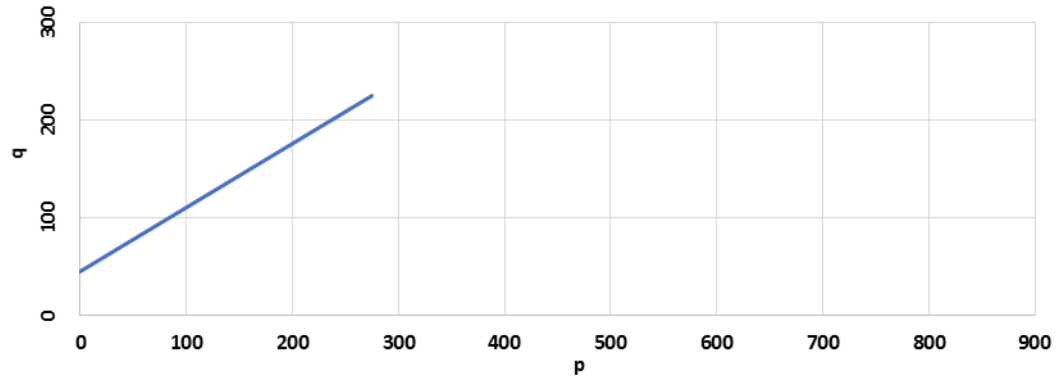

Figure F-4. First part of the bilinear envelope

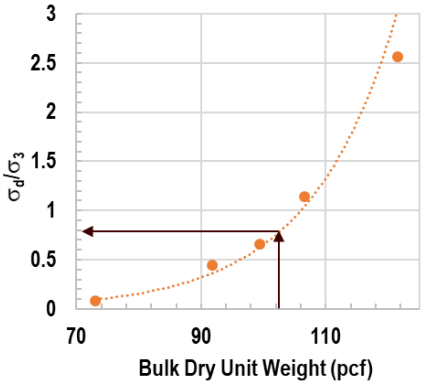

Figure F-5. Obtaining σ_d/σ_3 corresponding to γ_{dtw}

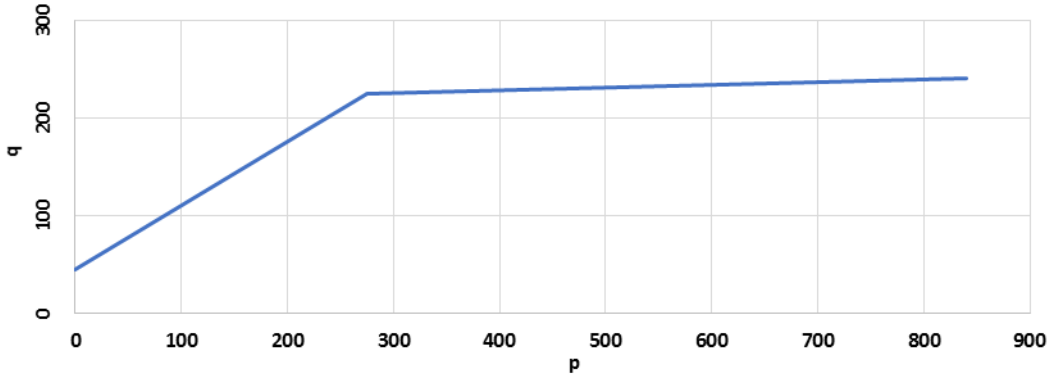

Figure F-6. Completion of bilinear envelope for intact rock

From Figure F-6, the 2nd slope in p-q diagram can be calculated:

$\tan\beta = \frac{240-224.6}{840-274.6} = 0.0272$

$\beta = 1.56$ and $\sin\omega = \tan\beta$, thus $\omega = 1.56$

Figure F-6 presents the mean value for strength envelope of intact rock. A more conservative envelope for intact rock can be obtained by reducing all the q_u, q_{dt}, and γ_{dt} by the standard deviation of the bias.

For rock mass, the mean value for REC for all core runs is 60%:

$$a_m = 60\%*a = 26.8 \quad \text{(F-16)}$$

$$\tan\alpha_m = 60\%*\tan\alpha = 60\%*0.6555 = 0.3933 \quad \text{(F-17)}$$

$$\tan\beta_m = 60\%*\tan\beta = 60\% * 0.0272 = 0.0163 \quad \text{(F-18)}$$

$$p_{pm} = p_p = 274.6 \quad \text{(F-19)}$$

So, the rock mass envelope is the bilinear curve below, which is presented in Figure F-7:

If $p < 274.6$ psi: $q = 26.8 + 0.3933\ p$

If $p \geq 274.6$ psi: $q = 26.8 + 0.3933*274.6 + 0.0163\ p$

$= 134.8 + 0.0163\ p$

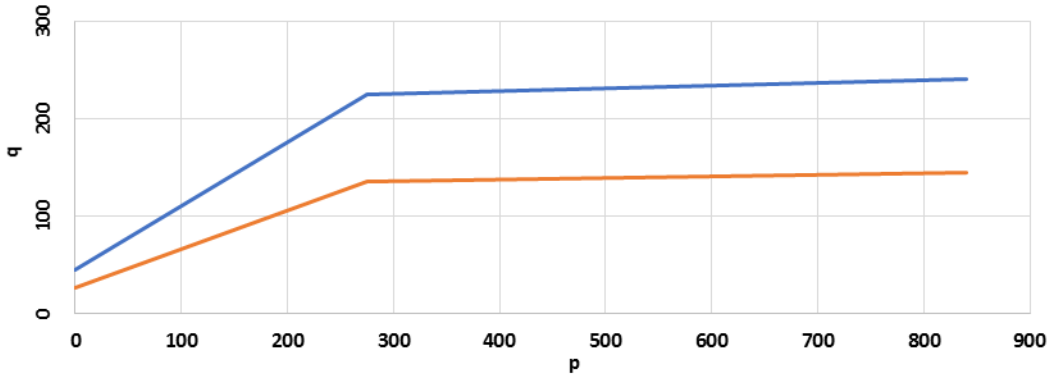

Figure F-7. Envelopes for intact rock and rock mass

APPENDIX G
FEM SIMULATION RESULTS IN SI UNIT

Table G-1. FEM simulation results – Bearing capacity (MPa) on rock subsurface

Note: The shaded texts have no significances. They only help with readability across the columns. The dim texts mean that they have the same results as the above row(s), thus, the differences in results of other rows are easily distinguished.

	B = 2 m; D = 0 m				B = 4 m; D = 0 m					B = 2 m; D = 1 m			B = 4 m; D = 2 m			
#	Strip B/L=0	L/B=10 B/L=0.1	L/B=5 B/L=0.2	square	Strip ν=0.2	Strip ν = 0.1	L/B=10 B/L=0.1	L/B=5 B/L=0.2	square	L/B=10 B/L=0.1	L/B=5 B/L=0.2	square	Strip B/L=0	L/B=10 B/L=0.1	L/B=5 B/L=0.2	square
1	0.56	0.58	0.61	0.70	1.61	0.58	0.60	0.63	0.72	0.72	0.75	0.86	0.69	0.74	0.78	0.89
2-27	same	results														
28	0.72	0.75	0.80	0.92	2.08	0.76	0.78	0.83	0.95	0.93	0.99	1.13	0.90	0.97	1.03	1.18
29	0.72	0.75	0.80	0.92	2.23	0.76	0.78	0.83	0.95	0.93	0.99	1.13	0.90	0.97	1.03	1.18
30	0.72	0.75	0.80	0.92	2.55	0.76	0.78	0.83	0.95	0.93	0.99	1.13	0.90	0.97	1.03	1.18
31	0.72	0.75	0.80	0.92	2.10	0.76	0.78	0.83	0.95	0.93	0.99	1.13	0.90	0.97	1.03	1.18
32	0.72	0.75	0.80	0.92	2.25	0.76	0.78	0.83	0.95	0.93	0.99	1.13	0.90	0.97	1.03	1.18
33	0.72	0.75	0.80	0.92	2.57	0.76	0.78	0.83	0.95	0.93	0.99	1.13	0.90	0.97	1.03	1.18
34	0.72	0.75	0.80	0.92	2.12	0.76	0.78	0.83	0.95	0.72	0.99	1.13	0.90	0.74	1.03	1.18
35	0.72	0.75	0.80	0.92	2.27	0.76	0.78	0.83	0.95	0.93	0.99	1.13	0.90	0.97	1.03	1.18
36	0.72	0.75	0.80	0.92	2.60	0.76	0.78	0.83	0.95	0.93	0.99	1.13	0.90	0.97	1.03	1.18
37	0.72	0.75	0.80	0.92	2.16	0.76	0.78	0.83	0.95	0.93	0.99	1.13	0.90	0.97	1.03	1.18
38	0.72	0.75	0.80	0.92	2.30	0.76	0.78	0.83	0.95	0.93	0.99	1.13	0.90	0.97	1.03	1.18
39	0.72	0.75	0.80	0.92	2.63	0.76	0.78	0.83	0.95	0.93	0.99	1.13	0.90	0.97	1.03	1.18
40	0.72	0.75	0.80	0.92	2.19	0.76	0.78	0.83	0.95	0.93	0.99	1.13	0.90	0.97	1.03	1.18
41	0.72	0.75	0.80	0.92	2.35	0.76	0.78	0.83	0.95	0.72	0.99	1.13	0.90	0.74	1.03	1.18
42	0.72	0.75	0.80	0.92	2.67	0.76	0.78	0.83	0.95	0.93	0.99	1.13	0.90	0.97	1.03	1.18
43	0.72	0.75	0.80	0.92	2.22	0.76	0.78	0.83	0.95	0.93	0.99	1.13	0.90	0.97	1.03	1.18
44	0.72	0.75	0.80	0.92	2.40	0.76	0.78	0.83	0.95	0.93	0.99	1.13	0.90	0.97	1.03	1.18
45	0.72	0.75	0.80	0.92	2.70	0.76	0.78	0.83	0.95	0.93	0.99	1.13	0.90	0.97	1.03	1.18
46	0.72	0.75	0.80	0.92	2.27	0.76	0.78	0.83	0.95	0.93	0.99	1.13	0.90	0.97	1.03	1.18
47	0.72	0.75	0.80	0.92	2.45	0.76	0.78	0.83	0.95	0.93	0.99	1.13	0.90	0.97	1.03	1.18
48	0.72	0.75	0.80	0.92	2.73	0.76	0.78	0.83	0.95	0.72	0.99	1.13	0.90	0.74	1.03	1.18
49	0.72	0.75	0.80	0.92	2.36	0.76	0.78	0.83	0.95	0.93	0.99	1.13	0.90	0.97	1.03	1.18
50	0.72	0.75	0.80	0.92	2.50	0.76	0.78	0.83	0.95	0.93	0.99	1.13	0.90	0.97	1.03	1.18
51	0.72	0.75	0.80	0.92	2.81	0.76	0.78	0.83	0.95	0.93	0.99	1.13	0.90	0.97	1.03	1.18
52	0.72	0.75	0.80	0.92	2.48	0.76	0.78	0.83	0.95	0.93	0.99	1.13	0.90	0.97	1.03	1.18
53	0.72	0.75	0.80	0.92	2.62	0.76	0.78	0.83	0.95	0.93	0.99	1.13	0.90	0.97	1.03	1.18
54	0.72	0.75	0.80	0.92	2.92	0.76	0.78	0.83	0.95	0.93	0.99	1.13	0.90	0.97	1.03	1.18
55	1.49	1.55	1.64	1.87	2.27	1.56	1.60	1.70	1.94	1.91	2.03	2.32	1.85	1.98	2.10	2.40
56	1.49	1.55	1.64	1.87	2.45	1.56	1.60	1.70	1.94	1.91	2.03	2.32	1.85	1.98	2.10	2.40
57	1.49	1.55	1.64	1.87	2.81	1.56	1.60	1.70	1.94	1.91	2.03	2.32	1.85	1.98	2.10	2.40
58	1.49	1.55	1.64	1.87	2.31	1.56	1.60	1.70	1.94	1.91	2.03	2.32	1.85	1.98	2.10	2.40
59	1.49	1.55	1.64	1.87	2.50	1.56	1.60	1.70	1.94	1.91	2.03	2.32	1.85	1.98	2.10	2.40
60	1.49	1.55	1.64	1.87	2.84	1.56	1.60	1.70	1.94	1.91	2.03	2.32	1.85	1.98	2.10	2.40
61	1.49	1.55	1.64	1.87	2.37	1.56	1.60	1.70	1.94	1.91	2.03	2.32	1.85	1.98	2.10	2.40
62	1.49	1.55	1.64	1.87	2.53	1.56	1.60	1.70	1.94	1.91	2.03	2.32	1.85	1.98	2.10	2.40
63	1.49	1.55	1.64	1.87	2.88	1.56	1.60	1.70	1.94	1.91	2.03	2.32	1.85	1.98	2.10	2.40
64	1.49	1.55	1.64	1.87	2.43	1.56	1.60	1.70	1.94	1.91	2.03	2.32	1.85	1.98	2.10	2.40
65	1.49	1.55	1.64	1.87	2.61	1.56	1.60	1.70	1.94	1.91	2.03	2.32	1.85	1.98	2.10	2.40

Table G- 1. Continued

	B = 2 m; D = 0 m				B = 4 m; D = 0 m				B = 2 m; D = 1 m				B = 4 m; D = 2 m			
#	Strip B/L=0	L/B=10 B/L=0.1	L/B=5 B/L=0.2	square	Strip ν=0.2	Strip ν = 0.1	L/B=10 B/L=0.1	L/B=5 B/L=0.2	square	L/B=10 B/L=0.1	L/B=5 B/L=0.2	square	Strip B/L=0	L/B=10 B/L=0.1	L/B=5 B/L=0.2	square
66	1.49	1.55	1.64	1.87	2.94	1.56	1.60	1.70	1.94	1.91	2.03	2.32	1.85	1.98	2.10	2.40
67	1.49	1.55	1.64	1.87	2.49	1.56	1.60	1.70	1.94	1.91	2.03	2.32	1.85	1.98	2.10	2.40
68	1.49	1.55	1.64	1.87	2.68	1.56	1.60	1.70	1.94	1.91	2.03	2.32	1.85	1.98	2.10	2.40
69	1.49	1.55	1.64	1.87	3.03	1.56	1.60	1.70	1.94	1.91	2.03	2.32	1.85	1.98	2.10	2.40
70	1.49	1.55	1.64	1.87	2.55	1.56	1.60	1.70	1.94	1.91	2.03	2.32	1.85	1.98	2.10	2.40
71	1.49	1.55	1.64	1.87	2.73	1.56	1.60	1.70	1.94	1.91	2.03	2.32	1.85	1.98	2.10	2.40
72	1.49	1.55	1.64	1.87	3.13	1.56	1.60	1.70	1.94	1.91	2.03	2.32	1.85	1.98	2.10	2.40
73	1.49	1.55	1.64	1.87	2.68	1.56	1.60	1.70	1.94	1.91	2.03	2.32	1.85	1.98	2.10	2.40
74	1.49	1.55	1.64	1.87	2.87	1.56	1.60	1.70	1.94	1.91	2.03	2.32	1.85	1.98	2.10	2.40
75	1.49	1.55	1.64	1.87	3.30	1.56	1.60	1.70	1.94	1.91	2.03	2.32	1.85	1.98	2.10	2.40
76	1.49	1.55	1.64	1.87	2.86	1.56	1.60	1.70	1.94	1.91	2.03	2.32	1.85	1.98	2.10	2.40
77	1.49	1.55	1.64	1.87	3.08	1.56	1.60	1.70	1.94	1.91	2.03	2.32	1.85	1.98	2.10	2.40
78	1.49	1.55	1.64	1.87	3.46	1.56	1.60	1.70	1.94	1.91	2.03	2.32	1.85	1.98	2.10	2.40
79	1.49	1.55	1.64	1.87	3.17	1.56	1.60	1.70	1.94	1.91	2.03	2.32	1.85	1.98	2.10	2.40
80	1.49	1.55	1.64	1.87	3.47	1.56	1.60	1.70	1.94	1.91	2.03	2.32	1.85	1.98	2.10	2.40
81	1.49	1.55	1.64	1.87	3.87	1.56	1.60	1.70	1.94	1.91	2.03	2.32	1.85	1.98	2.10	2.40
82	2.09	2.18	2.30	2.64	2.43	2.19	2.25	2.38	2.73	2.68	2.84	3.26	2.59	2.78	2.95	3.38
83	2.29	2.37	2.51	2.87	2.63	2.39	2.46	2.59	2.97	2.94	3.09	3.55	2.83	3.04	3.21	3.68
84	2.64	2.73	2.89	3.30	2.99	2.75	2.83	2.98	3.41	3.38	3.56	4.07	3.26	3.50	3.69	4.22
85	2.12	2.20	2.33	2.66	2.50	2.21	2.27	2.40	2.75	2.71	2.87	3.28	2.62	2.81	2.97	3.41
86	2.31	2.39	2.54	2.89	2.70	2.41	2.48	2.62	2.99	2.96	3.13	3.57	2.85	3.07	3.24	3.70
87	2.66	2.75	2.91	3.32	3.07	2.77	2.85	3.01	3.44	3.40	3.59	4.11	3.28	3.53	3.73	4.26
88	2.15	2.22	2.36	2.69	2.57	2.24	2.30	2.43	2.78	2.75	2.90	3.32	2.65	2.85	3.01	3.44
89	2.35	2.43	2.58	2.93	2.76	2.45	2.52	2.66	3.04	3.01	3.18	3.63	2.90	3.12	3.29	3.77
90	2.68	2.77	2.94	3.35	3.15	2.79	2.87	3.03	3.47	3.42	3.62	4.14	3.30	3.55	3.75	4.30
91	2.21	2.28	2.42	2.76	2.63	2.30	2.37	2.50	2.86	2.83	2.98	3.41	2.72	2.93	3.10	3.54
92	2.37	2.45	2.60	2.96	2.82	2.47	2.54	2.68	3.07	3.03	3.20	3.67	2.93	3.14	3.32	3.80
93	2.70	2.80	2.97	3.38	3.23	2.82	2.90	3.06	3.50	3.46	3.65	4.18	3.34	3.59	3.79	4.33
94	2.22	2.30	2.44	2.78	2.77	2.32	2.39	2.52	2.88	2.85	3.01	3.44	2.75	2.96	3.12	3.57
95	2.38	2.46	2.61	2.97	2.97	2.48	2.55	2.69	3.08	3.04	3.21	3.68	2.94	3.16	3.33	3.81
96	2.72	2.82	2.99	3.41	3.37	2.84	2.92	3.08	3.53	3.48	3.68	4.21	3.36	3.61	3.81	4.37
97	2.23	2.31	2.45	2.79	2.82	2.33	2.40	2.53	2.89	2.87	3.02	3.45	2.76	2.97	3.13	3.58
98	2.39	2.47	2.62	2.98	3.01	2.49	2.56	2.70	3.09	3.05	3.22	3.69	2.95	3.17	3.34	3.83
99	2.74	2.83	3.00	3.42	3.49	2.85	2.93	3.09	3.54	3.50	3.69	4.23	3.38	3.63	3.83	4.38
100	2.26	2.34	2.48	2.83	3.02	2.36	2.43	2.56	2.93	2.90	3.06	3.50	2.80	3.01	3.17	3.63
101	2.41	2.50	2.65	3.02	3.23	2.52	2.59	2.73	3.13	3.09	3.26	3.74	2.98	3.21	3.38	3.88
102	2.75	2.85	3.02	3.45	3.67	2.87	2.95	3.11	3.57	3.52	3.71	4.26	3.40	3.65	3.85	4.42
103	2.28	2.36	2.50	2.86	3.31	2.38	2.45	2.58	2.96	2.92	3.08	3.53	2.82	3.03	3.19	3.67
104	2.45	2.53	2.68	3.06	3.56	2.55	2.62	2.77	3.17	3.13	3.31	3.79	3.02	3.24	3.43	3.93
105	2.79	2.86	3.03	3.46	3.99	2.88	2.96	3.13	3.58	3.53	3.74	4.27	3.41	3.67	3.88	4.43
106	2.31	2.39	2.54	2.89	3.73	2.41	2.48	2.62	2.99	2.96	3.13	3.57	2.85	3.07	3.24	3.70
107	2.47	2.56	2.71	3.10	4.03	2.58	2.65	2.80	3.21	3.16	3.34	3.83	3.06	3.28	3.47	3.98
108	2.82	2.89	3.06	3.49	4.56	2.91	2.99	3.16	3.62	3.57	3.77	4.32	3.45	3.70	4.91	4.48
109	2.93	3.02	3.20	3.65	3.71	3.04	3.12	3.30	3.78	3.72	3.94	4.51	3.58	3.86	4.09	4.68
110	2.93	3.02	3.20	3.65	4.41	3.04	3.12	3.30	3.78	3.72	3.94	4.51	3.58	3.86	4.09	4.68
111	2.93	3.02	3.20	3.65	5.17	3.04	3.12	3.30	3.78	3.72	3.94	4.51	3.58	3.86	4.09	4.68
112	2.93	3.02	3.20	3.65	3.77	3.04	3.12	3.30	3.78	3.72	3.94	4.51	3.58	3.86	4.09	4.68
113	2.93	3.02	3.20	3.65	4.45	3.04	3.12	3.30	3.78	3.72	3.94	4.51	3.58	3.86	4.09	4.68

Table G- 1. Continued

	B = 2 m; D = 0 m				B = 4 m; D = 0 m				B = 2 m; D = 1 m				B = 4 m; D = 2 m			
#	Strip B/L=0	L/B=10 B/L=0.1	L/B=5 B/L=0.2	square	Strip ν=0.2	Strip ν = 0.1	L/B=10 B/L=0.1	L/B=5 B/L=0.2	square	L/B=10 B/L=0.1	L/B=5 B/L=0.2	square	Strip B/L=0	L/B=10 B/L=0.1	L/B=5 B/L=0.2	square
114	2.93	3.02	3.20	3.65	5.20	3.04	3.12	3.30	3.78	3.72	3.94	4.51	3.58	3.86	4.09	4.68
115	2.93	3.02	3.20	3.65	3.83	3.04	3.12	3.30	3.78	3.72	3.94	4.51	3.58	3.86	4.09	4.68
116	2.93	3.02	3.20	3.65	4.50	3.04	3.12	3.30	3.78	3.72	3.94	4.51	3.58	3.86	4.09	4.68
117	2.93	3.02	3.20	3.65	5.27	3.04	3.12	3.30	3.78	3.72	3.94	4.51	3.58	3.86	4.09	4.68
118	2.93	3.02	3.20	3.65	3.93	3.04	3.12	3.30	3.78	3.72	3.94	4.51	3.58	3.86	4.09	4.68
119	2.93	3.02	3.20	3.65	4.60	3.04	3.12	3.30	3.78	3.72	3.94	4.51	3.58	3.86	4.09	4.68
120	2.93	3.02	3.20	3.65	5.30	3.04	3.12	3.30	3.78	3.72	3.94	4.51	3.58	3.86	4.09	4.68
121	2.93	3.02	3.20	3.65	4.03	3.04	3.12	3.30	3.78	3.72	3.94	4.51	3.58	3.86	4.09	4.68
122	2.93	3.02	3.20	3.65	4.71	3.04	3.12	3.30	3.78	3.72	3.94	4.51	3.58	3.86	4.09	4.68
123	2.93	3.02	3.20	3.65	5.38	3.04	3.12	3.30	3.78	3.72	3.94	4.51	3.58	3.86	4.09	4.68
124	2.93	3.02	3.20	3.65	4.16	3.04	3.12	3.30	3.78	3.72	3.94	4.51	3.58	3.86	4.09	4.68
125	2.93	3.02	3.20	3.65	4.79	3.04	3.12	3.30	3.78	3.72	3.94	4.51	3.58	3.86	4.09	4.68
126	2.93	3.02	3.20	3.65	5.43	3.04	3.12	3.30	3.78	3.72	3.94	4.51	3.58	3.86	4.09	4.68
127	2.93	3.02	3.20	3.65	4.29	3.04	3.12	3.30	3.78	3.72	3.94	4.51	3.58	3.86	4.09	4.68
128	2.93	3.02	3.20	3.65	4.96	3.04	3.12	3.30	3.78	3.72	3.94	4.51	3.58	3.86	4.09	4.68
129	2.93	3.02	3.20	3.65	5.54	3.04	3.12	3.30	3.78	3.72	3.94	4.51	3.58	3.86	4.09	4.68
130	2.93	3.02	3.20	3.65	4.53	3.04	3.12	3.30	3.78	3.72	3.94	4.51	3.58	3.86	4.09	4.68
131	2.93	3.02	3.20	3.65	5.17	3.04	3.12	3.30	3.78	3.72	3.94	4.51	3.58	3.86	4.09	4.68
132	2.93	3.02	3.20	3.65	5.75	3.04	3.12	3.30	3.78	3.72	3.94	4.51	3.58	3.86	4.09	4.68
133	2.93	3.02	3.20	3.65	5.02	3.04	3.12	3.30	3.78	3.72	3.94	4.51	3.58	3.86	4.09	4.68
134	2.93	3.02	3.20	3.65	5.56	3.04	3.12	3.30	3.78	3.72	3.94	4.51	3.58	3.86	4.09	4.68
135	2.93	3.02	3.20	3.65	6.02	3.04	3.12	3.30	3.78	3.72	3.94	4.51	3.58	3.86	4.09	4.68
136	3.58	3.68	3.90	4.45	4.03	3.71	3.82	4.04	4.61	4.56	4.82	5.51	4.44	4.73	5.00	5.71
137	4.26	4.39	4.65	5.30	4.82	4.42	4.55	4.82	5.49	5.43	5.75	6.56	5.26	5.63	5.97	6.80
138	4.29	4.42	4.68	5.34	5.63	4.45	4.58	4.85	5.53	5.46	5.79	6.60	5.31	5.67	6.01	6.85
139	3.60	3.71	3.93	4.49	4.13	3.74	3.85	4.08	4.65	4.59	4.87	5.55	4.47	4.76	5.05	5.76
140	4.26	4.39	4.65	5.30	4.90	4.42	4.55	4.82	5.49	5.43	5.75	6.56	5.26	5.63	5.97	6.80
141	4.29	4.42	4.68	5.34	5.72	4.45	4.58	4.85	5.53	5.46	5.79	6.60	5.31	5.67	6.01	6.85
142	3.64	3.75	3.98	4.54	4.21	3.78	3.89	4.12	4.70	4.64	4.92	5.61	4.52	4.81	5.10	5.82
143	4.26	4.39	4.65	5.30	4.99	4.42	4.55	4.82	5.49	5.43	5.75	6.56	5.26	5.63	5.97	6.80
144	4.29	4.42	4.68	5.34	5.81	4.45	4.58	4.85	5.53	5.46	5.79	6.60	5.31	5.67	6.01	6.85
145	3.66	3.70	4.00	4.56	4.33	3.80	3.91	4.14	4.72	4.67	4.94	5.64	4.54	4.84	5.13	5.85
146	4.26	4.39	4.65	5.30	5.13	4.42	4.55	4.82	5.49	5.43	5.75	6.56	5.26	5.63	5.97	6.80
147	4.29	4.42	4.68	5.34	5.93	4.45	4.58	4.85	5.53	5.46	5.79	6.60	5.31	5.67	6.01	6.85
148	3.70	3.81	4.04	4.61	4.52	3.84	3.95	4.19	4.77	4.71	5.00	5.70	4.59	4.89	5.19	5.91
149	4.26	4.39	4.65	5.30	5.33	4.42	4.55	4.82	5.49	5.43	5.75	6.56	5.26	5.63	5.97	6.80
150	4.29	4.42	4.68	5.34	6.13	4.45	4.58	4.85	5.53	5.46	5.79	6.60	5.31	5.67	6.01	6.85
151	3.72	3.82	4.05	4.62	4.70	3.85	3.96	4.20	4.78	4.73	5.02	5.71	4.60	4.90	5.20	5.92
152	4.26	4.39	4.65	5.30	5.48	4.42	4.55	4.82	5.49	5.43	5.75	6.56	5.26	5.63	5.97	6.80
153	4.29	4.42	4.68	5.34	6.28	4.45	4.58	4.85	5.53	5.46	5.79	6.60	5.31	5.67	6.01	6.85
154	3.73	3.84	4.07	4.63	5.01	3.87	3.98	4.22	4.80	4.75	5.04	5.73	4.63	4.93	5.23	5.95
155	4.26	4.39	4.65	5.30	5.80	4.42	4.55	4.82	5.49	5.43	5.75	6.56	5.29	5.63	5.97	6.80
156	4.29	4.42	4.68	5.34	6.59	4.45	4.58	4.85	5.53	5.46	5.79	6.60	5.31	5.67	6.01	6.85
157	3.76	3.87	4.10	4.68	5.37	3.90	4.01	4.25	4.85	4.78	5.07	5.79	4.66	4.96	5.26	6.01
158	4.26	4.39	4.65	5.30	6.18	4.42	4.55	4.82	5.49	5.43	5.75	6.56	5.29	5.63	5.97	6.80
159	4.29	4.42	4.68	5.34	7.01	4.45	4.58	4.85	5.53	5.46	5.79	6.60	5.31	5.67	6.01	6.85
160	3.79	3.90	4.13	4.71	6.04	3.93	4.04	4.28	4.88	4.82	5.11	5.83	4.70	5.00	5.30	6.04
161	4.26	4.39	4.65	5.30	6.96	4.42	4.55	4.82	5.49	5.43	5.75	6.56	5.29	5.63	5.97	6.80

Table G- 1. Continued

	B = 2 m; D = 0 m				B = 4 m; D = 0 m				B = 2 m; D = 1 m				B = 4 m; D = 2 m			
#	Strip B/L=0	L/B=10 B/L=0.1	L/B=5 B/L=0.2	square	Strip ν=0.2	Strip ν = 0.1	L/B=10 B/L=0.1	L/B=5 B/L=0.2	square	L/B=10 B/L=0.1	L/B=5 B/L=0.2	square	Strip B/L=0	L/B=10 B/L=0.1	L/B=5 B/L=0.2	square
162	4.29	4.42	4.68	5.34	7.68	4.45	4.58	4.85	5.53	5.46	5.79	6.60	5.31	5.67	6.01	6.85
163	3.88	3.99	4.23	4.83	4.36	4.02	4.14	4.38	5.00	4.94	5.23	5.97	4.81	5.12	5.42	6.19
164	4.68	4.82	5.10	5.82	5.27	4.85	4.99	5.29	6.03	5.95	6.32	7.20	5.81	6.18	6.55	7.47
165	5.48	5.64	5.98	6.82	6.13	5.68	5.84	6.19	7.06	6.97	7.39	8.43	6.80	7.23	7.67	8.74
166	3.93	4.04	4.28	4.90	4.47	4.07	4.19	4.44	5.07	5.01	5.30	6.05	4.87	5.19	5.50	6.28
167	4.74	4.88	5.17	5.89	5.35	4.91	5.05	5.35	6.11	6.03	6.39	7.30	5.88	6.25	6.63	7.57
168	5.51	5.67	6.01	6.86	6.27	5.71	5.87	6.22	7.11	7.01	7.43	8.49	6.84	7.27	7.70	8.81
169	3.98	4.11	4.36	4.97	4.63	4.14	4.26	4.51	5.15	5.08	5.38	6.15	4.96	5.27	5.58	6.38
170	4.79	4.94	5.23	5.97	5.50	4.97	5.11	5.42	6.18	6.10	6.47	7.38	5.95	6.32	6.71	7.65
171	5.54	5.71	6.05	6.91	6.40	5.75	5.92	6.27	7.15	7.06	7.49	8.54	6.89	7.33	7.76	8.86
172	4.05	4.17	4.42	5.04	4.83	4.20	4.32	4.58	5.22	5.15	5.47	6.23	5.03	5.35	5.67	6.47
173	4.83	4.98	5.27	6.02	5.77	5.01	5.15	5.46	6.23	6.15	6.52	7.44	6.01	6.37	6.76	7.72
174	5.58	5.75	6.09	6.95	6.60	5.79	5.96	6.31	7.20	7.11	7.53	8.60	6.93	7.38	7.81	8.92
175	4.10	4.23	4.48	5.11	5.07	4.26	4.38	4.64	5.30	5.23	5.54	6.33	5.10	5.42	5.75	6.56
176	4.88	5.03	5.32	6.08	5.99	5.06	5.21	5.52	6.30	6.22	6.59	7.52	6.06	6.45	6.84	7.80
177	5.63	5.80	6.14	7.02	6.92	5.84	6.01	6.37	7.27	7.17	7.61	8.68	6.99	7.44	7.89	9.01
178	4.17	4.30	4.56	5.20	5.27	4.33	4.45	4.72	5.38	5.31	5.64	6.42	5.19	5.51	5.85	6.66
179	4.92	5.08	5.38	6.13	6.27	5.11	5.26	5.57	6.35	6.28	6.65	7.58	6.12	6.51	6.90	7.87
180	5.65	5.82	6.17	7.05	7.21	5.86	6.03	6.39	7.30	7.20	7.63	8.72	7.01	7.46	7.91	9.04
181	4.28	4.41	4.67	5.33	5.71	4.44	4.57	4.84	5.52	5.45	5.78	6.59	5.32	5.66	5.99	6.84
182	4.99	5.14	5.45	6.22	6.71	5.18	5.33	5.65	6.44	6.36	6.75	7.69	6.20	6.60	7.00	7.98
183	5.70	5.88	6.23	7.11	7.65	5.92	6.09	6.45	7.36	7.27	7.70	8.79	7.09	7.54	7.99	9.12
184	4.39	4.53	4.80	5.47	6.32	4.56	4.69	4.97	5.67	5.60	5.93	6.77	5.46	5.80	6.15	7.02
185	5.08	5.23	5.54	6.32	7.32	5.27	5.42	5.75	6.55	6.47	6.87	7.82	6.31	6.71	7.12	8.11
186	5.76	5.94	6.29	7.18	8.38	5.98	6.15	6.52	7.44	7.34	7.78	8.88	7.16	7.61	8.08	9.22
187	4.54	4.68	4.96	5.66	7.33	4.71	4.85	5.13	5.86	5.79	6.12	7.01	5.64	6.01	6.35	7.26
188	5.19	5.35	5.67	6.47	8.53	5.39	5.55	5.88	6.70	6.62	7.02	8.00	6.46	6.87	7.28	8.30
189	5.89	6.07	6.43	7.34	9.51	6.11	6.29	6.66	7.60	7.51	7.95	9.08	7.32	7.78	8.25	9.41
190	4.11	4.23	4.48	5.12	4.63	4.26	4.38	4.64	5.30	5.23	5.54	6.33	5.10	5.42	5.75	6.56
191	4.99	5.14	5.45	6.22	5.61	5.18	5.33	5.65	6.44	6.36	6.75	7.69	6.20	6.60	7.01	7.98
192	5.85	6.03	6.39	7.29	6.53	6.07	6.24	6.62	7.55	7.45	7.90	9.02	7.27	7.72	8.20	9.35
193	4.18	4.30	4.56	5.19	4.76	4.33	4.45	4.72	5.38	5.31	5.64	6.42	5.19	5.51	5.85	6.67
194	5.06	5.21	5.52	6.30	5.73	5.25	5.40	5.72	6.53	6.44	6.83	7.80	6.29	6.68	7.08	8.09
195	5.90	6.08	6.44	7.35	6.73	6.12	6.30	6.67	7.61	7.52	7.96	9.09	7.33	7.80	8.26	9.43
196	4.27	4.40	4.66	5.32	4.96	4.43	4.56	4.83	5.51	5.44	5.77	6.58	5.30	5.64	5.98	6.82
197	5.12	5.27	5.59	6.37	5.96	5.31	5.46	5.79	6.60	6.51	6.91	7.88	6.36	6.76	7.17	8.17
198	5.98	6.16	6.52	7.44	6.97	6.20	6.38	6.76	7.71	7.61	8.07	9.21	7.43	7.90	8.37	9.55
199	4.38	4.51	4.78	5.46	5.16	4.54	4.67	4.95	5.65	5.57	5.91	6.75	5.44	5.78	6.13	7.01
200	5.22	5.37	5.69	6.50	6.17	5.41	5.57	5.90	6.73	6.65	7.04	8.04	6.48	6.89	7.31	8.34
201	6.07	6.25	6.62	7.55	7.20	6.29	6.47	6.86	7.82	7.72	8.19	9.34	7.53	8.01	8.50	9.69
202	4.47	4.60	4.87	5.56	5.50	4.63	4.76	5.05	5.76	5.68	6.03	6.88	5.55	5.89	6.25	7.13
203	5.31	5.47	5.80	6.61	6.51	5.51	5.67	6.01	6.85	6.77	7.18	8.18	6.60	7.02	7.44	8.48
204	6.15	6.34	6.71	7.66	7.56	6.38	6.56	6.96	7.93	7.83	8.31	9.47	7.64	8.12	8.62	9.82
205	4.52	4.66	4.93	5.63	5.85	4.69	4.82	5.11	5.83	5.75	6.10	6.96	5.62	5.97	6.33	7.22
206	5.38	5.54	5.87	6.70	6.89	5.58	5.74	6.08	6.94	6.85	7.26	8.29	6.68	7.10	7.53	8.60
207	6.24	6.43	6.81	7.76	7.97	6.47	6.66	7.05	8.04	7.95	8.42	9.60	7.75	8.24	8.73	9.96
208	4.71	4.85	5.13	5.86	6.27	4.88	5.02	5.32	6.07	5.99	6.35	7.25	5.85	6.21	6.59	7.52
209	5.54	5.70	6.04	6.89	7.47	5.74	5.91	6.26	7.14	7.05	7.47	8.53	6.88	7.31	7.75	8.84

Table G- 1. Continued

	B = 2 m; D = 0 m				B = 4 m; D = 0 m				B = 2 m; D = 1 m				B = 4 m; D = 2 m			
#	Strip B/L=0	L/B=10 B/L=0.1	L/B=5 B/L=0.2	square	Strip ν=0.2	Strip ν = 0.1	L/B=10 B/L=0.1	L/B=5 B/L=0.2	square	L/B=10 B/L=0.1	L/B=5 B/L=0.2	square	Strip B/L=0	L/B=10 B/L=0.1	L/B=5 B/L=0.2	square
210	6.37	6.56	6.94	7.93	8.55	6.60	6.79	7.19	8.21	8.10	8.58	9.80	7.91	8.40	8.90	10.17
211	4.85	5.00	5.29	6.04	7.03	5.03	5.17	5.48	6.26	6.17	6.54	7.48	6.02	6.40	6.79	7.75
212	5.71	5.88	6.23	7.11	8.36	5.92	6.09	6.45	7.36	7.27	7.70	8.79	7.09	7.54	7.99	9.12
213	6.55	6.74	7.14	8.15	9.48	6.79	6.99	7.40	8.44	8.34	8.84	10.08	8.13	8.65	9.16	10.45
214	5.10	5.25	5.57	6.35	8.20	5.29	5.44	5.77	6.58	6.49	6.89	7.86	6.34	6.73	7.15	8.15
215	5.96	6.14	6.50	7.42	9.70	6.18	6.36	6.74	7.68	7.59	8.05	9.17	7.40	7.87	8.35	9.51
216	6.80	6.99	7.42	8.47	10.99	7.05	7.25	7.69	8.77	8.65	9.18	10.47	8.44	8.97	9.52	10.86
217	4.07	4.20	4.45	6.31	5.50	4.23	4.35	4.61	6.54	5.19	5.50	7.81	5.09	5.38	5.71	8.10
218	4.07	4.20	4.45	6.31	6.23	4.23	4.35	4.61	6.54	5.19	5.50	7.81	5.09	5.38	5.71	8.10
219	4.07	4.20	4.45	6.31	6.96	4.23	4.35	4.61	6.54	5.19	5.50	7.81	5.09	5.38	5.71	8.10
220	4.07	4.20	4.45	6.31	5.57	4.23	4.35	4.61	6.54	5.19	5.50	7.81	5.09	5.38	5.71	8.10
221	4.07	4.20	4.45	6.31	6.28	4.23	4.35	4.61	6.54	5.19	5.50	7.81	5.09	5.38	5.71	8.10
222	4.07	4.20	4.45	6.31	7.01	4.23	4.35	4.61	6.54	5.19	5.50	7.81	5.09	5.38	5.71	8.10
223	4.07	4.20	4.45	6.31	5.67	4.23	4.35	4.61	6.54	5.19	5.50	7.81	5.09	5.38	5.71	8.10
224	4.07	4.20	4.45	6.31	6.35	4.23	4.35	4.61	6.54	5.19	5.50	7.81	5.09	5.38	5.71	8.10
225	4.07	4.20	4.45	6.31	7.07	4.23	4.35	4.61	6.54	5.19	5.50	7.81	5.09	5.38	5.71	8.10
226	4.07	4.20	4.45	6.31	5.76	4.23	4.35	4.61	6.54	5.19	5.50	7.81	5.09	5.38	5.71	8.10
227	4.07	4.20	4.45	6.31	6.45	4.23	4.35	4.61	6.54	5.19	5.50	7.81	5.09	5.38	5.71	8.10
228	4.07	4.20	4.45	6.31	7.17	4.23	4.35	4.61	6.54	5.19	5.50	7.81	5.09	5.38	5.71	8.10
229	4.07	4.20	4.45	6.31	5.93	4.23	4.35	4.61	6.54	5.19	5.50	7.81	5.09	5.38	5.71	8.10
230	4.07	4.20	4.45	6.31	6.59	4.23	4.35	4.61	6.54	5.19	5.50	7.81	5.09	5.38	5.71	8.10
231	4.07	4.20	4.45	6.31	7.30	4.23	4.35	4.61	6.54	5.19	5.50	7.81	5.09	5.38	5.71	8.10
232	4.07	4.20	4.45	6.31	6.05	4.23	4.35	4.61	6.54	5.19	5.50	7.81	5.09	5.38	5.71	8.10
233	4.07	4.20	4.45	6.31	6.73	4.23	4.35	4.61	6.54	5.19	5.50	7.81	5.09	5.38	5.71	8.10
234	4.07	4.20	4.45	6.31	7.40	4.23	4.35	4.61	6.54	5.19	5.50	7.81	5.09	5.38	5.71	8.10
235	4.07	4.20	4.45	6.31	6.31	4.23	4.35	4.61	6.54	5.19	5.50	7.81	5.09	5.38	5.71	8.10
236	4.07	4.20	4.45	6.31	6.92	4.23	4.35	4.61	6.54	5.19	5.50	7.81	5.09	5.38	5.71	8.10
237	4.07	4.20	4.45	6.31	7.60	4.23	4.35	4.61	6.54	5.19	5.50	7.81	5.09	5.38	5.71	8.10
238	4.07	4.20	4.45	6.31	6.68	4.23	4.35	4.61	6.54	5.19	5.50	7.81	5.09	5.38	5.71	8.10
239	4.07	4.20	4.45	6.31	7.26	4.23	4.35	4.61	6.54	5.19	5.50	7.81	5.09	5.38	5.71	8.10
240	4.07	4.20	4.45	6.31	7.92	4.23	4.35	4.61	6.54	5.19	5.50	7.81	5.09	5.38	5.71	8.10
241	4.07	4.20	4.45	6.31	7.27	4.23	4.35	4.61	6.54	5.19	5.50	7.81	5.09	5.38	5.71	8.10
242	4.07	4.20	4.45	6.31	7.81	4.23	4.35	4.61	6.54	5.19	5.50	7.81	5.09	5.38	5.71	8.10
243	4.07	4.20	4.45	6.31	8.33	4.23	4.35	4.61	6.54	5.19	5.50	7.81	5.09	5.38	5.71	8.10
244	5.17	5.34	5.66	6.46	5.97	5.38	5.53	5.86	6.69	6.60	7.01	7.99	6.51	6.84	7.26	8.29
245	5.95	6.14	6.50	7.41	6.78	6.18	6.36	6.74	7.68	7.59	8.05	9.17	7.47	7.87	8.35	9.51
246	5.95	6.14	6.50	7.41	7.57	6.18	6.36	6.74	7.68	7.59	8.05	9.17	7.47	7.87	8.35	9.51
247	5.20	5.37	5.69	6.50	6.10	5.41	5.57	5.90	6.73	6.65	7.04	8.04	6.54	6.89	7.31	8.34
248	5.95	6.14	6.50	7.41	6.88	6.18	6.36	6.74	7.68	7.59	8.05	9.17	7.47	7.87	8.35	9.51
249	5.95	6.14	6.50	7.41	7.67	6.18	6.36	6.74	7.68	7.59	8.05	9.17	7.47	7.87	8.35	9.51
250	5.24	5.40	5.72	6.53	6.23	5.44	5.60	5.93	6.76	6.68	7.08	8.07	6.58	6.93	7.34	8.37
251	5.95	6.14	6.50	7.41	7.03	6.18	6.36	6.74	7.68	7.59	8.05	9.17	7.47	7.87	8.35	9.51
252	5.95	6.14	6.50	7.41	7.83	6.18	6.36	6.74	7.68	7.59	8.05	9.17	7.47	7.87	8.35	9.51
253	5.27	5.44	5.77	6.59	6.40	5.48	5.64	5.97	6.81	6.73	7.13	8.13	6.63	6.98	7.39	8.44
254	5.95	6.14	6.50	7.41	7.21	6.18	6.36	6.74	7.68	7.59	8.05	9.17	7.47	7.87	8.35	9.51
255	5.95	6.14	6.50	7.41	7.99	6.18	6.36	6.74	7.68	7.59	8.05	9.17	7.47	7.87	8.35	9.51
256	5.37	5.54	5.87	6.70	6.67	5.58	5.74	6.08	6.94	6.85	7.26	8.29	6.75	7.10	7.53	8.60
257	5.95	6.14	6.50	7.41	7.46	6.18	6.36	6.74	7.68	7.59	8.05	9.17	7.47	7.87	8.35	9.51

Table G- 1. Continued

	B = 2 m; D = 0 m				B = 4 m; D = 0 m				B = 2 m; D = 1 m				B = 4 m; D = 2 m			
#	Strip B/L=0	L/B=10 B/L=0.1	L/B=5 B/L=0.2	square	Strip ν=0.2	Strip ν = 0.1	L/B=10 B/L=0.1	L/B=5 B/L=0.2	square	L/B=10 B/L=0.1	L/B=5 B/L=0.2	square	Strip B/L=0	L/B=10 B/L=0.1	L/B=5 B/L=0.2	square
258	5.95	6.14	6.50	7.41	8.26	6.18	6.36	6.74	7.68	7.59	8.05	9.17	7.47	7.87	8.35	9.51
259	5.40	5.57	5.90	6.74	6.97	5.61	5.77	6.12	6.98	6.89	7.31	8.34	6.79	7.14	7.58	8.65
260	5.95	6.14	6.50	7.41	7.73	6.18	6.36	6.74	7.68	7.59	8.05	9.17	7.47	7.87	8.35	9.51
261	5.95	6.14	6.50	7.41	8.57	6.18	6.36	6.74	7.68	7.59	8.05	9.17	7.47	7.87	8.35	9.51
262	5.44	5.61	5.94	6.79	7.37	5.65	5.81	6.16	7.03	6.93	7.35	8.40	6.84	7.19	7.63	8.71
263	5.95	6.14	6.50	7.41	8.17	6.18	6.36	6.74	7.68	7.59	8.05	9.17	7.47	7.87	8.35	9.51
264	5.95	6.14	6.50	7.41	8.93	6.18	6.36	6.74	7.68	7.59	8.05	9.17	7.47	7.87	8.35	9.51
265	5.47	5.64	5.98	6.82	7.92	5.68	5.84	6.19	7.06	6.97	7.39	8.43	6.87	7.23	7.67	8.75
266	5.95	6.14	6.50	7.41	8.77	6.18	6.36	6.74	7.68	7.59	8.05	9.17	7.47	7.87	8.35	9.51
267	5.95	6.14	6.50	7.41	9.60	6.18	6.36	6.74	7.68	7.59	8.05	9.17	7.47	7.87	8.35	9.51
268	5.51	5.68	6.02	6.87	9.01	5.72	5.88	6.24	7.11	7.02	7.45	8.49	6.92	7.28	7.73	8.81
269	5.95	6.14	6.50	7.41	9.73	6.18	6.36	6.74	7.68	7.59	8.05	9.17	7.47	7.87	8.35	9.51
270	5.95	6.14	6.50	7.41	10.60	6.18	6.36	6.74	7.68	7.59	8.05	9.17	7.47	7.87	8.35	9.51
271	5.76	5.94	6.29	7.18	6.47	5.98	6.16	6.52	7.44	7.35	7.78	8.89	7.25	7.62	8.07	9.22
272	6.59	6.79	7.20	8.22	7.37	6.84	7.04	7.46	8.51	8.40	8.91	10.17	8.29	8.71	9.24	10.54
273	7.37	7.60	8.05	9.18	8.27	7.65	7.87	8.34	9.51	9.39	9.96	11.36	9.27	9.74	10.33	11.78
274	5.82	6.00	6.35	7.25	6.63	6.04	6.21	6.58	7.51	7.41	7.86	8.97	7.32	7.69	8.15	9.30
275	6.65	6.85	7.26	8.28	7.53	6.90	7.10	7.52	8.58	8.47	8.98	10.25	8.36	8.79	9.31	10.63
276	7.42	7.65	8.10	9.24	8.40	7.70	7.92	8.39	9.57	9.45	10.02	11.43	9.33	9.80	10.39	11.85
277	5.89	6.07	6.43	7.34	6.83	6.11	6.29	6.66	7.60	7.51	7.95	9.08	7.40	7.79	8.25	9.41
278	6.71	6.91	7.32	8.35	7.73	6.96	7.16	7.59	8.65	8.54	9.06	10.33	8.43	8.86	9.40	10.71
279	7.48	7.71	8.16	9.32	8.63	7.76	7.98	8.46	9.65	9.52	10.10	11.52	9.40	9.88	10.48	11.85
280	5.95	6.13	6.49	7.41	7.11	6.17	6.35	6.73	7.67	7.58	8.04	9.16	7.48	7.86	8.33	9.50
281	6.77	6.97	7.39	8.43	8.01	7.02	7.22	7.65	8.73	8.62	9.13	10.43	8.51	8.94	9.47	10.81
282	7.54	7.77	8.23	9.40	8.93	7.82	8.05	8.52	9.73	9.61	10.17	11.62	9.48	9.96	10.55	12.05
283	6.06	6.25	6.62	7.55	7.47	6.29	6.47	6.86	7.82	7.72	8.19	9.34	7.62	8.01	8.50	9.69
284	6.81	7.02	7.44	8.49	8.40	7.07	7.27	7.71	8.79	8.67	9.21	10.50	8.57	9.01	9.55	10.89
285	7.59	7.82	8.28	9.45	9.32	7.87	8.10	8.58	9.79	9.67	10.24	11.69	9.54	10.03	10.63	12.13
286	6.12	6.31	6.68	7.63	7.87	6.35	6.53	6.92	7.90	7.79	8.26	9.43	7.69	8.08	8.57	9.79
287	6.86	7.07	7.49	8.55	8.83	7.12	7.32	7.76	8.85	8.73	9.27	10.57	8.63	9.06	9.61	10.96
288	7.63	7.87	8.33	9.51	9.77	7.92	8.15	8.63	9.85	9.73	10.30	11.76	9.60	10.09	10.69	12.20
289	6.22	6.41	6.79	7.74	8.49	6.45	6.64	7.03	8.02	7.92	8.39	9.58	7.82	8.22	8.71	9.93
290	6.95	7.16	7.59	8.66	9.43	7.21	7.42	7.86	8.97	8.85	9.38	10.71	8.74	9.18	9.73	11.12
291	7.72	7.96	8.43	9.62	10.46	8.01	8.24	8.73	9.96	9.83	10.43	11.89	9.71	10.20	10.81	12.34
292	6.36	6.56	6.94	7.93	9.33	6.60	6.79	7.19	8.21	8.10	8.58	9.80	7.99	8.40	8.90	10.17
293	7.09	7.31	7.74	8.84	10.37	7.36	7.57	8.02	9.15	9.03	9.58	10.93	8.92	9.37	9.93	11.33
294	7.84	8.07	8.55	9.76	11.40	8.13	8.36	8.86	10.11	9.98	10.58	12.07	9.85	10.35	10.97	12.52
295	6.53	6.73	7.13	8.14	10.83	6.78	6.98	7.39	8.43	8.33	8.82	10.07	8.22	8.64	9.15	10.44
296	7.28	7.50	7.94	9.07	11.93	7.55	7.77	8.23	9.39	9.27	9.83	11.21	9.15	9.62	10.19	11.63
297	7.98	8.22	8.71	9.95	13.01	8.28	8.52	9.03	10.30	10.17	10.78	12.30	10.03	10.55	11.18	12.76
298	6.16	6.34	6.71	7.66	6.87	6.38	6.56	6.96	7.93	7.83	8.31	9.47	7.78	8.12	8.62	9.83
299	7.04	7.25	7.68	8.77	7.80	7.30	7.51	7.96	9.08	8.96	9.50	10.84	8.90	9.30	9.86	11.25
300	7.83	8.07	8.54	9.75	8.79	8.12	8.35	8.85	10.10	9.96	10.57	12.06	9.90	10.33	10.96	12.51
301	6.24	6.43	6.81	7.77	7.10	6.47	6.66	7.05	8.05	7.95	8.42	9.61	7.89	8.24	8.73	9.97
302	7.12	7.33	7.76	8.86	8.03	7.38	7.59	8.05	9.18	9.06	9.61	10.96	8.99	9.39	9.97	11.37
303	7.93	8.16	8.65	9.87	8.99	8.22	8.46	8.96	10.22	10.09	10.70	12.21	10.02	10.47	11.10	12.66
304	6.34	6.53	6.91	7.89	7.30	6.57	6.76	7.16	8.17	8.07	8.55	9.76	8.01	8.37	8.87	10.12
305	7.23	7.44	7.88	8.99	8.31	7.49	7.71	8.17	9.31	9.20	9.75	11.12	9.13	9.54	10.12	11.53

Table G- 1. Continued

	B = 2 m; D = 0 m				B = 4 m; D = 0 m				B = 2 m; D = 1 m				B = 4 m; D = 2 m			
#	Strip B/L=0	L/B=10 B/L=0.1	L/B=5 B/L=0.2	square	Strip ν=0.2	Strip ν = 0.1	L/B=10 B/L=0.1	L/B=5 B/L=0.2	square	L/B=10 B/L=0.1	L/B=5 B/L=0.2	square	Strip B/L=0	L/B=10 B/L=0.1	L/B=5 B/L=0.2	square
306	8.02	8.25	8.74	9.97	9.32	8.31	8.55	9.06	10.33	10.20	10.82	12.34	10.13	10.58	11.22	12.80
307	6.43	6.61	7.01	8.00	7.67	6.66	6.85	7.26	8.28	8.17	8.67	9.89	8.12	8.48	8.99	10.26
308	7.31	7.53	7.97	9.10	8.67	7.58	7.80	8.26	9.43	9.31	9.86	11.26	9.24	9.65	10.23	11.68
309	8.14	8.38	8.88	10.13	9.67	8.44	8.68	9.20	10.49	10.36	10.98	12.53	10.29	10.74	11.39	12.99
310	6.60	6.79	7.20	8.22	8.10	6.84	7.04	7.46	8.51	8.40	8.91	10.16	8.34	8.71	9.24	10.54
311	7.40	7.62	8.07	9.21	9.13	7.67	7.89	8.36	9.54	9.41	9.98	11.39	9.35	9.77	10.35	11.82
312	8.26	8.50	9.01	10.28	10.19	8.56	8.81	9.33	10.65	10.51	11.14	12.72	10.43	10.90	11.55	13.19
313	6.70	6.90	7.31	8.34	8.62	6.95	7.15	7.58	8.64	8.53	9.05	10.32	8.47	8.85	9.39	10.70
314	7.54	7.77	8.23	9.40	9.67	7.82	8.05	8.52	9.73	9.61	10.17	11.62	9.53	9.96	10.55	12.05
315	8.43	8.68	9.20	10.50	10.77	8.74	8.99	9.53	10.87	10.73	11.38	12.98	10.65	11.13	11.80	13.46
316	6.87	7.07	7.49	8.55	9.33	7.12	7.32	7.76	8.86	8.73	9.27	10.58	8.68	9.06	9.61	10.98
317	7.79	8.02	8.49	9.69	10.49	8.07	8.30	8.80	10.04	9.90	10.51	11.99	9.84	10.27	10.90	12.44
318	8.59	8.84	9.36	10.69	11.65	8.90	9.16	9.70	11.07	10.93	11.58	13.22	10.85	11.34	12.01	13.71
319	7.20	7.41	7.85	8.96	10.43	7.46	7.67	8.13	9.28	9.15	9.71	11.08	9.09	9.49	10.07	11.50
320	7.99	8.22	8.71	9.95	11.67	8.28	8.52	9.03	10.30	10.17	10.78	12.30	10.09	10.55	11.18	12.76
321	8.76	9.02	9.55	10.90	12.91	9.08	9.34	9.90	11.29	11.15	11.82	13.48	11.07	11.56	12.26	13.99
322	7.57	7.80	8.26	9.42	12.31	7.85	8.08	8.56	9.76	9.64	10.22	11.67	9.58	10.01	10.60	12.09
323	8.35	8.59	9.10	10.39	13.66	8.65	8.90	9.43	10.76	10.62	11.26	12.85	10.54	11.02	11.68	13.33
324	9.08	9.35	9.91	11.31	14.99	9.42	9.69	10.27	11.71	11.56	12.27	13.98	11.48	11.99	12.72	14.51

Table G-2. FEM simulation results – Bearing capacity (MPa) on 1.5 to 2-m rock over sand subsurface – Plane strain only

Note: The shaded texts have no significances. They only help with readability across the columns. The dim texts mean that they have the same results as the above row(s), thus, the differences in results of other rows are easily distinguished. E_{rock} = 300 MPa and E_{soil} is indicated in the table.

#	Rock (T) = 1.5 m				Rock (T) = 1.5 m				Rock (T) = 2 m			
	E=10MPa B = 2m D = 0m	E=10MPa B = 4m D = 0m	E=10MPa B = 4m D = 2m	E=10MPa B = 2m D = 1m	E=5MPa B = 2m D = 0m	E=5MPa B = 4m D = 0m	E=5MPa B = 4m D = 2m	E=5MPa B = 2m D = 1m	E=10MPa B = 2m D = 0m	E=10 MPa B = 4m D = 0m	E=10MPa B = 4m D = 2m	E=10MPa B = 2m D = 1m
1	0.35	0.36	0.44	0.42	0.29	0.30	0.37	0.34	0.37	0.38	0.47	0.45
2-27	same	results										
28	0.45	0.47	0.58	0.56	0.37	0.39	0.48	0.46	0.48	0.50	0.61	0.59
29	0.45	0.47	0.58	0.56	0.37	0.39	0.48	0.46	0.48	0.50	0.61	0.59
30	0.45	0.47	0.58	0.56	0.37	0.39	0.48	0.46	0.48	0.50	0.61	0.59
31	0.45	0.47	0.58	0.56	0.37	0.39	0.48	0.46	0.48	0.50	0.61	0.59
32	0.45	0.47	0.58	0.56	0.37	0.39	0.48	0.46	0.48	0.50	0.61	0.59
33	0.45	0.47	0.58	0.56	0.37	0.39	0.48	0.46	0.48	0.50	0.61	0.59
34	0.45	0.47	0.58	0.56	0.37	0.39	0.48	0.46	0.48	0.50	0.61	0.59
35	0.45	0.47	0.58	0.56	0.37	0.39	0.48	0.46	0.48	0.50	0.61	0.59
36	0.45	0.47	0.58	0.56	0.37	0.39	0.48	0.46	0.48	0.50	0.61	0.59
37	0.45	0.47	0.58	0.56	0.37	0.39	0.48	0.46	0.48	0.50	0.61	0.59
38	0.45	0.47	0.58	0.56	0.37	0.39	0.48	0.46	0.48	0.50	0.61	0.59
39	0.45	0.47	0.58	0.56	0.37	0.39	0.48	0.46	0.48	0.50	0.61	0.59
40	0.45	0.47	0.58	0.56	0.37	0.39	0.48	0.46	0.48	0.50	0.61	0.59
41	0.45	0.47	0.58	0.56	0.37	0.39	0.48	0.46	0.48	0.50	0.61	0.59
42	0.45	0.47	0.58	0.56	0.37	0.39	0.48	0.46	0.48	0.50	0.61	0.59

Table G-2. Continued

#	Rock (T) = 1.5 m				Rock (T) = 1.5 m				Rock (T) = 2 m			
	E=10MPa B = 2m D = 0m	E=10MPa B = 4m D = 0m	E=10MPa B = 4m D = 2m	E=10MPa B = 2m D = 1m	E=5MPa B = 2m D = 0m	E=5MPa B = 4m D = 0m	E=5MPa B = 4m D = 2m	E=5MPa B = 2m D = 1m	E=10MPa B = 2m D = 0m	E=10 MPa B = 4m D = 0m	E=10MPa B = 4m D = 2m	E=10MPa B = 2m D = 1m
43	0.45	0.47	0.58	0.56	0.37	0.39	0.48	0.46	0.48	0.50	0.61	0.59
44	0.45	0.47	0.58	0.56	0.37	0.39	0.48	0.46	0.48	0.50	0.61	0.59
45	0.45	0.47	0.58	0.56	0.37	0.39	0.48	0.46	0.48	0.50	0.61	0.59
46	0.45	0.47	0.58	0.56	0.37	0.39	0.48	0.46	0.48	0.50	0.61	0.59
47	0.45	0.47	0.58	0.56	0.37	0.39	0.48	0.46	0.48	0.50	0.61	0.59
48	0.45	0.47	0.58	0.56	0.37	0.39	0.48	0.46	0.48	0.50	0.61	0.59
49	0.45	0.47	0.58	0.56	0.37	0.39	0.48	0.46	0.48	0.50	0.61	0.59
50	0.45	0.47	0.58	0.56	0.37	0.39	0.48	0.46	0.48	0.50	0.61	0.59
51	0.45	0.47	0.58	0.56	0.37	0.39	0.48	0.46	0.48	0.50	0.61	0.59
52	0.45	0.47	0.58	0.56	0.37	0.39	0.48	0.46	0.48	0.50	0.61	0.59
53	0.45	0.47	0.58	0.56	0.37	0.39	0.48	0.46	0.48	0.50	0.61	0.59
54	0.45	0.47	0.58	0.56	0.37	0.39	0.48	0.46	0.48	0.50	0.61	0.59
55	0.94	0.97	1.20	1.16	0.77	0.80	1.00	0.95	0.98	1.02	1.26	1.22
56	0.94	0.97	1.20	1.16	0.77	0.80	1.00	0.95	0.98	1.02	1.26	1.22
57	0.94	0.97	1.20	1.16	0.77	0.80	1.00	0.95	0.98	1.02	1.26	1.22
58	0.94	0.97	1.20	1.16	0.77	0.80	1.00	0.95	0.98	1.02	1.26	1.22
59	0.94	0.97	1.20	1.16	0.77	0.80	1.00	0.95	0.98	1.02	1.26	1.22
60	0.94	0.97	1.20	1.16	0.77	0.80	1.00	0.95	0.98	1.02	1.26	1.22
61	0.94	0.97	1.20	1.16	0.77	0.80	1.00	0.95	0.98	1.02	1.26	1.22
62	0.94	0.97	1.20	1.16	0.77	0.80	1.00	0.95	0.98	1.02	1.26	1.22
63	0.94	0.97	1.20	1.16	0.77	0.80	1.00	0.95	0.98	1.02	1.26	1.22
64	0.94	0.97	1.20	1.16	0.77	0.80	1.00	0.95	0.98	1.02	1.26	1.22
65	0.94	0.97	1.20	1.16	0.77	0.80	1.00	0.95	0.98	1.02	1.26	1.22
66	0.94	0.97	1.20	1.16	0.77	0.80	1.00	0.95	0.98	1.02	1.26	1.22
67	0.94	0.97	1.20	1.16	0.77	0.80	1.00	0.95	0.98	1.02	1.26	1.22
68	0.94	0.97	1.20	1.16	0.77	0.80	1.00	0.95	0.98	1.02	1.26	1.22
69	0.94	0.97	1.20	1.16	0.77	0.80	1.00	0.95	0.98	1.02	1.26	1.22
70	0.94	0.97	1.20	1.16	0.77	0.80	1.00	0.95	0.98	1.02	1.26	1.22
71	0.94	0.97	1.20	1.16	0.77	0.80	1.00	0.95	0.98	1.02	1.26	1.22
72	0.94	0.97	1.20	1.16	0.77	0.80	1.00	0.95	0.98	1.02	1.26	1.22
73	0.94	0.97	1.20	1.16	0.77	0.80	1.00	0.95	0.98	1.02	1.26	1.22
74	0.94	0.97	1.20	1.16	0.77	0.80	1.00	0.95	0.98	1.02	1.26	1.22
75	0.94	0.97	1.20	1.16	0.77	0.80	1.00	0.95	0.98	1.02	1.26	1.22
76	0.94	0.97	1.20	1.16	0.77	0.80	1.00	0.95	0.98	1.02	1.26	1.22
77	0.94	0.97	1.20	1.16	0.77	0.80	1.00	0.95	0.98	1.02	1.26	1.22
78	0.94	0.97	1.20	1.16	0.77	0.80	1.00	0.95	0.98	1.02	1.26	1.22
79	0.94	0.97	1.20	1.16	0.77	0.80	1.00	0.95	0.98	1.02	1.26	1.22
80	0.94	0.97	1.20	1.16	0.77	0.80	1.00	0.95	0.98	1.02	1.26	1.22
81	0.94	0.97	1.20	1.16	0.77	0.80	1.00	0.95	0.98	1.02	1.26	1.22
82	1.33	1.38	1.69	1.63	1.09	1.14	1.41	1.34	1.39	1.44	1.76	1.70
83	1.45	1.50	1.84	1.77	1.19	1.23	1.53	1.45	1.51	1.57	1.92	1.85
84	1.67	1.73	2.12	2.04	1.37	1.42	1.77	1.67	1.74	1.80	2.21	2.13
85	1.34	1.39	1.71	1.65	1.10	1.14	1.42	1.35	1.40	1.45	1.78	1.72
86	1.46	1.51	1.86	1.79	1.19	1.24	1.55	1.47	1.52	1.58	1.94	1.87
87	1.68	1.74	2.14	2.06	1.37	1.43	1.78	1.69	1.76	1.82	2.23	2.15
88	1.36	1.41	1.73	1.67	1.11	1.16	1.44	1.37	1.42	1.47	1.80	1.74
89	1.48	1.54	1.89	1.82	1.21	1.27	1.57	1.49	1.55	1.61	1.97	1.90

Table G-2. Continued

#	Rock (T) = 1.5 m				Rock (T) = 1.5 m				Rock (T) = 2 m			
	E=10MPa B = 2m D = 0m	E=10MPa B = 4m D = 0m	E=10MPa B = 4m D = 2m	E=10MPa B = 2m D = 1m	E=5MPa B = 2m D = 0m	E=5MPa B = 4m D = 0m	E=5MPa B = 4m D = 2m	E=5MPa B = 2m D = 1m	E=10MPa B = 2m D = 0m	E=10 MPa B = 4m D = 0m	E=10MPa B = 4m D = 2m	E=10MPa B = 2m D = 1m
90	1.69	1.75	2.15	2.07	1.38	1.44	1.79	1.70	1.77	1.83	2.25	2.17
91	1.40	1.45	1.77	1.71	1.14	1.19	1.47	1.40	1.46	1.51	1.85	1.78
92	1.49	1.55	1.91	1.84	1.22	1.28	1.59	1.51	1.56	1.62	1.99	1.92
93	1.71	1.77	2.18	2.10	1.40	1.46	1.82	1.72	1.78	1.85	2.27	2.19
94	1.41	1.46	1.79	1.73	1.15	1.20	1.49	1.42	1.47	1.52	1.87	1.80
95	1.50	1.56	1.91	1.84	1.23	1.28	1.59	1.51	1.57	1.63	2.00	1.93
96	1.72	1.78	2.19	2.11	1.41	1.47	1.82	1.73	1.79	1.86	2.29	2.21
97	1.41	1.46	1.80	1.74	1.15	1.20	1.50	1.43	1.48	1.53	1.88	1.81
98	1.50	1.56	1.92	1.85	1.23	1.28	1.60	1.52	1.58	1.64	2.01	1.94
99	1.73	1.79	2.20	2.12	1.41	1.47	1.83	1.74	1.80	1.87	2.30	2.22
100	1.43	1.48	1.82	1.75	1.17	1.22	1.52	1.44	1.49	1.55	1.90	1.83
101	1.52	1.58	1.94	1.87	1.24	1.30	1.62	1.53	1.59	1.65	2.03	1.96
102	1.74	1.80	2.21	2.13	1.42	1.48	1.84	1.75	1.81	1.88	2.31	2.23
103	1.45	1.50	1.84	1.77	1.19	1.23	1.53	1.45	1.50	1.56	1.92	1.85
104	1.54	1.60	1.97	1.90	1.26	1.32	1.64	1.56	1.61	1.67	2.05	1.98
105	1.75	1.81	2.22	2.14	1.43	1.49	1.85	1.76	1.82	1.89	2.32	2.24
106	1.46	1.51	1.86	1.79	1.19	1.24	1.55	1.47	1.52	1.58	1.94	1.87
107	1.56	1.62	1.99	1.92	1.28	1.33	1.66	1.58	1.63	1.69	2.08	2.01
108	1.76	1.83	2.25	2.17	1.44	1.51	1.87	1.78	1.84	1.91	2.34	2.26
109	1.84	1.91	2.35	2.27	1.50	1.57	1.96	1.86	1.94	2.01	2.47	2.38
110	1.84	1.91	2.35	2.27	1.50	1.57	1.96	1.86	1.94	2.01	2.47	2.38
111	1.84	1.91	2.35	2.27	1.50	1.57	1.96	1.86	1.94	2.01	2.47	2.38
112	1.84	1.91	2.35	2.27	1.50	1.57	1.96	1.86	1.94	2.01	2.47	2.38
113	1.84	1.91	2.35	2.27	1.50	1.57	1.96	1.86	1.94	2.01	2.47	2.38
114	1.84	1.91	2.35	2.27	1.50	1.57	1.96	1.86	1.94	2.01	2.47	2.38
115	1.84	1.91	2.35	2.27	1.50	1.57	1.96	1.86	1.94	2.01	2.47	2.38
116	1.84	1.91	2.35	2.27	1.50	1.57	1.96	1.86	1.94	2.01	2.47	2.38
117	1.84	1.91	2.35	2.27	1.50	1.57	1.96	1.86	1.94	2.01	2.47	2.38
118	1.84	1.91	2.35	2.27	1.50	1.57	1.96	1.86	1.94	2.01	2.47	2.38
119	1.84	1.91	2.35	2.27	1.50	1.57	1.96	1.86	1.94	2.01	2.47	2.38
120	1.84	1.91	2.35	2.27	1.50	1.57	1.96	1.86	1.94	2.01	2.47	2.38
121	1.84	1.91	2.35	2.27	1.50	1.57	1.96	1.86	1.94	2.01	2.47	2.38
122	1.84	1.91	2.35	2.27	1.50	1.57	1.96	1.86	1.94	2.01	2.47	2.38
123	1.84	1.91	2.35	2.27	1.50	1.57	1.96	1.86	1.94	2.01	2.47	2.38
124	1.84	1.91	2.35	2.27	1.50	1.57	1.96	1.86	1.94	2.01	2.47	2.38
125	1.84	1.91	2.35	2.27	1.50	1.57	1.96	1.86	1.94	2.01	2.47	2.38
126	1.84	1.91	2.35	2.27	1.50	1.57	1.96	1.86	1.94	2.01	2.47	2.38
127	1.84	1.91	2.35	2.27	1.50	1.57	1.96	1.86	1.94	2.01	2.47	2.38
128	1.84	1.91	2.35	2.27	1.50	1.57	1.96	1.86	1.94	2.01	2.47	2.38
129	1.84	1.91	2.35	2.27	1.50	1.57	1.96	1.86	1.94	2.01	2.47	2.38
130	1.84	1.91	2.35	2.27	1.50	1.57	1.96	1.86	1.94	2.01	2.47	2.38
131	1.84	1.91	2.35	2.27	1.50	1.57	1.96	1.86	1.94	2.01	2.47	2.38
132	1.84	1.91	2.35	2.27	1.50	1.57	1.96	1.86	1.94	2.01	2.47	2.38
133	1.84	1.91	2.35	2.27	1.50	1.57	1.96	1.86	1.94	2.01	2.47	2.38
134	1.84	1.91	2.35	2.27	1.50	1.57	1.96	1.86	1.94	2.01	2.47	2.38
135	1.84	1.91	2.35	2.27	1.50	1.57	1.96	1.86	1.94	2.01	2.47	2.38
136	2.25	2.33	2.86	2.76	1.84	1.92	2.38	2.26	2.36	2.45	3.01	2.90

Table G-2. Continued

#	Rock (T) = 1.5 m				Rock (T) = 1.5 m				Rock (T) = 2 m			
	E=10MPa B = 2m D = 0m	E=10MPa B = 4m D = 0m	E=10MPa B = 4m D = 2m	E=10MPa B = 2m D = 1m	E=5MPa B = 2m D = 0m	E=5MPa B = 4m D = 0m	E=5MPa B = 4m D = 2m	E=5MPa B = 2m D = 1m	E=10MPa B = 2m D = 0m	E=10 MPa B = 4m D = 0m	E=10MPa B = 4m D = 2m	E=10MPa B = 2m D = 1m
137	2.68	2.78	3.41	3.29	2.19	2.29	2.84	2.70	2.82	2.92	3.59	3.46
138	2.70	2.80	3.43	3.31	2.21	2.31	2.86	2.72	2.84	2.94	3.61	3.48
139	2.27	2.35	2.89	2.79	1.86	1.93	2.41	2.29	2.38	2.47	3.04	2.93
140	2.68	2.78	3.41	3.29	2.19	2.29	2.84	2.70	2.82	2.92	3.59	3.46
141	2.70	2.80	3.43	3.31	2.21	2.31	2.86	2.72	2.84	2.94	3.61	3.48
142	2.29	2.38	2.92	2.81	1.87	1.96	2.43	2.31	2.41	2.50	3.07	2.96
143	2.68	2.78	3.41	3.29	2.19	2.29	2.84	2.70	2.82	2.92	3.59	3.46
144	2.70	2.80	3.43	3.31	2.21	2.31	2.86	2.72	2.84	2.94	3.61	3.48
145	2.30	2.39	2.93	2.82	1.88	1.97	2.44	2.31	2.42	2.51	3.09	2.98
146	2.68	2.78	3.41	3.29	2.19	2.29	2.84	2.70	2.82	2.92	3.59	3.46
147	2.70	2.80	3.43	3.31	2.21	2.31	2.86	2.72	2.84	2.94	3.61	3.48
148	2.32	2.41	2.96	2.85	1.90	1.98	2.47	2.34	2.45	2.54	3.12	3.01
149	2.68	2.78	3.41	3.29	2.19	2.29	2.84	2.70	2.82	2.92	3.59	3.46
150	2.70	2.80	3.43	3.31	2.21	2.31	2.86	2.72	2.84	2.94	3.61	3.48
151	2.33	2.42	2.97	2.86	1.90	1.99	2.47	2.35	2.46	2.55	3.13	3.02
152	2.68	2.78	3.41	3.29	2.19	2.29	2.84	2.70	2.82	2.92	3.59	3.46
153	2.70	2.80	3.43	3.31	2.21	2.31	2.86	2.72	2.84	2.94	3.61	3.48
154	2.34	2.43	2.99	2.88	1.91	2.00	2.49	2.36	2.47	2.56	3.14	3.03
155	2.68	2.78	3.41	3.29	2.19	2.29	2.84	2.70	2.82	2.92	3.59	3.46
156	2.70	2.80	3.43	3.31	2.21	2.31	2.86	2.72	2.84	2.94	3.61	3.48
157	2.36	2.45	3.01	2.90	1.93	2.02	2.51	2.38	2.49	2.58	3.17	306.00
158	2.68	2.78	3.41	3.29	2.19	2.29	2.84	2.70	2.82	2.92	3.59	3.46
159	2.70	2.80	3.43	3.31	2.21	2.31	2.86	2.72	2.84	2.94	3.61	3.48
160	2.44	2.47	3.03	2.92	1.99	2.03	2.52	2.40	2.51	2.60	3.19	308.00
161	2.68	2.78	3.41	3.29	2.19	2.29	2.84	2.70	2.82	2.92	3.59	3.46
162	2.70	2.80	3.43	3.31	2.21	2.31	2.86	2.72	2.84	2.94	3.61	3.48
163	2.44	2.53	3.10	2.99	1.99	2.08	2.58	2.45	2.57	2.66	3.26	3.14
164	2.94	3.05	3.74	3.61	2.40	2.51	3.12	2.96	3.10	3.21	3.94	3.80
165	3.44	3.57	4.38	4.22	2.81	2.94	3.65	3.46	3.63	3.76	4.61	4.45
166	2.47	2.56	3.14	3.03	2.02	2.11	2.62	2.49	2.59	2.69	3.30	3.18
167	2.98	3.09	3.79	3.65	2.44	2.54	3.16	2.99	3.13	3.25	3.99	3.85
168	3.46	3.59	4.41	4.25	2.83	2.96	3.67	3.49	3.65	3.78	4.64	4.48
169	2.51	2.60	3.19	3.08	2.05	2.14	2.66	2.53	2.64	2.74	3.36	3.24
170	3.01	3.12	3.84	3.70	2.46	2.57	3.20	3.04	3.17	3.29	4.04	3.90
171	3.48	3.61	4.44	4.28	2.85	2.97	3.70	3.51	3.66	3.80	4.67	4.50
172	2.55	2.64	3.24	3.12	2.08	2.17	2.70	2.56	2.68	2.78	3.41	3.29
173	3.04	3.15	3.87	3.73	2.49	2.59	3.22	3.06	3.19	3.31	4.07	3.93
174	3.51	3.64	4.47	4.31	2.87	3.00	3.72	3.54	3.69	3.83	4.70	4.53
175	2.58	2.68	3.29	3.17	2.11	2.21	2.74	2.60	2.72	2.82	3.46	3.34
176	3.07	3.18	3.90	3.76	2.51	2.62	3.25	3.08	3.23	3.35	4.11	3.96
177	3.54	3.67	4.51	4.35	2.89	3.02	3.76	3.57	3.72	3.86	4.74	4.57
178	2.62	2.72	3.34	3.22	2.14	2.24	2.78	2.64	2.76	2.86	3.52	3.40
179	3.09	3.21	3.94	3.80	2.53	2.64	3.28	3.12	3.26	3.38	4.15	4.00
180	3.55	3.68	4.52	4.36	2.90	3.03	3.77	3.58	3.73	3.87	4.76	4.59
181	2.69	2.79	3.43	3.31	2.20	2.30	2.86	2.72	2.84	2.94	3.60	3.47
182	3.14	3.26	4.00	3.86	2.57	2.68	3.33	3.17	3.30	3.42	4.21	4.06
183	3.59	3.72	4.57	4.41	2.93	3.06	3.81	3.62	3.77	3.91	4.81	4.64

Table G-2. Continued

#	Rock (T) = 1.5 m				Rock (T) = 1.5 m				Rock (T) = 2 m			
	E=10MPa B = 2m D = 0m	E=10MPa B = 4m D = 0m	E=10MPa B = 4m D = 2m	E=10MPa B = 2m D = 1m	E=5MPa B = 2m D = 0m	E=5MPa B = 4m D = 0m	E=5MPa B = 4m D = 2m	E=5MPa B = 2m D = 1m	E=10MPa B = 2m D = 0m	E=10 MPa B = 4m D = 0m	E=10MPa B = 4m D = 2m	E=10MPa B = 2m D = 1m
184	2.77	2.87	3.52	3.39	2.26	2.36	2.93	2.78	2.90	3.01	3.70	3.57
185	3.19	3.31	4.07	3.92	2.61	2.73	3.39	3.22	3.36	3.48	4.28	4.13
186	3.63	3.76	4.61	4.44	2.97	3.10	3.84	3.64	3.81	3.95	4.86	4.69
187	2.85	2.96	3.63	3.50	2.33	2.44	3.02	2.87	3.00	3.11	3.82	3.68
188	3.27	3.39	4.16	4.01	2.67	2.79	3.47	3.29	3.43	3.56	4.38	4.22
189	3.70	3.84	4.72	4.55	3.02	3.16	3.93	3.73	3.90	4.04	4.96	4.78
190	2.58	2.68	3.29	3.17	2.11	2.21	2.74	2.60	2.72	2.82	3.46	3.34
191	3.14	3.26	4.00	3.86	2.57	2.68	3.33	3.17	3.30	3.42	4.21	4.06
192	3.67	3.81	4.68	4.51	3.00	3.14	3.90	3.70	3.87	4.01	4.93	4.76
193	2.62	2.72	3.34	3.22	2.14	2.24	2.78	2.64	2.76	2.86	3.52	3.40
194	3.18	3.30	4.05	3.90	2.60	2.72	3.37	3.20	3.35	3.47	4.26	4.11
195	3.71	3.85	4.72	4.55	3.03	3.17	3.93	3.73	3.91	4.05	4.97	4.79
196	2.68	2.78	3.42	3.30	2.19	2.29	2.85	2.71	2.83	2.93	3.60	3.47
197	3.22	3.34	4.10	3.95	2.63	2.75	3.42	3.24	3.39	3.51	4.31	4.16
198	3.76	3.90	4.78	4.61	3.07	3.21	3.98	3.78	3.95	4.10	5.03	4.85
199	2.75	2.85	3.50	3.37	2.25	2.35	2.92	2.76	2.90	3.01	3.69	3.56
200	3.28	3.40	4.17	4.02	2.68	2.80	3.47	3.30	3.45	3.58	4.39	4.23
201	3.81	3.95	4.85	4.68	3.11	3.25	4.04	3.84	4.01	4.16	5.11	4.93
202	2.81	2.91	3.57	3.44	2.30	2.40	2.97	2.82	2.95	3.06	3.76	3.63
203	3.34	3.46	4.25	4.10	2.73	2.85	3.54	3.36	3.51	3.64	4.47	4.31
204	3.87	4.01	4.92	4.74	3.16	3.30	4.10	3.89	4.07	4.22	5.18	5.01
205	2.84	2.95	3.62	3.49	2.32	2.43	3.02	2.86	2.99	3.10	3.81	3.67
206	3.38	3.51	4.31	4.15	2.76	2.89	3.59	3.40	3.56	3.69	4.53	4.37
207	3.92	4.07	4.99	4.81	3.20	3.35	4.16	3.95	4.13	4.28	5.25	5.06
208	2.96	3.07	3.77	3.63	2.42	2.53	3.14	2.98	3.12	3.23	3.96	3.82
209	3.48	3.61	4.43	4.27	2.85	2.97	3.69	3.50	3.66	3.79	4.66	4.49
210	4.00	4.15	5.09	4.91	3.27	3.42	4.24	4.03	4.20	4.36	5.36	5.17
211	3.05	3.16	3.88	3.74	2.49	2.60	3.23	3.07	3.21	3.33	4.08	3.94
212	3.59	3.72	4.57	4.41	2.93	3.06	3.81	3.62	3.77	3.91	4.81	4.64
213	4.12	4.27	5.24	5.05	3.37	3.52	4.37	4.14	4.33	4.49	5.51	5.31
214	3.20	3.32	4.08	3.93	2.62	2.73	3.40	3.22	3.38	3.50	4.29	4.14
215	3.74	3.88	4.77	4.60	3.06	3.19	3.97	3.77	3.94	4.09	5.02	4.84
216	4.27	4.43	5.44	5.24	3.49	3.65	4.53	4.30	4.49	4.66	5.72	5.32
217	2.56	2.66	3.26	3.14	2.09	2.19	2.72	2.58	2.70	2.80	3.43	3.31
218	2.56	2.66	3.26	3.14	2.09	2.19	2.72	2.58	2.70	2.80	3.43	3.31
219	2.56	2.66	3.26	3.14	2.09	2.19	2.72	2.58	2.70	2.80	3.43	3.31
220	2.56	2.66	3.26	3.14	2.09	2.19	2.72	2.58	2.70	2.80	3.43	3.31
221	2.56	2.66	3.26	3.14	2.09	2.19	2.72	2.58	2.70	2.80	3.43	3.31
222	2.56	2.66	3.26	3.14	2.09	2.19	2.72	2.58	2.70	2.80	3.43	3.31
223	2.56	2.66	3.26	3.14	2.09	2.19	2.72	2.58	2.70	2.80	3.43	3.31
224	2.56	2.66	3.26	3.14	2.09	2.19	2.72	2.58	2.70	2.80	3.43	3.31
225	2.56	2.66	3.26	3.14	2.09	2.19	2.72	2.58	2.70	2.80	3.43	3.31
226	2.56	2.66	3.26	3.14	2.09	2.19	2.72	2.58	2.70	2.80	3.43	3.31
227	2.56	2.66	3.26	3.14	2.09	2.19	2.72	2.58	2.70	2.80	3.43	3.31
228	2.56	2.66	3.26	3.14	2.09	2.19	2.72	2.58	2.70	2.80	3.43	3.31
229	2.56	2.66	3.26	3.14	2.09	2.19	2.72	2.58	2.70	2.80	3.43	3.31
230	2.56	2.66	3.26	3.14	2.09	2.19	2.72	2.58	2.70	2.80	3.43	3.31

Table G-2. Continued

#	Rock (T) = 1.5 m				Rock (T) = 1.5 m				Rock (T) = 2 m			
	E=10MPa B = 2m D = 0m	E=10MPa B = 4m D = 0m	E=10MPa B = 4m D = 2m	E=10MPa B = 2m D = 1m	E=5MPa B = 2m D = 0m	E=5MPa B = 4m D = 0m	E=5MPa B = 4m D = 2m	E=5MPa B = 2m D = 1m	E=10MPa B = 2m D = 0m	E=10 MPa B = 4m D = 0m	E=10MPa B = 4m D = 2m	E=10MPa B = 2m D = 1m
231	2.56	2.66	3.26	3.14	2.09	2.19	2.72	2.58	2.70	2.80	3.43	3.31
232	2.56	2.66	3.26	3.14	2.09	2.19	2.72	2.58	2.70	2.80	3.43	3.31
233	2.56	2.66	3.26	3.14	2.09	2.19	2.72	2.58	2.70	2.80	3.43	3.31
234	2.56	2.66	3.26	3.14	2.09	2.19	2.72	2.58	2.70	2.80	3.43	3.31
235	2.56	2.66	3.26	3.14	2.09	2.19	2.72	2.58	2.70	2.80	3.43	3.31
236	2.56	2.66	3.26	3.14	2.09	2.19	2.72	2.58	2.70	2.80	3.43	3.31
237	2.56	2.66	3.26	3.14	2.09	2.19	2.72	2.58	2.70	2.80	3.43	3.31
238	2.56	2.66	3.26	3.14	2.09	2.19	2.72	2.58	2.70	2.80	3.43	3.31
239	2.56	2.66	3.26	3.14	2.09	2.19	2.72	2.58	2.70	2.80	3.43	3.31
240	2.56	2.66	3.26	3.14	2.09	2.19	2.72	2.58	2.70	2.80	3.43	3.31
241	2.56	2.66	3.26	3.14	2.09	2.19	2.72	2.58	2.70	2.80	3.43	3.31
242	2.56	2.66	3.26	3.14	2.09	2.19	2.72	2.58	2.70	2.80	3.43	3.31
243	2.56	2.66	3.26	3.14	2.09	2.19	2.72	2.58	2.70	2.80	3.43	3.31
244	3.26	3.38	4.15	4.00	2.67	2.78	3.46	3.28	3.43	3.56	4.37	4.22
245	3.74	3.88	4.77	4.60	3.06	3.19	3.97	3.77	3.94	4.09	5.02	4.84
246	3.74	3.88	4.77	4.60	3.06	3.19	3.97	3.77	3.94	4.09	5.02	4.84
247	3.28	3.40	4.17	4.02	2.68	2.80	3.47	3.30	3.45	3.58	4.39	4.23
248	3.74	3.88	4.77	4.60	3.06	3.19	3.97	3.77	3.94	4.09	5.02	4.84
249	3.74	3.88	4.77	4.60	3.06	3.19	3.97	3.77	3.94	4.09	5.02	4.84
250	3.30	3.42	4.20	4.05	2.70	2.82	3.50	3.32	3.47	3.60	4.42	4.26
251	3.74	3.88	4.77	4.60	3.06	3.19	3.97	3.77	3.94	4.09	5.02	4.84
252	3.74	3.88	4.77	4.60	3.06	3.19	3.97	3.77	3.94	4.09	5.02	4.84
253	3.32	3.44	4.23	4.08	2.71	2.83	3.52	3.35	3.49	3.62	4.45	4.29
254	3.74	3.88	4.77	4.60	3.06	3.19	3.97	3.77	3.94	4.09	5.02	4.84
255	3.74	3.88	4.77	4.60	3.06	3.19	3.97	3.77	3.94	4.09	5.02	4.84
256	3.38	3.51	4.31	4.15	2.76	2.89	3.59	3.40	3.56	3.69	4.53	4.37
257	3.74	3.88	4.77	4.60	3.06	3.19	3.97	3.77	3.94	4.09	5.02	4.84
258	3.74	3.88	4.77	4.60	3.06	3.19	3.97	3.77	3.94	4.09	5.02	4.84
259	3.40	3.53	4.33	4.17	2.78	2.91	3.61	3.42	3.58	3.71	4.55	4.39
260	3.74	3.88	4.77	4.60	3.06	3.19	3.97	3.77	3.94	4.09	5.02	4.84
261	3.74	3.88	4.77	4.60	3.06	3.19	3.97	3.77	3.94	4.09	5.02	4.84
262	3.42	3.55	4.36	4.20	2.80	2.92	3.63	3.45	3.61	3.74	4.59	4.43
263	3.74	3.88	4.77	4.60	3.06	3.19	3.97	3.77	3.94	4.09	5.02	4.84
264	3.74	3.88	4.77	4.60	3.06	3.19	3.97	3.77	3.94	4.09	5.02	4.84
265	3.44	3.57	4.38	4.22	2.81	2.94	3.65	3.46	3.63	3.76	4.61	4.45
266	3.74	3.88	4.77	4.60	3.06	3.19	3.97	3.77	3.94	4.09	5.02	4.84
267	3.74	3.88	4.77	4.60	3.06	3.19	3.97	3.77	3.94	4.09	5.02	4.84
268	3.46	3.59	4.41	4.25	2.83	2.96	3.67	3.49	3.65	3.78	4.64	4.48
269	3.74	3.88	4.77	4.60	3.06	3.19	3.97	3.77	3.94	4.09	5.02	4.84
270	3.74	3.88	4.77	4.60	3.06	3.19	3.97	3.77	3.94	4.09	5.02	4.84
271	3.63	3.76	4.61	4.44	2.97	3.10	3.84	3.64	3.81	3.95	4.86	4.69
272	4.15	4.30	5.28	5.09	3.39	3.54	4.40	4.18	4.36	4.52	5.55	5.35
273	4.64	4.81	5.90	5.69	3.79	3.96	4.92	4.67	4.88	5.06	6.21	5.99
274	3.66	3.80	4.66	4.49	2.99	3.13	3.88	3.68	3.85	3.99	4.90	4.73
275	4.18	4.34	5.32	5.13	3.42	3.57	4.43	4.21	4.40	4.56	5.60	5.40
276	4.67	4.84	5.94	5.73	3.82	3.98	4.95	4.70	4.91	5.09	6.25	6.03
277	3.70	3.84	4.72	4.55	3.02	3.16	3.93	3.73	3.90	4.04	4.96	4.78

Table G-2. Continued

#	Rock (T) = 1.5 m				Rock (T) = 1.5 m				Rock (T) = 2 m			
	E=10MPa B = 2m D = 0m	E=10MPa B = 4m D = 0m	E=10MPa B = 4m D = 2m	E=10MPa B = 2m D = 1m	E=5MPa B = 2m D = 0m	E=5MPa B = 4m D = 0m	E=5MPa B = 4m D = 2m	E=5MPa B = 2m D = 1m	E=10MPa B = 2m D = 0m	E=10 MPa B = 4m D = 0m	E=10MPa B = 4m D = 2m	E=10MPa B = 2m D = 1m
278	4.21	4.37	5.37	5.18	3.44	3.60	4.47	4.25	4.44	4.60	5.65	5.45
279	4.70	4.88	5.99	5.77	3.84	4.02	4.99	4.73	4.95	5.13	6.30	6.08
280	3.74	3.88	4.76	4.59	3.06	3.19	3.97	3.77	3.93	4.08	5.01	4.83
281	4.25	4.41	5.42	5.22	3.47	3.63	4.52	4.28	4.47	4.64	5.70	5.50
282	4.73	4.91	6.03	5.81	3.87	4.04	5.02	4.77	4.99	5.17	6.35	6.12
283	3.81	3.95	4.85	4.68	3.11	3.25	4.04	3.84	4.01	4.16	5.11	4.93
284	4.28	4.44	5.46	5.26	3.50	3.66	4.55	4.32	4.50	4.67	5.74	5.54
285	4.77	4.95	6.07	5.85	3.90	4.08	5.06	4.80	5.02	5.20	6.39	6.16
286	3.85	3.99	4.90	4.72	3.15	3.28	4.08	3.87	4.05	4.20	5.16	4.98
287	4.31	4.47	5.49	5.29	3.52	3.68	4.57	4.34	4.54	4.71	5.78	5.58
288	4.80	4.98	6.11	5.89	3.92	4.10	5.09	4.83	5.05	5.24	6.43	6.20
289	3.90	4.05	4.98	4.80	3.19	3.33	4.15	3.94	4.11	4.26	5.24	5.05
290	4.37	4.53	5.56	5.36	3.57	3.73	4.63	4.40	4.60	4.77	5.85	5.64
291	4.85	5.03	6.18	5.96	3.97	4.14	5.15	4.89	5.11	5.30	6.50	6.27
292	4.00	4.15	5.09	4.91	3.27	3.42	4.24	4.03	4.20	4.36	5.36	5.17
293	4.46	4.63	5.68	5.48	3.65	3.81	4.73	4.50	4.70	4.87	5.98	5.77
294	4.93	5.11	6.27	6.04	4.03	4.21	5.22	4.95	5.18	5.37	6.60	6.37
295	4.11	4.26	5.23	5.04	3.36	3.51	4.36	4.13	4.32	4.48	5.50	5.31
296	4.57	4.74	5.83	5.62	3.74	3.90	4.86	4.61	4.81	4.99	6.13	5.91
297	5.01	5.20	6.39	6.16	4.10	4.28	5.32	5.05	5.28	5.47	6.72	6.48
298	3.87	4.01	4.92	4.74	3.16	3.30	4.10	3.89	4.07	4.22	5.18	5.00
299	4.43	4.59	5.63	5.43	3.62	3.78	4.69	4.45	4.66	4.83	5.93	5.72
300	4.92	5.10	6.27	6.04	4.02	4.20	5.22	4.95	5.18	5.37	6.59	6.36
301	3.92	4.07	4.99	4.81	3.20	3.35	4.16	3.95	4.13	4.28	5.25	5.06
302	4.47	4.64	5.70	5.49	3.65	3.82	4.75	4.50	4.71	4.88	5.99	5.78
303	4.98	5.17	6.34	6.11	4.07	4.26	5.28	5.01	5.24	5.43	6.67	6.43
304	3.98	4.13	5.07	4.89	3.25	3.40	4.22	4.01	4.19	4.34	5.33	5.14
305	4.54	4.71	5.78	5.57	3.71	3.88	4.82	4.57	4.77	4.95	6.08	5.86
306	5.03	5.22	6.41	6.18	4.11	4.30	5.34	5.07	5.29	5.49	6.75	6.51
307	4.04	4.19	5.14	4.95	3.30	3.45	4.28	4.06	4.24	4.40	5.41	5.22
308	4.59	4.76	5.85	5.64	3.75	3.92	4.87	4.63	4.83	5.01	6.15	5.93
309	5.11	5.30	6.51	6.28	4.18	4.36	5.42	5.15	5.38	5.58	6.85	6.61
310	4.15	4.30	5.28	5.09	3.39	3.54	4.40	4.18	4.36	4.52	5.55	5.35
311	4.65	4.82	5.92	5.71	3.80	3.97	4.93	4.68	4.89	5.07	6.23	6.01
312	5.19	5.38	6.61	6.37	4.24	4.43	5.51	5.23	5.46	5.66	6.95	6.70
313	4.21	4.37	5.36	5.17	3.44	3.60	4.47	4.24	4.43	4.59	5.64	5.44
314	4.73	4.91	6.03	5.81	3.87	4.04	5.02	4.77	4.99	5.17	6.35	6.12
315	5.29	5.49	6.74	6.50	4.32	4.52	5.62	5.33	5.57	5.78	7.10	6.85
316	4.31	4.47	5.49	5.29	3.52	3.68	4.57	4.34	4.54	4.71	5.78	5.58
317	4.89	5.07	6.23	6.01	4.00	4.17	5.19	4.93	5.15	5.34	6.55	6.32
318	5.39	5.59	6.87	6.62	4.41	4.60	5.72	5.43	5.67	5.88	7.23	6.97
319	4.52	4.69	5.76	5.55	3.70	3.86	4.80	4.55	4.75	4.93	6.06	5.85
320	5.01	5.20	6.39	6.16	4.10	4.28	5.32	5.05	5.28	5.47	6.72	6.48
321	5.51	5.71	7.01	6.76	4.50	4.70	5.84	5.55	5.79	6.00	7.37	7.11
322	4.75	4.93	6.06	5.84	3.88	4.06	5.05	4.79	5.01	5.19	6.37	6.15
323	5.24	5.44	6.68	6.44	4.28	4.48	5.57	5.28	5.52	5.72	7.02	6.77
324	5.71	5.92	7.27	7.01	4.67	4.87	6.06	5.75	6.01	6.23	7.65	7.38

Table G-3. FEM simulation results – Bearing capacity (MPa) on 2 to 4-m rock over sand subsurface – Plane strain only

Note: The shaded texts have no significances. They only help with readability across the columns. The dim texts mean that they have the same results as the above row(s), thus, the differences in results of other rows are easily distinguished.

#	Rock (T) = 2 m				Rock (T) = 4 m				Rock (T) = 4 m			
	E=5MPa B = 2m D = 0m	E=5MPa B = 4m D = 0m	E=5MPa B = 4m D = 2m	E=5MPa B = 2m D = 1m	E=10MPa B = 2m D = 0m	E=10MPa B = 4m D = 0m	E=10MPa B = 4m D = 2m	E=10MPa B = 2m D = 1m	E=5MPa B = 2m D = 0m	E=5MPa B = 4m D = 0m	E=5MPa B = 4m D = 2m	E=5MPa B = 2m D = 1m
1	0.33	0.33	0.42	0.40	0.48	0.50	0.62	0.60	0.48	0.50	0.62	0.60
2-27	same	results										
28	0.43	0.44	0.54	0.52	0.64	0.66	0.81	0.78	0.64	0.66	0.81	0.78
29	0.43	0.44	0.54	0.52	0.64	0.66	0.81	0.78	0.64	0.66	0.81	0.78
30	0.43	0.44	0.54	0.52	0.64	0.66	0.81	0.78	0.64	0.66	0.81	0.78
31	0.43	0.44	0.54	0.52	0.64	0.66	0.81	0.78	0.64	0.66	0.81	0.78
32	0.43	0.44	0.54	0.52	0.64	0.66	0.81	0.78	0.64	0.66	0.81	0.78
33	0.43	0.44	0.54	0.52	0.64	0.66	0.81	0.78	0.64	0.66	0.81	0.78
34	0.43	0.44	0.54	0.52	0.64	0.66	0.81	0.78	0.64	0.66	0.81	0.78
35	0.43	0.44	0.54	0.52	0.64	0.66	0.81	0.78	0.64	0.66	0.81	0.78
36	0.43	0.44	0.54	0.52	0.64	0.66	0.81	0.78	0.64	0.66	0.81	0.78
37	0.43	0.44	0.54	0.52	0.64	0.66	0.81	0.78	0.64	0.66	0.81	0.78
38	0.43	0.44	0.54	0.52	0.64	0.66	0.81	0.78	0.64	0.66	0.81	0.78
39	0.43	0.44	0.54	0.52	0.64	0.66	0.81	0.78	0.64	0.66	0.81	0.78
40	0.43	0.44	0.54	0.52	0.64	0.66	0.81	0.78	0.64	0.66	0.81	0.78
41	0.43	0.44	0.54	0.52	0.64	0.66	0.81	0.78	0.64	0.66	0.81	0.78
42	0.43	0.44	0.54	0.52	0.64	0.66	0.81	0.78	0.64	0.66	0.81	0.78
43	0.43	0.44	0.54	0.52	0.64	0.66	0.81	0.78	0.64	0.66	0.81	0.78
44	0.43	0.44	0.54	0.52	0.64	0.66	0.81	0.78	0.64	0.66	0.81	0.78
45	0.43	0.44	0.54	0.52	0.64	0.66	0.81	0.78	0.64	0.66	0.81	0.78
46	0.43	0.44	0.54	0.52	0.64	0.66	0.81	0.78	0.64	0.66	0.81	0.78
47	0.43	0.44	0.54	0.52	0.64	0.66	0.81	0.78	0.64	0.66	0.81	0.78
48	0.43	0.44	0.54	0.52	0.64	0.66	0.81	0.78	0.64	0.66	0.81	0.78
49	0.43	0.44	0.54	0.52	0.64	0.66	0.81	0.78	0.64	0.66	0.81	0.78
50	0.43	0.44	0.54	0.52	0.64	0.66	0.81	0.78	0.64	0.66	0.81	0.78
51	0.43	0.44	0.54	0.52	0.64	0.66	0.81	0.78	0.64	0.66	0.81	0.78
52	0.43	0.44	0.54	0.52	0.64	0.66	0.81	0.78	0.64	0.66	0.81	0.78
53	0.43	0.44	0.54	0.52	0.64	0.66	0.81	0.78	0.64	0.66	0.81	0.78
54	0.43	0.44	0.54	0.52	0.64	0.66	0.81	0.78	0.64	0.66	0.81	0.78
55	0.87	0.90	1.12	1.08	1.30	1.35	1.66	1.60	1.29	1.34	1.65	1.59
56	0.87	0.90	1.12	1.08	1.30	1.35	1.66	1.60	1.29	1.34	1.65	1.59
57	0.87	0.90	1.12	1.08	1.30	1.35	1.66	1.60	1.29	1.34	1.65	1.59
58	0.87	0.90	1.12	1.08	1.30	1.35	1.66	1.60	1.29	1.34	1.65	1.59
59	0.87	0.90	1.12	1.08	1.30	1.35	1.66	1.60	1.29	1.34	1.65	1.59
60	0.87	0.90	1.12	1.08	1.30	1.35	1.66	1.60	1.29	1.34	1.65	1.59
61	0.87	0.90	1.12	1.08	1.30	1.35	1.66	1.60	1.29	1.34	1.65	1.59
62	0.87	0.90	1.12	1.08	1.30	1.35	1.66	1.60	1.29	1.34	1.65	1.59
63	0.87	0.90	1.12	1.08	1.30	1.35	1.66	1.60	1.29	1.34	1.65	1.59
64	0.87	0.90	1.12	1.08	1.30	1.35	1.66	1.60	1.29	1.34	1.65	1.59
65	0.87	0.90	1.12	1.08	1.30	1.35	1.66	1.60	1.29	1.34	1.65	1.59
66	0.87	0.90	1.12	1.08	1.30	1.35	1.66	1.60	1.29	1.34	1.65	1.59
67	0.87	0.90	1.12	1.08	1.30	1.35	1.66	1.60	1.29	1.34	1.65	1.59
68	0.87	0.90	1.12	1.08	1.30	1.35	1.66	1.60	1.29	1.34	1.65	1.59

Table G-3. Continued

#	Rock (T) = 2 m				Rock (T) = 4 m				Rock (T) = 4 m			
	E=5MPa B = 2m D = 0m	E=5MPa B = 4m D = 0m	E=5MPa B = 4m D = 2m	E=5MPa B = 2m D = 1m	E=10MPa B = 2m D = 0m	E=10MPa B = 4m D = 0m	E=10MPa B = 4m D = 2m	E=10MPa B = 2m D = 1m	E=5MPa B = 2m D = 0m	E=5MPa B = 4m D = 0m	E=5MPa B = 4m D = 2m	E=5MPa B = 2m D = 1m
69	0.87	0.90	1.12	1.08	1.30	1.35	1.66	1.60	1.29	1.34	1.65	1.59
70	0.87	0.90	1.12	1.08	1.30	1.35	1.66	1.60	1.29	1.34	1.65	1.59
71	0.87	0.90	1.12	1.08	1.30	1.35	1.66	1.60	1.29	1.34	1.65	1.59
72	0.87	0.90	1.12	1.08	1.30	1.35	1.66	1.60	1.29	1.34	1.65	1.59
73	0.87	0.90	1.12	1.08	1.30	1.35	1.66	1.60	1.29	1.34	1.65	1.59
74	0.87	0.90	1.12	1.08	1.30	1.35	1.66	1.60	1.29	1.34	1.65	1.59
75	0.87	0.90	1.12	1.08	1.30	1.35	1.66	1.60	1.29	1.34	1.65	1.59
76	0.87	0.90	1.12	1.08	1.30	1.35	1.66	1.60	1.29	1.34	1.65	1.59
77	0.87	0.90	1.12	1.08	1.30	1.35	1.66	1.60	1.29	1.34	1.65	1.59
78	0.87	0.90	1.12	1.08	1.30	1.35	1.66	1.60	1.29	1.34	1.65	1.59
79	0.87	0.90	1.12	1.08	1.30	1.35	1.66	1.60	1.29	1.34	1.65	1.59
80	0.87	0.90	1.12	1.08	1.30	1.35	1.66	1.60	1.29	1.34	1.65	1.59
81	0.87	0.90	1.12	1.08	1.30	1.35	1.66	1.60	1.29	1.34	1.65	1.59
82	1.23	1.27	1.57	1.51	1.83	1.90	2.34	2.26	1.82	1.89	2.33	2.25
83	1.34	1.38	1.71	1.64	2.01	2.08	2.55	2.46	2.00	2.07	2.54	2.45
84	1.54	1.59	1.97	1.89	2.31	2.39	2.93	2.83	2.30	2.38	2.92	2.82
85	1.24	1.28	1.59	1.53	1.85	1.92	2.36	2.28	1.84	1.91	2.35	2.27
86	1.35	1.39	1.73	1.66	2.02	2.09	2.57	2.48	2.01	2.08	2.56	2.47
87	1.56	1.60	1.99	1.91	2.33	2.41	2.95	2.85	2.32	2.40	2.94	2.84
88	1.26	1.30	1.61	1.55	1.88	1.95	2.39	2.31	1.87	1.94	2.38	2.30
89	1.38	1.42	1.76	1.69	2.05	2.13	2.61	2.52	2.04	2.12	2.60	2.51
90	1.57	1.61	2.01	1.93	2.33	2.42	2.98	2.88	2.32	2.41	2.97	2.87
91	1.30	1.33	1.65	1.58	1.93	2.00	2.45	2.36	1.92	1.99	2.44	2.35
92	1.38	1.43	1.78	1.70	2.06	2.14	2.63	2.54	2.05	2.13	2.62	2.53
93	1.58	1.63	2.03	1.94	2.36	2.45	3.01	2.90	2.35	2.44	2.99	2.89
94	1.30	1.34	1.67	1.60	1.94	2.01	2.47	2.38	1.93	2.00	2.46	2.37
95	1.39	1.44	1.78	1.71	2.07	2.15	2.64	2.55	2.06	2.14	2.63	2.54
96	1.59	1.64	2.04	1.96	2.38	2.47	3.03	2.92	2.37	2.46	3.01	2.91
97	1.31	1.35	1.68	1.61	1.95	2.02	2.48	2.39	1.94	2.01	2.47	2.38
98	1.40	1.45	1.79	1.72	2.08	2.16	2.66	2.57	2.07	2.15	2.65	2.56
99	1.60	1.65	2.05	1.97	2.38	2.47	3.04	2.93	2.37	2.46	3.02	2.92
100	1.32	1.37	1.70	1.62	1.98	2.05	2.52	2.43	1.97	2.04	2.51	2.42
101	1.41	1.45	1.81	1.74	2.11	2.19	2.69	2.60	2.10	2.18	2.68	2.59
102	1.61	1.66	2.06	1.98	2.40	2.49	3.06	2.95	2.39	2.48	3.04	2.94
103	1.33	1.38	1.71	1.64	2.01	2.07	2.54	2.45	2.00	2.06	2.53	2.44
104	1.43	1.47	1.83	1.76	2.13	2.21	2.72	2.62	2.12	2.20	2.71	2.61
105	1.62	1.67	2.07	1.99	2.41	2.50	3.07	2.96	2.40	2.49	3.05	2.95
106	1.35	1.39	1.73	1.66	2.02	2.09	2.57	2.48	2.01	2.08	2.56	2.47
107	1.45	1.49	1.86	1.78	2.16	2.24	2.75	2.65	2.15	2.23	2.74	2.64
108	1.63	1.68	2.09	2.01	2.44	2.53	3.10	2.99	2.43	2.52	3.08	2.98
109	1.72	1.77	2.20	2.11	2.55	2.64	3.24	3.13	2.54	2.63	3.22	3.11
110	1.72	1.77	2.20	2.11	2.55	2.64	3.24	3.13	2.54	2.63	3.22	3.11
111	1.72	1.77	2.20	2.11	2.55	2.64	3.24	3.13	2.54	2.63	3.22	3.11
112	1.72	1.77	2.20	2.11	2.55	2.64	3.24	3.13	2.54	2.63	3.22	3.11
113	1.72	1.77	2.20	2.11	2.55	2.64	3.24	3.13	2.54	2.63	3.22	3.11
114	1.72	1.77	2.20	2.11	2.55	2.64	3.24	3.13	2.54	2.63	3.22	3.11
115	1.72	1.77	2.20	2.11	2.55	2.64	3.24	3.13	2.54	2.63	3.22	3.11

Table G-3. Continued

#	Rock (T) = 2 m				Rock (T) = 4 m				Rock (T) = 4 m			
	E=5MPa B = 2m D = 0m	E=5MPa B = 4m D = 0m	E=5MPa B = 4m D = 2m	E=5MPa B = 2m D = 1m	E=10MPa B = 2m D = 0m	E=10MPa B = 4m D = 0m	E=10MPa B = 4m D = 2m	E=10MPa B = 2m D = 1m	E=5MPa B = 2m D = 0m	E=5MPa B = 4m D = 0m	E=5MPa B = 4m D = 2m	E=5MPa B = 2m D = 1m
116	1.72	1.77	2.20	2.11	2.55	2.64	3.24	3.13	2.54	2.63	3.22	3.11
117	1.72	1.77	2.20	2.11	2.55	2.64	3.24	3.13	2.54	2.63	3.22	3.11
118	1.72	1.77	2.20	2.11	2.55	2.64	3.24	3.13	2.54	2.63	3.22	3.11
119	1.72	1.77	2.20	2.11	2.55	2.64	3.24	3.13	2.54	2.63	3.22	3.11
120	1.72	1.77	2.20	2.11	2.55	2.64	3.24	3.13	2.54	2.63	3.22	3.11
121	1.72	1.77	2.20	2.11	2.55	2.64	3.24	3.13	2.54	2.63	3.22	3.11
122	1.72	1.77	2.20	2.11	2.55	2.64	3.24	3.13	2.54	2.63	3.22	3.11
123	1.72	1.77	2.20	2.11	2.55	2.64	3.24	3.13	2.54	2.63	3.22	3.11
124	1.72	1.77	2.20	2.11	2.55	2.64	3.24	3.13	2.54	2.63	3.22	3.11
125	1.72	1.77	2.20	2.11	2.55	2.64	3.24	3.13	2.54	2.63	3.22	3.11
126	1.72	1.77	2.20	2.11	2.55	2.64	3.24	3.13	2.54	2.63	3.22	3.11
127	1.72	1.77	2.20	2.11	2.55	2.64	3.24	3.13	2.54	2.63	3.22	3.11
128	1.72	1.77	2.20	2.11	2.55	2.64	3.24	3.13	2.54	2.63	3.22	3.11
129	1.72	1.77	2.20	2.11	2.55	2.64	3.24	3.13	2.54	2.63	3.22	3.11
130	1.72	1.77	2.20	2.11	2.55	2.64	3.24	3.13	2.54	2.63	3.22	3.11
131	1.72	1.77	2.20	2.11	2.55	2.64	3.24	3.13	2.54	2.63	3.22	3.11
132	1.72	1.77	2.20	2.11	2.55	2.64	3.24	3.13	2.54	2.63	3.22	3.11
133	1.72	1.77	2.20	2.11	2.55	2.64	3.24	3.13	2.54	2.63	3.22	3.11
134	1.72	1.77	2.20	2.11	2.55	2.64	3.24	3.13	2.54	2.63	3.22	3.11
135	1.72	1.77	2.20	2.11	2.55	2.64	3.24	3.13	2.54	2.63	3.22	3.11
136	2.09	2.16	2.69	2.58	3.11	3.22	3.96	3.82	3.09	3.20	3.94	3.80
137	2.50	2.57	3.20	3.07	3.70	3.84	4.71	4.55	3.68	3.82	4.69	4.53
138	2.52	2.59	3.22	3.09	3.72	3.86	4.75	4.58	3.70	3.84	4.73	4.56
139	2.11	2.18	2.71	2.60	3.14	3.25	3.99	3.85	3.12	3.23	3.97	3.83
140	2.50	2.57	3.20	3.07	3.70	3.84	4.71	4.55	3.68	3.82	4.69	4.53
141	2.52	2.59	3.22	3.09	3.72	3.86	4.75	4.58	3.70	3.84	4.73	4.56
142	2.14	2.20	2.74	2.63	3.16	3.28	4.03	3.89	3.14	3.26	4.01	3.87
143	2.50	2.57	3.20	3.07	3.70	3.84	4.71	4.55	3.68	3.82	4.69	4.53
144	2.52	2.59	3.22	3.09	3.72	3.86	4.75	4.58	3.70	3.84	4.73	4.56
145	2.15	2.21	2.76	2.65	3.18	3.30	4.05	3.91	3.16	3.28	4.03	3.89
146	2.50	2.57	3.20	3.07	3.70	3.84	4.71	4.55	3.68	3.82	4.69	4.53
147	2.52	2.59	3.22	3.09	3.72	3.86	4.75	4.58	3.70	3.84	4.73	4.56
148	2.17	2.24	2.78	2.67	3.21	3.33	4.10	3.96	3.19	3.31	4.08	3.94
149	2.50	2.57	3.20	3.07	3.70	3.84	4.71	4.55	3.68	3.82	4.69	4.53
150	2.52	2.59	3.22	3.09	3.72	3.86	4.75	4.58	3.70	3.84	4.73	4.56
151	2.18	2.25	2.79	2.68	3.22	3.34	4.11	3.97	3.20	3.32	4.09	3.95
152	2.50	2.57	3.20	3.07	3.70	3.84	4.71	4.55	3.68	3.82	4.69	4.53
153	2.52	2.59	3.22	3.09	3.72	3.86	4.75	4.58	3.70	3.84	4.73	4.56
154	2.19	2.26	2.80	2.69	3.24	3.36	4.13	3.99	3.22	3.34	4.11	3.97
155	2.50	2.57	3.20	3.07	3.70	3.84	4.71	4.55	3.68	3.82	4.69	4.53
156	2.52	2.59	3.22	3.09	3.72	3.86	4.75	4.58	3.70	3.84	4.73	4.56
157	2.21	2.27	2.83	2.71	3.27	3.39	4.16	4.01	3.25	3.37	4.14	3.99
158	2.50	2.57	3.20	3.07	3.70	3.84	4.71	4.55	3.68	3.82	4.69	4.53
159	2.52	2.59	3.22	3.09	3.72	3.86	4.75	4.58	3.70	3.84	4.73	4.56
160	2.23	2.29	2.85	2.73	3.29	3.41	4.19	4.04	3.27	3.39	4.17	4.02
161	2.50	2.57	3.20	3.07	3.70	3.84	4.71	4.55	3.68	3.82	4.69	4.53
162	2.52	2.59	3.22	3.09	3.72	3.86	4.75	4.58	3.70	3.84	4.73	4.56

Table G-3. Continued

#	Rock (T) = 2 m				Rock (T) = 4 m				Rock (T) = 4 m			
	E=5MPa B = 2m D = 0m	E=5MPa B = 4m D = 0m	E=5MPa B = 4m D = 2m	E=5MPa B = 2m D = 1m	E=10MPa B = 2m D = 0m	E=10MPa B = 4m D = 0m	E=10MPa B = 4m D = 2m	E=10MPa B = 2m D = 1m	E=5MPa B = 2m D = 0m	E=5MPa B = 4m D = 0m	E=5MPa B = 4m D = 2m	E=5MPa B = 2m D = 1m
163	2.28	2.34	2.91	2.79	3.37	3.49	4.29	4.14	3.35	3.47	4.27	4.12
164	2.75	2.83	3.52	3.37	4.06	4.21	5.17	4.99	4.04	4.19	5.14	4.97
165	3.22	3.31	4.11	3.95	4.76	4.93	6.06	5.85	4.74	4.91	6.03	5.82
166	2.30	2.37	2.94	2.82	3.41	3.53	4.34	4.19	3.39	3.51	4.32	4.17
167	2.78	2.87	3.56	3.42	4.11	4.26	5.24	5.06	4.09	4.24	5.21	5.03
168	3.24	3.33	4.14	3.98	4.79	4.96	6.09	5.88	4.77	4.94	6.06	5.85
169	2.34	2.42	3.00	2.88	3.47	3.60	4.42	4.27	3.45	3.58	4.40	4.25
170	2.81	2.90	3.61	3.46	4.17	4.32	5.30	5.11	4.15	4.30	5.27	5.08
171	3.25	3.35	4.17	4.00	4.81	4.99	6.13	5.92	4.79	4.97	6.10	5.89
172	2.38	2.45	3.04	2.92	3.52	3.65	4.48	4.32	3.50	3.63	4.46	4.30
173	2.83	2.92	3.63	3.49	4.20	4.35	5.34	5.15	4.18	4.33	5.31	5.12
174	3.28	3.38	4.19	4.02	4.85	5.03	6.17	5.95	4.83	5.00	6.14	5.92
175	2.41	2.49	3.09	2.97	3.57	3.70	4.54	4.38	3.55	3.68	4.52	4.36
176	2.87	2.95	3.67	3.52	4.24	4.39	5.40	5.21	4.22	4.37	5.37	5.18
177	3.30	3.40	4.23	4.06	4.89	5.07	6.23	6.01	4.87	5.04	6.20	5.98
178	2.45	2.52	3.14	3.02	3.63	3.76	4.62	4.46	3.61	3.74	4.60	4.44
179	2.89	2.98	3.70	3.55	4.28	4.44	5.45	5.26	4.26	4.42	5.42	5.23
180	3.31	3.41	4.25	4.08	4.91	5.09	6.25	6.03	4.89	5.06	6.22	6.00
181	2.52	2.59	3.21	3.08	3.72	3.86	4.73	4.56	3.70	3.84	4.71	4.54
182	2.93	3.01	3.76	3.61	4.34	4.50	5.52	5.33	4.32	4.48	5.49	5.30
183	3.35	3.45	4.29	4.12	4.96	5.14	6.31	6.09	4.94	5.11	6.28	6.06
184	2.57	2.65	3.30	3.17	3.82	3.96	4.86	4.69	3.80	3.94	4.84	4.67
185	2.98	3.07	3.82	3.67	4.42	4.58	5.62	5.42	4.40	4.56	5.59	5.39
186	3.38	3.48	4.34	4.16	5.01	5.19	6.38	6.16	4.98	5.16	6.35	6.13
187	2.66	2.74	3.41	3.27	3.95	4.09	5.02	4.84	3.93	4.07	4.99	4.82
188	3.04	3.14	3.91	3.75	4.52	4.68	5.75	5.55	4.50	4.66	5.72	5.52
189	3.46	3.56	4.43	4.24	5.12	5.31	6.52	6.29	5.09	5.28	6.49	6.26
190	2.41	2.49	3.09	2.97	3.57	3.70	4.54	4.38	3.55	3.68	4.52	4.36
191	2.93	3.01	3.76	3.61	4.34	4.50	5.52	5.33	4.32	4.48	5.49	5.30
192	3.44	3.54	4.40	4.23	5.08	5.27	6.47	6.24	5.05	5.24	6.44	6.21
193	2.45	2.52	3.14	3.02	3.63	3.76	4.62	4.46	3.61	3.74	4.60	4.44
194	2.97	3.06	3.80	3.65	4.40	4.56	5.60	5.40	4.38	4.54	5.57	5.37
195	3.47	3.57	4.44	4.25	5.12	5.31	6.53	6.30	5.09	5.28	6.50	6.27
196	2.51	2.58	3.21	3.08	3.71	3.85	4.72	4.55	3.69	3.83	4.70	4.53
197	3.01	3.09	3.85	3.69	4.45	4.61	5.66	5.46	4.43	4.59	5.63	5.43
198	3.51	3.61	4.49	4.31	5.19	5.38	6.61	6.38	5.16	5.35	6.58	6.35
199	2.57	2.65	3.29	3.16	3.80	3.94	4.84	4.67	3.78	3.92	4.82	4.65
200	3.06	3.16	3.92	3.76	4.53	4.70	5.77	5.57	4.51	4.68	5.74	5.54
201	3.56	3.67	4.56	4.38	5.27	5.46	6.71	6.48	5.24	5.43	6.68	6.45
202	2.62	2.70	3.36	3.22	3.88	4.02	4.94	4.77	3.86	4.00	4.92	4.75
203	3.12	3.21	3.99	3.83	4.61	4.78	5.88	5.67	4.59	4.76	5.85	5.64
204	3.61	3.72	4.62	4.45	5.34	5.54	6.80	6.56	5.31	5.51	6.77	6.53
205	2.65	2.73	3.40	3.26	3.93	4.07	5.00	4.83	3.91	4.05	4.98	4.81
206	3.16	3.25	4.04	3.88	4.68	4.85	5.95	5.74	4.66	4.83	5.92	5.71
207	3.67	3.77	4.68	4.49	5.42	5.62	6.90	6.66	5.39	5.59	6.87	6.63
208	2.77	2.85	3.53	3.39	4.09	4.24	5.20	5.02	4.07	4.22	5.17	4.99
209	3.25	3.34	4.16	3.99	4.80	4.98	6.12	5.91	4.78	4.96	6.09	5.88

Table G-3. Continued

#	Rock (T) = 2 m				Rock (T) = 4 m				Rock (T) = 4 m			
	E=5MPa B = 2m D = 0m	E=5MPa B = 4m D = 0m	E=5MPa B = 4m D = 2m	E=5MPa B = 2m D = 1m	E=10MPa B = 2m D = 0m	E=10MPa B = 4m D = 0m	E=10MPa B = 4m D = 2m	E=10MPa B = 2m D = 1m	E=5MPa B = 2m D = 0m	E=5MPa B = 4m D = 0m	E=5MPa B = 4m D = 2m	E=5MPa B = 2m D = 1m
210	3.73	3.84	4.78	4.59	5.53	5.73	7.04	6.79	5.50	5.70	7.00	6.76
211	2.85	2.94	3.64	3.50	4.22	4.37	5.36	5.17	4.20	4.35	5.33	5.14
212	3.35	3.45	4.29	4.12	4.96	5.14	6.31	6.09	4.94	5.11	6.28	6.06
213	3.84	3.96	4.92	4.71	5.69	5.90	7.24	6.99	5.66	5.87	7.20	6.96
214	3.00	3.09	3.83	3.68	4.43	4.59	5.64	5.44	4.41	4.57	5.61	5.41
215	3.50	3.61	4.48	4.30	5.18	5.37	6.59	6.36	5.15	5.34	6.56	6.33
216	3.99	4.11	5.10	4.72	5.90	6.12	7.52	7.26	5.87	6.09	7.48	7.22
217	2.40	2.47	3.06	2.94	3.54	3.67	4.51	4.35	3.52	3.65	4.49	4.33
218	2.40	2.47	3.06	2.94	3.54	3.67	4.51	4.35	3.52	3.65	4.49	4.33
219	2.40	2.47	3.06	2.94	3.54	3.67	4.51	4.35	3.52	3.65	4.49	4.33
220	2.40	2.47	3.06	2.94	3.54	3.67	4.51	4.35	3.52	3.65	4.49	4.33
221	2.40	2.47	3.06	2.94	3.54	3.67	4.51	4.35	3.52	3.65	4.49	4.33
222	2.40	2.47	3.06	2.94	3.54	3.67	4.51	4.35	3.52	3.65	4.49	4.33
223	2.40	2.47	3.06	2.94	3.54	3.67	4.51	4.35	3.52	3.65	4.49	4.33
224	2.40	2.47	3.06	2.94	3.54	3.67	4.51	4.35	3.52	3.65	4.49	4.33
225	2.40	2.47	3.06	2.94	3.54	3.67	4.51	4.35	3.52	3.65	4.49	4.33
226	2.40	2.47	3.06	2.94	3.54	3.67	4.51	4.35	3.52	3.65	4.49	4.33
227	2.40	2.47	3.06	2.94	3.54	3.67	4.51	4.35	3.52	3.65	4.49	4.33
228	2.40	2.47	3.06	2.94	3.54	3.67	4.51	4.35	3.52	3.65	4.49	4.33
229	2.40	2.47	3.06	2.94	3.54	3.67	4.51	4.35	3.52	3.65	4.49	4.33
230	2.40	2.47	3.06	2.94	3.54	3.67	4.51	4.35	3.52	3.65	4.49	4.33
231	2.40	2.47	3.06	2.94	3.54	3.67	4.51	4.35	3.52	3.65	4.49	4.33
232	2.40	2.47	3.06	2.94	3.54	3.67	4.51	4.35	3.52	3.65	4.49	4.33
233	2.40	2.47	3.06	2.94	3.54	3.67	4.51	4.35	3.52	3.65	4.49	4.33
234	2.40	2.47	3.06	2.94	3.54	3.67	4.51	4.35	3.52	3.65	4.49	4.33
235	2.40	2.47	3.06	2.94	3.54	3.67	4.51	4.35	3.52	3.65	4.49	4.33
236	2.40	2.47	3.06	2.94	3.54	3.67	4.51	4.35	3.52	3.65	4.49	4.33
237	2.40	2.47	3.06	2.94	3.54	3.67	4.51	4.35	3.52	3.65	4.49	4.33
238	2.40	2.47	3.06	2.94	3.54	3.67	4.51	4.35	3.52	3.65	4.49	4.33
239	2.40	2.47	3.06	2.94	3.54	3.67	4.51	4.35	3.52	3.65	4.49	4.33
240	2.40	2.47	3.06	2.94	3.54	3.67	4.51	4.35	3.52	3.65	4.49	4.33
241	2.40	2.47	3.06	2.94	3.54	3.67	4.51	4.35	3.52	3.65	4.49	4.33
242	2.40	2.47	3.06	2.94	3.54	3.67	4.51	4.35	3.52	3.65	4.49	4.33
243	2.40	2.47	3.06	2.94	3.54	3.67	4.51	4.35	3.52	3.65	4.49	4.33
244	3.04	3.14	3.90	3.75	4.51	4.67	5.74	5.54	4.49	4.65	5.71	5.51
245	3.50	3.61	4.48	4.30	5.18	5.37	6.59	6.36	5.15	5.34	6.56	6.33
246	3.50	3.61	4.48	4.30	5.18	5.37	6.59	6.36	5.15	5.34	6.56	6.33
247	3.06	3.16	3.92	3.76	4.53	4.70	5.77	5.57	4.51	4.68	5.74	5.54
248	3.50	3.61	4.48	4.30	5.18	5.37	6.59	6.36	5.15	5.34	6.56	6.33
249	3.50	3.61	4.48	4.30	5.18	5.37	6.59	6.36	5.15	5.34	6.56	6.33
250	3.08	3.17	3.94	3.78	4.55	4.72	5.80	5.60	4.53	4.70	5.77	5.57
251	3.50	3.61	4.48	4.30	5.18	5.37	6.59	6.36	5.15	5.34	6.56	6.33
252	3.50	3.61	4.48	4.30	5.18	5.37	6.59	6.36	5.15	5.34	6.56	6.33
253	3.10	3.19	3.97	3.81	4.59	4.76	5.84	5.64	4.57	4.74	5.81	5.61
254	3.50	3.61	4.48	4.30	5.18	5.37	6.59	6.36	5.15	5.34	6.56	6.33
255	3.50	3.61	4.48	4.30	5.18	5.37	6.59	6.36	5.15	5.34	6.56	6.33
256	3.16	3.25	4.04	3.88	4.65	4.85	5.95	5.74	4.63	4.83	5.92	5.71

Table G-3. Continued

#	Rock (T) = 2 m				Rock (T) = 4 m				Rock (T) = 4 m			
	E=5MPa B = 2m D = 0m	E=5MPa B = 4m D = 0m	E=5MPa B = 4m D = 2m	E=5MPa B = 2m D = 1m	E=10MPa B = 2m D = 0m	E=10MPa B = 4m D = 0m	E=10MPa B = 4m D = 2m	E=10MPa B = 2m D = 1m	E=5MPa B = 2m D = 0m	E=5MPa B = 4m D = 0m	E=5MPa B = 4m D = 2m	E=5MPa B = 2m D = 1m
257	3.50	3.61	4.48	4.30	5.18	5.37	6.59	6.36	5.15	5.34	6.56	6.33
258	3.50	3.61	4.48	4.30	5.18	5.37	6.59	6.36	5.15	5.34	6.56	6.33
259	3.18	3.27	4.06	3.90	4.70	4.87	5.98	5.77	4.68	4.85	5.95	5.74
260	3.50	3.61	4.48	4.30	5.18	5.37	6.59	6.36	5.15	5.34	6.56	6.33
261	3.50	3.61	4.48	4.30	5.18	5.37	6.59	6.36	5.15	5.34	6.56	6.33
262	3.20	3.30	4.10	3.93	4.74	4.91	6.03	5.82	4.72	4.89	6.00	5.79
263	3.50	3.61	4.48	4.30	5.18	5.37	6.59	6.36	5.15	5.34	6.56	6.33
264	3.50	3.61	4.48	4.30	5.18	5.37	6.59	6.36	5.15	5.34	6.56	6.33
265	3.22	3.31	4.11	3.95	4.76	4.93	6.06	5.85	4.74	4.91	6.03	5.82
266	3.50	3.61	4.48	4.30	5.18	5.37	6.59	6.36	5.15	5.34	6.56	6.33
267	3.50	3.61	4.48	4.30	5.18	5.37	6.59	6.36	5.15	5.34	6.56	6.33
268	3.24	3.33	4.14	3.98	4.79	4.97	6.10	5.89	4.77	4.95	6.07	5.86
269	3.50	3.61	4.48	4.30	5.18	5.37	6.59	6.36	5.15	5.34	6.56	6.33
270	3.50	3.61	4.48	4.30	5.18	5.37	6.59	6.36	5.15	5.34	6.56	6.33
271	3.38	3.48	4.34	4.16	5.01	5.19	6.38	6.16	4.98	5.16	6.35	6.13
272	3.87	3.98	4.95	4.75	5.73	5.94	7.29	7.04	5.70	5.91	7.25	7.00
273	4.33	4.46	5.54	5.32	6.41	6.64	8.16	7.87	6.38	6.61	8.12	7.83
274	3.42	3.52	4.37	4.20	5.06	5.25	6.44	6.21	5.03	5.22	6.41	6.18
275	3.91	4.02	5.00	4.79	5.78	5.99	7.36	7.10	5.75	5.96	7.32	7.06
276	4.36	4.49	5.58	5.35	6.45	6.69	8.21	7.92	6.42	6.66	8.17	7.88
277	3.46	3.56	4.43	4.24	5.12	5.31	6.52	6.29	5.09	5.28	6.49	6.26
278	3.94	4.06	5.04	4.84	5.83	6.04	7.42	7.16	5.80	6.01	7.38	7.12
279	4.39	4.52	5.62	5.40	6.50	6.74	8.28	7.99	6.47	6.71	8.24	7.95
280	3.49	3.60	4.47	4.29	5.17	5.36	6.58	6.35	5.14	5.33	6.55	6.32
281	3.97	4.09	5.09	4.88	5.89	6.10	7.49	7.23	5.86	6.07	7.45	7.19
282	4.43	4.56	5.67	5.43	6.55	6.79	8.34	8.05	6.52	6.76	8.30	8.01
283	3.56	3.67	4.56	4.38	5.27	5.46	6.71	6.48	5.24	5.43	6.68	6.45
284	3.99	4.12	5.12	4.92	5.92	6.14	7.54	7.28	5.89	6.11	7.50	7.24
285	4.46	4.58	5.70	5.47	6.59	6.83	8.39	8.10	6.56	6.80	8.35	8.06
286	3.59	3.70	4.60	4.42	5.32	5.51	6.77	6.53	5.29	5.48	6.74	6.50
287	4.03	4.15	5.16	4.95	5.96	6.18	7.59	7.32	5.93	6.15	7.55	7.28
288	4.48	4.62	5.74	5.51	6.64	6.88	8.45	8.15	6.61	6.85	8.41	8.11
289	3.65	3.76	4.68	4.48	5.40	5.60	6.88	6.64	5.37	5.57	6.85	6.61
290	4.08	4.21	5.22	5.01	6.04	6.26	7.69	7.42	6.01	6.23	7.65	7.38
291	4.54	4.67	5.80	5.57	6.71	6.96	8.54	8.24	6.68	6.93	8.50	8.20
292	3.73	3.84	4.78	4.59	5.53	5.73	7.04	6.79	5.50	5.70	7.00	6.76
293	4.17	4.29	5.34	5.12	6.16	6.39	7.85	7.58	6.13	6.36	7.81	7.54
294	4.60	4.73	5.89	5.66	6.81	7.06	8.67	8.37	6.78	7.02	8.63	8.33
295	3.83	3.95	4.91	4.71	5.68	5.89	7.23	6.98	5.65	5.86	7.19	6.95
296	4.27	4.40	5.47	5.25	6.33	6.56	8.05	7.77	6.30	6.53	8.01	7.73
297	4.69	4.82	6.00	5.75	6.94	7.19	8.83	8.52	6.91	7.15	8.79	8.48
298	3.61	3.72	4.62	4.44	5.34	5.54	6.80	6.56	5.31	5.51	6.77	6.53
299	4.14	4.26	5.29	5.08	6.12	6.34	7.78	7.51	6.09	6.31	7.74	7.47
300	4.60	4.73	5.88	5.65	6.80	7.05	8.66	8.36	6.77	7.01	8.62	8.32
301	3.67	3.77	4.68	4.49	5.42	5.62	6.90	6.66	5.39	5.59	6.87	6.63
302	4.18	4.30	5.35	5.13	6.18	6.41	7.87	7.59	6.15	6.38	7.83	7.55
303	4.65	4.79	5.95	5.71	6.89	7.14	8.77	8.46	6.86	7.10	8.73	8.42

Table G-3. Continued

#	Rock (T) = 2 m				Rock (T) = 4 m				Rock (T) = 4 m			
	E=5MPa B = 2m D = 0m	E=5MPa B = 4m D = 0m	E=5MPa B = 4m D = 2m	E=5MPa B = 2m D = 1m	E=10MPa B = 2m D = 0m	E=10MPa B = 4m D = 0m	E=10MPa B = 4m D = 2m	E=10MPa B = 2m D = 1m	E=5MPa B = 2m D = 0m	E=5MPa B = 4m D = 0m	E=5MPa B = 4m D = 2m	E=5MPa B = 2m D = 1m
304	3.72	3.83	4.76	4.56	5.51	5.71	7.01	6.76	5.48	5.68	6.97	6.73
305	4.23	4.36	5.43	5.20	6.27	6.50	7.99	7.71	6.24	6.47	7.95	7.67
306	4.70	4.84	6.02	5.78	6.97	7.22	8.86	8.55	6.94	7.18	8.82	8.51
307	3.76	3.88	4.83	4.64	5.58	5.78	7.10	6.85	5.55	5.75	7.06	6.82
308	4.29	4.42	5.49	5.27	6.35	6.58	8.08	7.80	6.32	6.55	8.04	7.76
309	4.78	4.92	6.11	5.87	7.07	7.33	9.00	8.69	7.03	7.29	8.96	8.65
310	3.87	3.98	4.95	4.75	5.73	5.94	7.29	7.04	5.70	5.91	7.25	7.00
311	4.34	4.47	5.56	5.34	6.43	6.66	8.18	7.89	6.40	6.63	8.14	7.85
312	4.85	4.99	6.20	5.95	7.17	7.43	9.13	8.81	7.13	7.39	9.08	8.77
313	3.93	4.05	5.03	4.83	5.83	6.04	7.41	7.15	5.80	6.01	7.37	7.11
314	4.43	4.56	5.67	5.43	6.55	6.79	8.34	8.05	6.52	6.76	8.30	8.01
315	4.94	5.10	6.34	6.08	7.32	7.59	9.32	8.99	7.28	7.55	9.27	8.95
316	4.03	4.15	5.16	4.95	5.96	6.18	7.59	7.32	5.93	6.15	7.55	7.28
317	4.57	4.71	5.85	5.61	6.76	7.01	8.61	8.31	6.73	6.97	8.57	8.27
318	5.03	5.18	6.45	6.19	7.46	7.73	9.49	9.16	7.42	7.69	9.44	9.11
319	4.22	4.35	5.41	5.19	6.25	6.48	7.96	7.68	6.22	6.45	7.92	7.64
320	4.69	4.82	6.00	5.75	6.94	7.19	8.83	8.52	6.91	7.15	8.79	8.48
321	5.14	5.29	6.58	6.31	7.61	7.89	9.68	9.34	7.57	7.85	9.63	9.29
322	4.45	4.58	5.68	5.46	6.58	6.82	8.37	8.08	6.55	6.79	8.33	8.04
323	4.90	5.04	6.26	6.01	7.25	7.51	9.22	8.90	7.21	7.47	9.17	8.86
324	5.33	5.49	6.83	6.55	7.89	8.18	10.05	9.70	7.85	8.14	10.01	9.65

Table G-4. Additional FEM simulations – Bearing capacities (MPa) on rock subsurface

D	a MPa	α_0	β_0	p_p MPa	B = 1 m L = 3 m	B = 1 m L= 10 m	B = 1.5 m L = 3 m	B = 1.5 m L = 15 m	B = 3 m L = 4.5 m	B = 3 m L = 30 m
0 m	0.1	27	0	1.2	0.44	0.42	0.54	0.45	0.65	0.47
	0.5	29	10	2.0	2.58	2.43	3.28	2.62	4.74	2.74
	0.7	32	-10	3.0	4.08	3.84	5.18	4.01	7.21	4.32
	0.8	33	0	4.0	5.29	4.98	6.72	5.35	9.22	5.85
0.5 m	0.1	27	0	1.2	0.46	0.43	0.55	0.47	0.68	0.51
	0.5	29	10	2.0	2.76	2.54	3.45	2.75	4.87	2.99
	0.7	32	-10	3.0	4.74	4.37	5.88	4.82	8.66	5.21
	0.8	33	0	4.0	6.26	5.77	7.78	6.22	10.89	6.72
1.0 m	0.1	27	0	1.2	0.49	0.46	0.59	0.50	0.73	0.54
	0.5	29	10	2.0	2.93	2.72	3.68	2.93	5.18	3.16
	0.7	32	-10	3.0	5.49	5.11	6.71	5.51	9.88	5.93
	0.8	33	0	4.0	6.70	6.23	8.13	6.71	11.85	7.24

Table G-5. Additional FEM simulation – Bearing capacities (MPa) on rock (E = 300 MPa) over sand subsurface

D	a MPa	α ^{0}	β ^{0}	p_p MPa	B = 1 m L = 3 m T = 3 m E_{soil}=60 MPa	B = 1 m L = 10 m T = 4 m E_{soil}=20 MPa	B=1.5 m L=3 m T = 3 m E_{soil}=25 MPa	B=1.5 m L=15 m T = 5 m E_{soil}=15 MPa	B=3 m L=4.5 m T = 5 m E_{soil}=20 MPa	B=3 m L=30 m T = 4 m E_{soil}=25 MPa
0 m	0.1	27	0	1.2	0.40	0.37	0.41	0.44	0.64	0.42
	0.5	29	10	2.0	2.32	2.13	2.47	2.58	4.69	2.43
	0.7	32	-10	3.0	3.67	3.37	3.90	3.95	7.15	3.82
	0.8	33	0	4.0	4.75	4.37	5.06	5.27	9.11	5.21
0.5 m	0.1	27	0	1.2	0.41	0.38	0.41	0.46	0.67	0.47
	0.5	29	10	2.0	2.48	2.23	2.60	2.71	4.81	2.68
	0.7	32	-10	3.0	4.26	3.83	4.42	4.75	8.59	4.62
	0.8	33	0	4.0	5.63	5.06	5.85	6.13	10.76	5.99
1.0 m	0.1	27	0	1.2	0.44	0.40	0.44	0.49	0.72	0.49
	0.5	29	10	2.0	2.63	2.39	2.77	2.89	5.12	2.83
	0.7	32	-10	3.0	4.93	4.48	5.05	5.43	9.75	5.35
	0.8	33	0	4.0	6.02	5.46	6.12	6.61	11.77	6.43